

International Publications Awards

Cairo University

Vol. 7 Issue 1 (A)

May 2013

Dear colleagues,

We are pleased to introduce vol. 7(1) issue of the international publications of Cairo University. It is a further step and distinct contribution, reflecting the scientific ability of staff members, which conforms to international quality standards.

The purpose of issuing these publications is mainly to introduce this work to the academic community, demonstrate the different research abilities of Cairo University researchers, and encourage them to increase the quality and quantity of their research.

We would like to assure you that the administration will spare no effort to support and reinforce these goals.

We congratulate all colleagues who were granted the awards for their international publications of the year 2012 and wish them all the best for their future endeavors.

We are also pleased to inform you that this policy will continue to be in effect for the years to come.

Prof. Gamal Esmat

**Vice - President for post-graduate
studies and research
Cairo university**

Prof. Hossam Kamel

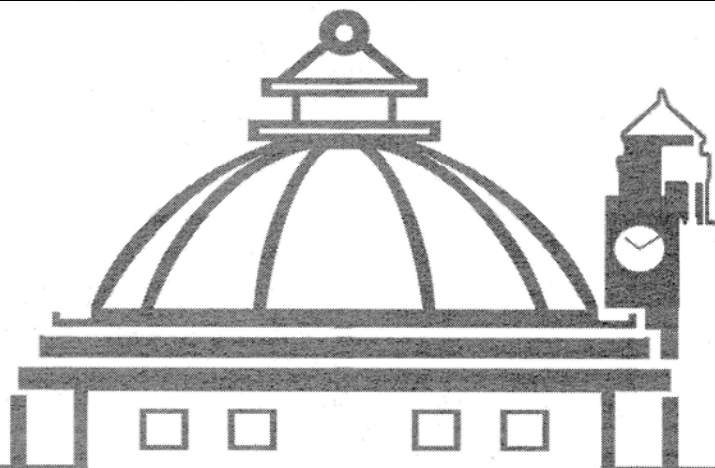
**President
Cairo university**

Table of Contents

	Page
Preface	i
1. Basic Sciences Sector	1
1-1 Faculty of Agriculture	3
1-2 Faculty of Science	43
1-3 Faculty of Veterinary Medicine	144
1-4 Institute of Statistical Studies and Research	169
Authors' Index	179



**International Publications Awards
Cairo University**



**(1)
Basic
Sciences Sector**

1-1 Faculty of Agriculture

1-2 Faculty of Science

1-3 Faculty of Veterinary Medicine

**1-4 Institute of Statistical Studies and
Research**

Faculty of Agriculture

Dept. of Agricultural Biochemistry

1. Enhancement of Lipid Accumulation in *Scenedesmus Obliquus* by Optimizing CO₂ and Fe³⁺ Levels for Biodiesel Production

Hanaa H. Abd El Baky, Gamal S. El-Baroty, Abderrahim Bouaid, Mercedes Martinez and José Aracil

Bioresource Technol, 119: 429-432 (2012) IF: 4.98

The effects of cultivation of *Scenedesmus obliquus* in nutrient medium supplemented with 0.03%, 3, 9% and 12% CO₂ or 2.5–20 mg L⁻¹ of Fe³⁺ on dry weight of biomass (DW), total lipid accumulation (TL contents) and total lipid productivity (TLP) were evaluated under indoor conditions. The accumulation of TL and TLP showed an increasing trend with increasing of CO₂ or Fe³⁺ levels. In cultures with 12% CO₂ or 20 mg/L Fe³⁺, maximum TL contents of 33.14% and 28.12%, respectively were obtained. These lipids displayed a fatty acid profile which is suitable for biodiesel production as the most abundant compounds were oleic (32.19–34.44%), palmitic (29.54–25.12%) and stearic (12.26–16.58% of total FAMES) acids. The properties of biodiesel obtained from *S. obliquus*, were the same with those specification for biodiesel standards including ASTM D 6751 (American Society for Testing Material) and the European Standard EN 14214. Thus, *S. obliquus* biomass could be used as suitable feedstock for biodiesel production.

Keywords: *Scenedesmus obliquus*; Microalgae biodiesel; Fatty acid; Microalgae oils and physiochemical properties of biodiesel.

2. Protein Solubility, Digestibility and Fractionation After Germination of Sorghum Varieties

Abd El-Moneim M. R. Afify, Hossam S. El-Beltagi, Samiha M. Abd El-Salam and Azza A. Omran

Plos One, 7: (2012) IF: 4.092

The changes in crude protein, free amino acids, amino acid composition, protein solubility, protein fractionation and protein digestibility after germination of sorghum were investigated. Sorghum varieties were soaked for 20 h followed by germination for 72h, the results revealed that crude protein and free amino acids in raw sorghum varieties ranged from 10.62 to 12.46% and 0.66 to 1.03 mg/g, respectively. Shandaweel-6 was the highest variety in crude protein and free amino acids content. After germination, crude protein was decreased and free amino acids were increased. There was an increase in content of amino acids valine and phenylalanine after germination. On the other hand, there was a decrease in most of amino acids after germination. After germination protein solubility was significantly increased. Regarding protein fractions, there was an increase in albumin, globulin and kafirin proteins and a decrease in cross linked kafirin and cross linked glutelin after germination.

Keywords: Sorghum; Germination; Amino Acids; Protein Fractions; Protein Digestibility.

3. Recombination Suppression at the Dominant *Rhg1/Rfs2* Locus Underlying Soybean Resistance to the Cyst Nematode

Ahmed J. Afzal, Ali Srouf, Navinder Saini, Naghmeh Hemmati, Hany A. El Shemy and David A. Lightfoot

Theor Appl Genet, 124 (6): 1027-1039 (2012) IF: 3.297

Host resistance to “yellow dwarf” or “moonlight” disease cause by any population (Hg type) of *Heterodera glycines* I., the soybean cyst nematode (SCN), requires a functional allele at *rhg1*. The host resistance encoded appears to mimic an apoptotic response in the giant cells formed at the nematode feeding site about 24–48 h after nematode feeding commences. Little is known about how the host response to infection is mediated but a linked set of 3 genes has been identified within the *rhg1* locus. This study aimed to identify the role of the genes within the locus that includes a receptor-like kinase (RLK), a laccase and an ion transporter. Used were near isogenic lines (NILs) that contrasted at their *rhg1* alleles, gene-based markers and a new Hg type 0 and new recombination events.

Keywords: Soybean; Cyst Nematode; *Rhg1/Rfs2*.

4. Anti-Cancer Characteristics of Mevinolin Against Three Different Solid Tumor Cell Lines Was Not Solely P53-Dependent

Ali Mokhtar Mahmoud, Ahmed M. Al-Abd, David A. Lightfoot and Hany A. El-Shemy

J Enzym Inhib Med Ch, 27: 673-679 (2012) IF: 1.617

Mevinolin (MVN) has been used clinically for the treatment of hypercholesterolemia with very good tolerance by patients. Based on epidemiological evidences, MVN was suggested strongly for the treatment of neoplasia. Early experimental trials suggested the mixed apoptotic/necrotic cell death pathway was activated in response to MVN exposure. Herein, the cytotoxic profile of MVN was evaluated, compared to the robust and frequently used anticancer drug doxorubicin (DOX), against breast (MCF-7), cervical (HeLa) and liver (HepG₂) transformed cell lines. MVN was showed comparable results in cytotoxic profile with DOX in all tested solid tumor cell lines. In addition, the MVN-induced cytotoxicity was inferred to be multi-factorial and not solely dependent on p53 expression. It was concluded that molecular and genetic assessment of MVN-induced cell death would be useful for developing cancer therapeutic treatments.

Keywords: Mevinolin; Doxorubicin; Solid tumors; Natural products; P53.

5. Characterization and Bioactivity of Phycocyanin Isolated from *Spirulina Maxima* Grown Under Salt Stress

Hanaa H. Abd El-Baky and Gamal S. El-Baroty

Food Function, 3: 381-388 (2012) IF: 1.179

In this study, *Spirulina maxima* (SM) has been selected following preliminary investigations, for cultivation in either normal (0.02M) or stress (0.1M) NaCl medium (Zarrouk) under room conditions to evaluate the possibility of increasing the total phycobiliprotein content (TPC) and their chemical constituents: C-phycocyanin (C-PC), allophycocyanin (APC) and phycoerythrin

(PE). TPC material was separated, purified and characterized by various spectroscopic techniques (UV-Vis and IR spectra). The antioxidant activity against free radicals of DPPH, ABTS, superoxide ($-\text{O}_2$), hydroxy (OH) and reducing power potential were determined. Results indicated a highly significant correlation between increased TPC content in SM cells and the increasing concentration of NaCl in medium and its chemical constituents were significantly different ($P > 0.05$). TPC of SM (grown in stress NaCl) containing high amounts of C-PC groups, showed strong antioxidant activity compared with ascorbic acid (standard antioxidant). Although, its activity against different free radicals were found to be variable and dose-dependent. Moreover, the TPC showed lower antimicrobial activity (MIC values in the range of $250\text{--}300\mu\text{g mL}^{-1}$) than that of chloramphenicol ($30\mu\text{g mL}^{-1}$, reference antimicrobial). Therefore, *Spirulina maxima* could be cultivated in a salinated open pond and considered as highly healthy foods and source of natural pigments.

Keywords: Bioactivity; Phycocyanin; *Spirulina Maxima* and Stress.

6. Studies on the Hypolipidemic Effects of Coconut Oil When Blended with Tiger Nut Oil and Fed to Albino Rats

A.M. El-Anany and R.F.M. Ali

Grasas Aceites, 63: 303-312 (2012) IF: 1.138

Hyperlipidemia is a predominant risk factor for atherosclerosis and associated cardiovascular diseases (CVD). The international guidelines issued by the World Health Organization recommend a reduction in dietary saturated fat and cholesterol intake as a means to prevent hypercholesterolemia and CVD. The main objective of the current investigation was to evaluate the effects of feeding blended oils consisting of coconut oil (CNO) with different proportions of Tiger nut oil (TNO) on serum lipid levels in Albino rats. GLC analysis was performed to illustrate the fatty acid composition of the blended oils. Blended oils were obtained by mixing tiger nut oil with coconut oil at the volume ratios of 100:0, 70:30, 50:50, 25:75, 10:90 and 0:100. Fifty-six male albino rats were randomly divided into 7 groups of 8 rats each according to the oil type. The blended oils were fed to rats for a period of up to 10 weeks. Total cholesterol (T-Ch), high-density lipoprotein cholesterol (HDL-Ch), low-density lipoprotein cholesterol (LDL-Ch) and triglycerides (TG), were determined. The atherogenic Index (AI) was calculated. The results showed that non-significant changes in all nutritional parameters were observed between the control group and the rats fed with the tested oils. The results also indicate that coconut oil had 86% saturated fatty acids. On TNO contains 66% oleic acid. Therefore, blending coconut oil with tiger nut oil can reduce the proportions of saturated to unsaturated fatty acids in CNO. The rats that were fed blended oils showed significantly reduced levels of serum cholesterol as compared to those fed CNO. The HDL levels were marginally enhanced in the rats that were fed blended oils. The total cholesterol and LDL cholesterol levels were controlled when TNO/CNO proportions varied between 25/75 and 70/30. This was reflected in the calculation of the atherogenic index. Similar changes were observed with serum triglyceride levels.

Keywords: Albino rats; Blood lipid; Coconut; Fatty acids; Hyperlipidemia; Oil blends; Tiger nut.

7. Physicochemical Studies on Sunflower Oil Blended with Cold Pressed Tiger Nut Oil During the Deep Frying Process

Rehab F. M. Ali and A. M. El Anany

Grasas Aceites, 63 (2012) IF: 1.138

Blends consisting of Sunflower oils were blended with different levels of coldpressed tiger nut oil. Blended oils were obtained by mixing tiger nut oil with sunflower oil at the volume ratios of 0:100, 10: 90, 20: 80, 30: 70, 40: 60, 50:50 and 100: 0. The effects of deep frying on physico-chemical parameters (Free Fatty Acid (FFA), Peroxide Value (PV), thiobarbituric acid value (TBA), iodine value, Total Polar Compounds (TPC), color and viscosity) were evaluated over 30 hours of the frying process. The total phenolic content of native oils was determined. GLC analysis was performed to illustrate the fatty acid composition of sunflower oil, tiger nut oil and binary mixtures of them as well as their oxidation rates. The pure and blended oils were heated at $180\text{ }^\circ\text{C} \pm 5\text{ }^\circ\text{C}$, then frozen French fried potatoes were fried every 30 min. Oil samples were taken every 5 h and the entire continuous frying period was 30 h. The results showed that fresh sunflower oil had significantly the highest value of COX (7.25); while tiger nut oil had significantly the lowest (2.24). Mixing sunflower oil with different levels of tiger nut oil led to an increase in its stability against oxidation. The phenolic content of cold pressed tiger nut oil was about 3.3 times as high as that of sunflower oil. The analytical data showed that the lowest deterioration during the frying process occurred in tiger nut oil and the highest in sunflower. The changes in the physico-chemical parameters were controlled and significantly ($P < 0.05$) decreased when tiger nut /sunflower oil (W/W) proportions were varied between 20/80 to 50/50. The obtained results indicate that mixing sunflower oil with cold pressed tiger nut oil increased the stability and hence improved the quality of sunflower oil during the frying process.

Keywords: Antioxidants; Blending; Cox Value-Fatty Acids; Oxidation; Tiger nut oil; Sunflower oil; Stability.

8. Hepatoprotective Effects of Antioxidants Against Non-Target Toxicity of the Bio-Insecticide Spinosad in Rats

Ahmed M. Aboul-Enein, Mourad A. M. Aboul-Soud, Hamed K. Said, Hanaa F. M. Ali, Zeinab Y. Ali, Amany M. Mahdi and John P. Giesy

African Journal of Pharmacy And Pharmacology, 6 (8): 550-559 IF: 0.839

The bio-insecticide spinosad (SPD) is increasingly being used in pest management programmes. In order to further assess its toxic effects to non-target species, male rats were exposed sub-chronically to SPD at a dose equivalent to $1/20\text{ LD}_{50}$ for four weeks. In order to assess the toxicity of SPD, parameters such as the activities of enzymes and concentrations of non-enzymatic antioxidant components, histopathological examination, DNA fragmentation and chromosomal aberrations in liver were analysed. Protection by an antioxidants mixture (AM), containing vitamin C, vitamin E and silymarin, against the effects of SPD was investigated. Exposure to SPD inhibited the activity of acetylcholinesterase and depleted contents of reduced glutathione and malondialdehyde. SPD caused significant inhibition of

activity of key antioxidant enzymes (GST, SOD) and induction in GPx. Treatment with AM attenuated all SPD-mediated effects. Histological examination of the liver revealed that SPD caused focal necrosis and degenerative changes in hepatocytes, along with cytoplasmic vacuolation. All of these lesions were significantly less in rats fed with AM. SPD accelerated formation of internucleosomal DNA fragmentation, which was attenuated by treatment with AM. Similarly, SPD caused significant structural chromosomal aberrations in bone marrow cells, the frequency of which was diminished by AM

Keywords: Antioxidants; Dna damage; Silymarin; Spinosa; Vitamin C; Vitamin E.

9. The Impact of γ -Irradiation, Essential Oils and Iodine on Biochemical Components and Metabolism of Potato Tubers During Storage

Abd El-Moneim M.R. Afify, Hossam S. El-Beltagi, Amina A. Aly and Abeer E. El-Ansary

Not Bot Horti Agrobo, 40 (2): 129-139 (2012) IF: 0.652

Several methods have been suggested as effective for inhibition of sprouting of potato tubers during storage. Three methods; γ -irradiation, volatile oils and iodine vapor were used for the inhibition of potato tuber cv. 'Diamond'. Gamma irradiation, essential oils (caraway, clove, carvone, eugenol) and Iodine vapor were used to achieve the purpose. The results proved that γ -irradiation and essential oils maintain potato as well as inhibit sprouting for 9 weeks while iodine vapor maintain potato for six weeks. Alpha amylase activity showed an increase after six weeks and then reduced to lower value compared to control. During the metabolic pathway the concentration of lactate was decreased and reached to the level of control when potato tuber treated even with essential oils, radiation as well as with iodine vapor. The levels of NADP and NADPH+H were decreased during potato storage proving that synthesis of this metabolite were very low. The level of glycoalkaloids was fluctuated during storage depending on the treatments.

Keywords: Essential oils; Gamma irradiation; Iodine; Metabolism; Potato tubers.

10. Effect of Soaking, Cooking, Germination and Fermentation Processing on Proximate Analysis and Mineral Content of Three White Sorghum Varieties (*Sorghum Bicolor* L. Moench)

Abd El-Moneim M. R. Afify, Hossam S. El-beltagi, Samiha M. and Azza A. Omran

Asian Pacific Journal of Tropical Biomedicine, 40: 92-98 (2012) IF: 0.652

The changes in chemical composition, amylose and minerals content after soaking, cooking, germination and fermentation of three white sorghum varieties, named 'Dorado', 'Shandaweel-6' and 'Giza-15' were investigated. The chemical composition concluded including crude protein, oils, crude fiber and ash. Crude protein content ranged from 10.62 to 12.46% in raw sorghum. 'Shandaweel-6' was the highest variety in crude protein content (12.46%). 'Dorado' was the highest variety in oils and ash (3.91 and 1.45%). 'Shandaweel-6' was the highest variety in crude fiber (1.85%). Amylose content ranged from 18.30 to

20.18% in raw sorghum. Amylose was higher in 'Giza-15' than other varieties. Minerals content i.e., Zn, Fe, Ca, K, Na, Mg, Mn and Cu were investigated. Results indicated that raw 'Dorado' was the highest variety in K, Mg, Ca, Fe and Mn (264.53, 137.14, 33.09, 7.65 and 1.98 mg/100g). While, 'Shandaweel-6' was the highest variety in Zn and Cu (5.02 and 0.84 mg/100 g). Finally 'Giza-15' was the highest variety in P and Na (381.37 and 119.29 mg/100 g). After treatments chemical composition, amylose and minerals were decreased. Processing techniques reduce the levels of antinutritional organic factors, which including phytates, phenols, tannins and enzyme inhibitors by releasing exogenous and endogenous enzymes such as phytase enzyme formed during processing.

Keywords: Amylose; Chemical composition; Minerals; Processing; Sorghum.

11. Oil and Fatty Acid Contents of White Sorghum Varieties Under Soaking, Cooking, Germination and Fermentation Processing for Improving Cereal Quality

Abd El-Moneim M.R. Afify, Hossam S. El-Beltagi, Samiha M. Abd El-Salam and Azza A. Omran

Not Bot Horti Agrobo, 40 (1): 86-92, 40: 86-92 (2012) IF: 0.652

The changes in lipid and fatty acid contents after soaking, cooking, germination and fermentation of three white sorghum varieties were studied to improve cereal quality. The results revealed that oil in raw sorghum varieties ranged from 3.58 to 3.91%, respectively and 'Dorado' represents the highest variety in oil content. As general trend after germination, oil content was decreased. Fatty acid contents of raw sorghum contains palmitic (12.10 to 13.41%), palmitoleic (0.47 to 1.31%), stearic (1.13 to 1.36%), oleic (33.64 to 40.35%), linoleic (42.33 to 49.94%), linolenic (1.53 to 1.72%), arachidic (0.10 to 0.18%) and eicosenoic acid (0.24 to 0.39% of total lipid). 'Dorado' was the highest variety in oleic acid while 'Shandaweel-6' was the highest variety in palmitic, stearic, linolenic, arachidic, eicosenoic acid and total saturated fatty acids. 'Giza-15' was the highest variety in palmitoleic, linoleic, total unsaturated fatty acids and ratio of unsaturated to saturated fatty acids. Fatty acids relative percentage changed after soaking, cooking, germination and fermentation

Keywords: Cooking; Fatty acid; Fermentation; Germination; Oils; Soaking; Sorghum.

12. Response of Antioxidant Substances and Enzymes Activities as a Defense Mechanism Against Root-Knot Nematode Infection

Hossam S. El-Beltagi, Ahmed A Farahat, Alsayed A. Alsayed and Nomer M. Mahfoud

Notulae Botanicae Horti Agrobotanici Cluj-Napoca, 40: 132-142 (2012) IF: 0.652

The organic amendments, composts (1, 2, 3), neem and poultry as well as inorganic fertilizers (NPK compound and commercial, A three®) and the nematicide nemacur 10 G applied singly were effective in reducing *M. incognita* number of galls, nematode reproduction and fecundity. The effectiveness seemed to be material origin dependent. Neem, compost 1, 3 (5 g/pot) gave the best results. Yet, achieved results were less than those of nemacur

10% G. The antioxidant substances content and enzymes activities due to nematode infection and application of organic and inorganic fertilizers pointed to significant increase of lipid peroxidation and hydrogen peroxide as a result of nematode infection and nematic treatment. While all organic and inorganic fertilizers reduced such materials with significant differences among treatments. Likewise, nematode infection resulted in slight but significant increase in glutathione and ascorbic acid in tomato shoots and roots. All treatments increased antioxidant substances comparing to healthy and infected plants. Glutathione-S-transferase activity highly increased in infected roots but the lowest activities were achieved by organic fertilizers. Nematode infection and nematic treatment increased slightly phenylalanine ammonia lyase activity but enormous increase was observed in shoots and roots of treated plants with organic fertilizers followed by NPK treatments.

Keywords: Antioxidant enzymes; Lipid peroxidation; Meoildogyne incognita.

13. Antioxidant Effect of Celery Against Carbon tetrachloride Induced Hepatic Damage in Rats

Abdou H. S, Salah S. H, Hoda Booles F and Abdel Rahim E. A.

African Journal of Microbiology Research, 6: 5657-5667 (2012) IF: 0.53

Ethanol extract of celery (*Apium graveolens*) and its diet were evaluated for antioxidant and hepatoprotective activities in rats. Celery is valuable in weight loss diets and regulate lipid metabolism. Albino male rats were used to evaluate its antioxidant and hepatoprotective activities against carbon tetrachloride induced toxicity. Chromosomal aberration, sperm abnormalities, biochemical and molecular assay were used to evaluate its antioxidant activity. Liver damage was assessed by estimating biochemical parameters such as total soluble protein, DNA and RNA contents. Celery showed significant antioxidant effect by reducing chromosomal aberration, sperm abnormalities and increasing DNA bands number and pattern as the control. It also showed a significant hepatoprotective effect by readjusting the toxic effect of CCl₄ on the total soluble protein, DNA and RNA contents around that of the normal.

Keywords: Celery (*Apium Graveolens*); Albino male rats; Carbon tetrachloride; Dna and rna contents and biochemical parameters.

14. Recovery of Used Frying Sunflower Oil with Sugar Cane Industry Waste and Hot Water

Rehab F. M. Ali and A. M. El Anany

Journal of Food Science and, 1-2 (2012) IF: 0.498

The main goal of the current investigation was to use sugar cane bagasse ash (SCBA) and to compare its adsorption efficiency with Magnesol XL as synthetic adsorbents to regenerate the quality of used frying sunflower oil. In addition, to evaluate the effect of water washing process on the quality of used frying oil and the treated oil. The metal patterns of sugar cane bagasse ash and Magnesol XL were determined. Some physical and chemical properties of unused, used frying and used-treated sunflower oil were determined. Sunflower oil sample was heated at 180 °C+5 °C, then frozen French fries potato were fried every 30

min. during a continuous period of 20 h. Oil samples were taken every 4 h. The filter aids were added individually to the used frying oil at levels 1, 2 and 3% (w / v), then mechanically stirred for 60 min at 105 °C. The results indicate that all the filter aids under study were characterized by high levels of Si and variable levels of other minerals. The highest level of Si was recorded for sugar cane bagasse ash (SCBA) was 76.79 wt. %. Frying process caused significant (P0.05) increases in physico-chemical properties of sunflower oil. The treatments of used frying sunflower oil with different levels of sugar cane bagasse ash and Magnesol XL caused significant (P0.05) increase in the quality of treated oil, however the soap content of treated oil was increased, therefore, the effect of water washing process on the quality of used frying and used-treated sunflower oil was evaluated. The values of soap and Total polar compounds after water.

Keywords: Sugarcane; Industrial waste; Frying; Ash.

15. Control of *Tetranychus Urticae* Koch by Extracts of Three Essential Oils of Chamomile, Marjoram and Eucalyptus

Abd El-Moneim MR Afify, Fatma S Ali and Turkey AF

Asian Pacific Journal of Tropical Biomedicine, 24-30 (2012)

To evaluate the acaricidal activity of extracts of three essential oils of chamomile and Eucalyptus against *Tetranychus urticae* (T. urticae) Koch.

Materials and Methods: Three essential oils of chamomile, marjoram and Eucalyptus with different concentrations (0.5%, 1%, 2%, 3%, 4%) were used to control T. urticae Koch.

Results: The results showed against Tetranychus (Chuha mfoolmloiwlead rbecyu tmitaar) j orerapmre sented the most potent efficient acaricidal agent values of chamomile, marjoram and Eucalyptus (Ms aforrj oardaunlats hwoerttee nsis) and Eucalyptus.

The LC₅₀ and for eggs 0.65, 1.84 and 2.18, respectively transferase, eslt.e1r7a, s6e. 26 and 7.33, respectively. Activities of enzymes including glutathione-S- were determined and (ac-teivstietireass eo fa enndz ym-cess tienvaoselv) eadn din a tlhkea lrinesei sphanosceph oaft aaseca riinc isduessc ewptrieb lpe rmovieteds. Pwriothte apsoes ietinvzey mcoen wtraosl. significantly decreased at LC₅₀ of both chamomile and marjoram compared compositions of Chamo Gmasil Leah reocmuatittoag raarpeh y-mass spectrometer (GC-MS) proved that the major-bisabolol oxide A (35.251%) and trans--farersene (7.758%), while the main components of Marjorana hortensis are terpinene-4-ol (23.860%), p-cymene (23.404%) and sabinene (10.904%). **Conclusions:** It can be concluded that extracts of three essential oils of chamomile, marjoram and Eucalyptus possess acaricidal activity against T. urticae.

Keywords: Tetranychidae; Plant essential; Oils enzymes; Glutathione-S; Transferase non specific esterase alkaline; Phosphatase protease chamomile marjoram eucalyptus.

16. A Modified Multi-Residue Method for Analysis of 150 Pesticide Residues in Green Beans using Liquid Chromatography-Tandem Mass Spectrometry

Abd El-Moneim M.R. Afify, Emad R. Attallah and Hassan A. El-Gammal

Advances Food Science, 34 (1): 24-35 (2012)

Three methods of sample preparation and analysis of 150 pesticides in green beans were evaluated and compared for a wide range of physicochemical properties followed by LC-MS/MS detection. One method, dubbed the quick, easy, cheap, effective, rugged and safe (QuEChERS) method for pesticide residue analysis, entailed extraction of 15 g sample with 15 mL acetonitrile. The second method was the ethyl acetate extraction method of 15 g sample without clean up and the third method by luke with extraction procedure of acetone and partitioning by dichloromethane:petroleum (3:1), extract solution of three methods were redissolved in methanol,buffer solution (1:1) ammonium formate 10 mM in pH 4 as modification to increased injection volume to 25 µl without losing our good peak shape. Stabilities of tested pesticides in five different calibration mixture pH stored for two weeks were studied.

Quantitation and identity confirmation was attained by using atmospheric pressure electrospray positive ionization LC-MS/MS in multiple reaction monitoring (MRM) mode, the 150 pesticides signal intensities were studied by three different pH and four concentrations to showed the effect of mobile phase on mention pesticides intensity due to ionization power. The recoveries at three different concentration levels (0.01, 0.05 and 0.1 mg/kg) ranged from 70 to 120% were carried out.

17. Antioxidant Enzyme Activities and Lipid Peroxidation as Biomarker Compounds for Potato Tuber Stored by Iodine Vapor

Abd El-Moneim M.R. Afify, Hossam S. El-Beltagi, Amina A. Aly and Abeer E. El-Ansary

Advances in Food Sciences, (2012)

The present study was conducted to evaluate effect of four iodine vapor concentrations: 9.375g/m³, 18.75g/m³, 37.5g/m³ and 75g/m³ as sprout inhibitors of potato tubers. The activities of biochemical enzymes: catalase, Glutathione-S-transferase, peroxidase, polyphenol oxidase and superoxide dismutase, in addition to lipid peroxidation level (MDA) were tested in potato tubers stored for 3, 6 and 9 weeks of storage. The four iodine vapor concentrations were used to inhibit sprouting process of potato tubers during storage.

The results of enzyme activities were varied depending on the function of enzymes. As general trend the activity of the enzymes recorded are significantly found on the range of enzyme control or less, which prevent potato tuber from sprouting. Glutathione-S-transferase activity was significantly decreased and reached to minimum activity to 2.8±2.41 when treated with high concentration of iodine vapor 75g/m³. Polyphenol oxidase and peroxidase activity increased in its activities and recovered to the level of control in which maintain potato tuber for 6 weeks. The results proved that inhibition of catalase enzyme inhibit germination while increasing catalase activity broken potato dormancy and initiate germination.

Keywords: Antioxidant Enzymes; Iodine; Potato Tubers; Storage.

18. Antioxidant Activity and Biological Evaluations of Probiotic Bacteria Strains

Abd El-Moneim M.R. Afify, Ramy M. Romeilah, Shaimaa I.M.sultan and Mona M. Hussein

International Journal of Academic Research Part A, 4 (6):131-139 (2012)

The antioxidant activity of four probiotics strains belongs to the genera *Lactobacillus* (two strains), *Bifidobacterium* as well as *Probionebacterium* were investigated through the DPPH• and ABTS•+ scavenging ability of the cell free extract of bacteria of the probiotic strains comparing with the standard antioxidant ascorbic acid and BHT. The results of the DPPH scavenging potential of cell free extract showed that the maximum antioxidant activity with *Probionebacterium freudenreichii* (97.75 %) and it was significant increased compared with vit.c and BHT followed by *Lactobacillus reuteria* (96.74 %) activity. All cell free extracts showed highly scavenging potential against ABTS radical. The present study evaluated the survival of free probiotic bacteria under acidic conditions (pH 2 and pH3) during 3h, *L.GG* showed intolerance to pH2, but showed more acid tolerance at pH3. In contrast, the other strains showed more acid tolerance at pH values where incubation of strains for 3h at pH2 resulted in a decrease of about one log cycle, while at pH3 the decrease ranged from 0.2 to 0.7 log cycles. A similar decrease in cell viability was observed in the case of 1% and 2% bile salt for *L.reuteri* and *B.breve*, the decrease ranged from 0.4 to 0.6 log cycles, while in case of *L.GG* and *P. Jensenii* the decrease in cell viability was about 1.5 log cycle. However, free cells were survived at 2 % bile salt. The biological evaluations of biscuit incorporated with four encapsulated probiotic bacteria strains and biscuit without encapsulated probiotic bacteria were studied in albino rats. The results showed that non significant change in (Total cholesterol and HDL-C) but there were significant change in (serum triglycerides and LDL-C). The safety of experimental diet was studied through serum liver and kidney functions where non significant change in liver function (serum alanine aminotransferase, aspartate aminotransferase and alkaline phosphatase). Also non significant change in kidney function (Creatinine & Urea).

Keywords: Antioxidant; Probiotic bacteria; Biochemical evaluation.

19. Biochemical Changes in Phenols, Flavonoids, Tannins, Vitamin E, Carotene and Antioxidant Activity During Soaking of Three white Sorghum Varieties

Abd El-Moneim MR Afify, Hossam S El-Beltagi, Samiha M Abd El-Salam and Azza A Omran

Asian Pacific Journal of Tropical Biomedicine, 2: 203-209 (2012)

To investigate the changes in total phenols, flavonoids, tannins, vitamin E, carotene and antioxidant activity during soaking of three white sorghum varieties. Methods: The change in total phenols, total flavonoids, tannins, phenolic acids compounds, flavonoid were determined. Results : Total phenols, total

flavonoids, tannins vitamin E , and-carotene and antioxidant activity during soaking in raw sorghum were ranged from mg/ 109.21 to 116.70, 45.91 to 54.69, 1.39 to 21.79 100 g, 1.74 to 5.25, 0.54 to 1.19 mg/kg and 21.72% to 27.69% and 25.29% to 31.97%, respectively. The above measured compounds were significantly decreased after soaking . p- hydroxybenzoic acid ,vanillic acid ,syringic acid and cinnamic acid represent the major phenolic in Dorado variety.

While freulic acid ,p-coumaric acid ,gallic acid and caffeic acid acid represent the major phenolic in Shandaweell-6 .On the other hand, protocatechuic acid represents the major phenolic in Giza - 15 .Regarding flavonoid compounds, Dorado was the highest variety in kampferol and naringenine while Shandweel -6 was the highest variety in luetulin ,apegnine, hypersoid,quercetin and chisrtin . Finally Giza -15 was the highest variety in catechin,phenolic acid and flavonoid compounds and antioxidant activities were decreased after soaking. Conclusions: Sorghum varieties have moderate quantities from total phenols, total flavonoids and antioxidant activity were decreased after soaking.

Keywords: Sorghum Soaking; Total Phenols; Flavonoids; Tannins; Vitamin E;-Carotene; Antioxidant Activity; Phenolic Acids; Flavonoid Components.

20. Antioxidant Enzyme Activities and Lipid Peroxidation as Biomarker Compounds for Potato Tuber Stored by Gamma Radiation

Abd El-Moneim MR Afify, Hossam S El-Beltagi, Amina A Aly and Abeer E El-Ansary

Asian Pacific Journal of Tropical Biomedicine, 2: 1548-1555 (2012)

To study the capability of gamma irradiation for inhibiting sprouting of potato tubers. Methods: The enzymes activities i.e. peroxidase (POD), polyphenol oxidase (PPO), glutathione- S-transferase (GST), superoxide dismutase (SOD) and catalase (CAT), in peroxidation level were tested in potato tubers stored for 3, 6 and 9 weeks. Gama radiation with five treatments (0, 30, 50,100 and 200 Gy) was used to control germination process of potato tubers .Results: Gama radiation was able to maintain potatoes for 6 weeks.

The main biomarkers for validity of potato tuber during storage were studying antioxidant enzyme activities i.e. POD, PPO, GST, SOD, CAT enzyme activities as well as lipid peroxidation during storage time. Conclusions: The optimum dose was 50 Gy which prevented the sprouting initiation all over the storage period without casting undesirable rotting for potato tuber . At this dose all antioxidant enzyme activities i.e. POD,PPO,GST, SOD,CAT enzyme activities as well as peroxidase level during storage time recorded the best rate.

Keywords: Antioxidant enzymes; Gamma irradiation; Lipid peroxidation; Superoxide dismutase; Peroxidase.

21. Antioxidant Enzyme Activities and Lipid Peroxidation as Biomarker for Potato Tuber Stored by two Essential Oils from Caraway and Clove and its Main Component Carvone and Eugenol

Abd El-Moneim MR Afify, Hossam S El-Beltagi, Amina A Aly and Abeer E El-Ansary

Asian Pacific Journal of Tropical Biomedicine, 2: 772-780 (2012)

The present study was conducted to evaluate two essential oils Caraway and Clove and its main component Carvone and ugenol as sprout inhibitors on germination of potato tubers. **Methods** :The enzymes activities: catalase, Glutathione-S-transferase, peroxidase, polyphenol oxidase and superoxide dismutase, in addition to lipid peroxidation level were tested in potato tubers stored for 3, 6 and 9 weeks. Essential oils; Caraway, Clove, Carvone and Eugenol with three concentration (100ppm, 200ppm and 300ppm) were used to control germination process of potato tubers. **Results:** The results of enzyme activities were varied depending on the function of enzymes involved.

As general trend the activities of the enzymes recorded are significantly found on the range of enzyme control or less , which prevent of potato tuber from germination . Glutathione – S-transferase activity was significantly increased after treatment with essential oils and the activity of enzyme reached 23.3±5.15 (100pmm) Caraway, 18.8±0.00(100 pmm) carvone, 10.4±0.00 (100pmm) colve and 14.1±0.0(100ppm) eugenol respectively compared to control 7.86±3.26. **Conclusions:** Polyphenol oxidase and peroxidase activity increased in its activity and recovered to the level of control after treatment with essential oils which maintain potato tuber for 9 weeks. The pure essential oils especially carvone have more potent as suppressor of potato tuber germination.

Keywords: Antioxidant enzymes; Essential oils; Caraway; Carvone; Clove; Eugenol; Mda; Lipid peroxidation; Potato tubers.

22. Traditional Medicinal Plants Research in Egypt Studies of Antioxidant and Anticancer Activities

Ahmed M. Aboul Enein, Faten Abu El-Ela, Emad A. Shalaby and Hany A. Elhemy

Journal Of Medicinal Plants Research, 6 (5): 689-703 (2012)

Plants have played a significant role in the treatment of cancer and infectious diseases for the last four decades. Natural products have been rediscovered as important tools for drug development despite advances in combinatorial chemistry. Egyptian flora, the most diverse in the world, has become an interesting spot to prospect for new chemical leads or hits due to its species diversity. Screening programs have been established in Egypt as a strategy to identify potentially active substances. High throughput screening techniques allow for the analysis of large numbers of extracts in a relatively short period of time and can be considered one of the most efficient ways of finding new leads from natural products. In our study, 23 wild plants were extracted by ethanol and water in addition to 24 ethanolic and aqueous extracts from spices and herbs and tested in vitro as anticancer agents. The trypan blue technique was used for the anticancer activity against Ehrlich Ascites Carcinoma Cells (EACC) while SRB technique was used against HepG2 cells. The antioxidant activity of the 90 plant extracts was determined by 2, 2 diphenyl-1-picrylhydrazyl

(DPPH) assay. Results showed that both of ethanolic and water extracts of some plant possessed high cytotoxic and antioxidant activities and inhibited the cell growth of cancer cells. On the other hand, some ethanolic extract gave cytotoxic and antioxidant activities more than aqueous extract but other aqueous extracts possessed the opposite trend. We believe that the flora of Egypt can be a valuable source of plants rich in, cytotoxic compounds and antioxidant agents.

Keywords: Anticancer; Antioxidant; Polar Extracts; Egyptian Flora.

23. Effect of Zingiber of ficinale on Paracetamol-Induced Genotoxicity in Male Rats

Salah S. H., Abdouh S, Hodaf Boolesand and Abdel - Rahim E. A.

Journal of Medicinal Plants R, 6: 5425-5434 (2012)

The mutagenic effects of paracetamol (acetaminophen) in male rat using *in vivo* mutagenicity tests, chromosomal aberrations of somatic and germ cells, molecular assay and biochemical were studied. Paracetamol genotoxicity on normal divided cells has been reported. The data obtained showed that the ability of paracetamol to bind and interact with genetic material lead to changes in chromosomal behavior and structure during mitosis. The significant increase in chromosomal aberration, the changes in the number, position and intensity of bands, liver and renal damages induced by paracetamol may be attributed to the fact that paracetamol can induce genotoxicity through DNA damage. Paracetamol also stimulated AST and ALT activity, these stimulations indicated liver cell necrosis. Paracetamol-induced acute renal damage by the elevations in blood urea, uric acid and creatinine levels. Paracetamol showed abnormal values of protein profile in blood. The treatments with ginger presented hepatoprotective effect, also ginger can protect against oxidative kidneys tissue damage that reduced lipid peroxidation in liver and kidneys. The possible mechanism by which ginger exhibited significant protection against paracetamol-induced genotoxicity and hepatotoxicity may be due to its antioxidant effect. It may also be responsible for the hepatoprotective activity and attainment of normal frequencies of chromosomal aberration in ginger-treated rats. Thus, the present study indicated that the genotoxicity products at low concentration and for long time treatment showed the hazard of paracetamol addiction on human's life.

Keywords: Zingiber officinale; Paracetamol; Chromosomal aberrations; Genotoxicity.

24. Antioxidant Mechanism of Active Ingredient Separated from Eucalyptus Globulus

N. M. El-Moein, E. A. Mahmoud and Emad A. Shalaby

Organic Chemistry Current Research, 1: 1-7 (2012)

The present study aimed to evaluate the antioxidant activity of petroleum ether, methanolic extracts and active ingredients separated from Eucalyptus globulus using three different antioxidant assays: 2,2-diphenyl picryl hydrazyl (DPPH), 2,2'-azino-bis [ethylbenzthiazoline-6-sulfonic acid] (ABTS) and β -carotene bleaching assay and identify the mode of action. The results revealed that, crude methanolic extract showed higher antioxidant activity against both DPPH and ABTS radicals than petroleum ether extract. The promising methanol soluble fraction

of Eucalyptus globulus wood was fractionated on a silica gel column, using hexane, chloroform and ethyl acetate as the mobile phase to give three fractions (C1, C2 and C3) and both the antioxidant activity and chemical composition for raw and fractions were determined. One of the fractions isolated (C2) showed a remarkable antioxidant activity (EC_{50} of 64.4 μ g/ml, in comparison with 52.74 μ g/ml for crude extracts) against ABTS radical method and the chemical structures of separated active ingredients were identified using different spectroscopic methods such as 17-pentatricontene (C1), N,N-diphenyllauramide (C2) and O-benzyl-N-tert-butoxycarbonyl-D-serine (C3). Also, the mode of action of the promising fraction was determined.

Keywords: Eucalyptus globulus; Antioxidant activity; Chemical constituents; Mode of action.

25. Isolation and Sequencing of the Cryc-Like Delta Endotoxin Gene from Egyptian Strains of Bacillus Thuringiensis Toxic Against Lepidoptera

Marwa E. Elkashef, Alaa M. Heikal, Mohe El-Din M. Solliman, Mohamed I. Kobeasy and Hany A. El-Shemy

African Journal of Biotechnology, 11: 3235-3243 (2012)

The aim of the present work was to explore the diversity of Bacillus thuringiensis (Bt) among local Egyptian isolates that produce parasporal crystalline inclusions. On the basis of bioactivities, nine isolates were collected from different ecological environments within Egypt. The Bt2K isolate was effective against Lepidoptera as compared to B. thuringiensis ssp. Kurstawi that was used as a reference standard. The gene isolated from the strain was shown to be homologous to the Lepidoptera active cryIC gene from B. thuringiensis ssp. ansawai as shown by PCR and alignment of the complete nucleotide sequences (98% identical). Therefore, a cryIC insecticidal toxin coding gene was cloned from an Egyptian isolate of B. thuringiensis. Sequence analyses of the cryIC gene showed the absence of potential polyadenylation signal sequences within the coding region and a less biased codon usage than most cryIC like genes. Therefore, the gene may be a suitable candidate for expression in plants without extensive modification.

This possibility was examined by subcloning the cryIC gene into a plant expression vector and then transferring it to tobacco and potato through Agrobacterium mediated transformation. Tobacco and potato plants with a stably integrated native cryIC gene were completely protected from predation by Lepidoptera. It was concluded that novel insecticidal genes exist in nature that may not require extensive modifications for efficient expression in plants.

Keywords: Bacillus thuringiensis; CryIC gene; Plant transformation; Bt toxins; Dna sequencing.

26. Biochemical Studies of Some Natural Antioxidants on Diabetic Rats

Fouad A. Ahmed, Nermien Z. Ahmed and Dalia A. Hashim

Advances in Food Sciences, 34: 6-13 (2012)

The aim of this study was to evaluate the effect of ethanolic extracts of different flavonoids, such as Vitis vinifera (seeds), Olea europaea (fruits), Vitis vinifera (fruits), Solanum melongena (aerial parts), and Morus alba (leaves), at three concentrations (25, 50 and 100 μ g/ml). DPPH (2,2-diphenyl-1-picrylhydrazyl)

assay in-vitro of these extracts compared with rutin as standard antioxidant was determined. Liver lysosomes were isolated from rats by ultra-cooling centrifugation at different speeds and the lysosomal fractions were incubated for 30 min with *Vitis vinifera* (seeds) and *Olea europaea* (fruits) extracts (1, 5 and 10 mg/ml) to perform and determine the in vitro activity of the released enzymes (acid phosphatase "ACP"; β -galactosidase " β -GAL" and β -N-acetyl glucosaminidase " β -NAG") in rat liver. Also, the labilizing and stabilizing effects on lysosomal membrane permeability were determined. In addition, the effects of the combination between *Vitis vinifera* (seeds) and *Olea europaea* (fruits) extracts (3 concentrations) were investigated. The release rate of the enzymes indicated the labilizing effect but the decrease rate was observed as the stabilizing effect of the lysosomal membrane. The release rate of the 3 lysosomal enzymes appeared to be significantly decreased ($P < 0.05$) compared to control. Under the effect of the 3 concentrations of each compound, different percentage values of inhibition were observed. A low dose of each antioxidant compound exerted a high percentage inhibition on the release of each lysosomal enzyme, while a high dose revealed a less stabilizing effect on membrane permeability and this stabilizing effect was dose-dependent. The medium concentration level caused a moderate inhibitory effect. It was observed that the protective effect of each flavonoid under investigation varied according to concentration and type of enzyme. The most potent inhibitory effect was observed for the extracts of *Vitis vinifera* (seeds), followed by those of rutin (control), *Olea europaea* (fruits) and the mixtures. These inhibitory effects on the lysosomal enzymes were dose- and enzyme type-dependent.

Keywords: Dpph; Antioxidant; Lysosomal enzyme.

27. Performance of "Le Conte" Pear Trees in Response to Biological Control of Fire Blight Disease

Sanaa S.A. Kabeil; Mohamed H. El-Sheikh; Elsabagh, A. Said and A.M. aboulenein

Journal of Applied Sciences Research, 8: 4511-4524 (2012)

Two isolated *Pseudomonas fluorescens* (DQ201414) and *Pantoea agglomerans* strain KB64, were obtained and used for bioassays and field applications against *Erwinia amylovora*, these isolates showed high activity against the pathogenic bacteria. Intergeneric mixtures of the two antagonists could reduce variation in control by establishing a robust community on plant surfaces and greater competition to the pathogen during its critical epiphytic growth stage. So, *Pseudomonas fluorescens* (DQ201414), whose nucleotide sequence data were reported in the NCBI nucleotide sequence database (GenBank) under the accession number GU168575 and *Pantoea agglomerans* strain KB64, could be used as bacterial antagonists for the management of fire blight of pome fruit trees and represented examples of field trials bacterial antagonists. DQ201414 suppressed colonization caused by *E. amylovora* through competitive exclusion. The strain *Pantoea agglomerans* KB64 suppressed pathogen growth by competition and production of an important small peptide antibiotic. Results of field trial proved that the highest number of fruits per tree, fruit weight, yield, fruit diameter, fruit firmness, TSS%, TSS/acid ratio and Total Sugar % resulted from *Pantoea agglomerans* strain KB64 treatment at the third concentration in both seasons followed by the third concentration of the mixture (*Pantoea agglomerans* strain KB64 (B1) + (*Pseudomonas fluorescens* DQ201414) (B2)) and the second concentration of *Pantoea*

agglomerans strain KB64 (B1) in both 2011 and 2012 seasons of the study. The highest average of leaf area, chlorophyll (A) and chlorophyll (B) was achieved by *Pantoea agglomerans* strain KB64 at the third concentration in both seasons followed by the third concentration of the mixture (*Pantoea agglomerans* KB64 (B1) + (*Pseudomonas fluorescens* DQ201414) (B2) and the second concentration of *Pantoea agglomerans* KB64 in both seasons of the study compared to the control. There was no constant trend for shoot length in both seasons. The highest significant amount of Fe, Zn, Mn, N, P and K resulted from *Pantoea agglomerans* KB64 at the third concentration in both seasons followed by the second concentration of *Pantoea agglomerans* KB64 and the third concentration of the mixture in both seasons of the study. In conclusion, the use of some strains of bacteria as a biological control of fire blight proved to be a useful, cheap and safe method to reduce shoot, blossom and immature fruit infection in addition to improving fruit quality

Keywords: "Le Conte" pear; Physical and chemical Characteristics; Biological control; *Pseudomonas fluorescens* DQ201414; *Pantoea agglomerans* strain KB64; Field experiments; Integrated control; Fire blight disease.

28. Hepatoprotective Effect of Red Grape Seed Extracts Against Ethanol-Induced Cytotoxicity

Hazem M.M. Hassan

Global Journal of Biotechnology & Biochemistry, 7: 30-37 (2012)

The hepatoprotective activity of red grape seed extracts (GSEs) was investigated against ethanol-induced cytotoxicity. In this study, liver slice culture model was used to demonstrate hepatoprotective activity of two GSEs (water and ethanol) *in vitro*. The hepatoprotective activity was evaluated by measuring the levels of lipid peroxidation, protein carbonyls, lactate dehydrogenase (LDH) leakage and antioxidant enzymes (catalase and peroxidase) in liver slice culture. The results revealed that the pre-treatment or treatment along of liver slices with water and ethanol grape seed extracts, significantly inhibited the ethanol-induced oxidative stress in the liver by suppressing lipid peroxidation and protein carbonylation. Parallel to these changes, the GSEs prevented the ethanol induced increases in the LDH leakage from liver cells and maintained the levels of antioxidant enzymes. The ethanol grape seed extract (EGSE) was more effective than water grape seed extract (WGSE) against hepatotoxicity of alcohol. Hepatoprotective activity of the grape seed extracts could be attributed to the antioxidant effect of the constituents and enhanced antioxidant defenses.

Keywords: Hepatoprotective; Red grape Seed; Ethanol; Cytotoxicity; Liver slice culture.

29. Effect of Sodium Nitroprusside, Putrescine and Glycine Betaine on Alleviation of Drought Stress in Cotton Plant

Magdy A. Shallan, Hazem M.M. Hassan, Alia A.M. Namich and Alshaimaa A. Ibrahim

American-Eurasian J. Agric. and Environ. Sci., 12: 1252-1265 (2012)

Drought stress is one of the major abiotic stresses in agriculture worldwide. This study was carried out to investigate the effect of sodium nitroprusside (SNP), putrescine (Put) and glycine betaine

(GB) on alleviation of drought stress in cotton plant. The cotton plants pre-treated with three concentrations of SNP (0.05, 0.1 and 1 mM), Put (200, 400 and 600 ppm) or GB (400, 600 and 800 ppm) then exposed to drought stress. In general, the drought stress reduced the growth characters, yield characters, pigments, total soluble sugars, total free amino acids, total phenols, total soluble proteins and catalase activity, while increased proline content, total antioxidant capacity and peroxidase activity in comparison with control. The results showed that pretreatment of cotton plants under drought stress with SNP, Put or GB caused enhancement of growth and yield characters and increasing of pigments content, total soluble sugars, proline content, total free amino acids, total phenols, total soluble proteins, total antioxidant capacity and antioxidant enzyme activities. The optimum concentration of SNP, Put and GB to alleviate the drought stress in cotton plant was 0.05 mM, 600 ppm and 800 ppm, respectively. Finally, it can be concluded that foliar application of SNP, Put or GB could improve the drought tolerance of cotton plants.

Keywords: Drought stress; Cotton; Sodium nitroprusside; Putrescine; Glycine betaine.

30. Effect of Pomegranate Pretreatment on Genotoxicity and Hepatotoxicity Induced by Carbon Tetrachloride (Ccl4) in Male Rats

Abdou H. S., Salah. S. H., Hoda F. Boolesand and Abdel - Rahim E. A.

Journal of Medicinal Plants Research, 6: 3370-3380 (2012)

Several in vivo studies had documented that pomegranate plant had antioxidants that were powerful and beneficial to overall health. They were called polyphenols and flavonoids. It was also a highly regarded defender against free-radicals in the body. In the present study, the anti-oxidant properties of pomegranate peel and seed (diet or extract) were investigated in CCl₄ – induced rat genotoxicity and hepatotoxicity.

The studied male Sprague-Dawley albino rats were divided into seven groups (control, CCl₄, CCl₄ + silymarin, CCl₄ + pomegranate peel diet, CCl₄ + peel extract, CCl₄ + seed diet and CCl₄ + seed extract). Chromosomal aberration, sperm abnormalities, molecular assay and determination of nucleic acid (DNA and RNA) of testes were carried out.

Results documented that CCl₄ produced genotoxicity as it increased chromosomal aberrations, sperm abnormalities and the number of amplified fragments DNA and decrease the content of total soluble protein. Administration of silymarin and pomegranate (diet or extract) after CCl₄ significantly decrease the genotoxicity of CCl₄, yet it failed in complete protection against toxic alterations caused by CCl₄.

Treatment with pomegranate appeared to have highly protective effect especially in animals treated with pomegranate seed extract. It can be concluded that pomegranate possess protective effects against CCl₄ genotoxicity and hepatotoxicity in animal models. This protective effect might be attributed to its antioxidant and free radical scavenger effects.

Keywords: Pomegranate peel and seeds; Sprague; Dawley albino male rats; Ccl4; Genotoxicity; Hepatotoxicity.

31. Resistance to Soybean Cyst Nematode: Rhg1

Ahmed J. Afzal, Ali Srouf, Aparna Natarajan, Navinder Saini, M. Javed Iqbal, Matt Geisler, Hany. El Shemy and David. Lightfoot

Journal of Plant Genome Sciences, 1: 39-45 (2012)

The genes underlying rhg1 lie at a sometimes dominant sometimes co-dominant locus, necessary for resistance to all Hg types of the soybean (*Glycine max* (L.) Merr.) cyst nematode (*Heterodera glycines*). Genomic research identified; nucleotide changes within a candidate gene encoding a receptor-like kinase (RLK) that were capable of altering root development and thereby part of the resistance to Hg types 0 (race 3); changes in a laccase that are capable of altering cyst development; and genes underlying changes in membrane biology. This set of three genes are subject to co-selection with a modifier locus on another linkage block. Root development is slowed in the resistant seedling and results in end of season yield loss when SCN is not present. However, in the presence of SCN resistant seedling roots grow just as vigorously as the now slower growing parasitized susceptible roots and therefore show little loss to SCN parasitism. In some genotypes but not others the RLK can act alone to confer resistance. Functional paralogs of the three gene cluster have been found on other linkage groups including A1, B1, G, and O and these can be functional in different sources of resistance like *G. soja*, PI 437654 and PI438489B. At rhg1 the allele differences change the structure, interacting partners and activity of the LRR protein and the laccase. The changes between the alleles result in about 30 other proteins (judged by 2 D gels), 112 metabolites (by FTICRMS) and 8 metabolites (by GCMS) to increase in abundance in roots during SCN infection in the resistant NILs. Understanding the basis of root stunting by resistance alleles will be used to improve methods for developing new nematode resistant soybean cultivars that do not suffer from the yield suppression and low seed germination rates of existing cultivars.

Keywords: Soybean cyst nematode (Scn); Nematode; Resistance; Proteomics; Soybean roots.

32. Cytotoxic Profiling of Some Compounds of Natural Origin Against Hepg 2 Liver Cancer Cell Line In-Vitro

Ali M. Mahmoud and Hany A. El-Shemy

Journal of Arid Land Studies, 22: 191-194 (2012)

Cancer is so far a national and international health problem. WHO reports showed constant rates of mortality caused by various types of cancer through the years 1950-2000. There is a wide gap between the disease incidence (0.16%), disease burden (5.6%) and the mortality caused by cancer (12.5%) worldwide. These gaps denote clearly the lack of effective treatment for cancer compared to other mortality causes. Despite the availability of several anticancer agents, the treatment of cancer remains a medical hurdle in the developed and developing countries. Discovery of natural products with potential anti cancer activity is a very initiative trend in countries with rich botanical flora. Liver cancer is a very serious solid tumor which is highly abundant in areas endemic with hepatitis viruses such as middle and Far East. Herein, we have assessed the cytotoxic characteristics of several natural molecules (cerulinin, chrysin, honiokiol, limonin, mevinolin, resveratrol, salicin, retinol, ascorbic acid and calciferol) against HepG2 liver solid tumor cell line. After exposure to serial concentrations of the test compounds for

72 h, SRB-u assay was undertaken and viability assessment was performed via fitting to Emax model to identify the cytotoxicity parameters such as, IC50 and resistant fraction (R-value). Most of tested compound showed sort of cytotoxic effects against HepG2 cell line with IC50's ranged from 1.1 to 33.1 µg/ml. Cerulinin and mevinolin showed the highest potency with IC50 less than 5 µg/ml. Chrysin, honikiol and resveratrol showed moderate potency with IC50 ranging from 5-10 µg/ml. Ascorbic acid was weak cytotoxic agent against HepG2 cell line. Limonine, salicin and retinol failed to exert any cytotoxicity against liver cancer cell line in-vitro. Impressively, molecules of potent and moderate potency (except chrysin) showed low resistant fraction in HepG2 liver cancer cell line. In conclusion, our data showed wide range of variable efficacy of several molecules of natural origin against liver solid tumor.

Keywords: Anti-Cancer screening; L Cytotoxicity; Liver cancer; Natural products.

33. Efficacy Assessment for Several Natural Products with Potential Cytotoxic Activity Against Breast and Cervix Cancers

Ali M. Mahmoud and Hany A. EL-Shemy

Journal of Arid Land Studies, 22: 107-110 (2012)

Over more than five decades, cancer remains a national and international health problem regardless of the discovery of several dozens of novel anticancer drugs (natural and synthetic). Accordingly, screening of natural products for promising anti cancer activity is very initiative field of studies in several countries with diversity of gardenia. Breast and cervix cancers are of the most common gynecological female solid tumors that represent major health problem. Herein, we have assessed the cytotoxic characteristics of several molecules of natural origin (cerulinin, chrysin, honikiol, limonin, mevinolin, resveratrol, salicin, retinol, ascorbic acid and calciferol) against two different gynecological breast (MCF-7) and Cervix (HeLa) solid tumor cell lines. After exposure to serial concentrations of the test compounds, SRB-u assay was undertaken and viability assessment was performed via fitting to Emax model to identify the cytotoxicity parameters such as, IC50 and resistant fraction (R-value). Tested compounds showed cytotoxic efficacy against both gynecological solid tumor cell lines (MCF-7 and HeLa) with IC50's ranged from 0.61 to 131.1 µg/ml. In MCF-7 breast cancer cell line; cerulinin, honikiol, mevinolin and calciferol showed the highest potency with IC50 less than 5 µg/ml. Chrysin showed moderate potency with IC50 of 7.27 µg/ml. Ascorbic acid and resveratrol showed the weakest cytotoxic activity with IC50 more than 10 µg/ml. In HeLa cervix cancer cell line; cerulinin and mevinolin showed the highest potency with IC50 less than 5 µg/ml. Chrysin, honikiol, resveratrol and calciferol showed moderate potency with IC50 of ranging from 5-10 µg/ml. Ascorbic acid was the weakest cytotoxic molecule with IC50 more than 10 µg/ml. Limonine, salicin and retinol failed to exert any cytotoxic effect against MCF-7 or HeLa cancer cell lines in-vitro. RT-PCR analysis revealed that the cytotoxicity of these products is multi-factorial and not solely dependent on p53 expression.

Keywords: Anti-Cancer screening; Breast cancer; Cervix cancer; Cytotoxicity; Natural products.

34. Two Steps Alkaline Transesterification of Waste Cooking Oil and Quality Assessment of Produced Biodiesel

Emad A. Shalaby and Nour Sh. El-Gendy

International Journal Of Chemical and Biochemical Sciences, 1: 30-35 (2012)

Biodiesel is an environmentally friendly renewable diesel fuel alternative. In Egypt, millions liters of waste cooking oil (WCO) are discarded annually into sewage systems, pollute water streams and adds to the cost of treating effluents. In an attempt to reduce the cost of biodiesel and pollution caused by WCO, this study aimed to investigate the feasibility of biodiesel production from WCO by applying two steps alkaline transesterification process using methanol, KOH as a catalyst and hot distilled water for purification. The produced biodiesel was physico-chemically characterized. From the results it was clear that the produced biodiesel was within the recommended standards of biodiesel fuel ($r > 0.95$) and met the criteria required to be a diesel substitute compared with the Egyptian petro-diesel fuel standards ($r = 0.999$).

Keywords: Biodiesel; Waste cooking oil; Physico-Chemical characterization.

35. Cultivating Microalgae in Domestic Wastewater for Biodiesel Production

Soha S.M. Mostafa, Emad A. Shalaby and Ghada Mahmoud

Not Sci Biol, 4 (1): 56-65 (2012)

The objective of this study was to evaluate the growth of nine species of microalgae (green and blue green microalgae) on domestic wastewater obtained from Zenein Wastewater Treatment Plant (ZWWTP), Giza governorate, Egypt. The species were cultivated in different wastewater treatments namely: without treatment; after sterilization; with nutrients with sterilization and with nutrients without sterilization. The experiment was conducted in triplicate and cultures were incubated at $25 \pm 1^\circ\text{C}$ under continuous shaking (150 rpm) and illumination (2000 Lux) for 15 days. Algal growth parameters i.e., pH, electric conductivity (EC), optical density (OD), dry weight (DW) and chlorophyll-a (Ch-a) were measured at zero-time and at the end of the experimental period; while, the percentages of total lipids, biodiesel and the residual sediments (glycerine, pigments, etc) were determined in the harvested algal biomass. The data revealed that domestic wastewater with nutrients and with sterilization (T_3) was promising for cultivating five algal species as compared to the synthetic media. Moreover, the sterilized-domestic wastewater (T_2) was the selective medium for cultivating *Oscillatoria* sp. and *Phormidium* sp; however, T_1 medium (wastewater without treatment) was the promising medium for cultivating *Nostoc humifusum*. Biodiesel production from the algal species cultivated in synthetic media was ranging between 3.90% (*Wollea saccata*) and 12.52% (*Nostoc muscorum*). On the other hand, the highest biodiesel production from algal biomass cultivated in wastewater was obtained by *Nostoc humifusum* (11.80%) when cultivated in wastewater without treatment (T_1) and the lowest (3.80%) was recorded by *Oscillatoria* sp. when cultivated on the sterilized-domestic wastewater (T_2). The results of this study suggest that cultivating microalgae on domestic wastewater combines nutrients removal and algal lipid production for potential use as a biodiesel

feedstock. Additionally, using the domestic wastewater, as nutrient media for microalgae cultivation, is suitable and non-expensive method as compared to the conventional cultivation methods for sustainable biodiesel and glycerol production.

Keywords: Biodiesel production; Domestic wastewater; Growth parameters; Microalgae.

36. Aqueous Extracts of Microalgae Exhibit Antioxidant and Anticancer Activities

Sanaa MM Shana, Soha SM Mostafa, Emad A Shalaby and Ghada Mahmoud

Asian Pacific Journal of Tropical Biomedicine, 608-615 (2012)

To investigate the antioxidant and anticancer activities of aqueous extracts of nine microalgae species, the antioxidant and anticancer activities of aqueous extracts of nine microalgae species were investigated. The antioxidant activity was determined using DPPH and ABTS radical cation assays, which revealed 30.1-72.4% and 32.0-75.9% respectively. The anticancer efficiency of the algal water extracts was investigated against Ehrlich ascites carcinoma cell line (EACC) and Human Hepatocellular cancer cell line (HepG2) with an 87.25% and 89.4% respectively. Culturing the promising cyanobacteria species; *Nostoc muscorum* and *Oscillatoria* sp. under nitrogen stress conditions (increasing and decreasing nitrate concentration) revealed that the nitrate concentration of 10 mg/L and 50 mg/L showed the highest nitrate content. The results revealed that crude methanolic extract showed higher antioxidant activity against both DPPH and ABTS radicals than petroleum ether extract. The promising methanol soluble fraction

Keywords: Microalgae; Antioxidant; Anticancer; Nitrogen Starvation; Cyanobacteria.

37. Antioxidant Mechanism of Active Ingredients Separated from Eucalyptus Globulus

N. M. El-Moein, E. A. Mahmoud and Emad A. Shalaby

Organic Chem Curr Res, 1 (2): 1-7 (2012)

The present study aimed to evaluate the antioxidant activity of petroleum ether, methanolic extracts and active ingredients separated from *Eucalyptus globulus* using three different antioxidant assays: 2,2-diphenyl picryl hydrazyl (DPPH), 2,2'-azino-bis [ethylbenzthiazoline-6-sulfonic acid] (ABTS) and β -carotene bleaching assay and identify the mode of action. The results revealed that crude methanolic extract showed higher antioxidant activity against both DPPH and ABTS radicals than petroleum ether extract. The promising methanol soluble fraction

of *Eucalyptus globulus* wood was fractionated on a silica gel column, using hexane, chloroform and ethyl acetate as the mobile phase to give three fractions (C1, C2 and C3) and both the antioxidant activity and chemical composition for raw and fractions were determined. One of the fractions isolated (C2) showed a remarkable antioxidant activity (EC_{50} of 64.4 μ g/ml, in comparison with 52.74 μ g/ml for crude extracts) against ABTS radical method and the chemical structures of separated active ingredients were identified using different spectroscopic methods such as 17-pentatriacontene (C1), N,N-diphenyllaurylamide (C2) and O-benzyl-N-tert-butoxycarbonyl-D-serine (C3). Also, the mode of action of the promising fraction was determined.

Keywords: *Eucalyptus globulus*; Antioxidant activity; Chemical constituents; Mode of action.

38. Biological Activities and Anticorrosion Efficiency of Water Hyacinth (*Eichhornia Crassipes*)

Sanaa M. M. Shanab and Emad A. Shalaby

J Med Plants Res, 6: 3950-3962 (2012)

Eichhornia crassipes (Mart) Solms is an invasive macrophyte, causing serious problems to the network of irrigation and drainage canals in the Nile Delta region and different places around the world. Plants and hydrophytes (as water hyacinth) have increasingly been shown to provide rich source of natural bioactive compounds with antimicrobial, antitumoral, antiviral and antioxidant activities. Spectroscopic methods of the separated fractions revealed the presence of different compounds of variable anticancer and antioxidant activities which acted synergistically in the crude extract leading to its greatest activities.

Keywords: Water hyacinth; Chemical composition; Biological activities.

39. Impact of Organic and Inorganic Fertilizers on Nematode Reproduction and Biochemical Alterations on Tomato

Ahmed A. Farahat, Alsayed A. Alsayed, Hossam S. El-Beltagi and Nomair M. Mahfoud

Notulae Scientia Biologicae, 4: 48-55 (2012)

The organic amendments, compost, neem and poultry as well as inorganic fertilizer, N P K and nematicide Nematicur 10% G applied singly at two different doses were effective in reducing *M. incognita* number of galls, nematode reproduction and fecundity. Also, they ameliorated growth criteria of treated tomato plants. The effectiveness seemed to be material origin and concentration dependent. Neem, compost 1, 3 at higher doses (5 g/pot) gave the best results. Yet, achieved results were less than those of Nematicur 10% G which overmatched all the organic and inorganic fertilizers. Nematode infection reduced total soluble sugars in roots but the opposite was the case in all treatments. Nematode infection supported root contents of amino acids, total phenols and tannins but they were diminished as a result of almost all treatments. Total soluble sugars and total carbohydrates in shoots decreased as a result of nematode infection but they were regained only by application of inorganic fertilizer. Total amino acids increased in shoots of infected plants and more increase was observed in almost all treatments. Nematode infection impaired tomato uptake of N P K; organic and inorganic

fertilizers provoked plants up take, however nemacur improved plants up take of nitrogen only.

Keywords: Meloidogyne incognita; Organic fertilizers; Inorganic fertilizers; Biochemical alterations.

40. Anti-Ulcer Activity of Oregano (*Origanum Syriacum* L.) Against Gastric Ulcer in Rats

Abd EL-Moneim M.R Afify, Sherif H. Esawy, Eshak M. El-Hadidy and Mostafa A.L. Abdel-Salam

Advances Food Science, 34: 145-149 (2012)

Ethanol extract of oregano (*Origanum syriacum* L.) and oregano volatile oil were evaluated for the antiulcer activity indomethacin suspension induced of Wistar albino rats (150-170g) by oral administration of indomethacin suspension. The antiulcer activity was assessed by determining and comparing the ulcer index in the test drug groups with that of the vehicle control and standard omeprazole, the volatile oil and ethanol extracts showed significant reduction of ulcers in a dose dependent manner. The parameters taken to assess antiulcer activity were volume of gastric juice, total acidity and ulcer index. The extracts and volatile oil significantly decreased the gastric secretion, total acidity on gastric ulcers in the indomethacin induced rats and the effects were compared with Omeprazole.

Keywords: Oregano; Anti; Ulcer.

41. Biological Activities of Superfood, Spirulina Sp

Emad Ahmed Shalaby

Book Published by Lambert Academic Publishing, 199 (2012)

The ethanol and its successive extracts of the marine red macroalga, *Gracilaria verrucosa*, were measured for antioxidant activity, using the α,α -diphenyl- β -picrylhydrazyl radical-scavenging assay system and compared with those of the positive controls of butylated hydroxytoluene (BHT) and Butylated hydroxyanisole (BHA). The crude ethanolic extract was further fractionated to afford four fractions (PE, EA, BuOH and Water fractions), of which the pet.ether (PE) and ethyl acetatesoluble (EA) fraction exhibited the strongest antioxidant activity in the assay system. The EA fraction was further separated into eleven subfractions, designated as EA1–EA11, by silica gel column chromatography. In most cases, EA3 and EA4 were found to possess the strongest antioxidant activity. The total phenolic contents and reducing powers of the extract, fractions and subfractions were also determined. Significant associations between the antioxidant potency and the total phenolic content, as well as between the antioxidant potency and the reducing power, were found for the tested fractions and subfractions.

Keywords: Antioxidant activity; DPPH; *Gracilaria verrucosa*; Phenolic compounds; Reducing power; Seaweeds.

42. Primary and Secondary Metabolites of Marine Macroalgae

Emad Ahmed Shalaby

Book Published by Lambert Academic Publishing, 179 (2012)

The ethanol and its successive extracts of the marine red macroalga, *Gracilaria verrucosa*, were measured for antioxidant activity, using the α,α -diphenyl- β -picrylhydrazyl radical-

scavenging assay system and compared with those of the positive controls of butylated hydroxytoluene (BHT) and Butylated hydroxyanisole (BHA). The crude ethanolic extract was further fractionated to afford four fractions (PE, EA, BuOH and Water fractions), of which the pet.ether (PE) and ethyl acetatesoluble (EA) fraction exhibited the strongest antioxidant activity in the assay system. The EA fraction was further separated into eleven subfractions, designated as EA1–EA11, by silica gel column chromatography. In most cases, EA3 and EA4 were found to possess the strongest antioxidant activity. The total phenolic contents and reducing powers of the extract, fractions and subfractions were also determined. Significant associations between the antioxidant potency and the total phenolic content, as well as between the antioxidant potency and the reducing power, were found for the tested fractions and subfractions.

Keywords: Antioxidant activity; DPPH; *Gracilaria verrucosa*; Phenolic compounds; Reducing power; Seaweeds.

Dept. of Agricultural Botany

43. 24-Epibrassinolide Ameliorates the Saline Stress and Improves the Productivity of Wheat (*Triticum Aestivum* L)

Neveen B. Talaat and Bahaa T. Shawky

Environ Exp Bot, 82: 80-88 (2012) IF: 2.985

Two wheat (*Triticum aestivum* L.) cultivars, Sids 1 and Giza 168, were grown under non-saline or saline conditions (4.7 and 9.4 dS m⁻¹) and were sprayed with 0.00, 0.05 and 0.10 mg l⁻¹ 24-epibrassinolide (EBL). Salt stress considerably decreased plant productivity, membrane stability index, photochemical reactions of photosynthesis, the content of relative water, chlorophyll and nitrate, the activity of nitrate reductase and carbonic anhydrase and the level of carbohydrate and protein. The reduction was more pronounced in Giza 168.

The follow-up treatment with 0.1 mg l⁻¹ EBL detoxified the stress generated by salinity and significantly improved the above parameters, especially in Sids 1. Glycinebetaine concentration was sharply elevated by salt stress and/or EBL treatments, particularly in Sids 1.

Salinity increased putrescine level in Sids 1 and Giza 168, however, spermidine and spermine increased in Sids 1 and decreased in Giza 168. Exogenously applied EBL had a varying effect on polyamines pool under saline condition, an increase in putrescine level associated with low contents of spermidine and spermine in Giza 168 was observed, while Sids 1 showed a decrease in putrescine and high increase in spermidine and spermine. EBL prevented diamine oxidase and polyamine oxidase inhibition, indicating a positive correlation between salt tolerance and polyamines accumulation.

Obviously, EBL can be a practical strategy toward generating high-yielding plants under saline condition by enhancing carbon and nitrogen metabolisms. This is the first report dealing with EBL effect on polyamines pool under salt stress.

Keywords: 24-Epibrassinolide; Wheat; Salinity; Productivity; Carbon metabolism; Nitrogen metabolism.

44. Morphological Characteristics of Vegetative and Reproductive Growth of *Senna Sophera* (L.) Roxb. (Caesalpiaceae)

M.A.A. Nassar, H.R.H. Ramadan and H.M.S. Ibrahim

Journal of Horticulture Science and Ornamental Plants, 4: 299-306 (2012)

In this study, morphological information is produced as evidence for proper delimitation of *Senna sophera* (L.) Roxb. taxonomy. The field work was carried out during the growing season of 2008 in order to follow up the morphology of vegetative and reproductive growth of studied species throughout the successive stages of its entire life span. Germination of seeds and yield components at harvest time were also taken in consideration. Such knowledge may fulfill information acquisition in this concern. The morphology of vegetative growth includes: plant height, length and diameter of the main stem, number of internodes of the main stem, number of primary branches developed on the main stem, lengths of primary branches at maturity, fresh weight of leafless shoot per plant, total number of leaves per plant, total leaf area per plant and fresh weight of leaves per plant. Moreover, keen observations and descriptive morphology of the root and the shoot were under consideration. The morphology of reproductive growth includes: flower bud differentiation, full blooming, fruit set and maturity. In addition, the yield characters at harvest time were investigated; i.e., number of matured dry pods per plant, number of seeds per pod, number of seeds per plant, yield of matured dry seeds per plant and specific weight of seeds.

Keywords: *Senna Sophera*; Caesalpiaceae; Morphology; Vegetative Growth; Reproductive Growth.

45. Morphological and Anatomical Study on Some Wheat Cultivars and their Response to Seasonal Variations

Sawsan M. Abou-Taleb and Elham F. Gomaa

Australian Journal of Basic and Applied Sciences, 6: 13-22 (2012)

An experiment was conducted at The Agricultural Experimental and Research Station, Faculty of Agriculture, Cairo University, Egypt during the two successive seasons of 2007/2008 and 2008/2009. Two wheat species were adopted to evaluate some morphological and anatomical features as well as some yield and yield attributes. Seasonal influences on performance of cultivated genotypes have been considered. Six cultivars, three of bread wheat (*Triticum aestivum*) viz., Sids1, Gemmeiza7 and Sakha93 & others of macaroni wheat (*Triticum durum*) viz., Beni Sweif1, Beni Sweif3 and Sohag3, were utilized. Regarding the bread wheat, plants of Sids1 cv. were the tallest ones in both seasons. Plants of Sakha93 cv. was the superior with respect to number of leaves/plant in the first season and Gemmeiza7 in the second one. Wider leaf area/plant was for Sids1. The highest dry weight of shoot was produced by Gemmeiza7 plants in both seasons with significant differences compared to the other two cultivars. Regarding the durum wheat, insignificant differences were detected between the three studied cultivars with respect to plant height in both seasons and number of developed tillers/plant in the first season. Plants of Beni Sweif1 produced the highest shoot dry weight in the first season with significant difference. In the second season, maximum shoot dry weight/plant was recorded by Sohag3 plants with significant differences. Regarding seasonal effect, pronounced increase was achieved in shoot dry weight and

weight of 1000 kernels in majority of the studied cultivars in the second season compared to the first one. Main spike length and number of spikelets /main spike were reduced as higher temperature was prevailed in the second season. As to the seasonal effect on performance of the two species, insignificant differences were detected between seasons except for seed index of the species *T. aestivum*. The trait was significantly increased by 27.4% in the second season over that in the first one. Considerable but insignificant increment was recorded in shoot dry weight of both species in the second season. The percentages of increment were 63.8% and 103.3% for *T. aestivum* and *T. durum* respectively. Means of number of grains/plant were reduced in the second season by 8.3% and 10% for *T. aestivum* and *T. durum* respectively. Weight of grain yield/plant was increased in the second season by (27.5%) and (3.4%) for *T. aestivum* and *T. durum* respectively. Comparing between the studied species, higher numbers of spikelet/spike were produced by *T. aestivum* cvs. compared to *T. durum* ones in both seasons, the latter possessed shorter spikes. Insignificant differences were detected between the two species except for number of grains/plant in both seasons and weight of grain yield/plant in the first season, *T. durum* was the superior. Seed index was increased by 21% in *T. durum* over that of *T. aestivum* in the first season while it reduced by 9.6% in the second one. No great differences were recognized comparing the anatomical features of main stems as well as flag leaves of the studied cultivars. Stem transection of Sids1 cv. exhibited narrower chlorenchyma adjacent to the peripheral bundles. Stem outlines of Beni Sweif1 and Sohag3 were slightly ridged as the peripheral bundles located. Stem bundles of Sohag3 cv. seemed to arrange in three concentric rings, the inner ring contains the larger vascular bundles. Peripheral larger bundles, occasionally found in stems of Gemmeiza7 and Sakha93, are separated from the epidermis by layers of sclerenchyma. In Gemmeiza7 stem, chlorenchyma adjacent to the outer peripheral bundles occasionally extended tangentially seemed in connection between the nearby bundles. Flag leaf of Sakha93 cv. obviously differed. It possessed thicker midrib, contains the largest vascular bundle, than the two sided lamina. The laminar bundles appeared in zigzag manner. Flag leaves of the other cultivars possessed midribs slightly thicker than the lamina.

Keywords: Wheat; *T. Aestivum*; *T. Durum*; Cultivars; Morphology; Anatomy; Yield component.

46. Comparative Study on Four Cereal Genotypes: 1-Morphological and Anatomical Characteristics

Sawsan M. Abou-Taleb

Journal of Applied Sciences Research, 8: 3834-3844 (2012)

A field and pot experiments were conducted during 2011/2012 winter season at the Agricultural Experimental and Research station, Faculty of Agriculture, Cairo University, Giza, Egypt. Four cereal crops belonging to different species were adopted to create comparative investigation. Cultivar Sakha93 (*Triticum aestivum*), cultivar Beni Sweif1 (*Triticum durum*), rye (*Secale cereale*) and triticale (*Triticale* spp.) were included in this study. Plants of Beni Sweif1 cv. possessed longer main stems with significant differences. Rye plants were the shortest ones with the shortest uppermost internode and possessed tillers 4-6 folds compared to those developed by the other genotypes. Widest leaves, either flag or determined foliage leaves, were developed on main stems of *Triticale* spp. The differences were mostly

significant. The lowest area was recorded for flagleaves of Secale cereale. Main spike length of Triticale spp. with or without awns was significantly longer than that of the other three genotypes. Cluster analysis created by either arithmetic averages or individuals revealed finally four genotypes located in four separated groups. The latter (involved nine characteristics of 40 individuals) exhibited the aggregation of Sakha 93 cv., Triticale spp. and Secale cereale between 91%-94% level. Meanwhile, the durum cultivar Beni Sweif was located separately. This may indicate that triticale is a resultant of crossing Triticum aestivum and Secale cereale. Regarding the anatomical features, higher numbers of protoxylem points were counted for the lateral seminal roots of all genotypes compared to the primary root. Two metaxylem vessels were observed in lateral seminal root of Sakha 93 cv. and main root at tip of Triticale spp. Numbers of lysigenous cavities in varying sizes were observed between cortex parenchyma of primary and lateral seminal roots of Beni Sweif and Secale cereale. Coleoptile transection of Sakha 93 exhibited three stomata outwardly to both coleoptile bundles. Stomata were also found towards the adaxial first leaf surface. In Secale cereale one stoma was observed outwardly to each bundle. Moreover, stomata were found in outer epidermis towards the abaxial surface of the first leaf. Bundles of foliage leaves of Sakha 93 and triticale spp., even the largest main one, are bounded by incomplete undulate sheaths. Cells of outer parenchyma layer are hardly recognized from ordinary mesophyll cells and contain fewer chloroplasts. Also, wide intercellular spaces were observed between mesophyll chlorenchyma. Foliage leaf of Secale cereale was characterized by 12 bundles along the lamina transection. Also, abaxial epidermis curved as the bundles located. Upper epidermal cells above ridges were apparently larger than those in grooves except for Beni Seif 1, both were uniform. Peripheral larger bundles in stems of each of Sakha 93 cv., Secale cereale and Triticale spp. seemed apart from epidermis by bands of lignified sclerenchyma cells. Band thickness and width was varied according to genotype. Wing-shaped chlorenchyma was recognized. Outer smaller vascular bundles of Secale cereale stem were separated from epidermis by layers of chlorenchyma. The inner bundles appeared smaller compared to those of the other genotypes. Flag leaf of Sakha 93 cv. exhibited thicker midrib, contains the largest vascular bundle, than the two sided lamina. In Secale cereale, no great difference was detected in size between the main bundle and the larger laminar ones. Flag leaf of the latter genotype appeared with reduced lamina thickness. Great similarity could be recognized between flag leaf of the durum cultivar Beni Sweif and that of Triticale spp. The bulliform cells are greatly typical in shape and size.

Keywords: T. Aestivum; T. Durum; Triticale; Triticale Spp.; Rye; Secale Cereale Morphology; Anatomy.

47. Response of Sesame Plant (*Sesamum Orientale* L.) to Treatments with Mineral and Bio-Fertilizers

Mohamed S. Boghdady, Rania M.A. Nassar and Fouad A. Ahmed

Research Journal of Agriculture And Biological Sciences, 8: 127-137 (2012)

Field experiments were carried out in a private farm at Met Raba village, Bilbas, Sharkia Governorate, Egypt during the two growing summer seasons of 2010 and 2011 in order to study the effect of different levels of mineral fertilizers from nitrogen and phosphorus (25, 50 and 100% of the recommended dose) alone or in combination with a mixture of biofertilizers containing

nitrogen fixers (nitrobein) and phosphate dissolving bacteria (phosphorein) on morphological characters, photosynthetic pigments, stem and leaf anatomy, yield and seed oil percentage of sesame cv. Shandaweel-3. The obtained results revealed that increasing level of the used mineral fertilizers induced significant increases in all investigated morphological and yield characters as well as in seed oil percentage of sesame cv. Shandaweel-3. Likewise, prominent increases in photosynthetic pigments of sesame leaves were recorded in this respect. Worthy to note that the rate of promotion increased gradually as the rate of mineral fertilizers increased up to 100% of the recommended dose. Data also indicated that sesame plants obtained from biofertilized seeds and grown in biofertilized soil showed prominent increases in all investigated morphological and yield characters as well as in seed oil percentage and in photosynthetic pigments when compared with control plants which were obtained from uninoculated seeds and grown in uninoculated soil. The interaction among the used levels of mineral fertilizers and biofertilizers proved promotive effect for all investigated characters. It is noted that the promotion induced by raising the level of the used mineral fertilizers was equal to that induced by biofertilizers treatment which substituted half of the recommended dose from the used NP and this decreased the environmental pollution caused by repeated application of mineral fertilizers. Worthy to mention that the effect of the used mineral and biofertilizers on stem and leaf anatomy of sesame cv. Shandaweel-3 was also investigated.

Keywords: Mineral Fertilizers; Bio-Fertilizers; Sesame; *Sesamum Orientale* L; Morphological Characters; Photosynthetic Pigments; Yield Characters; Seed Oil Percentage; Stem Anatomy; Leaf Anatomy.

48. Minimizing the Harmful Effects of Cadmium on Vegetative Growth, Leaf Anatomy, Yield and Physiological Characteristics of Soybean Plant [*Glycine Max* (L.) Merrill] by Foliar Spray with Active Yeast Extract or with Garlic Cloves Extract

Fatma A. Abdo, Dalia M.A. Nassar, Elham F. Gomaa and Rania M.A. Nassar

Research Journal of Agriculture And Biological Sciences, 8: 24-35 (2012)

Pot experiments were carried out during the two successive summer seasons of 2010 and 2011 in the greenhouse of Crops Physiology Research Department, Field Crops Research Institute, Agricultural Research Center, Giza, Egypt to investigate the effect of pollution with cadmium at concentrations of 50, 100 and 200 ppm on vegetative growth, leaf anatomy, yield and certain physiological aspects of soybean 'Giza 35'. In addition, the use of natural extracts from active yeast (60ml/L.) and garlic cloves (30 ml/L.) for minimizing the harmful effects of environmental pollution caused by cadmium on vegetative and reproductive growth as well as on leaf anatomy and physiological behaviour of soybean was also investigated. The obtained results revealed that all assigned concentrations of cadmium induced significant decrease in all investigated morphological characters of vegetative growth and in all studied yield characters of soybean 'Giza 35'. Moreover, the significant decrease in morphological and yield characters got higher as the concentration of cadmium increased in irrigation water. Worthy to note that, soybean plants grown under stress of pollution with different levels of cadmium

and sprayed with either yeast or garlic extract had better growth behavior and yield than those of unsprayed with natural extracts. Likewise, the concentrations of photosynthetic pigments (Chl. a, Chl. b and carotenoids), total sugars and phytohormones from IAA and GA3 in leaves of cadmium polluted soybean plants were decidedly lower than those of control plants. In this respect, increasing cadmium concentration in irrigation water decreased gradually photosynthetic pigments, total sugars, IAA and GA3. It was found that yeast as well as garlic extracts were able to minimize the harmful effect of cadmium and improve the concentrations of photosynthetic pigments, total sugars, IAA and GA3 in leaves of cadmium polluted soybean plants. Also, the percentage of crude protein and total lipids in seeds of cadmium polluted soybean plants were decidedly lower than those in seeds of control plants and increasing cadmium concentration in irrigation water decreased gradually the percentage of crude protein and of total lipids. It is clear that foliar application with yeast or garlic extract was sufficient for reducing the harmful effect of cadmium and improve the percentage of crude protein and of total lipids in seeds of cadmium polluted soybean plants. At the same time, the concentration of phytohormone ABA in leaves and of cadmium in leaves and seeds of soybean plants was increased due to cadmium treatments and the application of yeast or garlic extract on soybean plants grown under stress of pollution with cadmium minimized the harmful effect of such heavy metal on concentration of ABA in leaves and on cadmium accumulation in leaves and seeds of cadmium polluted soybean plants. Concerning the anatomical structure of leaflet blades, the application of yeast or garlic extract caused enhancement in leaflets structure of polluted plants.

Keywords: Soybean; Pollution; Cadmium; Natural Extracts; Vegetative Growth; Leaf Anatomy; Yield; Physiological Aspects.

49. Response of Sesame Crop to the Biofertilizer Cerealine with or Without Mineral Nitrogen Fertilization

Sawsan M. Abou-Taleb

Research Journal of Agriculture And Biological Sciences, 8: 45-54 (2012)

Two field experiments were conducted during the two successive seasons 2007 and 2008 at the Agricultural Experimental and Research Station, Faculty of Agriculture, Cairo University, Giza, Egypt. The biofertilizer Cerealine (*Azospirillum brasilense*) was adopted as soil inoculant, either alone or as a supplement to mineral fertilization. Their effect on growth and yield of sesame plant (*Sesamum indicum* L.) was studied. Three treatments were applied, i.e. the recommended rate of mineral nitrogen (40kgMN/fed.), half rate of MN combined with half rate of Cerealine or the recommended dose of Cerealine (400g/fed.). Two cultivars of sesame viz. Tushki 1 and Schandweel 2000 were studied. Regardless of cvs. effect, dry weight of shoots tended to be doubled in plants, those received Cerealine alone in the first season. While maximum dry weight of shoots was achieved in plants which received the recommended dose of MN in the second season. Moreover, most of growth characters varied in their response to the applied treatments comparing the two growing seasons. Highest values were obtained where the plants received the biofertilizer alone in the first season and vice versa in the second one. As to the cultivar effect, results revealed insignificant differences between cultivars in most of growth traits. In the second season, the cultivar Schandweel 2000 was

apparently vigorous than Tushki 1. Concerning the cultivars vs. the treatments, the investigation exhibited the existence of genotypic variability under the influence of various treatments. Most growth traits gave insignificant differences; due to various treatments. Tushki 1 significantly behaved better in root length and dry weight separated leaves by combined treatment in the first season. Means of main stem height and root length varied significantly in the second one, as the cultivars received the recommended dose of MN, higher values were for Schandweel 2000 cv. Significant differences were detected also between the cultivars in the number of primary branches as affected by both mineral nitrogen or Cerealine treatments, Tushki 1 cv. was the superior. Yield attributes were insignificantly higher as detected by Cerealine application in the first season. Number of capsuled nodes and capsules/plants and seed yield/plant were positively affected by applying the MN alone in the second season. Highest seed index was insignificantly obtained in plants with combined treatment. Variable seasonal influences were detected due to the applied treatments on growth and yield attributes. The results revealed that the biofertilizer Cerealine could be replaced partially instead of inorganic nitrogen approaching to reducing the harmful effect of chemical fertilization. This may lead to clean and sustainable agriculture. Variable anatomical responses were detected between the studied cultivars under the effect of the applied treatments. Most of stem tissues of Tushki 1 cv. were negatively affected by applying the combination treatment comparing to MN or Cerealine treatments, thickness of fiber groups was drastically reduced. In other words stem diameter was surpassed in Tushki 1 plants those received the bio fertilizer treatment compared to the other treatments. Most of stem tissues of Schandweel 2000 cv. Consequently whole stem diameter were reduced as the plants received either the combination treatment or Cerealine one compared to MN treatment.

Keywords: Inoculation; *Azospirillum brasilense*; Mineral nitrogen; Sesame Growth and Yield.

50. Two Closely Linked Tomato HKT Coding Genes are Positional Candidates for the Major Tomato QTL Involved in Na^+/K^+ Homeostasis

Maria Jose Asins, Irene Villalta, Mohamed M. Aly, Raquel Olas, Paz Lvarez De Morales, RaL Huertas, Jun Li, Noelia Jaime-Perez, Rosario Haro, VerNica Raga, Emilio A. Carbonell and Andres Belver

Plant, Cell And Environment, : 1-21 (2012)

The location of major quantitative trait loci (QTL) contributing to stem and leaf $[\text{Na}^+]$ and $[\text{K}^+]$ was previously reported in chromosome 7 using two connected populations of recombinant inbred lines (RILs) of tomato. HKT1;1 and HKT1;2, two tomato Na^+ -selective class I-HKT transporters, were found to be closely linked, where the maximum logarithm of odds (LOD) score for these QTLs located. When a chromosome 7 linkage map based on 278 single-nucleotide polymorphisms (SNPs) was used, the maximum LOD score position was only 35 kb from HKT1;1 and HKT1;2. Their expression patterns and phenotypic effects were further investigated in two near-isogenic lines (NILs): 157-14 (double homozygote for the *cheesmaniae* alleles) and 157-17 (double homozygote for the *lycopersicum* alleles). The expression pattern for the HKT1;1 and HKT1;2 alleles was complex, possibly because of differences in their promoter sequences. High salinity had very little effect on root dry and fresh weight and

consequently on the plant dry weight of NIL 157-14 in comparison with 157-17. A significant difference between NILs was also found for $[K^+]$ and the $[Na^+]/[K^+]$ ratio in leaf and stem but not for $[Na^+]$ arising a disagreement with the corresponding RIL population. Their association with leaf $[Na^+]$ and salt tolerance in tomato is also discussed.

Keywords: Solanum cheesmaniae; Solanum lycopersicum; Candidate gene analysis; Hkt1-Like genes; K^+ And Na^+ Concentration.

51. Influence of Arbuscular Mycorrhizae on Root Colonization, Growth and Productivity of Two Wheat Cultivars Under Salt Stress

Neveen B. Talaat and Baha T. Shawky

Archives of Agronomy and Soil Science, 58: 85-100 (2012)

Two pot experiments were conducted in the greenhouse of the National Research Center, Egypt during 2003/2004 and 2004/2005 to investigate the efficacy of arbuscular mycorrhizae (AM) on root colonization, growth and productivity in two wheat cultivars, Sakha 8 and Giza 167, under salt stress. The extent of the AM effect on wheat development varied with plant cultivar and salinity level. Maximum root colonization and spore production were observed with the Sakha 8 cultivar, which resulted in greater plant growth and productivity at all salinity levels. AM and plant development were adversely affected by increasing salinity. However, the presence of mycorrhizal fungi protected wheat against the detrimental effect of salinity and stimulated growth, productivity, total crude protein concentration and nitrate reductase activity. The average enhancement in grain yield due to AM inoculation was 76 and 68% at 0.15 mS cm^{-1} , 93 and 84% at 3.13 mS cm^{-1} , 130 and 115% at 6.25 mS cm^{-1} and 154 and 120% at 9.38 mS cm^{-1} salinity for Sakha 8 and Giza 167, respectively. In general, mycorrhizal inoculation enhanced the ability of wheat to cope with saline conditions and using AM inoculants can help plants to thrive in degraded arid/semi-arid areas.

Keywords: Wheat cultivars; Arbuscular mycorrhizae; Salt stress; Root colonization; Growth; Productivity.

Dept. of Agricultural Microbiology

52. El-Salam Canal is A Potential Project Reusing the Nile Delta Drainage Water for Sinai Desert Agriculture: Microbial and Chemical Water Quality

Amal A. Othman, Saleh A. Rabeih, Mohamed Fayez, Mohamed Monib and Nabil A. Hegazi.

Journal Of Advanced Research, 3: 99-108 (2012) IF: 3

More than $12 \times 10^9 \text{ m}^3/\text{year}$ of Nile Delta drainage water is annually discharged into the Mediterranean Sea. El-Salam (peace) canal, having a mixture of such drainage water and the Nilewater (1:1 ratio), crosses the Suez canal eastward to the deserts of north Sinai. The suitability of the canal water for agriculture is reported here. Representative samples were obtained during two successive years to follow effects of seasonal and spatial distribution, along the first 55 km course in north Sinai, on the water load of total bacteria, bacterial indicators of pollution and chemical and heavy metals contents. In general, the canal water is acceptable for irrigation, with much concern directed towards the chemical

contents of total salts (EC), Na and K, as well as the trace elements Cd and Fe. Extending the canal course further than 30 km significantly lowered the fecal pollution rate to the permissible levels of drinking water. Results strongly emphasize the need for effective pre-treatment of the used drainage water resources prior mixing with the Nile water.

Keywords: El-Salam canal; North Sinai; Drainage water; Reuse of Nile water; Water pollution; Diazotrophs.

53. Isolation of Probiotic Lactobacilli Strains Harboring L-Asparaginase and Arginine Deiminase Genes from Human Infant Feces for their Potential Application in Cancer Prevention

Mai N. Amer, Nahla M. Mansour, Ahmed I. El-Diwany, Insaaf E. Dawoud and Ferial M. Rashad

Annals of Microbiology, 1-2 (2012) IF: 0.689

The aim of this work was to isolate novel lactobacilli probiotic strains from human feces and screen them for the presence of two valuable antitumor genes—the arginine deiminase-encoding gene *arcA* and L-asparaginase-encoding gene *ansA*—for future potential therapeutic application in cancer prevention. Feces samples were collected from Egyptian infants. Forty-two isolates were determined as *Lactobacillus* sp. and selected for further characterization. Only 20 isolates exhibited good tolerance to pH 1.5, 0.3 % bile salts and moderate tolerance to pancreatic enzymes in addition to antagonistic action. These isolates were screened by PCR for the presence of the *arcA* and *ansA* genes. Three strains were selected and identified to subspecies levels by amplification and sequencing of 16S rRNA genes as *Lactobacillus gasserii* NM112 containing the *ansA* gene; *Lactobacillus fermentum* NM212; and *Lactobacillus casei* NM312 containing the *arcA* gene and confirmed by determining enzyme activity. We conclude that these three strains can be suggested as probiotics with potential therapeutic effect against cancer.

Keywords: Lactobacillus; Probiotics; Identification; 16S Rna Sequencing analysis; Antitumor genes; L-Asparaginase; Arginine deiminase.

54. Identification of Mosquito Larvicidal Bacterial Strains Isolated from North Sinai in Egypt

Ferial M Rashad, Waleed D Saleh, M Nasr and Hayam M Fathy

Amb Express, 2: 1-15 (2012)

In the present study, two of the most toxic bacterial strains of *Bacillus sphaericus* against mosquito were identified with the most recent genetic techniques. The PCR product profiles indicated the presence of genes encoding Bin A, Bin B and Mtx1 in all analyzed strains; they are consistent with protein profiles. The preliminary bioinformatics analysis of the binary toxin genes sequence revealed that the open reading frames had high similarities when matched with nucleotides sequence in the database of other *B. sphaericus* strains. The biological activity of *B. sphaericus* strains varied according to growing medium and cultivation time. The highest yield of viable counts, spores and larvicidal protein were attained after 5 days. Poly(P) medium achieved the highest yield of growth, sporulation, protein and larvicidal activity for all tested strains compared to the other tested media. The larvicidal protein produced by local strains (*B.*

sphaericus EMCC1931 and EMCC1932) in P medium was more lethal against the 3rd instar larvae of *Culex pipiens* than that of reference strains (*B. sphaericus* 1593 and *B. sphaericus* 2297). The obtained results revealed that P medium was the most effective medium and will be used in future work in order to optimize large scale production of biocide by the locally isolated *Bacillus sphaericus* strains.

Keywords: *Bacillus Sphaericus*; Pcr; Sequencing; Conventional Media; *Culex Pipiens*; Larvicidal; Activity.

55. Microbiota Are Necessary to Ameliorate Broccoli Vegetative Growth, Yield and Quality

Badawi, H. Mona, EL-Helaly, M.A. and Shalaby. E.A.

Journal of Applied Sciences Research, 8 (11): 5512-5520 (2012)

This work was conducted at the Experimental Station of the Faculty of Agriculture, Cairo University during the winter seasons of 2010/2011 and 2011/2012 to throw a flashlight on the impact of the diazotrophic bioformulation "Biofertile" and *Saccharomyces cerevisiae* in presence of N fertilization on vegetative growth and head quality of broccoli yield. Rhizosphere soil of Biofertile-treated plants accommodated total culturable bacteria of > 108 cfu g⁻¹, corresponding estimate for total diazotrophs approximated 107 cfu g⁻¹. In general, rhizospheric diazotrophs represented 12.1 - 50.0 % of total bacterial load. The highest records for head diameter, average head weight, economic yield and harvest index were attributed to Biofertile in combination with 50 % of recommended N fertilization regime. This unique treatment resulted in respective increases of ca. 5 and 4.7 tonnes fed⁻¹ head yield during the two successive experimental seasons while in the other biotic treatments, they did not exceed 1.9 tonnes fed⁻¹ compared to control. The presence of yeast strain in the applied treatments had no effect on the majority of determined traits. As high as 224.0 mg /100 g ascorbic acid was accumulated in heads due to Biofertile treatment. Incorporation into soil of 40 kg N fed⁻¹ resulted in the highest total chlorophyll content (3.06 mg g⁻¹) in broccoli heads. More than 250% increase over full N-dressed plants was attributed to inoculation with Biofertile plus yeast strain in presence of 20 kg N fed⁻¹. Antioxidant activity significantly supported due to microbiota treatments. Biofertile treatment significantly modified the N budget of soil where a net N gain of ca. 23 kg fed⁻¹ was estimated. Findings of the present study proved saving of 50% of needed mineral N fertilizer by Biofertile application besides improving both quality and quantity of broccoli yield.

Keywords: Broccoli; Biofertile; *Saccharomyces Cerevisiae*; N Fertilizer; Growth Formula; Head Yield .

Dept. of Agricultural Microbiology

56. El-Salam (Peace) Canal in North Sinai, Egypt

Nabil Hegazi and Mohamed Fayed Fouad Ibrahim

Book Published by Lambert Academic Publishing, 133 (2012)

More than 12 x10⁹ m³/year of Nile Delta drainage water is annually discharged into the Mediterranean Sea. El-Salam (peace) canal, having a mixture of such drainage water and the Nile water (1:1 ratio), crosses the Suez Canal eastward to the deserts of north Sinai. The chemical and microbiological quality of the canal water were monitored along two successive years, to follow

effects of seasonal and spatial distribution along the first 55 km course in north Sinai. It appeared that the canal water is acceptable for irrigation, with much concern directed towards the chemical contents of total salts, Na and K, as well as the trace elements Cd and Fe. Extending the canal course further than 30 km deep in the desert significantly lowered the faecal pollution rate to the permissible levels of drinking water. However, results obtained strongly emphasize the need for effective pre-treatment of the used drainage water resources prior mixing with the Nile water. The book with its 5 chapters is providing specialists in various fields of environment, agriculture and water resources with original data on the potential reuse of drainage water particularly in desert agriculture

Keywords: El-Salam Canal; North Sinai; Egypt, Nile Delta; Desert Agriculture; Drainage Water; Reuse of Water; Microbial Load; Water Quality; Water Pollution

57. Diversity of Microflora Associated to the Flora of North Sinai, Egypt

Samia Mahmoud El-Dieb, Mohamed Mohamed Metwally and Alaa Mohamed Abd El-Fattah

Book Published by Lambert Academic Publishing, 60 (2012)

The unique Sinai environment is currently subjected to changes due to the on-going agricultural and urban development projects. This includes the mega project of Al-Salam canal, that reuses the agricultural drainage water of the Delta mixed with Nile water (2:1, v/v), for cultivating ca 400,000 acres in north Sinai. As dramatic environmental changes and upsets are anticipated, efforts are made to survey and document the diversity of native flora and associated microflora in the major areas assigned to agricultural development. Microorganisms associated with the various root spheres (Ecto-rhizosphere, endo-rhizosphere) and plant canopy (phyllosphere) were cultured and estimated, e.g. Total bacteria, spore-formers and nitrogen-fixers (diazotrophs). The book presents the wonder of diversity and richness of north Sinai plant-microbe environments. Detailed information is presented regarding botanical information of dominant plants, associated bacteria in the root spheres and phyllosphere, as well as the taxonomic position of the hundreds of diazotrophs isolated

Dept. of Agricultural Zoology and Nematology

58. Effects of Insect Growth Regulators on the Mosquito-Parasitic Nematode *Romanomermis Iyengari*

Suman DS, Brey CW, Wang Y, Sanad M, Shamseldean MS and Gaugler R.

Parasitol Res, 112: 817-824 (2012) IF: 2.149

Pyriproxyfen, a juvenile hormone analogue, diflubenzuron, a chitin synthesis inhibitor and azadirachtin, anecdysone agonist, are three insect growth regulators (IGRs) considered as selective and effective insecticides for mosquitoes. *Romanomermis iyengari* (Welch) is a mosquito parasitic mermithid that can provide biological control against many medically important mosquito species. The compatibility of these two control tactics was tested by evaluating the sublethal effects of exposure to IGR on nematode developmental stages (preparasitic, parasitic and parasitic + parasitic) using *Culex pipiens* larvae as the host. Sublethal concentrations of IGRs were 90 %

emergence inhibition of host mosquito. Preparasitic exposure to pyriproxyfen, azadirachtin and diflurbenzuron had no effect on infectivity, parasite load, sex ratio, or male size but reduced nematode female length and increased male sex ratio at one parasite/larva.

When IGRs treatments were made against the parasitic and preparasitic + parasitic stages, pyriproxyfen and azadirachtin reduced *R. iyengari* infectivity, parasite load and male nematode length, whereas pyriproxyfen exposure increased male sex ratio and reduced the female *R. iyengari* length. Thus, IGRs have significant negative impact on different stages of mosquito mermithid that can destabilize the balance of host-parasite population interaction. Therefore, IGRs should be used with caution in mosquito habitats where these parasites have established.

59. Pathogenicity of Three Phytoparasitic Nematode Species Infecting Papaya and their Economic Thresholds in Egypt

H. H. Kesba, A. A. Al-Sayed and A. A. Farahat

International Journal of Nematology, 22: 103-111 (2012)

Susceptibility of papaya, *Carica papaya* L., cv. Solo to different inoculum levels of the root-knot, the reniform and the citrus nematodes was evaluated for the first time in Egypt under greenhouse conditions. The plants were found to be highly susceptible to the root-knot nematode, *Meloidogyne incognita* and the reniform nematode, *Rotylenchulus reniformis*, but moderately susceptible to the citrus nematode, *Tylenchulus semipenetrans* according to the rates of nematode multiplication. The highest rates of nematode reproduction were observed with the lowest levels of inocula.

The root-knot nematode reduced plant growth more than either citrus or reniform nematodes. The economic threshold of the citrus nematode was 2000 infective stage individuals (J_2)/pot; however, 4000 J_2 /pot was the economic threshold for root-knot or reniform nematodes. Infection with three nematode species, in general, increased shoot content of N, P and K and decreased the reducing sugars and total carbohydrates. In roots, different inoculum levels of the three nematode species decreased total phenols, tannins and increased total proteins.

Keywords: Chemical analysis; *Meloidogyne*; *Rotylenchulus*; Papaya; *Tylenchulus*.

Dept. of Agronomy

60. Moisture Balance and Tracer Gas Technique for Ventilation Rates Measurement and Greenhouse Gases and Ammonia Emissions Quantification in Naturally Ventilated Buildings

M. Samer, C. Ammon, C. Loebstin, M. Fiedler, W. Berg, P. Sanftleben and R. Brunsch

Build Environ, 50: 10-20 (2012) IF: 2.4

Experiments were performed to study the ventilation rates in a naturally ventilated animal building through four summer seasons and three winter seasons. The ventilation rates were determined using moisture (H_2O) balance, tracer gas technique (TGT) and CO_2 -balance. The statistical analyses were correlation analysis, regression model and t-test. Continuous measurements of gaseous

concentrations (NH_3 , CH_4 , CO_2 and N_2O), temperature and relative humidity inside and outside the building were performed. The H_2O -balance showed reliable results through winter seasons and acceptable results to some extent through summer seasons. The CO_2 -balance showed unexpected high differences to the other methods in some cases.

The TGT showed reliable results compared to H_2O -balance and CO_2 -balance. The air exchange rates (AERs) were 37.2, 61.6 and 63 h^{-1} through summer seasons and 40.3, 38.9 and 60.5 h^{-1} through winter seasons subject to H_2O -balance, TGT and CO_2 -balance, respectively. The emission rates through summer seasons, subject to TGT, were 191, 855, 73,877 and 45.6 $g d^{-1} AU^{-1}$; and through winter seasons were 88, 463, 55,976 and 47.3 $g d^{-1} AU^{-1}$, for NH_3 , CH_4 , CO_2 and N_2O , respectively.

Keywords: CO_2 -Balance; Gaseous Emissions; Livestock Buildings; Moisture (H_2O) Balance; Natural Ventilation; Tracer Gas Technique.

61. Numerical Simulation Study of A Tree Windbreak

Jessie P. Bitog, In-Bok Lee, Hyun-Seob Hwang, Myeong-Ho Shin, Se-Woon Hong, Il-Hwan Seo, Kyeong-Seok Kwon, Ehab Mostafa and Zhenzhen Pang

Biosyst Eng, 111: 40-48 (2012) IF: 1.354

In this study, computational fluid dynamics (CFD) was utilised to investigate the flow characteristics around tree windbreaks. The efficiency of windbreaks depends on many factors which can be investigated in field experiments, though this is limited due to several reasons such as unstable weather conditions, few measuring points, etc. Fortunately, the investigation is possible via computer simulations.

The simulation technique allows the trees to be modelled as a porous media where the aerodynamic properties of the trees are utilised in the model.

The trees employed are Black pine trees (*Pinus thunbergii*) with a drag coefficient value of 0.55. The simulation provides analysis of the effect of gaps between trees, rows of trees and tree arrangements in reducing wind velocity.

The simulations revealed that 0.5 m gap between trees was more effective in reducing wind velocity than 0.75 and 1.0 m. The percentage reduction in velocity at the middle of the tree section for 0.5, 0.75 and 1.0 m gap distance was found to be 71, 65 and 56%, respectively.

Two-rows of alternating trees were also found to be more effective than one-row and two-rows of trees. The reduction at the middle of the tree region for one-row and two-rows of trees and two-rows arranged alternately was 71, 88 and 91%, respectively. Results revealed that the percentage reduction in wind velocity measured at distance 15H, where H is the tree height, for one-row, two-rows of trees and two-rows arranged alternately was approximately 20, 30 and 50%, respectively.

Keywords: Cfd; Aerodynamic porosity; Black pine Tree; Drag coefficient; Tree windbreak.

62. Computational Fluid Dynamics Simulation of Air Temperature Distribution Inside Broiler Building Fitted with Duct Ventilation System

Ehab Mostafa , In-Bok Lee, Sang-Hyeon Song, Kyeong-Seok Kwon, Il-Hwan Seo, Se-Woon Hong, Hyun-Seob Hwang, Jessie Bitog Hwa and Taek Han

Biosyst Eng, 112: 293-303 (2012) IF: 1.354

An investigation was conducted to develop ventilation systems to prevent cold air drafts during the winter season and create a suitable atmosphere inside the broiler rearing building. In the cold weather, ventilation ducts and low ventilation rates are used to maintain the required air temperature. Perforated ducts are preferred for heating spaces because they provide efficient and uniform distribution of the entire air volume. Four ventilation systems were designed in order to establish a comfortable zone for the broilers during winter season. To investigate these different systems under realistic conditions, computational fluid dynamic simulation was used. Field experiments were conducted to validate the designed cases. From the validation results, very low errors were observed. The improved designs were compared with the standard design in terms of ventilation rate, air temperature distribution and indoor gas concentration reduction. Case four (C-4) of the improved designs achieved the highest ventilation rate in the broiler zone. In C-4, the inlet duct was installed in building side and the outlet duct in the opposite side. It achieved about 54% of the ventilation in comparison to standard design. All improved designs showed high uniformity ranging around 60-70% compared to the standard design. For gas dilution in broiler zone, C-4 showed 15% ammonia reduction efficiency 3 min after operating the ventilator.

Keywords: Cfd; Pipe ventilation; Broiler; Air temperature distribution; Stability.

63. An Expert System for Planning and Designing Dairy Farms in Hot Climates

M. Samer, M. Hatem, H. Grimm, R. Doluschitz and T. Jungbluth

Agricultural Engineering International: Cigr Journal, 14 (1): 1-15 (2012)

Eleven simulation models were developed to plan and design several dairy farm facilities. Subsequently, an electronic spark map (decision tree) was developed for each simulation model and then the simulation models were integrated into the relevant spark maps. Afterwards, C# language (C Sharp), which is an object-oriented programming language, was used to develop an expert system via the simulation models and the electronic spark maps. The developed expert system is able to plan and design several dairy farm facilities, e.g. housing system (corrals system), shade structure and roof material, concrete base, cooling system, milking parlour, forage storage and manure handling system. Subsequently, it plans the farmstead layout and it leads to implement the technologies, equipments and machines required for performing several farm operations. Furthermore, it studies water and electricity requirements of the planned dairy farm and the available sources on site. Moreover, it calculates the capital investment and the fixed, variable and total costs. Data of six dairy farms were used to carry out the expert system validation and evaluation. The differences between the actual and calculated values were determined and the standard deviations were

calculated. The coefficients of variation range between 3% and 7%. The accuracy of the developed expert system is 94.5%.

Keywords: Expert systems; Simulation models; Spark maps; Precision livestock farming; Dairy cows.

64. A Tool to Design the Concrete Constructions of Horizontal Silos

Mohamed Samer, Mohamed Hatem, Hartmut Grimm, Reiner Doluschitz and Thomas Jungbluth

International Journal of Scientific Research and Application, 1 (1): 13-19 (2012)

A tool is developed in order to plan and design concrete structures for horizontal silos. A mathematical model was developed. Subsequently, the tool is developed by integrating the mathematical model into an electronic spark map. The spark map (decision tree) specifies the horizontal silo dimensions according to the planned storage volume, computes the required amounts of construction materials to build the horizontal silo and calculates the capital investment and the fixed, variable and total costs. On the other hand, the mathematical model of the spark map requires some input data. According to these data, the spark map will make calculations and show the output data automatically. Data of 4 horizontal silos were used to carry out the model validation. The differences between actual and calculated values were determined and the standard deviations were calculated. The coefficients of variation were 3.4%, 5.5%, 5%, 7% and 4.5% for amounts of concrete, gravels, cement, sand and iron rods, respectively.

Keywords: Concrete structures; Mathematical modeling; Silage structures; Cement based materials; Horizontal silos; Forage storage; Spark mapping; Costs calculation.

65. Air-Polluted with Particulate Matters from Livestock Buildings

Ehab Mostafa

Air Quality – New Perspective, Intech, 287-312 (2012)

Livestock production has a harmful effect on the environment during the breeding period, such as the emittance of dust, odour and ammonia into the surrounding environment through the ventilation system as well as its harmful influence on the animals and workers inside these animal houses. Airborne dusts is normally considered to be one of the contaminants in livestock buildings. Particle matter reduces the air quality within the livestock buildings compromising the health of farmers and animals. Commercial livestock production facilities are always associated with some level of airborne particles. High concentrations of airborne particles could affect the external environment, production efficiency, health and welfare of humans and animals. The improvement of the farm animal health is an important goal to ensure proper livestock production. Apart from management factors the internal environmental conditions play a key role for ensuring the well-being of intensively housed livestock and farm workers. Livestock farmers are exposed to dust concentrations inside their animal houses that are a factor of 10 to 200 times higher than those of the outside air. The ventilation system of a building discharges dust particles into the environment, considering the high dilution rate with the outside air, the following discussion focuses on the dust level and control inside

the livestock building. Requirements for good management and ventilation in animal husbandry systems ensure that the quality of indoor air is acceptable for animals' and humans' health.

Keywords: Livestock; Airborne dust; Animal health; Environment; Farm workers.

66. Biogas Plant Constructions

Mohamed Samer

Biogas, Intech, chapter (17): 343-368 (2012)

The chapter concerns with the constructions of the commercial biogas plants as well as the small and household units. Furthermore, the chapter aims at providing a clear description of the structures and constructions of the anaerobic digesters and the used building materials. Ultimately, the chapter answers an important question: how to build a commercial biogas plant and a household unit and what are the construction steps.

Keywords: Constructions; commercial biogas plants; household units; structures and constructions; anaerobic digesters; building materials; construction steps.

Dept. of Animal Production

67. Molecular Mechanisms and Pathways Involved in Bovine Embryonic Genome Activation and the Regulation by Alternative in Vivo and in Vitro Culture Conditions¹

Gad A, Hoelker M, Besenfelder U, Havlicek V, Cinar U, Rings F, Held E, Dufort I, Sirard MA, Schellander K and Tesfaye D.

Biology of Reproduction, 87 (4): 1-13 (2012) IF: 4.009

Understanding gene expression patterns in response to altered environmental conditions at different time points of the preimplantation period would improve our knowledge on regulation of embryonic development. Here we aimed to examine the effect of alternative in vivo and in vitro culture conditions at the time of major embryonic genome activation (EGA) on the development and transcriptome profile of bovine blastocysts. Four different blastocyst groups were produced under alternative in vivo and in vitro culture conditions before or after major EGA. Completely in vitro- and in vivo-produced blastocysts were used as controls. We compared gene expression patterns between each blastocyst group and in vivo blastocyst control group using EmbryoGENE's bovine microarray. The data showed that changing culture conditions from in vivo to in vitro vice versa, either before or after the time of major EGA, had no effect on the developmental rates; however, in vitro conditions during that time critically influenced the transcriptome of the blastocysts produced. The source of oocyte had a critical effect on developmental rates and the ability of the embryo to react to changing culture conditions. Ontological classification highlighted a marked contrast in expression patterns for lipid metabolism and oxidative stress response between blastocysts generated in vivo versus in vitro, with opposite trends. Molecular mechanisms and pathways that are influenced by altered culture conditions during EGA were defined. These results will help in the development of new strategies to modify culture conditions at this critical stage to enhance the development of competent blastocysts.

Keywords: Bovine; Culture conditions; Embryonic genome activation; Gene expression; Lipid metabolism; Oxidative stress.

68. Endometrial Response of Beef Heifers on Day 7 Following Insemination to Supraphysiological Concentrations of Progesterone Associated with Superovulation

N. Forde, F. Carter, S. di Francesco, J. P. Mehta, M. Garcia-Herreros, A. Gad, D. Tesfaye, M. Hoelker, K. Schellander and P. Lonergan

Physiological Genomics, 44: 1107-1115 (2012) IF: 2.73

Endometrial response of beef heifers on day 7 following insemination to supraphysiological concentrations of progesterone associated with superovulation. *Physiol Genomics* 44: 1107–1115, 2012. First published September 25, 2012; doi:10.1152/physiolgenomics.00092.2012.—Ovarian stimulation is a routine procedure in assisted reproduction to stimulate the growth of multiple follicles in naturally single-ovulating species including cattle and humans. The aim of this study was to analyze the changes induced in the endometrial transcriptome associated with superovulation in cattle and place these observations in the context of our previous data on changes in the endometrial transcriptome associated with elevated progesterone (P4) concentrations within the physiological range and those changes induced in the embryo due to superovulation. Mean serum P4 concentrations were significantly higher from day 4 to day 7 in superovulated compared with unstimulated control heifers ($P < 0.05$). Between-group analysis revealed a clear separation in the overall transcriptional profile of endometria from unstimulated control heifers ($n = 5$) compared with superovulated heifers ($n = 5$). This was reflected in the number of differentially expressed genes (DEGs) identified between the two groups with 795 up- and 440 downregulated in superovulated endometria. Ten times more genes were altered by superovulation ($n = 1,234$) compared with the number altered due to elevated P4 within physiological ranges by insertion of a P4-releasing intravaginal device ($n = 124$) with only 22 DEGs common to both models of P4 manipulation. Fewer genes were affected by superovulation in the embryo compared with the endometrium, (443 vs. 1,234 DEGs, respectively) and the manner in which genes were altered was different with 64.5% of genes up- and 35.5% of genes downregulated in the endometrium, compared with the 98.9% of DEGs upregulated in the embryo. In conclusion, superovulation induces significant changes in the transcriptome of the endometrium which are distinct from those in the embryo.

Keywords: Bovine; Gene expression; Embryo; Uterus; Progesterone.

69. Incidence of Apoptosis and Transcript Abundance in Bovine Follicular Cells is Associated with the Quality of the Enclosed Oocyte

D. Janowski, D. Salilew-Wondim, H. Torner, D. Tesfaye, N. Ghanem, W. Tomek, A. El-Sayed, K. Schellander and M. Hlker

Theriogenology, 78: 656-669 (2012) IF: 1.963

The close contact and interaction between the oocyte and the follicular environment influence the establishment of oocyte developmental competence. Moreover, it is assumed that

apoptosis in the follicular cells has a beneficial influence on the developmental competence of oocytes. The aim of this study was to investigate whether bovine oocytes with varied developmental competence show differences in the degree of apoptosis and gene expression pattern in their surrounding follicular cells (cumulus and granulosa cells). Oocytes and follicular cells from follicles of 3 to 5 mm in diameter were grouped as brilliant cresyl blue (BCB) + and BCB- based on glucose-6-phosphate dehydrogenase (G6PDH) activity in the ooplasm by BCB staining. In the follicular cells initial, early and late apoptotic events were assessed by analyzing caspase-3 activity, annexin-V and TUNEL, respectively. Global gene expression was investigated in immature oocytes and corresponding follicular cells. BCB + oocytes resulted in a higher blastocyst rate (19.3%) compared to the BCB- group (7.4%, $P < 0.05$). Moreover, the analysis of apoptosis showed a higher caspase-3 activity in the follicular cells and an increased degree of late apoptotic events in granulosa cells in the BCB + compared with the BCB- group. Additionally, the global gene expression profile revealed a total of 34 and 37 differentially expressed genes between BCB + and BCB- cumulus cells and granulosa cells, respectively, whereas 207 genes showed an altered transcript abundance between BCB + and BCB- oocytes. Among these, EIF3F, RARRES2, RNF34, ACTA1, GSTA1, EIF3A, VIM and CS gene transcripts were most highly enriched in the BCB + oocytes, whereas OLFM1, LINGO1, ALDH1A3, PTHLH, BTN3A3, MRPS2 and PPM1K were most significantly reduced in these cells. Therefore, the follicular cells enclosing developmentally competent oocytes show a higher level of apoptosis and a different pattern of gene expression compared to follicular cells enclosing non-competent bovine oocytes.

Keywords: Bovine; Oocyte; Granulosa; Cumulus; Apoptosis; Gene expression.

70. Cdna Microarray Analysis of Gene Expression in Parthenotes and in Vitro Produced Buffalo Embryos

Abdoon AS, Ghanem N, Kandil OM, Gad A, Schellander K and Tesfaye D.

Theriogenology, 77: 1240-1251 (2012) IF: 1.963

The retarded development of parthenote embryo could be due to aberrant epigenetic imprinting, which may disrupt many aspects and lead to conceptus demise. The present work was conducted to: 1) compare the development of in vitro produced (IVP) and parthenogenetically developed (P) buffalo embryos from the 2-cell to blastocyst stage; 2) investigate the global gene expression profile and search for new candidate transcripts differing between IVP and P buffalo blastocyst using cDNA microarray analysis (validated by Real Time PCR); 3) follow the particular expression patterns of PLAC8 and OCT4 genes at five different stages of preimplantation development by Real Time PCR; and 4) study the expression of CDX2 at the blastocyst stage. Cleavage rate was higher ($P < 0.05$) in P than IVP buffalo embryos, while, progression to blastocyst and number of cells per blastocyst were lower ($P < 0.05$) in P than IVP blastocysts. Microarray analysis indicate that 56 differentially expressed genes between the two groups, of which 51 genes (91.07%) were up-regulated and five genes were downregulated in IVP blastocyst, using 1.4 fold-changes as a cutoff. Differentially expressed genes are related to translation, nucleic acid synthesis, cell adhesion and placentation. Validation of candidate genes revealed that the transcript abundance of PTGS2, RPS27A, TM2D3, PPA1, AIOX15, RPL0

and PLAC8 were downregulated (7/8) in parthenote blastocyst compared to the IVP blastocyst. PLAC8 gene expression was higher ($P < 0.05$) at 2-cell, morula and blastocyst stages in IVP embryos compared with parthenote embryos. The OCT4 gene expression was higher ($P < 0.05$) in 2-cell, 4-cell, 8-cell and blastocysts produced in vitro. In conclusion, the retarded development of parthenogenetic buffalo embryos could be due to downregulation of genes related to translation, nucleic acid synthesis, cell adhesion and placental development. The low expression of PLAC8 and OCT4 during the different stages of development may be responsible, in part, to the failure of development of parthenote buffalo embryos.

Keywords: Buffalo Embryos; Parthenogenesis; Ivp; Microarray Analysis; Gene Expression.

71. Transcriptome Profile of Early Mammalian Embryos in Response to Culture Environment

A. Gada, K. Schellander, M. Hoelker and D. Tesfaye

Anim Reprod Sci, 134: 76-83 (2012) IF: 1.75

Early embryonic development, the period from maturation until blastocyst formation, is one of the most critical periods of mammalian development involves various morphological, cellular and biochemical changes related to genomic activity. During the post-fertilization period, several major developmental events occur in the embryo which are regulated by a harmonized expression of genes and strongly influenced by culture conditions. The products of these genes are involved in various biological processes including metabolism, growth factor/cytokine signaling, stress adaptation, transcription and translation, epigenetic regulation of transcription, apoptosis, compaction and blastocyst formation.

Post-fertilization culture environment is known to be the most important factor determining the quality of the resulting embryos as indicated in terms of cryo-tolerance and relative abundance of transcripts. However, the exact effect of culture conditions on gene expression and subsequent influences on molecular pathways controlling early development is still unknown.

A number of culture environmental factors can influence the gene expression of produced embryos such as media composition, serum supplementation, number of embryos present in the culture drop and gas atmosphere. During the last ten years several studies were concerned with differences in the transcriptome profile of embryos produced under different environmental conditions and its subsequent influence on embryo developmental competence. From these studies, several genes have been determined as candidate genes controlling preimplantation embryo development and affecting its quality.

Here we will discuss results of different experiments investigated the effect of different culture conditions on the transcriptome profile of bovine blastocyst. These experiments identified molecular mechanisms and pathways that influenced by culture conditions and this will enable to launch strategies to modify culture conditions to enhance the development of competent blastocyst.

Keywords: Gene Expression; Culture Conditions; Mammalian Embryos.

72. Metabolic and Reproductive Status are Not Improved from 11 to 25 Day Post-Partum in non-Weaned Primiparous Rabbit Does

R.M. Garcia-Garcia, I. O.G. Sakr, M. Arias-Alvarez, B. Velasco, P.L. Lorenzo and P.G. Rebollar

Anim Reprod Sci, 131: 100-106 (2012) IF: 1.75

The aim of present work was to analyze the body reserves and ovarian features of lactating primiparous rabbit does under extensive reproductive management (artificial insemination (AI) at 25 days post-partum (dpp)) compared with the common insemination rhythm at 11 dpp. A total of 48 primiparous Californian × New Zealand White rabbit does suckling 8 kits were used to assess liveweight, estimated body composition, serum metabolic and endocrine parameters (oestradiol and progesterone concentrations) and ovarian features like follicle population and atresia rate and oocyte maturation. Rabbit does were randomly allocated in two experimental groups: (a) lactating does euthanized at early post-partum period (11 dpp) according to a semi intensive rhythm (n = 24) and (b) lactating does euthanized at later post-partum period (25 dpp) according to a more extensive rhythm (n = 24). Liveweight, body energy content, lipid depots and serum non-esterified fatty acids (NEFA) concentrations decreased from parturition to post-partum period (P < 0.05). In addition, serum protein and glucose concentrations increased in the post-partum period (P < 0.05). Similar oestradiol and progesterone levels were found in rhythms as well as similar follicle population and nuclear and cytoplasmic maturation rates measured as metaphase II and cortical granule migration, respectively in both post-partum times. However, the number of preovulatory follicles on the ovarian surface was lower (P < 0.05) and the atresia rate tended to be higher with a lower percentage of healthy follicles (P < 0.1) in ovaries from females of extensive group. In conclusion, the body reserves, serum metabolic parameters and oocyte quality of primiparous non-weaned rabbits does at the late post-partum time (25 days) were not improved. Thus this reproductive management did not present any advantages compared to earlier post-partum (11 days) reproductive rhythm.

Keywords: Lactating; Primiparous rabbits; Reproductive; Management; Metabolic status; Ovarian characteristics.

73. The Effect of Backfat Thickness at Mating on the Reproductive and Productive Performances of Ewes

I.I. Abdel-Mageeda and A.M. Abo El-Maaty

Small Ruminant Research, 105: 148-153 (2012) IF: 1.295

Three Egyptian sheep breeds (Rahmani, n = 40; Barki, n = 50; Ossimi, n = 36) were used to investigate the effect of backfat thickness of ewes, at mating, on their subsequent reproductive and productive performances. Ewes were assigned to four groups, according to their backfat thickness (<1; 1 to <1.5; 1.5 to <2; ≥2 mm) respectively.

The experimental design was thus completely randomized with the 12 groups arranged factorially (3 × 4), according to breed and backfat thickness. Ewe breeds did not significantly affect the studied reproductive and productive traits. However, the backfat thickness of the ewes significantly affected all the reproductive and productive traits, except for ewes conceived/ewes joined and lambs born/ewe lambing. Superior performances were recorded for ewes with a backfat thickness of 1.5 to <2 mm and those

having ≥2 mm – where the lambs weaned/ewe joined increased from 43% in the lowest backfat thickness group (<1 mm) to 73% and 77% in the higher backfat thickness groups (1.5 to <2 mm and ≥2 mm groups, respectively).

The kg lamb weaned/ewe joined increased gradually by increasing the backfat thickness of the ewes from 6.2 kg in the lowest backfat thickness group, to 14 kg in the highest backfat thickness group. However, no significant differences were recorded for ewes with a backfat thickness of 1.5 to <2 mm and those having ≥2 mm regarding all the reproductive and productive traits, except for ovulation rate. Therefore, to optimize the profitability in sheep flocks, it is recommended to control the backfat thickness of ewes at mating between 1.5 and 2 mm.

Keywords: Ewes; Backfat thickness; Sheep breeds; Reproduction; Lambing rate.

74. Effect of Feed Additive "Exogenous Enzymes" on Growth Performance of Maghraby Camels

Adel E. M. and H. EL-Metwaly

Life Science Journal, 9: 4830-4835 (2012) IF: 0.073

This experiment aimed to evaluate the effects of a mixture of exogenous enzymes (ZADO[®]) from anaerobic bacteria on growth performance, feed intake, nutrient digestibility and blood parameters. Eighteen growing Maghraby camels averaged, 268.83 kg body weight; 1.5-2 years. Camels were randomly divided into 3 equal groups (6 in each) of similar weight and age, which were offered complete rations with low levels of ZADO[®] product. The first group was Zero g/h/d (control), the second group take 20 g/h/d of ZADO[®] and the third group 40 g/h/d, over a period of 90 days. Results indicated that 40 g supplementation showed the best response in DM and OM digestibility. Carbohydrate results showed significant effects of ZADO supplementation on crude fiber and Nitrogen free extract in R40 being, 78.23 %, 80.60% and R20 being, 75.56%, 77.23%, respectively with insignificant difference between R20 and C ration. NDF digestibility was significantly with R40 (75.77%) followed by R20 (72.99%) and C (71.17 %). Blood parameters of control and tested groups of camels were in normal range with slight decrease in total lipid. Total body gain and average daily gain (ADG) significantly differed among experimental groups being 61.87, 84.82 and 88.65 kg and 0.69, 0.94 and 0.98, in C, R20 and R40 kg, respectively. Data related to feed intake as DM, TDN showed insignificant difference among groups of camels. It could be concluded that growing male Maghraby camels fed on the diet containing ZADO[®] performed better than those offered the control ration. Moreover, adding ZADO[®] in camel ration (40g/h/d) was the better, as confirmed by the highest body weight gain, most of blood metabolites and digestibility.

Keywords: Camel; Zado; Digestibility; Daily gain.

75. Microsatellite Markers Associated with Body and Carcass Weights in Broiler Breeders

F. S. Nassar, R. E. A. Moghaieb, A. M. Abdou and F. K. R. Stino

African Journal of Biotechnology, 11(15): 3514-3521 (2012)

Microsatellite markers are presently used in selection to facilitate the genetic improvement of growth and carcass traits in chickens. The genetic improvement of six weeks live body and carcass weights of Cairo B-2 line, after six generation of selection, was

compared with the control line (C line). Cairo B-2 line had higher body weight, breast meat and carcass parts than the C line. Seven microsatellites, associated with body and carcass weights, were efficiently used to study the effect of selection on the microsatellite marker frequencies of Cairo B-2 line. The allelic number of the microsatellite markers ADL0328, MCW0097 and ROS0025 associated with live body, breast, carcass and wings weights increased in the Cairo B-2 line than the C line. The association between these important economic characteristics and microsatellite loci will facilitate the selection process by applying marker assisted selection in future breeding programs.

Keywords: Marker assisted selection; Microsatellite; Carcass; Breast meat.

76. Fertilization Capacity of Rooster Spermatozoa in Response to the Modification in the Semen Composition

Essam A. El-Gendy, Marwa M. Ahmed, Shoukry M. El-Tantawy and Shawki A. Ibrahim

International Journal of Poultry Science, 11(11): 683-688 (2012)

An experiment was carried out to study the changes in fertilization capacity of rooster sperms in response to the modification in the biochemical composition of the semen. Chickens of two lines (CE2 and CE4) were used. Seven treatments of semen were designed and included the incubation of sperm with the plasmid, with a mixture of the plasmid and lipofectin at 2.5 or 5% concentration and the incubation of spermatozoa with lipofectin and a semen extender (BPSE). The progenies were obtained from the insemination of hens by the semen of different treatments. Sperm motility was greatly influenced by the treatments. Motility was significantly the highest in the control semen and averaged 92.42% and highly significantly declined to 52.08 and 58.75% in the semen samples treated with the plasmid, lipofectin at 2.5 or 5% concentration and diluted with BPSE. The percentage of live sperm was not affected by the addition of the plasmid. The addition of the plasmid and lipofectin or the diluted BPSE resulted in a significant reduction in the percentage of live sperms. The percentage of live sperms was 59-62% when the plasmid, lipofectin and BPSE were all together added to the semen samples. The percentages of dead and abnormally-shaped sperm reached to 26.88 and 17.13%, respectively, in the semen treated with plasmid, lipofectin 5% and BPSE. Fertility averaged 88.22% in the eggs of hens inseminated with the control semen and significantly decreased to 42.14% when semen was incubated with the plasmid pUC18 and reached to 58.98% when semen was treated with plasmid, lipofectin (5%) and BPSE.

Keywords: Bacterial Plasmid; Rooster Spermatozoa; Lipofectin; Semen Dilution.

Dept. of CROP Sciences

77. Evaluation of Some Faba Bean Genotypes Against Chocolate Spot Disease using Cdna Fragments of Chitinase Gene and Some Traditional Methods

S.R.E. Abo-Hegazy, Noha F. El-Badawy, I.V.I.V.I. Mazen and H. Abd El-Menem

Asian Journal of Agriculture Research, 6 (2): 60-72 (2012)

Thirteen faba bean (*Vicia faba* L.) genotypes were assessed under greenhouse and field conditions in 2008/2009 and 2009/2010 seasons, using morphological and molecular characterization methods for resistance to chocolate spot diseases caused by *Botrytis fabae*. A significant variation among the tested genotypes and their reaction to the disease was found under greenhouse condition. Sakha 1, Sakha 2 and Nubaria-1 were resistant, indicating by the lowest disease severity. Whereas Giza 40, line 375 and Cairo 25 were susceptible. Other faba bean genotypes were moderately susceptible. Reverse-Transcription (RT-PCR) showed that Chitinase gene is expressed at early stages in infected faba bean leaves. By using of Chitinase specific primers DNA fragment at molecular weight 900 bp appeared at 48 hrs. in six faba bean genotype upon infection with the pathogen 48 hrs after inoculation and disappeared in the healthy plants. This fragment detected only in the resistance cultivars Sakha-1, Sakha-2 and Nubaria-1 and some moderate resistance genotype including Giza-3, line-24H and line 36. At the same time no signal was detected in other infected genotypes or healthy ones. Field results of testing genotype against chocolate spot diseases differed slightly than that of greenhouse. The estimates of heritability in broad sense ranged from 0.90 to 0.99, High values of heritability were obtained for seed yield/plant (0.99), followed by plant dryweight, plant height, seeds/pod across the two seasons. However, No relationship was found between resistance of genotypes against *B. fabae* and their morphological characteristics under field conditions.

Keywords: Faba Bean; Chocolate Spot; Phenotypic Correlation; Heritability; Chitinase; Rna; Cdna; Rt; Per.

78. Yield and Soybean Characters Under Some Intercropping Patterns with Corn

A A Metwally, M M Shafik, K. E. El-Habbak and Sh Abd elwahab

Soybean Research, 10: 24-42 (2012)

Two experiments were conducted at Gemmeiza Agricultural Experimental and Research Station, ARC, El-Gharbia Governorate, Egypt, during 2006 and 2007 summer seasons to investigate the possibility of increasing intercropped soybean yield by raising each of soybean plant density and intercepted light on soybean through intercropping patterns. Intercropping patterns comprised alternating and mixed ridges between corn and soybean. Alternating ridges (70 cm/ridge) between corn and soybean were used as 2:2 and 2:4, respectively, soybean was grown in alternating ridges by two rows per ridge (N) in normal plant population density (2:2 and 2:4), in addition to another single row on the other adjacent side of corn ridges (H) to increase the density of the intercropped soybean plants by about 25 per cent than normal density (N) for the two intercropping patterns 2:2 and 2:4. In mixed pattern, four rows of soybean were planted on the wide ridge (140 cm/ridge) by two rows on each side, while, corn was grown on middle of the ridge. Two patterns of solid planting were adopted as those of alternating and mixed patterns. Soybean plants were grown in 2 plants per hill (15 cm apart), while, corn was distributed in two plants per hill (30 cm apart) and four plants per hill (60 cm apart). One corn variety and two soybean varieties were used. Solid planting patterns had higher values for soybean seed yield and its components as compared with intercropping patterns, whereas, the reverse was true for seed protein content. Growing corn and soybean in 2:4 ridges under high soybean plant density (H) gave higher values for yields of seed, oil and protein

as compared with those of normal population of 2:4(N) and other patterns. The soybean variety Giza 22 had higher values for all the studied parameters, except seed index, than the other variety. All the studied parameters were increased by doubling distance between hills of corn from 30 to 60 cm apart, whereas, the reverse was true for seed protein content.

Keywords: Intercropping; Light Intensity; Plant Density; Seed Yield; Soybean Varieties.

79. Effect of Intercropping Corn on Egyptian Cotton Characters

Abd El-Alim A. Metwally, Magdy M. Shafik, Mohamed N. Sherief and Tamer I. Abdel-Wahab

Journal of Cotton Science, 16: 210-219 (2012)

Two experiments were conducted at Gemmeiza Agric. Exp. and Res. Station, A.R.C., El-Gharbia Governorate, Egypt, during 2006 and 2007 summer seasons to study the effects of intercropping corn with cotton on seed cotton yield and its components. Intercropping patterns included alternating ridges between cotton and corn at 2:1 and 3:1, respectively, (60 cm per ridge), a mixed intercropping pattern (120 cm per ridge) for growing the two crops and two additional solid planting patterns of cotton. Intercropping corn with cotton resulted in lower values for number of open bolls plant-1, seed cotton yield plant-1 and seed cotton yield acre-1 as compared with recommended solid planting of cotton. Alternating ridges between cotton and corn in a 3:1 ratio had higher values for number of open bolls plant-1, seed cotton yield plant-1, grain yield plant-1 and lint percentage as compared with the other intercropping patterns. Mixed intercropping pattern gave the highest yields for both crops. Seed cotton yield in intercropping patterns was affected by intercepted light on cotton plants through adjacent corn plants and the ratio of occupied cotton plants in the intercropping area. Cotton fiber properties were not affected significantly by any of the different cropping systems, corn varieties or their distributions. Seed yield of intercropped cotton reached 80.45 % of that obtained from recommended solid planting of cotton in addition to 2.90 ton acre-1 of corn grains. Intercropping corn with cotton increased total and net returns as compared with recommended solid planting of cotton. Mixed intercropping pattern gave the highest financial return value when using high population densities of both crops and distributing the corn plants at a wide distance between hills.

Keywords: Intercropping; Cotton; Corn Varieties.

80. Analysing and Modeling the Relationship Between Yield and yield components in sunflower under different planting dates

Ashraf Abd El-Aal Abd El-Mohsen

Journal of Plant Breeding and Crop Science, 4(8): 125-135 (2012)

The relationships between planting dates and yield and its components in sunflower was evaluated through orthogonal polynomial regression analysis. Five field experiments were conducted during the summer season of 2011 to study the effect of five planting dates and three oilseed sunflower genotypes and their interactions on yield and yield components of sunflower. The highest seed yield, oil yield, plant height, head diameter, 1000-

seed weight, seed yield plant-1 and oil content were obtained at the earliest planting date (1st May). The evaluated genotypes differed significantly for all the studied traits. Sakha 53 cultivar was the best cultivar in seed yield, oil yield, plant height, head diameter, thousand seed weight and seed yield plant plant-1 followed by Giza 102 and Pioneer hybrid 63M02, respectively. Orthogonal polynomial regression analysis revealed that, yield and yield components were significantly affected by planting date in linear responses. Multiple linear regression analysis indicated that seed yield plant-1, head diameter and thousand seed weight were the most important variables contributing toward higher seed yield (kg ha-1). Finally, it can be concluded that planting sunflower cultivar Sakha 53 on 1st May was recommended for maximizing seed and oil yields per unit area under the environmental conditions of this study.

Key words: Sunflower; planting date; genotype; regression analysis; yield; yield components.

81. Genotypic and Phenotypic Interrelationships Among Yield and Yield Components in Egyptian Bread Wheat Genotypes

Ashraf A. Abd El- Mohsen, Samir R. Abo Hegazy and Moemen H. Taha

Journal of Plant Breeding And Crop Science, 4 (1): 9-16 (2012)

Two field experiments were conducted in 2008/2009 and 2009/2010 growing seasons at the experimental farm of the Faculty of Agriculture, Cairo University, Giza, Egypt. Ten Egyptian bread wheat genotypes were planted in a randomized complete block design with three replications and evaluated for eight characters.

The aim was to study the phenotypic and genotypic correlations and genotypic path analysis for grain yield and yield components. Highly significant differences were observed among genotypes for all the eight studied traits. Statistical analysis showed that genotypic correlation coefficients were higher than the corresponding phenotypic correlation coefficients in most of the traits.

The results revealed positive association in between number of tillers plant-1, number of spikelets spike-1, spike length, number of grains spike-1 and 1000 grain weight with grain yield plant-1 at both genotypic and phenotypic levels. However, days to 50% heading and plant height contributed negatively towards grain yield at both levels.

Path analysis showed that maximum positive direct effect on grain yield plant-1 was contributed mostly by number of grains spike-1, followed by number of tillers plant-1 and 1000-grain weights were the major contributors towards grain yield. Since these three characters had high correlation and also high direct effect thus direct selection for these three characters should be of a major concern for a plant breeder. It was, therefore, suggested that number of grains spike-1, number of tillers plant-1 and 1000-grain weight should be given emphasis for future wheat yield improvement programs.

Keywords: Wheat; Variability; Phenotypic and genotypic correlation; Path coefficients; Yield; Yield components.

Dept. of Dairy Sciences**82. the Growth Behaviour and Enhancement of Probiotic Viability in Bioyoghurt**

S.M. El-Dieb, F.H.R. Abd Rabo, S.M. Badran, A.M. Abd El-Fattah and F.M.F. Elshaghabe

Int Dairy J, 22: 44-47 (2012) IF: 2.401

The growth behaviour of *Lactobacillus casei*-01 and *Bifidobacterium bifidum* Bb-12 in bioyoghurt made with three different yoghurt starter cultures (YC-Fast 1, YC-380 and YC-180) and the enhancement of probiotic viability, were investigated. The titratable acidity (TA) increased rapidly in yoghurt samples made with YC-Fast 1. The fermentation times were 3, 3.5 and 4 h for bioyoghurts made with YC-Fast 1, YC-380 and YC-180, respectively. The total viable counts of *L. casei* and *B. bifidum* were the highest in bioyoghurt samples made with YC-180. Microencapsulation of *L. casei* and *B. bifidum* enhanced their viability and this technique can be used with normal yoghurt starter. Also, utilization of heat shock yoghurt starter enhanced the viability of probiotics.

Keywords: Probiotic; Bioyoghurt; Growth Behaviour.**83. The Influence of Fat Globule Membrane Material on the Microstructure of Low-Fat Cheddar Cheese**

Ehab Ali Romeih, Kim Marius Moe and Siv Skeie

Int Dairy J, 26: 66-72 (2012) IF: 2.401

The microstructural characteristics of low-fat Cheddar cheese differing in the content of milk fat globule membrane (MFGM) material achieved by addition of either buttermilk powder (BMP) or skim-milk powder (SMP) to the cheese milk were investigated. Scanning electron microscopy (SEM) and confocal scanning laser microscopy (CSLM) were used to study the cheese structure and the distribution of the starter culture and fat globules. Variations in the microstructure were observed relating to the MFGM content. The structure of the control cheese (SMP) was more irregular with inhomogeneous large voids. Whereas, cheese with BMP had a homogeneous protein network with small voids, showing a smoother, more compact and less coarse structure accompanied by more pronounced fat globules that were uniformly scattered throughout the protein matrix. The starter bacteria were located within the protein networks in clusters which were distributed homogeneously throughout the cheese matrix regardless of treatment.

Keywords: Cheddar Cheese; Buttermilk; Scanning Electron Microscopy.**84. Changes in Composition of Colostrum of Egyptian Buffaloes and Holstein Cows**

Alaa M Abd El -Fattah, Fawzia HR Abd Rabo, Samia M EL-Dieb and Hany A El-Kashef

Bmc Veterinary Research, 8: 1-7 (2012) IF: 2

Changes in colostrum composition of Egyptian buffaloes and Holstein cows collected at calving, 6, 12, 24, 48, 72, 96, 120 h and after 14 days of parturition were studied. Total solids, total protein, whey proteins, fat, lactose and ash contents were determined. Macro- and micro-elements, IgG, IgM, IGF-1,

lactoferrin and vitamins (A and E) were also estimated. Results: At calving, the total protein and whey proteins concentration did not differ between buffalo and cow colostrum, while total solids, fat, lactose and ash concentrations were higher in buffalo than in cow colostrum.

All components decreased gradually as the transition period advanced except lactose which conversely increased. On the fifth day post-partum, concentration of total protein, whey proteins, fat, ash and total solids decreased by 69.39, 91.53, 36.91, 45.58 and 43.85% for buffalo and by 75.99, 94.12, 53.36, 33.59 and 52.26% for cow colostrum.

However, lactose concentration increased by 42.45% for buffalo and 57.39% for cow colostrum. The macro-and micro-elements concentration of both colostrums tended to decline slightly toward normality on the fifth day of parturition. Buffalo colostrum had a higher concentration of vitamin E than cow colostrum during the experimental period.

At calving, the concentration of vitamin A in buffalo colostrum was found to be approximately 1.50 times lower than in cow colostrum. The concentrations of IgG, IgM, IGF-1 and lactoferrin decreased by 97.90, 97.50, 96.25 and 96.70% for buffalo and 76.96, 74.92, 76.00 and 77.44% for cow colostrum, respectively after five days of parturition. Conclusions: There is a dramatic change in buffalo and cow colostrum composition from the first milking until the fifth day of parturition. There are differences between buffalo and cow colostrum composition during the five days after calving. The composition of both colostrums approaches to those of normal milk within five days after parturition.

Keywords: Colostrum; Egyptian Buffaloes; Holstein Cows.**85. The Changes in Uht Milk Properties During Storage**

Samia Mahmoud El-Dieb, Mohamed Mohamed Metwally and Alaa Mohamed Abd El-Fattah

Book Published by Lambert Academic Publishing, 60 page (2012)

Different heat treatments are given to raw milk in order to destroy pathogenic organisms, increase the shelf life, help subsequent processing, e.g. warming before separation and homogenization or prepare milk for cheese making, yoghurt manufacture and production of evaporated and dried milk products (1). Ultra-high temperature (UHT) process is a method of milk preservation.

UHT process should reduce both the bacterial and enzymes content of the product to a commercially acceptable level that will ensure consumer safety and extending shelf life of milk. However, during this heat treatment as well as storage, number of changes undergo in chemical, physical and microbiological characteristics of the product.

These changes may render the product unacceptable because of the development of off-flavor and color or gelation. Milk in the UHT-treatment is exposed to a heat treatment of 130-149°C for 2-4 sec either in the indirect or direct heating method. Both processes differ in the heat treatment / time curve and for O₂ left in the product. Continuous UHT processes used commercially are summarized in Fig. (1). Changes in the UHT milk could be divided to: A: changes occurring during the heat treatment itself; B: changes developed on storage.

Dept. of Economic Entomology and Insecticides

86. Susceptibility of Different Life Stages of Sawtoothed Grain Beetle *Oryzaephilus Surinamensis* (L) (Coleoptera: Silvanidae) to Modified Atmospheres Enriched with Carbon Dioxide

Mohamed Y. Hashem, Sayeda S. Ahmed, Mohsen A. El-Mohandes and Mahrous A. Gharib

Journal of Stored Products Research, 48: 46-51 (2012)
IF: 1.414

The susceptibility of the different life stages of the saw-toothed grain beetle *Oryzaephilus surinamensis* to different modified atmospheres (MAs) containing various concentrations of carbon dioxide (CO₂) was studied as an alternative to methyl bromide fumigation at 30C and 65±5% relative humidity (r.h.).

The tested MAs were 55%, 65%, 75% and 85% CO₂ gas in the air. Mortality (%) was recorded after exposure periods of 3, 6, 12, 24, 48, 72 and 96 h. Larvae and adults were more susceptible while eggs and pupae were more tolerant to CO₂. A two-day exposure period was adequate to completely kill larvae and adults under all tested MAs. All eggs and pupae were killed after four days of exposure to the high-CO₂ atmospheres (75% and 85%).

Keywords: Control; Carbon Dioxide; Modified Atmospheres; *Oryzaephilus Surinamensis*.

87. Susceptibility of Different Life Stages of Indian Meal Moth *Plodia interpunctella* (Hübner) and Almond Moth *Ephestia cautella* (Walker) (Lepidoptera: Pyralidae) to Modified Atmospheres Enriched with Carbon Dioxide

Sayeda S. Ahmed and Mohamed Y. Hashem

Journal of Stored Products Research, 51: 49-55 (2012)
IF: 1.414

The susceptibility of the different life stages of the Indian meal moth *Plodia interpunctella* and almond moth *Ephestia (Cadra) cautella* to different modified atmospheres (MAs) containing various concentrations of carbon dioxide (CO₂) was studied as an alternative to methyl bromide fumigation at 27C and 60±5% relative humidity (r.h.).

The MAs tested were 40%, 60% and 80% CO₂ in air at different exposure times. Results showed that five days were adequate to kill all eggs and pupae of the two moths under all tested MAs. Exposure time needed to be extended to 6 and 7 days at 80% CO₂ to obtain complete mortality of larva of *E. cautella* and *P. interpunctella*, respectively.

The order of sensitivity of *P. interpunctella* to MAs was: egg = pupa > larva, while for *E. cautella* it was: pupa > egg > larva. Generally, eggs and pupae of *P. interpunctella* were more sensitive to MAs than those of *E. cautella* but the larvae of the latter were more sensitive.

Keywords: Control; Storage Moths; Egg; Larva; Pupa; Mortality; Toxicity.

88. The Effect of Modified Atmospheres, an Alternative to Methyl Bromide, on the Susceptibility of Immature Stages of Angoumois Grain Moth *Sitotroga Cerealella* (Olivier) (Lepidoptera: Gelechiidae)

Mohamed Y. Hashem, El-Sayed M. Risha, Samir I. El-Sherif and Sayeda S. Ahmed

Journal of Stored Products Research, 50: 57-61 (2012) IF: 1.414

The Angoumois grain moth, *Sitotroga cerealella* is recognized as a common pest of grains world-wide. This investigation aimed at determining the most effective CO₂ concentration in air against the immature stages of the pest in laboratory tests. The sensitivity of newly-laid eggs (<24 h old), 4th instar larvae and 3-day-old pupae to 4 modified atmospheres (MAs) containing 30%, 45%, 65% and 75% CO₂ in air was investigated at 27C and exposure periods between 2 h and 264 h. The percentage mortality of the newly-laid eggs, as well as the reduction of adult emergence from 4th instar larvae and 3-day-old pupae tended to increase with the increase of CO₂ concentrations in air and exposure period. According to LT95 values, the order of sensitivity of the three developmental stages of *S. cerealella* to the four MAs tested was as follows: eggs > pupae > larvae.

Keywords: *Sitotroga Cerealella*; Modified Atmospheres; Carbon Dioxide; Cereal Grains.

89. Genetic Variability Among Some Quantitative Characters, Insecticidal Activity and Essential Oil Composition of two Egyptian and French Sweet Basil Varieties

Ottai, M.E.S, Sayeda S. Ahmed and Mona Magd El Din

Australian Journal of Basic and Applied Sciences, 6: 185-192 (2012)

Inbred seeds of Egyptian and French sweet basil *Ocimum basilicum* varieties were cultivated to test their variation among some phenotypic quantitative characters, insecticidal activity and essential oil composition. Six phenotypic quantitative characters were recorded and had high significant variation between the two varieties. According to c.v.% values, the two varieties had homogeneous plants.

The insecticidal activity of essential oil and four successive extracts, petroleum ether, chloroform, acetone and ethanol was monitored against adults of lesser grain borer *Rhizopertha dominica* Fabricus (Coleoptera: Bostrichidae). The values of LC and LT decreased with increasing of concentrations and times, respectively for all extracts in the two varieties. All French basil extracts appeared stronger effects than those of Egyptian basil. The essential oil and petroleum ether exhibited the higher insecticidal activity than the others.

The constituents of essential oils and their contents were different between the two basil varieties. The correlation of oil components with LT50 was negative in the two basil varieties. This confirms that the combined fractions will be more toxic than a single compound.

Keywords: Essential Oil Composition; Insecticidal Activity; *Ocimum Basilicum*; Quantitative Characters; *Rhizopertha. Dominica*.

90. First Record in Egypt of Two Thrips Species Infesting Cucumber Crop

A.S. Abd EL-Wahab, S. Salah, S. Elnagar and M.A.K. El-Sheikh

Academic Journal of Entomology, 5: 164-168 (2012)

Direct inspection of weekly leaf samples revealed that two thrips species *Chirothrips texanus* Andre and *Thrips palmi* Karny were detected for the first time in Egypt, in addition to *Thrips tabaci* Lindeman and *Frankliniella occidentalis* (Pergande). The highest number of thrips species was recorded in August plantations for *Thrips tabaci* (923 individuals/25 leaves) followed by *Ch. texanus* (679 individuals/25 leaves). *F. occidentalis* recorded the lowest number (368 individuals/25 leaves). The present finding updates

the list of thrips species in Egypt.

Keywords: *Chirothrips Texanus*; Cucumber; Thrips; *Thrips Palmi*.

91. Effect of three the rmal Factors onthe foraging Activity of the Ground Nesting Subterranean Termite *Anacanthotermes Ochraceus* (Burmeister) (Isoptera: Hodotermitidae) at Fayoum Governorate Egypt

S I El-Sherif and N A Abd El-latif

Research Journal of Agricultural Sciences, 3: 804-809 (2012)

The current study investigates the statistical relationships between the foraging activities of *A. ochraceus* and 3 thermal factors in 2 years at Fayoum Governorate, Egypt. The results revealed that the direct effect of thermal factors on soil translocation varied from one year to another. In 1st year, AT reflected the strongest effect followed by ST20 then ST10 while in 2nd year ST20 was the most effective thermal factor followed by ST10 then AT. The direct influence of the 3 factors on soil translocation was considerably stronger during 1st year than 2nd year. The true effect of tested thermal factors on both food consumption and soil translocation, as revealed by partial regressions, was statistically insignificant during both years of investigation except for ST20 during the 2nd year only where that effect was significantly positive. In general, the effect of tested thermal factors on food consumption and soil translocation was rather stronger during 2nd than 1st year. However, the 3 thermal factors simultaneously expressed a highly significant true effect on food consumption during the 1st year with 82% explained variance while during the 2nd year this effect was significant, but relatively less, with 64% explained variance. In both years of investigation, the simultaneous effect of the 3 thermal factors on soil translocation was highly significant with explained variance percentages of 85.6% for 1st year and 77.5% for 2nd year. Partial regression values indicated that the influence of the 3 tested thermal factors was generally markedly stronger on soil translocation than on food consumption. The influence of tested thermal factors on food consumption was the strongest in the case of ST20 followed by ST10 then AT while for soil translocation, ST20 induced the strongest effect followed by AT then ST10.

Keywords: *Anacanthotermes Ochraceus*; Soil Temperature; Air Temperature; Foraging Activity; Ground Nesting.

92. New Quality Assured Educational Programs for Post Graduate Studies in Economic Entomology in Egypt

Samir-El-Sherif, S A Sayeda and A H Hanan

Research Journal of Agricultural Sciences, 3: 330-335 (2012)

The government of Egypt is highly concerned with raising awareness of educational quality assurance and accreditation among Egyptian academic institutes. In 2007, NAQAAE (The National Authority for Quality Assurance and Accreditation of Education) was established by a Presidential Decree. The main goals of NAQAAE are supporting Egyptian educational institutes by fostering their quality assurance practices through establishing an integrated system for accreditation, setting up educational standards and performance assessment indicators and supporting Egyptian educational institutions in their preparation of self assessment. In accordance with these goals, Egyptian educational institutions are strongly urged to revise and improve their educational programs to meet with the international standards for quality assurance and accreditation. The Department of Economic Entomology and Pesticides, Faculty of Agriculture, Cairo University pioneered in that direction and developed two new educational postgraduate programs for studies towards M. Sc. and Ph.D. degrees in economic entomology. Both programs were designed to meet with the international standards of quality assured education and the official bylaws related to postgraduate studies. The two programs have been reviewed by internal and external highly recognized scientists then submitted to NAQAAE for final approval and accreditation. For M. Sc. degree, the student is required to study 39 credit hours (1 credit hour = 1 theoretical hour or 2 practical hours) and submit and discuss a scientific thesis. For Ph. D. degree, the student is required to study 53 credit hours and submit and discuss a scientific thesis. M. Sc. and Ph. D. Students must score 400 and 450, respectively, in International Toefl, get ICDL and publish at least one scientific paper. Ph.D. students must also pass written and oral qualifying examinations.

Keywords: Educational Programs; Economic Entomology; Egypt.

93. Cutworm Pest Species in Egypt

S.I. El-Sherif and S.A. Abd El-Rahman

Ann. Entomol, 30: 41-46 (2012)

Cutworms from the Family Noctuidae and Order Lepidoptera are a group of polyphagous insect pests threatening the seedlings of many cultivated economically important plants. There is a noticeable discrepancy in the number of cutworm species in Egypt as 5 to 16 species had been reported in different references. Therefore, this investigation aimed at a precise survey of the currently occurring cutworm species in Egypt. Survey included cutworm larvae and pupae in many fields cultivated with a variety of crops in the different governorates throughout 2 successive years, as well as cutworm adult moths attracted to light traps operated at 3 ecologically different regions for 3 successive years. Larval and pupal surveys revealed the occurrence of only 4 species; *Agrotis ipsilon* (Hufn.), *Agrotis spinifera* (Hb.) (= *A. biconica* Hbn), *Agrotis segetum* Schiff. and *Noctua* (= *Agrotis*) *pronuba* L. The larvae and pupae of *A. ipsilon* were abundant all over the country, those of *A. spinifera* were of frequent occurrence, those of *A. segetum* were of

occasional presence while those of *N. pronuba* were rarely found. Meanwhile, light trap catches revealed the occurrence of the moths of 7 cutworm species; *Agrotis ipsilon*, *Agrotis spinifera*, *Agrotis segetum*, *Noctua pronuba*, *Agrotis trux* Huben., *Agrotis herzogii* Rebel and *Agrotis puta* Hubner. *A. ipsilon* was the most abundant species while *A. spinifera* was of frequent occurrence. *A. segetum*, *N. pronuba* and *A. trux* were of occasional occurrence. Both *A. herzogii* and *A. puta* were rare and very rare, respectively.

Keywords: Cutworm Species; Survey; Egypt.

94. Transmission Efficiency of Lettuce Mosaic Virus (Lmv) by Different Aphid Species and New Aphid Vectors in Egypt

A.S. Abd El-Wahab

Academic Journal of Entomology, 5 (3): 158-163 (2012)

Seven different aphid species (Homoptera: Aphididae) were recorded on lettuce crops cultivated in the field at Giza region, Egypt, throughout 2010/2011 growing season. The most abundant species was the green peach aphid, *Myzus persicae* (Sulzer). On the other hand, 14 different aphid species (winged forms) were recorded in the yellow pan-water traps. The most dominant two aphid species were *M. persicae* followed by the lettuce aphid *Hypomyzus lactucae* (Lin.), Lettuce mosaic virus (LMV) was isolated from naturally infected lettuce plants grown at Giza region, Egypt. Infected lettuce plants having syndromes including, mosaic, mottling, leaf distortion and stunting, were collected and the causative agent was identified according to: symptomatology, diagnostic hosts, serology (DAS-ELISA) and transmission tests (mechanical and aphids). LMV produced symptoms on 12 different diagnostic hosts: *Chenopodium quinoa*, *Chenopodium amaranticolor*, *Chenopodium murale*, *Chenopodium album*, *Lactuca sativa*, *Nicotiana tabacum*, *Nicotiana rustica*, *Datura innoxia*, *Gomphrina globosa*, *Sonchus oleraceae*, *Cichorium endivia* and *Spinacia oleracea*. Sixteen different aphid species were tested as vectors of LMV the most efficient vector was *Myzus persicae* (86%). Both *Acyrtosiphon lactucae* and *Acyrtosiphon kondi* recorded as vectors of LMV for the first time in Egypt.

Keywords: Aphid Vectors; Lettuce Mosaic Virus; Transmission; Efficiency.

95. Tropical Grasshopper Glutathione-S-transferase and Detoxification of Plant Allelochemicals in *Calotropis Procera*

G. Elsayed, Mohamed M. Ahmed, Samy M.H. Sayed and Sayed A.M. Amer

Archives of Phytopathology and Plant Protection, 45: 707-711 (2012)

Poecilocus bufonius inhabits Saudi Arabia and uses *Calotropis procera* as its main host plant. Cardenolids of this plant are used by this grasshopper as chemical defence against the natural enemies. The activity of enzyme detoxification in mid-gut wall for these allelochemicals has been determined in this study. Results indicate that the activity of glutathione-S-transferase (GST) was significantly higher after 24 hours of feeding on the main host plant but no difference has been found after one, two, four and five hours of feeding.

Keywords: Tropical Grasshopper; *C. Procera*; Glutathione; S; Transferase; Detoxification.

Dept. of Food Science and Technology

96. Chemical Composition and Antimicrobial Activity of Basil, Thyme, Sage and Clove Essential Oils and their Major Constituents

Shahinaz A. Helmy

International Journal of Advanced Research, 4: 124-137 (2012)

Investigation was carried out to recognize the chemical constituents of basil, thyme, sage and clove essential oils by GC/MS, beside, evaluate the in vitro antimicrobial activity of such oils and their major components as well, to utilize them as natural food preservatives. Results purported that the oil content recorded 0.63, 1.52, 2.23 and 12.73% (v/w, on dry wt. basis) from basil, thyme, sage and clove plants, respectively. The analysis of the chemical composition by GC/MS ascertained that the principal component of basil essential oil was methyl chavicol (78.22%). Meanwhile, the major components of thyme essential oil were thymol (46.21%), followed by cymene (17.12%) and terpinene (10.21%). On the other hand, thujone represented the dominant component in sage oil (41.12%), followed by camphor (12.34%) and 1,8-cineole (10.96%). The main components of clove oil were eugenol (71.88%), followed by eugenyl acetate (12.96%) and caryophyllene (5.92%). Antimicrobial screening of such essential oils by using Paper Disc Diffusion method purported that both thyme and clove essential oils exhibited markedly the strongest antimicrobial activity against all tested bacterial and fungal strains at all tested concentrations (5, 10 and 20 µL/disc), compared with gentamycin (an antibiotic, used as a positive control, at 20 µg/disc), at P0.05. Meanwhile, basil essential oil exhibited weak to moderate antimicrobial activity. Furthermore, *Staphylococcus aureus* ATCC 20231, *Bacillus subtilis* ATCC 3321, *Saccharomyces cerevisiae* NRRLY 2034 and *Candida lipolytica* NRRL 1095, were sensitive to sage essential oil. On the other hand, major components of our tested essential oils (methyl chavicol, thymol, carvacrol, eugenol, camphor, thujone, borneol and 1,8-cineole) were evaluated at 1, 1.5 and 2 µg/disc, for their antimicrobial potency compared with their neat oils. Results revealed that among all tested pure components, thymol and carvacrol possess the highest notable antimicrobial activity against all tested strains (but less than the inhibition zones of its neat oil, thyme), followed by eugenol (in a less efficiency than that of their neat oil, clove, sage and thyme). In general, Gram-positive bacterial strains were higher sensitivity to all tested essential oils as well as pure compounds, compared to the Gram-negative ones. Also, thujone and borneol showed a moderate antimicrobial potency, especially, against *Staphylococcus aureus* ATCC 20231 and *Bacillus subtilis* ATCC 3321. While, methyl chavicol was the weakest compound, compared with its neat oil (basil) and other components. In conclusion, the results confirmed the antimicrobial potency of the essential oils, which results from the combination effect of compounds which have synergistic effects with each others.

Keywords: Basil; Thyme; Sage; Clove; Chemical Constituents; Active Components; Antimicrobial Activity.

97. Extending the Shelf Life of Minced Beef Meat by Some Essential Oils Under Refrigeration and Freezing Storage

Shahinaz A. Helmy

International Journal of Advanced Research, 4: 14-24 (2012)

An investigation was carried out to explore the possibilities of utilizing essential oils; clove(CEO), thyme (TEO), sage (SEO) at 0.1% or their mixture (MEO) at 0.05% each as phytopreservatives of the minced beef meat (MBM) during storage at 4 C for 15 days and -18 C for 90 days to extend the shelf life. The evaluation criteria included pH value, TBA value, color, psychrophilic bacterial count and sensory attributes. Results ascertained that fresh MBM sample contained 65.21% moisture, 17.23% ether extract, 17.29% crude protein, 1.41% total ash and 0.28% crude fibers (fresh wt. basis).

The main constituents of CEO is eugenol(71.88%), followed by eugenyl acetate (12.96%), while-thujone is the dominant component in SEO. However, camphor and camphene were found to be the main components in TEO (32.11 and 16.33 %, respectively). The pH value of the control sample increased rapidly after 3 days of storage at 4C, where it reached 6.57 after 15 days (initial pH was 5.94). Although, pH value of samples treated with the tested essential oils slightly increased throughout the storage, these increments were not significant. Significant differences were noticed between the control samples and the other treatments.

Meanwhile, the increment rate was little in the treated samples stored at frozen temperature for 90 days, while the increment rate in the control sample was significantly higher. Considering the TBA value, results ascertained that lipid oxidation started to increase in the control MBM sample, after 3 days of storage at 4C and then increased rapidly throughout storage (15 days). Meanwhile, addition a mixture of the tested essential oils (MEO), or the individual essential oils to the MBM could retard the oxidative rancidity of the meat samples during storage with the superior effect of their mixture (synergistic effect). The findings also showed an antimicrobial potency of the tested essential oils as psychrophilic bacterial load significantly decreased (P 0.05) throughout the storage period at 4C and -18C, compared with the control sample.

On the other hand, color of samples was measured by Hunter lab color meter. Results purported that 'L' and 'b' values significantly decreased, while 'a' value increased in the control sample, during storage. Meanwhile, no significant differences were recorded in the samples treated with different essential oils during storage either at 4C or -18 C. Furthermore, sensory evaluation of the samples implied that MBM samples treated with a mixture of our tested essential oils recorded the highest scores of acceptability for all sensory criteria, followed by MBM samples treated by individual essential oils (CEO, TEO and SEO), where no significant differences could be recorded among these treatments, even after refrigeration storage at 4C for 15 days, or freezing storage at -18C for 90 days. Meanwhile, significant differences were recorded between these treatments and the control sample, which recorded the lowest overall acceptability.

Keywords: Essential Oils; Minced Meat; Refrigeration; Freezing Storage; Tba; Sensory Attributes; Shelf Life.

98. Microencapsulation of Peppermint Oil by Spray Drying

Suzan M. Ragheb, Aymen S. Yassin and Magdy A. Amin

Australian Journal of Basic And Applied Science, 66 307-317 2012)

Notable progress has been made in methods that encourage the use of polymerase chain reaction (PCR) as a rapid and accurate tool in microbiological testing of pharmaceuticals. In this study, the detection of the four main specified microorganisms according to the pharmacopeial recommendations, *Salmonella* spp, *Escherichia coli*, *Pseudomonas aeruginosa* and *Staphylococcus aureus*, was optimized in different pharmaceutical dosage forms and raw materials. Uniplex PCR was performed for the detection of each microorganism individually targeting the conserved region in each bacterial genome. Further optimizations were done to perform duplex and multiplex PCR assays considering relative concentrations of competitor primers used in the reaction. The uniplex PCR amplicons were successfully sequenced, confirming the conservation of used primers. Other validation parameters such as specificity, sensitivity and robustness were examined closely. The method provides a high-throughput screening method to test different pharmaceutical preparations for specified microorganisms for the detection of microbiological contamination.

Keywords: PCR; USP; Indicator pathogens; Nonsterile pharmaceuticals; Technology transfer.

Dept. of Genetics

99. The Involvement of Arabidopsis Glutathione Peroxidase 8 in the Suppression of Oxidative Damage in the Nucleus and Cytosol

Ahmed Gaber, Tomoya Ogata, Takanori Maruta, Kazuya Yoshimura, Masahiro Tamoi and Shigeru Shigeok

Plant Cell Physiol, 53: 1596-1606 (2012) IF: 4.702

A family of eight genes with homology to mammalian glutathione peroxidase (GPX) isoenzymes, designated AtGPX1–AtGPX8, has been identified in *Arabidopsis thaliana*. In this study we demonstrated the functional analysis of Arabidopsis AtGPX8 with peroxidase activity toward H₂O₂ and lipid hydroperoxides using thioredoxin as an electron donor. The transcript and protein levels of AtGPX8 in Arabidopsis were up-regulated coordinately in response to oxidative damage caused by high-light (HL) stress or treatment with paraquat (PQ). Furthermore, the knockout Arabidopsis mutants of AtGPX8 (KO-gpx8) exhibited increased sensitivity to oxidative damage caused by PQ treatment in root elongation compared with the wild-type plants. In contrast, transgenic lines overexpressing AtGPX8 (Ox-AtGPX8) were less sensitive to oxidative damage than the wild-type plants. The levels of oxidized proteins in the KO-gpx8 and Ox-AtGPX8 lines were enhanced and suppressed, respectively, compared with the wild-type plants under HL stress or PQ treatment. The fusion protein of AtGPX8 tagged with green fluorescent protein was localized in the cytosol and nucleus of onion epidermal cells. In addition, the AtGPX8 protein was detected in the cytosolic and nuclear fractions prepared from leaves of Arabidopsis plants using the AtGPX8 antibody. Oxidative DNA damage under treatment with PQ increased in the wild-type and KO-gpx8 plants, while it decreased in the Ox-

AtGPX8 plants. These results suggest that AtGPX8 plays an important role in the protection of cellular components including nuclear DNA against oxidative stress.

Keywords: Arabidopsis; Glutathione; Peroxidase; Oxidative Stress.

100. Embryonic Stem Cell-Derived Factors Inhibit T Effect or Activation and Induce T Regulatory Cells by Suppressing Pkc-H Activation

Kanishka Mohib, Bodour AlKhamees, Haggag S. Zein, David Allan and Lisheng Wang

Plos One, 7: 1-11 (2012) IF: 4.092

Embryonic stem cells (ESCs) possess immune privileged properties and have the capacity to modulate immune activation. However, the mechanisms by which ESCs inhibit immune activation remain mostly unknown. We have previously shown that ESC-derived factors block dendritic cell maturation, thereby indirectly affecting T cell activation. Here, we show that ESC-derived factors also directly affect T cell activation. We provide the first demonstration that ESC-derived factors significantly down-regulated the expressions of IL-2 and IFN- γ , while markedly up-regulating the expression of IL-10, TGF- β and Treg transcription factor Foxp3 in CD4⁺ CD25⁺ T cells. Furthermore, ESC-derived factors robustly suppressed T cell proliferation in response to the protein kinase C- δ (PKC- δ) activator phorbol 12-myristate 13-acetate (PMA). Western blot analysis indicated that ESC-derived factors prevented PKC- δ phosphorylation without influencing total PKC- δ levels. Moreover, I κ B- α degradation was abrogated, confirming absence of PKC- δ activity. The impact of ESC-derived factors on PKC- δ activation appeared to be specific since other upstream T cell signaling components were not affected. In conclusion, ESCs appear to directly impact T cell activation and polarization by negatively regulating the PKC- δ pathway.

Keywords: Embryonic Stem Cells; Dendritic Cell; Pkc-H Pathway.

101. Mouse Nkrp1-Clr Gene Cluster Sequence and Expression Analyses Reveal Conservation of Tissue-Specific Mhc Independent Immunosurveillance

Zhang Q, Rahim MM, Allan DS, Tu MM, Belanger S, Abou-Samra E, Ma J, Sekhon HS, Fairhead T, Zein HS, Carlyle JR, Anderson SK and Makrigiannis AP.

Plos One, 7:(2012) IF: 4.092

The Nkrp1 (Klrb1)-Clr (Clec2) genes encode a receptor-ligand system utilized by NK cells as an MHC-independent immunosurveillance strategy for innate immune responses. The related Ly49 family of MHC-I receptors displays extreme allelic polymorphism and haplotype plasticity. In contrast, previous BAC-mapping and aCGH studies in the mouse suggest the neighboring and related Nkrp1-Clr cluster is evolutionarily stable. To definitively compare the relative evolutionary rate of Nkrp1-Clr vs. Ly49 gene clusters, the Nkrp1-Clr gene clusters from two Ly49 haplotype-disparate inbred mouse strains, BALB/c and 129S6, were sequenced. Both Nkrp1-Clr gene cluster sequences are highly similar to the C57BL/6 reference sequence, displaying the same gene numbers and order, complete pseudogenes and gene fragments. The Nkrp1-

Clr clusters contain a strikingly dissimilar proportion of repetitive elements compared to the Ly49 clusters, suggesting that certain elements may be partly responsible for the highly disparate Ly49 vs. Nkrp1 evolutionary rate. Focused allelic polymorphisms were found within the Nkrp1b/d (Klrb1b), Nkrp1c (Klrb1c) and Clr-c (Clec2f) genes, suggestive of possible immune selection. Cell-type specific transcription of Nkrp1-Clr genes in a large panel of tissues/organs was determined. Clrb (Clec2d) and Clr-g (Clec2i) showed wide expression, while other Clr genes showed more tissue-specific expression patterns. In situ hybridization revealed specific expression of various members of the Clr family in leukocytes/hematopoietic cells of immune organs, various tissue-restricted epithelial cells (including intestinal, kidney tubular, lung and corneal progenitor epithelial cells), as well as myocytes. In summary, the Nkrp1-Clr gene cluster appears to evolve more slowly relative to the related Ly49 cluster and likely regulates innate immunosurveillance in a tissue-specific manner.

Keywords: Nkrp1; Clr; Natural Killer Cell; in Situ Hybridization; Genomic Sequencing.

102. Discrimination Capacity of Rapd, Issr and Ssr Markers and of the ir Effectiveness in Establishing Genetic Relationship and Diversity Among Egyptian and Saudi Wheat Cultivars

Salah El-Din El-Assal and Ahmed Gaber

American Journal of Applied Sciences, 9: 724-735 (2012)

Problem statement: Yield crop cultivars and landraces are valuable sources of genetic variations that the knowledge and implication of these variations are critical in the plant breeding programs. Our major objective of this study is investigating the discriminating capacity of RAPD, ISSR and SSR markers and of their effectiveness in establishing genetic relationship and diversity among Egyptian and Saudi wheat cultivars. Approach: Eleven wheat cultivars and landraces collected from Egypt and Saudi Arabia, five Egyptian wheat (Sakha 93, Sods 1, Sods 4, Gmiza 9 and Sohag 3) and six Saudi wheat landrace cultivars (Hmees, Al-Kaseem, Hegazi, Abo-Sakr, Dubai 1 and Nagran) were characterized using RAPD, ISSR and SSR molecular markers as efficient tools. Ten and nine oligonucleotide primers of RAPD and ISSR respectively and four primer pairs of SSR were used in wheat samples analysis. Only clear and repeatable band profile of 6 RAPD, 8 ISSR and 2 SSR primers were obtained. In RAPD analyses, 74 out of 141 bands (52%) were polymorphic. Results: The number of alleles ranged from 8-21 per primer, with an average of 14.1 per primer. In ISSR analyses, a total of 78 alleles were detected, along with 36 alleles (46%) were polymorphic. The number of alleles per primer ranged from 5-10 with an average of 8.6 alleles per ISSR primer. SSR reactions recorded 6 alleles, of which 5 alleles (83%) were polymorphic. Cluster analysis was conducted using Unweighted Pair Group Method that depends on Arithmetic Average (UPGMA). The dendrogram cluster diagram classified the evaluated genotypes in three major clusters corresponding to the cultivation regions. The first group contains Sakha 93, Sods 1 and Sods 4 with more than 80% Genetic Similarity (GS). The GS between Sakha 93 and Sods 1, Sakha 93 and Sods 4 or Sods 1 and Sods 4 were 83.6%, 83.9 and 85.4 respectively. The second group contains Gmiza 9 and Sohag 3 with GS 83.1%. The third group contains most of the Saudi landrace cultivars, Hmees, Al-Kaseem, Dubai 1, Abo-Sakr and Nagran, which are genetically

closed to each other with GS of 81%. The last Saudi wheat landrace cultivar, Hegazi, was falling outside the three major clusters, revealing around 78% similarity with the rest of the five Saudi landrace cultivars. Conclusion/Recommendations:

These analyses fit together with geographical distribution of the 11 wheat cultivars and landraces. Moreover, some morphological characterizations as fresh and dry or flowering time between the selected cultivars were analyzed under different salt concentration. We recognized differences in the fresh and dry weight between the selected cultivars. Wheat cultivars Sods 4 and Sohag 3 were the most sensitive cultivars to the salt treatment, while Sods 1 and Sakha 93 cultivars were less sensitive to the salt treatments. Additionally, Sods 4 and Sakha 93 cultivars were the earliest among the five wheat cultivars (flowering time 68.0 ± 5.04 and 71 ± 6.97 days respectively), while Sohag 3 and Gmiza 9 have flowered later than the other five cultivars (111 ± 12 and 105 ± 11.1) respectively. In conclusion, the long term objective of this study was to use these fingerprints to identify molecular markers that co-segregate and could be used in isolating gene(s) which controlling some important traits.

Keywords: Genetic Similarity (Gs); Random Amplified Polymorphic Dna (Rapid); Inter-Simple Sequence Repeat Polymorphic Dna (Issr); Simple Sequence Repeat (Ssr); Landrace Cultivars (Lcs).

103. A Cyanobacterium *Synechocystis* Sp. Pcc 6803 Glutaredoxin Gene (Slr1562) Protects *Escherichia Coli* Against Abiotic Stresses

Ahmed Gaber and Salah El-Din El-Assal

American Journal of Agricultural and Biological Sciences, 7: 88-96 (2012)

Problem statement: Glutaredoxins (GRXs) are ubiquitous small heat stable glutathione dependent oxidoreductase enzymes that play a crucial role in plant development and response to oxidative stress.

Approach: Cyanobacterium *Synechocystis* strain PCC 6803 contains two genes (slr1562 and ssr2061) encoding glutaredoxins. In the present investigation the slr1562 gene (grxC) was isolated and characterized.

Results: The results revealed that the amino acid sequence deduced from GrxC protein share high identity with those of GRXs from other organisms and contain the consensus GRX family domain with a CPFC active site. Northern blotting analysis revealed that the expression of slr1562 gene could be induced by oxidative and salt stresses. Moreover, the protein GrxC was successfully overexpressed as a soluble fraction in *Escherichia coli* JM109. The overexpression of GrxC in *Escherichia coli* cells significantly increased resistance of cells to oxidative, drought and salt stresses.

Conclusion/Recommendations: These results suggest that the slr1562 gene could play an important role in regulating abiotic tolerance against oxidative, drought and salt stresses in different organisms.

Keywords: Luria-Bertani (Lb); Different Stress Conditions; Glutaredoxins (Grxs); *Synechocystis* Pcc 6803; Slr1562; Recombinant Enzyme; Abiotic Stress.

Dept. of Horticulture Pomology

104. Effects of Some Dormancy Breaking Agents on Flowering, Fruiting and Fruit Characteristics of 'Canino' Apricot Cultivar

Ayman A. Hegazi

World Journal of Agricultural Sciences, 8: 169-173 (2012)

This study was carried out during two successive seasons (2009 and 2010) on nine year old Canino apricot trees (*Prunus armeniaca* L.) budded on Nemaguard peach rootstock growing in sandy soil at a private orchard, Noubaria, Behira Governorate, Egypt. The aim of this investigation is to study the effect of the following treatments: Urea at 5, 10 and 15%, zinc sulphate at 5, 10 and 15%, hydrogen cyanamide (H CN 49%) 2.2 at 1, 2 and 3% and control (sprayed with water), sprayed at four weeks before full bloom on flowering and harvesting time, flower and vegetative bud percentage, initial and final fruit set and fruit characteristics (fruit length, diameter, weight, volume, length/diameter ratio, seed weight, total soluble solids, firmness and fresh weight). From the obtained results, it was noticed that flowering and harvesting time were enhanced and earlier by treatments, flower and vegetative bud percentage were increased also initial and final fruit set were improved. Also, fruit characteristics were improved by spraying these chemicals while hydrogen cyanamide at 1, 2, 3% and zinc sulphate 10 and 15% were more effective than urea and control treatments.

Keywords: Apricot; Canino Cultivar; Urea; Zinc Sulphate; Hydrogen Cyanamide; Flower Buds; Vegetative Buds; Fruit Set; Fruit Characteristics.

105. Performance of 12 Introduced Olive Cultivars Under Egyptian Conditions

Ayman A. Hegazi

Research Journal of Agriculture And Biological Sciences, 8: 98-107 (2012)

Performance of 12 olive cvs. introduced to Egypt in 1984 (Thrombolia, Strogylia, Villalonga, Cerasicola, Dermlali, Leccio Dela Corna, Roseciola, Boutellian, Ouslati, Mouslati, Enduri and Tansh) included vegetative characteristics, floral biology, fruit set, fruit characteristics and oil percentage of these cvs. were investigated under Egyptian conditions, (Giza Governorate), for two seasons 2008 and 2009. Julian dates of full bloom (FB) in the first season showed that bud break of Tansh, Roseciola and Leccio Dela Corna cvs. were significantly late compared to other cvs. while, the earliest date was observed in Mouslati cv. Growing degree days (GDD) at FB was significantly higher in Mouslati cv. compared to other cvs. While it was significantly lower in Tansh cv. Leaves density was the highest in Boutellian cv., while it was the lowest in Ouslati and Villalonga cvs. There was no significant difference between average leaf area of Villalonga, Mouslati, Leccio Dela Corna, Ouslati, Cerasicola, Roseciola, Boutellian and Strogylia cvs, while it was the lowest in Enduri, Tansh, Dermlali and Thrombolia cvs. compared to other cvs. Flowering density was significantly higher in Enduri, Ouslati, Cerasicola and Villalonga cvs. than in other cvs. Number of perfect flowers/inflorescence was significantly higher in Dermlali cv. while it was the lowest in Leccio Dela Corna and Enduri cvs. Fruit set was the highest in Tansh, Ouslati and Leccio Dela Corna and it was the lowest in Thrombolia cv. Fruit length,

diameter, weight and flesh weight of Strogylia and Boutellian cvs. were the highest, while the lowest averages of previous characteristics were observed in Ouslati cv. Oil % of Leccio Dela Corna, Boutellian and Mouslati was the highest compared to other cvs, while the lowest oil % was observed in Cerasicola and Strogylia cvs. It could be concluded that, Leccio Dela Corna, Boutellian and Mouslati olives were superior in oil content. On the other hand, Strogylia and Boutellian were superior in fruit characteristics.

Keywords: Olive Cultivars; Performance; Vegetative Characteristics; Floral Biology; Fruit Set; Fruit Characteristics; Oil Percentage.

106. Resistance of Some Olive Cultivars to Verticillium Wilt

El Said S. Hegazi, Ayman A. Hegazi and Abdou M. Abd Allatif
Journal of Applied Sciences Research, 8: 2758-2765 (2012)

The current study was conducted on twelve olive cvs. to investigate the resistance to Verticillium wilt disease caused by Verticillium dahlia. One-year-old olive transplants were inoculated at green house with NET-5 isolate of V. dahliae during the period of October 2011 to March 2012. Resistance was evaluated by assessing symptom severity using (0 – 5) rating scale and the percentage of dead plants. Cultivars were classified into a defined category. Chlorosis was the most common disease symptoms appeared on the infected olive transplants, the chlorosis severity was determined in all the studied cultivars. Dolce cv. recorded the highest percentage of defoliation, while Picual cv. recorded the lowest percentage. The percentage of disease incidence recorded the highest percentage (83.33%) in Dolce cv, while Cairo 7 recorded the lowest percentage (27.78). Disease severity ranged from (2.50 to 0.48). Dolce cv. recorded the highest disease severity (2.50) followed by Eggizi and Coratina cvs. (1.43 and 1.07, respectively), while Frantoio and Cairo 7 cvs. recorded the lowest values (0.48 and 0.56, respectively). The percentage of dead plants ranged from (0 to 12.50%). Dolce cv. recorded the highest percentage of dead plants (12.50%) followed by Eggizi cv. (10.00%), while Frantoio, Arbequina, Verdal and Cairo 7 recorded the lowest.

Keywords: Olive; Verticillium Wilt; V. Dahliae; Disease Resistance.

107. Physiological Studies on Development Flower Bud In Vitro of 'Le Conte' Pear Trees

Taher A. Yehia, Ayman A. Hegazi, Malaka A. Saleh, Dorria M. Ahmed, Nagwa S. Zaied and Sayed A. Hassan

Middle-East Journal of Scientific Research, 12: 864-869 (2012)

Flower bud explants from Le Conte pear were cultured individually on MS medium supplemented with 0.1 mg/L 6-benzylaminopurine (BAP), 30 g/L sucrose and 7.0 g/L Difco Bacto agar. Different root pruning treatments (0.0, 30, 60 and 90 cm) from the trunk of mother plants during bud break and full bloom stages and Medium strength (Full, one-half and one-fourth) were tested. Data indicated that bud break stage surpassed full bloom stage in all parameters under study (shoot length, number of node, number of branch, explants development, fresh weight, number of leaves and greening). Moreover, using root pruning treatments (30 cm) was better than (0.0, 60 and 90 cm).

Also, one-half treatment enhanced the proliferation percentage and shoot number compared with the other treatments.

Keywords: Le Conte Pear; In Vitro; Medium Strength; Flower Bud; Root Pruning.

108. Safe Postharvest Treatments for Controlling Penicillium Molds and Its Impact Maintaining Navel Orange Fruits Quality

Sahar M. Abdel Wahab and Ismail A. S. Rashid

American-Eurasian J. Agric. & Environ. Sci., 12 (7): 973-982 (2012)

Postharvest diseases caused by Penicillium digitatum (green mold) and Penicillium italicum (blue mold) are the most important negative factors affecting market local and export of citrus fruits in Egypt. The effectiveness of postharvest treatments of 4% chitosan, 2% potassium sorbate (PS), or 2% potassium sorbate in wax to control green and blue molds decay and keeping quality were studied on Navel oranges during storage. Intact orange or orange artificially inoculated with Penicillium digitatum or Penicillium italicum, coated and stored up to 45 days at 5°C and relative humidity (RH) 90-95%. The results indicated that fruit rot and quality characteristics (weight loss and juice percentages, Total soluble solids (TSS), total acidity (TA), firmness, vitamin C content) were affected positively by application of the antifungal coatings. Antifungal coatings significantly reduced incidence and severity of both green (GM) and blue (BM) molds. Coating fruits decreased decay, weight loss and delayed changes loss in the firmness, acidity, ascorbic acid, juice percentage and total soluble solids concentration compared with control fruits. The study suggests that coating might be a promising candidate for controlling decay, maintaining navel orange quality and extending its postharvest marketing life.

Keywords: Navel Orange Chitosan; Wax Potassium Sorbate Quality Postharvest Decay; Green Mold; Blue Mold.

109. Effect of Humic Acid and Amino Acids on Pomegranate Trees Under Deficit Irrigation. I: Growth, Flowering and Fruiting

Magda M. Khattab, Ayman E. Shaban, Arafa H. El-Shrief and Ahmed S. El-Deen Mohamed

Journal of Horticultural Science and Ornamental Plants, 4: 253-259 (2012)

This experiment was carried out during 2007 and 2008 seasons on 20 years old pomegranate trees of Manfalouty cultivar. Trees under investigation were grown in a sandy soil at El-Kassasien Research Station, Ismailia Governorate. The trees received humic acid (32- 48 gm / tree/season) or amino acids (8- 16 gm/ tree/season) incorporated with irrigation levels 7 and 9 m³/tree/year in comparison to farm control (11 m³). The results showed that, shoot length, number of leaves per shoot, leaf area, number of flowers per shoot, fruit set percentage, fruit retention percentage, number of fruits per tree and yield (kg/tree) significantly increased by increasing water level from 7 and 9 to 11 m³. On the other side increasing irrigation water amount from 7 and 9 to 11 m³ decreased fruit drop percentage significantly. Increasing humic acid doses from 32 to 48 g and amino acids from 8 to 16 g/tree enhanced vegetative growth and fruiting. When the lower water levels 7 or 9 m³/tree/ season were supplemented by

the higher doses of either humic acid (48g) or amino acids (16g) all studied parameters were improved.

Keywords: Pomegranate; Irrigation; Humic Acid; Amino Acids; Growth; Flowering; Fruiting.

110. Effect of Gibberellic Acid Spraying on Alternate Bearing of Olive Trees

Abd El-Naby, S.K.M.; M.R.El-Sonbaty; E.S. Hegazi; M.M. Samira and T.F. El-Sharony

Journal of Applied Sciences Research, 8(10): 5114-5123 (2012)

The present study was carried out for three successive seasons 2008/2009, 2009/2010 and 2010/2011 on fifteen years old of olive trees cv. Picual to reduce the degree of alternate bearing of olive through spraying gibberellic acid (GA) on first or mid of December or on first or mid of January at concentrations, 0, 25, 50 and 75 ppm.

The results showed that, spraying the olive trees with GA3 at 75 ppm on first December impact on reducing the density of flowering, fruit set, decreased the yield of 2009 season as compared with most GA concentrations, while control gave the highest yield.

On the contrary, in 2010 season GA at 75 ppm on first December gave the highest yield, while control gave the lowest yield. In 2011 season, the control gave the highest yield while the lowest yield was observed when trees were sprayed with GA at 75 ppm at mid January. Spraying the olive trees with GA3 at 75 ppm on first December reduced the alternate bearing index (ABI) in comparison with other GA concentrations in different times. Spraying the olive trees with GA3 at 75 ppm on first December led to an increase in vegetative growth and to improve in fruit characteristics and increase the oil percentage.

Keywords: Alternate Bearing; Flowering; Fruit Set; Fruit Characteristics; Gibberellic Acid (Ga3); Oil Content; Olive; Vegetative Growth; Yield.

111. Effect of Increasing Fertilization Levels on Alternate Bearing of Olive Cv. "Picual"

El-Sonbaty, M.R., S.K.M. Abd El-Naby, E.S. Hegazi, M.M. Samira and T.F. El-Sharony

Australian Journal of Basic And Applied Sciences, 6 (10): 608-614 (2012)

The present study was carried out for three successive seasons 2008/2009, 2009/2010 and 2010/2011 on fifteen years old of olive trees cv. Picual to reduce the degree of alternate bearing through fertilization by NPK over than the rates recommended by the Ministry of Agriculture and Lands Reclamation.

The obtained results showed that, fertilizing olive trees with 50% over NPK recommended doses in heavy crop year "on year" had a positive effect on improving the vegetative growth and increase yield in application year and the next year and reduce the degree of alternate bearing and improves fruit characteristics and oil content. alternate bearing fruit characteristics.

Keywords: Alternate Bearing; Fruit Characteristics; Npk Fertilization; Oil Content; Olive; Vegetative Growth; Yield.

112. The Relationship Between the Histological Features in the Grafting Areas and the Compatibility Degrees of Some Mango Cultivars Onto Nucellar Seedlings

Omima A. Kilany, M.H. Abd El-Zaher and H.H. Hamed

Journal of Horticultural Science and Ornamental Plants, 4: 58-65 (2012)

These studies were carried out during the period from 2010 to 2011 at the nursery and laboratory of Pomology department, Faculty of Agriculture, Cairo University at Giza. Two experiments with two rootstock ages (21 days and 9 months) were conducted to classify their grafts, according to their compatibility between the scions and the rootstocks (degree of their anatomical connection) as following:

The first experiment: Mango Keitt, Alphonso and Ewais were saddle grafted onto 21 days old of Zebda and Sukkary seedlings and top-cleft grafted onto 9 months old of the same rootstocks. Also, each of the rootstock was grafted on the other one. The obtained results of first experiment indicated that, there are two degrees of anatomical connection at both ages of the two rootstocks. 1- The rootstocks of 21 days age: a- High compatibility grafts: These included the grafts of Sukkary/Sukkary (S.), Keitt (K.)/Sukkary, Alphonso (Al.)/Sukkary, Zebda/Zebda (Z.), Keitt/Zebda and Alphonso/Zebda. B - Moderate compatibility grafts: These included the grafts of S./Z., Z./S., E./S. and E./Z.. 2-

The rootstocks of 9 months age: a- High compatibility grafts: These included the grafts of S./S., K./S., Al./S., Z./S., E./S.. b- The moderate compatibility grafts: These included the grafts of K./Z., Al./Z., S./Z. and E./Z.. Meanwhile, in the second experiment: Mango Keitt scion was top-cleft grafted onto compound rootstocks Keitt/Sukkary, Alphonso/Sukkary, Keitt/Zebda and Alphonso/Zebda.

The results of second experiment indicated that, there are two degrees of anatomical connection at both ages of the ground rootstock: 1- The rootstocks of 21 days old: a- High compatibility grafts: These included the grafts of K./K./S., K./Al./S. and K./K./Z.. b- The moderate compatibility grafts: These included the grafts of K./Z., Al./Z.. 2- The rootstocks of 9 months age: a- High compatibility grafts: These included the grafts of K./K./S., K./K./Z., K./Al./S. and K./Al./Z.. b-

The moderate compatibility grafts: This was not noticed in the experimental graft. The histological features of the studies cross section illustrated that necrotic layers, which are scattered and get browning because of enzymatic reactions, characterized all successful graft union regions. Different intensities of an regular disposition uniformly callus tissues were originated from parenchymatic cells of xylem ray of both scion and rootstock, this callus fill the spaces (gaps) between the rootstocks and the scions; and finally, the vascular connection (mechanically strong graft union) form without apparent disruption of the necrotic layer, these new vessels originated by some meristematic cells in the callus. On the contrary, the lower successful grafts exhibited other histological features at the graft union region, where forming the collapsed cells, necrotic layer of dead cells, numerous free callus positions and separation zones overall grafting margins. These bad structures lead to separate the graft partners.

Keywords: Mango; Rootstocks; Interstocks; Scions; Histology; Grafting Area; Compatibility.

113. Molecular Characterization of Local and Imported Olive Cultivars Grown in Egypt using Issr Technique

El Saied S. Hegazi, Ayman A. Hegazi, Ahmed A. Tawfik and Hossam A. Sayed

Journal of Horticultural Science and Ornamental Plants 4, 2: 148-154 (2012)

Olive *Olea europaea* L. is one of the most economically important crops in the Mediterranean area and known for having large genetic variability. Consequently, genetic variation among 22 olive cultivars (Twelve local cultivars grown in Egypt and ten foreign cultivars) was assessed using inter-simple sequence repeats (ISSRs) markers. Ten (ISSRs) primers amplified 71 fragments of which 38 were polymorphic. The number of polymorphic bands per primer varied from 4 to 10 with 7.1 bands per primer on average. Genetic similarities were calculated using the Jaccard similarity coefficient. The resulting similarity matrix was subjected to the UPGMA clustering method for dendrogram construction and cultivar differentiation. Our results indicate that ISSR can be useful for genetic diversity studies, to provide practical information for parental selection and to assist breeding and conservation strategies. Also, the present results along with those of other researchers show that ISSRs can be used for cultivar differentiation in *Olea europaea* L.

Keywords: Olive *Olea europaea* L.; Genetic Diversity Issr Marker.

114. Effect of Some Soil Conditioners and Organic Fertilizers on Vegetative Growth and Quality of Crimson Seedless Grapevines

M.A. Gawad Shaheen, Sahar M. Abdel-Wahab, Emad A. Hassan and Adel M.R.A. AbdelAziz

Journal of Horticultural Science and Ornamental Plants, 4: 260-266 (2012)

This experiment was carried out during the two successive seasons of 2009 and 2010 on six years old Crimson seedless grapevines cultivar grown in a private orchard at Behaira Governorate. Two different compost types, plant residues (compost A) and plant + animal residues (compost B) at rates 3.26, 4.19 and 5.13 ton/fed., (equal 7.9 and 11 kg compost/vine) with two natural rocks, rock phosphate and feldspar at rates of 0.250 and 0.500 kg/vine respectively. All used treatments were applied with or without NPK biofertilizers and humic acid. Results clearly showed that the vegetative growth for treatments received compost (B) at rate of 11 kg compost (35 g N), 0.250 rock phosphate and 0.500 kg feldspar/ vine, in presence of biofertilizers NPK and humic acid gave the highest values for main shoot length, leaf area, cane thickness and leaf nutrient content (N, P and K). At harvest, the same treatment gave a significant differences for fruit yield per vine, number of cluster, cluster weight as well as chemical properties of fruit, i.e. T.S.S., total acidity and total sugars content as compared to mineral fertilizers (control) and received recommended doses of mineral NPK fertilizers. Therefore, these organic and neutral fertilizers in combination with NPK biofertilizers and humic acid can be recommended for Crimson grapevine to improve productivity and quality and produce a healthy product.

Keywords: Grapevines; Crimson Seedless; Organic Compost Biofertilizers; Humic Natural Rocks.

Dept. of Ornamental Horticulture

115. Growth, Chemical Constituents and Histological Structure Responses of Schinus Terebinthifolius Raddi Seedlings as Affected by Irrigation Rates, Periods and Treated Wastewater

Mohamed S. Hanafy, Amira F.Y. El-Kady and Doaa A.H. Korym

World Journal Of Agricultural Sciences, 8(5): 485-505 (2012)

Treated wastewater is being considered a highly valued water source for irrigation. A pot experiment was conducted to assess the impact of using municipal wastewater for irrigating *Schinus terebinthifolius* Raddi seedlings by evaluating its growth, chemical constituents and histological structure responses as affected by irrigation rates, periods and treated wastewater types. The study was carried out during seasons of 2009/2010 and 2010/2011 at the nursery of the Ornamental Horticulture Department, Faculty of Agriculture, Cairo University, Egypt. The seedlings were irrigated with potable tap water (control) and three treated wastewater types (primary, aeration and secondary) at two rates (75 and 100% field capacity (F.C.)) and the data was collected after four, eight and twelve months from the beginning of the experiment. Growth traits (seedling height and leaves and main roots number) and chemical constituents (total nitrogen (N), phosphorus (P), potassium (K), copper (Cu), zinc (Zn), manganese (Mn), iron (Fe) and total carbohydrates) were measured. Histological structure (lamina and midrib thicknesses, length and width of midrib main vascular bundles and number of oil glands) was also conducted. The irrigation with wastewater performed best under all irrigation rates and periods as compared to the control. Increasing irrigation rates from 75 to 100% F.C. as well as prolonging the irrigation periods from 4, 8 to 12 months caused a progressive increase in all the studied traits. Primary wastewater surpassed aeration and secondary wastewater. Moreover, the interaction of the three factors proved that primary wastewater treatment at the rate of 100% F.C. over a period of 12 months was superior to all other treatments. The data revealed that usage of treated municipal wastewater under different irrigation rates over different periods proved to be an economic way to dispose wastewater and a promising solution for plantation.

Keywords: Wastewater Types; Irrigation Rates; Irrigation Periods; *Schinus Terebinthifolius*; Growth Characters; Nutrient Contents; Histological Structure.

Dept. of Plant Pathology

116. Using Virulence Genes *HrpB*, *Egl* and *Flic* in Differentiation Between Virulent and Avirulent Isolates of *Ralstonia Solanacearum*, the Causal Agent of Potato Brown Rot

M. S. Mikhail, Maggie E. Mohamed, A. I. Abdel-Alim and Mary M. Youssef

Afr J Microbiol Res, 6: 225-235 (2012) IF: 0.528

To characterize the genetic variation between virulent and avirulent isolates of *Ralstonia solanacearum* race 3 (biovar II), the

causal agent of potato brown rot. Nine isolates of *R. solanacearum* recovered from the natural habitats (potato tubers, weeds, soil and water) were used. Six virulent and three avirulent isolates were characterized in terms of pathogenicity and molecular level using PCR technique with specific primers targeting three-virulence related genes located on the megaplasmid which was involved directly or indirectly in the disease process. Both virulent and avirulent forms of *R. solanacearum* were pathogenic to potato plants causing different symptoms. The two forms of the pathogen were containing the megaplasmid which carry three genes *hrpB*, *egl* and *fliC*. Detection and digestion of the amplification PCR of the three genes by two restriction endonuclease enzymes *EcoRI* and *DraI* showed differences between the two forms of *R. solanacearum*, whereas digested *egl* gene by the *DraI* enzyme gave two bands with all virulent isolates, while it gave only one band with the avirulent isolates. On the other hand, there were no differences in bands with the two genes *hrpB* and *fliC*.

Keywords: *Ralstonia Solanacearum*; Virulent; Avirulent; Pathogenicity; Potato; Pcr; Megaplasmid; Restriction Enzymes.

Dept. of Soil Sciences

117. Sustainable Multivariate Analysis for Land use Management in El-Sharkiya, Egypt

W. A. Abdel Kawy and Kh. M. Darwish

Arabian Journal of Geosciences, 9: (2012) IF: 1.14

In Egypt, major sustainability variables could be identified as scarce of soil and water resources, environmental degradation, rapid population growth, institutional arrangement that includes land tenure and farm fragmentation, agricultural administration, lack of infrastructure and credit utilization.

The main objective of the current work is to evaluate the sustainable land use management (SLM) model through biophysics and socioeconomic elements for the purpose of combating sustainability constraints that preclude the agricultural development geospatially.

In this research, from the geomorphologic point of view, the obtained results showed three main landscapes. They were identified in the study area as: fluviolacustrine plain, Aeolian deposits and flood plain. The study area was dominated by some physical and chemical degradation processes with different scales breaking down the equilibrium of soil stability. The SLM model was implemented and assessed from multivariate perspective points of productivity, security, protection, economic viability and social acceptability. Four SLM classes were outlined as follows: class I, land management practices that did meet sustainability requirements with a score 0.65, which represented 31.0 % of the considered agricultural study area; class II, land management practices that were marginally above the sustainability threshold and represented 12.6 %; class III, land management practices that were slightly below the threshold of sustainability and represented 8.60 %; class IV, land management practices that did not meet sustainability requirements with index values >0.1 that represented 47.86 %. As a general conclusion, it is found that land management practices tend to be unsustainable in the area under investigation for certain constraints that play motivated roles in lowering the targeted land sustainability.

Keywords: Multicriteria Decision Analysis; Sustainable Land Management (Slm); Socioeconomic Evaluation El-Sharkiya Governorate.

118. Assessing Crop Water Requirements on the Bases of Land Suitability of the Soils South El Farafra Oasis, Western Desert, Egypt

W. A. Abdel Kawy and Islam H. Abou El-Magd

Arabian Journal of Geosciences, (2012) IF: 1.14

The aims of this study are: (1) producing a geometrically corrected physiographic soil map scale 1:50,000 reduced to the attached map; (2) crop water requirements calculation for the suitable crops in this area. To fulfill the first aim, ten soil profiles were selected to represent the different mapping units. Morphological description was carried out and soil samples were collected for physical and chemical analysis. Based on the Enhanced Thematic Mapper Plus images and the geographic information system, coupled with the field work and laboratory analysis data, the physiographic soil map was produced. Satellite images interpretation indicated that the investigated area includes the main physiographic units are plateaus, hillland, mountain and depression floor. With respect to the second aim, the main land qualities of the different mapping units and the crop requirement were rated and matched to obtain the current and potential land suitability using Automated Land Evaluation system. The most suitable crops for the studied area were: clover, wheat, beans, sugar beet, onions, maize, sunflower, tomato, potato, groundnut, pea, lentil, barley, sesame and carrots. The crop water requirements for the selective crops were calculated using CROPWAT 8.0 for Windows program as: 781.80, 571.70, 383.20, 641.55, 395.45, 771.80, 693.90, 880.32, 432.00, 510.30, 205.05, 201.30, 284.20, 487.95 and 254.85 mm, respectively.

Keywords: Gis; Optimum Land Use; Consumptive Use . El Farafra Oasis.

119. Land Degradation Risk Assessment of El Fayoum Depression, Egypt

R. R. Ali and W. A. M. Abdel Kawy

Arabian Journal of Geosciences, (2012) IF: 1.14

The main objective of this study is to assess the land degradation risk of cultivated land in El Fayoum depression. The physiographic map of the depression was produced by using remote sensing and land surveying data. The depression comprises lacustrine plain, alluvial-lacustrine plain and alluvial plain representing 12.22%, 53.58% and 34.20% of the total area, respectively. The soil, climate and topographic characteristics of the depression were extracted from land surveying, laboratory analyses, digital elevation model and available reports. A simple model was designed to employ these data for assessing the chemical and physical risk of land degradation using Arc-GIS 9.2 software. The obtained results indicate that severe risk to chemical and physical degradation affect 54.15% and 29.23% of the depression, respectively. The current status of soil salinity, sodicity and water table indicate that most of lacustrine and alluvial-lacustrine soils are actually degraded by salinization, sodification and waterlogging. The results of degradation risk and the actual hazard indicate that the human activities are not sufficient to overcome the degradation processes in the most of the depression (80.22%). Moreover, a negative human impact affects 26.29% of the area mostly in the alluvial plain. Great efforts related to the land management are required to achieve the agriculture sustainability.

Keywords: Soil Degradation; Physiography; Remote Sensing; Gis; El Fayoum; Egypt.

120. Land Suitability Decision Support for Assessing Land use Changes in Areas West of Nile Delta, Egypt

Kh. M. Darwish and W. A. Abdel Kawy

Arabian Journal of Geosciences, (2012) IF: 1.14

The main objective of this study was to discuss the efficiency of agricultural land suitability for assessing land use types in rural areas. In this research, El-Nubaryia area west of Nile Delta was selected as a case study site, which considers one of the high priority regions for future development in Egypt. As input, a total of ten representative soil profiles and number of observations points were used for collecting soil samples. Based on the field survey, laboratory analysis and satellite image interpretation in cooperation with Geographic Information System GIS, the physiographic map was executed. Three main landscape units were identified as follow: Marine Deposits (M), Eolian Deposits (E) and River terraces (T). The soils were classified mainly as Typic Torripsamments; Typic Paleorthids and Typic Calciorthids. Land suitability assessment was done to define maps of the suitable areas for agricultural production using MicroLEIS micro-computer program and ALESarid-GIS system as well. According to the crop suitability results, the most suitable crops to grow in the study area were maize, melon, potato, sunflower, onion, garlic, olive and date palm in the order indicated. Generally, the data on land suitability resulting from the evaluation models indicated that 56.1% of the area is considered as suitable, 30.8% is moderately to marginally suitable and 13.1% is not suitable. The main limitation factors for land suitability are the excess of salts, shallow soil depth and inadequate drainage conditions. The output results are presented as georeferenced soil suitability maps using GIS utilities.

Keywords: Land Suitability; Decision Support for Assessing Land Use Changes.

121. Use of Satellite Data and Gis for Assessing the Agricultural Potentiality of the Soils South Farafra Oasis, Western Desert, Egypt

Kh. M. Darwish and W. A. Abdel Kawy

Arabian Journal of Geosciences, (2012) IF: 1.14

Overpopulation and food security are the main global problems alert decision makers. In developing countries, such problem put extra pressure for horizontal expansion for agricultural development. The rapid sprawl of urbanized areas on the alluvial land of the River Nile and delta to accommodate the population growth has encouraged governmental and private sector for agricultural expansion in the desert. Unless there are reliable information and accurate studies for land and soil suitability, there will be a collapse of such investment. To evaluate the potential suitability of soil for agriculture development in areas of the western desert, satellite images, geographic information and field survey including soil profiles and artesian water samples with laboratory analysis were integrated to classify the soils according their suitability for specific crop. The main land qualities of the different mapping units and the crop requirement were rated and matched to obtain the current and potential land suitability using

Automated Land Evaluation System "ALES". The study found that the main physiographic units are plateaus, hilland, mountain and depression floor. But there are three limiting parameters for land suitability which are the lack of nutrient elements, wind erosion vulnerability and soil texture. The study concluded that the best crops adapted with the soil conditions and could be feasible for economic use are:(1) native vegetation such as agol, sand trees, sammar, halfaa, bawaal, qordaob, bardi and qortom; (2) filed crops such asonion, garlic, watermelon and wheat; and (3) fruits such as olive and date palms.

Keywords: Land Suitability; Agriculture Potentiality; South Frafra Oasis; Gis; Remote Sensing.

122. Crop Water Requirements in Selective Wetland Areas, West Suez Canal, Egypt

W. A. Abdel Kawy, Abdel-Aziz Belal and Kh. M. Darwish

Journal of Agricultural Extension and Rural Development, 4: 11-18 (2012)

The present research aims to generate a geometrical corrected physiographic map with a scale (1:50,000) and calculating crop water requirements for the suitable crops in this area. To fulfill these requirements, eight soil profiles were chosen to represent the different mapping units. Morphological description was carried out and soil samples were collected for the physical and chemical analyses. Based on satellite ETM+ images of the area and the geographic information system integrated with field work and laboratory routine analyses data, the physiographic soil map was produced. In this study, two main landscape units were identified, named: Coastal plain (the Fluvio Marine deposits) and Young sub-deltaic deposits. Subsequently, the main land qualities of different mapping units with the corresponding crop requirement were rated and matched to obtain the current and potential land suitability using automated land evaluation system (ALES). In this study, it is found that the most suitable crops for the study area in regard to its crop water requirements were: Clover, wheat, beans, onion, maize, sunflower, tomato and potato.

Keywords: Soil Mapping; Water Requirements; West Suez Canal; East Delta.

123. Detecting Soil Productivity Changes and Degradation Processes in the Irrigated Agriculture Eastof the Nile Delta, Egypt

Rafat Ramadan Ali and Wael Ahmed Abd El Kawy

International Journal of Environmental Sciences, 1: 11-18 (2012)

This study aims to detect the changes of soil productivity and soil degradation processes in the irrigated agriculture east of the Nile Delta. The study area extends between longitudes 3120' and 32 15' E & latitudes 2954 ' and 3112 ' N. The main landforms of the area were delineated by using remote sensing and land surveying data. The recognized landforms include flood plain, fluvio-lacustrine and Aeolian deposits. A semi detailed survey was carried out in order to verify landform units and collecting soil samples. The historical data of the soils has been extracted from the available studies of the year 1975. Results indicate that the degradation processes are sweeping the investigated soils, where 69.73 % of the area has been degraded during the period of 1975 - 2011. The soil productivity was shifted from low to high grade only in 30.27 % of the total area. Soil Salinity, alkalinity,

water logging and compaction are the main degradation process prevail the area. The agriculture development in the area requires improved drainage network through governmental support and proper land management by farmers themselves.

Keywords: Remote Sensing; Landforms; Soil Productivity; Soil Degradation; East Nile Delta; Egypt.

124. Maize Yield as Influenced by Some Plowing Practices and Fertilization

H.A. Khaler, MM Kamel and T.I. Borham

American-Eurasian J. Agric. & Environ. Sci., 12: 664-668 (2012)

A field experiment was conducted for two consecutive years at El Nubaria station to study the effect of two plowing methods (chisel and moldboard) and fertilization on yield of maize crop and its irrigation water requirements under calcareous soil. The obtained data showed a significant effect of deep tillage on seed yield of maize. Highest yield was noted with moldboard plough compared to chisel plough. Also, seed yield of maize crop was influenced by the fertilizer treatments in both investigated seasons. Data indicated that seed yield of maize crop was increased with increasing the application rates of nitrogen, phosphorous and potassium in both seasons. Concerning, the water use efficiency (W.U.E), the highest value of W.U.E was obtained under the highest level of N fertilizers under using moldboard plow in the both seasons.

Keywords: Crop Water Requirements; Chisel And Moldboard; Maize Crop.

125. Effect of Different Sources and Rates of Some Organic Manure on Content of Some Heavy Metals in Different Soils and Plants Grown the rein: Ii. Effect on Corn Plants

Hala Kandil, M.I. El- Kherbawy, S. Ibrahim, A. Abd-Elfattah, M.R. Abd El-Moez and S.H. Badawy

Soil Forming Factors and Processes From The Temperate Zone, 11: 19-32 (2012)

This experiment was conducted to study the influence of different sources and rates of some organic manure on growth and heavy metals concentration in spinach plants grown on two different soils. The important results could be summarized in the following: Results show that values of dry weight (DW) of roots, shoots and total plant of corn grown on Abou-Rawash and El-Nobaria soils significantly increased by using all the organic manure sources (sewage sludge(SS), banana and cottoncomposts (BC and CC) and rates (11, 22 and 44 t/fed)) as compared with control treatment. There is no significant effect between all the used organic manures (SS, BC and CC) on dry weight production of roots, shoots and total plant of corn grown on Abou-Rawash sandy soil, but in El-Nobaria sandy calcareous soil, the SS and BC treatments significantly increased dry weight of roots, shoots and total plant of corn in comparison with those obtained by using CC treatment. Furthermore, there is no any significant effect between sewage sludge (SS) and (BC) on the production of the dry weight of different organs of corn plant grown on El-Nobaria soil. Dry weight of corn plants grown on both soils significantly increased by increasing the application rate from all the used organic manures up to 44 t/fed. The highest DW of corn plants grown on both soils were obtained by using BC and

rate of 44 t/fed, while the lowest values were attained by using CC and rate of 11 t/fed. All the organic manures (SS, BC and CC) led to more significantly increases in the concentration of Zn, Cu, Pb, Cd and Ni in both roots and shoots of corn plants grown on both soils as compared with control. The concentrations of Zn, Cu, Pb, Cd and Ni in corn plants grown on Abou-Rawash significantly increased when BC was applied as compared with CC. Moreover, there is no clear difference could be found between BC and CC used in sandy calcareous soil of El-Nobaria and the concentration of all the heavy metals in corn plants followed the order of SS > BC > CC in decreasing order. All the concentration of Zn, Cu, Pb, Cd and Ni in corn plants grown on both soils were within the normal range of heavy metals in plants and did not reach phytotoxic studies in the literature. Application of organic manures (SS, BC and CC) resulted in significantly increases of the extractable DTPA and the total metals of Zn, Cu, Pb, Cd and Ni in both used soils after corn plantation as compared with untreated control. Application of SS significantly increased both extractable and total heavy metals (Zn, Cu, Pb, Cd and Ni) in Abou-Rawash and El-Nobaria soils after plantation of corn as compared with CC and BC. Also, the addition of banana compost to Abou-Rawash and El-Nobaria soils significantly increased the extractable as well as the total heavy metals (Zn, Cu, Pb, Cd and Ni) after corn plantation when compared with addition of cotton compost. Generally, the highest values of extractable and total heavy metals in the two tested soils after corn plantation were attained by using sewage sludge (SS) following by BC and CC in decreasing order (SS > BC > CC). The values of extractable and total of content of heavy metals took the following order: Zn > Cu > Pb > Ni > Cd after corn plantation. The extractable heavy metals in Abou-Rawash sandy soil were higher than those obtained in El-Nobaria sandy calcareous soil under all the organic manure treatments and the tested soils. The obtained values of DTPA heavy metals in the used soils are in the normal range and less than tolerable levels of all studied heavy metals and could be used as the background level of the heavy metals in uncontaminated soil of Egypt.

Keywords: Banana Compost; Cotton Compost; Heavy Metals; Sewage Sludge; Corn Plant.

126. Effect of Different Sources and Rates of Some Organic Manure on Content of Some Heavy Metals in Different Soils and Plants Grown the rein: I. Effect on Spinach Plants

Hala Kandil; S. Ibrahim; M.I. El- Kherbawy, A. Abd-Elfattah; M.R. Abd El-Moez and S.H. Badawy

Soil Forming Factors and Processes from the Temperate Zone, 11: 9-18 (2012)

This experiment was conducted to study the influence of different sources and rates of some organic manure on growth and heavy metals concentration in spinach plants grown on two different soils. Results showed that values of dry weight (DW) of roots, shoots and total plant of spinach grown on Abou-Rawash and El-Nobaria soils significantly increased by using all the organic manure sources (sewage sludge(SS), banana and cottoncomposts (BC and CC)) and rates (11, 22 and 44 t/fed)) as compared with control treatment. The highest dry weight of roots, shoots and total spinach plants grown on both soils were obtained by using cottoncompost (CC) followed by banana compost (BC) and sewage sludge (SS) in decreasing order (CC > BC > SS). The obtained results revealed that DW of spinach plants grown on

sandy calcareous soil of El-Nobaria was higher under all the organic manure treatments than those obtained from sandy soil of Abou-Rawash. Moreover, dry weight of spinach plants grown on Abou-Rawash and El-Nobaria soils significantly increased by increasing the application rate from all the used organic manures up to 44 t/fed. Organic manures (SS, BC and CC) led to more significant increases in the concentration of Zn, Cu, Pb, Cd and Ni in both roots and shoots of spinach plants grown on Abou-Rawash and El-Nobaria soils as compared with control treatment. The concentration of Zn, Cu, Pb, Cd and Ni in roots and shoots of spinach plants grown on sandy and calcareous soils were higher when SS was applied to the tested soils in comparison with the addition of the other organic composts (BC and CC). The tested sources of organic manures could be arranged due to their inducing effect on Zn, Cu, Pb, Cd and Ni concentrations in roots and shoots of spinach plants grown on both soils in the following decreasing order: SS > CC > BC. The efficiency of studied materials on heavy metal concentrations was varied in accordance to sources and rates of application and / or the part of the grown plant. All the concentrations of Zn, Cu, Pb, Cd and Ni in spinach plants grown on Abou-Rawash and El-Nobaria soils were within the normal ranges of heavy metal in plants and did not reach the phytotoxic levels obtained in the literature. The highest values of extractable and total heavy metals in the two tested soils after spinach plantation were attained by using sewage sludge (SS) following by BC and CC in decreasing order (SS > BC > CC). The values of extractable and total of studied heavy metals in the used soils after spinach plantation follow the order: Zn > Cu > Pb > Ni > Cd. It could be concluded that all the obtained values of DTPA-heavy metals in the used soils are in the normal range and less than tolerable levels of all studied heavy metals and could be used as the background level of the heavy metals in uncontaminated soils of Egypt.

Keywords: Banana Compost; Cotton Compost; Heavy Metals; Sewage Sludge; Spinach Plant.

Dept. of Vegetable Crops

127. Cassia Oil for Controlling Plant and Human Pathogens on Fresh Strawberries

Mohamed M. El-Mogy and Beatrix W. Alsanii

Food Control, 28: 157-162 (2012) IF: 2.656

The inhibitory effects of cassia oil on the human pathogen *Escherichia coli* serotype O157:H7 and the plant pathogen *Botrytis cinerea* were tested in vitro at different concentrations (200e800 ppm). Cassia oil exhibited antibacterial and antifungal activity against both pathogens. Cassia oil at 400e800 ppm inhibited the growth of *E. coli* O157:H7 in vitro and on the surface of treated strawberries. Cassia oil also completely inhibited the growth of *B. cinerea* at 400e800 ppm. Spore germination and germ tube elongation of the pathogens in potato dextrose broth were strongly inhibited in the presence of 100 ppm cassia oil. Cassia oil at all concentrations reduced the percentage of decayed strawberries. Experiments on reducing the development of natural decay in strawberries gave similar results. None of the quality parameters tested (colour, total soluble solids, pH, total acidity and ascorbic acid) was affected by cassia oil treatment. Storage experiments on strawberry showed that the percentage weight loss was reduced by cassia oil treatment. Hence, cassia oil could be an alternative to synthetic chemicals for controlling

human and plant pathogens on fruits such as strawberries during postharvest and storage.

Keywords: *Escherichia coli*; Essential Oils; Grey Mould; Postharvest; Quality; Strawberry.

128. Propagation of Potato (*Solanum Tuberosum* L.) by Seedlings

M.A. El-Helaly

American-Eurasian J. Agric. and Environ. Sci., 12: 1117-1121 (2012)

This study was conducted at the Experimental Station of the Faculty of Agriculture Cairo University, Egypt during two winter seasons of 2008/2009 and 2009/2010 to investigate the potato propagation by seedlings compared to traditional method of potato planting (tuber seeds) on growth, tuber yield and some associated characters. The treatments consisted of the combination of two planting methods (tuber seeds and seedlings) with two planting dates (November 4 and December 4). No differences between means of planting methods or planting dates in stem length. Seedling in the second planting date had the lowest stem length, tuber numbers per plant, tuber yield and above ground dry weight. No statically differences between plants grown from seedlings and tuber seeds in first planting date and plants grown from tuber seeds in second planting date in tuber numbers. The method of tuber seeds had the highest tuber numbers per plant and no differences between planting dates in tuber numbers per plant. No statically differences between tuber seeds in second planting date and seedlings in the first planting date in tuber yield and harvest index.

Keywords: Potato (*Solanum Tuberosum* L.); Seedling; Tuber Seeds; Biological Yield -Harvest Index.

129. Influence of Aquaculture Effluent on Broccoli Yield and Quality

M.A. El-Helaly and Ashraf Suloma

Australian Journal of Basic And Applied Sciences, 6: 505-510 (2012)

This experiment was conducted at Fish Nutrition Laboratory of the Faculty of Agriculture, Cairo University, Giza Governorate during 2010/2011 and 2011/2012 seasons, to study the influence of Nile Tilapia (*Oreochromis niloticus* L.) aquaculture effluents as irrigation and fertilizer sources on broccoli yield and quality. Two types of tilapia aquaculture effluent production systems viz., Bio-floc and Intensive culture were used as irrigation water compared with mineral nutrient solution. Randomized Complete Block Design with three replications was used. Results showed that there were no significant differences between treatments in leaf area average and head dry matter percentage. Average head weight and harvest index were significantly affected by treatments on the two seasons, the highest head weight was recorded with the mineral nutrient solution. Meanwhile, no differences between Intensive culture and Bio-floc effluent in head weight average were detected. Hence, Intensive culture delayed ten days to harvest. The highest harvest index was recorded with the mineral nutrient solution followed by Bio-floc effluent. While, intensive culture had the lowest harvest index in the two seasons. It could be concluded that despite the superiority of the control (mineral nutrient solution) in head weight and

harvest index. However, the most important finding is fish effluent treatments had less nitrogen accumulation in head and this healthier and reduces fertilizer costs.

Keywords: Broccoli; Aquaculture Effluents; Bio;Floc; Intensive Culture; Harvest Index.

130. Effect of Some Pre- and Postharvest Treatments on Browning Inhibition in Fresh Cut Lettuce During Cold Storage

Shehata S.A. El-Sheikh, T.M Mohamed and M. El Saleh M.A.

Journal of Applied Sciences Research, 8: 25-33 (2012)

An experiment was carried out at the Agricultural Experiments and Researches Station, Faculty of Agriculture, Cairo University during the winter season of 2008/2009 and 2009/2010 seasons, to study the influence of foliar spray of citric acid at 1.0 and 2.0 g/L (0.1 and 0.2%), in addition to potassium sulfate at 2.5g/L (0.25%) [pre-harvest treatment] and evaluate the effect of dipping the lettuce cut stem of all the previous field experiment with dipping in citric acid at 5 g/ 0.1 L (5%) or coated by sugar syrup at 100% (post harvest treatment) and determine those which the prevention of butt discoloration (browning of the cut stem lettuce) and maintained quality during storage at 0°C and 95 % relative humidity (RH) for 12 days. Results indicated that spraying the lettuce plants with 2 g/L of citric acid + 2.5 gm/L of potassium sulfate reduced the weight loss percentage, total phenolic contents and inhibited polyphenol oxidase (PPO) activity and gave good appearance in their heads when compared with the control. Treating cut stem lettuce with citric acid at 5% or sugar syrup as postharvest treatments is the most effective for controlling the enzymatic of browning reaction and protected phenolic compounds from oxidation during storage. The best and beneficial results were obtained when spraying lettuce plants in the field with 2 g/L citric acid + 2.5 g/L potassium sulfate, in addition to, dipping their cut stem lettuce in sugar syrup 100% solution before storage. This completely inhibited browning on lettuce stem cutting (indicating by lower chroma value and higher hue angle), maintained quality and gave lettuce heads with good appearance for 12 days at 0°C and 95% RH.

Keywords: Lettuce; Pre and Post Harvest; Browning Inhibition; Cold Stage.

131. Response of Cucumber Plants to Foliar Application of Chitosan and Yeast Under Greenhouse Conditions

Said A. Shehata, Zakaria. F. Fawzy and Hassan R. El-Ramady

Australian Journal of Basic And Applied Sciences, 6 (4): 63-71 (2012)

The present study was carried out in two successive seasons of 2010 and 2011 to study the effect of foliar application of chitosan rates (1, 2, 3 and 4 mL⁻¹) and yeast rates (1, 2, 3 and 4 gL⁻¹) on growth, yield and quality as well as chemical constituents of cucumber plants. Results of this work showed that foliar application with yeast and chitosan increased significantly the vegetative growth, yield and its quality of cucumber. Meanwhile, foliar spraying with active dry yeast at rates of 4 g L⁻¹ recorded highest values of T.S.S., N (%), Fe, Zn, Cu and Mn (mg kg⁻¹) in cucumber fruits. However, foliar application of chitosan at rates of 4 mL⁻¹ gave highest contents of P and K % in the two seasons of

study. It can be concluded that foliar application with chitosan at rates of 4 mL⁻¹ recorded the best treatment to obtain the highest vegetative growth, yield and quality of cucumber plants.

Keywords: Cucumber (Cucumis Sativus L); Chitosan; Yeast; Foliar Application; Growth; Yield;

132. Influence of Planting Date on the Production and Quality of Onion Seeds

M.A. El-Helaly and S.S. Karam

Journal of Horticultural Science and Ornamental Plants, 4: 275-279 (2012)

A field experiment was conducted at Experiment Station of the Faculty of Agriculture, Cairo University, Giza Governorate during 2008/2009 and 2009/2010 seasons, to study the influence of planting date (15 November, 15 December and 15 January) on seed production of onion (*Allium cepa* L.) cv. Giza 20. Results of planting date showed significant effect for most of studied characters. The highest significant increases of scapes number/plant, scape diameter, main scape length, umbel diameter, seed yield /plant, seed yield /fed, weight of 1000-seeds and percentage of seed germination were resulted from planting on mid of November. Meanwhile the lowest significant values were recorded with delaying planting up to mid of January. On the other hand, sprouts number/plant was not affected by planting dates. It could be concluded that the favorable planting date to produce high seed yield with best quality is mid of November for Onion Giza 20 cultivars under Giza region.

Keywords: Onion % *Allium Cepa* L.; Planting Date; Seed Yield; Seed Germination.

133. Effect of Some Pre-Harvest Treatments on Onion Seeds Production Under Sandy Soil Conditions

Shehata S.A., Hashem M.Y., Ghada I. Mahmoud and Karima F. Abd El-Gawad

Journal Of Applied Sciences Research, 8: 763-769 (2012)

This study was conducted at the Agricultural Experiment Station of the Faculty of Agriculture, Cairo University, Wady Al-Natron farm, Egypt, during winter seasons of 2008/2009 and 2009/2010 to investigate the effect of spray with 12 commercial compounds and untreated treatment (spray with water) on onion seeds production and quality under sandy soils conditions. One commercial onion cultivar was selected for this study viz., Giza 20. The spray with union feer, union Mn, boron, elgae 600 and amino x had the higher inflorescence diameter. While the foliar application of union Mn, shams K, boron, magnesium, amica and shetocare had the highest flower stalks length (cm). The highest number of seed stem/plant was recorded with the foliar application with union feer, shams K and shetocare. The foliar application with union Zn, union feer, shams K, Magnesium, caboron, hummer and amino x had the highest seed yield. The highest germination percentage was recorded with the spray with boron, union feer, union Mn shams K.

Keywords: Onion Seeds; Sandy Soil; Foliar Application; Union Zink; Union Feer; Union Manganese; Shams K; Boron; Magnesium Sulfate; Elga 600; Caboron; Amica; Shetocare; Hummer; Amino X.

134. Response of Green Bean to Pulse Surface Drip Irrigation

Mohamed M. El-Mogy, Mohamed E. Abuarab and Amal L. Abdullatif

Journal of Horticultural Science and Ornamental Plants, 4: 329-334 (2012)

Effects of pulse irrigation on yield and nutritional elements of green beans (*Phaseolus vulgaris* L.), irrigated with a subsurface drip irrigation system, were evaluated over two years under field conditions in the Mediterranean region of Egypt. The irrigation system consisted of four irrigation treatments based on the number of pulses which ranged from T1 where the irrigation water requirement applied at one time to T4 where the irrigation water requirement applied using four pulses. Maximum and minimum yields were obtained from T4 and T1 treatments as 4.83 and 3.78 t/fed. in the first experimental year 2008 and 4.73 and 4.06 t/fed. in the second experimental year 2009, respectively. WUE ranged from 4.59 kg/ m³ in T1 to 6.84 kg/ m³ in T4 for the first experimental year and varied from 4.44 kg/ m³ in T1 to 6.64 kg/ m³ in T4 in the second experimental year. Results showed that the vegetative growth of green bean plants (plant height, number of leaves, plant fresh weight, plant dry weight, total leaf area as well as chlorophyll content) were improved by increasing number of pulses per each irrigation. It was found that the highest concentration of all determined nutrient elements was obtained in the high pulse irrigation T4. While, the lowest concentration was obtained in the low pulse irrigation T1.

Keywords: Phaseolus Vulgaris; Drip Irrigation; Yield; Growth; Nutrients.

135. Effects of Regulated Deficit Irrigation and Phosphorus Fertilizers on Water use Efficiency, Yield and Total Soluble Solids of Tomato

Mohamed M. Shahein, Mohamed E. Abuarab and Ahmed M. Hassan

American-Eurasian J. Agric. and Environ. Sci., 12: 1295-1304 (2012)

A field experiment was carried out on a sandy clay loam soil at the Experimental Farm of Faculty of Agriculture, Cairo University, Giza, Egypt. The experiment was consisted of 4 drip irrigation water levels (I : 1.0 IETc (potential crop evapotranspiration), I : 0.9 ETC, I : 0.8 ETC and I : 0.7 ETC) accompanied with two kinds of 2 3 4 phosphorus fertilizers (F : Calcium super phosphate and F : El-Mowfer-Bio). Yield was significantly (P = 0.05) I 2 affected by irrigation level, fertilizers and their interaction. The highest fruit yield, equal to 75049.33 kg/ha was recorded for F I , while the lowest fruit yield, equal 58524.20 kg/ha was recorded under F I . IWUE values varied I 1 2 4 from 4.326 to 4.730 kg/m³ in 2010-2011 and from 3.893 to 4.247 kg/m³ in 2011-2012. WUE values varied from 4.266 to 4.643 kg/m³ in 2010-2011 and from 3.893 to 4.180 kg/m³ in 2011-2012. The highest values of IWUE and WUE increased with water shortage till I (80% ETC). The effects of deficit irrigation on fruit quality were conversely 3 of those on fruit yield, whereas the amount of water applied through drip irrigation increased, the percentage of solids level decreased, so the lowest TSS (5.867 % Brix) value was corresponded to the full irrigation and calcium super phosphate fertilizer (F I). The results indicated that the crop does not benefit from the water I 1 when the last is supplied to

fulfill total crop requirements (100% ETC). Indeed, it is possible to save water, improving its use efficiency in processing tomato at a low rate (80% ETC), to achieve adequate fruit yield, minimizing fruit losses and maintaining high fruit quality levels. Tomato yield under calcium super phosphate was higher than of those under El-Mowfer-Bio, while the quality parameters like TSS and hardness were higher under El-Mowfer-Bio so it is recommended to use it if the main purpose is the quality.

Keywords: Deficit Irrigation; Drip Irrigation; Phosphorus Fertilizers; Wue; Yield; Tss.

136. Compost and its Application in Egypt (Effect of Rates and Time on Snap Beans Growth)

Said Abdalla Shehata, Yasser Mohamed Ahmed and Omaima Dareish Salah

Book Published by Lambert Academic Publishing, 67 (2012)

Compost is one of the most major sources of organic fertilization. The application of compost positively affects the structure, porosity, water holding capacity, compression strength, nutrient content and organic matter content of the soil (Mays et al., 1973; Pinamonti and Zorzi, 1996; Smith, 1996) consequently improves plant growth, crop yield and crop quality (Pinamonti and Zorzi, 1996; Rodrigues et al., 1996; Smith, 1996). The utilization of compost and manure in agriculture is an age old practice. However, during the Green Revolution, the high yielding varieties of used seeds required heavy nutrient input and chemical synthetic fertilizers largely superseded the use of organic materials. The extensive use of synthetic fertilizers is not without problems. In many places, degradation of the environment has been linked to the injudicious use of fertilizers (Lalljee, 2006). Compost had positive effects on plant growth and yield due to their high organic matter content which improved not only soil physical and biological properties, but also chemical characteristics resulting in more available nutrient elements (Gupta et al., 1995). The main aim of this study was to investigate the effect of the application of different compost rates and time of application on vegetative growth traits, yield and chemical composition of snap beans in comparison with two different sources of inorganic fertilizers.

137. Pre - And Postharvest of Vegetable Crops (Effects on Onion Seed Production and Longevity in Egypt)

Said Abdalla Shehata, Mohamed Hashim and Karima Abd El Gawad

Book Published by Lambert Academic Publishing, 172 (2012)

Onion (*Allium cepa* L.) is a species of the alliaceae family it is of great economic importance in Egypt. It is the most important cash crop after rice in Egypt. The total planted area for onion seed production is 2752 fed. Producing 742 tons with an average of 270 kg/ fed according to the Egyptian Ministry of Agriculture report (2008). Increasing its yield with consequent economic return is the major concern of the farmers (Sliman et al. 1999). Onion seeds are eaten, especially in some Indian dishes, they do not affect the breath as the bulbs and nevertheless, their commercial availability is currently limited. Perhaps, if consumers were much more acquainted with onion seed nutritional and functional properties, there would be a boost in the trade market for this product (Ostrowska et al. 2004 cited after Diniet al. 2008). Onion seeds in

general have poor longevity and lose viability rapidly within 1-2 years (Yasseen, 1994). It is unnecessary to store seeds for a period of several months to a year or more. However, no storage procedure guarantees that seeds will remain viable forever. Seeds eventually lose vigor and then viability with time (Cantliffe, 1998 cited after Korkmaz et al. 2004).

138. Contemporary Environmental Readings

Said Abdalla Shehata

Book Published By Lambert Academic Publishing, 296 (2012)

Climate change is a natural phenomenon, but humankind has drastically altered the process. When we use computers to model only the natural influences on the climate, we cannot explain the rapid rise in global temperatures we have seen during the 20th century. It is only when we include the influence of our emissions of greenhouse gases into the atmosphere over the last 150 years that we can replicate the temperature rises seen in recent decades. To help to avoid unacceptably dangerous climate change in the future, many countries and regions have set targets for reducing their greenhouse gas emissions. According to the IPCC (2008), climate change is any "change in climate over time whether due to natural variability or as a result of human activity". It is general consensus among IPCC researchers that increases in atmospheric concentrations of greenhouse gases (mainly CO₂, CH₄, N₂O and O₃) since pre-industrial times have led to a warming of the surface of the earth. During the last 250 years, the atmospheric concentrations of CO₂, CH₄ and N₂O have increased by 30%, 145% and 15%, respectively. The emissions are mainly due to the use of fossil fuels, but changes of land use as well as agriculture are also major sources of emissions (Raberg, 2008).

Faculty of Science

Dept. of Astronomy and Meteorology

139. Non-Hydrostatic Hybrid-Coordinate Modelling: Simulation of Extreme Weather Event on 20–22 April 2005 in Cairo, Egypt

AbdelTawab A.A. Shalaby, M.M. Abdel Wahab and R.O. Anyah A. Yousef

Atmos Res, 108: 74-85 (2012) IF: 1.911

We demonstrate in this study that by modifying a hydrostatic numerical weather prediction (Eta) model to incorporate some non-hydrostatic processes leads to significant improvement in the simulation of extreme weather (sand storm and rainfall) event that occurred over Cairo, Egypt during 20–22 April 2005. We compare simulations of the event by both the original version of the hydrostatic (HY) and modified version (hereafter non-hydrostatic (NH)) models to evaluate any improvement in skill due to incorporation of non-hydrostatic processes in the latter (NH). The computed skill score of sand storms as simulated by both (NH) and (HY) models for our case show that NH model correctly captures 278 cases from the total 539 events forecast and falsely captures 261 events compared to 108 and 431 cases for HY, respectively.

The NH model reaches perfect skill for the Probability of Detection (POD) and the Detection Failure Ratio (DFR) by the second day and third day of integration. Critical Success Index (CSI) indicates no skill for HY forecast after first day, also

no skill of (POD), but has perfect skill of False Alarm Ratio (FAR). True Skill Statistic (TSS) and Heidke reach its highest values at second day of NH and lowest values at third day for HY. The HY model reproduces fairly well the correct non-rainy day events although the false alarm rate increases after the third day of model integration. However, the NH model captures the correct number of rainy-day events as well as the episodic events. The rainfall simulated (forecast) by NH and HY models have Probability of Detection (POD) approximately 65% and less than 20%, respectively.

The False Alarm Ratio (FAR) by the NH model approaches 87% on second and third days during the 72-hour integration period, while it is 92% and 85% for the HY model by the second and third day, respectively.

Keywords: Weather extremes; Sandstorms; Numerical modeling; Egypt.

140. Some Characteristic Parameters of Gaussian Plume Model

M. Abdel-Wahab, Khaled S. M. Essa, M. Embab and Sawsan E. M. Elsaid

Mausam, 63, 1: 123-128 (2012) IF: 0.17

The Gaussian solution of the diffusion equation for line source is used to have the first four moments of the vertical concentration distribution (centroid, variance, skewness and kurtosis). The magnitude and position of maximum concentration level were evaluated. Also the plume advection wind speed is estimated. Equations for the ground level concentration were compared with wind tunnel measurements.

Keywords: Key words; Moments; Diffusion equation; Plume advection wind speed.

141. J₂ Gravity Perturbed Motion of Artificial Satellite in Terms of Euler Parameters

Z. M. Hayman

The Open Astronomy Journal, 5: 12-18 (2012)

In this paper the solution of an artificial satellite motion under the influence of the Earth's gravitational field with axial symmetry of any conic section with zonal harmonics J₂ in terms of Euler parameters is established. Applications of this method enable anyone to predict the motion of artificial satellites.

Keywords: Satellite; Euler; Conic sections; Classical newtonian equations.

142. Invariant Relative Orbits Taking Into Account Third-Body Perturbation

Walid Ali Rahoma and Gilles Metris

Applied Mathematics, 3, 113-120 (2012)

For a satellite in an orbit of more than 1600 km in altitude, the effects of Sun and Moon on the orbit can't be negligible. Working with mean orbital elements, the secular drift of the longitude of the ascending node and the sum of the argument of perigee and mean anomaly are set equal between two neighboring orbits to negate the separation over time due to the potential of the Earth and the third body effect. The expressions for the second order conditions that guarantee that the drift rates of two neighboring

orbits are equal on the average are derived. To this end, the Hamiltonian was developed. The expressions for the non-vanishing time rate of change of canonical elements are obtained.

Keywords: Invariant relative orbits; Third-Body perturbation; Hamiltonian.

143. Visual Contact Between Two Earth'S Satellites

Awad, M.E., M.A. Sharaf and E.H. Khattab

American Journal of Applied Sciences, 9 (5): 620-623 (2012)

Problem statement: In this study, an analytical expression for predicting mutually visible between Earth's satellites is developed.

Approach: A relative visibility function of two satellites to each other is developed in terms of orbital elements for two satellites in the same orbital plane. Also, a computational algorithm is expressed to compute the visibility function.

Results: This study presents a method to rapidly determine the visibility times of satellite-satellite in the same orbital plane.

The problem of visibility is calculated by using an algorithm which used a simple treatment to construct the visibility function versus time.

Conclusion: This study presented a method to rapidly determine the visibility of satellite-satellite visibility periods. This study calculated the problem by using an algorithm which used a simple treatment to construct the visibility function versus time.

Keywords: Visibility problem; Rise; Set function.

144. Solar Forcing on Makkah Al-Mukaramah Flash Floods

Yousef, Shahinaz; Algafari, Yasser H. O. Al-Mostafa and Zak Kordi Mutaz

Journal of Earth Science And Engineering, 2, 77-83 (2012)

Severe solar events manifested by highly energetic X-Ray events accompanied by coronal mass ejections and proton flares caused flash floods in Makkah Al-Mukaramah, Al-Madinah Al-Munawarah and Jeddah.

The responses can be prompt, delayed or prompt-delayed, suggesting that the protons entered the troposphere either through the opening of a direct gate in the magnetosphere to the location concerned due to magnetic reconnection, through the polar gates or through those two paths respectively.

The authors suggest that there is a magnetic anomaly in Makkah Al-Mukaramah area which makes it liable to be subjected to flash floods. The width of the solar streams determines the width of the gate opened in the magnetosphere via magnetic reconnection and thus narrow streams affect only one location of the three cities while extended width streams can cause flash floods in all of Makkah Al-Mukaramah, Al-Madinah Al-Munawarah and Jeddah. In addition, the November 24-26 Jeddah flash flood could be attributed to a prompt event due to a moderately fast solar stream that arrived the earth on those days.

Keywords: Makkah Al-Mukaramah; Al-Madinah Al-Munawarah; Jeddah; Coronal mass ejections; X-Ray events; Flash floods.

145. Evolution of the Motion Around A Slowly Rotating Body

Z. M. Hayman and W. M. El-Mahy

The Open Astronomy Journal, 5: 1-6 (2012)

The motion of a satellite about a rotating triaxial body will be investigated, stressing on the case of slow rotation. The Hamiltonian of the problem will be formed including the zonal harmonic J_2 and the leading tesseral harmonics C_{22} and S_{22} . The small parameter of the problem is the spin rate (σ) of the primary. The solution proceeds through three canonical transformations to eliminate in succession; the short, intermediate and long-period terms. Thus secular and periodic terms are to be retained up to orders four and two respectively.

Keywords: Hamiltonian; Perturbation; Motion; Satellite.

146. Satellite to Satellite Visibility

M.A. Sharaf, Z.M. Hayman and M.E. Awad

The Open Astronomy Journal, 5: 26-40 (2012)

In this paper, general analytical and computational technique for satellite - to-satellite visibility will be established. The developments are general in the sense that the visibility conditions can be used whatever the types of the satellite orbits may be. Numerical applications are also included.

Keywords: Satellite; Visibility; Orbit; Numerical solution.

147. The Other Side of Gravity and Geometry: Antigravity and Anticurvature

M. I. Wanas

Adv. High Energy Phys., 1-10 (2012) IF: 4.522

Gravity is one of the four known fundamental interactions used to study and interpret physical phenomena. It governs diverse phenomena, especially those connected with large-scale structures. From more than one decade, existing gravity theories have suffered from some problems, when confronting their predictions with the results of some experiments and observations.

This situation has led to many suggestions, none of which is final, so far. Here, we show that the assumption of existence of another side of gravity, a repulsive gravity or antigravity, together with its attractive side, may give a satisfactory solution to gravity problems. We caught here two pieces of evidence for the existence of antigravity in nature.

The first is on the laboratory scale, the COW experiment and the second is on the cosmic scale, SN type Ia observation. On the other hand, we show how gravity theories can predict antigravity, using a new defined geometric object called parameterized anticurvature.

This shows clearly how Einstein's geometrization philosophy can solve recent gravity problems in a satisfactory and easy way. Also, it may throw some light on the mystery of physical nature of "Dark Energy."

148. Cosmological Applications in Kaluza Klein the Ory

M. I. Wanasa, Gamal G. L. Nashed and A. A. Nowayae

Chin. Phys. B, 21, (4) 4980-4987 (2012) IF: 1.376

The field equations of Kaluza–Klein (KK) theory have been applied in the domain of cosmology. These equations are solved for a flat universe by taking the gravitational and the cosmological constants as a function of time t . We use Taylor's expansion of cosmological function, (t) , up to the first order of the time t . The cosmological parameters are calculated and some cosmological problems are discussed.

Keywords: Kaluza; Klein Theory; Cosmology; Taylor's Expansion of Cosmological Function.

Dept. of Biophysics

149. CBX4-Mediated SUMO Modification Regulates BMI1 Recruitment at Sites of DNA Damage

Ismail IH, Gagné JP, Caron MC, McDonald D, Xu Z, Masson JY, Poirier GG and Hendzel MJ

Nucleic Acids Res, 40 (12): 497-510 (2012) IF: 8.026

Polycomb group (PcG) proteins are involved in epigenetic silencing where they function as major determinants of cell identity, stem cell pluripotency and the epigenetic gene silencing involved in cancer development. Recently numerous PcG proteins, including CBX4, have been shown to accumulate at sites of DNA damage. However, it remains unclear whether or not CBX4 or its E3 sumo ligase activity is directly involved in the DNA damage response (DDR). Here we define a novel role for CBX4 as an early DDR protein that mediates SUMO conjugation at sites of DNA lesions. DNA damage stimulates sumoylation of BMI1 by CBX4 at lysine 88, which is required for the accumulation of BMI1 at DNA damage sites. Moreover, we establish that CBX4 recruitment to the sites of laser micro-irradiation-induced DNA damage requires PARP activity but does not require H2AX, RNF8, BMI1 nor PI-3-related kinases. The importance of CBX4 in the DDR was confirmed by the depletion of CBX4, which resulted in decreased cellular resistance to ionizing radiation. Our results reveal a direct role for CBX4 in the DDR pathway.

Keywords: Dna repair; Dna damage; Polycomb group proteins.

150. Interaction of Doxorubicin and Dipalmitoylphosphatidylcholine Liposomes

Mohsen M. Mady Medhat W. Shafaa, Eman R. Abbase and Amine H. Fahium

Cell Biochem Biophys, 62: 481-486 (2012) IF: 3.743

The interaction between doxorubicin (DOX), an anthracycline antibiotic frequently used in chemotherapy and zwitterionic dipalmitoylphosphatidylcholine (DPPC) was investigated using Fourier transform infrared (FTIR) spectroscopy, differential scanning calorimetry (DSC) and rheological measurements. FTIR results showed that DOX shifted the wavenumber of the PO_2^- band for pure DPPC to a higher wavenumber. This may be due to the strong interactions between the NH_3^+ group in DOX and the phosphate (PO_2^-) group in the polar head of DPPC. The main

transition temperature of DPPC liposomes was slightly shifted to a lower temperature for DPPC liposome-encapsulated DOX. This suggested that DOX had a significant effect on the acyl chains in the DPPC bilayers and that its presence decreased the transition cooperativity of lipid acyl chains. There was also the appearance of an additional transition peak at nearly 136°C for the DPPC/DOX sample. These interactions between DOX and DPPC phospholipid would cause a decrease in the DPPC liposomes plastic viscosity and increase membrane fluidity. A better understanding of the interactions between DOX and lipid bilayers could help in the design and development of improved liposomal drug delivery systems.

Keywords: Liposome; Dppc; Doxorubicin; Ftir; Dsc; Viscosity.

151. Assessment of Genotoxic and Cytotoxic Hazards in Brain and Bone Marrow Cells of Newborn Rats Exposed to Extremely Low-Frequency Magnetic Field.

Monira M. Rageh, Reem H. EL-Gebaly and Nihal S. El-Bial

J Biomed Biotechnol, 1-7 (2012) IF: 2.436

The present study aimed to evaluate the association between whole body exposure to extremely low frequency magnetic field (ELFMF) and genotoxic, cytotoxic hazards in brain and bone marrow cells of newborn rats. Newborn rats (10 days after delivery) were exposed continuously to 50Hz, 0.5mT for 30 days. The control group was treated as the exposed one with the sole difference that the rats were not exposed to magnetic field. Comet assay was used to quantify the level of DNA damage in isolated brain cells. Also bone marrow cells were flushed out to assess micronucleus induction and mitotic index. Spectrophotometric methods were used to measure the level of malondialdehyde (MDA) and the activity of glutathione (GSH) and superoxide dismutase (SOD). The results showed a significant increase in the mean tail moment indicating DNA damage in exposed group ($P < 0.01, 0.001, 0.0001$). Moreover ELF-MF exposure induced a significant ($P < 0.01, 0.001$) four folds increase in the induction of micronucleus and about three folds increase in mitotic index ($P < 0.0001$). Additionally newborn rats exposed to ELF-MF showed significant higher levels of MDA and SOD ($P < 0.05$). Meanwhile ELF-MF failed to alter the activity of GSH. In conclusion, the present study suggests an association between DNA damage and ELF-MF exposure in newborn rats.

Keywords: Genotoxic and Cytotoxic Hazards; Brain and Bone marrow Cells; Extremely Low-Frequency magnetic Field.

152. Enhancement of Photovoltaic Characteristics of Nanocrystalline 2,3-Naphthalocyanine Thin Film-Based Organic Devices

A.A.M. Farag, W.G. Osiris and A.H. Ammar

Applied Service Science, 259: 600-609 (2012) IF: 2.103

Nanocrystalline thin films of 2,3-naphthalocyanine (NPC) were successfully deposited by a thermal evaporation technique at room temperature under high vacuum ($\sim 10^{-4}$ Pa). The crystal structure and surface morphology were measured using X-ray diffraction (XRD) and scanning electron microscopy (SEM), respectively. A preferred orientation along the (001) direction was observed in all the studied films and the average crystallite size was calculated. SEM images of NPC films at different thermal

treatment indicated significant changes on surface level patterns and gave clear evidence of agglomeration of nanocrystalline structures. The molecular structural properties of the thin films were characterized using Fourier transform infrared spectroscopy (FTIR), which revealed the stability of the chemical bonds of the compound under thermal treatment. The dark electrical conductivity of the films at various heat treatment stages showed that NPC films have a better conductivity than that of its earlier reported NPC films and the activation energy was found to decrease with annealing temperature. The absorption edge shifted to the lower energy as a consequence of the thermal annealing of the film and the fundamental absorption edges correspond to a direct energy gap. The temperature coefficient of the onset and optical band gaps for the film was calculated to be -4.4×10^{-4} and -1.76×10^{-3} eV/K, respectively. The effect of thermal annealing on the photovoltaic properties of Al/NPC/ITO devices was also considered. The as-deposited device showed maximum power conversion efficiency about 0.70% under illumination of 100 mW/cm², whereas 2.65% power conversion efficiency was achieved after annealing the samples at 500 K for 1 h.

Keywords: Al/Npc/Ito Device; Optical band gap; Activation energy; Thermal annealing; Nanostructured film.

153. Effect of Zincon the Physical Properties of Borate Glasses

Ghada E. El-Falaky and Osiris W. Guirguis

Journal of Non-Crystalline Solids, 358, (15): 1746-1752 (2012)
IF: 1.537

This manuscript presents a theoretical analysis of the elastic properties of ZnONa2OAl2O3B2O3 (in molar %) glass. The elastic moduli were calculated in terms of Makishima–Mackenzie theory and bond compression model. Addition effect of ZnO on the elastic moduli was investigated according to bond compression model in terms of the number of network bonds, the mean cross-link density, average stretching force constant, atomic ring size and the ratio K_{bc}/K_e of the glass systems. Young's modulus, packing density and Poisson's ratio have been calculated and analyzed according to Makishima–Mackenzie model. The results indicate that the elastic moduli and the dimensionality of these glasses are sensitive to the increase in the zinc oxide content.

Keywords: Borate Glasses; Elastic Properties; Cross; Link Density; Bond Compression Model; Makishima; Mackenzie Model.

154. A Comparison of Three Commercial Imrt Treatment Planning Systems for Selected Pediatric Cases

Ismail Eldesoky, Ehab M. Attalla, Wael M. Elshemey and Mohamed S. Zaghoul

J Appl Clin Med Phys, 13, (2): (2012) IF: 1.291

This work aimed at evaluating the performance of three different intensity-modulated radiotherapy (IMRT) treatment planning systems (TPSs) — KonRad, XiO and Prowess — for selected pediatric cases. For this study, 11 pediatric patients with different types of brain, orbit, head and neck cancer were selected. Clinical step-and-shoot IMRT treatment plans were designed for delivery on a Siemens ONCOR accelerator with 82-leaf multileaf

collimators (MLCs). Plans were optimized to achieve the same clinical objectives by applying the same beam energy and the same number and direction of beams. The analysis of performance was based on isodose distributions, dose-volume histograms (DVHs) for planning target volume (PTV), the relevant organs at risk (OARs), as well as mean dose (Dmean), maximum dose (Dmax), 95% dose (D95), volume of patient receiving 2 and 5 Gy, total number of segments, monitor units per segment (MU/Segment) and the number of MU/cGy. Treatment delivery time and conformation number were two other evaluation parameters that were considered in this study. Collectively, the Prowess and KonRad plans showed a significant reduction in the number of MUs that varied between 1.8% and 61.5% (p-value = 0.001) for the different cases, compared to XiO. This was reflected in shorter treatment delivery times. The percentage volumes of each patient receiving 2 Gy and 5 Gy were compared for the three TPSs. The general trend was that KonRad had the highest percentage volume, Prowess showed the lowest (p-value = 0.0001). The KonRad achieved better conformality than both of XiO and Prowess. Based on the present results, the three treatment planning systems were efficient in IMRT, yet XiO showed the lowest performance. The three TPSs achieved the treatment goals according to the internationally approved standards.

Keywords: Konrad; Xio; Prowess; Imrt.

155. A.C. Conductivity and Relaxation Dynamics in Zinc–Borate Glasses

Ghada E. El-Falaky, Osiris W. Guirguis and Nadia S. Abd El-Aal

Progress in Natural Science: Materials International, 22 (2): 86-93 (2012) IF: 1.099

The frequency-dependent dielectric dispersion of ZnO–Na₂O–Al₂O₃–B₂O₃ (in mol%) glass prepared by the melt quenching technique is investigated in the temperature ranges from room temperature to 420 K. Dielectric relaxation has been analyzed based on the behavior of electric modulus behavior. An analysis of the real and imaginary parts of dielectric is performed assuming the ideal Debye behavior as confirmed by Cole–Cole plot. The activation energy associated with the dielectric relaxation determined from the electric modulus spectra was found to be 1.863 eV, which is close to that the activation energy for d.c. conductivity (1.871 eV), indicating the similar nature of relaxation and conductivity.

Keywords: Zinc; Borate Glasses; A.C. Conductivity; Dielectric Properties; Impedance Properties.

156. Biophysical Characterization of Gold Nanoparticles-Loaded Liposomes

Mohsen Mahmoud Mady, Mohamed Mahmoud Fathy, Tareq Youssef.W and afaa Mohamed Khalil

Phys Medica, 28: 288-295 (2012) IF: 1.068

Gold nanoparticles were prepared and loaded into the bilayer of dipalmitoylphosphatidylcholine (DPPC) liposomes, named as gold-loaded liposomes. Biophysical characterization of gold-loaded liposomes was studied by transmission electron microscopy (TEM) and Fourier transform infrared (FTIR) spectroscopy as well as turbidity and rheological measurements. FTIR measurements showed that gold nanoparticles made

significant changes in the frequency of the CH₂ stretching bands, revealing that gold nanoparticles increased the number of gauche conformers and create a conformational change within the acyl chains of phospholipids. The transmission electron micrographs (TEM) revealed that gold nanoparticles were loaded in the liposomal bilayer. The zeta potential of DPPC liposomes had a more negative value after incorporating of Au NPs into liposomal membranes. Turbidity studies revealed that the loading of gold nanoparticles into DPPC liposomes results in shifting the temperature of the main phase transition to a lower value. The membrane fluidity of DPPC bilayer was increased by loading the gold nanoparticles as shown from rheological measurements. Knowledge gained in this study may open the door to pursuing liposomes as a viable strategy for Au NPs delivery in many diagnostic and therapeutic applications.

Keywords: Liposome; Dppc; Gold Nanoparticles; Ftir; Characterization.

157. The Influence of Low Power Microwave on the Properties of Dppc Vesicles

Mohsen M. Mady and Mousa A. Allam.

Phys Medica, 28: 48-53 (2012) IF: 1.068

The effect of microwave exposure on liposome at non-thermal level is studied. Dipalmitoyl phosphatidylcholine (DPPC) liposomes were exposed to 950 MHz at power densities of 2.5 mW/cm², which is equivalent to specific absorption rate (SAR) of 0.238 W/K. The interaction of microwave with liposomes was investigated by membrane solubilization measurements using a non-ionic detergent, octylglucoside (OG), as well as Fourier transform infrared (FTIR) spectroscopy and flow activation energy measurements. The amount of detergent needed to completely solubilize the liposomal membrane was increased after exposure of liposomes to microwave irradiation, indicating an increased membrane resistance to the detergent and hence a change in the natural membrane permeation properties. In the analysis of FTIR spectra the symmetric and antisymmetric CH₂ (at 2070 cm⁻¹) band and the C=O (at 1640 cm⁻¹) stretching bands were investigated after liposomal exposure to microwave irradiation. It is clearly shown from the flow activation energy measurements, that low-power microwave induce changes in the liposomes deformability (decreases the liposome fluidity and increases the liposome rigidity). Finally it could be concluded that low-power microwave of 950 MHz induced structural and functional changes in liposomes as a membrane model system.

Keywords: Microwave; Liposome; Dppc; Solubilization; Ftir; Viscosity.

158. Physical Study of Poly(Methyl Methacrylate) - Rare Earth Composite Luminescent Materials

Osiris W. Guirguis, Wedad A. Alharbi and Jamila H. Alzahrani

Materials Science (an Indian Journal), 8 (11): 423-433 (2012) IF: 0.299

In the present work, mixture of five different concentrations (2, 4, 6, 8 and 10 wt%) of an alkali earth aluminate photoluminescent pigment powder (AREAPP) with poly (methyl methacrylate) (PMMA) were prepared. The pigment has the composition formula of MeO.xAl₂O₃.ySiO₂:Eu (Me = Ca, Mg, Sr, Ba, x = 0.5-2.0, y = 0.005-0.5) which is activated by rare earth element

(Eu). Thermal analyses (DSC and TGA) as well as FTIR spectroscopy were employed to characterize and reveal the miscibility map and the relationship of the structure properties. From the results, we can find that the organic parts are attached with the inorganic parts in the PMMA/AREAPP mixtures. Also, the obtained results of the thermal analyses showed variations in the phase transition temperature on the lower temperature side indicating the miscibility of the systems. The changes in the phase transition temperature on the high temperature side, shape and area were attributed to the different degrees of crystallinity.

Keywords: Poly (Methyl Methacrylate); Rare Earth Element; Luminescent Materials; Structural Properties; Thermal Analyses; Ftir Spectroscopy.

159. Optical Studies of Fast Neutron Irradiated Composites of Poly(Vinyl Alcohol) and Bovine Serum Albumin

Nabawia A. Abdel Zaher and Osiris W. Guirguis

Materials Science (An Indian Journal), 8 (9): 370-382 (2012)

IF: 0.229

The proposal in this study was to evaluate the optical properties of different biopolymers films before and after irradiation with fast neutrons. The materials used were: poly(vinyl alcohol) (PVA) and bovine serum albumin (BSA). PVA-BSA blends were prepared by casting technique. The effects of different BSA concentrations (2.5-15 wt%) on the optical properties by near infrared and transmittance in the spectral region 400-2500 nm of the films were studied before and after irradiation with fast neutrons of fluence 1×10^7 n/cm². Transmittance spectra were used for the determination of the optical constants. The results indicate that variation in the optical band gap was derived from Tauc's extrapolation with the BSA contents. The results obtained by the effect of different weight percent of BSA were compared with that detected by the effect of fast neutron.

Keywords: Pva; Bsa; Near Infrared; Extinction Coefficient; Transmittance Spectra; Optical Parameters.

160. A 50 Hz 0.5 Mt Magnetic Field Induces Cytogenetic Effects and Biological Alterations in Wistar Rat

Reem H. El-Gebaly, Nihal S. El-Bialy and Monira M. Rageh

Life Science Journal, 9(4): 1906-1912 (2012) IF: 0.073

The effects of continuous whole body exposure to extremely low frequency magnetic fields (ELF-MF) (50Hz, 0.5 mT for 30 days 24 hrs) on cytogenecity, bone parameters and some hematological and biochemical parameters were evaluated. Male rats were exposed continuously to ELF-MF for a period of 30 days. The exposure effects were assessed by measurements of micronucleus formation, DNA fragmentation and bone parameters. Additionally the levels of some liver and blood parameters were calculated. Moreover, osmotic fragility of erythrocytes was also considered. Exposure to ELF-MF resulted in a 6.5 fold increase in the micronucleus formation and a decrease in polychromatic erythrocytes (PCE)/normochromatic erythrocytes (NCE) ratio, in addition to a significant increase in the level of aspartate transaminase (AST) alanine aminotransferase (ALT), alkaline phosphatase (ALP), Magnesium (Mg) and uric acid in serum was observed. However, 0.5 mT ELF-MF was unable

to cause either direct DNA primary damage or changes in bone parameters and erythrocytes lyses percent. The present results provide evidence that continuous exposure to ELF-MF causes micronucleus formation and some physiological disturbance but had no effect on DNA structure and bone parameters. Furthermore, the levels of glucose, creatinine, cholesterol and the percentage of erythrocytes lyses were not affected.

Keywords: Extremely Low Frequency Magnetic Field (Elf-Mf); Micronucleus Test; Dna Fragmentation; Bone Mineral Density.

161. Studies on Hematological Parameters and Dna Structure in Newborn Rats Exposed to Extremely Low Frequency Magnetic Fields

Nihal S. El-Bialy, Reem H. El-Gebaly and Monira M. Rageh

Life Science Journal, 9 (1): 489-495 (2012) IF: 0.073

The aim of this study was to evaluate the possible effects of in vivo exposure to extremely low frequency magnetic fields (ELF-MF) on some hematological parameters, pathological variations and DNA structure in newborn rats. Six female pregnant Wistar rats were obtained from the National Research centre in Egypt and gave birth to 30 rats at the animal house of Cairo University. The newborn rats were divided into two separate groups: one exposed group (50 Hz, 0.5 mT, 30 days, 24 h/day) and one control (sham). Red blood cells (RBCs), hemoglobin and hematocrit levels decreased significantly ($P < 0.02$) while white blood cells (WBCs) and platelets levels significantly increased ($P < 0.04$) in newborn rats that were exposed to ELF-MF. There was no significant difference in mean corpuscular hemoglobin (MCH), mean corpuscular hemoglobin concentration (MCHC), mean corpuscular volume (MCV) levels and DNA structure between the exposed and sham-exposed groups. ELF-MF induced a marked necro-degenerative change in kidney tissue and periportal fibrosis in liver tissues. Our results indicate that the applied ELF-MF exposure may induce statistically significant alterations in some hematological parameters, kidney and liver tissues of newborn rats.

Keywords: Electromagnetic Field; Hematological Parameters; Dna; Pathological Tissues.

162. The Thermal and Structural Studies of Poly(Vinyl Alcohol) and Hydroxypropyl Cellulose Blends

Osiris W. Guirguis and Manal T. H. Moselhey

Natural Science, 4 (1): 57-67 (2012)

Polymers and polymeric composites have steadily reflected their importance in our daily life. Blending poly(vinyl alcohol) (PVA) with a potentially useful natural biopolymers such as hydroxypropyl cellulose (HPC) seems to be an interesting way of preparing a polymeric blends. In the present work, blends of PVA/HPC of compositions (100/0, 90/10, 75/25, 50/50, 25/75 and 0/100 wt/wt%) were prepared to be used as bio-equivalent materials. Thermal analyses [differential scanning calorimetry (DSC) and thermo-gravimetric analysis (TGA)] and X-ray diffraction (XRD) were employed to characterize and reveal the miscibility map and the structural properties of such blend system. The obtained results of the thermal analyses showed variations in the glass transition temperature (T_g) indicating the miscibility of the blend systems. Moreover, the changes in the melting temperature (T_m), shape and area were attributed to the

different degrees of crystallinity and the existence of polymer-polymer interactions between PVA and HPC molecules. The X-ray diffraction (XRD) analysis showed broadening and sharpening of peaks at different HPC concentrations with PVA. This indicated changes in the crystallinity/amorphosity ratio and also suggested that the miscibility between the amorphous components of homo-polymers PVA and HPC is possible. The results showed that HPC doped in PVA film can improve the thermal stability of the film under investigation, leading to interesting technological applications.

Keywords: Pva; Hpc; Dsc; Tga; Xrd.

163. Rheological Parameters Assessment in Serum, Plasma and Whole Blood of Rats After Administration of Gold Nanoparticles of Different Sizes: in Vivo

Mohamed Anwar K Abdelhalim and Mohsen Mahmoud Mady

J. Nanomed Nanotechnol, 3-6 (2012)

The evaluation of blood rheology has been underutilized in clinical practice. We performed an array of rheological parameters measurements to quantify the responses of rat plasma, serum and whole blood to gold nanoparticles (GNPs) of different sizes.

Methods: GNPs of various sizes were used in this study. Doses of 0.05 ml of the GNPs were administered to the animals via intraperitoneal injection for a period of 3 days. Blood samples with volumes of nearly 2 ml were obtained from each rat. Various rheological parameters, such as %torque, shear stress (SS), shear rate (SR), viscosity, plastic velocity, yield stress, consistency index and flow index, were measured in rat plasma, serum and whole blood.

Results: The relationship between SS and SR for rat serum, plasma and whole blood showed linear behaviour with the 10, 20 and 50 nm GNPs. The viscosities of rat serum, plasma and whole blood with GNPs were decreased with increasing the SR and showed non-linear behaviour. The viscosity of blood serum and plasma was measured at a range of shear rates from 200 to 1375 s⁻¹, while the viscosity of whole blood was measured at 75 to 600 s⁻¹.

Conclusions: The GNP size has a considerable influence on the various rheological parameters for rat blood at a fixed temperature of 37°C. The decrease in viscosity of 50 nm GNPs compared to 10 and 20 nm GNPs may be attributed to decrease in number of NPs and GNP surface area. It can be concluded that the GNPs probably cause erythrocyte deformability and their interactions with blood proteins may cause a decrease in serum, plasma and whole blood viscosities under a given level of applied SS and SR compared to the control. This study suggests that further experimental work taking nanoparticle surface properties into consideration should be performed.

Keywords: Gold Nanoparticle Sizes; Serum; Plasma; Whole Blood; Rheological Parameters; Rats.

164. Effect of Gamma Irradiation on Biophysical and Protection Properties of Melanin

Magdy M. Ghannam and Mohsen M. Mady

International J of Physical Sciences, 7 (23): 2952-2959 (2012)

Melanins are natural pigments distributed in living organisms and they are responsible for pigmentation of surface structure. In the present work, gel exclusion chromatography, spectrophotometric

and dielectric relaxation techniques were used to characterize DOPA melanin before and after irradiation with ^{60}Co gamma rays in the range of 5 to 50 Gy. The results show that the studied melanin is composed of two structural groups. The extinction absorption coefficient and relative permittivity and conductivity of melanin sample increased after irradiation with gamma rays and were dose dependent in manner. These increases were attributed to the formation of melanin aggregation and crosslinks which result from the growing number of the formed free radicals by radiation. It was concluded from the results that melanin goes through some structural changes after irradiation with the gamma doses demonstrated. Further studies were recommended to investigate and evaluate whether these changes could affect its efficiency as a radio protector against gamma radiation.

Keywords: Melanin structure; Gamma irradiation; Gel chromatography absorption spectra; Relative permittivity and conductivity.

165. Quantitative Structure Activity Relationship: History, Development and Application

Noha A. Saleh and Wael M. Elshemey

Recent Trends on Qsar In The Pharmaceutical Preceptions, Bentham Science, 12: 360-391 (2012)

The Quantitative Structure Activity Relationship (QSAR) is a technique which quantifies the relationship between a physicochemical property of a drug and its biological activity. The present chapter aims at presenting some basic considerations concerning QSAR.

These considerations include a historic background, some selected developments and some important descriptors including; electronic parameters, hydrophobic (Lipophilic) parameters and steric parameters. Finally, the application of QSAR on some selected biological structures is presented. Among these are 3'-azido-2',3'-dideoxythymidine (AZT); fulleropyrrolidine-1-carbodithioic acid 2; 3 and 4-substituted-benzyl esters; hydroxychalcone-acetic acid-(4-pyrrolidin-1-yl-phenyl) ester and hydroxy-chalcone-acetic acid-[2-(2-hydroxy-acetylchalconyl)-4-pyrrolidin-1-yl-phenyl] ester.

Keywords: AZT; Chitosan; Fulleropyrrolidine; Hammett constant; Hansche equation; HIV; protease; Hydroxyapatite; Molecular modeling; QSAR descriptors.

166. Rat Sleep under the Effect of Electromagnetic Radiation

Haitham Sharaf El-Din Mohamed

Book Published by Lambert Academic Publishing, 85 (2012)

The electromagnetic radiation emitted from new technological devices forms a real hazard to the biological structure. The most important biological structure ever known is the brain. The interaction of such fields with the brain causes changes in its function and consequently puts the whole organism in danger. Research is now carried on to investigate the interaction mechanisms of EMF with the biological structures and the impact of such fields on the integrity of the organism.

Keywords: Electromagnetic radiation (EMR); Electroencephalogram (EEG); slow wave sleep (SWS); Rapid eye movement (REM).

167. Crystal Structure of N-Glycosylated Human Glypican-1 Core Protein

Gabriel Svensson, Wael Awad, Maria Hkansson, Katrin Mani and Derek T. Logan

The Journal of Biological Chemistry, 287 (17): 14040-14051 (2012) IF: 4.773

The glypican family of cell-surface proteoglycans regulates growth factor signaling during development through their core proteins and heparan sulfate chains. Results: The crystal structure of N-glycosylated human glypican-1 is described. Conclusion: The structure reveals the complete disulfide bond arrangement for the conserved Cys residues in glypicans. Significance: Increased structural knowledge of glypicans will help elucidate their important functions in shaping animal development.

Keywords: Proteoglycans; Cell Surface Receptor; Glypican 1; Crystallography; Protein Structure.

168. Fullerene Derivative as Anti-Hiv Protease Inhibitor: Molecular Modeling and Qsar Approaches

M. Ibrahim, N.A. Saleh, W.M. Elshemey and A.A. Elsayed

Mini-Reviews In Medicinal Chemistry, 12: 447-451 (2012) IF: 2.528

A Fullerene based system is modified in order to increase its solubility and enhance its ability to carry a protein-like structure. The modified structure, which is proposed to act as HIV-1 protease inhibitor, is $[\text{C}_{60}\text{-C}_2\text{H}_4\text{N}-(2,4\text{-XCOCH}_2\text{OH})\text{C}_6\text{H}_4]$, where the X atom is either O, S or Se. The geometry optimization, vibrational spectra and thermodynamics were performed using semiempirical quantum mechanical PM3 method in order to study the proposed compounds. Furthermore, the quantitative structure activity relationship (QSAR) properties of the compounds are calculated at the same level of theory. Results indicate a possible use of the investigated structures as HIV-1 protease inhibitors. The compounds containing oxygen are more stable as compared to the other two compounds.

Keywords: Fulleropyrrolidine; Hiv-1 Protease; Hydroxymethylcarbonyl Group (Hmc); Molecular Modeling; Qsar.

169. Hexapeptide Functionality of Cellulose as NS3 Protease Inhibitors

Medhat Ibrahim Noha A. Saleh, Wael M. Elshemey and Anwar A. Elsayed

Medicinal Chemistry, 8 (5): (2012) IF: 1.496

Two novel groups of hexapeptide inhibitors for NS3 serine protease of the hepatitis C virus (HCV) are redesigned. The hexapeptide is an amino acid sequence of NS5A/NS5B substrate (Glu-Asp-Val-Val-Cys-Cys). In the first group, the hexapeptide binds to a cellulose monomer at the positions 2, 3 or 6 while in the second group, the hexapeptide binds to a cellulose dimer at the positions 2, 3, 6, 2', 3' or 6'. Molecular modeling semiempirical PM3 calculations are used to optimize the geometry and calculate the electronic properties of the suggested inhibitors compared to that of natural substrate. Computational results show that the second group has the maximum stability and reactivity indicating

that it would be considered as a promising HCV NS3 protease inhibitor.

Keywords: Molecular Modeling; Pm3; Hcv; Ns3 Protease; Subtype 4A and Ns5a / Ns5b Junction.

170. A Novel Peptidomimetic Compounds as Hcv- Ns3 Protease Inhibitors: Spectroscopic Analysis

Medhat Ibrahim, Noha A. Saleh, Wael M. Elshemey and Anwar A. Elsayed

The Open Spectroscopy Journal, 6: 15-21 (2012)

The presented molecular modeling is utilized to innovate new peptidomimetic compounds. These proposed compounds are redesigned to act as HCV NS3 protease antiviral. The suggested antivirals are divided into two groups. The first group has hexapeptide (Glu-Asp-Val-Val-Cys-Cys) binding to cellulose monomer at positions 2, 3 or 6 while the second group has hexapeptide (Glu-Asp-Val-Val-Cys-Cys) binding to cellulose dimer at positions 2, 3, 6, 2', 3' or 6'. Semi-empirical PM3 quantum mechanical method is first utilized for optimization, then to calculate the vibrational spectra of these novel compounds. It is found that higher dipole moment (11.907 Debye) corresponds to the hexapeptide (Glu-Asp-Val-Val-Cys-Cys) binding to cellulose dimer at position 2' compound. Accordingly, calculation is repeated at HF/3-21^a and B3LYP/3-21^b, for such compound for verification.

Keywords: Ftir; Hcv; Molecular Modeling; Ns3 Protease; Ns5a/Ns5b Junction; Pm3 And Subtype 4A.

Dept. of Botany

171. Molecular Characterization of Diarrheogenic Escherichia Coli from Libya

Mostafa Mohamed M. Ali, Zienat Kamel Mohamed, John D. Klena and Salwa Fouad Ahmed

Am. J. Trop. Med. Hyg. 86 (5): 866-871 (2012) IF: 2.59

Diarrheogenic *Escherichia coli* (DEC) are important enteric pathogens that cause a wide variety of gastrointestinal diseases, particularly in children. *Escherichia coli* isolates cultured from 243 diarrheal stool samples obtained from Libyan children and 50 water samples were screened by polymerase chain reaction (PCR) for genes characteristic of enteroaggregative *E. coli* (EAEC), enteropathogenic *E. coli* (EPEC), enterotoxigenic *E. coli* (ETEC), enterohemorrhagic *E. coli* (EHEC) and enteroinvasive *E. coli* (EIEC). The DEC were detected in 21 (8.6%) children with diarrhea; 10 (4.1%) cases were identified as EAEC, 3 (1.2%) as EPEC and 8 (3.3%) were ETEC; EHEC and EIEC were not detected. All DEC were grouped phylogenetically by PCR with the majority (> 70%) identified as phylogenetic groups A and B1. The EAEC isolates were also tested for eight genes associated with virulence using PCR. Multi-virulence (3 virulence factors) was found in 50% of EAEC isolates. Isolated EAEC possessed different virulence traits and belonged to different phylogenetic groups indicating their heterogeneity.

Keywords: *Escherichia Coli*; Enteric Pathogens; Diarrhea.

172. Morphological and Molecular Differentiation Between Egyptian Species of *Pancratium L* (Amaryllidaceae)

Azza El-Hadidy, Monier Abd El-Ghani, Wafaa Amer and Rania Hassan

Acta Biologica Cracoviensia Series Botanica, 54 (1): 7-18 (2012) IF: 0.565

Three problems exist in the taxonomy of *Pancratium* in Egypt. These involve lack of publications, lack of clarity about the relationship between recently distinguished species and lack of markers for examining the levels and patterns of variation in rare and endemic species; the latter hinders work in plant conservation genetics. In this study we reassessed the taxonomic status of the *Pancratium* species of Egypt and examined morphological and genetic variation within and between species, using specimens from different populations collected throughout its distribution range in the country. Our assessment was based on 38 macromorphological characters mainly representing vegetative parts, flowers, fruits and seeds, in addition to RAPD data. The results revealed five morphologically distinguished *Pancratium* species in Egypt, of which *P. trianthum* Herb. is newly recorded. Species identification was confirmed by two phenetic dendrograms generated with 26 quantitative morphological characters and RAPD data, while species delimitation was verified by principal component analysis. The diagnostic floral characters are those of the perianth, corona teeth, pistil, stamens, aerial scape, spathe and number of flowers. The retrieved RAPD polymorphic bands show better resolution of the morphologically and ecologically closely allied *Pancratium* species (*P. arabicum* and *P. maritimum*) and also confirm the morphological and ecological divergence of *P. tortuosum* from the other studied species. These results are supported by the constructed UPGMA dendrogram.

Keywords: Taxonomic Revision; Morphometrics; Rapd; Monocotyledons; Upgma; Reappraisal; Species Separation.

173. Biodegradation of Some Polycyclic Aromatic Hydrocarbons by *Aspergillus Terreus*

Mohamed I. A. Ali, Neveen M. Khalil and Mohamed N. Abd El-Ghany

African Journal of Microbiology Research, 6 (16): 3783-3790 (2012) IF: 0.539

In our search for new fungal isolates capable of degrading polycyclic aromatic hydrocarbons (PAHs) in soil, twenty one fungal isolates were recovered from Orman Garden, Wadi Degla Protectorate and benzene station soils. All tested fungi exhibited lignin peroxidase and manganese peroxidase activities in solid as well as in liquid cultures. However, laccase was detected in low amounts by some of the tested fungal isolates. Accordingly, laccase was eliminated from further work. *Aspergillus terreus* was superior in ligninolytic enzyme production. Hence, it was chosen for the following studies. The statistical optimum temperatures for lignin peroxidase and manganese peroxidase production by *A. terreus* were 33.6 and 33.1°C, respectively. Meanwhile lignin peroxidase and manganese peroxidase yields were maximal at pH 4.1 and 5.8, respectively. Highest ligninolytic enzyme secretions were established on D-glucose and sodium nitrate. An experiment to study biodegradation of PAHs in soil was conducted. *A. terreus*

was able to degrade 98.5% of naphthalene and 91% of anthracene in soil models.

Keywords: Biodegradation; Fungi; Polycyclic Aromatic Hydrocarbons (Pahs) Lignolytic Enzymes; Soil Model.

174. Antimicrobial Potential of Licorice: Leaves Versus Roots

Rasha H. Bassyouni, Zeinat Kamel, Ahmed Megahid and Eman Samir

African Journal of Microbiology Research, 6 (49): 7485-7493 (2012) IF: 0.539

Medicinal plants play a vital role in covering the basic health needs. They may offer a new source of antibacterial agents. The aim of this study was to screen in-vitro the antimicrobial activity of some Egyptian medicinal plants against clinical methicillin-resistant *Staphylococcus aureus* (MRSA) strains isolated from different hospitals in Egypt followed by studying the MIC and cytotoxicity of the most active one. Screening of antimicrobial activities of 70% ethanolic extracts obtained from 19 plants against 59 MRSA clinical isolates were tested by agar well diffusion method. Licorice showed the highest antimicrobial effect against all 59 MRSA isolates (leaves were more active than roots). Minimum inhibition concentrations (MICs) of licorice leaves were 8 g/ml, whereas that of Flucloxacillin range between 32 to <128 ug/ml when tested against five MRSA strains. Colorimetric cytotoxicity assay of licorice leaves extract was done on HEPG² and HCT116 cell lines and revealed that the IC₅₀ were 19.5 and 15g/ml respectively. Separation of the components in licorice leaves using thin layer chromatography (TLC) results in two active fractions identified with the help of spectroscopic analysis as inflacoumarin A and Licochalcone A. Our results reveal that the Egyptian licorice leaves extract represent a new candidate for antimicrobial agent against MRSA more than that achieved by root. This is the first report which highlights the antimicrobial activity of licorice leaves.

Keywords: Plant Extracts; Licorice; Mrsa; Antimicrobial.

175. Evaluation of the Roles of Physical (Osmotic, Gamma Irradiation and/or Heat Shock) Stress Factors on Enzyme Activities and Protein Accumulation in *Pleurotus Ostreatus* Mushroom and Its Descendent Progenies

M. E. A. Dawoud and Amira Abu-Taleb

Journal of Food, Agriculture and Environment, 10 (2): 22-32 (2012) IF: 0.517

Applications of agricultural and industrial wastes in the field of fermentation technology results in the production of many biomaterials as amino acids, enzymes, organic acids and proteins. The aim of this study was to increase the protein content of mushrooms grown on semisynthetic medium (APCEB substrate formulated from digested slaughter wastes, plant remains and KH₂PO₄ salt) by application of physical stresses on spore and mycelial inocula.

The inocula of *Pleurotus ostreatus* divisions representing three groups of spores and mature mycelia were gradually or abruptly stressed (one division was gamma irradiated, 0.0-3.0 kGy; the second was heat shocked, 25-50C and the third was osmotically stressed 0.00-150 mM NaCl). Different stressed inocula were

allowed to grow in liquid fermentation medium (APCEB) and at the end of the fermentation period different nitrogen and carbon fractions and enzyme activities were estimated in the fungal tissues.

The result showed that combined heat shock and gradual gamma irradiation of the parent developing spores (PDS) and their progenies (GDS) produced significantly higher amount of tissue proteins (166.67, 170.88%) compared to parent mature spores (PMS) and their progenies (GMS) 122.60 and 88.89%, respectively. The total amino acid content of GDS was significantly higher amount 132.77% compared with PDS, PMS and GMS (118.11, 120.20 and 84.36%, respectively). Also combined heat shock and gradual gamma irradiation resulted in the maximum increase in the activities of GOT, GPT, glutamate synthase (Gts) and glutamine synthetase (Gns) in parent developing spore (PDS) and their progenies (GDS), while glutamate dehydrogenase (G-H2) activity was decreased. Electrophoretogram down regulated 47.0 kDa intense and 12 and 80 light protein bands/GMS.

Heat shock resulted in an upregulation of light protein bands (120.0, 110.0, 96.0, 63.0 and 60.0)/GDS, PDS and PMS and down regulated intense 53.0 kDa and light 80.0, 19.0 protein bands/ GMS. Heat shock and irradiation stresses had an accumulative effects. GDS spore inocula responded to physical stress (gradual gamma irradiation, 1.75 kGy and heat shock 35-40C) and produced the maximum percent control of protein and amino acids. The new acquired characters of the PDS were transferred to their progenies GDS while that of the parent mature spore PMS did not.

Keywords: *Pleurotus Ostreatus*; Progenies; Protein Production; Gamma Irradiation; Heat Shock; Osmotic Stress; Semisynthetic Media; Protein Profile; Enzyme Activities; Nitrogen Compounds; Keto Acids.

176. Characterization of Lactic Acid Bacteria Isolated from Dairy Products in Egypt as A Probiotic

Rasha H. Bassyouni., Walla S. Abdel-all , Mostafa G. Fadl Saed Abdel-all and Zeinat kamel

Life Science Journal, 9 (4): 2924-2933 (2012) IF: 0.073

Lactobacilli belong to lactic acid bacteria (LAB), generally recognized as safe primary fermentation end product from sugars is lactic acid and that is why foods are conserved. Lactic acid bacteria have been used for improving health host. Therefore, they are an important part of intestinal flora in human and animals as probiotic. This research aimed to isolate lactic acid bacteria with significant probiotic character from different dairy products.

In this study, homo- fermentative LAB were isolated from different dairy products in Egypt. Isolates were identified by morphological, biochemical and physiological methods. Probiotic properties of isolates were investigated. The isolated bacteria were studied for antagonistic effects on clinically isolated *E.coli*, *Salmonella* spp. *Micrococcus* spp., *Staphylococcus* spp. A collection of fifty four isolates were obtained. Eight isolates from different dairy products were observed as potential probiotic safe for human use; where they found to be tolerant to low pH and bile salt and effective against isolated *E.coli*, *Salmonella* spp. *Micrococcus* spp. All isolates were screened for enzymatic activity using API ZYM Kits and antibiotic sensitivity. Biochemical and physiological results indicated that they were found to be related to the genus *Lactobacillus* and suggested to belong to *L. casei* (4 isolates), *L. Acidophilus* (3 isolates) and *L.*

lactis (1 isolates) and that were effective on the isolated E. coli, Salmonella spp. Staphylococcus spp. and they have enzymatic activity galactosidase was produced, which is beneficial for lactose intolerance. Lactobacillus spp. produced enzymes including leucine arylamidase, cysteine arylamidase, acid phosphatase, naphthol-AS-BI-phosphohydrolase, galactosidase, galactosidase, -glucosidase, -glucosidase and N-acetyl--glucosamidase so we concluded that human milk, yogurt and raw milk are considered a good source of potential probiotic strains also the isolated bacteria had no haemolytic activity so it is considered as a great potential probiotic and safe for human use.

Keywords: Lactobacilli; Probiotic; Bile Salt; Acid Tolerance; Enzymatic Activity; Antimicrobial Activity; Hemolytic Activity.

177. Solid-State Fermentation for the Production of Dextran from *Saccharomyces Cerevisiae* and Its Cytotoxic Effects

Tarek A. A. Moussa and Neveen M. Khalil

Life Science Journal, 9 (4): 2210-2218 (2012) IF: 0.07

Maximum yield of dextran was obtained when using ground date seeds. Different concentrations of date seeds were applied and the highest dextran production was achieved at 6 g/flask. Extraction of dextran was carried out using ethanol. The molecular weight of the purified dextran was 67 kDa by GPC. Spectral analysis showed that dextran contains D-glucose units in a linear chain with consecutive (1,6) linkages. The melting temperature (T_m) was 70.56°C and the value of ΔH was -290.57 mJ, as determined by DSC analysis. The TGA clearly showed the thermal stability of purified dextran. The analysis showed three stages of degradation process. An initial loss of about 0.577 mg (2.17%) weight occurred at 30-75°C, second loss of about 0.822 mg (3.1%) weight occurred at 75-125°C and the third loss of about 0.427 mg (1.61%) weight occurred at 125-175°C. Surface morphology of dextran using scanning electron microscopy showed dextran has a crystalline form which is attributed to the presence of hydroxyl groups which increase crystallinity of dextran, also, dextran showed a compact structure characterized by transverse arrangement which reflects brittleness of dextran and seems to have a porous structure. The cytotoxicity assays on human normal melanocytes (HFB 4) revealed no toxic effect. However, a clear decrease in cell survival was observed in case of human liver carcinoma (HEPG 2) and cervical carcinoma (HELA) tumor cell lines.

Keywords: Solid State Fermentation; Agricultural Wastes; *Saccharomyces Cerevisiae*; Dextran; FT-IR; Antitumor.

178. Potential for Improving Healthy and Productivity of Soybean by Plant Growth Promoting Rhizobacteria

Heba S. Shehata, Eman R. Hamed and Mona E. Eleiwa

Aust. J. Basic And Appl. Sci, 6 (4): 98-107 (2012)

A pot and field experiment were conducted to evaluate some rhizobacteria namely *Pseudomonas fluorescens* and *Bacillus subtilis*. The pot experiment was executed to evaluate the probable suppressive effect of rhizobacteria as bioagents against *Macrophomina phaseolina*, *Rhizoctonia solani* and *Sclerotium rolfsii* under artificially infested soil. Results showed that co-

inoculation of soybean with rhizobacteria led to a significant decrease in pre- and post-emergence damping-off caused by all pathogens under investigation. In addition to enhance the nodulation status under uninfested or infested soil. Field experiments were carried out in Etay-El Barooud to evaluate the promotive and suppressive disease effects of rhizobacteria on nodulation, plant growth and yield of soybean. Results showed that the inoculation with rhizobacteria led to a significant increase in the nodulation status, shoot dry matter and N-content after 30, 60, 90 days of planting. Moreover, the co-inoculation of *Bacillus subtilis* with *Bradyrhizobium* sp. Salient superiority in suppressive disease. The obtained results explained that the synergy between rhizobacteria (*Bacillus subtilis*, *Pseudomonas fluorescens*) and *Bradyrhizobium* sp. considered the efficient manner to save the protection against the phytopathogens and promote the nodulation and symbiotic nitrogen fixation leading to a high quality yield of soybean.

Keywords: *Bradyrhizobium* Sp.; Rhizobacteria; *Bacillus Subtilis*; *Pseudomonas Fluorescens*; PGR; Damping-off; Soybean.

179. Nutritional Value and Biomass Yield of the Edible Mushroom *Pleurotus Ostreatus* Cultivated on Different Wastes in Egypt

Ramy S. Yehia

Innovative Romanian Food Biotechnology, 11: 9-14 (2012)

Mushroom yield (number of fruit bodies, fresh biomass gain and pileus diameter) and biochemical composition (proteins, fats, carbohydrates, ash, fiber, moisture, metals and amino acids). *Pleurotus ostreatus* was evaluated using different natural wastes for cultivation either singly or in combination. The most suitable substrate for fresh, high number, large sized pileus yield with high nutritional facts was the combined mixture of wheat and rice straws (1:1). This mushroom was rich in proteins, fibers, carbohydrates, metals with low fat content. *P. ostreatus* cultivated in the combined mixture was found to be rich in amino acids with glutamic and aspartic acids being of the highest quantities. Paddy and bamboo leaves not suited the quality and quantity of mushroom gain.

Keywords: Natural Wastes; *P. Ostreatus*.

180. The Role of Biofertilizers and/Or Some Micronutrients on Wheat Plant (*Triticum Aestivum* L.) Growth in Newly Reclaimed Soil

Mona E. Eleiwa, Eman R. Hamed and Heba Sh. Shehata

Journal of Medicinal Plants Research, 6 (17): 3359-3369 (2012)

The effect of biofertilizers (inoculation with different bacterial isolates), foliar spraying with some micronutrients and their interaction on growth, physiological parameters and nutrient content of wheat plants grown on newly reclaimed soil were studied. The growth parameters, some physiological parameters and nutrient contents of wheat plants were significantly increased by inoculating wheat grains with different bacteria as compared with un-inoculated (control). The highest values of all mentioned parameters were obtained by using *Azospirillum brasilense* followed by *Azotobacter chroococcum* and *Bacillus polymyxa* in decreasing order. Foliar spraying treatments significantly increased the growth parameters, physiological parameters as well as nutrient content of wheat plants.

compared with control treatment. Highest values were obtained by using (Mn+Fe+Zn) treatment followed by Zn, Fe and Mn in decreasing order. Micronutrients in wheat plants differed as the foliar treatments were differed, so application of any micronutrient individually significantly increased its content and enhanced the content of other micronutrients in wheat. Used biofertilizers and foliar spraying with micronutrients significantly affected all the studied parameters of wheat plants, the highest were obtained by inoculating wheat grains with *A. brasilense* and spraying the plants with (Mn+Fe+Zn) treatment, while the lowest values were attained by un-inoculated grains (control) and spraying the wheat plants with tap water (control). It can be concluded that the data collected proves that the use of *Azospirillum*, *azotobacter* or *Bacillus*, in combination with foliar application with micronutrients (Mn+Fe+Zn) can lead to higher wheat yield.

Keywords: Biofertilizers; Wheat Plants; Nutrients Content; Physiological Parameters; Foliar Spray; Micronutrient; Bacterial Isolates.

181. Antifungal Activity of Rice Straw Extract on Some Phytopathogenic Fungi

Ramy S. Yehia and Ahmed M. Saleh

African Journal Of Biotechnology, 11(71): 13586-13590 (2012)

The antifungal activity of allelochemicals extracted from rice straw on the radial growth rate and the activity of some hydrolyzing enzymes of *Aspergillus flavus*, *Alternaria alternata* and *Botrytis cinerea* were studied in vitro. Five different concentrations (2, 4, 6, 8 and 10%, w/v) of water, methanol and acetone extracts of rice straw were tested. All extracts significantly ($P < 0.05$) inhibited the radial growth rate and protease, carboxymethyl cellulase (CMCase) and amylase activities of the tested fungal species. The most potent solvent was methanol. The present study suggests that rice straw extract had antifungal properties, thus it can be used as a natural alternative approach to synthetic fungicide.

Keywords: Rice Straw; Allelochemicals; Antifungal; *Aspergillus flavus*; *Alternaria Alternata*; *Botrytis Cinerea*; Amylase; Protease; Carboxymethyl Cellulase.

182. Effect of the Purification of Antidermatophytic Proteins from *Nigella Sativa* on Four Zoophilic Species

Neveen S. Geweely and Saleha Y. M. Alakilli

African Journal of Biotechnology, 11(39): 9422-9434 (2012)

The antidermatophytic activities of proteins which are extracted from four plant species (*Carum carvi*, *Cymbopogon citratus*, *Moringa oleifera* and *Nigella sativa*) on four zoophilic dermatophytes (*Microsporum canis*, *Microsporum equinum*, *Trichophyton mentagrophytes* and *Trichophyton verrucosum*) were evaluated in this study. The crude proteins of *N. sativa* had the broadest significant spectrum of antidermatophytic activity on the tested dermatophytes as well as the greatest antioxidant activity (95.11%) and the highest protein content (82 mg/ml). 17 amino acids were found in the four tested plant proteins with *N. sativa* protein having the highest content of amino acid (347.21g/ml). *N. sativa* protein had the greatest effect on the fungal cell permeability of all the tested zoophilic dermatophytes. Purification of *N. sativa* protein on Sephadex G-100 column

showed two peaks of protein (Pr1 and Pr2) as well as increasing antidermatophytic activities. Complete purification of the most active fraction (Pr2) on diethylaminoethyl (DEAE)-Sephadex eluted one single peak with increasing antidermatophytic activity (7.6 cm) against the most sensitive pathogen (*M. canis*), representing 1.43 fold purification of the crude protein. The molecular weights of the purified *N. sativa* proteins (Pr1 and Pr2) were 42.7 and 31 kDa, respectively. The highest antidermatophytic activity of Pr2 was observed at a pH of 7 and temperature of 20°C. Na⁺, K⁺, Ca²⁺ and Mg²⁺ decreased the antidermatophytic activity of the pure protein of *N. sativa*.

Keywords: Dermatophytes; Plant; Protein; Purification.

183. The First Record of Biological Activities of the Egyptian Red Algal Species *Compsopogon helwanii* Helwanii

Sanaa M. M. Shanab and Emad A. Shalaby

Int. J. Of Bioscience, Biochemistry And Bioinformatics, (2012)

Compsopogon helwanii is a new Egyptian species of the genus *compsopogon*, collected (in 1999) from Ain Helwan Spring. It dominated all over the year. Neither this new red alga species, nor the other known eight *compsopogon* species were subjected to any physiological or biochemical studies. This is the first investigation concerning the biological activities of this new algal species. Methanolic extract of this alga was tested for antimicrobial (G+ve, G-ve bacteria, yeast, fungi), anti-algal (green and cyanobacteria), antioxidant (DPPH and ABTS assays) and anticancer (EACC) activities. The obtained results correlated the biological activities to the contents of phycobilin pigments, spermine derivatives (GC/MS) and other active constituents in this algal extract.

Keywords: Anticancer; Antimicrobial; Antioxidant; *Compsopogon Helwanii*; New Species.

184. Bioremoval Capacity of Three Heavy Metals by Some Microalgae Species (Egyptian Isolates)

Sanaa Shanab, Ashraf Essa and Emad Shalaby

Plant Signaling & Behavior, 7(3): 1-8 (2012)

Three fresh water microalgal isolates [*Phormidium ambiguum* (Cyanobacterium), *Pseudochlorococcum typicum* and *Scenedesmus quadricauda* var *quadrispina* (Chlorophyta)] were tested for tolerance and removal of mercury (Hg²⁺), lead (Pb²⁺) and cadmium (Cd²⁺) in aqueous solutions as a single metal species at conc. 5–100mg/ L under controlled laboratory conditions. The obtained results showed that Hg²⁺ was the most toxic of the three metal ions to the test algae even at low concentration (20 mg/L). While lower concentration of Pb²⁺ and Cd²⁺ (5–20mg/ L) enhanced the algal growth (chlorophyll a and protein), elevated concentrations (40–100mg/ L) were inhibitory to the growth. The results also revealed that *Ph. ambiguum* was the most sensitive alga to the three metal ions even at lower concentrations (5 and 10mg/ L) while *P. typicum* and *S. quadricauda* were more tolerant to high metal concentrations up to 100 mg / L. The bioremoval of heavy metal ions (Hg²⁺, Pb²⁺ and Cd²⁺) by *P. typicum* from aqueous solution showed that the highest percentage of metal bioremoval occurred in the first 30 min of contact recording 97% (Hg²⁺), 86% (Cd²⁺) and 70% (Pb²⁺). Transmission electron microscopy (TEM) was used to

study the interaction between heavy metal ions and *P. typticum* cells. At ultrastructural level, an electron dense layers were detected on the algal cell surfaces when exposed to Cd, Hg and Pb. At the same time, dark spherical electron dense bodies were accumulated in the vacuoles of the algal cells exposed to Pb. Excessive accumulation of starch around the pyrenoids were recorded as well as deteriorations of the algal cell organelles exposed to the three metal ions.

Keywords: Microalgae; Heavy Metals; Bioremoval; Histological Studies.

Dept. of Chemistry

185. Rheokinetics of Ring-Opening Metathesis Polymerization of Bio-Based Castor Oil the rmoset

Samy A. Madbouly, Ying Xia and Michael R. Kessler

Macromolecules, 45: 7729-7739 (2012) IF: 5.167

Ring-opening metathesis polymerization (ROMP) of *forbornenyl*-functionalized castor oil has been evaluated using small-amplitude oscillatory shear flow experiments as a function of angular frequency, temperature and curing time. At the onset temperature of the curing process, an abrupt increase in dynamic shear modulus, G' and G'' and complex shear viscosity, η^* , was observed during the dynamic temperature ramps (2 °C/min heating rate) of the sample over a wide range of angular frequencies. A dramatic increase in zero-shear viscosity, η_0 , was also observed at the gelation temperature, T_{gel} . The value of T_{gel} obtained from the abrupt increase in η_0 was found to be in good agreement with the value evaluated from the crossover point of G' and G'' . The real time curing kinetics was investigated under isothermal conditions over a wide range of angular frequencies at different constant curing temperatures (40, 45, 50 and 55 °C). The isothermal gelation kinetics was found to be strongly curing temperature dependent; i.e., the higher the curing temperature, the faster the gelation process. Both G' and G'' showed a power law relationship with angular frequency at the gel point, with critical power law exponents at the gel point in good agreement with the value predicted using percolation theory. Furthermore, η_0 and the equilibrium storage modulus, G_{eq} , were found to be well described by power law scaling functions with the relative distance from the gel point. The molecular dynamics and thermal stability of the fully cured sample were also investigated by dynamic mechanical analysis and thermogravimetry, respectively.

Keywords: Rheology; Gelation Kinetics; Ring Opening Polymerization.

186. Electrocatalytic Oxidation of Methanol At Tantalum Oxide-Modified Pt Electrodes

Jahangir Masud, Muhammad T. Alam, Zaenal Awaludin, Mohamed S. El-Deab-Takeyoshi Okajima and Takeo Ohsaka

J Power Sources, 220: 399-404 (2012) IF: 4.951

The current study addresses the electrocatalytic activity of tantalum oxide (TaOx)-modified Pt electrode as a novel catalyst for methanol oxidation in acidic media. The modified Pt electrode is shown to support a larger oxidation current of methanol compared to that obtained at the unmodified Pt electrode concurrently with a favorable significant shift of the onset potential of methanol oxidation. Tafel plots, with a slope close to

0.118 V decade⁻¹, were obtained for methanol oxidation at the unmodified and TaOx-modified Pt electrodes, reflecting that the methanol oxidation proceeds with the first electron transfer as the rate-determining step. The observed enhancement was attributed to a favorable d-d metal-metal oxide interaction which changes the electronic property of Pt and hence enhances the oxidation of the adsorbed reaction intermediates (e.g., COads). Moreover, a possible contribution of the OH spillover via a so-called "bifunctional mechanism" is proposed. The influence of the temperature on the oxidation current of methanol at the TaOx-modified Pt electrode is investigated and apparent activation energy, E_a , for methanol oxidation is calculated as 39 kJ mol⁻¹ at a specific potential. The proposed catalyst showed a good enhancement for methanol oxidation for a prolonged time of continuous potentiostatic electrolysis.

Keywords: Electrocatalysis; Metal Oxides; Fuel Cells; Electronic Interaction; Methanol Oxidation.

187. Construction and Performance Characteristics of New Ion Selective Electrodes Based on Carbon Nanotubes for Determination of Meclofenoxate Hydrochloride

Rasha M. El-Nashar, Nour T. Abdel Ghani and Sherif M. Hassan

Analytica Chimica Acta, 730: 99-11 (2012) IF: 4.555

This work offers construction and comparative evaluation the performance characteristics of conventional polymer (I), carbon paste (II) and carbon nanotubes chemically modified carbon paste ion selective electrodes (III) for meclofenoxate hydrochloride are described. These electrodes depend mainly on the incorporation of the ion pair of meclofenoxate hydrochloride with phosphomolybdic acid (PMA) or phosphotungstic acid (PTA). They showed near Nernstian responses over usable concentration range 1.0×10^{-5} to 1.0×10^{-2} M with slopes in the range 55.15–59.74 mV (concentration decade)⁻¹. These developed electrodes were fully characterized in terms of their composition, response time, working concentration range, life span, usable pH and temperature range. The electrodes showed a very good selectivity for Meclo with respect to a large number of inorganic cations, sugars and in the presence of the degradation product of the drug (p-chloro phenoxy acetic acid). The standard additions method was applied to the determination of MecloCl in pure solution, pharmaceutical preparations and biological samples. Dissolution testing was also applied using the proposed sensors.

Keywords: Meclofenoxate Ion Selective Electrode Potentiometry Polyvinyl Chloride Membrane Carbon Paste Electrodes Carbon Nanotube Chemically Modified Carbon Paste Electrodes.

188. A Novel Sensor of Cysteine Self-Assembled Monolayers Over Gold Nanoparticles for the Selective Determination of Epinephrine in Presence of Sodium Dodecyl Sulfate

Nada F. Atta, Ahmed Galal and Ekram H. El-Ads

Analyst, 137: 2658-2668 (2012) IF: 4.23

A novel sensor of cysteine self-assembled monolayers over gold nanoparticles modified gold electrode has been constructed for the determination of epinephrine in presence of sodium dodecyl sulfate (Au/Aunanano-Cys...SDS). Electrochemical investigation

and characterization of the modified electrode are achieved using cyclic voltammetry, linear sweep voltammetry and scanning electron microscopy. The Au/Aunano-Cys...SDS electrode current signal is remarkably stable via repeated cycles and long term stability, due to the strong Au–S bond, compared to the Au/Aunano electrode. The catalytic oxidation peak currents obtained from linear sweep voltammetry (LSV) increased linearly with increasing epinephrine concentrations in the range of 2 to 30 mol L⁻¹ and 35 to 200 mol L⁻¹ with correlation coefficients of 0.9981 and 0.9999 and a limit of detection of 0.294 nmol L⁻¹ and 1.49 nmol L⁻¹, respectively. The results showed that Au/Aunano-Cys...SDS can selectively determine epinephrine in the coexistence of a large amount of uric acid and glucose. In addition, a highly selective and simultaneous determination of tertiary mixture of ascorbic acid, epinephrine and acetaminophen is explored at this modified electrode. Excellent recovery results were obtained for determination of epinephrine in spiked urine samples at the modified electrode. Au/Aunano-Cys...SDS can be used as a sensor with excellent reproducibility, sensitivity and long term stability.

Keywords: Sensor; Gold Nanoparticles; Self-Assembly Monolayer; Epinephrine; Surfactant.

189. Synthesis and Characterization of SiC and SiC/Si₃N₄ Composite Nano Powders from Waste Material

M.F. Zawrah, M.A. Zayed and Moustafa R.K. Ali

J Hazard Mater, 227-228: 250-256 (2012) IF: 4.173

In the present work, nano silicon carbide has been prepared by pyrolysis of rice-husk ashes as starting materials. Three rice-husk ash samples having different features were used. The first was coarse-grained rice husk ash (fired husk as is), the second was fine rice husk ash (hand-ground), while the third was ball milled one. Effect of ball milling of the starting ashes for 6 h on the formation of nano SiC was investigated and compared with those prepared without milling. The particle sizes of the prepared SiC materials were affected by the milling process. The particle sizes of the obtained nano SiC from ball milled starting materials were smaller than those prepared without milling. The pyrolysis conditions, i.e. the temperature and atmosphere were optimized. The optimum firing temperature to obtain well crystalline nano SiC was 1550°C. The effect of pyrolysis atmosphere, i.e. argon, vacuum and nitrogen was also demonstrated. The pyrolysis in argon exhibited lower efficiency on the formation of SiC than vacuum; while the pyrolysis in nitrogen atmosphere led to formation of SiC/Si₃N₄ nano-composite.

Keywords: Nano SiC; Rice Husk Ash; Pyrolysis; SiC/Si₃N₄ Nano-Composite.

190. Enhancement of Stabilizing Properties of Double-Base Propellants using Nano-Scale Inorganic Compounds

M.A. Zayed, Salah E.M. El-Begawy and Hossam E.S. Hassan

J. Hazard Mater, 227-228: 274-279 (2012) IF: 4.173

The use of inorganic stabilizers for double-base propellants in literature is scanty; therefore five samples (S1–S5) of different percentages (2–4%) of nano-clinoptilolite were investigated as new inorganic stabilizers for double-base propellants (DBPs). The

grain size of clinoptilolite stabilizer played an important role in the stabilization effect. As the grain size of stabilizer decreases, the surface area of stabilizer increases and the ability to absorb pronounce amount of hazardous nitrogen oxides increases. In this work clinoptilolite in nano-scale (30 nm) has been used to obtain higher stabilizing effect for DBPs. The evaluation process has been performed through the classical thermal stability tests (Bergmann–Junk and calorimetric tests), in comparison with thermal analyses measurements (TGA and DSC) and kinetic parameters calculation such as activation energy (E_a), enthalpy of activation (H), Gibbs free energy of activation (G), entropy of activation (S) and frequency factor (A), which calculated using Coats–Redfern and Horowitz–Metzger methods. The results for the new stabilizers were compared with that for the classical one (N, N-diethyldiphenyl urea, C1). It has been found that the samples containing new stabilizer with percentages (3.0, 3.5 and 4.0%) showed better stability effect for DBPs than the classical one. The efficiency of stabilization of each inorganic stabilizer to DBPs is also rationalized and correlated with its structure.

Keywords: Inorganic Stabilizers; Double-Base Propellants; Classical Thermal Stability Tests; Thermal Analyses (Tg And Dsc).

191. Influence of Cerium (Iii) Ions on Corrosion and Hydrogen Evolution of Carbon Steel in Acid Solutions

F. El-Taib Heakal, N.S. Tantawy and O.S. Shehata

Int J Hydrogen Energ, 37: 19219-19230 (2012) IF: 4.054

This paper intended to investigate the influence of rare earth Ce(III) ions on the corrosion behavior of carbon steel in two acid solutions (0.5 M HCl and 0.25 M H₂SO₄) in order to control the rate of hydrogen evolution in those systems. Potentiodynamic polarization and electrochemical impedance spectroscopy (EIS) tests were used for corrosion rate and electrochemical impedance evaluation. SEM was used to examine the sample surfaces immersed in acid solutions containing the optimal threshold Ce(III) concentration (0.1 mM). All results reveal that the corrosion resistance of carbon steel in HCl is superior to that in H₂SO₄ due to the higher rate of hydrogen production in the latter. A model for the corrosion process mechanism and inhibition by Ce(III) salt for carbon steel in the two tested media is proposed.

Keywords: A. Carbon Steel; B. EIS; B. SEM; C. Acidic Corrosion; C. Hydrogen Evolution.

192. Electrocatalytic Activity of Nickel Oxide Nanoparticles-Modified Electrodes: Optimization of the Loading Level and Operating Ph Towards the Oxygen Evolution Reaction

Ibrahim M. Sadiq, Ahmad M. Mohammad, Mohammed E. El-Shakre and Mohamed S. El-Deab

Int J Hydrogen Energ, 37: 68-77 (2012) IF: 4.054

The current study addresses the superior electrocatalytic activity of nickel oxide nanoparticles (nano-NiOx) modified GC, Au and Pt electrodes towards the OER. The electrodeposition of nickel oxide nanoparticles (with an average particle size of 80 nm) are believed to enhance the OER reaction. NiOOH phase, as shown from XRD data, participates in the OER mechanism in such a way to facilitate the charge transfer during various steps in the

reaction mechanism through a reversible transformation of NiOOH to NiO₂. Optimizing the loading level and the operating pH of the proposed catalyst has been carried out.

Keywords: Nanostructures; Water Electrolysis; Metal Oxides; Electrocatalysis.

193. the rmodynamicsof the Interaction of Ruthenium (Iii) PolyaminecarboxylateComplexes with Bio-Relevant Ligands. Deactivationof the Complexes as no Scavengers by Thiol Ligands Scavengers by Thiol Ligands

Safaa S. Hassan, Mohamed M. Shoukry and Rudi van Eldik

Dalton Trans., 41: 13447-13453 (2012) IF: 3.838

The acid–base and complex-formation equilibria of [Ru (H₂dtpa) (H₂O)], where dtpa = diethylenetriaminepentaacetate, with a series of bio-relevant ligands having various functional groups, viz. thiol, amine, imidazole and carboxylate, were investigated using potentiometric and spectrophotometric techniques. The pK_a values for [Ru(H₂dtpa)(H₂O)] were found to be 2.28 and 3.48 for the uncoordinated carboxylic acid groups and 8.83 for the coordinated water molecule. The complexes formed are of 1 : 1 stoichiometry and their formation-constants were determined. The effect of dioxane on the acid–base and complex formation equilibria of the RuIII complex was studied. The displacement reaction of coordinated NO by the investigated ligands showed that thiols can compete with NO in their reaction with RuIII(dtpa)(H₂O)]₂. The results reveal that the RuIII complex is deactivated as a NO scavenger by thiolate ligands.

Keywords: Ru(III) Complexes; Ethylenetriaminepentaacetate; Thiols; No Scavenger.

194. Synthesis, Characterization and Application of Enrofloxacin Complexes as the rmal Stabilizers for Rigid Poly (Vinyl Chloride)

Nadia E. A. El-Gamel Riham R. Mohamed and M. A. Zayed

Dalton Trans., 41: 1824-1831 (2012) IF: 3.838

Synthesis and characterization of both binary Co(II)- (1), Ni(II)- (2) complexes with enrofloxacin drug, (HL1) and ternary Co(II)- (3), Ni(II)- (4) complexes in presence of DL-alanine (H₂L₂) are reported using physico-chemical techniques. The antimicrobial activity of these complexes has been screened against two Gram-positive and two Gram-negative bacteria. Antifungal activity against two different fungi has been evaluated and compared with reference drug. All the binary and ternary complexes showed remarkable potential antimicrobial activity higher than the recommended standard agents. Ni (II)- complexes exhibited higher potency as compared to the parent drug against bacterial and fungal strain. In addition, it was of interest to investigate the reported complexes as thermal stabilizers and co-stabilizers for rigid PVC in air at 180°C. Their high stabilizing efficiency is detected by their high induction period values (T_s) compared with some of the common reference stabilizers used industrially, such as dibasic lead carbonate (DBLC) and calcium-zinc soap. Blending these complexes with some of the reference stabilizers in different ratios had a synergistic effect on both induction period as it gave better thermal stability and lower extent of discoloration. The stabilizing efficiency is attributed at least

partially to the ability of the metal complex stabilizer to be incorporated in the polymeric chains, thus disrupting the chain degradation and replace the labile chlorine atoms on PVC chains by a relatively more s moiety of the inorganic stabilizer. Their amenability to use as a biomedical additives for PVC, has afforded them great potential for various medical applications.

Keywords: Synthesis; Characterization; Application; Enrofloxacin.

195. The Role of Ni in the Surface Stability of Cu-Al-Ni Ternary Alloys in Sulfate-Chloride Solutions

W.A. Badawy, M. El-Rabee and N.H. Helal H. Nady

Electrochim Acta, 71: 50-57 (2012) IF: 3.832

The stability of Cu-Al-Ni ternary alloys used in the manufacturing of NaCl and Na₂SO₄ from Lake Qaroun in Egypt was investigated in sulfate-chloride electrolytes. Different electrochemical techniques were used. The results show that the increase in the nickel content improves the stability of the ternary alloys due to formation of a stable barrier film. The barrier film behaves like an ideal capacitor and its stability is affected by the chloride ion concentration. An equivalent circuit model for the electrode/electrolyte interface was proposed and the experimental impedance data were fitted to theoretical data according to this model. The surface morphology and barrier layer constituents were investigated by SEM/EDAX unit.

Keywords: Chloride Ions; Cu-Al-Ni Alloys; Cyclic Voltammetry; Impedance; Passive Films.

196. Gold Nanoparticles-Coated Poly (3,4-Ethylene-Dioxythiophene) for the Selective Determination of Sub-Nano Concentrations of Dopamine in Presence of Sodium Dodecyl Sulfate

Nada F. Atta, Ahmed Galal and Ekram H. El-Ads

Electrochim Acta, 69: 102-111 (2012) IF: 3.832

For the first time, a novel electrochemical sensor; gold nanoparticles-coated poly(3,4-ethylenedioxythiophene) polymer modified gold electrode in presence of SDS (Au/PEDOT-Aunano...SDS) was developed by the electrodeposition of gold nanoparticles on poly(3,4-ethylene-dioxythiophene) (PEDOT) modified gold electrode for the selective determination of dopamine (DA) in presence of uric acid (UA) and ascorbic acid (AA) in presence of sodium dodecyl sulfate (SDS). Synergism between the composite of conducting polymer matrix and gold nanoparticles in presence of SDS for electron transfer enhancement of DA is explored. Electrochemical investigation and characterization of the modified electrode are achieved using cyclic voltammetry, electrochemical impedance spectroscopy, scanning electron and atomic force microscopies. The oxidation current signal of DA is remarkably stable via repeated cycles and has unique long term stability. Very small peak potential separation (E_p), almost zero or 15 mV is also obtained by repeated cycles indicating unusual high reversibility. The use of SDS in the electrochemical determination of DA using linear sweep voltammetry at Au/PEDOT-Aunano modified electrode resulted in determining DA at very low concentrations. The DA concentration could be measured in the linear range of 0.5–20 mol L⁻¹ and 25–140 mol L⁻¹ with correlation coefficients of 0.9978 and 0.9987 and detection limits of 0.39 nmol L⁻¹ and 1.55 nmol L⁻¹,

respectively. The validity of using this method in the determination of DA in human urine was also demonstrated. It has been shown that modified electrode can be used as a sensor with high reproducibility, sensitivity, selectivity and long term stability.

Keywords: Sensor; Pedot; Gold Nanoparticles; Sds; Dopamine; Ascorbic Acid.

197. Probing Cysteine Self-Assembled Monolayers Over Gold Nanoparticles-Towards Selective Electrochemical Sensors

Ahmed Galal, Nada F. Atta and Ekram H. El-Ads

Talanta, 93: 264-273 (2012) IF: 3.794

Cysteine forms self-assembled monolayers over gold nanoparticles. Based on this knowledge, a novel electrochemical sensor (Au-Aunano-Cys-SDS) has been constructed by the formation of self-assembly monolayer (SAM) of cysteine on gold-nanoparticles modified gold electrode (Au-Aunano-Cys) to be utilized for determination of dopamine in the presence of sodium dodecyl sulfate (SDS). Electrochemical investigation and characterization of the modified electrode sensor was achieved using cyclic voltammetry, electrochemical impedance spectroscopy, scanning electron and atomic force microscopies. Au-Aunano-Cys electrode in the presence of SDS gave comparable high current response to that of the gold nanoparticles modified gold electrode (Au-Aunano). The Au-Aunano-Cys-SDS electrode current signal was remarkably stable via repeated cycles and long term stability due to the strong Au S bond. Very small peak separation, almost zero or 15 mV peak separation was also obtained by repeated cycles indicating unusual high reversibility. The oxidation peak current was determined to be linearly dependent on the dopamine concentration. A resulting calibration curve using square wave voltammetry (SWV) was obtained over concentration range of 30–100 mol L⁻¹ and 120–320 mol L⁻¹ with correlation coefficients of 0.996 and 0.994 and a limit of detection of 16 and 57 nmol L⁻¹, respectively. Using differential pulse voltammetry (DPV), a highly selective and simultaneous determination of tertiary mixture of ascorbic acid AA, dopamine and acetaminophen APAP was explored at this modified electrode. It has been demonstrated that Au-Aunano-Cys-SDS electrode can be used as a sensor with excellent reproducibility, sensitivity and long term stability.

Keywords: Electrochemical Sensor; Gold Nanoparticles; Self-Assembly Monolayer; Neurotransmitters; Ascorbic Acid.

198. Potentiometric Determination of Tolterodine in Batch and Flow Injection Conditions

Marwa M. Sakr and Rasha M. El Nashar

Talanta, 96 153-160 (2012) IF: 3.794

Two new ion-selective electrodes of the plastic membrane type for the determination of Tolterodine (Tol) were prepared. These electrodes depend on the incorporation of the ion-exchangers of the above mentioned drug with phosphotungestic acid (PTA) or Silicotungestic acid (STA) in a PVC matrix. A comparative study is made between the performance characteristics of electrodes containing ion-exchanger in batch and FIA conditions. The usable concentration range of the electrodes was found to be (1.0 × 10⁻⁵–1.0 × 10⁻² and 5.0 × 10⁻⁵–1.0 × 10⁻² M) in batch and FIA

conditions, respectively. The electrodes have nearly the same usable concentration, pH range and exhibited high selectivity toward Tol in the presence of many inorganic cations and can be used in biological fluids such as urine and plasma. The dissolution profile of the investigated drug as well as its assay in pure and pharmaceutical preparations was performed and the results were relatively accurate and precise as indicated by the recovery values and coefficients of variation.

Keywords: Tolterdine; Pharmaceutical Analysis; Dissolution Testing.

199. Flow Injection Catalase Activity Measurement Based on Gold Nanoparticles/ Carbon Nanotubes Modified Glassy Carbon Electrode

Rasha Mohamed El Nashar

Talanta, 96 161-167 (2012) IF: 3.794

Amperometric flow injection method of hydrogen peroxide analysis was developed based on catalase enzyme (CAT) immobilization on a glassy carbon electrode (GC) modified with electrochemically deposited gold nanoparticles on a multiwalled carbon nanotubes/chitosan film. The resulting biosensor was applied to detect hydrogen peroxide with a linear response range 1.0 × 10⁻⁷–2.5 × 10⁻³ M with a correlation coefficient 0.998 and response time less than 10 s. The optimum conditions of film deposition such as potential applied, deposition time and pH were tested and the flow injection conditions were optimized to be: flow rate of 3 ml/min, sample volume 75 µl and saline phosphate buffer of pH 6.89. Catalase enzyme activity was successfully determined in liver homogenate samples of rats, raised under controlled dietary plan, using a flow injection analysis system involving the developed biosensor simultaneously with spectrophotometric detection, which is the common method of enzymatic assay.

Keywords: Catalase; Gold Nanoparticles; Carbon Nanotubes; Flow Injection Analysis; Biosensors; Modified Glassy Carbon Electrode; Amperometric Detection

200. Novel Sensor Based on Carbon Paste/Nafion® Modified with Gold Nanoparticles for the Determination of Glutathione

Nada F. Atta, Ahmed Galal and Shereen M. Azab

Analytical And Bioanalytical Chemistry, 404: 1661-1672 (2012) IF: 3.778

Several problems for the direct electrochemical oxidation of reduced glutathione (GSH) challenge the usage of electroanalytical techniques for its determination. In this work, the electrochemical oxidation of GSH catalyzed by gold nanoparticles electrodeposited on Nafion® modified carbon paste electrode in 0.04 mol L⁻¹ universal buffer solution (pH 7.4) is proved successful. The effect of various experimental parameters including, pH, scan rate and stability on the voltammetric response of GSH was investigated. At the optimum conditions, the concentration of GSH was determined using differential pulse voltammetry (DPV) in two concentration ranges: 0.1 × 10⁻⁷ to 1.6 × 10⁻⁵ mol L⁻¹ and 2.0 × 10⁻⁵ to 2.0 × 10⁻⁴ mol L⁻¹ with correlation coefficients 0.9988, 0.9949 and the limit of detections (LOD) are 3.9 × 10⁻⁹ mol L⁻¹ and 8.2 × 10⁻⁸ mol L⁻¹, respectively which confirmed the sensitivity of the electrode. The high

sensitivity, wide linear range, good stability and reproducibility and the minimal surface fouling make this modified electrode useful for the determination of spiked GSH into urine samples and in tablet with excellent recovery results were obtained.

Keywords: Glutathione; Sensor; Carbon Paste Electrode; Gold Nanoparticles; Nafion.

201. Enhanced Corrosion Resistance of Magnesium Alloy Am60 by Cerium (Iii) in Chloride Solution

F. El-Taib Heakal, O.S. Shehata and N.S. Tantawy

Corros Sci, 56: 86-95 (2012) IF: 3.734

Cerium(III) was utilised to enhance the corrosion resistance of AM60 in NaCl solution. Ce³⁺ can suppress corrosion deterioration up to 1.0 mM. Beyond that level corrosion rate increases till a steady value. Surface film resistance increases with time evolution until 24 h, then decreases and stabilizes. The converted film after 240 h immersion exhibits self-healing and thickening when re-exposed to plain chloride solution. SEM and EDX confirmed that when Ce is present as additive in solution, more compact coating is formed better than its presence as a post coating on the alloy surface before being immersed in the corrosive environment

Keywords: A. Magnesium; B. Eis; B. Polarisation; B. Sem; C. Neutral Inhibition.

202. Impact of Chloride and Fluoride Additions on Surface Reactivity and Passivity of Am60 Magnesium Alloy in Buffer Solution

F. El-Taib Heakal, N.S. Tantawy and O.S. Shehata

Corros Sci, 64: 153-163 (2012) IF: 3.734

The electrochemical behaviour of AM60 alloy was investigated in pH 9.2 borate buffer solution including anions. The extent of surface reactivity and passivity is always a function of solution composition. Increasing Cl concentration increases corrosion attack and decreases slightly surface film resistance (R₁). Nevertheless, F addition (>0.01 M) strongly passivates the surface, as it enhances formation of fluorinated film with superior corrosion resistance. At 0.01 M, fluoride induces surface activation and R₁ decreases. Thus, fluoride can efficiently inhibit AM60 corrosion in chloride-containing solution, where it forms highly protective film with refined structure as confirmed by SEM and EDX examinations.

Keywords: A. Magnesium; B. Eis; B. Sem; C. Alkaline Corrosion; C. Passive Film.

203. Removal of Some Pesticides from the Simulated Waste Water by Electrocoagulation Method Using Iron Electrode

Soha A. Abdel-Gawad, Amin M. Baraka, Kawther A. Omran and Mohamed M. Mokhtar

International Journal of Electrochemical Science, 7: 6654 - 6665 (2012) IF: 3.729

This work deals with the possibility of using electrocoagulation method for the removal of some pesticides (malathion, imidacloprid and chlorpyrifos). The effect of various operational parameters of the removal efficiency was investigated and

optimized. The removal of pesticides using iron sacrificial oxide was affected by the initial pH, the current density, the amount of NaCl and the initial pesticide concentration. The removal % for pesticides was ~ 98-99%. When iron used as a sacrificial anode under the operating conditions of initial pH of 6-7, current density of 1mA/cm², electrolysis time of 10 min, initial pesticide concentration of 0.5% and NaCl concentration of 1g/L. the obtained results showed that pseudo-second-order equation was found to be in a good agreement with the experimental results.

Keywords: Iron Electrode; Electrocoagulation; Pesticides; Chemical Oxygen Demand (Cod).

204. Electrocatalytic Oxidation of formic Acid At Manganese Oxide Nanorods Modified Electrodes: Effect of Substrate

Mohamed S. El-Deab and Takeo Ohsaka

International Journal of Electrochemical Science, 7: 5115-5121 (2012) IF: 3.729

Electrochemical oxidation of formic acid (FA) has been investigated at manganese oxide nanorods (nano-MnOx) modified electrodes (i.e., Au, Pt, GC and Pd). The electrocatalytic activity of the aforementioned anodes depends markedly on the nature of the underlying substrate. That is, the nano-MnOx at Pt electrode enhances the direct oxidation of FA. However, it does not show any significant enhancing effect on the poor catalytic activity of Au and GC electrodes. The catalytic role of nano-MnOx is inherently connected with a substrate suitable for FA adsorption (case of Pt, but not Au or GC) and/or the generation of a poisoning CO intermediate (case of Pt but not Pd, Au or GC). At Pt electrode, nano-MnOx facilitates the electrooxidation of the generated poisoning CO intermediate at a reasonably low anodic potential, while it does not affect the catalytic activity of Pd electrode towards the direct oxidation of FA to CO₂ (which occurs with no CO formation).

Keywords: Nanostructures; Electrocatalysis; Metal Oxides; Formic Acid; Fuel Cells.

205. Electropolymerization of Aniline Over Chemically Converted Graphene-Systematic Study and Effect of Dopant

Hagar K. Hassan, Nada F. Atta and Ahmed Galal

International Journal of Electrochemical Science, 7: 11161-11181 (2012) IF: 3.729

Graphene was chemically prepared using microwave irradiation. Aniline was electropolymerized over graphene immobilized on glassy carbon substrate potentiostatically in a three-electrode-one compartment cell. A systematic study of chemically converted graphene/PANI composites in both monomer free solution and potassium ferricyanide/ferrocyanide redox system was performed. The resulted chemically converted graphene/poly(aniline) (CCG/PANI) composite was characterized using surface techniques such as field emission scanning electron microscope (FE-SEM) and atomic force microscope (AFM). The effect of different dopants on the electrochemical behavior of CCG/PANI in several protonic acids was also investigated. The diffusion coefficients of proton and counterion (anion) as well as the average diffusion coefficients in these protonic acids were calculated. The results revealed that the presence of graphene

enhances the electrochemical performance of PANI in both monomer free solution and potassium ferricyanide. A synergetic electrocatalytic effect resulted when combining PANI and CCG as manifested by a noticeable increase in current signals.

Keywords: Chemically Converted Graphene (Ccg); Polyaniline (Pani); Protonic Acids; Doping Process; Electropolymerization.

206. The Counter Ion Influence of Cationic Surfactant and Role of Chloride Ion Synergism on Corrosion Inhibition of Mild Steel in Acidic Media

A. Khamis, M. M. Saleh and M.I. Awad

Int. J. Electrochem. Sci., 7: 10487-10500 (2012) IF: 3.729

The corrosion inhibition of mild steel in 0.5 M H₂SO₄ solution by cationic surfactants, cetylpyridinium chloride (CPC) and cetylpyridinium bromide (CPBr) was studied by potentiodynamic polarization curves. The results showed that the counter ions of these surfactants, i.e., chloride and bromide and the addition of chloride ion to any of the surfactants significantly influenced the protection efficiency (Picor) and mode of inhibition. Surfactants alone and in combination with chloride ions were found to obey Temkin adsorption isotherm. Chemical adsorption was proposed from the obtained thermodynamic parameters such as the free energy of adsorption. The synergism parameter (S), as a quantitative estimation of the interaction of surfactants and chloride, was found to be greater than unity indicating that the enhanced protection efficiency caused by the addition of chloride ions to the surfactants is due to a co-operative adsorption of both species. The experimental data and the extracted thermodynamic parameters confirmed the role of the counter ions (Cl⁻ and Br⁻) which has been confirmed by the addition of Cl⁻ ions as additive for synergism effects.

Keywords: Cationic; Surfactant; Corrosion; Inhibition; Synergism.

207. Characterization of Air Plasma Sprayed Al₂O₃ and Laser-Sealed ZrO₂-MgO Coatings on Ni-Base Superalloys of Aero-Engine

Soha A. Abd El Gwad, Mohamed S. Morsi and Khalid. F. Ahmed

Int. J. Electrochem. Sci., 7: 13020-13043 (2012) IF: 3.729

Aerospace gas turbine engines are now designed such that the heat resistant super alloys operate at temperature very close to their melting, so current strategies for performance improvement are centered on thermal barrier coatings. Lower thermal conductivities lead to temperature reductions at the substrate/bond coat interface which slows the rate of the thermally induced failure mechanisms. Alternatively, lower thermal conductivity of thermal barrier coating (TBC) layers might allow designers to reduce the TBC thickness there by decreasing the significant centrifugal load that the mass of the TBC imposes on the rotating turbine engine components. One approach to improve TBC system is to optimize the pore morphologies in order to reduce the thermal conductivity while still retaining high in-plane compliance. The second approach to improve TBC system performance is to optimize the surface microstructure, surface densification, phase structures mechanical characteristic, chemical structure and thermo-physical properties. The main focus of this work is to study the influence of Al₂O₃ (and laser)-sealed ZrO₂-MgO coatings on thermal barrier coating system

comprised of zirconia stabilized with magnesia top coat to predict the best improvement of TBC system and to optimize the surface microstructure, surface densification, phase structures, mechanical characteristic, chemical structure and thermo-physical properties as well as their properties with those obtained using reference techniques. Thermal expansion studies were used to study the high temperature stability of the different coatings (reference and modified coatings) structures. As low thermal conductivity is one of the most important features of TBC, thermal diffusivity and specific heat measurements were carried out. Also the mechanical measurements (e.g. micro-hardness, tensile bond strength, young's modulus), phase analyses using XRD and chemical analysis using electron dispersive X-ray (EDX) for elemental analysis in scanning microscopy studies.

Keywords: Thermal Barrier Coating; Air Plasma Spray; Heat Treatment; Thermal Expansion Coefficient; Thermal Conductivity; Zirconia Stabilized With Magnesia; Nickel Alumina Coatings; Laser Sealed Zirconia Coatings And Laser Sealed ZrO₂-MgO Coatings.

208. Effect of Air Plasma Sprays Parameters on Coating Performance in Zirconia-Based Thermal Barrier Coatings

Mohamed S. Morsi, Soha A. Abd El Gwad, Madiha. A. Shoeib and Khalid. F. Ahmed

Int. J. Electrochem. Sci., 7: 2811-2831 (2012) IF: 3.729

Advanced ceramic multilayered coatings are commonly used as protective coatings for engine metal components, where, aerospace gas turbine engines are now designed such that the heat resistant super alloys operate at temperature very close to their melting, so current strategies for performance improvement are centered on thermal barrier coatings. The main focus of this work is to study the effect of different parameters of air plasma spraying technique for various thermal barrier coatings comprised of zirconia stabilized with magnesia top coat and nickel-aluminum bond coat as well as their properties with those obtained using reference techniques. The deviations of the parameters from the optimum conditions are discussed. The investigation shows that: the deviation of the plasma spray parameters from the optimum conditions led to create a poor contact between the bond coat and the Ni-base-super alloy substrate, increase of the cracks resulting from the relaxation of residual stresses in the planer direction (open porosity), increase of the voids resulting from poor deformation of partially melted particle (few micrometer void) and present of the un-melted particles. The conclusions of this experimental study are in good agreement with theoretical predictions resulting from a sensitivity analysis reported in a previous study.

Keywords: Thermal Barrier Coating; Air Plasma Spray; Heat Treatment; Thermal Expansion Coefficient; Thermal Conductivity; Zirconia Stabilized With Magnesia.

209. Sulphur Dioxide Poisoning and Recovery of Platinum Nanoparticles: Effect of Particle Size

M. M. Saleh, M. I. Awad and F. Kitamura and T. Ohsaka

Int. J. Electrochem. Sci., 17: 12004-12020 (2012) IF: 3.729

The effect of the size of platinum nanoparticles (nano-Pt) deposited onto glassy carbon (GC) electrode (GC/nano-Pt) on the

SO₂ poisoning and recovery of these particles is examined. Both hydrogen adsorption and oxygen reduction reaction (ORR) are utilized for the quantification of the extent of poisoning and recovery of these electrodes. Cyclic voltammetry (CV) and scanning electron microscopy (SEM) were used to characterize the GC/nano-Pt. Two procedures were used in the recovery of the electrodes activity, i.e., the short-range (1.0 to 0.1 V (vs. RHE)) and long-range (0 to 1.5 V) recovery. GC/nano-Pt electrode showed poisoning-recovery behavior that depends on the Pt particle size. For the smallest Pt particle size (20 nm) used in the present study the largest extent of the recovery was achieved using either the short-range or long-range recovery procedure. The particles of 20 nm showed ~ 83% current recovery after the short-range recovery and ~100% after the long-range recovery, while those of the highest particle size (480 nm) used in this investigation showed only 67 and 87% current recovery after short-range and long-range recovery, respectively. An attempt to interpret the effects of the nanoparticle size on the poisoning and recovery behavior is introduced. The present experimental framework and analyses may help in the optimization of the Pt particle size in the ORR and the choice of the recovery approach of SO₂ poisoning.

Keywords: Nano; Platinum; Oxygen; Particle Size; So₂; Fuel Cell.

210. Development of Tailor-Designed Gold-Platinum Nanoparticles Binary Catalysts for Efficient formic Acid Electrooxidation

Islam M. Al-Akara, Ahmad M. Mohammad, Mohamed S. El-Deab and Bahgat E. El-Anadouli

International Journal of Electrochemical Science, 7: 3939-3946 (2012) IF: 3.729

The modification of a glassy carbon (GC) electrode with platinum (PtNPs) and gold (AuNPs) nanoparticles is targeted to fabricate efficient anodes for the electrooxidation of formic acid (FA). A proper adjustment of the deposition sequence of PtNPs and AuNPs could eventually enhance the electrocatalytic activity of the electrode in such a way that suppresses the CO poisoning effect during FA oxidation. The highest catalytic activity is obtained at the Au/Pt/GC electrode (with PtNPs firstly deposited on the GC electrode followed by AuNPs). This superb enhancement is quantified by comparing the relative ratio of the direct vs. the indirect oxidation peaks at 0.3 and 0.65 V, respectively, at each electrode. The fundamental role of AuNPs (in Au/Pt/GC electrode) imparts immunity to the underlying PtNPs against CO poisoning by interrupting the contiguity of the Pt surface sites, thus, prevents the deterioration of the catalytic activity of the anode.

Keywords: Catalytic Activity; Carbon Monoxide; Fuel Cells; Poisoning; Nanoparticles.

211. Graphene Supported-Pt-M (M=Ru Or Pd) for Electrocatalytic Methanol Oxidation

Ahmed Galal, Nada F. Atta and Hagar K. Hassan

International Journal of Electrochemical Science, 7: 768-784 (2012) IF: 3.729

Different methods for preparation of a highly efficient catalyst made of a hybrid of graphene and sub-micron structured Pt-Ru or

Pt-Pd is illustrated for methanol oxidation. Graphene is prepared chemically using microwave method or electrochemically by reducing graphene oxide (GO). Glassy carbon (GC) electrodes are modified with the catalyst. The electrocatalytic activity of the surface is examined for methanol oxidation with cyclic voltammetry (CV), chronoamperometry (CA) and chronocoulometry (CC). The electrocatalytic activity is doubled when graphene is modified with Pt-Pd and increases five times in case of Pt-Ru compared to GC - Pt-Pd and Pt-Ru electrodes, respectively. SEM and AFM are used to characterize the catalyst morphology and surface roughness of the catalyst. Effect of catalyst loading, temperature, stability and methanol concentration on the catalyst efficiency are presented.

Keywords: Graphene; Electrocatalysis; Composite Electrodes; Methanol Oxidation; Afm; Sem.

212. Determination of the Diffusion Coefficients for Charge Transfer Through Homo-, Bilayered- and Co- Polymers of 3-Methylthiophene and N-Methyl Pyrrole

Nada F. Atta, Ahmed Galal and Shima M. Ali

International Journal of Electrochemical Science, 7: 785-805 (2012) IF: 3.729

Conducting homo-, bilayered- and co-polymers of 3-methylthiophene (MT) and N-methylpyrrole (NMPy) were electrochemically deposited on platinum electrode. Electrochemical investigation of the resulting films was achieved using cyclic voltammetry and chronocoulometry. The diffusion coefficients were calculated in case of using different films of different thicknesses. The synthesis and testing the films in presence of different types of electrolytes and solvents were studied. The results showed that a memory effect caused by the synthesis anion affects further interaction between the film and the test anion which consequently affect the diffusion coefficient. The charge spacing effect caused by the type of electrolyte is more pronounced in the case of PMPy compared to PMT. Also, diffusion coefficient values were calculated for films with different thickness prepared from different monomers feed ratios in different electrolytes and solvents. Some of them showed similar trend to the homo-polymers. For conducting bilayers, the inner layer influences the redox process of the bilayer. This can be showed from the cyclic voltammetry measurements and diffusion coefficient calculations. FTIR measurements proved the incorporation of both individual monomers in the copolymer films. TGA proved that the thermal stability of the copolymer increased by increasing NMPy content. On the other hand, surface morphology revealed by SEM showed a distinct difference between homo- and co-polymeric structures.

Keywords: Conducting Polymers; Bilayers; Copolymers; Diffusion Coefficients; Ftir; Tga; Sem.

213. The Catalytic Activity of Ruthenates ARuO₃ (A= Ca, Sr Or Ba) for the Hydrogen Evolution Reaction in Acidic Medium

Nada F. Atta, Ahmed Galal and Shima M. Ali

Int. J. of Electrochemical Science, 7: 725-746 (2012) IF: 3.729

Ruthenate perovskites ARuO₃, (A= Ca, Sr or Ba) were prepared by coprecipitation method. The electrocatalytic activity of the

prepared perovskites was investigated toward the hydrogen evolution reaction (HER). X-ray diffraction analysis suggested successful incorporation of Ru⁴⁺ at the Ca²⁺, Sr²⁺ and Ba²⁺ cations sites confirming the formation of the orthorhombic perovskite phases of CaRuO₃ and SrRuO₃ and the hexagonal perovskite phase of BaRuO₃. The average particle size for the prepared perovskites was 39.0, 42.2 and 101.4 nm for Ca, Sr and BaRuO₃, respectively. Scanning electron micrographs showed a well-defined hexagonal crystal structure in case of BaRuO₃, while CaRuO₃ and SrRuO₃ composed of agglomerations of nearly spherical grains. CaRuO₃ showed smaller agglomerations and more cavities than SrRuO₃. The influence of the type of A-cation on the catalytic activity for HER was studied by Tafel linear polarization. The order of the electrocatalytic activity was BaRuO₃CaRuO₃SrRuO₃. This was shown from the values of the exchange current density, -60.7, -13.1 and -884.6A.cm⁻² for Ca, Sr and BaRuO₃, respectively. This suggested that the A-site metal ion not only has a strong effect on the stability of the whole crystal configuration but also provides the possibility to improve catalyst performance by synergetic interactions with the B-site metal ion. The activation energy, reaction order and reaction mechanism have been investigated using the electrochemical techniques, Tafel linear polarization and impedance. Again, the calculated values of the activation energy gave similar trend for catalytic activity; 42.6, 86.3 and 17.7 kJ/mol for Ca, Sr and BaRuO₃ respectively. Both Tafel and the impedance data showed that the volmer step is the rate determining step. In addition, the effect of the partial substitution at the A-site in Sr_{1-x}Ca_xRuO₃ was also studied. The catalytic activity of ternary perovskites was about twice higher than that of binary ones. The catalytic activity of ternary oxides increased with increasing the fraction of Ca-doped.

Keywords: Perovskites; Catalyst; Tafel; Impedance; Sem And Xrd.

214. Synthesis and Photoelectrochemical Behavior of A Hybrid Electrode Composed of Polyaniline Encapsulated in Highly Ordered TiO₂ Nanotubes Array

Nada F Atta, Ahmed Galal and Hatem M. A. Amin

International Journal of Electrochemical Science, 7: 3610-3626 (2012) IF: 3.729

Polyaniline (PANI) nanostructures encapsulated in highly ordered TiO₂ nanotubes (NTs) array was obtained by formation of TiO₂ NTs array in HF-H₃PO₄ solution using constant potential anodization method; followed by electropolymerization of aniline to be encapsulated in the TiO₂ NTs array, The electrochemical, morphological and structural characteristics of PANI/TiO₂ nanocomposite electrode were examined by cyclic voltammetry (CV), electrochemical impedance spectroscopy (EIS), scanning electron microscope (SEM), X-ray diffraction (XRD) and infrared (IR) spectroscopy. Thermal behavior of PANI film was studied by thermogravimetric analysis (TGA). Studies showed that anatase phase of TiO₂ prevailed and PANI-modified TiO₂ composite did not change the crystalline structure of neat TiO₂. Dye sensitized photogalvanic cell based on PANI/TiO₂ nanocomposite electrode was also examined. Different metal phthalocyanine dyes were examined as the photosensitizer for composites formed of PANI nanostructures encapsulated in TiO₂ NTs array. The Photoelectrochemical properties and the conversion efficiency of the modified CoPC dye sensitized PANI/TiO₂ nanocomposite

were enhanced compared to "neat" TiO₂ NTs. The photogalvanic cell showed good stability for many turnovers.

Keywords: TiO₂ Nanotubes; Dye Sensitized Solar Cell; Polyaniline; Phthalocyanine; Photoelectrochemical Properties.

215. Electrochemical Behavior of Al-Si Alloy in Phosphoric Acid Containing Halogen or Oxyhalogen Anions

A. A. Ghoneim, M. A. Ameer and A.M. Fekry

International Journal of Electrochemical Science, 7: 10851-10864 (2012) IF: 3.729

Electrochemical techniques were used to characterize the corrosion behavior of aluminum die casting alloy (A 383) in phosphoric acid without and with the individual addition of various halide anions (chloride Cl, bromide Br, iodide I⁻) or their oxyhalide ions of chlorate ClO₃, bromate BrO₃ and iodate IO₃. The electrochemical impedance spectroscopy (EIS) and potentiodynamic polarization measurements indicate that the solution of 0.5 M H₃PO₄ containing iodide ions is the most effective solution towards protective film formation with an inhibition efficiency (IE%) reaches to 88.9 %. However, the bromide ions have the most aggressive nature among the halides and oxyhalide ions as indicated from its higher corrosion current density *i*_{corr} value. The results were confirmed by surface examination via scanning electron microscope.

Keywords: EIS; Polarization; Corrosion; Phosphoric Acid; Halides.

216. Corrosion Inhibition of Steelin Hydrochloric Acid Solution using A Triazole Derivative Electrochemical and Computational Studies

Yahia H. Ahmad and Walid M. I. Hassan

Int. J. Electrochem. Sci., 7: 12456-12469 (2012) IF: 3.729

The efficiency of 5,5'-[butane-1,4-diylbis(sulfanediy)]bis(4-amino-4H-1,2,4-triazole-3-thiol) (BATT) as a corrosion inhibitor for mild steel in 2 M HCl was studied using polarization and electrochemical impedance spectroscopy (EIS). The adsorption of the investigated inhibitor onto the steel surface was found to follow Langmuir isotherm. The negative value of the free energy of adsorption, G_{ads} ensures the spontaneity of the adsorption process. The temperature effect on the corrosion of steel in 2 M HCl with and without inhibitor was also studied. Moreover, density functional theory (DFT) calculations give a clear indication of strong molecular interaction between inhibitor molecules and iron surface.

Keywords: Mild steel; Triazole; Polarization; EIS; Acid inhibition; Dft.

217. Electrochemical Behavior of Magnesium Alloys as Biodegradable Materials in Phosphate Buffer Saline Solution

A.M. Fekry and R.H. Tammam

Int. J. Electrochemical Science, 7: 12254-12261 (2012) IF: 3.729

The electrochemical behavior of extruded AZ31E and AZ91E alloys was investigated in Phosphate Buffer Saline (PBS)

Solution of pH 7.4 at 37C. The behavior of the two alloys was studied with immersion time by using electrochemical impedance spectroscopy (EIS). Polarization measurements are carried out to study the corrosion rate. It was found that the corrosion resistance of AZ91E alloy is higher than that of AZ31E using EIS tests and this is confirmed by polarization tests. Also, the effect of adding 10⁻³ M concentration of 2-thiouracil and L-tyrosine as inhibitor in PBS solution for AZ91E alloy was studied. The corrosion was inhibited by addition of L-tyrosine more than 2-thiouracil.

Keywords: Az31e; Az91e; Eis; Pbs Solution.

218. Electrochemical Corrosion Inhibition of Al-Si Alloy in Phosphoric Acid

M.A. Ameer, A.A. Ghoneim and A.M. Fekry

International Journal of Electrochemical Science, 7: 4418-4431 (2012) IF: 3.729

Electrochemical corrosion inhibition of aluminum die casting alloy (A383) in H₃PO₄ has been studied using different electrochemical techniques. The results of electrochemical impedance spectroscopy (EIS) and potentiodynamic polarization measurements confirm the inhibition effects of K₂CrO₄ which describe the increase in the effectiveness of a corrosion inhibitor in the presence of 0.1M K₂CrO₄ in 0.5 M H₃PO₄. The results indicated that both concentration and the immersion time affect the inhibition efficiency (IE%). Langmuir adsorption isotherm was found to fit well with the experimental data. The obtained results were confirmed by surface examination using scanning electron microscope.

Keywords: A383; Polarization; Eis; Sem; Acid inhibition

219. Carbon Nanotubes Modified and Conventional Selective Electrodes for Determination of Selegiline Hydrochloride and Its Pharmaceutical Preparations

Nour T. Abdel Ghani, Rasha M. El-Nashar and Sherif M. Hassan

International Journal of Electrochemical Science, 7 7235-7252 (2012) IF: 3.729

The construction and performance characteristics of selegiline (Sel) carbon paste (CPEs) and plastic membranes electrodes are described. The cited electrodes are based on the ion associates selegiline phosphomolybdate (Sel-PMA) or phosphotungstate (Sel-PTA). Matrix composition of each electrode is optimized on the basis of effects of type and concentration of the ionophore as well as influence of the selected plasticizers. Carbon nanotubes (CNTs) have a good conductivity which helps the transduction of the signal in carbon paste electrode, so the addition small quantity of multi-wall carbon nanotubes (MWCNTs) particles to the composition of carbon paste electrode gave a better performance characteristics for Sel-electrodes with Nernstian slope of 59.50 and 58.20 mV at 25C for Sel-PMA and Sel-PTA ion associates, respectively within a linear concentration range from 1.0x10⁵ to 1.0x10² M for MWCNTs modified paste electrodes. The mean recovery of the amounts taken of pure and pharmaceutical preparations ranged from 95.2 to 103.5% with RSD = 0.2–0.8%. While for urine and plasma samples, the recovery values ranged from 96.2 to 103.5% with RSD = 0.2–0.7%, with limit of detection (LOD), ranged from 1.52 to 21.26g/L, while the limit of quantification (LOQ) ranged from 1.52 to 20.36g/L for the studied electrodes.

Keywords: Selegiline; Potentiometry; Pvc Membrane; Carbon Nanotubes.

220. Potentiometric Determination of Chlorpromazine Hcl Using Carbon Paste Electrode in Pure and Pharmaceutical Preparations

Eman Y.Z. Frag, M.A. Zayed, M.M. Omar, Sally E.A. Elashery and Gehad G. Mohamed

Int. J. Electroche. Sci., 7: 650-662 (2012) IF: 3.729

Carbon paste electrode has been developed for the potentiometric determination of chlorpromazine HCl drug. This work has focused on the fabrication of carbon paste ion selective electrode for determination of the drug under investigation using potentiometric titration with sodium tetraphenyl borate. The performance of such sensor in the potentiometric determination of chlorpromazine HCl is compared with those of PVC membrane, coated wire and coated graphite electrodes. This carbon paste electrode was applied to the determination of chlorpromazine HCl in pharmaceutical preparations. The repeatability and accuracy of measurements performed in the analysis of these pharmaceutical matrices using new carbon paste sensor were evaluated. The influence of the electrode composition, conditioning time of the electrode and pH of the test solution, on the electrode performance were investigated. The drug electrode showed Nernstian response in the concentration range from 1×10⁻⁷ to 1×10⁻² mol L⁻¹ with slope of 58.06 ± 0.34 mV decade⁻¹ and was found to be very precise and usable within the pH range 2–6. This sensor exhibited a low detection limit (1×10⁻⁷ mol L⁻¹), a long lifetime (>2 months) and good stability. The percentage recovery obtained is 97.72 % with a relative standard deviation 0.28%.

Keywords: Chlorpromazine Hcl; Carbon Paste Electrode; Potentiometric Determination; Tablets; Official Method.

221. Construction of Different Types of Ion-Selective Electrodes Characteristic Performances and Validation for Direct Potentiometric Determination of Orphenadrine Citrate

Eman Y.Z. Frag, Tamer Awad Ali, Gehad G. Mohamed and Yusra H.H. Awad

Int. J. Electrochem. Sci., 7: 4443-4464 (2012) IF: 3.729

Three types of ion-selective electrodes (carbon paste, PVC membrane and screen printed electrodes) have been proposed for determining orphenadrine citrate (OphC) in pure solution and pharmaceutical preparation based on the ion-pair formation between OphC with sodium tetraphenylborate. The three types of electrodes were prepared using five types of plasticizers with each type of electrodes. The electrodes showed a linear response with a good Nernstian slope of 57.20 ± 0.70, 56.81 ± 1.6 and 57.09 ± 0.2 mV decade⁻¹ over the concentration range 10⁻⁶ to 10⁻² mol L⁻¹ with CPE, PVC membrane and SPEs, respectively. The standard electrode potentials, E°, were determined at 10, 20, 30, 40 and 50 °C and used to calculate the isothermal coefficient (dE°/dT) of the electrodes. Temperatures higher than 60 °C affect the electrodes performance. The electrodes proved highly selective with selectivity coefficients ranging from 1.063-5.573, 1.323-6.798 and 1.073-6.504 for CPE, PVC membrane and SPE, respectively. The detection limits (signal/noise [S/N] = 3) were 1.016×10⁻⁶, 0.984×10⁻⁶ and 0.992×10⁻⁶ mol L⁻¹ for CPE, PVC membrane

and SPE, respectively. The practical applications of these electrodes were demonstrated by measuring the concentrations of OphC in pure solutions and pharmaceutical preparations with satisfactory results. The reliability and stability of the electrodes gave a good possibility for applying the technique to routine analysis.

Keywords: Orphenadrine Citrate; Pharmaceutical Analysis; Potentiometry; Tetraphenyl Borate; Cpe; Pvc; Spe.

222. Modified Screen Printed and Carbon Paste Ion Selective Electrodes for Potentiometric Determination of Naphazoline Hydrochloride in Pure and Pharmaceutical Preparations

F.A. Nour El-Dien, Gehad G. Mohamed, Eman Y.Z. Frag and Marwa El-Badry Mohamed

Int. J. Electrochem. Sci., 7: 10266-10281 (2012) IF: 3.729

In this study, a comparison between modified screen printed (SPE) and carbon paste (CPE) electrodes is described for determination of naphazoline hydrochloride in pure and pharmaceutical formulations. The performance characteristics of the electrodes were evaluated in terms of composition, life span, pH and temperature. The electrodes show Nernstian slope values of 55.4 ± 2.2 and 59.6 ± 1.3 mV decade⁻¹ at 25 °C, over the concentration ranges of 5.0×10^{-7} – 3.5×10^{-2} and 3.0×10^{-7} – 2.5×10^{-2} mol L⁻¹ with a limit of detection of 2.512×10^{-7} and 3.162×10^{-7} mol L⁻¹ for modified SPE and CPE, respectively. The potentiometric response of the electrodes is independent of the pH of the solution within the pH range of 2.5-8.5 and 2.7-8.5 for modified SPE and CPE, respectively. The electrodes showed good selectivity for naphazoline hydrochloride (NPZ.HCl) with respect to some inorganic cations, sugars and glycine. The electrodes exhibited relatively long operational lifetime of 47 and 32 days for modified SPE and CPE sensors, respectively. The developed modified sensors have been used successfully for the determination of naphazoline hydrochloride in pharmaceutical preparation using standard addition, potentiometric titration and calibration methods. The direct potentiometric determination of naphazoline hydrochloride using the prepared sensors gave recoveries 98% and 97.4% using modified SPE and CPE, respectively. The method avoids any interference of coexistent NPZ.HCl in the compounding drug. The obtained results were in a good agreement with those obtained using the official method. The results obtained were satisfactory with excellent percentage recovery comparable and sometimes better than those obtained by other routine methods for the assay.

Keywords: Modified Screen Printed And Carbon Paste Electrodes; Naphazoline Hydrochloride; Calibration; Method Validation.

223. Direct and Sensitive Determination of Atropine Sulfate at Polymer Electrode in Presence of Surface Active Agents

Nada F. Atta, Ahmed Galal and Rasha A. Ahmed

Int. J. of Electrochemical Science, 7:10365-10379 (2012) IF: 3.729

A novel, selective, rapid and simple electrochemical method is demonstrated for the first time for the determination of atropine sulfate, using poly (3,4-ethylene-dioxythiophene) (PEDOT) electrode film modified platinum electrode in presence of sodium

dodecyl sulfate (SDS). The modified electrode displays an obvious increase in the peak current (8 times) compared to the bare platinum electrode (Pt). The results indicate that PEDOT/Pt electrode in presence of SDS remarkably enhances the electrocatalytic activity towards the oxidation of Atropine sulfate. Cyclic voltammetry (CV), linear sweep voltammetry (LSV) and Electrochemical impedance spectroscopy (EIS) are used to verify the voltammetric behavior of Atropine sulfate in micelles media. Simultaneous determination of Atropine and morphine and selective determination of atropine sulfate in presence of codeine, ascorbic acid and uric acid are obtained with high sensitivity and good resolution. The PEDOT/Pt in presence of SDS has also been successfully applied to the determination of Atropine sulfate in atropine sulfate injection in the linear ranges of 0.1 to 0.8 mol L⁻¹ and 2.5 to 100 mol L⁻¹ with low detection limits of 27 and 64 nM, respectively. The results indicate that the PEDOT/Pt electrode can successfully be applied for the analysis of pharmaceuticals in biological fluids.

Keywords: Pedot; Sds; Atropine Sulfate; Morphine; Codeine; Electrochemical Analysis.

224. Sensitive Electrochemical Determination of Morphine using Gold Nanoparticles-Ferrocene Modified Carbon Paste Electrode

Nada F. Atta, Ahmed Galal, Anwar A. Wassel and Asmaa H. Ibrahim

Int. J. of Electrochemical Science, 7:10501-10518 (2012) IF: 3.729

An effective electrochemical sensor based on carbon paste (CP) electrode with ferrocene/gold nanoparticles GNFCPE, is introduced for selective determination of morphine (MO) in presence of interference compounds as ascorbic acid (AA) and uric acid (UA). Furthermore, the modified electrode is used for simultaneous determination in presence of dopamine (DA) or l-norepinephrine (NEP) in 0.04 mol L⁻¹ universal buffer solution (B-R) (pH 7.4), a well defined oxidation peaks with high current response and good potential peak separation is obtained compared to the unmodified electrode. The electrochemistry of MO is investigated by cyclic voltammetry (CV), differential pulse voltammetry (DPV) and electrochemical impedance measurements (EIS). The morphine concentration could be measured in the concentration range of 1.0×10^6 to 18.0×10^4 mol L⁻¹ with a detection limit of 3.507×10^{-9} mol L⁻¹ and a correlation coefficient of 0.9994. The sensor has also been successfully applied to the determination of morphine spiked into diluted urine samples with a low detection limit and satisfied recovery. The good results indicate that GNFCPE holds great promise in practical application.

Keywords: Sensor; Carbon Paste Electrode; Ferrocene Carboxylic Acid; Gold Nanoparticles; Morphine; Urine Samples.

225. Nanocomposite Graphene-Based Material for Fuel Cell Applications

Ahmed A. Elzatahry, Aboubakr M. Abdullah, Taher A. Salah El-Din, Abdullah M. Al-Enizi, Ahmed A. Maarouf, Ahmed Galal, Hagar K. Hassan, Ekram H. El-Ads, Salem S. Al-Theyab and Attiah A Al-Ghamd

Int. J. of Electrochemical Science, 7: 3115-3126 (2012) IF: 3.729

Cobalt and nickel oxides-graphene nanocomposites have been prepared by a simple chemical route. The structure, morphology

and properties were characterized using X-ray diffraction (XRD) and Transmission Electron Microscope (TEM). The electrocatalytic activity for the methanol oxidation reaction in acidic medium of these nanocomposites compared to platinum has been confirmed using cyclic voltammetry technique.

Keywords: Graphene; Graphene Oxide; Nanocomposite; Methanol Oxidation; Fuel Cells Electrocatalysis.

226. Electrocatalytic Evolution of Oxygen Gas At Cobalt Oxide Nanoparticles Modified Electrodes

Ibrahim M. Sadiek, Ahmad M. Mohammad, Mohamed E. El-Shakre, M. Ismail Awad, Mohamed S. El-Deab and Bahgat E. El-Anadouli

International Journal of Electrochemical Science, 7: 3350-3361 (2012) IF: 3.729

The electrocatalysis of oxygen evolution reaction (OER) at cobalt oxide nanoparticles (nano-CoOx) modified GC, Au and Pt electrodes has been examined using cyclic voltammetry. The OER is significantly enhanced upon modification of the electrodes with nanoCoOx, as demonstrated by a negative shift in the polarization curves at the nano-CoOx modified electrodes compared to that obtained at the unmodified ones. Scanning electron microscopy (SEM) revealed the electrodeposition of nanometer-size CoOx (average particle size of 200 nm) onto GC electrode. Optimization of the operating experimental conditions (i.e., solution pH and loading level of nano-CoOx) has been achieved to maximize the electrocatalytic activity of nano-CoOx modified electrodes. It has been found that the electrocatalytic activity of the nano-CoOx modified electrodes towards the OER is pH and loading level dependent, while it is substrate independent. The low cost as well as the marked stability of the thus-modified electrodes make them promising candidates in industrial water electrolysis process.

Keywords: Nanostructures; Water Electrolysis; Cobalt Oxide; Electrocatalysis.

227. Potentiometric Determination of Imatinib under Batch and Flow Injection Analysis Conditions

Shereen E. Abdel Karim, Rasha M. El-Nashar and Ashraf H. Abadi

International Journal of Electrochemical Science, 7: 9668-9681 (2012) IF: 3.722

A new potentiometric electrochemical sensor (ion-selective electrode) based on the formation of ion associate of Imatinib mesylate with sodium tetraphenyl borate in polyvinyl chloride plasticized with dioctylphthalate was developed. Such electrode was prepared for the assay of the cited drug in its pure form and pharmaceutical formulations under batch and flow injection analysis conditions. The life span of the electrode is 30 days on continuous soaking and several months when kept in dry conditions. It is characterized by usable concentration range of (1.0×10^{-5} - 1.0×10^{-3} M) and (5.0×10^{-6} - 1.0×10^{-2} M) in batch and FIA conditions, respectively. The change of pH does not affect the potential reading or peak heights of the electrode in the range of 4.00-7.50 in batch condition. While in FIA, the peak heights representing the pH are almost stable in the range 4.00-6.00. The electrode is highly selective towards many inorganic cations and

neutral molecules. The obtained results indicated high accuracy and precision of the studied electrode as sensor for the drug.

Keywords: Imatinib; Fia; Potentiometric Determination; Ion-Selective Electrode; Imatinib Mesylate.

228. Potentiometric Membrane Sensors for the Selective Determination of Memantine Hydrochloride in Pharmaceutical Preparations

Rasha M. El Nashar, Aliaa S. M. El-Tantawy and Saad S. M. Hassan

International Journal of Electrochemical Science, 7: 10802-10817 (2012) IF: 3.722

Three potentiometric sensors responsive to Memantine HCl (MEM) drug are described, characterized, compared and used for drug assessment. The sensors are based on the use of the ion-association complex of (MEM) cation with Flavianate (FA), 5-Nitro-barbiturate (NBA) and phosphomolybdate (PMA) anions as electroactive materials in plasticized poly(vinyl chloride) membranes. The sensors demonstrate fast near-Nernstian response for MEM with lower limits of quantification of: 4.76×10^{-6} , 5.22×10^{-5} and 9.08×10^{-6} M with detection limits of 1.74×10^{-6} , 9.17×10^{-6} and 2.93×10^{-6} M, with slopes of 55.45, 45.84 and 54.58 mV/concentration decade over a pH range of 2.66-9.54, 4.64-8.51 and 4.60-9.07 for Flavianate (FA), 5-Nitro-barbiturate (NBA) and phosphomolybdate (PMA), respectively. The three sensors showed good selectivity for MEM drug over several inorganic cations, nitrogenous excipients and diluents commonly used in drug formulations. The dissolution profile was also plotted using the proposed sensor at optimum electrode conditions.

Keywords: Potentiometric sensors; Memantine; Flow injection analysis (Fia); Dissolution test; Drug analysis.

229. Synthesis and Characterization of Antibacterial Semi-Interpenetrating Carboxymethyl Chitosan/Poly (Acrylonitrile) Hydrogels

Riham R. Mohamed, Rania S. Seoudi and Magdy. W. Sabaa

Cellulose, 19: 947-958 (2012) IF: 3.6

Blend hydrogels composed of carboxymethylchitosan (CMCh) and poly (acrylonitrile)(PAN) were synthesized via crosslinking method. Several analyses were made to investigate both physical and thermal properties of CMCh/PAN hydrogels like; FTIR, scanning electron microscope, XRD and thermogravimetric analysis (TGA). TGA results showed that CMCh/PAN hydrogels are thermally more stable than CMCh and their thermal stability increases as PAN content increases in the hydrogel. Moreover, the swelling behavior of CMCh/PAN hydrogels was studied in different buffer solutions. It was found that CMCh/PAN hydrogels swell much more than PAN especially at pH 9. The hydrogel sorption for different dye stuff and various metal ions like; Cu^{2+} , Cd^{2+} and Co^{2+} were also studied. In this work, antibacterial characteristic of hydrogels was mainly investigated towards Escherichia coli (E. coli) as a serious disease-leading bacterium. All tested hydrogels have clearly presented good antibacterial activity as CMCh content increases in the hydrogels.

Keywords: Hydrogels; Swelling; Metal uptake; Dye uptake; Thermal analysis; Physical analysis.

230. Recent Advances in the the rapeutic Applications of Pyrazolines

Mohamed R Shaaban, Abdelrahman S Mayhoub and Ahmad M Farag

Expert Opin Ther Pat, 22, (3): 253-291 (2012) IF: 3.571

Pyrazoline heterocycle provides a structural core for building huge variety of biologically active compounds. The pharmacological activity of pyrazoline-based compounds extends from central nervous system(CNS) applications to antimicrobials. The most predominant pharmacological activity was observed for the class of 'antimicrobials'. Cannabinoid receptor type 1 (CB1) pyrazoline modulators are very useful in treatment of obesity and schizophrenia. Pyrazoline-containing cytotoxic compounds are not only useful in treatment of cancer, but also some of them act as cancer chemopreventive agents. There are many reports centered on the antimycobacterium activity of pyrazoline-containing compounds, most of them have been assayed versus the vaccine-strain H37Rv.

Keywords: Pyrazolines; Antimicrobials; Chemopreventive Agents.

231. Ultrasound Assisted one-Pot, Three-omponents Synthesis of pyrimido[1,2-a]Benzimidazoles and Pyrazolo[3,4-B]Pyridines: A New Access Via Phenylsulfone Synthron

Tamer S. Saleh, Taha M.A. Eldebss and Hassan M. Albishri

Ultrason Sonochem, 19 (2012): 49-55 (2012) IF: 3.567

A simple, facile, efficient and three-components procedure for the synthesis of pyrimido[1,2-a]benzimidazoles and pyrazolo[3,4-b]pyridines utilizing phenylsulfone synthron, under ultrasonic irradiation was Developed.

Keywords: 2-Aminobenzimidazole5; Aminopyrazolesmulticom; ponent Reactions (Mcrs).

232. Novel Palladium (II) and Platinum (II) Complexes with 1H-Benzimidazol-2-Ylmethyl-N-(4-Bromo-Phenyl)-Amine: Structural Studies and Anticancer Activity

Nour T. Abdel Ghani and Ahmed M. Mansour

Eur J Med Chem, 47: 399-411 (2012) IF: 3.346

[MLCl₂] (L= (1H-benzimidazol-2-ylmethyl)-N-(4-bromo-phenyl)-amine; M = Pd & Pt) and [PdL(OH₂)₂]₂X_zH₂O (X = Br, I, z = 2; X = SCN, z = 1; X = NO₃, z = 0) complexes have been synthesized as potential anticancer compounds and their structures were elucidated using elemental analysis, spectral, thermal analysis and X-ray powder diffraction. The benzimidazole (L) crystallizes in the space group P2_{1/c} with a = 8.6660 (3) Å, b = 16.6739(7) Å, c = 9.8611(4) Å and β = 113.505(3)° and forms an infinite chain structure with a trans-zigzag type along the crystallographic axis "a", through the intermolecular H-bond. FT-IR and ¹H NMR studies revealed that the ligand L is coordinated to the metal ion via the pyridine-type

nitrogen (N_{Dv}) of the benzimidazole ring and secondary amino group (NHsec). Quantum mechanical calculations of energies, geometries, vibrational wavenumbers and ¹H NMR of the benzimidazole L and its complexes were carried out by DFT/B3LYP method combined with 6-31G(d) and LANL2DZ basis sets. Natural bond orbital (NBO) analysis and frontier molecular orbitals (FMO) were performed at B3LYP/LANL2DZ level of theory. The benzimidazole L, in comparison to its metal complexes was screened for its antibacterial activity. The complexes showed cytotoxic effects against human breast cancer (MCF7), hepatocarcinoma (HepG₂) and colon carcinoma cells (HCT). The platinum complex (6) exhibited a moderate antitumor activity against MCF7 with IC₅₀ = 10.2M comparing to that reported for cis-platin 9.91M.

Keywords: Biological activity; Benzimidazole; Dft; Nbo; Lanl2dz.

233. Synthesis and Characterization of Pirylogens Possessing Low Excitation Energies– Substituent Modification in Order to Improve Solar Energy Collection

Tamer T. El-Idreesy

European Journal of Organic Chemistry, 2012 Issue 24: 4515-4522 (2012) IF: 3.329

The synthesis and characterization of the first di-β-naphthylsubstituted pyrylogens, N-methyl-2,6-di-β-naphthyl-4,4'-pyrylogen bis(tetrafluoroborate) and N-methyl-2,6-di-β-naphthyl-4,2'-pyrylogen bis(tetrafluoroborate) are reported.

The photophysical and electrochemical behaviors of these new pyrylogens are examined and compared to the previously reported diphenyl-substituted analogs, N-methyl-2,6-diphenyl-4,4'-pyrylogen bis(tetrafluoroborate) and N-methyl-2,6-diphenyl-4,2'-pyrylogen bis(tetrafluoroborate) as well as to 2,4,6-triphenylpyrylium tetrafluoroborate, the typical electron-transfer photocatalyst. The newly synthesized pyrylogens exhibit substantially lower excitation energies. The results are supported by theoretical calculations using the B3LYP/6-31G(d) and time-dependent DFT (TD-DFT) CAM-B3LYP/6-31G(d) computational models. In addition, insight into the reduction reactions of the new pyrylogens to their radical cation and neutral redox partners is also provided.

Keywords: Pyrylogens; Pyrylium Salts; Photochemistry; Computational Chemistry; Electron Transfer.

234. Controlled Experimental Soil Organic Matter Modification for Study of Organic Pollutant Interactions in Soil

Ashour A. Ahmed, Oliver Kühn and Peter Leinweber

Science of the Total Environment, 441: 151-158 (2012) IF: 3.29

Interactions of organic pollutants with soil organic matter can be studied by adsorption of the pollutants on well-characterized soil samples with constant mineralogy but different organic matter compositions. Therefore, the objectives of the current study are establishing a set of different, well-characterized soil samples by systematic modifications of their organic matter content and molecular composition and prove these modifications by advanced complementary analytical techniques. Modifications were done by off-line pyrolysis and removal/addition of hot-water

extracted organic fraction (HWE) from/to the original soil sample. Both pyrolysis-field ionization mass spectrometry (Py-FIMS) and synchrotron-based C- and N- X-ray absorption near-edge structure spectroscopy (XANES) were applied to investigate the composition of the soil organic matter. These complementary analytical methods in addition to elemental analysis agreed in showing the following order of organic matter contents: pyrolyzed soil/soil residue/original soil/soil+3 HWE/soil+6 HWE/HWE. The addition of HWE to the soil sample increases the relative proportions of carbohydrates, N-containing heterocyclic compounds and peptides and decreases the relative proportions of phenols, lignin monomers and dimers and lipids. The most abundant organic compound classes in the pyrolyzed sample are aromatics, aliphatic nitriles, aldehydes, five- and six-membered N-containing heterocyclic compounds and aliphatic carboxylic acids. It can be expected that removal or addition of HWE, that mimic biomass inputs to soil or soil amendments, change the binding capacity for organic pollutants less intensively than heat impact, e.g. from vegetation burning. It will be possible to interpret kinetic data on the pollutants adsorption by these original and modified soil samples on the basis of the bond- and element-specific speciation data through C-XANES and N-XANES and the molecular-level characterization through Py-FIMS. Finally, this combination of analytical techniques can be recommended for similar problems that require characterizing the bulk, non-extracted SOM instead of pre-selected compounds or compound classes.

Keywords: Soil organic matter; Pollutants; Hot-water extraction; Pyrolysis; Mass spectrometry; Xanes.

235. Synthesis of Spiro-Heterocycles Via 1,3-Dipolar Cycloadditions of Nitrilimines to Exoheterocyclic Enones Site-, Regio- and Stereo-Selectivities Overview

Sami Shawali Ahmad and Osman Abdelhamid Abdou

Current Organic Chemistry, 16, 22: 2673-2689 (2012) IF: 3.064

This review provides a survey on the reactions of nitrilimines, generated in situ by dehydrohalogenation of the corresponding hydrazonoyl halides, with heterocyclic enones. These reactions proved useful for synthesis of various spiroheterocycles possessing chiral centers and some biological activities.

Keywords: Heterocycles; Hydrazonoyl Halides; Nitrilimines; Spiroheterocycles.

236. Effect of Solvent on the Regioselective Synthesis of Spiropyrazoles

Sayed M. Riyadh and Thoraya A. Farghaly

Tetrahedron, 68: 9056-9060 (2012) IF: 3.025

1,3-Dipolar cycloaddition reactions of 6-arylmethylene-6,7,8,9-tetrahydro-5H-benzocyclohepten-5-ones (1) with nitrilimines 3 were investigated in benzene and chloroform. The reaction products were 20,40,6,7,8,9-hexahydro-20,40,50-triaryl spiro[benzocycloheptene-6(5H),30(3H-pyrazol)-5-ones (4) or 20,30,6,7,8,9-hexahydro-20,30,50-triarylspirobenzocycloheptene-6(5H),40(4H-pyrazol)-5-ones (5). X-ray crystallographic analysis was carried out for compound 5b. It was found that the regioselectivity of the produced compounds was altered based on changing solvent type.

Keywords: Benzocyclohepten-5-Ones; Nitrilimines; Regioselectivity; X-Ray Crystallographic Analysis; Hydrazonoyl Halides.

237. Kinetics of the Electropolymerization of Aminoanthraquinone from Aqueous Solutions of the Polymer Film and Analytical Applications of the Polymer Film

Shymaa S. Medany, Khaled M. Ismail and Waheed A. Badawy

J. Adv. Res., 3: 261-268 (2012) IF: 3

Poly 1-amino-9,10-anthraquinone (PAAQ) films were prepared by the electropolymerization of 1-amino-9,10-anthraquinone (AAQ) on platinum substrate from aqueous media, where $5.0 \cdot 10^{-3}$ mol L⁻¹ AAQ and 6.0 mol L⁻¹ H₂SO₄ were used. The kinetics of the electropolymerization process was investigated by determining the change of the charge consumed during the polymerization process with time at different concentrations of both monomer and electrolyte. The results have shown that the process follows first order kinetics with respect to the monomer concentration. The order of the reaction with respect to the aqueous solvent i.e. H₂SO₄ was found to be negative. The polymer films were successfully used as sensors for the electroanalytical determination of many hazardous compounds, e.g. phenols and biologically important materials like dopamine. The electroanalytical determination was based on the measurements of the oxidation current peak of the material in the cyclic voltammogram measurements. The cyclic voltammograms were recorded at a scan rate of 100 mV s⁻¹ and different analyte concentrations. A calibration curve was constructed for each analyte, from which the determination of low concentrations of catechol and hydroquinone (HQ) as examples of hazardous compounds present in waste water.

Keywords: Ascorbic Acid; Catechol; Dopamine; Hydroquinone; Polyaminoanthraquinone.

238. Platinum Nanoparticles–Manganese Oxide Nanorods as Novel Binary Catalysts for formic Acid Oxidation

Mohamed S. El-Deab

Journal of Advanced Research, 3: 65-71 (2012) IF: 3

The current study proposes a novel binary catalyst system (composed of metal/metal oxide nanoparticles) as a promising electrocatalyst in formic acid oxidation. The electro-catalytic oxidation of formic acid is carried out with binary catalysts of Pt nanoparticles (nano-Pt) and manganese oxide nanorods (nano-MnO_x) electrodeposited onto glassy carbon (GC) electrodes. Cyclic voltammetric (CV) measurements showed that unmodified GC and nano-MnO_x/GC electrodes have no catalytic activity. Two oxidation peaks were observed at nano-Pt/GC electrode at ca. 0.2 and 0.55 V (corresponding to the direct oxidation of formic acid and the oxidation of the poisoning CO intermediate, respectively). The combined use of nano-MnO_x and nano-Pt results in superb enhancement of the direct oxidation pathway. Nano-MnO_x is shown to facilitate the oxidation of CO (to CO₂) by providing oxygen at low over-potential. This leads to retrieval of Pt active sites necessary for the direct oxidation of formic acid. The higher catalytic activity of nano-MnO_x/nano-Pt/GC electrode (with Pt firstly deposited) compared to its mirror image electrode

(i.e., with MnO_x firstly deposited, nano-Pt/nano-MnO_x/GC) reveals that the order of the electrodeposition is an essential parameter.

Keywords: Nanostructures; Electrocatalysis; Co oxidation; Manganese oxide; Binary catalysts.

239. A New Convenient Synthesis of 3-Hetaryl-Pyrazolo[5,1-C][1,2,4]Triazines

Ahmad S. Shawali

Journal of Advanced Research, 3: 185-188 (2012) IF: 3

Reactions of enamines 2 with diazotized 5-amino-3-henylpyrazole provide a convenient route to 3-[(4,5-disubstituted-pyrazol-3-yl)carbonyl]-pyrazolo[5,1-c][1,2,4]triazines.

Condensation of the latter with hydrazine hydrate yielded the title compounds. The structures of the compounds prepared were elucidated on the basis of their spectral and elemental analyses.

Keywords: Hydrazonoyl Halides; Heterocycles; Enamines; Pyrazoles.

240. New Copper(II)-Selective Chemically Modified Carbon Paste Electrode Based on Etioporphyrin I Dihydrobromide

Yousry M. Issa, Hosny Ibrahim and Ola R. Shehab

J. Electroanal. Chem., 666: 11-18 (2012) IF: 2.905

A new chemically modified carbon paste electrode (CMCPE) based on etioporphyrin I has been developed for the determination of Cu²⁺ in real samples. The performance of this electrode was investigated using potentiometric measurements. The developed sensor exhibits a good linear response with a slope of 30.30 mV per decade over the concentration range of 1.28 × 10⁻⁶–1.28 × 10⁻² mol L⁻¹. It has a very low limit of detection, 8.99 × 10⁻⁷ mol L⁻¹, with response time of 5 s. The proposed electrode revealed very good selectivities with respect to alkali, alkaline earth and some transition metal ions and could be used in pH range of 4.5–8.5. The thermal stability of the electrode was studied. This modified electrode was successfully applied as an indicator electrode for potentiometric titration of Cu²⁺ with EDTA and CDTA. Also the electrode was applied for direct determination of copper in different water samples, milk powder, brass powder and copper rod.

Keywords: Copper carbon paste; Potentiometry; Etioporphyrin.

241. Gold Nanoparticles Modified Electrode for the Determination of an Antihypertensive Drug

Nada F. Atta, Ahmed Galal and Shereen M. Azab

Electroanalysis, 24 (6) : 1431-1440 (2012) IF: 2.872

The nature of binding between Terazosin (TR) and gold nanoparticles (Au-Nps) is investigated using UV-vis and fluorescence spectroscopies, cyclic voltammetry, SEM and EIS. The results suggest that Au-Nps are effective carriers for TR. An electrochemical sensor for TR is introduced using Au-Nps electrodeposited on carbon paste electrode. The effect of parameters including pH and scan rate on the response was investigated. A linear range from 8.0 × 10⁻⁹ to 5.4 × 10⁻⁵ mol L⁻¹ with correlation coefficient of 0.9995 and detection limit of 1.2 ×

10⁻¹⁰ mol L⁻¹ was obtained. This sensor was used for determining TR spiked in urine and excellent recovery results are achieved.

Keywords: Terazosin; Gold nanoparticles; Electrochemical sensor; Impedance spectroscopy.

242. Monodispersed Gold Nanoparticles Decorated Carbon Nanotubes as an Enhanced Sensing Platform for Nanomolar Detection of Tramadol

Nada F. Atta, Rasha A. Ahmed, Hatem M. A. Amin and Ahmed Galal

Electroanalysis, 24, (11) 2135-2146 (2012) IF: 2.872

A promising composite-modified glassy carbon electrode is fabricated by electrodeposition of mono-dispersed gold nanoparticles onto carbon nanotubes (AuNPs/CNTs/GCE). The electroanalysis of Tramadol (TRA) was achieved by different electrochemical techniques. The effect of different parameters including pH, concentration and potential scan on the oxidation current signal of TRA was investigated. Large excess of ascorbic acid (AA) and uric acid (UA) with a maximum molar ratio of 1/1000 and 1/100, respectively, did not interfere with the response of TRA. The detection limit with high sensitivity is 68 nM. TRA was successfully determined in pharmaceutical dosage forms, without any pretreatment of the samples.

Keywords: Electrochemical sensor; Carbon nanotubes; Gold nanoparticles; Tramadol; Uric acid; Ascorbic acid.

243. Reaction of Pregnenolone with Cyanoacetylhydrazine: Novel Synthesis of Hydrazide-Hydrazone, Pyrazole, Pyridine, Thiazole, Thiophene Derivatives and the *in vitro* Cytotoxicity Evaluations

Rafat M. Mohareb and Fatima Al-Omran

Steroids, 77: 1551-1559 (2012) IF: 2.829

Pregnenolone (1) was used as a template to develop new anticancer compounds. Ring D modification of 1 through its reaction with cyanoacetylhydrazine (2) gave the hydrazide-hydrazone derivative 3. The latter compound underwent heterocyclization reactions to give the pyrazole, pyridine, thiazole and thiophene derivatives of pregnenolone. The cytotoxicity of the newly synthesized heterocyclic steroids against three human tumor cell lines namely breast adenocarcinoma (MCF-7), non-small cell lung cancer (NCI-H460) and CNS cancer (SF-268) were studied. Some of tested compounds were found to exhibit much higher inhibitory effects towards the three tumor cell lines than the reference drug, doxorubicin.

Keywords: Cytotoxicity; Pregnenolone; Hydrazide-Hydrazone; Pyrazole.

244. Heterocyclizations of Pregnenolone: Novel Synthesis of Thiosemicarbazone, Thiophene, Thiazole, Thieno[2,3-*b*]Pyridine Derivatives and the *in vitro* Cytotoxicity Evaluations

Rafat M. Mohareb, Wagnat W. Wardakhan, Gamal A. Elmegeed and Rehab M.S. Ashour

Steroids, 77: 1560-1569 (2012) IF: 2.829

Pregnenolone (1) was used as a template to develop new anticancer compounds. Ring D modification of 1 through its reaction with 4-phenyl-3-thiosemicarbazide gave the thiosemicarbazone derivative 3. The latter compound underwent heterocyclization reactions to give the thiazolyl hydrazonoandrostane and pyrazolyl semicarbazidoandrostane derivatives 5a-d and 9a-d, respectively. On the other hand compound 1 reacted with either malononitrile or ethyl cyanoacetate to give the Knoevenagel condensed products 11a and 11b, respectively. Compounds 11a,b afforded the thiophenyl pregnane derivatives 12a and 12b, respectively, their reactivity toward some chemical reagents was studied. The cytotoxicity of the newly synthesized heterocyclic steroids against three human tumor cell lines namely breast adenocarcinoma (MCF-7), non-small cell lung cancer (NCI-H460) and CNS cancer (SF-268) were studied. Some of tested compounds were found to exhibit much higher inhibitory effects toward the three tumor cell lines than the reference drug, doxorubicin.

Keywords: Cytotoxicity; Pregnenolone; Thiosemicarbazides.

245. Chitosan Based Nanofibers, Review

Maher Z. Elsabee, Hala F. Naguib and Rania Elsayed Morsi

Mat Sci Eng C-Mater, 32: 1711-1726 (2012) IF: 2.686

Chitin and chitosan are natural polymers with a huge potential in numerous fields, namely, biomedical, biological and many industrial applications such as waste water treatment due to the fact that they can absorb and chelate many metal cations. Electrospinning is a growing field of research to produce submicron fibers with promising applications in biomedical fields like tissue engineering scaffolds and wound healing capabilities. Both chitin and chitosan polymers were found to be hard to electrospin, however, many researchers manage to produce nanofibers using special solvents; for example, 90% acetic acid was found to reduce the surface tension making electrospinning feasible. Mixtures of organic acids were also experimented to produce homogenous and uniform fibers. Bigger attention was given to electrospinning of their soluble derivatives such as dibutyl and carboxymethyl chitin. More derivatives of chitosan were investigated to produce nano-fibers such as hexanoyl, polyethyleneglycol, carboxymethyl and a series of quaternized chitosan derivatives. The obtained nano-fibers were found to have much better qualities than normal chitosan fibers. Several polymer blends of chitin/chitosan with many commercial polymers were found to be amenable for electrospinning producing uniform beads free fibers. The review surveys the various approaches for successful electrospinning of chitin, chitosan, their derivatives and blends with several other polymers.

Keywords: Chitin; Chitosan; Electrospinning; Chemical modifications; Blends; Nano-fibers.

246. Eclipsed Acetaldehyde as A Precursor for Producing Vinyl Alcohol

Osman I. Osman, Abdulrahman O. Alyoubi, Shabaan A. K. Elroby, Rifaat H. Hilal and Saadullah G. Aziz

International Journal of Molecular Sciences, 13: 15360-15372 (2012) IF: 2.598

The MP2 and DFT/B3LYP methods at 6-311++G(d,p) and aug-cc-pdz basis set have been used to probe the origin of relative

stability preference for eclipsed acetaldehyde over its bisected counterpart. A relative energy stability range of 1.02 to 1.20 cal/mol, in favor of the eclipsed conformer, was found and discussed. An NBO study at these chemistry levels complemented these findings and assigned the eclipsed acetaldehyde preference mainly to the vicinal antiperiplanar hyperconjugative interactions. The tautomeric interconversion between the more stable eclipsed acetaldehyde and vinyl alcohol has been achieved through a four-membered ring transition state (TS). The obtained barrier heights and relative stabilities of eclipsed acetaldehyde and the two conformers of vinyl alcohol at these model chemistries have been estimated and discussed.

Keywords: Acetaldehyde; Eclipsed; Bisected; Vinyl alcohol; Tautomerization; Hyperconjugation; Mp2; B3lyp; Nbo.

247. Synthesis and Antimicrobial Studies of Some Novel Bis-[1,3,4]Thiadiazole and Bis-Thiazole Pendant Thieno[2,3-b]Thiophene Moiety

Nabila Abdelshafy Kheder and Yahia Nasser Mabkhot

International Journal of Molecular Sciences, 13: 3661-3670 (2012) IF: 2.598

The synthetic utility of 3,3'-(3,4-dimethylthieno[2,3-b]thiophene-2,5-diyl) bis (3-oxopropanenitrile) (1) in the synthesis of some novel bis-[1,3,4-thiadiazole] 6a-g and bis-thiazole 10 and 13 derivatives with thieno[2,3-b]thiophene moiety is reported. Antimicrobial evaluation of some selected examples from the synthesized products was carried out and showed promising results.

Keywords: Thieno[2,3-b]Thiophene; Nucleophilic addition; Hydrasonoyl Halides.

248. Toward the Understanding of the Metabolism of Levodopa I. DFT Investigation of the Equilibrium Geometries, Acid-Base Properties and Levodopa-Water Complexes

Shabaan A. K. Elroby, Mohamed S. I. Makki, Tariq R. Sobahi and Rifaat H. Hilal

International Journal of Molecular Sciences, 13: 4321-4339 (2012) IF: 2.598

Levodopa (LD) is used to increase dopamine level for treating Parkinson's disease. The major metabolism of LD to produce dopamine is decarboxylation. In order to understand the etabolism of LD; the electronic structure of levodopa was investigated at the Density Functional DFT/B3LYP level of theory using the 6-311+G** basis set, in the gas phase and in solution. LD is not planar, with the amino acid side chain acting as a free rotator around several single bonds. The potential energy surface is broad and flat. Full geometry optimization enabled locating and identifying the global minimum on this Potential energy surface (PES). All possible protonation/deprotonation forms of LD were examined and analyzed. Protonation/deprotonation is local in nature, i.e., is not transmitted through the molecular framework. The isogyric protonation/deprotonation reactions seem to involve two subsequent steps: First, deprotonation, then rearrangement to form H-bonded structures, which is the origin of the extra stability of the deprotonated forms. Natural bond orbital (NBO) analysis of

LD and its deprotonated forms reveals detailed information of bonding characteristics and interactions across the molecular framework. The effect of deprotonation on the donor-acceptor interaction across the molecular framework and within the two subsystems has also been examined. Attempts to mimic the complex formation of LD with water have been performed.

Keywords: Levodopa; Parkinson'S Disease; Dft; Protonation/ Deprotonation; Nbo.

249. Catalytic Activity Toward Oxygen Evolution of LaFeO₃ Prepared by the Microwave Assisted Citrate Method

Shimaa M. Ali, Yasser M. Abd Al-Rahman and Ahmed Galal

Journal of the Electrochemical Society, 159 (9): 600-605 (2012) IF: 2.59

LaFeO₃ was prepared by the microwave-assisted citrate method and the catalytic activity for oxygen evolution reaction was investigated in HClO₄ solution. The prepared sample was characterized by XRD, HRTEM and FESEM. XRD data showed that pure perovskite phase was indeed formed. The results suggested the successful incorporation of Fe³⁺ at the La³⁺ cations sites confirming the formation of the orthorhombic perovskite phase of LaFeO₃. The particle size calculated from Scherrer equation was found to be 80.56 nm. The orthorhombic phase and the particle size were also ascertained by the HRTEM picture. FESEM image showed a porous and rough surface. Anodic linear polarization was used to evaluate the catalytic activity. The presence of the perovskite modifier increased the electrocatalytic activity toward oxygen evolution reaction (OER) by about 100 times, the current densities obtained at 1.5 V are 3.6×10^{-5} and 1.2×10^{-3} A/cm² for unmodified and modified surfaces, respectively. The order of reaction with respect to [H⁺] is close to unity and the calculated activation energy is 20 kJ/mol, which is much less than the values reported for several catalysts used for OER including some precious metal oxides. EIS results proved the high electrocatalytic activity of LaFeO₃ toward OER.

Keywords: Perovskites; Catalyst; Microwave synthesis; Oer.

250. Synthesis and Antimicrobial Activity of Some Novel Cross-Linked Chitosan Hydrogels

Nadia Ahmed Mohamed and Mona Mohamed Fahmy

Int. J. Mol. Sci., 13: 11194-11209 (2012) IF: 2.59

Four novel hydrogels based on chitosan were synthesized via a cross-linking reaction of chitosan with different concentrations of oxalyl bis 4-(2,5-dioxo-2H-pyrrol- 1(5H)-yl)benzamide. Their structures were confirmed by fourier transform infrared X-ray(FTIR), scanning electron microscopy (SEM) and X-ray diffraction. The antimicrobialactivities of the hydrogels against two crop-threatening pathogenic fungi namely:Aspergillus fumigatus (A. fumigatus, RCMB 06002) and Aspergillus niger (A. niger,RCMB 06106) and five bacterial species namely: Bacillus subtilis (B. subtilis, RCMB6005), Staphylococcus aureus (S. aureus, RCMB 2004), Streptococcus pneumonia (S. pneumonia, RCMB 000101) as Gram positive bacteria and Salmonella typhimurium (S. typhimurium, RCMB 000104) and Escherichia coli (E. coli, RCMB 5003) as Gram negative bacteria have been investigated. The prepared hydrogels showed much higherantimicrobial activities than that of the parent

chitosan. The hydrogels were more potent in case of Gram-positive bacteria than Gram-negative bacteria. Increasing the degree ofcross-linking in the hydrogels resulted in a weaker antimicrobial activity.

Keywords: Chitosan; Chemical cross-Linking; Hydrogels; Antimicrobial activity.

251. Facilitated Electro-Oxidation of formic Acid at Nickel Oxide Nanoparticles Modified Electrodes

Gumaa A. El-Naga, Ahmad M. Mohammad, Mohamed S. El-Deab and Bahgat E. El-Anadouli

Journal of The Electrochemical Society, 159, (7): (2012) IF: 2.59

This study addresses the electrocatalytic oxidation of formic acid (FA) at nickel oxide nanoparticles (nano-NiOx) modified Pt, Au, GC anodes. FA oxidation proceeds at the unmodified Pt electrode with the appearance of two oxidation peaks at 0.25 and 0.65 V corresponding to the direct oxidation of FA to CO₂ and the oxidation of the poisoning intermediate, CO, to CO₂ with a current ratio of the two peaks less than 0.2. Interestingly, this ratio jumps up to more than 50, upon modifying Pt with nano-NiOx. This highlights the essential role of NiOx in enhancing the direct oxidation of FA (at 0.25 V) at Pt substrate. On the other hand, unmodified GC and Au anodes as well as those modified with nano-NiOx exhibit no catalytic response toward FA oxidation. This highlights the essential role of the underlying substrate and depicts also that nano-NiOx behaves as a catalytic mediator which facilitates the charge transfer during the oxidation of FA at Pt anode. Optimization of the surface coverage of nano-NiOx at Pt is achieved, aiming at maximizing the rate of the direct oxidation pathway of FA while suppressing the indirect oxidation route producing the poisoning CO. Moreover, nano-NiOx/Pt anode maintains its high catalytic activity for a prolonged time of continuous oxidation of FA.

Keywords: Nanostructures; Direct formic Acid fuel Cells; Nickel oxide; Electrocatalysis.

252. Electrochemical Determination of Neurotransmitters using Gold Nanoparticles on Nafion/ Carbon Paste Modified Electrode

Nada F. Atta, Ahmed Galal and Shereen M. Azab

J. of The Electrochemical Society, 159: 765-771 (2012) IF: 2.59

A promising electrochemical sensor was developed using carbon paste electrode, gold nanoparticles and Nafion. This sensor is sensitive for the determination of catecholamine compounds, namely dopamine (DA), epinephrine (EP), L-norepinephrine (NP) and L-DOPA, as well as serotonin (5-TH), in the presence of interference molecules such as uric acid (UA) and ascorbic acid (AA). Cyclic voltammetry, differential pulse voltammetry and electrochemical impedance spectroscopy were used to verify the behavior of the studied compounds in the physiological pH of the body. Simultaneous determinations of DA with 5-TH and L-DOPA with acetaminophen (ACOP) give very good peak separations. The linear response was obtained for L-DOPA in the ranges of 2.0×10^{-7} to 2.0×10^{-5} mol L⁻¹ with correlation coefficient 0.9990 and a second range of 5.0×10^{-5} to 3.0×10^{-3} mol L⁻¹ with correlation coefficient 0.9985. LOD was found to be 1.45×10^{-9} mol L⁻¹ and 2.84×10^{-6} mol L⁻¹, respectively. The

utility of this modified electrode was demonstrated for the determination of L-DOPA in human urine.

Keywords: Catecholamines; L-Dopa; Carbon paste electrode; Gold nanoparticles; Nafion.

253. Novel Screen-Printed Electrode for the Determination of Dodecyltrimethylammonium Bromide in Water Samples

Gehad G. Mohamed Tamer Awad Ali, M. F. El-Shahat, M. A. Migahed and A. M. Al-Sabagh

Drug Test. Analysis, 4: 1009-1013 (2012) IF: 2.537

The construction and electrochemical response characteristics of a screen-printed electrode (SPE) for the determination of dodecyltrimethylammonium bromide (DTAB) are described. The sensor was based on the use of DTA-tetraphenylborate ion association complex as an electroactive material in screen-printed electrode with dioctylsebacate (DOS) as a solvent mediator. In aqueous solution of pH 3, the sensor displayed a stable response for six months with reproducible potential and linear response for surfactant over the concentration range 1.20×10^{-2} - 5.6×10^{-7} mol L⁻¹ at 25°C with Nernstian slope of 55.95 ± 0.58 mV decade⁻¹ for detection limit of 6.8×10^{-6} mol L⁻¹. The response time was 6–10 s. The selectivity coefficients indicate excellent selectivity for DTAB over many common cations (e.g. Mg²⁺, Na⁺, K⁺, Co²⁺, Ni²⁺, Ca²⁺, Cl⁻, I⁻, SO₄²⁻ and cetylpyridinium chloride (CPC)). The sensor was used successfully for the determining of DTAB in pure form and water samples with average recoveries of 99.98, 98.78 and 99.99%. Copyright.

Keywords: Dodecyltrimethylammonium bromide; Screen-printed Electrode; Water samples.

254. The Thermal Properties of Biodegradable Poly (Phb/Pcl-Peg-Pcl) Urethanes Nanocomposites using Clay/Poly(-Caprolactone) Nanohybrid Based Masterbatch

Hala F. Naguib, Mohamed S. Abdel Aziz, Sherif M. Sherif and Gamal R. Saad

Applied Clay Science, 57: 55-63 (2012) IF: 2.474

Organoclay/polyurethanes nanocomposites (CPNs) based on bacterial poly(3-hydroxybutyrate), PHB and poly(-caprolactone)-b-poly(ethylene glycol)-b-poly(-caprolactone), PCL-PEG-PCL triblock copolymer with poly(-caprolactone) grafted montmorillonite, Mt-PCL, were prepared by dispersion intercalation method. The microstructure of the CPNs with different content of Mt-PCL was investigated with wide angle X-ray diffraction (WAXD) and transmission electron microscopy (TEM) revealed good dispersion of Mt-PCL within the polyurethane matrix. The thermal properties of the prepared CPNs were investigated with differential scanning calorimetry (DSC) and thermogravimetric analysis (TGA). DSC data revealed the increase in T_g and crystallization rate of both the PHB and PCL-PEG-PCL segments upon incorporation of Mt-PCL. The thermal stability of the nanocomposites was enhanced with increase of the Mt-PCL content. Activation energy (E_a) was evaluated applying both Flynn–Wall–Ozawa and Kissinger methods. The CPNs were found to exhibit a lower activation energy compared with pure polyurethanes, indicating that the

presence of Mt-PCL possesses an accelerating effect on the thermal decomposition of polyurethanes.

Keywords: Clay/Poly(-Caprolactone) Masterbatch; Poly(3-Hydroxybutyrate); Poly(Ester-Ether Urethane); Nanocomposites; Thermal Degradation; Activation Energy.

255. 3-Amino-8-Hydroxy-4-Imino-6-Methyl-5-Phenyl-4,5-Dihydro-3H-Chromeno[2,3-d]Pyrimidine: An Efficient Key Precursor for Novel Synthesis of Some Interesting Triazines and Triazepines as Potential Anti-Tumor Agents

Mohamed G. Badrey and Sobhi M. Gomha

Journal/Molecules, 17: 11538-11553 (2012) IF: 2.386

A number of interesting heterocycles were prepared through interaction of the intermediate 3-amino-8-hydroxy-4-imino-6-methyl-5-phenyl-4,5-dihydro-3H-chromeno-[2,3-d]pyrimidine (1) and reagents such as hydrazonyl halides 2 to furnish triazine derivatives 4a–l. Reaction of 1 with phenacyl bromide afforded compound 5. Moreover, the title compound 1 was subjected to condensation with active methylene compounds (ethyl acetoacetate and ethyl benzoylacetate) to give triazipinones 8a,b. The condensation with aromatic aldehydes afforded either the triazole derivatives 10a–d or Schiff base 11. In addition, the behaviour of compound 1 towards activated unsaturated compounds namely dimethyl acetylene dicarboxylate and ethoxymethylenemalonitrile was studied and it was found to furnish the triazine 13 and triazepine derivative 15, respectively. Combination of title compound 1 with chlorinated active methylene compounds delivered the triazine derivatives 18a–c. Reaction of 1 with chloroacetonitrile furnished compound 20. The structures of the products were elucidated based on their microanalyses and spectroscopic data. Finally, the antitumor activity of the new compounds 4a and 8a against human breast cell MCF-7 line and liver carcinoma cell line HepG2 were recorded.

Keywords: Pyrimidotriazines; Pyrimidotriazepinones; Triazolopyrimidines; Antitumor Activity; Hydrazonyl Halides.

256. A Convenient Ultrasound-Promoted Synthesis of Some New Thiazole Derivatives Bearing A Coumarin Nucleus and the *in vitro* Cytotoxic Activity

Sobhi M. Gomha and Khaled D. Khalil

Molecules, 17: 9335-9347 (2012) IF: 2.386

Successful implementation of ultrasound irradiation for the rapid synthesis of a novel series of 3-[1-(4-substituted-5-(aryldiazonyl)thiazol-2-yl)hydrazono]ethyl]-2H-chromen-2-ones 5a–h, via reactions of 2-(1-(2-oxo-2H-chromen-3-yl)ethylidene)thiosemicarbazide (2) and the hydrazonyl halides 3(4), was demonstrated. Also, a new series of 5-arylidene-2-(2-(1-(2-oxo-2H-chromen-3-yl)ethylidene)hydrazonyl)thiazol-4(5H)-ones 10a–d were synthesized from reaction of 2 with chloroacetic acid and different aldehydes. Moreover, reaction of 2-cyano-N'-(1-(2-oxo-2H-chromen-3-yl)ethylidene)acetohydrazide (12) with substituted benzaldehydes gave the respective arylidene derivatives 13a–c under the conditions employed. The structures of the synthesized compounds were assigned based on elemental analyses and spectral data. Also, the cytotoxic activities of the

thiazole derivative 5a was evaluated against HaCaT cells (human keratinocytes). It was found that compound 5a possess potent cytotoxic activity.

Keywords: Thiosemicarbazides; Thiazoles; Hydrazonoyl Halides; Ultra-Sound Irradiation; Cytotoxic Activity.

257. Synthesis and Antimicrobial Activity of Some New 1,3,4-Thiadiazole Derivatives

Thoraya A. Farghaly, Magda A. Abdallah and Mohamed R. Abdel Aziz

Molecules, 17: 14625-14636 (2012) IF: 2.386

New series of 1,3,4-thiadiazoles have been prepared via reaction of 1,3,4-thiadiazolenaminones 1 with N-phenyl 2-oxopropanehydrazonoyl chloride (2) in dioxane in the presence of triethylamine. Also, some new heterocycles incorporating 1,3,4-thiadiazole ring were obtained by reaction of 1,3,4-thiadiazolenaminones 1 with nitrogen-nucleophiles like hydrazine hydrate, 3-amino-1,2,4-triazole and 2-aminobenzimidazole. The structure of the new products was established based on elemental and spectral analysis. The relation between the structure of the products and their activity towards some microorganisms was studied and promising results were obtained.

Keywords: Antimicrobial Activity; Enaminone; 1;3;4-Thiadiazole; Hydrazonoyl Halides.

258. Synthesis, Tautomeric Structure and Antimicrobial Activity of 3-Arylhydrazono-4-Phenyl-[1,2,4]-Triazepino[2,3-A]Quinazoline-2,7(1H)-Diones

Thoraya Abdel Reheem Farghaly, Mastoura Mohamed Edrees and Mosselhi Abdelnabi Mosselhi

Molecules, 17: 8483-8493 (2012) IF: 2.386

A simple strategy for the synthesis of the hitherto unreported 3-arylazo-4-phenyl-[1,2,4]triazepino[2,3-a]quinazoline-2,7(1H)-diones is described. Spectral data indicated that the studied compounds exist predominantly in the hydrazine tautomeric form. The antimicrobial activity of the newly synthesized compounds was also evaluated. The results indicated that some of these compounds have moderate activity towards bacteria.

Keywords: Azo;Hydrazone; Tautomerism; [1;2;4] Triazepino; [2;3-A]Quinazolinidione.

259. Novel Self-Dyed Wholly Aromatic Polyamide-Hydrazides Covalently Bonded with Azo Groups in the ir Main Chains:1. Structure-Property Relationships

Nadia A. Mohamed, Mohammad H. Sammour and Ali M. Elshafai

Molecules, 17: 13969-13988 (2012) IF: 2.386

Twelve novel intrinsically colored wholly aromatic zopolyamide-hydrazides containing various proportions of para- and meta-phenylene units were successfully synthesized by a low temperature (10 °C) solution polycondensation reaction of either

4-amino-3-hydroxybenzhydrazide (4A3HBH) or 3-amino-4-hydroxybenzhydrazide (3A4HBH) with an equimolar amount of either 4,4'-azodibenzoyl chloride (4,4'ADBC), 3,3'-azodibenzoyl chloride (3,3'ADBC), or mixtures of various molar ratios of 4,4'ADBC and 3,3'ADBC in anhydrous N,N-dimethyl acetamide (DMAc) containing 3% (wt/v) LiCl as a solvent. The structures of the polymers were proven by elemental analysis, FTIR, 1H- and 13C-NMR spectroscopy. The polymers' properties were strongly affected by their various structures. The intrinsic viscosities of the polymers were ranged from 0.7 to 4.75 dL g⁻¹ and increased with the para-phenylene units content. The polymers are partially soluble in DMAc, dimethyl formamide (DMF) and N-methyl-2-pyrrolidone (NMP). Their solubility increases with the introduction of meta-phenylene moieties into the polymer chains. The polymers exhibit a great affinity for water sorption. Their hydrophilicity increases as a function of the content of meta-phenylene rings incorporated into the polymer. Mechanical properties of the polymer films are improved markedly by substitution of para-phenylene units for meta-phenylene units. The completely para-oriented type polymer has the best thermal and thermo-oxidative stability relative to those of the other polymers.

Keywords: Azopolyamide-Hydrazides; Intrinsic Viscosity; Solubility; Crystallinity; Mechanical Properties; Thermal Characteristics.

260. Novel Antimicrobial Organic the rmal Stabilizer and Co-Stabilizer for Rigid Pvc

Mona M. Fahmy, Riham R. Mohamed and Nadia A. Mohamed

Molecules, 17: 7927-7940 (2012) IF: 2.386

Biologically active N-benzoyl-4-(N-maleimido)-phenylhydrazide (BMPH) was synthesized and its structure was confirmed by elemental analysis and various spectral tools. It was examined as a thermal stabilizer and co-stabilizer for rigid poly(vinyl chloride) at 180 °C in air. Blending BMPH with reference samples in different ratios greatly lengthens the thermal stability value and improves the extent of discoloration of PVC. TGA confirmed the improved stability of PVC in presence of the investigated organic stabilizer. GPC measurements were done to investigate the changes occurred in the molecular masses of the degraded samples of blank PVC and PVC in presence of the novel stabilizer. BMPH showed good antimicrobial activity towards two kinds of bacteria and two kinds of fungi.

Keywords: Pvc; Thermal Stability; Discoloration; Antimicrobial Activity.

261. Uses of Cyanoacetylhydrazine in Heterocyclic Synthesis: Novel Synthesis of Pyrazole Derivatives with Anti-Tumor Activities

Rafat M. Mohareb, Nahed N. E. El-Sayed and Mahmoud A. Abdelaziz

Molecules, 17: 8449-8463 (2012) IF: 2.386

The reaction of cyanoacetylhydrazine with chloroacetyl chloride gave N'-(2-chloroacetyl)-2-cyanoacetohydrazide. The latter underwent cyclization to afford 1-(5-amino-3-hydroxy-1H-pyrazol-1-yl)-2-chloroethanone, which underwent nucleophilic substitution to give 3-(5-amino-3-hydroxy-1H-pyrazol-1-yl)-3-oxopropanenitrile. The latter two compounds were

used as key synthons to synthesize new thiophene, pyran, thiazole and some fused heterocyclic derivatives. The antitumor activity of the newly synthesized compounds was evaluated against three human tumor cells lines, namely breast adenocarcinoma (MCF-7), non-small cell lung cancer (NCI-H460) and CNS cancer (SF-268) and some of these compounds were found to exhibit much higher inhibitory effects towards the three tumor cell lines than the Gram positive control doxorubicin.

Keywords: Pyrazole; Thiophene; Thiazole; Antitumor

262. The Role of Ni Content on the Stability of Cu-Al-Ni Ternary Alloy in Neutral Chloride Solutions

H. Nady, N.H. Helal, M.M. El-Rabiee and W.A. Badawy

Materials Chemistry And Physics, 134: 945-950 (2012) IF: 2.234

The effect of systematic increase of Ni content on the electrochemical behavior of the Cu-Al-Ni ternary alloys in neutral chloride solutions was investigated. Alloys with Ni contents, 5, 10, 30 and 45 mass% were used. The effect of chloride ions on the electrochemical behavior of these alloys was investigated. The presence of Al in the alloy increases its stability. An increase in the nickel content decreases the corrosion rate of the alloys. Conventional electrochemical techniques and electrochemical impedance spectroscopy, EIS, were used. The impedance measurements have shown that the increase of the Ni content and the immersion time of the alloys in the chloride solution increase the corrosion resistance of the alloys. The experimental impedance data were fitted to theoretical data according to a proposed model representing the electrode/electrolyte interface and the equivalent circuit parameters were calculated.

Keywords: Cu-Al-Ni Alloys; Corrosion; Impedance; Passivation; Polarization.

263. Preparation, Characterization and Properties of Novel 0-3 Ferroelectric Composites of Ba_{0.95}Ca_{0.05}Ti_{0.8}Zr_{0.2}O₃-Poly(Vinylidene Fluoride-Trifluoroethylene)

E. El. Shafee and S.M. Behery

Materials Chemistry And Physics, 132: 740-746 (2012) IF: 2.234

The present work describes the preparation and properties of a novel ceramic-polymer composites using Ba_{0.95}Ca_{0.05}Ti_{0.8}Zr_{0.2}O₃ (BCTZ) as a ceramic filler and poly(vinylidene fluoride trifluoroethylene) [P(VDF-TrFE)] as a polymer matrix. The BCTZ ceramics were prepared by the conventional solid-state reaction route whereas the BCZT-P(VDF-TrFE) composites with various BCTZ volume fractions were prepared by the combined method of solvent casting and hot pressing. The microstructure of the composites was investigated using scanning electron microscopy and X-ray diffraction. The dependences of the dielectric properties of the composites on BCTZ volume fraction was reported and analyzed in terms of the effective medium theory (EMT). The P-E hysteresis loops of the composites are strongly dependent on the ceramic volume fraction. The composites with higher ceramic volume fractions showed larger remanent polarization and smaller coercive field. The mechanical properties of the composites were investigated. Tensile strength showed enhancement at lower ceramic content and decreased with higher ceramic loading while Young's modulus showed increase with respect to the ceramic loading.

Keywords: Composite materials; Ceramics; Mechanical properties; Ferroelectricity.

264. Effect of Li₂O – Doping on Physicochemical, Surface and Catalytic Properties of Nanosized CuO-Mn₂O₃ / Cordierite System

Gamil A. El-Shobaky, Hala G. El-Shobaky, Abdelrahman A. Badawy and Ghada M. Mohamed

Materials Chemistry And Physics, 136: 1143-1147 (2012) IF: 2.234

Physicochemical, surface and catalytic properties of pure and Li₂O-doped (0.75-3.0 mol.%) CuO-Mn₂O₃ supported on cordierite (commercial grade) preheated in air at 500 °C were investigated using XRD, EDX, nitrogen adsorption at -196 °C and catalysis of CO-oxidation by O₂ at 250 °C. The results revealed that treating the support material with 10 wt.% of both CuO and Mn₂O₃ followed by heating in air at 500 °C which much increased its SBET (several folds) led to the formation of nanosized CuO and CuMn₂O₄ phases. Li₂O-doping enhanced copper manganite (CuMn₂O₄) formation. The doping process increased effectively the surface concentration of both copper and manganese species due to an enhanced formation of CuMn₂O₄ on top surface layers of the doped system leading to an important increase in its catalytic activity.

Keywords: Co-Oxidation; Copper Manganite; Cordierite; Li₂O Dopant.

265. Molecular Structures of 2-Arylaminoethyl-1H-Benzimidazole: Spectral, Electrochemical, Dft and Biological Studies

Nour T. Abdel Ghani and Ahmed M. Mansour

Spectrochimica Acta Part A: Molecular and Biomolecular Spectroscopy, 91: 272-284 (2012) IF: 2.098

In the present work, structural studies on (1H-benzimidazol-2-ylmethyl)-N-(4-chloro-phenyl)-amine (L1) and (1H-benzimidazol-2-ylmethyl)-N-(4-iodo-phenyl)-amine (L2) have been done extensively by a variety of physico-chemical techniques. Optimized geometrical structures, harmonic vibrational frequencies, natural bonding orbital (NBO) analysis and Frontier molecular orbitals (FMO) were obtained by DFT/B3LYP method. TD-DFT calculations help to assign the electronic transitions. The polarizable continuum model (PCM) fails to describe the experimental chemical shift associated with the NH protons as calculated by applying Gauge-invariant atomic orbital (GIAO) method, but a very good correlation between the theoretical and experimental values was achieved by taking into account the specific solute solvent interactions. DFT calculations showed a good agreement between the theoretical and observed results. These compounds exhibited a high biological activity through the inhibition of the metabolic growth of the investigated bacteria.

Keywords: Benzimidazole; Hydrogen; Bonding; Crystal Structure; Nbo; Td-Dft.

266. A theoretical Dft Study on the Structural Parameters and Azide–Tetrazole Equilibrium in Substituted Azidothiazole Systems

Rafie H. Abu-Eittah and Khaled E. El-Kelany

Spectrochimica Acta Part A, 99: 316-328 (2012) IF: 2.098

The literature is rich in experimental data which report the effect of substituent on the azide-tetrazole equilibrium in the system: 2-azido-1,3-thiazole but without a theoretical basis. Here, the effect is investigated theoretically using the B3LYP/6311G level of theory. The two steps involved in the reaction, namely, azide group rotation from the trans to the cis conformer and the ring closure of the azide group to the tetrazole ring are investigated, the PES of each step is constructed, the TS of each step is identified and confirmed. Electron donor substituents shift the equilibrium to the tetrazole isomer and in some cases the azide isomer cannot be isolated. Electron withdrawing substituents shift the equilibrium to the azide isomer, in some cases, the tetrazole isomer cannot be isolated.

267. Preparation, Spectroscopic and the rmal Characterization of New Metal Complexes of Verlipride Drug, in Vitro Biological Activity Studies

M.H. Solimana and Gehad G. Mohamed

Spectrochimica Acta (Part A), 91: 11-17 (2012) IF: 2.098

Metal complexes of the general formula $[M(VER)_2Cl_2(H_2O)_2] \cdot yH_2O$ and $[Cr(VER)_2Cl_2(H_2O)_2]Cl \cdot H_2O$ (where VER = verlipride, M = Mn(II) (y = 2), Co(II) (y = 2), Ni(II) (y = 2), Cu(II) (y = 1) and Zn(II) (y = 0)) are prepared and characterized based on elemental analyses, IR, 1H NMR, magnetic moment, molar conductance and thermal analyses (TG and DTA) techniques. From the elemental analyses data, the complexes are formed in 1:2 [Metal]:[VER] ratio.

The molar conductance data reveal that all the metal chelates are non-electrolytes except Cr(III) complex, it is 1:1 electrolyte. IR spectra show that VER is coordinated to the metal ions in a neutral monodentate manner with O donor site of the carbonyl O atom.

On the basis of spectral studies and magnetic moment measurements an octahedral geometry has been assigned for the complexes. The thermal behavior of these chelates is studied using thermogravimetric analysis technique. The results obtained show that the complexes lose hydrated water, HCl and coordinated water molecules followed immediately by decomposition of the ligand molecules in the successive unseparate steps.

The VER drug, in comparison to its metal complexes is also screened for its biological activity against Gram positive bacterial (*Staphylococcus aureus*) and Gram negative bacteria (*Escherichia coli*) and fungi (*Candida albicans* and *Aspergillus flavus*) in vitro. The activity data show that most of the metal complexes have antibacterial activity like or higher than that of the parent VER drug against one or more species.

Keywords: Verlipride; Metal complexes; Ir; Molar conductance; Magnetic moment; 1H nmr; Thermal analyses; Biological activity.

268. Spectrophotometric Studies of Reactions Between Pseudo-Ephedrine with Different Inorganic and Organic Reagents and its Micro-Determination in Pure and in Pharmaceutical Preparations

M.A. Zayed and El-Gazy A. El-Rasheedy

Spectrochimica Acta Part A, 88: 156-161 (2012) IF: 2.098

Two simple, sensitive, cheap and reliable spectrophotometric methods are suggested for micro-determination of pseudoephedrine in its pure form and in pharmaceutical preparation (Sinofree Tablets). The first one depends on the drug reaction with inorganic sensitive reagent like molybdate anion in aqueous media via formation of ion-pair mechanism. The second one depends on the drug reaction with bi-acceptor reagent like DDQ in non-aqueous media via formation of charge transfer complex. These reactions were studied under various conditions and the optimum parameters were selected. Under proper conditions the suggested procedures were successfully applied for micro-determination of pseudoephedrine in pure and in Sinofree Tablets without interference from excipients. The values of SD, RSD, recovery %, LOD, LOQ and Sandell sensitivity refer to the high accuracy and precision of the applied procedures. The results obtained were compared with the data obtained by an official method, referring to confidence and agreement with DDQ procedure results; but it referred to the more accuracy of the molybdate data. Therefore, the suggested procedures are now successfully being applied in routine analysis of this drug in its pharmaceutical formulation (Sinofree) in Saudi Arabian Pharmaceutical Company (SPIMACO) in Boridah El-Qaseem, Saudi Arabia instead of imported kits had been previously used.

Keywords: Spectrophotometer; Pseudoephedrine; Molybdate.

269. Synthesis and Structural Characterization of Pd (N,N-Dimethylaminopropylamine)Cl₂Complex the Interaction with Bio-Relevant Ligands with Reference to the Effect of Cysteine on the Deactivation of Metal-Based Drug

Shehata MR, Shoukry MM and Ragab MS. Source

Spectrochimica Acta Part A: Molecular and Biomolecular Spectroscopy, 96: 809-814 (2012) IF: 2.098

The synthesis and X-ray structural characterization of Pd (DMPA) Cl₂ complex, where DMPA = N,N-dimethylaminopropylamine, is reported. The complex crystallizes in the space group P2₁/c, a=8.8923(4), b=10.9050(5), c=11.5006(7) Å, β=120.00(18)°, V=948.25(8)³, Z=4. The palladium centre has a typical square-planar geometry with a tetrahedral distortion. Stoichiometry and stability constants of the complexes formed between $[Pd(DMPA)(H_2O)_2]^{2+}$ and some selected DNA constituents and cysteine are investigated at 25°C and at constant 0.1 M ionic strength. The concentration distribution diagrams of the various species formed are evaluated. The equilibrium constants for the displacement of coordinated ligands as inosine by cysteine are calculated. The results are expected to contribute to the chemistry of tumour therapy.

Keywords: Crystal structure; N; N-Dimethylaminopropylamine; Pd(II) Complex; Stability constant; Displacement reaction.

270. Microplate Assay for Screening the Antibacterial Activity of Schiff Bases Derived From Substituted Benzopyran-4-One

Rehab M. Amina

Spectrochimica Acta Part A, 95: 517-525 (2012) IF: 2.098

Schiff bases (SB1–SB3) were synthesized from the condensation of 6-formyl-7-hydroxy-5-methoxy-2-methylbenzopyran-4-one with 2-aminopyridine (SB1), p-phenylenediamine (SB2) and o-phenylenediamine (SB3), while Schiff bases (SB4–SB6) were synthesized by condensation of 5,7-dihydroxy-6-formyl-2-methylbenzopyran-4-one with 2-aminopyridine (SB4), p-phenylenediamine (SB5) and o-phenylenediamine (SB6). Schiff bases were characterized using elemental analysis, IR, UV-Vis, ¹H-NMR, ¹³C NMR and mass spectroscopy.

These compounds were screened for antibacterial activities by micro-plate assay technique. *Escherichia coli* and *Staphylococcus capitis* were exposed to different concentrations of the Schiff bases. Results showed that the antibacterial effect of these Schiff bases on Gram-negative bacteria were higher than that on Gram-positive bacteria moreover, the Schiff bases containing substituent OCH₃ on position five have higher antibacterial activity than that containing hydroxy group on the same position.

Keywords: Schiff Bases; Antibacterial Effect; Benzopyran-4-One; Microplate Assay.

271. Molecular Structure of 2-Chloromethyl-1H-Benzimidazole Hydrochloride: Single Crystal, Spectral, Biological Studies and Dft Calculations

Abdel Ghani NT and Mansour AM

Spectrochimica Acta Part A: Molecular and Biomolecular Spectroscopy, 18:(2012) IF: 2.098

In the present work, structural studies on 2-chloromethyl-1H-benzimidazole hydrochloride have been performed extensively by X-ray crystallography, ¹H NMR, FT-IR, UV/vis and elemental analysis. The title compound crystallizes in a monoclinic space group P2₁/c with a = 7.1982 (3) Å, b = 9.4513 (5) Å, c = 14.0485 (7) Å and β = 102.440 (3)° forming an infinite chain structure parallel to “b” axis through the intermolecular hydrogen bond.

Optimized geometrical structure, harmonic vibrational frequencies, natural bonding orbital (NBO) and frontier molecular orbitals (FMO) were obtained by DFT/B3LYP method combined with 6-31G(d) basis set. TD-DFT calculations help to assign the electronic transitions.

The ¹H NMR chemical shifts were computed at the B3LYP/6-311 + G(2d,p) level of theory in different solvents by applying GIAO method using the polarizable continuum model (PCM). The title compound was screened for its antibacterial activity referring to Tetracycline as a standard antibacterial agent.

Keywords: Benzimidazole; Hydrogen-bonding; Crystal structure; Nbo; Td-Dft.

272. Synthesis and Characterization of New Chromium, Molybdenum and Tungsten Complexes of 2-[2-(Methylaminoethyl)] Pyridine

Saadia A. Alia, Ahmed A. Soliman, Amany H. Mareia and Doaa H. Nassar

Spectrochimica Acta, 94: 164-168 (2012) IF: 2.098

A green chemistry route of synthesis using direct sunlight irradiation for the reactions of [M(CO)₆] M = Cr, Mo or W with 2-[2-(methylaminoethyl)] pyridine (maepy) in THF. The reactions resulted in the formation of the oxo complex [Cr₂(O)₄(maepy)₂] (1) and the tetracarbonyl complexes [Mo(CO)₄(maepy)] (2) and [W(CO)₄(maepy)] (3). The prepared complexes were characterized by elemental analysis, IR, NMR, mass spectrometry and magnetic measurement. The complexes (1–3) were further investigated by thermo-gravimetric technique (TG). The biological activity of maepy and complexes as antibacterial and antifungal reagents have been investigated.

Keywords: Chromium; Molybdenum; Tungsten 2-[2-(Methylaminoethyl)]; Pyridine; Ppectral and biological investigation.

273. The Rmodynamics of the Interaction of Pd (Dmen) (H₂O)₂²⁺ with Bio-Relevant Ligands with Reference to the Deactivation of Metal Based Drug by Thiol Ligands

Mohamed R Shehata, Mohamed M Shoukry and Sara Ali

Spectrochimica Acta Part A: Molecular and Biomolecular Spectroscopy, (2012) IF: 2.098

Pd (dmen) Cl₂ complex was synthesized and characterized, where dmen = N,N-dimethylethylenediamine. Stoichiometry and stability constants of the complexes formed between [Pd(dmen)(H₂O)₂]²⁺ and various biologically relevant ligands such as amino acids, peptides and dicarboxylic acids are investigated at 25 °C and at constant 0.1 M ionic strength. The concentration distribution diagrams of the various species formed are evaluated. The equilibrium constants for the displacement of coordinated ligands as inosine, glycine or methionine by cysteine are calculated. The results are expected to contribute to the chemistry of tumour therapy.

Keywords: Palladium (II); Antitumour activity; Displacement reactions; Biorelevant ligands.

274. Synthesis, Characterization and Biological Activities of Some New Chromium Molybdenum and Tungsten Complexes with 2,6-Diaminopyridine

Ahmed A. Soliman, Saadia A. Ali, Amany H. Marei and Doaa H. Nassar

Spectrochimica Acta, 89: 329-332 (2012) IF: 2.089

The reactions of [M(CO)₆], M = Cr, Mo, W with 2,6-diaminopyridine (dap) in ethanol was carried out under sun light and microwave irradiation routes of synthesis and compared with the traditional thermal reflux method. All routes resulted in the formation of the binuclear oxo complexes with the general formulas [M₂(O)₄(dap)₂]. The prepared complexes were characterized using elemental analysis, IR, ¹H NMR, mass

spectrometry and magnetic measurement. The biological activity of dap and its complexes as antibacterial and antifungal reagents have been screened.

Keywords: Chromium; Molybdenum; Tungsten; 2,6 diaminopyridine (Dap); Spectral and biological study.

275. Synthesis, Characterization, Biological Activity and Equilibrium Studies of Metal (II) Ion Complexes with Tridentate Hydrazone Ligand Derived from Hydralazine

Ahmed A. El-Sherif, Mohamed M. Shoukry and Mohamed M.A. Abd-Elgawad

Spectrochimica Acta Part A: Molecular and Biomolecular Spectroscopy, 98: 307-321 (2012) IF: 2.04

In the present study, a new hydrazone ligand (2-((2-phthalazin-1-yl)hydrazono)methyl)phenol) prepared by condensation of hydralazine (1-Hydralazinophthalazine) with salicylaldehyde (SAH). The synthesized SAH-hydrazone and its metal complexes have been characterized by elemental analyses, IR, ¹H NMR, solid reflectance, magnetic moment, molar conductance, mass spectra, UV-vis and thermal analysis (TGA). The analytical data of the complexes show the formation of 1:1 [M:L] ratio, where M represents Ni(II), Co(II) and Cu(II) ions, while L represents the deprotonated hydrazone ligand. IR spectra show that SAH is coordinated to the metal ions in a tridentate manner through phthalazine-N, azomethine-N and phenolic-oxygen groups. The ligand and their metal chelates have been screened for their antimicrobial activities using the disc diffusion method against the selected bacteria and fungi. Proton-ligand association constants of (SAH) and the stepwise stability constants of its metal complexes are determined potentiometrically in 0.1 M NaNO₃ at different temperatures and the corresponding thermodynamic parameters were derived and discussed. The order of ΔG° and ΔH° were found to obey $Mn^{2+} < Co^{2+} < Ni^{2+} < Cu^{2+}$, in accordance with the Irving-Williams order. The complexes were stabilized by enthalpy changes and the results suggest that the complexation is an enthalpy-driven process. The concentration distribution diagrams of the complexes are evaluated.

Keywords: Hydrazones; Metal(Ii) Hydralazine; Electronic Spectra; Stability Constants; Biological Activity.

276. Degradable Polyurethane Soy Protein Shape-Memory Polymer Blends Prepared Via Environmentally Friendly Aqueous Dispersions

Samy A. Madbouly and Andreas Lendlein

Macromolecular Materials and Engineering, 297: 1213-1224 (2012) IF: 1.986

Degradable polyurethane/soybean protein (PU/SP) shape-memory polymer blends are synthesized using an environmentally-friendly aqueous dispersion technique. The effects of SP concentration on the blend miscibility, thermal properties, hydrolytic degradation and shape-memory behavior are investigated. The shape recovery rates are found to depend on SP concentration. A porous structure can be generated using scCO₂ foaming. This degradable blend may be an interesting multifunctional candidate material for potential biomedical applications.

Keywords: Aqueous dispersion; Soybean; Polymer blends; Miscibility.

277. Synthesis and Biological Evaluation of A Novel Series of Chalcones Incorporated Pyrazole Moiety as Anticancer and Antimicrobial Agents

Walid Salama, Mourtada El Aref and Reinhard Gaupp

Appl Biochem Biotechnol, 168: 1153-736 (2012) IF: 1.943

A newly synthesized series of chalcone derivatives containing pyrazole rings were synthesized and evaluated for their cytotoxic activities in vitro against several human cancer cell lines. Most of the prepared compounds showed potential cytotoxicity against human breast cancer cell lines MCF-7, HEPG-2 and HCT-116. Also the compounds were evaluated as antimicrobial agents. The three compounds 3, 4 and 5 were proved to be better anticancer agents than the positive standard doxorubicin with IC₅₀ values (4.7, 4.4 and 3.9g/ml) against the same human cancer cell lines, whereas compounds 5 and 6 showed the most active antimicrobial compounds in comparison to the other chalcones.

Keywords: Chalcones; Cancer cell lines (Mcf-7, Hepg-2 and Hct-116); Potential.

278. The Effect of Different Ethoxylations for Sorbitan Monolaurate on Enhancing Simultaneous Saccharification and Fermentation (SSF) of Wheat Straw to Ethanol

A. M. Badawi , A. A. Fahmy , Karima A. Mohamed , M. R. Noor El-Din and M. G. Riad

Appl Biochem Biotech, 166: 22-35 (2012) IF: 1.943

In this paper, four nonionic surfactants with different hydrophilic-lipophilic balance (HLB) based on sorbitan monolaurate were synthesized by introducing ethylene oxide gas ($n=20,40, 60$ and 80 ethylene oxide units). The chemical structure of the prepared ethoxylated surfactants was confirmed using Fourier transform-infrared and ¹H NMR spectroscopies. The surface tension and thermodynamic properties of the prepared surfactants have been studied. The simultaneous saccharification and fermentation (SSF) process for ethanol production from microwave/alkali pretreated wheat straw has been assayed using nonionic surfactants having different ethylene oxide units. Ethanol yield was 82% and 61% for *Kluyveromyces marxianus* and *Saccharomyces cerevisiae*, respectively, with the addition of 2.5 g/l of the prepared nonionic surfactant (HLB=18.2). Results show that the production of ethanol from microwave/alkali pretreated wheat straw increased with increasing the (HLB) value of the nonionic surfactant.

Keywords: Nonionic surfactants; Simultaneous; Yeast saccharification and fermentation (Ssf); Wheat straw; Ethanol.

279. Molecular Dynamics Study of Ethanol Solvated by Water on the Pt (111) Surface

Kholmimirz Kholmurodov, Ermuhammad Dushanov, Kenji Yasuoka, Hagar Khalil, Ahmed Galal, Sameh Ahmed, Nasser Sweilam and Hatem Moharram

Chem Phys, 402: 41-47 (2012) IF: 1.896

An analysis of the molecular dynamics of ethanol solvated by water molecules in the absence and presence of the Pt (1 1 1) surface has been performed using DL_POLY version 2.19. The structure and diffusion properties of an ethanol–water system have been studied at various temperatures from 250 to 350 K. We have measured the self-diffusion coefficients of a 50:50% ethanol–water system; in the absence of a Pt surface our results have shown an excellent agreement with the experimental data (within an error of 7.4%). The enhancement of self-diffusion coefficients with the inclusion of the Pt (1 1 1) surface has been observed and estimated. Graphs of radial distribution functions (RDF) have been built; RDF correlations with the self-diffusion coefficients of both ethanol and water molecules are also illustrated.

Keywords: Molecular Dynamics Simulations; Ethanol Molecule; Water Active Solvent; Diffusion Coefficient; Pt Surface.

280. Influence of Electrodeposition Parameters on the Characteristics of Nimop Film

Z. Abdel Hamid and H.B. Hassan

Surface and Coatings Technology, 212 (2012): 37-45 (2012)

IF: 1.867

In the present work, NiMoP thin films have been electrodeposited from citrate bath onto Cu sheets for the application as diffusion barriers and metal capping layers in the copper interconnect technology. The study focused on the effect of the electrodeposition parameters including $[\text{MoO}_4^{2-}]/\text{Ni}^{2+}$ molar ratio, temperature, pH and current density on the properties of NiMoP films. The morphology, textural components and phase structures of the coatings were evaluated using scanning electron microscopy (SEM), energy-dispersive X-ray (EDX) analysis and X-ray diffraction (XRD), respectively. The results revealed that the maximum deposition rate was found at 0.122 $[\text{MoO}_4^{2-}]/\text{Ni}^{2+}$ molar ratio. However, for the highest examined $[\text{MoO}_4^{2-}]/\text{Ni}^{2+}$ molar ratio, a considerable decrease in the rate of the process is subsequently observed. The influences of deposition current density, solution pH and deposition temperature at a certain $[\text{MoO}_4^{2-}]/\text{Ni}^{2+}$ molar ratio on the plating rate and chemical composition were studied. NiMoP alloys of high Mo at.% as-deposited films showed an irregular microcrack structure while those of low Mo at.% showed an amorphous/nanocrystalline structure. However, after heat treatment at 400 °C for 1 h, the deposited films converted into polycrystalline structure. The magnetic nature of coated materials has been studied by hysteresis loop measurements. The corrosion results were calculated from polarization Tafel lines and electrochemical impedance spectroscopy (EIS) for as-plated NiMoP coatings in a 3.5% NaCl solution.

Keywords: Nimop electrodeposition; Barrier layers; Capping layers; Thin films; Ferromagnetic; Corrosion.

281. Palladium (II) Complex Taken as A Model of An Antitumour Agent: Synthesis and Equilibrium Investigation Involving Biologically Relevant Ligands

Mohamed M. Shoukry, M.M. Hassouna and R.K. Mahmouda

Cr Chim, 15: 356-364 (2012) IF: 1.803

Pd (DHP)Cl₂ and Pd(DHP)(CBDCA) complexes (DHP = 1,3-diamino-2-hydroxopropane and CBDCA = 1,1-

cyclobutanedicarboxylate), were synthesized and characterized by elemental analysis, IR and NMR spectral measurements. The coordination of $[\text{Pd}(\text{DHP})(\text{H}_2\text{O})_2]^{2+}$ with some selected bio-relevant ligands, containing different functional groups was investigated. The ligands used are amino acids, peptides, DNA constituents and dicarboxylic acids. Stoichiometry and stability constants of the complexes formed are reported at 25 °C and 0.1 M ionic strength. The results show the formation of 1:1 complexes with amino acids and dicarboxylic acids. DNA constituents form 1:1 and 1:2 complexes. Peptides form both 1:1 complexes and the corresponding deprotonated amide species. The effect of chloride ion concentration and dioxane on the acid dissociation constants of 1,1-cyclobutane dicarboxylic acid (CBDCAH₂) and the formation constant of its complex with $\text{Pd}(\text{DHP})^{2+}$ was reported. The equilibrium constants for the displacement of coordinated ligands as uracil, glycine or methionine by cysteine are calculated. The results are expected to contribute to the chemistry of antitumour agents.

Keywords: Amino acids; Peptides; Dna; dicarboxylic Acids; 1;3-diamino-2-Hydroxopropane; Stability constants.

282. Electronic Structure and Decomposition Reaction Mechanism of Cyclopropanone, Phenylcyclopropanone and the ir Sulfur Analogues: A theoretical Study

Shabaan A. K. Elroby, Saadullah G. Aziz and Rifaat Hilal

Journal of Molecular Modeling, (2012) IF: 1.797

The electronic structure, the origin of the extraordinary stability and the reaction mechanisms of the decomposition reaction of the three-membered ring cyclopropanone (IO), its phenyl derivative (IIO) and its sulfur analogues (IS and IIS) have been investigated at the B3LYP/6-311+G. level of theory. All critical points on the reaction surface, reactants, transition states and intermediates were determined. Reaction rate constants and half-lives have been computed. Natural bond orbital (NBO) analysis has been used to investigate the type and extent of interaction in the studied species. Results indicate that the decomposition reaction occurs via a stepwise mechanism, with the formation of a short-lived intermediate. The characters of the intermediates for the decomposition of IIO and IIS are different. In case of IIO decomposition, the intermediate structure is of prevailing zwitterionic character, whereas that for the decomposition of IIS is of prevailing carbene character. Solvent effects are computed, analyzed and discussed.

Keywords:

Density functional theory; Phenylcyclopropanone; Natural Bond Orbital; Zwitterion; Decomposition Reaction.

283. Electrical Properties of Multi Walled Carbon Nanotubes Poly (Vinylidene Fluoride Trifluoroethylene) Nanocomposites

E. El Shafee, M. El Gamal and M. Isa

J Polym Res, 1-8 (2012) IF: 1.733

Poly (vinylidene fluoride-trifluoroethylene) (PVDF-TrFE)/multi-walled carbon nanotube (MWCNT) nanocomposites were prepared by the method of solution mixing/casting. The dispersity of the MWCNTs in the PVDF-TrFE matrix was investigated using transmission electron microscopy (TEM), revealing that MWCNT

are well distributed in the PVDF matrix. Both individual and agglomerations of MWCNT's were evident. The electrical properties were characterized by ac conductivity measurements. The conductivity was found to obey a percolation-like power law with a percolation threshold below 0.30 wt. %. The electrical conductivity of the neat PVDF-TrFE could be enhanced by seven orders of magnitude, with the addition of only 0.3 wt. % MWCNTs, suggesting the formation of a well-conducting network by the MWCNT's throughout the insulating polymer matrix. The intercluster polarization and anomalous diffusion models were used to explain the dielectric behaviors of the composites near the percolation threshold and the analyses of ac conductivity and dielectric constant imply that the intercluster polarization is more applicable to our systems.

Keywords: Nanocomposites. Electrical Conductivity. Percolation Threshold; Poly(Vinylidene Fluoride-Trifluoroethylene).

284. Novel Antimicrobial and Antitumor Organic Thermal Stabilizers for Rigid Poly (Vinyl Chloride)

M. W. Sabaa and R. R. Mohamed

J Therm Anal Calorim, 109: 1503-1513 (2012) IF: 1.604

Pyrazolodithiones of expected biological activity were examined as thermal stabilizers and co-stabilizers for rigid poly(vinyl chloride) (PVC) in air at 180 °C. Their high stabilizing efficiency were shown by their high thermal stability values (Ts), which is the time needed for the liberation of HCl gas, if compared with dibasic lead carbonate (DBLC) and calcium-zinc soap (Ca-Zn soap) reference stabilizers used industrially, with better extent of discoloration. Blending these derivatives with reference stabilizers in different ratios greatly lengthens the thermal stability value and improves the extent of discoloration of the PVC. The structure of the novel organic stabilizers was confirmed by elemental analysis, FTIR, Mass spectra and ¹H-NMR. Thermogravimetric analyses confirmed the improved stability of PVC in the presence of the investigated organic stabilizers, compared to blank PVC and PVC stabilized with the reference stabilizers. Also, GPC measurements were done to investigate the changes occurred in the molecular masses of the degraded samples of PVC in presence of the newly synthesized stabilizers. The stabilizing efficiency of pyrazolodithionesis attributed to the replacement of the labile chlorine atoms on the PVC chains by a relatively more stable moiety of the organic stabilizer. The investigated stabilizers showed a good antimicrobial activity toward two kinds of bacteria, *Escherichia coli* and *Staphylococcus aureus*; and also toward two kinds of fungi, *Aspergillus flavus* and *Candida albicans*. They also exhibited antitumor activity against both liver and colon human cell lines.

Keywords: Pvc; Pyrazolodithiones; Stabilizer.

285. The Thermal and Mass Spectral Characterization of Novel Azo Dyes of P-Aceto-Amido-Phenol in Comparison with Hammett Substituent Effects and Molecular Orbital Calculations

M. A. Zayed, Gehad G and Mohamed M. A. Fahmey

J Therm Anal Calorim, 107: 763-776 (2012) IF: 1.604

Four novel azo compounds were synthesized: o-phenylazo-C₁₄H₁₃N₃O₂ (I), p-bromo-o-phenylazo-(C₁₄H₁₃BrN₃O₂) (II),

p-methoxy-o-phenylazo-(C₁₅H₁₆N₃O₃) (III) and p-nitro-o-phenylazo-p-acetamidophenol (C₁₄H₁₃N₄O₄) (IV). These compounds were carefully investigated using elemental analyses, IR and thermal analyses (TA) in comparison with electron ionization (EI) mass spectral (MS) fragmentation at 70 eV. Semi-empirical MO calculation, PM3 procedure, has been carried out on the four azo dyes (I-IV), both as neutral molecules and the corresponding positively charged molecular ions. These included molecular geometries (bond length, bond order and charge distribution, heats of formation and ionization energies). The mass spectral fragmentation pathways and thermal decomposition mechanisms were reported and interpreted on the basis of molecular orbital (MO) calculations. They are found to be highly correlated to each other. Also, the Hammett's effects of p-methoxy, p-bromo and p-nitro-substituents of phenyl azo groups on the thermal stability of these dyes (I-IV) are studied by experimental (TA and MS) in comparison with MO calculations and the data obtained are discussed. This research aimed chiefly to throw more light on the structures of the four prepared azo derivatives of acetoamido-phenol (p-acetamol). The data referring to the thermal stability of these dyes can be used in industry for effective dyeing purposes under different thermal conditions.

Keywords: Acetamidophenol Azodyes; Hammett Effect; Ft-Ir; Mass Spectrometry; Thermal Analyses; Mo-Calculations.

286. Investigation of Ibuprofen Drug using Mass Spectrometry, the Thermal Analyses and Semi-Empirical Molecular Orbital Calculation

Mohamed A. Zayed and M. F. Hawash

J Therm Anal Calorim, 108: 315-322 (2012) IF: 1.604

Ibuprofen (C₁₅H₁₈O₂) is an anti-inflammatory drug. It is important to investigate its structure to know the active groups and weak bond responsible for its medical activity. Consequently in the present study, ibuprofen was investigated by mass spectrometry (MS) and thermal analyses (TAs) (TG/DTG and DTA) and confirmed by semi-empirical molecular orbital (MO) calculation using PM3 procedure, on the neutral and positively charged forms of the drug. These calculations included bond order, bond length and bond strain and charge distribution, heat of formation and ionization energy. The mass spectra and thermal analysis fragmentation pathways were proposed and compared to each other to select the most suitable scheme representing the correct fragmentation pathway of the drug in both techniques. From the electron ionization (EI) mass spectra, the primary cleavage site of the charged molecule is because of the rupture of COOH group (the lowest bond order) followed by propyl group loss. The TAs of the drug revealed high response of the drug to the temperature variation with very fast rate. It decomposed in several sequential steps in the temperature range 25–360 °C. The initial thermal decomposition is similar to that obtained by MS fragmentation of the first rupture (COOH), then subsequent one of propyl loss and finally of ethylene loss. These mass losses appear as endothermic peaks required energy values of -214.83, -895.95 and -211.10 J g⁻¹, respectively. The order of these losses is also related to the values of the MO calculation parameters. Therefore, the comparison between MS and TA helps in the selection of the proper pathway representing the decomposition of this drug to give its metabolites in vivo system. This comparison is also successfully confirmed by MO calculations.

Keywords: Ibuprofen; Mass Spectrometry; Thermal Analysis; Molecular Orbital Calculation; Pm3.

287. Synthesis, Spectroscopic, the rmal Characterization and Antimicrobial Activity of Miconazole Drug and its Metal Complexes

Hanan F. Abd El-Halim and F. A. Nour El-Dien

J Therm Anal Calorim, 109: 883-892 (2012) IF: 1.604

Metal complexes having the general composition $[MCl_2(H_2O)_2(L)_2] \cdot yH_2O$ (where $y = 1-3$, $M = Mn(II), Cu(II), Co(II), Ni(II)$ and $Zn(II)$ and $L =$ miconazole drug = MCNZ) and $[MCl_2(H_2O)_2(L)_2]Cl \cdot 3H_2O$ (where $M = Cr(III)$ and $Fe(III)$) have been synthesized. All the synthesized complexes were identified and confirmed by elemental analyses, IR, diffused reflectance and thermal analyses (TG and DTA) techniques as well as molar conductivity and magnetic moment measurements. The molar conductance data reveals that bivalent metal complexes are non-electrolytes while $Cr(III)$ and $Fe(III)$ complexes are electrolytes and of 1:1 type. IR spectral studies reveal that MCNZ is coordinated to the metal ions in a neutral unidentate manner with N donor site of the imidazole-N. On the basis of magnetic and solid reflectance spectral studies, an octahedral geometry has been assigned for the complexes. Detailed studies of the thermal properties of the complexes were investigated by thermogravimetry (TG) and differential thermal analyses (DTA) techniques and the activation thermodynamic parameters are calculated using Coats-Redfern method. The free MCNZ drug and its complexes were also evaluated against bacterial species (*P. aeruginosa*, *S. aureus*, *B. subtilis*, *E. Coli*) and fungi (*A. fumigatus*, *P. italicum* and *C. albicans*) in vitro. The activity data show that the metal complexes have higher biological activity than the parent MCNZ drug.

Keywords: Miconazole; Metal Complexes; Spectroscopic Studies; Thermal Analyses; Biological Activity.

288. Thermal Decomposition Study and Biological Characterization of Zinc(II) 2-Chlorobenzoate Complexes with Bioactive Ligands

Lenka Findorak, Katarina Gyory, Daniela Hudec, Dagmar Mudron, Jana Kovar, Katarina Homz and Faten A. Nour El-Dien

J Therm Anal Calorim, (2012) IF: 1.604

New zinc(II) 2-chlorobenzoates of general formula $[Zn(2-ClC_6H_4COO)_2(L)_2]$ (where $L =$ caffeine—caf, urea—u, methyl-3-pyridylcarbamate—mpc, phenazone—phen, theophylline—thp) were synthesised and characterised by elemental analysis and IR spectroscopy. The thermal behaviour of the complexes was studied by TG/DTG and DTA methods in nitrogen and in air atmosphere. During the thermal decomposition of the studied compounds the release of organic ligands take place followed by the decomposition of 2-chlorobenzoate anion. The volatile decomposition intermediates were proved by mass spectrometry. Zinc oxide was found as the final product of the thermal decomposition performed up to 1,000 K. The antimicrobial activity of the zinc(II) complexes against various strains of bacteria, yeasts and filamentous fungi has been investigated. It was found that the prepared compounds decreased the growth of *Staphylococcus aureus*, *Escherichia coli*, *Candida albicans*,

Rhizopus oryzae and *Microsporum gypseum*, respectively. The most resistant to all tested compounds was probiotic strain of *actobacillus plantarum*. The presence of zinc and ligands in the prepared compounds increased the inhibitory effect compared to sodium salt of prepared compounds and free ligands.

Keywords: Zinc; 2-Chlorobenzoate; Thermal; Spectral Properties; Bioactive Ligands.

289. The Rmoanalytical, Spectral and Biological Study of 4-Bromobenzoatozinc(II) Complexes Containing Bioactive Organic Ligands

Annamaria Krajnc, Katarina Gyory, Jana Kovar Daniela Hudec, Jana Huback, Faten Nour El-Dien and Marian Koman

J Therm Anal Calorim, 110: 177-185 (2012) IF: 1.604

New zinc(II) 4-bromobenzoate complex compounds with general formula $[Zn(4-BrC_6H_4COO)_2(L)_2] \cdot xH_2O$ (where $L =$ urea, nicotinamide, phenazone or thiourea, $x = 0-2$) were prepared and characterized by elemental analysis, IR spectroscopy and thermal analysis. The thermal decomposition of hydrated compounds started with dehydration process. During the thermal decomposition, the neutral organic ligand, bis(4-bromophenyl)methanone and carbon dioxide were evolved. The solid intermediates and volatile products of thermal decomposition were proved by IR spectroscopy and mass spectrometry. The final solid product of the thermal decomposition heated up to 800 °C was zinc oxide, which was confirmed by X-ray powder diffractometry. Antimicrobial activity of the prepared compounds was tested against various strains of bacteria, yeasts and filamentous fungi (*E. coli*, *S. aureus*, *C. albicans*, *R. oryzae*, *A. alternata* and *M. gypseum*). It was found that bacterium *S. aureus* and fungi *A. alternata* are the most sensitive to the studied compounds.

Keywords: Zinc 4-Bromobenzoate; Ir Spectroscopy; Thermal Behaviour; Biological Activity.

290. Some Electrical and Physical Properties of Castor Oil Adducts Dissolved in 1-Propanol

M.A. Saied, S.H. Mansour, M.Z. El Sabee, A.L.G. Saad and K.N. Abdel-Nour

Journal of Molecular Liquids, 172: 1-7 (2012) IF: 1.58

A series of castor oil (CO) adducts was synthesized by esterification with phthalic anhydride (PA), maleic anhydride (MA) and succinic anhydride (SA) and dissolved in different concentrations of 1-propanol. Permittivity, dielectric loss and electrical conductivity were studied at frequency range from 100 Hz to 100 kHz and temperature between 30 and 60 °C. Also some physical properties of the obtained adducts were measured in terms of viscosity and density. The permittivity decreased by increasing temperature to certain propanol mole fraction after which it starts to increase, while increased continuously by increasing both the temperature and the concentration of propanol. The electrical conductivity of such materials indicated that at certain propanol mole fraction, castor oil and adducts lose, to some extent, their insulating properties. The activation energy E was calculated from the correlation between the temperature and conductivity. It was found that the E decreased by increasing the propanol mole fraction up to 0.9, after which it starts to increase reaching that of propanol. The viscosity decreased by

increasing the amount of propanol and the activation energy E_a calculated from the viscosity showed a small decrease up to 0.8 mole fractions and then a sharp decrease was noticed. This finding is comparable with that given in the case of density measurements.

Keywords: Castor Oil; Adduct; Propanol; Physical Property; Electrical Property.

291. Mono- and Binuclear Complexes Involving [Pd(N,N-Dimethylethylenediamine)(H₂O)₂]²⁺, 4,4-Bipiperidine and Dna Constituents.

Mohamed R. Shehata, Mohamed M. Shoukry and Sara Ali

J Coord Chem, 65(8): 1311-1323 (2012) IF: 1.547

The Pd(dmen)Cl₂, where dmen = 1/2 N,N-dimethylethylenediamine, was synthesized and characterized by elemental analysis and spectroscopy.

The complex-formation equilibria in the reaction of [Pd(dmen)(H₂O)₂]²⁺ with 4,4'-bipiperidine (Bip) and DNA constituents were investigated at 25°C and 0.1 mol/l ionic strength. The results show the formation of (H₂O)₂ Pd (Bip) Pd (dmen) (H₂O)₄⁺. Inosine, uracil and thymine interact with the previously mentioned complex by the substitution of two-coordinated water molecules.

The formation constants of all possible mono- and binuclear complexes were determined and their speciation diagrams were evaluated.

Keywords: Palladium(Ii) Complexes; 4,4'-Bipiperidine; Dna Constituents; Binuclear Complexes; Equilibrium Constants.

292. Molecular Structures of Antitumor Active Pd (II) and Pt (II) Complexes of N,N-Donor Benzimidazole Methyl Ester

N.T. Abdel-Ghan and A.M. Mansour

J Coord Chem, 65(5): 763-779 (2012) IF: 1.547

[MLCl₂].zH₂O.C₂H₅OH (L = 2-[(1H-benzimidazol-2-ylmethyl)-amino]-benzoic acid methyl ester; M = Pd, z = 2; M = Pt, z = 0) complexes were synthesized as potential antitumor compounds and their structures were elucidated by elemental analysis and spectroscopic data. Theoretical molecular structures were investigated by the DFT/B3LYP method using the LANL2DZ basis set.

The calculated molecular parameters, bond distances and angles, revealed a square-planar geometry around the metal through pyridine-type nitrogen (N_{pv}) of benzimidazole and the secondary amino group (NH_{sec}).

The lone pair interaction LP(2)O48 of ethanol with anti-bonding σ^* (C(16)-H(29)) is an evidence for charge transfer from ethanol to platinum. The electronic movement and assignment of electronic spectra were carried out by TD-DFT calculations. The ligand in comparison to its metal complexes was screened for antibacterial activity and cytotoxicity.

Keywords: Benzimidazole; Hydrogen bonding; Td-Dft; Nbo; Cytotoxicity.

293. Synthesis, Characterization and Biological Activity of Some Transition Metal Complexes with Schiff Base Ligands Derived from 4-Amino-5-Phenyl-4H-1,2,4-Triazole-3-Thiol and Salicaldehyde

Farag M. A. Altalbawy, Gehad G. Mohamed, Mohsen Abou El-Ela Sayed and Mohamed I. A. Mohamed

Monatsh Chem, 143: 79-89 (2012) IF: 1.532

The coordination behaviour of a Schiff base with SNO donation sites, derived from condensation of 4-amino-5-phenyl-4H-1,2,4-triazole-3-thiol and salicaldehyde, towards some bi- and trivalent metal ions, namely Cr(III), Mn(II), Fe(III), Co(II) (Cl, ClO₄), Ni(II) (Cl, ClO₄), Cu(II) and Zn(II), is reported. The metal complexes were characterized on the basis of elemental analysis, IR, ¹H NMR, solid reflectance, magnetic moment, molar conductance and thermal analyses (TG, DTG and DTA). The ionization constant of the Schiff base under investigation and the stability constants of its metal chelates were calculated pH-metrically at 25 °C and ionic strength $\mu = 0.1$ M in 50% (v/v) ethanol-water mixture. The chelates were found to have octahedral (Mn(II)), trigonal bipyramidal (Co(II), Ni(II), Zn(II)) and tetrahedral (Cr(III), Fe(III) and Cu(II)) structures. The ligand and its binary chelates were subjected to thermal analyses and the different thermodynamic activation parameters were calculated from their corresponding DTG curves to throw more light on the nature of changes accompanying the thermal decomposition process of these compounds. The free Schiff base ligand and its metal complexes were tested in vitro against *Aspergillus flavus*, *Candida albicans*, *C. tropicalis* and *A. niger* fungi and *Bacillus subtilis* and *Escherichia coli* bacteria in order to assess their antimicrobial potential. The results indicate that the ligand and its metal complexes possess antimicrobial properties.

Keywords: 1,2,4-Triazole-3-Thiol schiff bases; Metal complexes; Stability constants; Molar conductance; Thermal analyses; Biological activity.

294. A DFT Study on the Structures and Stabilities of As-Doped Si_{n-1} (n = 2–15) Clusters

Annan Kodlaa and Sabry El-Taher

Journal of Molecular Structure, 992: 134-141 (2012) IF: 1.437

The structures and relative stability of pure Si_n and AsSi_{n-1} (n = 2–15) clusters have been investigated at the B3LYP/6-31++G(3d) level of density functional theory. In general, the As doping does not lead to fundamental changes in the geometry of the studied clusters; the effects are localized. Relative stabilities of these clusters have been analyzed based on the variation of their averaged binding energies (E_b), fragmentation energies (E_f), second differences in energy (Δ^2E) and the highest occupied and the lowest unoccupied molecular orbital (HOMO–LUMO) gaps (ΔE) with cluster size (n). The calculated values of E_f, Δ^2E and ΔE shed light on the relatively high stability of clusters Si₁₂ and Si₁₄ in addition to the well-known magic numbers Si₆ and Si₁₀. According to E_b, Δ^2E and E_f results both Si_n and AsSi_{n-1} clusters with n = 6, 10, 12 and 14 exhibit high stability when compared to their neighbors. This has been discussed in terms of their close-packed structures rather than electronic pairing effect. The analysis indicates that ΔE of AsSi_{n-1} clusters are significantly smaller than those of the corresponding Si_n clusters, especially for n > 4, which means that the metallic characters of AsSi_{n-1} clusters are enhanced by As doping.

Keywords: As-doped silicon clusters; Structure; Stability; Density functional method; Homo-lumo gap.

295. Kinetic Study of the Hydrolysis of Schiff Bases Derived From 2-Aminothiophenol

Hekmat B. Hassib, Nora S. Abdel-Kader and Yousry M. Issa

Journal of Solution Chemistry, 41: 2036-2046 (2012) IF: 1.415

The kinetics of the hydrolysis of Schiff bases derived from 2-aminothiophenol have been studied in aqueous sodium hydroxide media containing 40 % (v/v) methanol in the temperature range 22-45°C. The Schiff base molecular structure-hydrolysis reactivity relationship has been investigated and discussed. Suitable reaction mechanisms have been suggested. From the effect of temperature on the rate constant, various activation parameters have been evaluated. The work has been extended to study the hydrolysis mechanism in buffer solutions of pH = 2-13 at 22°C for Schiff base I (H). A rate profile diagram of pH-rate constant has been proposed.

Keywords: Kinetic Hydrolysis; Hydrolysis of Thio Schiff Bases; Hydrolysis Rate.

296. Complex formation Equilibria of Unusual Seven-Coordinate Fe (EDTA) Complexes with DNA Constituents and Related Bio-Relevant Ligands

Ahmed A. El-Sherif, Mohamed M. Shoukry, Wafaa M. Hosny and Mohamed G. Abd-Elmoghny

J. Solution Chem, 41: 813-827 (2012) IF: 1.415

Seven-coordinate Fe(EDTA)-L complexes, where L represents DNA constituent (uracil, uridine, thymine, thymidine and inosine), methylamine, ammonium chloride or imidazole were investigated to resolve the solution chemistry of this system. The results showed the formation of 1:1 complexes with DNA constituents and the other ligands supporting the hepta-coordination mode of Fe(III) ion. Stability constants of the complexes were measured by potentiometric titration at 25°C and ionic strength 0.1 mol.L⁻¹ NaNO₃. The hydrolysis constant of [Fe(EDTA)(H₂O)]⁻ and the formation constants of the complexes formed in solution were calculated using the non linear least-squares program MINQUAD-75. The concentration distributions of the various complex species were evaluated as a function of pH. The thermodynamic parameters ΔH^0 and ΔS^0 calculated from the temperature dependence of the equilibrium constants were investigated for Fe(EDTA)-uracil complex. The effect of dioxane as a solvent on the protonation constant of uracil, hydrolysis constants of [Fe(EDTA)(H₂O)]⁻ and the formation constants of Fe(EDTA)-uracil complex was discussed.

Keywords: Complex Formation Equilibria; Fe, Edta; Dna; Seven Coordinate; Stability Constants; Speciation.

297. Equilibrium Studies of Binary and Mixed-Ligand Complexes of Zinc (II) Involving 2-(Aminomethyl)-Benzimidazole and Some Bio-Relevant Ligands

M. Aljhdali and Ahmed A. El-Sherif

J. Solution Chemistry, 41: 1579-1776 (2012) IF: 1.415

Binary and mixed-ligand complexes of zinc(II) involving 2-(aminomethyl)-benzimidazole (AMBI) and amino acids, peptides (HL) or DNA constituents have been investigated. Ternary complexes of amino acids or peptides are formed by simultaneous mechanism. Amino acids form the complex Zn(AMBI)L, whereas amides form two complex species Zn(AMBI)L and Zn(AMBI)(LH-1). The ternary complexes of zinc(II) with AMBI and DNA are formed in a stepwise process, whereby binding of zinc(II) to AMBI is followed by ligation of the DNA constituents. The stability of ternary complexes was quantitatively compared with their corresponding binary complexes in terms of the parameters log₁₀ K, log₁₀ Stat and log₁₀ X. The effect of the side chains of amino acid ligands (R) on complex formation was discussed. The values of log₁₀ K indicate that the ternary complexes containing aromatic amino acids are significantly more stable than the complexes containing alkyl- and hydroxyalkyl-substituted amino acids. This may be taken as an evidence for a stacking interaction between the aromatic moiety of AMBI and the aromatic side chains of the bio-active ligands. The concentration distributions of various species formed in solution were also evaluated as a function of pH.

Keywords: 2-(Aminomethyl) – Benzimidazole; Amino Acids; Amides; Dna Constituents; Stability Constants.

298. Potentiometric Determination of the Stability Constants of Trimethyltin (IV) Chloride Complexes with Imino-Bis (Methylphosphonic Acid) in Water and Dioxane–Water Mixtures

Ahmed A. El-Sherif

J Solution Chemistry, 41: 392-409 (2012) IF: 1.415

The interaction of trimethyltin(IV) (TMT) with imino-bis(methyl phosphonic acid) (IDP) abbreviated as H₄L was investigated at 25 °C and ionic strength 0.1 mol·dm³ NaNO₃ using the potentiometric technique. The formation constants of the complexes formed in solution were calculated using the non linear least-squares program MINQUAD-75. The stoichiometry and stability constants for the complexes formed are reported. The results showed the formation of 1:1, 1:1, 1:2 and 1:1-1 for TMT-IDP complexes. The concentration distribution of the various complex species has been evaluated. The effect of dioxane as a solvent on both the protonation constants and the formation constants of trimethyltin(IV) complexes with IDP was discussed. The thermodynamic parameters ΔH^0 and ΔS^0 calculated from the temperature dependence of the equilibrium constants were investigated. The effect of ionic strength on the protonation constants of IDP was discussed.

Keywords: Trimethyltin (IV); Imino-Bis (Methylphosphonic Acid); Stability Constants; Speciation; Equilibria; Ionic Strength; Thermodynamic Parameters.

299. Kinetics and Mechanism for Hydrolysis of Amino Acid Esters in Mixed Ligand Complexes with Zn(II)–Nitrilo-Tris(Methyl Phosphonic Acid)

Ahmed A. El-Sherif

J Solution Chemistry, 41: 249-260 (2012) IF: 1.415

The kinetics of base hydrolysis of alanine ethyl ester in addition to glycine-, histidine and methionine methyl esters in the presence of Zn-NTP complex is studied in aqueous solution by pH-stat

technique. The kinetic data fits assuming that the hydrolysis proceeds through formation of a M-OH complex, followed by intramolecular OH- attack. The effect of organic solvent on the hydrolysis of coordinated esters is investigated by measuring the rate of hydrolysis in dioxane-water solutions of different compositions at T = 25.0 °C and I = 0.1 mol.dm⁻³. The kinetic of base hydrolysis of glycine methyl ester was studied at different temperatures. The activation parameters for the base hydrolysis of the complexes are evaluated.

Keywords: Zn(II); Formation Equilibria; Nitrido -Tris (Methylphosphonic Acid); Kinetics Of Hydrolysis; Rate Constant; Amino Acid Ester.

300. Solution Coordination Chemistry of Organotin (IV) Cation with Bio-Relevant Ligands

Ahmed A. El-Sherif

J. Solution Chemistry, 41: 1522-1554 (2012) IF: 1.415

A comprehensive review on organotin(IV)ⁿ⁺ hydrolysis and their complex formation equilibria with amino acids, peptides and DNA constituents is presented with special reference to their solution and coordination chemistry studies. The review focuses on results obtained in the author's laboratory and on related work of other groups. Also, these complexes are reviewed on literature taking into account their biological aspects.

Keywords: Organotin(IV)ⁿ⁺; Complex Formation Equilibria; Hydrolysis Dna; Peptides; Amino Acids And Biological Activity.

301. Spectrophotometric Determination of Carbamazepine and Mosapride Citrate in Pure and Pharmaceutical Preparations

Eman Y.Z. Frag, M.A. Zayed, M.M. Omar and Sally E.A. Elashery

Arabjc, 5: 375-382 (2012) IF: 1.367

Simple, rapid and sensitive spectrophotometric methods were developed for the determination of carbamazepine and mosapride citrate drugs in pure and pharmaceutical dosage forms. These methods are based on ion pair and charge transfer complexation reactions. The first method is based on the reaction of the carbamazepine drug with Mo (V)-thiocyanate in hydrochloric acid medium followed by an extraction of the coloured ion-pair with 1, 2-dichloroethane and the absorbance of the ion pair was measured at 470 nm. The second method is based on the formation of ion pairs between mosapride citrate and two dyestuff reagents namely bromothymol blue (BTB) and bromocresol green (BCG) in a universal buffer of pH 4 and 3, respectively. The formed ion-pairs are extracted with chloroform and methylene chloride and measured at 412 and 416 nm for BTB and BCG reagents, respectively. The third method is based on charge transfer complex formation between mosapride citrate (electron donor) and DDQ (p-acceptor reagent) and the absorbance of the CT complexes was measured at 450 nm. All the optimum conditions are established. The calibration graphs are rectilinear in the concentration ranges 10–350 for carbamazepine using Mo (V) – thiocyanate and 4–100, 4–60 and 10–150 g mL⁻¹ for mosapride citrate using BTB, BCG and DDQ reagents, respectively. The Sandell sensitivity (S), molar absorptivity, correlation coefficient, regression equations and limits of detection (LOD) and quantification (LOQ) are calculated. The

law values of standard deviation (0.04–0.09 for carbamazepine using Mo (V)-thiocyanate and 0.022–0.024, 0.013–0.018 and 0.013–0.020 for mosapride citrate using BTB, BCG and DDQ, respectively) and relative standard deviation (0.630–2.170 for carbamazepine using Mo (V)-thiocyanate and 0.123– 1.43, 0.102–0.530 and 0.226–1.280 for mosapride citrate using BTB, BCG and DDQ, respectively) reflect the accuracy and precision of the proposed methods. The methods are applied for the assay of the two investigated drugs in pharmaceutical dosage forms. The results are in good agreement with those obtained by the official method.

Keywords: Carbamazepine; Mosapride; Citrate; Ion-Pair Formation; Charge Transfer; Spectrophotometry.

302. The Structure of Cinnamic Acid and Cinnamoyl Azides, A Unique Localized π System: the Electronic Spectra and DFT- Treatment

Rafie H. Abu-Eittah, M. K. Khedr, M. Goma and W. Zordok

Int. J. of Quantum Chemistry, 112: 1256-1272 (2012) IF: 1.357

The electronic absorption spectra of cinnamic acid and some cinnamoylazides have been recorded in absolute methanol and investigated to explore the structure of the titled compounds. Cinnamic acid and its derivatives have a double bond, -C=C-, between the aromatic ring and the carboxyl group which disturbs the π electron system of the molecule and inhibits electron delocalization as compared with styrene or benzoic acid. The azide group is neither a strong electron donor nor a strong electron acceptor but it increases conjugation in the molecule. The observed spectra confirm that each of the cinnamic acid and cinnamoyl azide molecules is one of a kind of unique disturbed π system and not of different independent π systems, each on a fragment of the molecule as predicted by the quantum theory of atom in molecule calculations. The spectra of cinnamic acid and its derivatives are not the additive spectra of the different fragments of the molecule. The spectra are characterized by few number, low intensity and high-energy electronic transitions (absorption bands) in the UV-vis region. Molecular orbital calculations confirmed the spectral observations. The optimized geometry of the ground state of the studied compounds is calculated using the DFT/B3LYP/6-31G** level of theory and an explicit molecular orbital analysis is carried out. Excited states are calculated using the TD/DFT procedure as implemented by the Gamess 2009 package of programs. The correspondence between calculated and the observed transition energies is adequate.

Keywords: Cinnamic acid and cinnamoyl azides; Localized π system; Opposing dipoles in cinnamic acid and Cinnamoyl azides-unique -disturbed structure of cinnamic acid and cinnamoyl azides.

303. Poly (2-Aminobiphenyl), Preparation, Characterization, Mechanism and Kinetics of the Electropolymerization Process

Waheed A. Badawy, Khaled M. Ismail, Ziad M. Khalifa and Shymaa S. Medany

J Appl Polym Sci, 125: 3410-3418 (2012) IF: 1.289

Electropolymerization of 2-aminobiphenyl (ABP) was carried out on glassy carbon, gold and platinum electrodes, in aqueous-

organic solvent mixtures, using a potentiodynamic technique. The choice of organic solvent strongly influences the film formation. In a mixture of 60 % acetonitrile (ACN) and 40 % 1.0 M HClO₄ stable films were obtained.

The poly (2-aminobiphenyl) films were characterized with cyclic voltammetry where the electrochemical activity of the formed polymer films was investigated in acidic and neutral aqueous solutions containing perchlorates or in potassium ferrocyanide.

The prepared films possess a remarkable stability in acidic aqueous solutions and also are stable in some organic solvents. The stability of the polymer films depends on the pH of the solution and the mechanism of the polymerization process involves deprotonation and head-to-tail coupling of oxidized monomers with its oligomeric radical cations.

The kinetics of the electropolymerization process was investigated by determining the charge consumed during the electropolymerization as a function of time at different concentrations of the electrolyte components.

The electropolymerization process follows first-order kinetics with respect to the monomer and negative order with respect to HClO₄.

Keywords: Conducting polymers; Polymerization; Cyclic voltammetry; Poly (2-Aminobiphenyl).

304. Crosslinked Poly(Vinyl Alcohol)Carboxymethyl Chitosan Hydrogels for Removal of Metal Ions and Dyestuff from Aqueous Solutions

Magdy W. Sabaa, Riham R. Mohamed. S. H. Eltaweel and Rania S. Seoudi

J. Appl Polym Sci, 123: 3459-9469 (2012) IF: 1.289

Hydrogels composed of poly (vinyl alcohol) (PVA) and carboxymethyl chitosan (CMCh) were synthesized via ultraviolet (UV) irradiation that can be used in several industrial fields. Several analysis tools were used to characterize the physical and thermal properties of CMCh/PVA hydrogels namely FT-IR, scanning electron microscope (SEM), XRD, thermogravimetric analysis (TGA) and differential scanning calorimetry (DSC). TGA results showed that CMCh/PVA hydrogels are thermally more stable than CMCh and their thermal stability increases as PVA content increases in the hydrogel. Also, DSC results showed that CMCh/PVA hydrogels are at least partial miscible blends.

Moreover, the swelling behavior of the CMCh/PVA hydrogels was studied in different buffered solutions and in different salt solutions at various concentrations. CMCh/PVA hydrogels swell much more than CMCh especially at alkaline pH. Both metal and dye uptake were studied for CMCh/PVA hydrogels. The hydrogels adsorb much more dyestuff and metal ions like Cu²⁺, Cd²⁺ and Co²⁺ than CMCh itself. Much dyestuff and metal ions are adsorbed by the hydrogels as PVA content increases in the hydrogel.

Keywords: Hydrogels; Thermal analysis; Swelling; Metal uptake.

305. Preparation, Characterization and Antimicrobial Activity of Poly (3-Hydroxybutyrate – Co-3-Hydroxyvalerate) –G-Poly(N Vinylpyrrolidone) Copolymers

Gamal R. Saad, Moataz A. Elsayy and Maher Z. Elsabee

Polym-Plast Technol, 51: 1113-1121 (2012) IF: 1.279

Graft polymerization of N-vinylpyrrolidone onto poly(3-hydroxybutyrate-co-3-hydroxyvalerate), PHBV was carried out in solution. The evidence of grafting was provided by FTIR and ¹H-NMR. The DSC results showed that the cold crystallization temperature from the glass state increased with increasing of grafting %. TGA analysis revealed that the thermal stability of the host PHBV was improved remarkably with increasing extent of grafting. The swelling of the graft copolymer in water increases with increasing G%. The antibacterial activity of PHBV-g-PVP copolymers was improved dramatically with the extent of grafting. The biodegradability of PHBV and its graft copolymers was investigated in active soil.

Keywords: Antimicrobial Activity; Biodegradability; Graft Copolymers; N-Vinylpyrrolidone; Poly(3-Hydroxybutyrate-co-3-Hydroxyvalerate); Swelling; Thermal Analysis.

306. Antitumor and Antileishmanial Evaluation of Novel Heterocycles Derived from Quinazoline Scaffold: A Molecular Modeling Approach

Daisy H. Fleita Rafat M. Mohareb and Ola K. Sakka

Med Chem Res, 19 (7): 617-716 (2012) IF: 1.271

Novel thiazole, pyrimidine and benzylidene derivatives derived from quinazoline scaffold have been synthesized. The antitumor evaluation of the newly synthesized products against three cancer cell lines namely breast adenocarcinoma (MCF-7), non-small cell lung cancer (NCI-H460) and CNS cancer (SF-268) showed that the benzylidene-quinazoline derivative 12a showed remarkable activity against all three cell lines. The thiazolo-quinazoline derivative 10 showed greater activity than the control against breast adenocarcinoma (MCF-7) with a concentration of 0.01 μM. Moreover, the antileishmanial activity of the newly synthesized products tested on *Leishmania donovani* mastigotes showed that compounds 4, 14 and 18 had very promising activity.

Keywords: Quinazolines; Thiazole; Pyrimidine.

307. Site Selectivity in the Reaction of Hydrazine Hydrate with 3,4-Bis (Functionalized Carbonyl)-4,3-Bis (Pyrazolyl) Ketones. Synthesis of 4-(Pyrazol-3-Yl)-2H-Pyrazolo[3,4-d]Pyridazines.

Ahmad Sami Shawali and Adel J. M. Haboub

Arxivoc, (v): 301-311 (2012) IF: 1.252

Reaction of hydrazine hydrate with 3,4-bis-(functionalized carbonyl)-4,3-bis(pyrazolyl)ketones proceeds regioselectively affording the corresponding 4-(pyrazol-3-yl)-2H-pyrazolo[3,4-d]pyridazine derivatives in high yields. The structures of the products were determined by spectroscopic and elemental analyses and supported by comparison with the possible isomers prepared by an independent route.

Keywords: Hydrazonoyl halides; Enaminones; Pyrazoles; Pyrazolopyridazines.

308. Synthesis of New Pentaheterocyclic Ring Systems as Anti-Androgene, Anti-HCV and Anti-H1N1 Agents

Thoraya A. Farghaly, khlass M. Abbas, Mohamed M. Abdalla and Raghda O. A. Mahgoub

Arkivoc, 57-70 (2012) IF: 1.252

A new series of pentaheterocycles, namely, benzo[5',6']pyrano[4',3':4,5]pyrido[2,3-d]triazolo[4,3-a]pyrimidine-7,13(3H)-diones 10 was prepared via the reaction of hydrazonoylchlorides 7 with 2,4-dihydro-3-thioxo-benzo[5',6']pyrano[3',4':5,6]pyrido[2,3-d]pyrimidine-1,7-dione 4 in presence of chitosan as ecofriendly catalyst. The structure of the newly synthesized compounds were established on the basis of spectral data (Mass, IR, ¹H and ¹³C NMR) and elemental analyses.

Keywords: Hydrazonoyl Halides; 4-Hydroxycoumarine; Chitosan; Antiandrogene; Anti Hcv; Anti

309. Bis-Enaminones as Versatile Precursors for Terheterocycles: Synthesis and Reactions

Ahmad Sami Shawali

Arkivoc, (i): 383-431 (2012) IF: 1.252

This review summarizes the results of literature reports concerning synthesis and chemical reactions of bis(enaminones) reported by us and by other research groups from 1995 to mid 2011. It outlines their utility as versatile precursors for synthesis of various terheterocycles.

Keywords: Enaminones; Heterocycles; Nitrilimines; Condensation; Dmf; Dma.

310. Synthesis and Applications of Bipyrazole Systems

Bakr F. Abdel-Wahab and Kamal M. Dawood

Arkivoc, (i): 491-545 (2012) IF: 1.252

This review focuses on the synthetic methodologies towards ten main classes of bipyrazole systems (according to the type of connection between them): 1,1'-, 1,3'-, 1,4', 1,5'-, 3,3'-, 3,4'-, 3,5'-, 4,4'-, 4,5'- and 5,5'-junctions. The research and industrial applications of these bipyrazoles are reported as well.

Keywords: Pyrazoles; Bipyrazoles; Synthesis; Cycloaddition; Heterocycles.

311. Reaction with Hydrazonoyl Halides 64: Synthesis of Some New Triazolino[4,3-a]Pyrimidines, 1,3,4-Thiadiazoles and 5-Arylazothiazoles

Abdou O. Abdelhamid, Abdelgawad A. Fahmi and Basma S. Baoui

J. Heterocyclic Chem, 49: 1098-1107 (2012) IF: 1.22

2,3-Dihydro-1,3,4-thiadiazoles, 2,3-dihydro-1,3,4-selenadiazoles and triazolino[4,3-a]pyrimidines containing benzofuran moiety were prepared from the reaction of 2-(2-phenylhydrazono)-1-(5-

bromobenzofuran-2-yl)-2-chloroethanone with each of potassium thiocyanate, potassium selenocyanate, alkyl carbodithioate and pyrimidine-2-thione derivatives. All the newly synthesized compounds were confirmed by elemental analysis, spectral data and alternative route synthesis whenever possible.

Keywords: 1;3;4-Thiadiazoles; 1;3;4-Selenadiazoles; Benzofuran; Hydrazonoyl Halides; Nitrile Imine.

312. A New Approach for the Synthesis of Some Pyrazolo[5,1-C]Triazines and Pyrazolo[1,5-a]Pyrimidines Containing Naphthofuran Moiety

Abdou O. Abdelhamid, Shokry A. Shokry and Sayed M. Tawfik

J Heterocyclic Chem, 49: 116-124 (2012) IF: 1.22

Naphtho[2,1-b]furan-2-yl)(8-phenylpyrazolo[5,1-c][1,2,4]triazin-3-yl)methanone, ([1,2,4]triazolo[3,4-c][1,2,4]triazin-6-yl)(naphtho[2,1-b]furan-2-yl)methanone, enzo[4,5]imidazo[2,1-c][1,2,4]triazin-3-yl-naphtho[2,1-b]furan-2-yl-methanone, 5-(naphtho[2,1-b]furan-2-yl)pyrazolo[1,5-a]pyrimidine, 7-(naphtho[2,1-b]furan-2-yl)-[1,2,4]triazolo[4,3-a]pyrimidine, 2-naphtho[2,1-b]furan-2-yl-benzo[4,5]imidazo[1,2-a]pyrimidine, pyridine and pyrazole derivatives are synthesized from sodium salt of 5-hydroxy-1-naphtho[2,1-b]furan-2-ylpropanone and various reagents. The newly synthesized compounds were elucidated by elemental analysis, spectral data, chemical transformation and alternative synthetic route whenever possible.

Keywords: Pyridines; Pyrazoles; Pyrazolo[1;5-A]Pyrimidines; Pyrazolo[5;1-C]Triazines naphtho[2;1-B] Furan.

313. Synthetic Studies with 3-Oxo-N-[4-(3-Oxo-3-Phenylpropionylamino)-Phenyl]-3-Phenylpropionamide

Fathy M. Abdelrazek, Nehal A. Sobhy and Peter Metz

J Heterocyclic Chem, 49: 381-387 (2012) IF: 1.22

3-Oxo-N-[4-(3-oxo-3-phenylpropionylamino)-phenyl]-3-phenylpropionamide 1 and its derivative 2-benzoyl-N-[4-(2-benzoyl-3-(dimethylamino)acryloylamino)-phenyl]-3-dimethylaminoacrylamide 12 are used for the synthesis of the hitherto not known bis-heterocyclic amine and bis-heterocyclic carboxamide derivatives. Plausible mechanisms are discussed for the formation of the new compounds.

Keywords: 3-Oxo-N-[4-(3-Oxo-3-Phenylpropionylamino)-Phenyl]-3-Phenylpropionamide; Dmf; Dma; Bis Heterocycles.

314. Bis (α-Bromo Ketones): Versatile Precursors for Novel Bis(S-Triazolo[3,4-b][1,3,4]Thiadiazines) and Bis(As-Triazino[3,4-B][1,3,4]Thiadiazines)

Mohamed R. Shaaban and Ahmed H. M. Elwahy

J. Heterocyclic Chem, 49: 640-645 (2012) IF: 1.22

A synthesis of bis(α-bromo ketones) 5a-c and 6b,c was accomplished by the reaction of bis(acetophenones) 3a-c and 4b,c with N-bromosuccinimide in the presence of p-toluenesulfonic acid (p-TsOH). Treatment of 5a-c and 6b,c with each of 4-amino-3-mercapto-1,2,4-triazoles 9a,b and 4-amino-6-phenyl-3-mercapto-1,2,4-triazin-5(4H)-ones 13 in refluxing ethanol afforded the novel bis(s-triazolo[3,4-b][1,3,4]thiadiazines) 10a-d

and 11a-c as well as bis(as-triazino[3,4-b][1,3,4]thiadiazines) 14a-c and 15, respectively, in good yields. Compounds 11b and 11c underwent NaBH₄ reduction in methanol to give the target 1,?-bis{4-(6,7-dihydro-3-substituted-5H-1,2,4-triazolo[3,4-b][1,3,4]thiadiazin-6-yl)phenoxy}butanes 12a and 12b in 42 and 46% yields, respectively.

Keywords: Bis(A-Bromo Ketones); Bis(Acetophenones); Cyclocondensation; Triazolothiadiazines.

315. Microwave-Assisted Synthesis of Bis (Enaminoketones): Versatile Precursors for Novel Bis (Pyrazoles) Via Regioselective 1,3-Dipolar Cycloaddition with Nitrileimines

Ahmed H. M. Elwahy, Ahmed F. Darweesh and Mohamed R. Shaaban

J Heterocyclic Chem, 49: 1120-1125 (2012) IF: 1.22

Synthesis of bis(enaminones) 6a-c and 7a-c was accomplished by the reaction of bis(acetophenones) 3a-c and 4a-c with dimethylformamide-dimethylacetal, under microwave irradiation. 1,3-Dipolar cycloaddition of bis(enaminones) 6a and 7b,c with nitrileimines in refluxing benzene led to the regioselective synthesis of the novel bis(pyrazoles) 11a-h in 62-89% yield. The bis(pyrazoles) 11b,c underwent condensation with hydrazine hydrate to give the corresponding bis(pyrazolo[3,4-d]pyridazines) 14a,b in good yields.

Keywords: Bis (Enaminones); Bis (Pyrazoles); Dipolar Cycloaddition; Microwave.

316. The Interaction of [Pd (N,N-Dimethylaminopropylamine)(H₂O)]²⁺ with Dicarboxylic Acids and Inosine-Thermodynamic Model for Carboplatin Drug

Mohamed R. Shehate, Mohamed M. Shoukry and Mona S. Ragab

Central European Journal of Chemistry, 10(4): 1253-1281 (2012) IF: 1.073

Pd(DMPA)Cl₂ complex, where DMPA = N,N-dimethylaminopropylamine, was synthesized and characterized. The stoichiometry and stability constants of the complexes formed between various dicarboxylic acids and [Pd(DMPA)(H₂O)₂]²⁺ were investigated. The effect of solvent dielectric constant, chloride ion concentration of the medium and temperature on the stability constant of cyclobutanedicarboxylic acid (CBDCA) complex is investigated. The equilibrium constants for the displacement of coordinated CBDCA by inosine, taken as an example of DNA constituents, are calculated. The results are expected to contribute to the chemistry of antitumour agents.

Keywords: Complex - Formation equilibria; 3-Dimethylaminopropylamine; Pd(II); Amino Acid; Peptides; Dna Units; Dibasic Acids And Amino Acid Ester Hydrolysis.

317. A Convenient Synthesis of Polyaza-3,4-Bis (Hetaryl) Pyrazoles

Ahmad S. Shawalia and Adel J. M. Habouba

Synthetic Communications, (2012) IF: 1.062

Reactions of a new series of bis-enaminones with some N- and C-nucleophiles proved to be convenient routes for synthesis of novel

variety of 3,4-bis(heteroaryl)pyrazoles which have not been reported hitherto. The structures of the compounds prepared were elucidated on the basis of their spectral and elemental analyses and by alternative synthesis wherever possible.

Keywords: Enaminones; Heterocycles; Hydrazonoyl Halides; Pyrazoles.

318. Electroanalysis of A Ternary Disinfectant Mixture

M. I. Awad, A. M. Mohammad and Takeo Ohsaka

Anal Lett, 45: 1506-1518 (2012) IF: 1.016

The analysis of a ternary mixture containing ozone (O₃), sodium hypochlorite (NaClO) and hydrogen peroxide (H₂O₂), in their coexistence was simultaneously performed using a potentiometric method. In this method, the change in the open circuit potential of a Pt indicator electrode dipped in a potential buffer containing I/I₃ upon the addition of the ternary mixture is measured. The analysis was based on the different reaction kinetics of the three oxidants with I. The kinetics of the reaction of O₃ and I is about three orders of magnitude faster than that of sodium hypochlorite and the reaction of hydrogen peroxide and I is negligible compared with those of O₃ or hypochlorite ion and I unless a molybdate catalyst is added. Several factors, including the iodide concentration, pH and the molybdate concentration were investigated to optimize the analysis and achieve a reasonable separation among the reactions of the three oxidants and I. A theoretical model was developed to compare with the experimental results and a reasonable correlation was obtained.

Keywords: Electroanalysis; Hypochlorite; Ozone; Peroxide; Potentiometry.

319. Synthesis And Characterization of 6-(aryl)-2-Thioxo-1,2-Dihydropyridine-3-Carbonitriles

Fawzy A. Attaby, Ahmed H. El-Ghandour, Abdelwahed R. Sayed, Ashraf A. El Bassuony and Ahmed A.M. El-Reedy

J. of Sulfur Chemistry, 33, (2): 197-221 (2012) IF: 1.009

In the present study, 3-aminothieno[2,3-b]pyridines, pyrido[3,2:4,5]thieno[3,2-d]pyrimidinones and pyrido[3,2:4,5]thieno[3,2-d][1,3]oxazinones were prepared via the reaction of 6-(aryl)-2-thioxo-1,2-dihydropyridine-3-carbonitriles with active-halogen-containing compounds. The structures of all the newly synthesized heterocyclic compounds were established by considering elemental analysis and spectral data.

Keywords: Thienopyridines; Pyridinethiones; Pyridothienopyrimidinones; Pyridothienotriazines;

320. Bis-(Cyanoacetamide) Alkanes in Heterocyclic Synthesis: Synthesis of Bis-Hetaryl (Carboxymido) Alkanes and Bis-(Hetaryl) Alkanes of Thiophene, Pyrrole, Thiazole and Pyrimidinone Series

Mohamed A.A. Elneairy, Ahmed E.M. Mekky and Ahmed A.M. Ahmed

Journal of Sulfur Chemistry, 33, (3) : 373-383 (2012) IF: 1.009

Bis-N-substituted cyanoacetamides 3a and b reacted with active methylene-containing compounds 2a-c and elemental sulfur to

give bis-thiophene 4a and b and bis-pyrrole 6a and b derivatives. Compounds 4a and b reacted with ethyl cyanoacetate 2a to afford bis-thienopyrimidine derivatives 5a and b; on the other hand, 6a and b reacted with cyanothioacetamide 2c to give the corresponding bis-thioxopyrrolopyrimidine derivatives 7a and b. Compounds 7a and b reacted with methyl iodide to give the corresponding bis-2-S-methylpyrrolopyrimidine derivatives 8a and b, which could be, in turn, cyclized into the bispyrazolopyrrolopyrimidine derivatives 9a and b by refluxing with hydrazine hydrate. On the other hand, 7a and b reacted with ethyl chloroacetate to yield the corresponding bis-thienopyrrolopyrimidine derivatives 10a and b. Finally, compounds 3a and b reacted with phenylisothiocyanate and elemental sulfur to give the corresponding bis-2-thioxoaminothiazole derivatives 11a and b.

Keywords: Bis-Thiophene; Bis-Pyrrole; Bis; Thiazole; Bis-Pyrrolopyrimidine; Bis-Thienopyrimidine

321. A Facile and Convenient Synthesis of Novel Pyridine Derivatives Incorporating Antipyrine Moiety and Investigation of the *in vitro* Antimicrobial Activities

Kheder Nabila A, Riyadh Sayed M and Asiry Ahlam M

Heterocycles, 85(9): 2259-2268 (2012) IF: 0.999

A series of potentially bioactive piperidines and pyridines, pendant to antipyrine moiety, were synthesized and evaluated *in vitro* for their antimicrobial potential. Condensation of acetamide 1 with arylaldehydes in (2:1 molar ratio) gave hitherto unreported novel piperidine-3-carboxamide derivatives 4a-c. Also, reaction of acetamide 1 with ethyl 2-cyano-3-(4-nitrophenyl)acrylate afforded unexpected piperidine-3-carboxamide 4c. On the other hand, treatment of acetamide 1 with (arylmethylene)malononitriles 7a,b afforded pyridine-3,5-dicarbonitrile derivatives 10a,b. The structures of the synthesized products were confirmed by IR, ¹H NMR, ¹³C NMR and mass spectral techniques.

Keywords: Pyridine; Piperidines; Antipyrine; Acetamide; Antimicrobial Activities; Condensation.

322. Enaminones as Building Blocks in Heterocyclic Preparations: Synthesis of Novel Pyrazoles, Pyrazolo [3,4-*d*] Pyridazines, Pyrazolo[1,5-*a*] Pyrimidines, Pyrido [2,3-*d*] Pyrimidines Linked to Imidazo[2,1-*b*] Thiazole System

Sobhi M. Gomha and Hatem A. Abdel-Aziz

Heterocycles, 85 (9): 2291-2303 (2012) IF: 0.999

The unreported 2-[E-3-(N,N-dimethylamino)acryloyl]-3-methyl-5,6-diphenyl imidazo[2,1-*b*]thiazole 3 was prepared via the reaction of 2-acetyl-3-methyl-5,6-diphenylimidazo[2,1-*b*]thiazole 2 with dimethylformamide dimethyl acetal (DMF-DMA). Enaminone 3 underwent regioselective 1,3-dipolar cycloaddition with nitrilimines 5a-f, to afford the corresponding pyrazoles 7a-f. The reaction of 7a,d,g with hydrazine hydrate, afforded the pyrazolo[3,4-*d*]pyridazines 8a-c, respectively. Enaminone 3 also reacted with a hydrazines, hydroxylamine hydrochloride, 5-aminopyrazole 11, 6-aminothiouracil 15 and hippuric acid 22.

The structures of the newly synthesized compounds were confirmed by spectral data and elemental analyses.

Keywords: Pyrazoles; Imidazo[2;1-B] Thiazole; Pyrazolo[3;4-D]Pyridazines; Nitrilimines; 1;3-Dipolar Cycloaddition.

323. Synthesis of Some New Pyridine-2,6-Bis-Heterocycles

Korany A. Ali, Mohamed A. Elsayed and Ahmad M. Faragb,

Heterocycles, 85 (8): 1913-1923 (2012) IF: 0.999

The versatile multifunctional hitherto unreported pyridine-2,6-Bis[ethyl 2-(N,N-dimethylamino)methylene-3-oxopropanoate] (2) was prepared by the reaction of pyridine-2,6-bis(ethyl 3-oxopropanoate) (1) with 1,1-dimethoxytrimethylamine. Several new pyrazole, isoxazole, pyrimidine, pyrazolo[1,5-*a*]pyrimidine and imidazo[1,2-*a*]pyrimidine derivatives attached to pyridine ring at 2,6-positions have been synthesized by the reactions of the enaminone 2 with the appropriate nitrogen binucleophiles.

Keywords: Pyrazole; Isoxazole; Pyrazolo[1;5-A]Pyrimidine; Imidazo[1;2-*a*]Pyrimidine.

324. Synthesis of New Heterocycles Derived From 3-(3-Methyl-1*H*-Indol-2-yl)-3-Oxopropanenitrile as Potent Antifungal Agents

Sobhi M. Gomha and Hatem A. Abdel-Aziz

Bull. Korean Chem. Soc., 33 (9): 2985-2990 (2012) IF: 0.906

New thiazoline derivatives 7a-c and thiophenes 9a-c linked to indole moiety were easily prepared via the reaction of the acrylamide derivative 3 with phenacyl bromides 4a-c, depending on the reaction conditions. In addition, the reaction of compound 3 with hydrazonoyl chlorides 11a-f afforded a series of 1, 3, 4-thiadiazole derivatives 13a-f. Moreover, coupling of 3-(3-methyl-1*H*-indol-2-yl)-3-oxopropanenitrile (2) with the diazonium salts of 3-phenyl-5-aminopyrazole 16 or 3-amino-1, 2, 4-triazole 17 gave the corresponding hydrazones 18 and 19, respectively. Cyclization of the latter hydrazones yielded the corresponding pyrazolo[5,1-*c*]-1,2,4-triazine and 1,2,4-triazolo[5,1-*c*]-1,2,4-triazine derivatives 20 and 21, respectively. The structures of the synthesized compounds were assigned on the basis of elemental analysis, IR, ¹H NMR and mass spectral data. All the synthesized compounds were tested for *in vitro* activities against certain strains of fungi such as *Aspergillus niger*, *Aspergillus nodulans*, *Alternaria alternata*. Compounds showed marked inhibition of fungal growth nearly equal to the standards.

Keywords: 2-Cyanoacetyl -3-Methyl-Indole; Hydrazonoyl Chlorides; Thiazoles; 1; 3; 4- Thiadiazoles And Antifungal Activity.

325. Synthesis and Antimicrobial Evaluation of Novel Pyrazolones and Pyrazolone Nucleosides

Hassan AE, Moustafa AH, Tolbah MM, Zohdy HF and Haikal AZ.

Nucleosides, Nucleotides and Nucleic Acids, 31(11): 783-800 (2012) IF: 0.899

The synthesis of a novel series of 4-arylhydrazono-5-methyl-1,2-dihydropyrazol-3-ones 4a-h and their N2-alkyl and acylo, glucopyranosyl and ribofuranosyl derivatives is described. K₂CO₃ catalyzed alkylation of 4a-h with allyl bromide, propargyl bromide, 4-bromobutyl acetate, 2-cetoxyethoxymethyl bromide

and 2,3,4,6-tetra-O-acetyl- α -D-glucopyranosyl bromide proceeded selectively at the N2-position of the pyrazolinone ring. Glycosylation of 4a with 1,2,3,5-tetra-O-acetyl- β -D-ribofuranose under Vorbruggen glycosylation conditions gave the corresponding N2-4-arylhydrazonopyrazolone ribofuranoside 9a in good yield. Conventional deprotection of the acetyl-protected nucleosides furnished the corresponding 4-arylhydrazonopyrazolone nucleosides in good yields. Selected numbers of the newly synthesized compounds were screened for antimicrobial activity. Compounds 4b, 12a and 14d showed moderate activities against *Aspergillus flavus*, *Penicillium* sp and *Escherichia coli*.

Keywords: Pyrazolinone; Pyrazolone Nucleosides; Acyclic Nucleosides; N2-Alkyl Pyrazolones.

326. Grafting of 1-Cyanoethanoyl-4-Acryloylthiosemicarbazide Onto Chitosan and Biocidal Activity of the Graft Copolymers

Said S. Elkholy, Hend. A. Khalek and Maher Z. Elsabee

Journal Of Macromolecular Science, Part A: Pure And Applied Chemistry, 49: 720-728 (2012) IF: 0.887

Chitosan was grafted with a novel monomer 1-Cyanoethanoyl-4-acryloylthiosemi carbazide (CEATS). The graft copolymerization was conducted using potassium persulfate ($K_2S_2O_8$) and sodium bisulfite ($NaHSO_3$) as redox initiators. The grafted samples were characterized by FTIR spectroscopy, scanning electron microscopy, X-ray diffraction and thermogravimetric analysis. The data may indicate that grafting has occurred at the surface of chitosan. The grafted samples showed high water swelling. The antifungal behavior of chitosan and its graft copolymers was investigated in vitro and it has been found that grafting with CEATS noticeably enhances the antifungal activity.

Keywords: Chitosan; 1-Cyanoethanoyl-4-Acryloylthiosemicarbazide; Graft Copolymer; Swelling Behavior; Biological Activity.

327. Synthesis, Reactions and Characterization of 6-Amino-4-(Benzo[b]Thiophen-2-Yl)-2-Thioxo-1, 2-Dihydropyridine-3, 5-Dicarbonitrile (Benzo [B] Thiophen-2-Yl)-2-Thioxo-1, 2-Dihydropyridine-3, 5-Dicarbonitrile

Azza M. Abdel-Fattah and Fawzy A. Attaby

Phosphorus, Sulfur And Silicon and The Related Elements, 187 (5): 555-563 (2012) IF: 0.716

Benzothiophene -2- carbaldehyde 1 reacted with 2-cyanoethanethioamide 2 in 1:2 molar ratios to give the corresponding 6-amino-4-(benzo[b]thiophen-2-yl)-2-thioxo-1,2-dihydropyridine-3,5-dicarbonitrile 6. The synthetic potentiality of compound 6 was investigated via its reaction with active halogen-containing reagents to afford the corresponding thieno[2,3-b]pyridine derivatives 11a,b, 14, 16 and 19. Also, compound 6 reacted with hydrazine hydrate to give the pyrazolo[3,4-b]pyridine derivative 21. Compound 21 condensed with 4-(2-thienyl)benzaldehyde to afford pyrazolo[3,4-b]pyridine derivative 23. Structural elucidation of all the newly synthesized heterocyclic compounds was based on elemental analyses, IR, 1H NMR and mass spectra.

Keywords: 3; (Benzo[B]Thiophen-2-Yl); 2; Cyanoprop; 2; Enethioamide; 2-Cyanoethanethioamide.

328. Simultaneous Determination of Paracetamol, Caffeine, Domperidone, Ergotamine Tartrate, Propyphenazone, and Drotaverine Hcl By High Performance Liquid Chromatography

Yousry M. Issa, Mohamed E. M. Hassoun and Ashraf G. Zayed

J. Liq. Chrom. Related Tech., 2149-2161 (2012) IF: 0.706

A high performance liquid chromatographic (HPLC) method was developed for the simultaneous determination of paracetamol, (acetaminophen), caffeine, domperidone, ergotamine tartrate, propyphenazone and drotaverine HCl. The chromatography was performed in the isocratic mode on a Hypersil C18 BDS column using a mobile phase consisting of 0.02 mole L^{-1} tetrabutylammonium bisulphate and methanol (100:45, v=v) at 50° using UV detection at 210 nm. The method was validated by specificity, linearity, limit of detection and limit of quantification, accuracy and precision for the aforementioned drugs. The time required for a single analysis amounts to 14 min. The response was linear for the drug concentration ranges of 6.20–420.00, 0.80–80.00, 0.80–64.00, 2–40.00, 1.20–240.00 and 3.20–64.00, $\mu g mL^{-1}$ for PA, CA, DO, ET, PP and DH, respectively. Accuracy values for the method ranged from 99.40–101.94, 98.48–101.13, 98.97–100.54, 96.47–102.43, 98.92–101.82 and 97.63–100.45% for PA, CA, DO, ET, PP and DH, respectively.

Keywords: Caffeine; Domperidone; Drotaverine Hcl; Ergotamine Tartrate; Hplc; Method Validation; Paracetamol (Acetaminophen); Propyphenazone.

329. Hydrazonoyl Halides as Precursors for Synthesis of Novel Bioactive Thiazole and formazan Derivatives

Thoraya A. Farghaly and Eman M.H. Abbas

Journal of Chemical Research, 660-664 (2012) IF: 0.633

A new series of substituted 4-methyl-5-(aryloxy)-2-[N'-(6,7,8,9-tetrahydro-benzocyclohepten-5-ylidene) -hydrazino]-thiazoles and 5-(aryloxy)-2-[N'-(6,7,8,9-tetrahydro-benzocyclohepten-5-ylidene)-hydrazino] -thiazol-4-one were prepared by reaction of hydrazonoyl chlorides with a thiosemicarbazone derivative. The tautomeric structures of the products were studied using electronic absorption and NMR spectroscopy. The site-selectivities of the reactions of hydrazonoyl halides with benzocyclohepten-5-one hydrazone were also investigated. In addition, the antimicrobial activity of some of the products was evaluated. Many derivatives have promising activities against antibacterial and antifungal species.

Keywords: Thiosemicarbazone; Hydrazone; Thiazole; Hydrazonoyl Chlorides; Formazan; Antimicrobial Activity.

330. Synthesis and Tautomeric Structure of Novel 3-Aryloxyimidazo[1,2-b]Pyrazolo[4,3-d]Pyridazines

Thoraya A. Farghaly and Ahmad Sami Shawali

Journal of Chemical Research, 296-299 (2012) IF: 0.633

Treatment of 3-acetyl-5-amino-4-cyano-1-phenylpyrazole with hydrazine hydrate afforded the hydrazone derivative. Reaction of

the latter hydrazone with hydrazoneyl chlorides was found to be site selective as it afforded the corresponding formazan and not the amidrazones derivatives. The ^1H NMR spectra of the formazan derivatives indicated that they exist as the bis-hydrazone tautomers. Acid-catalysed cyclisation of these dihydroformazans afforded the respective 9-amino-3-aryloxy-6-methyl-8-phenyl-2-substituted-8*H*-imidazo [1,2-*b*] pyrazolo [4,3-*d*] pyridazines whose electronic absorption spectra revealed that they exist predominantly in the aryloxy tautomeric form.

The structures of all compounds prepared were confirmed by spectral and elemental analyses. Also the mechanism of the reactions studied are discussed.

Keywords: Hydrazoneyl Halides; Amidrazones; Hydrazones; Formazans.

331. Synthesis, Solvatochromic Properties and Substituent Effects of 3-Aryloxy-8*H*-Imidazo[1,2-*b*] Pyrazolo[4,3-*d*]Pyridazines

Ahmad S. Shawali, Thoraya A. Farghaly, and Tarek M.S. Nawar

Journal Of Chemical Research, 615-618 (2012) IF: 0.633

A series of new 3-aryloxy-6-methyl-2,8,9-triphenyl-8*H*-imidazo[1,2-*b*]pyrazolo[4,3-*d*]pyridazines was prepared via reaction of hydrazoneyl halides with 3-hydrazoneacetyl-4-cyano-1,5-diphenylpyrazole. The structures of the compounds prepared were confirmed by spectral and elemental analyses. The solvatochromic and substituent effects on the absorption spectra of these azo dyes were interpreted by correlation of absorption frequencies with Kamlet-Taft and Hammett equations, respectively.

Keywords: Aryloxyheterocycles; Pyrazole; Hydrazoneyl Bromides; Imidazo[1,2-*B*] Pyrazolo[4,3-*D*]-Pyridazines.

332. Effect of the Relative Orientation of the Two Fluoro-Substituents on the Mesophase Behavior of Phenylazophenyl Benzoates

M. M. Naoum, A. A. Fahmi and H. A. Ahmed

Mol. Cryst. Liq. Cryst., 562: 43-65 (2012) IF: 0.58

Four novel types of laterally di-fluoro substituted 4-(2-(or 3)-fluoro phenylazo)-2-(or 3)- fluoro phenyl-4-alkoxybenzoates were prepared and investigated for their mesophase behavior. In order to deduce the most probable conformation for each of the positional isomers investigated, the dipole moments for each of the four novel types have been determined experimentally in benzene at 30°C and compared with those theoretically calculated using molecular modeling program. Probable conformations deduced were found to vary according to the relative orientations of the two fluorine atoms.

The results were used to correlate the mesophase behavior, in pure and mixed derivatives, with the conformation deduced for each series. The study aims to investigate the effect of the spatial orientation of the two lateral fluoro-substituents on the mesomorphic properties in their pure and mixed states.

Keywords: Binary Mixtures; Dipole Moments; Fluorine; Liquid Crystals.

333. Induction, Purification and Molecular Characterization of Sulphydryl Oxidase from an Egyptian Isolate of *Aspergillus Niger* 1

H. Moubasher, A. A. Fahmi and M. AbdurRahman

Applied Biochemistry And Microbiology, 48, (3) : 323-327 (2012) IF: 0.56

The conditions for the sulphydryl oxidase (SOX) production and activity from an Egyptian isolate of *Aspergillus niger* were optimized. Purification and determination of the kinetic properties (K_m and V_{max}) of the purified enzyme have been done. The possibility for the SOX induction using L-Cys (as a natural substrate) was studied to determine whether SOX could be produced as an inducible enzyme in addition to being a constitutive one (i.e. whether induction leads to increase SOX production and activity or not). The optimum temperature and pH for its activity were found to be 60°C and 5.5, respectively. The activity of the induced intracellular SOX, was measured according to Ellman's method using the standard GSH oxidation where it reached 94% while that of noninduced one reached only 27.6%. This wide difference in activity between the induced and non-induced SOX indicates the successful L-Cys-induction of the SOX production (i.e. SOX from *A. niger* AUMC 4947 is an inducible enzyme). Molecular characterization of the pure SOX revealed that it is constituted of two 50–55 kDa subunits. K_m and V_{max} were found to be 6.0 mM and 100 U/min/mg respectively.

Keywords: Sulphydryl Oxidase; L-Cys; Ellman's Method.

334. Poly (n-Alkyl Itaconate-Co-Vinyl Acetate) as Pour Point Depressants for Lube Oil in Relation to Rheological Flow Properties

A. M. Al-Sabagh, T. M. Khalil, M. W. Sabaa, T. T. Khidr and G. R. Saad

Journal of Dispersion Science and Technology, 33: 1649-1660 (2012) IF: 0.56

In the present work, poly(n-alkyl itaconate-co-vinyl acetate) comb-like polymers were synthesized by radical copolymerization of n-alkyl itaconates of various alkyl chain length and vinyl acetate monomers for use as pour point depressants in lubricant oil. Initially four n-alkyl itaconate monomers were synthesized by esterification of itaconic acid with a series of n-alkyl alcohol, having different alkyl chain length $C_{16}/C_{18}/NAFOL+20A$ ($C_{av} \approx 20$)/NAFOL 1822B ($C_{av} \approx 22$). The copolymerization of these monomers with vinyl acetate was then performed using dibenzoyl peroxide in toluene at 120°C up to high conversion, with molar ratios of 0.25:0.75, 0.50:0.50 and 0.75:0.25 for alkyl itaconate: vinyl acetate. All products were characterized by FTIR, ^1H NMR and gel permeation chromatography (GPC). These copolymers were tested in terms of their suitability as pour point depressants and flow improvers for lube oil. The obtained data revealed that the prepared compounds depress the pour point of the lube oil successfully and the additive efficiency on the pour point reduction of the lube oil increases by increasing the concentration of these additives and by decreasing the alkyl chain length of n-alkyl itaconate. The rheological properties of lube oil (with and without copolymer additive) were studied in terms of shear rate, shear stress and viscosity. The results indicated that the performance of flow improver was dependent on the copolymer compositions and the size of alkyl chain length of n-alkyl itaconate monomers. Poly(hexadecyl itaconate-co-vinyl acetate)

with high content of vinyl acetate showed the best flow improver properties of lube oil. Comparison of morphologies and structures of wax crystals or aggregates in untreated and treated lube oil was also done by micro photographic studies which showed the modification in wax crystal morphology due to additives.

Keywords: Copolymer additives; Flow improver; Lube oil; Pour point depressant; Wax crystallization.

335. Petroleum Oil Dispersion Efficiency and Stability Using Eco-Friendly Chitosan-Based Surfactant and Nanoparticles

A. M. Al-Sabagh, R. E. Morsi, M. Z. Elsabee, H. F. Naguib and Y. M. Moustafa

Journal Of Dispersion Science and Technology, 33: 1661-1666 (2012) IF: 0.56

In this article, a new aspect of comparing oil dispersion efficiency and stability using eco-friendly surfactants and nanoparticles of the same natural origin was carried out. Nanoparticles effectively disperse oil in water as well as do surfactant but with different actions; surfactants act by reducing the interfacial tension between oil and water leading to the distribution of oil in water while nanoparticles give stable and uniform distribution of oil in water depending on oil trapping inside the polymer matrix. As a result, the dispersion stability of nanoparticles was found to be superior to that of surfactant.

Keywords: Chitosan; Chitosan Derivatives; Chitosan Nanoparticles; Petroleum Oil Dispersant.

336. Organosolv Pulping Of Cotton Linter. Ii. Effect of Dioxane And Anthraquinone on Cotton Linter Properties

Nahed a. Abd El-Ghany

Cellulose Chemistry And Technology, 2: 137-145 (2012) IF: 0.55

Compared to soda pulping, soda-dioxane pulping of cotton linter stabilizes the long-chain cellulose macromolecules against alkaline degradation.

The presence of dioxane also results in a more open and accessible fine structure, higher chemical reactivity (upon xanthation) and better viscose filterability. Soda dioxane anthraquinone (AQ) pulping increases the stabilization of cellulose in cotton and gives pulp with higher accessibility, higher chemical reactivity and better viscose filterability, especially at a higher anthraquinone charge – of 0.1%. Acid prehydrolysis of cotton linter prior to soda dioxane AQ pulping favors the penetration of AQ and dioxane molecules among cellulose chains and breaks the hydrogen bonds, thus providing better accessibility of the hydroxyl groups to the reactant molecules, which leads to a pulp with higher chemical reactivity and better viscose filterability. It is evident that both the soda and the prehydrolyzed soda dioxane AQ pulping methods give cotton linter with better reactivity than that of commercial softwood viscose pulp.

Keywords: Anthraquinone (AQ); Cotton Linters; Chemical Reactivity (Xanthation); Prehydrolysis Soda Pulping; Prehydrolysis Soda Dioxane Anthraquinone Pulping.

337. Enhancement of Ethanol Production by Simultaneous Saccharification and Fermentation (Ssf) of Rice Straw using Ethoxylated Span 20

A. M. Badawi, A. A. Fahmy, Karima A. Mohamed, M. R. Noor El-Din and M. G. Riad

Prep Biochem Biotech, 42: 44-59 (2012) IF: 0.466

In this work, four nonionic surfactants based on sorbitan monolaurate (Span 20) were synthesized by introducing ethylene oxide gas (n/20, 40, 60, 80 ethylene oxide units) into Span 20 to give four new surfactants with different hydrophilic-lipophilic balance (HLB), namely, E(20), E(40), E(60) and E(80).

The structures of the prepared nonionic surfactants were elucidated using Fourier-transform infrared (FT-IR) and ¹H-nuclear magnetic resonance (NMR) spectroscopy. The surface-tension measurements were recorded.

The effects of the prepared nonionic surfactants on the simultaneous saccharification and fermentation (SSF) of microwave-alkali pretreated rice straw to produce ethanol were investigated. From the obtained data, it was found that the addition of the nonionic surfactants at 2.5 g/L had a positive effect on SSF. The maximum ethanol yield (76 and 55%) was obtained after 72 hr for rice straw using *Glycyveromyces marxianus* and *Saccharomyces cerevisiae*, respectively.

Also, it was found that the ethanol yield increases with increasing HLB of the prepared nonionic surfactants by increasing ethylene oxide units. The adsorption of nonionic surfactants on lignocelluloses is proposed to be due to hydrophobic and hydrogen bonding interactions between nonionic surfactants and the lignin part in the lignocellulose.

It can be concluded that additions of surface-active compounds, such as nonionic surfactants, increase enzymatic conversion of rice straw for bioethanol purposes.

Keywords: Ethanol; Microwave Irradiation; Nonionic Surfactants; Rice Straw; Ssf; Yeast.

338. Synthesis and Antimicrobial Evaluation of Some New Pyrazole, Fused Pyrazolo[1,5-A] Pyrimidine and Pyrazolo[1,5-D]Pyrimido[4,5-D][1,2,3] Triazine Derivatives

Elham S. Darwish, Fivian F. Mahmoud and Farag M.A. Altalbawy

Asian J of Chemisrty, 4(7): 2997-3002 (2012) IF: 0.266

A variety of 3-aryloxy-5-amino and 7-amino pyrazolo[1,5-a] pyrimidines were obtained via reacting 1 with cinnamionitriles and methoxymethylene malononitrile. Diazotized 1 coupled with active methylene reagents to yield pyrazolo[5,1-c][1,2,4]triazines. The products were screened for their antifungal and antibacterial activity properties and showed promising results.

The mechanism of the studied reactions is discussed. The structures of the compounds prepared were elucidated on the basis of their elemental analyses, spectral data and alternate synthesis.

Keywords: Aryloxy; Pyrazolopyrimidine; Pyrazolotriazinethione; Pyrazolotriazine; Antimicrobial Activities.

339. Spectrophotometric Determination of Thrombin in Pure Samples and Biological Fluids using-Acceptors

Gehad Genidy Mohamed, Barsoum Nashed Barsoum, Shahira Morsi El Shafi and Fatma El Zahraa Ahmed Hafez

Afinidad, 217-223 (2012) IF: 0.138

Thrombin is the central enzyme of coagulation. It is engaged in opposing functions in blood. As a procoagulant factor, it converts fibrinogen into an insoluble fibrin clot and activate platelet, as anticoagulant when it activates Protein C. This knowledge is used for the pharmacologic control of blood coagulation, so monitoring its activity is reliable indicator of the rate and extent of coagulation. A simple, rapid, sensitive and accurate spectrophotometric method is suggested for the determination of thrombin in pure form and in biological fluids. The utility of some – acceptors as 2,3-dichloro-5,6-dicyanobenzoquinone (DDQ), 7,7,8,8-tetracyanoquinodimethane (TCNQ) and tetracyanoethylene (TCNE) for thrombin (as electron donor) determination is described. These acceptors give highly coloured complex species that have been spectrophotometrically studied. The optimum experimental conditions for these CT reactions have been studied carefully. Beer's law is obeyed over the concentration ranges of 10-130, 50-150 and 10-100g ml⁻¹ thrombin using DDQ, TCNQ and TCNE reagents, respectively. The percentage recovery amounts to 99.33-100.1% (SD = 0.032-0.075), 99.50-102.5% (SD = 0.016-0.076) and 99.5-101.4% (SD = 0.034-0.088) for four to six experiments. The reagents are utilized for the determination of thrombin in poor platelet plasma of dialysis patients with a percentage recovery amount to 98.76-103.3% (for n = 5). No endogenous compounds were found to interfere. The results obtained applying the acceptors reagents are comparable with those obtained by the official method.

Keywords: Thrombin; Ddq; Tcnq; Tcne; Spectrophotometry; Charge Transfer Complexes.

340. Determination of Aluminum (Iii) by using A Modified Carbon Paste Selective Electrode

Sameh S.F. Mehanny

Journal of Pharmacy Research, 3, (1) : 17-35 (2012)

A new chemically modified carbon paste Al(III) ion selective electrode based on 1,8-dihydroxyanthraquinone (DHAQ) as an ionophore is described. This sensor has a wide linear range of concentration (1.0×10⁻⁶ – 1.0×10⁻¹ mol L⁻¹) and a low detection limit of 5.0×10⁻⁷ mol L⁻¹ of Al(III) ion. It has a Nernstian response with slope of 20.7 ± 0.5 mV/decade and it is applicable in the pH range of 2.0–5.0 without any divergence in potential. The proposed electrode has a short response time of approximately 20 s and is stable at least for 3 months. The electrode shows a good selectivity for Al(III) ion towards a wide variety of metal ions. The proposed sensor was successfully applied for the determination of Al(III) ion in different real samples (aluminium-silicon alloy, pharmaceutical drug and water samples) with satisfactory results.

Keywords: Aluminum Determination; Chemically Modified Carbon Paste Ion Selective Electrode; 1;8-Dihydroxyanthraquinone; Pharmaceutical Preparations; Water Samples.

341. Development and Validation of Extractive Spectrophotometric Method for Determination of Venlafaxine Hydrochloride in Pure Solutions Pharmaceutical Dosage form and Urine Samples

M.S. Rizk, N.T. Abdeland Ghani M. Mostafa

Int. J. of Chemical and Analytical Science, 1(3): 215-232 (2012)

Simple, rapid, sensitive and economical spectrophotometric procedures have been described for the determination of antidepressant drug Venlafaxine hydrochloride (V-HCl) in bulk sample, dosage form and in spiked urine samples. The implemented procedures are based on the formation of a yellow colored ion-associates due to the interaction between the examined drug V-HCl with Picric acid (PA), Chlorophylline coppered trisodium salt (CLPH), alizarin red (AR), ammonium reineckate (RK) reagents. A suitable recommended buffer solution has been used and the extraction was carried out using chloroform, the ion associates exhibit absorption maxima at 407, 405, 430 and 530 nm for PA, CLPH, AR and RK respectively. (V-HCl) can be determined up to 8-125, 1.7-23, 9.6-200 and 8.28-160g mL⁻¹, respectively. Moreover, the optimum reaction conditions for quantitative analysis were carefully investigated. In addition the molar absorptivity and Sandell sensitivity were determined of the investigated drug. The correlation coefficient was 0.9983 (n = 6) with a relative standard deviation (RSD) 1.13 for five selected concentrations of the reagents. Therefore the concentration of V-HCl drug in its pharmaceutical formulation and spiked urine samples has been determined successfully.

Keywords: Venlafaxine Hydrochloride; Chlorophylline Coppered Trisodium Salt; Alizarin Red; Picric Acid; Ammonium Reineckate.

342. Synthesis and Antimicrobial Activities of Pyrido[2,3D]Pyrimidine, pyridotriazolopyrimidine, Triazolopyrimidine and Pyrido[2,3D:6,5D] Dipyrimidine Derivatives

Anhar AbdelAzim, Marwa Sayed ElGendy and Abdou Osman Abdelhamid.

European Journal of Chemistry, 3 (4): 455-460 (2012)

A new series of pyridotriazolopyrimidines were synthesized via reaction of hydrazonoylhalides with pyrido[2,3d]pyrimidines. The structures of the newly synthesized compounds were established by elemental analysis spectral data and alternative synthetic routes whenever possible. Some of synthesized compounds were also screened in vitro for their antimicrobial activity against a variety of bacterial and fungal samples.

Keywords: Nitrilimines; Pyridopyrimidine; Pyridotriazolopyrimidines; Pyridodipyrimidines .

343. Anti-Tumor and Anti-Leishmanial Evaluations of Novel Thiophene Derivatives Derived from the Reaction of Cyclopentanone with Elemental Sulphur and Cyano-Methylene Reagents

Rafat M. Mohareb and Fatma O. Al-farouk

Organic Chemistry: Current Research, 1: 1-6 (2012)

The reaction of cyclopentanone (1), elemental sulfur and either malononitrile or ethyl cyanoacetate gave the cyclopenta[b] thiophene derivatives 3a and 3b, respectively. The reaction of either 3a or 3b with either 2a or 2b afforded the cyclopenta[4,5]thieno[2,3-b]pyridine derivatives 5 and 6, respectively. The reactivity of the latter products toward different reagents was studied to give pyrazole, pyridine, pyrimidine derivatives. The antitumor evaluation of the newly synthesized products against the three cancer cells namely breast adenocarcinoma (MCF-7), non-small cell lung cancer (NCI-H460) and VNS cancer (SF-268) showed that some of them have high inhibitory effect towards three cell lines which is higher than the standard. Moreover, the anti-leishmanial activity of the newly synthesized products was tested on *Leishmania amastigotes* showed that some compounds have high activity.

Keywords: Cyclopenta[B]Thiophene; Coumrin; Anticonvulsant.

344. Recent Advances in the Chemistry of Nitriles and Enaminonitriles

Fathy M. Abdelrazeka and Mahmoud S. Bahbouh

Jjees, 4: 47-61 (2012)

Recent developments in the chemistry of nitriles and enaminonitriles are surveyed with emphasis on the most new findings of our group's work aimed at developing efficient approaches to different heterocyclic compounds as well as correcting some erroneous literature reports and reviews.

Keywords: Active Methylene Nitriles; Arylidene; Alkylidene; Dimethylformamide; Dimethylacetal; Enaminone; Heterocyclic Compounds.

345. Renal Leptin in Experimental Nephrotic Syndrome

Abdelgawad Ali Fahmi, Dawoud Fakhry Habib and Naglaa Mohamed Kholousy

Journal of Genetic Engineering and Biotechnology, 10: 87-92 (2012)

Leptin is a fat derived hormone involved in the regulation of metabolism and body composition. The kidney is the principle organ responsible for elimination of circulating leptin. Our aim is to evaluate if the nephrotic kidneys participate in the metabolism of leptin by comparing the serum leptin level in renal veins and in their renal arteries and to study the relationship between leptin and lipoprotein levels in healthy and nephrotic rats. Methods: Rats were divided into two equal groups: group 1 in which experimental nephrotic syndrome was produced by injecting them intraperitoneally with a supernatant of the homogenized mixture of their own kidney (obtained by previous unilateral nephrectomy) and complete Freund's adjuvant. Another group constituted the control group. Leptin and lipid profile were estimated in blood samples of renal veins and renal arteries. There was a highly significant increase in leptin and lipid profile levels in the nephrotic rats compared with the normal group. There was a high significant decrease in leptin in the renal venous blood compared with its level in the renal arterial blood of normal and nephrotic rats. This work has stressed the involvement of kidney and the nephrotic renal tissue in the process of leptin metabolism and lipogenesis.

Keywords: Leptin; Nephrotic Syndrome; Lipids; Lipoproteins; Apolipoproteins; Rats.

346. Sorptive Removal of Phosphate from Waste Water using Activated Red Mud

A.M. Baraka, Marwa M. EL-Tayieb, Maha El Shafai and Nouran Yussri Mohamed

Australian Journal of Basic and Applied Sciences, 6(10): 500-510 (2012)

Red mud (RM), is a kind of industrial waste produced in the process of alumina production. Because of the increasing demand for alumina during economic development, more and more RM is being produced. Hence, the disposal and management of RM remains a challenging issue to the alumina industry. This study examined the effect of acid activated red mud on phosphate removal. Thus, its use in phosphate removal can be also considered as a way of disposal. The removal capacity of RM for phosphate ions was studied as a function of solution pH, contact time, adsorbent dosage and adsorbate concentration. The maximum adsorption of the phosphate ions on the RM was observed at the pH values between 8 and 12. The equilibrium time was attained after 60 min. and the maximum removal percentage was achieved at an adsorbent loading weight of 0.5 gm/100ml. The equilibrium adsorption capacity of adsorbent used for phosphate was measured and extrapolated using linear Freundlich, Langmuir isotherms and the experimental data were found to fit the Freundlich isotherm model. The morphological characteristics of the adsorbent were evaluated by using a scanning electron microscope. SEM image for RM after adsorption of phosphate shows that phosphate ions appeared to cover the surface of RM. The optimized method was applied for the removal of phosphate from Zenin wastewater treatment plant (ZWWTP) and proctor and gamble (P&G) company for household products. The removal efficiency achieved was 94 %, 74% in the ZWWTP sample and 97% in the P&G sample.

Keywords: Adsorption; Batch; Rm; Phosphate; Wastewater; Isotherm.

347. Convenient Synthesis of Some New Pyrazolo[5,1-C]Triazines, Isoxazolo[3,4-D]Pyrimidine, Pyridine Derivatives Containing Benzofuran Moieties.

Abdou Osman Abdelhamid, Abdelgawad Ali Fahmi and Amna Ali Mohamed Alshefelo

European Journal Of Chemistry, 3 (2): 129-137 (2012)

Pyrazolo[5,1-c][1,2,4]triazine, [1,2,4]triazolo[3,4-c][1,2,4]triazine, benzo[4,5] - imidazo[2,1-c][1,2,4]triazine, isoxazole, isoxazolo[3,4-d]pyridazine, pyrazole, pyridine, substituted urea and phenyl carbamate derivatives containing benzofuran moieties were synthesized via reaction of sodium salt of 5-hydroxy-1-benzofuran - 2-ylpropanone or 1-(benzofuran-2-yl)-3-(dimethylamino)prop-2-en-1-one with diazotized heterocyclic amines, hydroxymoyl chlorides and active methylene compounds. The structures of all the newly synthesized compounds were confirmed by elemental analyses, spectral data and alternative routes synthesis whenever possible.

Keywords: Triazines; Pyridine; Pyrazole; Isoxazole; Hydrazone.

348. Synthesis of 5-Arylazothiazoles, Pyridines and Thieno[2,3-B]Pyridines Derivatives Containing 1,2,3-Triazole Moiety

Abdou Osman Abdelhamid, Nadia Abdelhamid AbdelRiheim, Tamer Tawhid ElIdreesy and Huda Refat Mahmoud Rashdan

European Journal Of Chemistry, 3 (3): 322-331 (2012)

1-(2-(4,5-Dihydro-3-(5-methylphenyl)-1H-1,2,3-triazol-4-yl)-5-phenylpyrazol-1-yl)-4-substituted-thiazol-5-yl)-2-phenyldiazene (4) and substituted pyridines (512) were synthesized via reaction of 1-(5-methylphenyl)-1H-1,2,3-triazol-4-yl)-3-phenylprop-2-en-1-one with hydrazonoyl halides and active methylene compounds. Also, thieno[2,3-b]pyridines (14ae) were prepared through reactions of 2-mercapto-6-(5-methylphenyl)-1H-1,2,3-triazol-4-yl)-4-phenylpyridine-3-carbonitrile with halo ester and halo ketones, respectively. The newly synthesized derivatives were elucidated by elemental analysis, spectral data and alternative synthetic routes wherever possible.

Keywords: Urea; Pyridines; Carbamates; Thieno[2;3-B]Pyridines.

349. Extractive Spectrophotometric Determination of Biperiden Hydrochloride in Pure Solutions, Pharmaceutical Dosage form and Urine Samples

M.S. Rizk N.T. Abdel-Ghani and M. Mostafa

International Journal of Applied Pharmaceutical Sciences and Biomedical Sciences, 1(3): 215-232 (2012)

Simple, rapid, sensitive and economical spectrophotometric procedures for the determination of anticholinergic drug iperiden hydrochloride (Bi-HCl) in bulk sample, dosage form and in spiked urine samples have been investigated. The suggested procedures are based on the formation of a yellow colored ion-associates due to the interaction between the examined drug Bi -HCl with Picric acid (PA), Bactophenol red (BPR), alizarin red (AR) and bromothymol blue (BTB) reagents. A buffer solution has been used and the extraction was carried out using chloroform, the ion associates exhibit absorption maxima at 415, 410, 430 and 420 nm for PA, BPR, AR and BTB respectively. (Bi -HCl) can be determined up to 35, 52, 90 and 42.5g mL⁻¹, respectively. The optimum reaction conditions for quantitative analysis were carefully investigated. The molar absorptivity and Sandell sensitivity were determined of the investigated drug. The correlation coefficient was 0.995 (n =6) with a relative standard deviation (RSD) 0.65 for five selected concentrations of the reagents. Therefore the concentration of Bi -HCl drug in its pharmaceutical formulation and spiked urine samples has been determined successfully.

Keywords: Biperiden Hydrochloride; Picric Acid; Bactophenol Red; Alizarin Red; Bromothymol Blue; Pharmaceutical Analysis; Spectrophotometry; Ion-Associates.

350. Evaluation of Tolerance of Some Elemental Impurities on Performance of Pb-Ca-Sn Positive Pole Grids of Lead-Acid Batteries

H.A. Abd El-Rahman, A.G. Gad-Allah, S.A. Salih and A. M. Abd El-Wahab

Journal of Electrochemical Science And Technology, 3, (3): 123-134 (2012)

The electrochemical performance of positive pole grids of lead-acid batteries made of Pb-0.08%Ca-1.1%Sn alloys without and with 0.1 wt% of each of Cu, As or Sb and with 0.1 wt% of Cu, As and Sb combined was investigated by electrochemical methods in 4.0 M H₂SO₄. The corrosion of alloys under open-circuit conditions and constant current charging of the positive pole, the positive pole gassing and the self-discharge of the charged positive pole were studied. All impurities (Cu, As, Sb) were found to decrease the corrosion resistance, R_{corr} after 1/2 hour corrosion, but after 24 hours an improvement in R_{corr} was recorded for Sb containing alloy and the alloy with the three impurities combined. While an individual impurity was found to enhance oxygen evolution reaction, the impurities combined significantly inhibited this reaction and the related water loss problem was improved. Impedance results were found helpful in identification of the species involved in the charging/discharging and the self-discharge of the positive pole. Impurities individually or combined were found to increase the self-discharge during polarization (33-68%), where Sb containing alloy was the worst and impurities combined alloy was the least. The corrosion of the positive pole grid in the constant current charging was found to increase in the presence of impurities by 5-10%. Under open-circuit, the self-discharge of the charged positive grids was found to increase significantly (92-212%) in the presence of impurities, with Sb-containing alloy was the worst. The important result of the study is that the harmful effect of the studied impurities combined was not additive but sometimes lesser than any individual impurity.

Keywords: Positive Pole; Pb-Ca-Sn Alloys; Lead-Acid Batteries; Recycled Lead.

351. Recent Progress in the Electrochemistry of Planar and Reticulated Vitreous Carbon: Fundamentals and Applications – Review Article

M. I. Awad, M. M. Saleh and T. Ohsaka

Current Topics in Electrochemistry, 17: 15-40 (2012)

This review outlines the recent published works on the fundamental studies and electrochemical applications of glassy carbon in both forms, i.e., planar glassy carbon (GC) and reticulated vitreous carbon (RVC) electrodes. Special attention is paid to our recent works for using glassy carbon electrode in hydrogen evolution reaction (HER), oxygen reduction reaction (ORR) and oxygen evolution reaction (OER) and the relevant literatures for the above applications. This includes the use of electrochemically pretreated GC and modified GC electrodes. The effects of surface modification via oxidation of the GC were outlined.

Keywords: Reticulated Vitreous Carbon; Glassy Carbon; Oxygen Evolution; Oxygen Reduction; Ozone Electrogeneration.

352. Solid Contact Sensors for Determination of the Antihistaminic Drug Ketotifen Fumarate

Yousry M. Issa, Motaza M. Khater and Sabre H. Mohamed

Sensing In Electroanalysis, 7: 373-391 (2012)

Reliable potentiometric sensing devices with unique advantages were constructed for determination of ketotifen fumarate (ketofuma). Five sensors based on Ag, Ag/Ag₂S, Ag/AgCl, graphite and glassy carbon solid beds were constructed. These sensors

were constructed based on ketotifen-tetraphenylborate (keto-TPB) as ion pairing material and dibutyl phthalate as solvent mediators. The sensors showed high sensitivity and near Nernstian slope in batch and flow injection conditions (FIA). According to the results obtained, the best behavior observed for coated graphite sensor was with slope $60.10 \text{ mV} \cdot \text{decade}^{-1}$, linear range 7×10^{-6} – $1 \times 10^{-2} \text{ M}$ and limit of detection $3.9 \times 10^{-7} \text{ M}$. Enhancement of the detection limit of the sensors was done by incorporating potassium tetraphenylborate (KTPB) and graphite in the membrane. The sensors were used for determination of keto-fuma in the pure form as well as in its pharmaceutical preparations. It was performed using potentiometric titration and standard addition methods with recoveries of 97.0-100.4% and relative standard deviations of 0.13-1.42%.

Keywords: Ketotifen Fumarate; Sensors; Graphite; Solid Contact.

353. Determination of Nitrite in Environmental Samples using Chemically Modified Carbon Paste Electrode Based on New Co(III)-Benzopyran-4-One Schiff Base Complex

Y. M. Issa, Hosny Ibrahim and Ola R. Shehab

Sensing In Electroanalysis, : 235-256 (2012)

Nitrite chemically modified carbon paste electrode based on Co(III)-benzopyran-4-one Schiff base complex is described. The electrode revealed a Nernstian response over a wide nitrite ion concentration range (9.1×10^{-6} – $1.5 \times 10^{-2} \text{ mol} \cdot \text{L}^{-1}$). The detection limit of the sensor is $7.0 \times 10^{-6} \text{ mol} \cdot \text{L}^{-1}$. The best performance was obtained with a paste composition of 4% Co(III)-benzopyran-4-one Schiff base, 2% cetylpyridinium chloride (CPC), 42% graphite and 52% dibutyl-butyl phosphonate (DBBP). The potentiometric response of the sensor is independent of the pH of solution in the pH range of 3.0–8.5. The electrode exhibits a very fast response time reaching to 20 s and good selectivity over a variety of common inorganic anions, including Cl^- , Br^- , NO_3^- , F^- , SO_4^{2-} , CO_3^{2-} , S^{2-} , HPO_4^{2-} , $\text{S}_2\text{O}_3^{2-}$ and CH_3COO^- . The selectivity behavior of the proposed sensor shows substantial improvements in comparison to many previously reported electrodes for nitrite ion. The electrode was successfully applied also to the monitoring of nitrite ion in drinking water, soil and for determination of nitrogen dioxide in the air.

Keywords: Nitrite; Carbon Paste Electrode; Co(III)-Benzopyran-4-One Schiff Base; Potentiometry.

354. Carbon Paste Electrode Modified with Chromium Thiopental for the Potentiometric Flow Injection Analysis of Chromium (Iii)

A.F.A. Youssef, Y.M. Issa and M.S. Mohamed

Tox. Environ. Chem., 94: 220-238 (2012)

A chemically modified carbon paste electrode for chromium (III) based on the formation of ion-association complex of chromium with 5-ethyl-6-oxo-5-pentan-2-yl-sulfanyl-pyrimidin-4-olate (thiopental, THP) as electroactive ion-exchanger (Cr-THP) was prepared and investigated. The electrode has a linear dynamic range of 1.7×10^{-6} – $1.3 \times 10^{-2} \text{ mol L}^{-1}$, with a Nernstian slope of $19.60.5 \text{ mV}$ per decade and a detection limit of $9.0 \times 10^{-7} \text{ mol L}^{-1}$. It has a fast response time of 15 s and can be used for at least 7

weeks without any considerable divergence in potential. The proposed sensor revealed good selectivity for Cr(III) over a wide variety of mono-, di- and trivalent cations and could be used in the pH range of 2.3–6.5. The proposed electrode was used in batch measurements and in flow injection analysis. The Cr-CMCPE was successfully applied for the determination of Cr(III) in real samples (wastewater of hot dip galvanizing unit and alloys). The present electrode was also used as an indicator electrode in potentiometric titration of Cr(III). The results were highly satisfactory.

Keywords: Ion-Selective Electrode; Chromium (Iii); Carbon Paste; Thiopental; Fia.

355. A Comparative Study of the in-Vitro Dissolution Profiles of Paracetamol and Caffeine Combination in Different formulations using Hplc

M.E.M. Hassouna, Y.M. Issa and A.G. Zayed

J Appl. Pharm. Sci, 02 (05): 52-59 (2012)

Dissolution testing is an in vitro technique of great importance in formulation and development of pharmaceutical dosage forms, as it can be used as a substitute for in vivo studies under strictly defined and specified conditions. The main objective of the present study is to conduct the comparative dissolution studies of various brands of same dosage forms and treatment of obtained dissolution data by using f_2 to determine whether all the formulations used were equivalent or significantly different. Five different brands of drug containing paracetamol and caffeine from different manufacturers were used in the study and dissolution testing in different dissolution media viz., water, 0.1 N HCl, phosphate buffer of pH 4.5 and phosphate buffer of pH 6.8 was conducted for 12 tablets from each brand for 60 min. by using dissolution testing apparatus USP type-II. Samples were withdrawn at 10 min. time interval and analyzed for drug content by using HPLC technique. Percent drug release at each time interval was calculated for tablets and the data obtained were treated with statistical technique to meet the FDA requirements for obtaining a waiver of bioavailability and bioequivalence studies.

Keywords: Acetaminophen (Paracetamol); Caffeine; Comparative Studies of in-Vitro Dissolution; Hplc

356. Simple and Accurate Rp-Hplc and Tlc Densitometric Methods for Determination of Carvedilol in Pharmaceutical formulations

Fatma M Abdel-Gawad, Yousry M Issa, Emad M Hussien, Magda M. Ibrahim and Saadia Barakat

J. Res. Pharm. Chem., 2(3): 741-748 (2012)

Simple and accurate two chromatographic methods were developed for the determination of carvedilol in raw material and in tablets. The first method uses isocratic reversed-phase high performance liquid chromatographic (RP-HPLC) method. Analysis was performed on Agilent C18 column using a mobile phase consisting of 0.05 M potassium dihydrogen phosphate (pH 2.5 ± 0.1) and acetonitrile (60:40, v/v) with a flow rate of 2.0 mL min⁻¹ and UV detection at 245 nm. The second method uses thin-layer liquid chromatography (TLC) separation of drug from its impurities followed by densitometric measurements of drug spots at 245 nm. The separation was carried out on silica gel 60 F254

using acetone-toluene-ethanol-ammonia solution 33% (45:45:10:1, v/v/v/v) as mobile phase. The methods were validated according to USP and ICH guidelines and the acceptance criteria for linearity, accuracy, precision, specificity and system suitability were met in all cases. The methods were linear in the range of 10-200g mL⁻¹ and 2.0-37.4g/spot for HPLC and TLC, respectively. The proposed methods were successfully applied for the determination of carvedilol in bulk and tablets forms. The results were compared statistically at 95% confidence level with each other. There was no significant difference between the mean percentage recoveries and precision of the two methods.

Keywords: Carvedilol; Rp-Hplc; Tlc-Densitometry; Tablets.

357. Spectrophotometric Determination of Carvedilol in Tablets by Charge-Transfer and Ion-Pair Complexation Reaction

Issa Y. M., Hussien E. M, Ibrahim M. M. AbdelGawad and F. M. Barakat S.

Int. J. Develop. Tech., 3(2): 131-147 (2012)

Simple, sensitive and accurate spectrophotometric methods are described for the assay of carvedilol. The first method is based on the charge-transfer (CT) reaction of drug as an n-electron donor with either 2,3-dichloro 5,6-dicyano-p-benzoquinone (DDQ) or 2,5-dichloro-3,6-dihydroxy-p-benzoquinone (p-chloranilic acid, p-CA) as-acceptors to give colored radical anions. The colored products are quantified spectrophotometrically at 455 and 520 nm for DDQ and p-CA, respectively. The second method is based on the formation of ion-pair complexes with the acidisulphonophthalein dyes bromophenol blue (BPB) and bromocresol purple (BCP) in dry chloroform to form stable yellow colored complexes with maximum absorbance at 412 and 407 nm, respectively. The proposed methods obeyed the Beer-Lambert law with a good correlation coefficient (0.9996–0.9999) in the concentration ranges 10.0-80.0, 30.0-300.0, 1.0-14.0 and 2.0-17.0g/mL for DDQ, p-CA, BPB and BCP, respectively. The parameters, molar absorptivity, precision, accuracy, recovery, robustness and stability constant were evaluated. The methods were applied successfully to the determination of carvedilol in tablets with mean recoveries of 100.35 ± 0.66%, 100.07±0.59%, 99.82±0.78% and 99.77±0.68% for DDQ, p-CA, BPB and BCP, respectively. The low values of the relative standard deviation (RSD < 1.0%) indicate the high accuracy and precision of the methods. The spectral characteristics of the CT- complexes are evaluated.

Keywords: Carvedilol; Spectrophotometry; Charge-Transfer and Ion-Pair Complexes; Tablets.

358. Synthesis and Structural Study of the Ion-Associates of Sildenafil Citrate with Chromotropic Acid Azo Dyes

Y.M. Iss, W.F. El-Hawary, A.F.A. Youssef and A.R. Senosy

Eur. Chem. Bull., 1(6): 205-209 (2012)

Five ion-associates of the drug sildenafil citrate (SC) with monochromotropic acid azo dyes, chromotrope 2B (I) and chromotrope 2R (II) and chromotropic acid bi-azo dyes, bis-3,6-(o-hydroxyphenylazo)-chromotropic acid (III), bis-3,6-(p-N,N-dimethylphenylazo)-chromotropic acid (IV) and 3-phenylazo-6-o-

hydroxyphenylazo-chromotropic acid (V) have been synthesized. Structural characterization of these novel sildenafil citrate ion-associates was carried out using elemental analysis and spectral techniques (VIS and IR). IR absorption spectra of the investigated ion-associates are studied and compared with those of the pure azo dyes and the drug. The spectral characteristics, oscillator strengths, transition dipole moments and resonance energy of the ion-associates in the ground state have also been calculated.

Keywords: Sildenafil Citrate; Chromotropic Acid Azo Dyes; Vis Spectrophotometry; Ir Spectra.

359. The Reaction of Cyanoacetylhydrazine with Furan-2-Aldehyde: Novel Synthesis of Thiophene, Azole, Azine and Coumarin Derivatives and the ir Antitumor Evaluation

Wagnat W. Wardakhan, Sherif M. Sherif, Rafat M. Mohareb and Amr S. Abouzied

International Journal of Organic Chemistry, 2: 321-331 (2012)

The reaction of cyanoacetylhydrazine 1 with furan-2-aldehyde 2 gives the hydrazide-hydrazone derivative 3. The latter compound undergoes a series of heterocyclization reactions to give new heterocyclic compounds. The antitumor evaluation of the newly synthesized products against three cancer cell lines, namely breast adenocarcinoma (MCF-7), non-small cell lung cancer (NCI-H460) and CNS cancer (SF-268) were recorded. Some of the synthesized compounds show high inhibitory effects.

Keywords: Acetylhydrazine; Hydrazide-Hydrazone; Thiophene; Thiazole; Pyridine; Coumarin; Antitumor.

360. Conducting Scientific Research: Research Hypothesis and Null Hypothesis

Rafat M. Mohareb

Organic Chemistry: Current Research, 1 (2): 1-2 (2012)

In the simplest forms, hypotheses are typically phrased as "if-then" statements. For example, a researcher may hypothesize that "if people exercise for 30 minutes per day at least three days per week, then their cholesterol levels will be reduced". This hypothesis makes a prediction about the effects of exercising on levels of cholesterol and the prediction can be tested by gathering and analyzing data. Your prediction is that variable A and variable B will be related (you don't care whether it's a positive relationship).

Keywords: Research Hypothesis; Null Hypothesis.

361. The Reaction of Cyanoacetylhydrazine with Chloroacetone: Synthesis of 1,2,4-Triazine, 1,3,4-Oxadiazine and the ir Fused Derivatives with Antitumor Activities

Rafat M. Mohareb and Eman M. Samir

Open Journal Of Medicinal Chemistry, 2: 1-9 (2012)

The reaction of cyanoacetylhydrazine with chloroacetone gave the N-(1-chloropropan-2-ylidene)-2-cyanoacetylhydrazide. This compound reacted with either hydrazine hydrate or phenylhydrazine to give the corresponding 1,2,4-triazine derivatives. On the other hand, its reaction with either

benzenediazonium chloride or benzaldehyde gave in each case the 1,3,4-oxadiazine derivatives. Moreover, the reaction of the cyanoacetylhydrazine with 2-bromocyclohexanone gave the corresponding hydrazine-hydrozone derivative. The antitumor evaluation of the newly synthesized products against three cancer cell lines, namely breast adenocarcinoma (MCF-7), non-small cell lung cancer (NCI-H460) and CNS cancer (SF-268) was recorded. Some of the tested compounds showed activities which were higher than the reference doxorubicin

Keywords: 1,2,4-Triazine; 1,3,4-Oxadiazine; Pyrazole; Antitumor.

362. Uses Of 1-Cyanoacetyl-4-Phenyl-3-Thiosemicarbazide in the Synthesis of Antimicrobial and Antifungal Heterocyclic Compounds

Rafat M. Mohareb and Abeer A. Mohamed

International Journal of Pure and Applied Chemistry, 2(2): 144-155 (2012)

The thiosemicarbazide synthesized from the reaction of cyanoacetylhydrazine phenylisothiocyanate reacted with acetoacetanilide gave the 2-pyridinone derivative 4. The reaction of the latter product with 1,3-dicarbonyl and halocarbonyl compounds gave the benzo[c]pyridine derivatives 6a,b and the thiazole derivatives 9a,b, respectively. The reaction with phenylisothiocyanate and elemental sulfur gave the thiazole derivative 14. The latter compound reacted with halocarbonyl compounds to give the thiazole products 16a-c. The antimicrobial and antifungal evaluations of the newly synthesized products showed that some compounds have high activity.

Keywords: Thiosemicarbazide; Pyridine; Thiazole; Antimicrobial

363. Coordination Behaviour and Biological Activity Studies of Transition Metal Complexes with Indapamide and Mixed Ligands of Indapamide and Glycine

Fatma S.M. Hassan, Gehad G. Mohamed, Ahmed F. Al Hossainy and Mostafa A.S. Khidr

Journal Of Pharmacy Research, 5(7): 3753-3763 (2012)

A series of binary and ternary metal(II)/(III) complexes of Cr(III), Mn(II), Fe(III), Co(II), Ni(II), Cu(II) and Zn(II) have been synthesized from the indapamide (IND) alone or in the presence of glycine. They were characterized by elemental analysis, spectral (IR, UV-Vis), magnetic moment measurements, molar conductance, thermal analysis and X-ray powder diffraction studies.

The electronic absorption spectra and magnetic susceptibility measurements of the complexes indicate octahedral geometry for all the complexes. The important infrared (IR) spectral bands corresponding to the active groups in the IND and the solid complexes under investigation were studied and implies that IND is coordinated to the metal ions in a neutral monodentate manner. The antibacterial and antifungal activities of the IND and its metal complexes were screened against bacterial species (*Staphylococcus aureus*, *Bacillus subtilis*, *Pseudomonas*

aeruginosa and *Escherichia coli*) and fungi (*Candida albicans*, *Aspergillus fumigatus*, *Geotrichum candidum* and *Syncephalastrum racemosum*). Penicillin G, Streptomycin, Itraconazole and Clotrimazole were used as references for antibacterial and antifungal studies. The activity data show that the metal complexes have a promising biological activity comparable with the parent IND drug against bacterial and fungal species. The X-ray powder diffraction reveals that the IND ligand and its binary Cr(III), Mn(II), Co(II), Ni(II) and Cu(II) complexes are crystalline while the Fe(III) complex is amorphous. In addition, the ternary chelates are crystalline, except Co(II) and Fe(III) chelates, they are amorphous.

Keywords: Binary and Ternary Complexes; Indapamide; Glycine; Spectroscopy; Thermal Analysis.

364. Cr(III), Mn(II), Fe(II), Co(II), Ni(II), Cu(II), Zn(II), Th(IV) and UO₂(II) Mixed Ligand complexes of Lomefloxacin and Dl-Alanine. Preparation, Spectroscopic Characterization, Biological and Anticancer Activity

Hanan F. Abd El-Halim, Gehad G. Mohamed, M.M.I. El-Dessouky and Walaa H. Mahmoud

Journal of Pharmacy Research, 5(11): 5084-5092 (2012)

Mixed ligand transition metal complexes with general formula $[M(LFX)(Ala)(H_2O)_2]Cl$ and $[M(LFX)(Ala)(H_2O)_m](X)_n \cdot yH_2O$ (LFX = lomefloxacin, Ala = alanine, M = Fe(III), Ni(II), Cu(II), X = Cl, m = 2, n = 1, 2, y = 1-2), $[M(LFX)(Ala)(H_2O)_m](X)_n$ (M = Cr(III), Co(II), Mn(II), Zn(II), X = Cl, n = 1-3, m = 2) and $[M(LFX)(Ala)](X)_n$ (M = UO₂(II), Th(IV), X = Cl or NO₃, n = 2, 3) have been synthesized and characterized using different spectroscopic tools, magnetic susceptibility, conductivity measurements and thermal analysis. The present results suggested that the lomefloxacin as bidentate coordinated with metal ions through carbonyl oxygen and carboxylate. The alanine as monodentate is coordinated with metal ions through the amino nitrogen atom and deprotonated carboxylate. LFX and its metal complexes were screened for their biological activity. Metal complexes exhibited higher antibacterial and antifungal than the free ligand. The anticancer activities against breast cancer cell line (MCF7) by using 100 µg / ml drug concentration were also tested. LFX and its metal complexes except Cr(III), Fe(III) and Th(IV) complexes were found to be very active against breast cancer cells with inhibition ratio values between 70-85.5 %.

Keywords: Lomefloxacin; Alanine; Mixed Ligand Complexes; Spectroscopic; Biological Activity; Anticancer Activity.

365. Development and validation of spectrophotometric and HPLC Methods for the determination of desloratadine in tablets and syrup.

Gehad G. Mohamed, Fekria M. Abou Attia and Neveen S. Ibrahim

Journal Of Pharmacy Research, 5(5): 2799-2825 (2012)

Two simple, rapid and selective methods were developed for the determination of desloratadine in drug substance and its pharmaceutical preparations. The first method (I) is based on ion-pair formation between desloratadine (DES) with bromocresol green (BCG) and bromothymol blue (BTB) reagents in 1,2-

dichloroethane where stable coloured ion-pairs were obtained and measured spectrophotometrically at 414 and 408 nm, respectively. All variables affecting the reaction were investigated and the conditions were optimized. Beer's law was obeyed over the concentration range from 0.622 to 18.66g mL⁻¹. The molar ratio of the formed ion-pair association complexes are found to be 1:1 as deduced by Job's method. The lower detection limits (LOD) and the limits of quantification (LOQ) were found to be 0.267 and 0.361 and 0.892 and 1.204g mL⁻¹ for BCG and BTB reagents, respectively. A high performance liquid chromatography (HPLC; method II) was used for DES determination in tablets. The method is based on separation of DES on a reversed phase, J'sphere ODS-H80 column, with 5m particle size and 250 x 4.5 mm dimensions using a mobile phase consists of a mixture of 0.0734 mol L⁻¹ phosphate buffer (pH 2.5), methanol and acetonitrile (50: 25: 25, v/v/v) at a flow rate of 1.5 ml min⁻¹ at ambient temperature with UV detection at 240 nm. The procedure provided a linear response over the concentration range from 1 to 300g mL⁻¹ with a mean accuracy of 100.4%±0.682. The LOD and LOQ were 0.432 and 1.439g mL⁻¹, respectively. The proposed methods were successfully applied for the determination of desloratadine in bulk powder and in dosage forms. There was no significant difference between each of the two methods and the reported one.

Keywords: Desloratadine; Spectrophotometry; Bromocresol Green; Bromothymol Blue; Hplc; Pharmaceutical Preparations.

366. Monitoring of Pesticide Residues in Different Agriculture Fields Effect of Different Home Processes on the Pesticides Elimination

Gehad G. Mohamed, M. Saleh and Hala M. Ibrahim.

Int. J. Res. Chem. Environ., 2 (3) : 236-253 (2012)

The effect of washing, storing, boiling, peeling, cooking with and without vinegar and frying on pesticide residue were investigated for vegetables and water/soil samples collected from Aghakahlia (Field 1), Nobaria, Behera (Field 2) and Giza (Field 3). Residues of organophosphorus, carbamate, organochlorine, fungicide, pyrethroid and abamectin pesticides in the processed were analysed by gas and HPLC chromatography. Statistical analysis showed that potatoes contained the highest levels of dimethoate and diazinon as organophosphorus pesticides. Residue of pirimiphos-methyl in green bean and potatoes and residues of methomyl, abamectin and dicofol in cucumber and tomatoes were found to be higher than their corresponding MRL's. Effect of some common food processing techniques (simple washing combined with cooking and/or frying techniques and drying of green bean) were also investigated and the results reported their effectiveness in residues reduction. It was found that, washing process eliminated approximately 13-60% of organophosphorus, 20-50% of carbamates, 19-25% of cypermethrin, 60% of dicofol, 100% of penconazole and 18-75% of abamectin residues. Peeling of washed cucumber removed 65% of malathion, 66% of methomyl, 80% of dicofol and 83% of abamectin. It might be concluded that a combination of simple washing and peeling removed 10 to 85% of insecticides if applied before consumption. As well, cooking and frying might help to remove 25-100% of the residual insecticides. Irrigation and drainage water were contaminated with pesticides such as malathion, dimethoate, methomyl, aldicarb, dicofol and abamectin. Effect of storage on the abamectin found with vegetables and soil after spraying suggested that the residue of abamectin was gradually decreased

with storage time. Final recommendations for this study is that monitoring programmes of pesticide residues in local produces must be expanded to include all food items and potentially harmful pesticide residues in order to generate information and establishing data based on food contaminants.

Keywords: Pesticides Residues; Home Processing; Soil; Irrigation Water; Drainage Water.

367. 5-Fluorouracil Induces Plasmonic Coupling in Gold Nanospheres: New Generation of Chemotherapeutic Agents

Mona B. Mohamed, Nour T. Adbel-Ghani, Ola M. El-Borady, and Mostafa A. El-Sayed

Nanomedicine and Nanotechnology, 3 (7) : 1-7 (2012)

Loading 5-Fluorouracil (5-FU) into gold nanoparticles (AuNPs) could enhance its activity as anticancer drug hugely by enhancing its ability for penetration through the cell membrane. Accordingly, this work is devoted to loading 5-FU into AuNPs surface and studying the binding mechanism of the drug to the surface of the gold nanoparticles. Our finding indicates that new absorption band appears at longer wavelength upon loading 5-FU into gold nanospheres capped with citrate. This near IR band is due to induced surface plasmon coupling via hydrogen bonding between 5-FU and surface capping AuNPs. This leads to great enhancement of the drug action as chemotherapeutic as well as photothermal agents. Factors which affect the binding between 5-FU and the AuNPs such as pH, time after mixing the drug with AuNPs, concentration of the 5-FU, have been studied in detail. Accordingly, the binding interaction is proven to be via hydrogen bonding. Upon the investigation of thermal and photo stability, the formed composite 5-FU@ AuNPs showed high stability towards these factors. The spectral and morphological studies were measured via UV-VIS spectroscopy and Transmission Electron Microscopy (HR-TEM). Remarkable increases in the drug anticancer activity upon loading into AuNPs were observed for the cell viability test of human colon cancer (HCT16).

Keywords: Gold Nanoparticles; Plasmonic Coupling; Cytotoxicity; Colon Cancer; 5-Fluorouracil.

368. Synthesis, Characterization and Antimicrobial Activity of Pyridine-3-Carbonitrile Derivatives

Azza M. Abdel-Fattah, Fawzy A. Attaby, Mohamed A. A. Elneairy and Mohmoud N. M. Gouda

Current Bioactive Compounds, 8: 176-187 (2012)

2-Cyanoethanethioamide (1) reacted with, unsaturated ketones 2a,b to afford the corresponding 2-thioxopyridine-3-carbonitrile derivatives 6a,b. The reactivity of the latter products towards various chemical reagents was studied to yield both thieno[2,3-b]pyridines 9a-r and 3-aminothieno[2,3-b]pyridine-2-carbohydrazides 10a,b which were used in turn, to prepare N-phenylmethylenethieno[2,3-b]pyridine-2-carbohydrazides 13a,b, pyrido[3',2':4,5]thieno[3,2-d]pyrimidinones (15a,b,16a,b) and pyrido[3',2':4,5]thieno[3,2-d]triazinones 17a,b. Considering the data of IR, ¹H NMR, mass spectra and elemental analyses the chemical structures of the newly synthesized heterocyclic compounds were elucidated.

Keywords: Pyridothienotriazinones; 2-Cyanoethanethioamide; Pyridothienopyrimidinones; N-Phenylmethylenethienopyridin.

369. Synthesis, Characterization of La (Iii), Nd(Iii) and Er(Iii) Complexes with Schiff Bases Derived From Benzopyran-4-One and the ir Fluorescence Study

Aida L. El-Ansary and Nora S. Abdel-Kader

International Journal of Inorganic Chemistry, 2012: 1-13 (2012)

The Schiff bases, L1, L2 and L3, are synthesized from the condensation of 5,7-dihydroxy-6-formyl-2-methylbenzopyran-4-one (L) with 2-aminopyridine (1), p-phenylenediamine (2) and o-phenylenediamine (3). The prepared Schiff bases react with lanthanum (III), neodymium (III) and erbium (III) nitrate to give complexes with stoichiometric ratio (1:1) (ligand : metal). The binuclear complexes of Er(III) with L3 and the three metal ions with L2 are separated. The complexes have been characterized by elemental analysis, molar conductance, electronic absorption and infrared, ¹H-NMR spectral studies. The presence of hydrated and coordinated water molecules is inferred from thermogravimetric analysis. Thermal degradation studies show that the final product is the metal oxide. The luminescence properties of the Nd(III) and Er(III) complexes in dimethylformamide (DMF) solutions were investigated.

Keywords: Schiff Bases; Benzopyran-4-One; Luminescence Properties.

370. Extractive Spectrophotometric Method for Determination of Meoxipril Hcl and Perindopril in Raw Materials and Tablets using Ion Pair formation

HM Elqudaby, FA Nour El-Dien, Eman YZ Farg, Noha M Kamal El-Dien and Gehad G Mohamed

National Organization for *International J. of Chemical and Analytical Science*, 3(3): 1334-1339 (2012)

A simple and rapid extraction spectrophotometric method has been developed for the determination of some angiotensin converting enzyme inhibitor drugs (ACE) such as perindopril (PRD) and meoxipril (MOEX) in pure and different dosage forms. The method involves the formation of tense yellow ion pairs between these drugs under investigation with methyl orange (MO) and bromocresol green (BCG) at pH 2.5 followed by their extraction with chloroform. The absorbance is measured at 414 and 416 nm for PRD and 414 and 413 nm for MOEX, using MO and BCG reagents, respectively. The analytical parameters and their effects on the proposed system are investigated. Experimental conditions for the method permits the determination of PRD and MOEX over the concentration ranges of 2 – 140 and 2 – 120 µg mL⁻¹ for PRD and 2 – 90 and 2 – 140 µg mL⁻¹ for MOEX using MO and BCG reagents, respectively. The sandell sensitivity is found to be 2.84 and 2.74 g cm⁻² and 2.67 and 0.169 g cm⁻² for PRD and MOEX using MO and BCG, respectively. The relative standard deviation and the limits of detection (LOD) were calculated. The proposed method has been applied successfully for the determination of the drugs under investigation in raw materials and commercial tablets. No significant interference was observed from the excipients commonly used as pharmaceutical aids with assay procedure. The results are in good agreement with those obtained by the official method.

Keywords: Ace; Angiotensin Extraction; Spectrophotometer; Converting Enzyme; Methyl Orange; Bromocresol Green.

371. Synthesis and Tautomeric Structure of 7-Arylhrazono-3,5-Diphenyl-5H-Pyrazolo[5,1-C][1,2,4]Triazol-6(7H)-Ones in its Ground and Excited States

Farag M. A. Altalbawy and Elham S. S. Darwish

Asian J Spectroscopy, 16: 45-54 (2012)

A series of 7-Arylhrazono-3,5-diphenyl-5H-pyrazolo[5,1-c][1,2,4]triazol-6(7H)-ones 4a-j were synthesized from the reactions of 4-phenylamino-5-phenyl-4H-1,2,4-triazole-3-thiol 1 and ethyl arylhydrazonochloro acetate 2 and their acid dissociation constant pKa and pKa*, in the ground and excited states, respectively, were determined. Both pKa and pKa* constants were correlated with the Hammett equation. The results of such correlations together with the spectroscopic data indicated that the studied compounds exist predominantly in the hydrazone tautomeric form in both ground and excited states.

372. Synthesis and Characterization of A Novel Schiff Base Metal Complexes and the ir Application in Determination of Iron in Different Types of Natural Water

Mostafa M. H. Khalil, Eman H. Ismai, Gehad G. Mohamed, Ehab M. and Zayed Ahmed Badr

Open Journal of Inorganic Chemistry, 2: 13-21 (2012)

A novel, simple approach to the synthesis of macro-cyclic Schiff base ligand resulted from the condensation of bisaldehyde and ethylenediamine was prepared (7, 8, 15, 16, 17, 18-hexahydrodibenzo (a, g) (14) annulene) (L) and its complexes were synthesized and characterized using different physicochemical studies as elemental analysis, FT-IR, ¹H NMR, conductivity, magnetic properties, thermal analysis and their biological activities. The spectroscopic data of the complexes suggest their 1:1 complex structures which are investigated by elemental analysis, FT-IR, ¹H NMR, conductivity, magnetic properties, thermal analysis and their biological activities. The spectroscopic studies suggested the octahedral structure for the all complexes. The spectroscopic data of the complexes suggest their structure in which (N2O2) group act as a tetradentate ligand and two chlorides as monodentate ligands. Also electronic spectra and magnetic susceptibility measurements indicate octahedral structure of these complexes. The synthesized Schiff base and its metal complexes also were screened for their anti-bacterial and antifungal activity. Here we report the effect of a neutral chelating ligand on the complexation with iron to determine it in different types of natural water using recovery test. The activity data show that the metal complexes to be more potent/ antibacterial than the parent Schiff base ligand against one or more bacterial species.

Keywords: Novel Schiff Base; Transition Metal Complexes And Natural Water.

373. Chemically Modified Carbon Paste Electrode for Determination of Cesium Ion by Potentiometric Method

Refat F. Aglan, Gehad G. Mohamed and Hala A. Mohamed

American Journal Of Analytical Chemistry, 3: 576-586 (2012)

A new chemically modified carbon paste electrode for cesium(I) ion determination based on potassium zinc hexacyanoferrate

(PZHCF) as an ionophore was prepared. The electrode exhibits a Nernstian response for Cs(I) ions over a wide concentration range from 1×10^{-6} to 1×10^{-1} mol•L⁻¹ with a slope of 58 ± 0.5 mV•decade⁻¹. It has a response time of about 35 s and can be used for a period of 3 months with good reproducibility. Detection limit obtained in the optimal conditions was 3×10^{-7} mol•L⁻¹. The potentiometric response is independent of the pH of the solution in the pH range 4.0 - 8.0. The electrode possesses the advantages of low resistance, fast response over a variety of other cations. The proposed electrode is applied as a sensor for the determination of Cs(I) ion concentration in different samples solutions. The results showed a good correlation with the data obtained by atomic absorption spectrometric method.

Keywords: Cesium Determination; Modified Ion Selective Electrode; Potassium Zinc Hexacyanoferrate Ionophore .

374. Spectrophotometric Determination of Aluminium in Different Water Sources and Alloys using Calcon and Eriochrome Cyanine R Reagents

Gehad G Mohamed, Fayza A Afify and Osama A Mohamed

International Journal of Chemical and Analytical Science, 3(12),: 1651-1655 (2012)

A sensitive spectrophotometric method is developed for the determination of Al(III). The method involves the formation of a ternary complex from this metal ion with calcon and eriochrome cyanine R in the presence of the cationic surfactant cetyltrimethylammonium bromide (CTAB). The optimum conditions for the ternary complex formation are established. The method permits the determination of Al(III) over a concentration range of 0.002 - 0.68g mL⁻¹. Sandell sensitivity is found to be 0.0012g cm⁻². The method is simple, rapid, reproducible and accurate for Al(III) determination without previous separation in presence of other ions. The method is applicable for the determination of Al(III) in different water and alloy samples. The results obtained are in a good agreement with those obtained by the reference ICP_OES technique.

Keywords: Spectrophotometry; Calcon; Eriochrome Cyanine R; Cationic Surfactant; Al(III).

375. Large Scale Production of Antitumor Cucurbitacins from Ecballium Elaterium using Bioreactor

Mahmoud M. Saker, Mai M. FaridAbdelgawad A. Fahmi, Sahar A. El-Mekkawy, Hussein S.Taha and Ahmed I. Amin.

African Journal of Biotechnology, 11(66): 12974-12982 (2012)

Bioreactor plays a vital role in the commercial production of secondary metabolites and pharmaceuticals from plant cells. Many physical factors, like the mixing intensity, shear stress and operation conditions were optimized as a first step in scaling up process. Qualitative and quantitative determination of cucurbitacins E and I in the extract were carried out using high-performance liquid chromatography (HPLC). After two weeks of equipping the reactor with marine impeller, both the growth rate and the concentration of cucurbitacins were increased. However, the increase in the aeration rate from 0.3 to 0.6 vvm induced the production of cucurbitacin E, it reduced the cucurbitacin I production. The highest recorded level of cucurbitacins was 0.3 and 0.1 g/L for cucurbitacin E and cucurbitacin I, respectively.

Crude cucurbitacins extract showed potent antitumor activity in a range of 15.6 to 23.5g/ml against various carcinoma cell lines. In the current study, the optimizing condition for the production of cucurbitacins E and I in Ecballium Elaterium and their biological activities as an antitumor and antimicrobial agent were evaluated.

Keywords: Ecballium Elaterium; Cucurbitacins E; Cucurbitacins I; Bioreactor; Antitumor.

376. Simple Validated Method for Determination of Deoxynivalenol and Zearalenone in Some Cereals using High Performance Liquid Chromatography

Ahmed S. Sebaei, Ahmed M. Gomaa, Gehad G. and Mohamed ZEANour El-Dien

American J. Of Food Technology, 7 (11): 668-678 (2012)

Deoxynivalenol (DON) and zearalenone (ZON) are two of the five most important naturally occurring mycotoxins in human feeds produced by Fusarium species. The aim of the present study was to develop a fast extraction and a cheap method that can be applied for the determination of DON and ZON in cereals using high performance liquid chromatography (HPLC) using diode array and fluorescence detectors. The method validation performance was tested on three varieties of cereal samples (maize, rice and wheat).

The within-laboratory reproducibility expressed as relative standard deviation (RSDWR) was less than 10% for both mycotoxins (9% for DON and 7% for ZON). The method is linear from the limit of quantification (LOQ) from 200 to 2000 µg kg⁻¹ levels for DON and 20 to 400 µg kg⁻¹ levels for ZON. The limits of detection (LOD) for maize, rice and wheat samples were 24, 32 and 40 µg kg⁻¹ for DON, respectively and 3 µg kg⁻¹ for ZON. The measurement of uncertainty in terms of expanded uncertainty expressed as relative standard deviation (at 95% confidence level and coverage factor of k = 2) is in the range of ±31% for DON and ±25% for ZON, the method is economically used in ZON and DON determination in safety and quality assurance programs.

Keywords: Deoxynivalenol; Zearalenone; Method Validation; Cereals; Mycotoxins.

377. Detection of Mutations in Gata4 and Nkx2.5 Genes in Patients with Fallot'S Tetralogy

Ibtessam R. Hussein, Mona , El-Ruby, Abdelgawad A. Fahmi, Mohamed A. El-Desouky and Alaa El-Deen G. Fayed

Middle East Journal of Medical Genetics, 2012, 1: 46-52 (2012)

The aim of this work was to screen for mutations in the GATA4 and Nkx2.5 genes in patients affected by tetralogy of Fallot (TOF) in order to assess the role of Nkx2.5 and GATA4 mutations in causing this defect.

We also aimed to assess the effectiveness of the single stranded conformation polymorphism method (SSCP) as a screening method for detecting Nkx2.5 and GATA4 mutations.

Keywords: Congenital Heart Disease; Fallot'S Tetralogy; Gata4; Nkx2.5; Point Mutation.

378. Microstructure and Corrosion Behaviour of Al-Si Alloy Treated by High Intensity Ultrasonic Vibrations

Rana. M. El nashar, Ahmed M. El-aziz, Waleed. K and Nour. T. Abd el ghany

Ochrona Przed Korozj, 55, nr 2: 7-11 (2012)

The effect of ultrasonic liquid metal treatment on the microstructure and the corrosion behaviour of the A356 Al-Si alloy was studied. The microstructures of the Al-Si were observed by means of optical and scanning electron microscopes. The corrosion behaviour was studied electrochemically and by gravimetric method.

The results showed that the microstructure was modified from a coarse acicular plate-like form when no ultrasonic vibration was used, to a finely dispersed rosette-like form when ultrasonic treatment was employed. The ultrasonically treated samples showed higher resistance to pitting than the untreated sample. The soaking process negatively affected the pitting resistance.

Keywords: Al-Si Alloy; Ultrasonic Treatment; Microstructure; Corrosion.

379. Ethyl 3-(2-(3-Methyl-1H-Indole-2-Carbonyl)Hydrazono) Butanoate

Thoraya A. Farghaly and Sobhi M. Gomha

Molbank, 749: 1-4 (2012)

The title compound, ethyl 3-{2-[(3-methyl-1H-indol-2-yl)carbonyl]hydrazinylidene} Butanoate (3), was prepared via reaction of 3-methyl-1H-indole-2-carbohydrazide (1) and ethyl 3-oxobutanoate (2) under reflux.

The structure of the synthesized compound was assigned on the basis of elemental analysis, IR, ¹H-NMR, mass spectral and X-ray data.

Keywords: 3-Methyl; 1H-Indole-2; Carbohydrazide; X-Ray

380. Synthesis of Trifluoromethyl-Substituted Fused Bicyclic Heterocycles and their Corresponding Benzo-Fused Analogues

Ahmed H. M. Elwahy and Mohamed R. Shaaban

Synthesis of Trifluoromethyladvances in Organic Synthesis, Bentham E Books, chapter 8, 411-457 (2012)

Development of efficient routes to many kinds of fluorine-containing heterocycles is an attractive area of research since these compounds are now widely recognized as important organic materials for their potential use in medicinal and agricultural scientific fields.

This review survey research works on trifluoromethylsubstituted fused bicyclic heterocycles and their corresponding benzo-fused analogues over the last twelve years. Different approaches for the synthesis of such systems are discussed.

381. Quantum Dots and Nano-Porous Materials for Solar Energy Conversion

Waheed A. Badawy

Fuelling The Future, Brown Walker Press Boca Raton, Florida, chapter 2, 235-242 (2012)

New synthetic strategies have been developed to design nanostructure architectures of semiconductors, metals, polymers and light harvesting assemblies. New sensitizer or semiconductor systems are necessary to broaden the photoresponse in solar spectrum. Hybrids of solar and conventional devices may provide an interim benefit in seeking economically valuable devices. New quantum dot solar cells based on CdSe-TiO₂ architecture have been developed. With increasing demand for clean energy alternatives an increasing interest from private sector and venture capitalist investment could be achieved, where major breakthroughs in developing economically viable solar energy conversion devices are expected.

Keywords: Nanotechnology; porous Si; quantum dots; solar cells; solar energy conversion.

382. Coordination Chemistry of Palladium (II) Ternary Complexes with Relevant Biomolecules

Ahmed A. El-Sherif

Stoichiometry And Research - The Importance of Quantity in Biomedicine, In Tech, chapter 4, 79-120-(2012)

In this chapter, a detailed survey of the formation equilibria of [Pd(diamine)(H₂O)₂]²⁺ with ligands of biological significance (amino acids, peptides, dicarboxylic acids and DNA constituents) is presented. The stability constants of the hydroxo complexes were investigated and discussed for the diaqua complexes of both aromatic and aliphatic diamines coordinated with Pd(II). The stability constants data of such diaqua-complexes with amino acids, peptides, dicarboxylic acids and DNA constituents were reported and discussed. The speciation of the metal complexes approximately for all types of ligands was discussed. This constitutes a powerful starting point for understanding the mode of action of such metal species under physiological conditions. The present study clearly shows that [Pd(diamine)(H₂O)₂]²⁺ complex can form strong bonds with peptides and promote easy deprotonation of the peptide. The effect of chloride on the anti-tumour Pt(II) amines which are usually administered as cis-dichloro complexes was discussed. Biological activity of mixed ligand Pd(II) complexes with biologically active ligands was discussed.

383. Rubber Types, Properties and Uses

Maher Z Elsabee

Rubber Types, Properties and Uses, Nova Science Publishing Inc, USA, chapter 5 (2012)

This review article deals with the different types of rubber, their properties and uses. Brief description of the various rubber processes and ingredients used for the preparation of the final rubber products is given. The last part of the article is devoted to rubber composites and nanocomposites describing rubber/carbon nanotubes, rubber/nanoclays.

384. Tailor - Designed Electrodeposited Metallic Thin Films, Nanostructures and Nanowires Towards Targeted Applications

A.M. Mohammed, Mohamed S. El - Deab and Bahgat E. El-Anadouli

Electrodeposition: Properties, Processes and Applications, Nova Science Publishers Inc., chapter 7 (2012)

This chapter describes our findings over the last few years, concerning the use of electrodeposition as a facile technique for the fabrication of several thin films of noble metals, nanostructures and nanorods onto various substrates. This includes three tasks. Firstly: the electrodeposition of metallic Ni or Cu thin films on reticulated vitreous carbon (RVC) and Pd or black Ni onto copper screens for use as electro-catalytically active cathodes for the hydrogen evolution reaction (HER). Moreover, the effects of some hydrodynamic and solution parameters concerning the performance of the electrodeposition process of heavy metal ions (e.g., lead ions) from flowing wastewater are briefly discussed. Secondly: the fabrication (via electrodeposition) of metallic (e.g., Au) and metal oxide (e.g., manganese oxide) nanostructures for application in fuel cell catalysis including the oxygen reduction and evolution reactions in addition to formic acid oxidation. Details of the morphological and electrochemical characterizations of the thus-electrodeposited nanostructures are outlined. This includes scanning electron microscope imaging (SEM), electron back scatter diffraction (EBSD) and X-ray diffraction (XRD) patterns. Thirdly: the fabrication of one-dimensional nanostructures, i.e., nanowires, for vital electronic, chemical, biological and medical applications. Several methodologies are outlined for this sake; however, the electrodeposition in templates seems more interesting in terms of cost and potential for high volume production. The recent work combining the electrodeposition and the template growth approach for nanofabrication is introduced. Special emphasis is dedicated to assembling metal-semiconductor nanowire contacts in which the contact interface is formed along the cross-section of the wire.

385. Applications of Polymers Surfactants in Oil Industry

Rania Elsayed Morsi, Maher Z Elsabee and Ahmed Elsabagh

Book Published By Lambert Academic Publishing Saarbrücken Germany, 116 (2012)

Crude oil production under deep water presents serious operational problems; its main implication is the paraffin blockage with serious economical consequences due to possible obstruction of flow pipes or production lines. Also, there are an increasing number of crude oil fields that produce both crude oil and water, naturally occurred or injected as a second stage recovery to maintain the reservoir operating pressure and fluid flow profile. The water in crude oil emulsion so produced will then be stabilized by the variety of surfactant indigenous to the crude oil called emulsifying agent. It is more economic to separate water before transportation. Polymers have been used extensively in the petroleum industry as pour point depressant and demulsifiers for economical transportation of crude oil since the former can prevent the deposition in the pipe lines which may cause blockage of the transportation lines. emulsifiers are class of surfactants used to destabilize the emulsions by reducing the

interfacial tension at the emulsion interface, often by neutralizing the effect of the other, naturally occurring surfactants which are stabilizing the emulsion.

386. Synthesis of New Thiazolo [3,2A] Benzimidazole Derivatives

Ahmad Mahmoud Farag

Book Published By: Lap Lambert Academic Publishing, 200 (2012)

In this book, a study, was undertaken to explore the utility of 1-(3-methylthiazolo [3,2-a] benzimidazol-2-yl) ethanone, 3-methylthiazolo [3,2-a]benzimidazole-2-carboxylic acid ethyl ester and thiazolo[3,2-a]benzimidazol-3(2H)-one for the synthesis of a great variety of fused heterocyclic ring systems which could possess interesting biological and pharmacological properties.

Keywords:Thiazolo [3,2-a] benzimidazole; pyrazolo[1,5-a]pyrimidin; pyrazol[5,1 - c] - 1,2,4-triazine; triazolotriazine; thiazole; 1,3,4-thiadiazole.

387. Chitosan Derivatives, Preparation, the rmal and Spectral Characterization, Metal Uptake Absorption Isotherm

Maher Zaki Elsabee

Book Published by Lambert Academic Publishing, Saarbrücken, Germany, 122, (2012)

The reaction of chitosan with either cinnamoyl chloride or ammonium thiocyanate/cinnamoyl chloride to afford two polymeric chitosan derivatives having [-NH-(C=O)-] and [-NH-(C=S)-NH-C=O] moieties has been investigated. The obtained polymers have different chelating sites which might be more effective for the metals uptake and could be used to remove Cu(II) Ni(II), Co(II), Cr(III) and Fe(III) from their solutions. The chelating behavior has been investigated under several conditions, different isotherms models were studied. Different physico/chemical and spectroscopic studies have been investigated to identify the chemical and geometrical structure around each metal center. Also the kinetic parameters of the thermal decomposition of the prepared polymers and their metal complexes have been calculated based on the Coats-Redfern method from the thermograms of the TGA curves.

388. Ni-P and Ni-Co-P Coated Aluminum Alloy 5251 Substrates as Metallic Bipolar Plates for Pem Fuel Cell Applications

Amani E. Fetohi, R.M. Abdel Hameed , K.M. El-Khatib and Eglal R. Souaya

Int J Hydrogen Energ, 37: 7677-7688 (2012) IF: 4.054

This study is aimed to replace graphite bipolar plates in PEM fuel cells with surface modified aluminum alloy. To improve the surface characteristics of aluminum alloy 5251 (AA5251) substrate, Ni-P and Ni-Co-P coatings were deposited using electroless and electroplating deposition techniques [power supply and chronoamperometry]. Surface morphology and chemical composition of prepared coatings have been investigated using scanning electron microscopy (SEM) and energy dispersive X-ray (EDX) techniques. The corrosion

behaviour of Ni-P and Ni-Co-P coated AA5251 was studied in (0.5 M H₂SO₄ + 2 ppm HF) solution by potentiodynamic polarization technique. Lower corrosion current densities and more positive corrosion potentials were gained after coating AA5251 with Ni-P and Ni-Co-P deposits. Much better corrosion resistance was shown by coatings containing cobalt. Potentiostatic tests were carried out at 160 mV (MMS) in air saturated solution to simulate cathode environment in PEM fuel cells. The current density of Ni-Co-P (1:1)/AA5251 was stabilized at a value lowered by 4 times relative to that at bare AA5251 substrate. Interfacial contact resistance values between coated substrates and carbon paper were measured. Ni-P and Ni-Co-P coatings prepared by electroless method showed ICR values, twice that at ones prepared by electroplating power supply technique.

Keywords: Bipolar Plate; Polymer Electrolyte Membrane Fuel Cell; Ni-P; Ni-Co-P; Interfacial Contact Resistance.

389. Study of different aluminum alloy substrates coated with ni-co-p as metallic bipolar plates for pem fuel cell applications

Amani E. Fetohi, R.M. Abdel Hameed K.M. El-Khatib and Eglal R. Souaya

Int J Hydrogen Energ. 37: 10807-10817 (2012) IF: 4.054

Pure Al and some of its alloys [Al alloy 6061 (AA6061), Al alloy 3004 (AA3004) and Al alloy 1050 (AA1050)] were coated with Ni-Co-P using electroplating power supply technique. Scanning electron microscopy (SEM) and energy dispersive X-ray (EDX) techniques were applied to study the surface morphology and chemical composition of coated aluminum substrates. Their performance against corrosion was examined using potentiodynamic polarization technique in (0.5 M H₂SO₄ + 2 ppm HF) solution. Corrosion potential values were shifted in the positive direction at all aluminum substrates after their coating with Ni-Co-P. Corrosion current density values at coated pure Al and AA1050 were decreased by 18.6 times, compared to those at bare substrates. The stability of coated aluminum alloys was investigated during long-time operation under cathodic environment in PEMFCs using potentiostatic polarization test at 160 mV (MMS) in air-saturated solution. Ni-Co-P/AA3004 substrate showed a high corrosion rate after short time, while coated AA6061 one slowly corroded. Interfacial contact resistance (ICR) values between metallic bipolar plates and gas diffusion layer were measured. Coating AA1050 with Ni-Co-P reduces its ICR value by 13 times. Accordingly, electroplated Ni-Co-P/AA1050 substrate can be chosen as an efficient bipolar plate material in PEMFCs.

Keywords: Electroplating; Ni,Co,P; Aluminum; Metallic bipolar plate; Polymer electrolyte membrane fuel.

390. Effect of Preparation Conditions on the Performance of Nano Pt-CuO/C Electrocatalysts for Methanol Electro-Oxidation

R.S. Amin, R.M. Abdel Hameed, K.M. El-Khatib, Hammam El-Abd and Eglal R. Souaya

Int J Hydrogen Energ. 37: 18870-18881 (2012) IF: 4.054

Nano PtCuO particles were deposited on Vulcan XC-72R carbon black using the impregnation and microwave irradiation methods. The prepared catalysts were characterized by XRD, TEM and

EDX analyses. TEM images indicated that the microwave method provides homogeneously distributed catalyst particles in smaller size, compared to the one prepared by the impregnation method. The electrocatalytic activity of PtCuO/C electrocatalysts was investigated to oxidize methanol in 0.5 M H₂SO₄ solution by applying cyclic voltammetry and chronoamperometry techniques. The oxidation current density of PtCuO/C electrocatalyst, prepared by the microwave method, showed two folds increment with a potential shift in the negative direction by 69 and 36 mV at the first and second oxidation peaks, respectively, relative to those at the catalyst prepared by the impregnation method. The effect of varying methanol concentration on the resulting oxidation current density of PtCuO/C electrocatalysts was studied. Some kinetic information about the reaction order with respect to methanol and Tafel slope values was calculated. Slower current density decay was observed in the chronoamperogram of PtCuO/C electrocatalyst, prepared by the microwave method, reflecting a lower degree of surface poisoning.

Keywords: Platinum; Copper oxide; Fuel cells; Acidic solution; Methanol oxidation; Microwave irradiation.

391. Pt-NiO/C Anode Electrocatalysts for Direct Methanol Fuel Cells

R.S. Amin, R.M. Abdel Hameed, K.M. El-Khatib M. Elsayed Youssef and A.A. Elzatahry

Electrochim Acta, 59: 499-508 (2012) IF: 3.832

Pt catalyst was supported on Vulcan XC-72R containing 5 wt.% NiO using NaBH₄ as a reducing agent. The prepared catalyst was heat-treated at 400°C. XRD, TEM and EDX analyses were applied to characterize Pt-NiO/C electrocatalyst. The introduction of NiO reduces the particle size of Pt crystallites. The electrocatalytic activity of Pt-NiO/C electrocatalysts was examined towards methanol oxidation reaction in 0.5 M H₂SO₄ solution using cyclic voltammetry and chronoamperometry techniques. A three fold increment in the oxidation current density was gained at Pt-NiO/C electrocatalyst compared to Pt/C one. The corresponding chronoamperograms showed high steady state current density values suggesting better stability of Pt-NiO/C electrocatalyst towards the carbonaceous poisoning species. The enhanced electrocatalytic performance and the long-term cycle durability of Pt-NiO/C electrocatalyst are attributed to the strong interaction between Pt and NiO and the formation of small Pt crystals.

Keywords: Platinum; Nickel oxide; Methanol oxidation; Fuel cells; Carbon black; Electrocatalyst.

392. Synthesis and Antimicrobial Activity of Some Novel Terephthaloyl Thiourea Cross-Linked Carboxymethylchitosan Hydrogels

Nadia A. Mohamed and Nahed A. Abd El-Ghany

Cellulose, 19: 1879-1891 (2012) IF: 3.6

Four novel hydrogels composed of carboxymethylchitosan (CM-chitosan) cross-linked with various contents of terephthaloyl thiourea moieties (TTUCM-chitosan-1, TTUCM-chitosan-2, TTUCM-chitosan-3, TTUCM-chitosan-4) have been successfully synthesized. The hydrogels were characterized by elemental analyses, FTIR, ¹³C NMR, SEM, XRD, solubility and swell ability in various solvents. The antimicrobial activities of these hydrogels against three crop-threatening pathogenic fungi

(*Aspergillus fumigatus*, *Geotrichum candidum* and *Candida albicans*) and against three bacterial species (*Bacillus subtilis*, *Staphylococcus aureus* and *Escherichia coli*) were investigated. The hydrogels showed higher antibacterial activity than the parent CM-chitosan as judged by their higher inhibition zone diameter and lower minimum inhibition concentration. They are more active against Gram-positive bacteria than against Gram-negative bacteria. The results also indicated that the hydrogels have effective antifungal activity as compared with CM-chitosan. The antimicrobial activity of the hydrogels increased with increasing their cross-linking density.

Keywords: Chitosan; Diisothiocyanate; Cross-Linking; Hydrogels; Synthesis; Characterization; Antimicrobial Activity.

393. Preparation and Antimicrobial Activity of Some Carboxymethyl Chitosan Acyl Thiourea Derivatives

Nadia A. Mohamed and Nahed A. Abd El-Ghany

International Journal of Biological Macromolecules, 50: 1280-1285 (2012) IF: 2.453

Acetyl, chloroacetyl and benzoyl thiourea derivatives of carboxymethyl chitosan (ATUCMCS, CATUCMCS and BZTUCMCS) with comparable grafting degree were synthesized and their structures were characterized by FTIR spectroscopy and elemental analyses. The antimicrobial behaviors of CMCS and its derivatives against three types of bacteria [*Bacillus subtilis* (*B. subtilis*), *Staphylococcus aureus* (*S. aureus*) and *Escherichia coli* (*E. coli*)] and three crop-threatening pathogenic fungi [*Aspergillus fumigatus* (*A. fumigatus*), *Geotrichum candidum* (*G. candidum*) and *Candida albicans* (*C. albicans*)] were investigated. The results indicated that the antibacterial and antifungal activities of the acyl thiourea derivatives are much higher than that of the parent CMCS. The acyl thiourea derivatives were more potent in case of Gram-positive bacteria than Gram-negative bacteria. This is illustrated for example by the values of minimum inhibitory concentration (MIC) of the ATUCMCS, CATUCMCS and BZTUCMCS against *B. subtilis* were 3.9, 15.6 and 62.5, respectively, while the MIC values of these derivatives against *E. coli* were 62.5, 125 and 500. Moreover, the antifungal activity of the CATUCMCS is higher than that of the acetyl and benzoyl thiourea derivatives. This may be due to the presence of chlorine atom.

Keywords: Carboxymethyl chitosan; Acyl thiourea derivatives; Antibacterial activity; Antifungal activity.

394. Synthesis, Characterization and Antimicrobial Activity of Carboxymethyl Chitosan-Graft-Poly(N-Acryloyl, N-Cyanoacetohydrazide) Copolymers of Carboxymethyl Chitosan-Graft-Poly(N-Acryloyl, N-Cyanoacetohydrazide) Copolymers

Nadia A. Mohamed and Nahed A. Abd El-Ghany

Carbohydrate Chemistry, 31: 220-240 (2012) IF: 0.631

Carboxymethyl chitosan was grafted with N-acryloyl, N-cyanoacetohydrazide in homogenous aqueous phase using potassium persulfate initiator. The maximum grafting yield achieved was 448% at 0.03 mol/L potassium persulfate, 0.75 mol/L N-acryloyl, N-cyanoacetohydrazide and 60°C within 2 h. The grafted copolymers showed better thermal stability than that

of carboxymethyl chitosan. The samples with percent grafting values up to 98% were soluble in water, but a higher grafting extent resulted in insoluble copolymers.

The grafted copolymers are nontoxic materials and showed an inhibition effect on both *Escherichia coli* and *Staphylococcus aureus* bacteria and *Aspergillus flavus* and *Candida albicans* fungi better than those of chitosan and carboxymethyl chitosan themselves.

Keywords: Carboxymethyl chitosan; N-acryloyl; N-carboxymethyl chitosan; Graft copolymerization; Characterization; Antimicrobial activity.

395. Development and Validation of Spectrophotometric and HPLC Methods for the Determination of Cefixime in Capsule and Suspension.

Eman Y. Frag, Z.A.B. Farag, Gehad G. Mohamed and Z.Eman B. Yussof

Insight Pharmaceutical Sciences, 2 (2): 8-16 (2012)

Cefixime is an oral third generation cephalosporin antibiotic. It is used to treat gonorrhea, tonsillitis and pharyngitis. Two simple, rapid and selective methods were developed for the determination of cefixime in drug substance and its pharmaceutical preparations. The first method (I) is based on charge transfer complex formation between cefixime (CF) with 7,7,8,8-tetracyanoquinodimethane (TCNQ) and I2 reagents in acetonitrile and 1,2-dichloromethane, respectively. Where coloured charge transfer complexes were obtained and measured spectrophotometrically at 842 and 360 nm, respectively.

All variables affecting the reaction were investigated and the conditions were optimized. Beer's law was obeyed over the concentration range from 10 to 240 and 0.25 to 17.5 µg mL⁻¹ for TCNQ and I2 reagents, respectively.

The molar ratio of the formed CF-TCNQ CT complexes are found to be 1:1 as deduced by Job's method where the molar ratio of the formed CF-I2 CT complexes are found to be 2:3. The lower detection limits (LOD) and the limits of quantification (LOQ) were found to be 1.10 and 3.80 and 3.21 and 1.07 µg mL⁻¹ for TCNQ and I2 reagents, respectively. A high performance liquid chromatography (HPLC; method II) was used for CF determination in capsule and suspension forms.

The method is based on separation of CF on a reversed phase, Waters, Symmetry C18 column (5m, 250x4.6 mm) using a mobile phase consists of a mixture of water, acetonitrile and glacial acetic acid and adjusted to pH 2 using orthophosphoric acid (72: 25: 3 (v/v/v)) at a flow rate of 1.5 ml min⁻¹ at ambient temperature with UV detection at 273 nm. The procedure provided a linear response over the concentration range from 1 to 500 µg mL⁻¹ with a mean accuracy of 100.9%±0.728. The LOD and LOQ were 0.432 and 1.439 µg mL⁻¹, respectively. The proposed methods were successfully applied for the determination of cefixime in bulk powder and in dosage forms. There was no significant difference between each of the two methods and the official one.

Keywords: Cefixime; Spectrophotometry; 7,7,8,8-Tetracyanoquinodimethane; I2; HPLC; Pharmaceutical Preparations.

396. Spectrophotometric Studies using Charge-Transfer Complexes of Orphenadrine Citrate in Pure and in Dosage forms with-Acceptors.

Gehad G. Mohamed, Eman Y.Z. Fragand Yusra H.H. Awad

Journal of Pharmacy Research, 5(3): 1774-1779 (2012)

Simple, rapid and sensitive spectrophotometric procedure is suggested for the determination of orphenadrine citrate (OphC) drug in pure form and in pharmaceutical formulations. The method was based on the reaction of OphC as n-electron donor with p-acceptors namely, 2,3-dichloro-5,6-dicyano-1,4-benzoquinone (DDQ) and 3,6-dichloro-2,5-dihydroxy-p-benzoquinone (p-CLA). The obtained complexes were measured spectrophotometrically at 480 and 520 nm for DDQ and p-CLA reagents, respectively. Beer's plots were linear in the concentration range of 10-300 µg mL⁻¹ OphC, with correlation coefficients not less than 0.9941 and 0.9979 using DDQ and p-CLA reagents, respectively. The Sandell sensitivity was found to be 0.477 and 0.742 µg cm⁻² for DDQ and p-CLA, respectively. Low values of standard deviation (SD = 0.21-0.57 and 0.26-0.87 for DDQ and p-CLA reagents, respectively) and relative standard deviation (RSD% = 1.40-2.10 and 2.63-2.90%) (n = 4 for DDQ and p-CLA reagents, respectively) indicate accuracy and precision of the method. These results were also confirmed by inter- and intra-day precision with percent recovery of 97.50-98.33% and 98.60-98.66% and 98.20-9.33% and 98.53-102.4% for DDQ and p-CLA reagents, respectively. This method was successfully applied for determination of OphC in norflex tablet. The calculated t- and F- values (95% confidence limit) indicate no significant differences between the proposed and official methods.

Keywords: Orphenadrine citrate; Spectrophotometry; Acceptors; Norflex tablet.

397. Optimized and Validated Spectrophotometric Methods for the Determination of Clomipramine and Paroxetine Hydrochloride in Drug formulations.

Elqudaby H. M, Frag E. Y. Z., Gehad G. M and Mohamed M. A.

International Journal Of Research In Ayurveda And Pharmacy, 3(4): 537-542 (2012)

Two simple and sensitive spectrophotometric methods have been developed for the determination of some antidepressant drugs such as clomipramine (CLO) and paroxetine (PRX). The methods involved the formation of ion-pairs between the inorganic complexes of molybdenum(V) thiocyanate and hexakis iron(III) solution followed by extraction with 1,2-dichloroethane. The optimum conditions for the ion-pairs formation were established under which Beer's law was obeyed for CLO and PRX in the concentration range 5-150 and 10-250 µg mL⁻¹ for the first method, while it was obeyed for the second method in the concentration range of 10-200 µg mL⁻¹ for both CLO and PRX drugs, respectively. The limits of detection were 0.0744 and 0.109 µg mL⁻¹ and 0.177 and 0.113 µg mL⁻¹ for CLO and PRX using the first and second methods, respectively. The limits of quantifications for the first method were 0.233 and 0.531 µg mL⁻¹ while they were 0.327 and 0.34 µg mL⁻¹ using the second method for CLO and PRX drugs, respectively. Both of the two methods have been successfully applied for the determination of the cited drugs in raw materials and in drug formulations and compared with the

official reference methods. Complete validation of the proposed methods were done.

Keywords: Ion-Pair; Molybdenum(V) Thiocyanate; Hexakis Iron(III)-Thiocyanate; Clomipramine; Paroxetine.

Dept. of Entomology

398. Characterization of Multisugar-Binding C-Type Lectin (SpliLec) from A Bacterial-Challenged Cotton Leafworm, *Spodoptera littoralis*

Alaa Eddeen M. Seufi, Fatma H. Galal and Elsayed E. Hafez

SpliLec Multisugar-Binding C-Type Lectin, 7 (8): 1-15(2012)

IF: 4.092

Background: Various proteins that display carbohydrate-binding activity in a Ca²⁺-dependent manner are classified into the C-type lectin family. They have one or two C-type carbohydrate-recognition domains (CRDs) composed of 110-130 amino acid residues in common. C-type lectins mediate cell adhesion, non-self recognition, and immuno-protection processes in immune responses and thus play significant roles in clearance of invaders, either as cell surface receptors for microbial carbohydrates or as soluble proteins existing in tissue fluids. The lectin of *Spodoptera littoralis* is still uncharacterized.

Methodology: A single orf encoding a deduced polypeptide consisting of an 18-residue signal peptide and a 291-residue mature peptide, termed SpliLec, was isolated from the haemolymph of the cotton leafworm, *S. littoralis*, after bacterial challenge using RACE-PCR. Sequence analyses of the data revealed that SpliLec consists of two CRDs. Short-form CRD1 and long-form CRD2 are stabilized by two and three highly conserved disulfide bonds, respectively. SpliLec shares homology with some dipteran lectins suggesting possible common ancestor. The purified SpliLec exhibited a 140-kDa molecular mass with a subunit molecular mass of 35 kDa. The hemagglutination assays of the SpliLec confirmed a thermally stable, multisugar-binding C-type lectin that binds different erythrocytes. The purified SpliLec agglutinated microorganisms and exhibited comparable antimicrobial activity against gram (+) and gram (-) bacteria too.

Conclusions: Our results suggested an important role of the SpliLec gene in cell adhesion and non-self recognition. It may cooperate with other AMPs in clearance of invaders of *Spodoptera littoralis*.

Keywords: Light; Electron microscopy; Mosquito; Aedes; Yolk formation.

399. Yolk Protein Uptake in the Oocyte of the Asian Tiger Mosquito *Aedes albopictus* (Skuse) (Diptera: Culicidae)

Abeer S. Yamany, Heinz Mehlhorn and Fatma K. Adham

Parasitol Res, 111, (3): 1315-1324 (2012) IF: 2.149

The formation and uptake of the yolk protein in the oocyte of the Asian Tiger, *Aedes albopictus* mosquito was investigated. Light and electron microscopy of the ovaries at early resting stage as well as the structural changes associated with yolk formation were described 16 h after blood meal. The deposition of the yolk protein in the oocyte was correlated with a 15-fold increase in 138-nm pit-like depressions on the oocyte surface. These pits result by invagination of the oocyte cell membrane. They have a 20-nm

bristle coat on their convex cytoplasmic side and a layer of protein on their concave extraoocyte space. The pits, by pinching off from the cell membrane become bristle coat vesicles which carry the adsorbed protein into the oocyte. These vesicles lose the coat and then fuse to form small crystalline yolk droplets, which subsequently coalesce to form the large protein yolk bodies of the mature oocyte. Preliminary radioautographs and certain morphological features of the fat body, ovary and midgut, suggest that the midgut is the principal site of the yolk protein synthesis in *A. albopictus*.

Keywords: Light; Electron microscopy; Mosquito; Aedes; Yolk formation.

400. Food Consumption and Utilization by Tribolium Confusum Du Val (Coleoptera:Tenebrionidae) Larvae and their Susceptibility to the Acetone Extract of Nerium Oleander L. (Apocynaceae) Leaves in Relation to Three Types of Flour

El-Sayed H. Shaurub and Genan M. Abou Gharsa

J Stored Prod Res, 51: 56-6051 (2012) IF: 1.414

The nutritional indices of *Tribolium confusum* larvae reared on wheat, barley and corn flour and their susceptibility to acetone extracts of *Nerium oleander* leaves were studied. In addition, the concentrations of total protein, carbohydrate and lipid in the flours and the larvae reared on them were also determined. Although the lowest consumption index and relative growth rate (RGR) were obtained in larvae reared on corn flour, these showed the highest weight gain. No significant difference was apparent between the three types of flour in terms of digestibility, or between the RGR of larvae reared on barley and corn flour. In contrast, the RGR of larvae reared on wheat flour was significantly higher than that for those reared on barley and corn flour. The highest food utilization, in terms of the efficiency of conversion of ingested and digested food into biomass, was reached in larvae reared on corn flour. Larvae reared on wheat and corn flour had the highest and lowest total protein contents, respectively, while larvae reared on corn and barley flour had the highest and lowest total lipid contents, respectively. On the other hand, no relationship was evident between larval and flour total carbohydrate content. The present study showed that larvae reared on corn flour were more tolerant to acetone extracts of *N. oleander* leaves than those reared on wheat or barley flour. The relationship between the total protein, carbohydrate and lipid contents in the flour and the larval nutritional indices and also the susceptibility of larvae to the botanical extract, were discussed.

Keywords: *Tribolium Confusum*; *Nerium Oleander*; Insecticidal Bioassay; Nutritional Indices.

401. Immunomodulation in Insects Post-Treatment with Abiotic Agents: A Review

El-Sayed H. Shaurub

European Journal of Entomology, 109: 303-316 (2012) IF: 1.061

The effects of different abiotic agents that may modulate the activity of an insect's immune system are reviewed. These agents include insecticides, chitin synthesis inhibitors, juvenile hormone analogues, inert particles, antibiotics, heavy metals, radiation and miscellaneous substances. The significance of studying immunomodulation in insects treated with abiotic agents in

relation to both insect control and insect-borne parasitic diseases and the link between immunomodulation in insects post-treatment with both abiotic and biotic agents are discussed.

Keywords: Insects; Insecticides; Chitin Synthesis Inhibitors; Juvenile Hormone Analogues; Inert Particles; Antibiotics; Heavy Metals; Radiation; Immunomodulation.

402. Incidence of Orthopteran Species (Insecta: Orthoptera) Among Different Sampling Sites Within Satoyama Area, Japan

S. Abu ElEla, W. ElSayed and K. Nakamura

Journal Of Threatened Taxa, 4(3): 2476-2480 (2012)

In a survey of the orthopteran assemblages in four different sampling sites in Satoyama area, fifty different species have been recorded. These species belong to 10 families, 17 subfamilies and 27 tribes. Family Acrididae was found to exhibit the highest number of subfamilies and tribes (four subfamilies and eight tribes). This was followed by Tettigoniidae with six tribes. However, both of Gryllidae and Tettigoniidae harbored the highest number of observed species (12 species). On the other hand, three families were considered comparatively poor families exhibiting a single subfamily, a single tribe and a single species. These families were Eneopteridae, Mecopodidae and Pyrgomorphidae.

Keywords: Distribution; Incidence; Orthoptera; Presence-Absence; Satoyama.

403. Ultrastructural Observations on the Gonads and Neurosecretory Cells of Schistocerca Gregaria after Treatment with Lufenuron (Cga-184699)

Nirvina Ghazawy

Journal of Orthoptera Research, 21(2): 141-148 (2012)

Topical application of a series of concentrations of lufenuron, a chitin synthesis inhibitor, on the neck membrane of newly molted fifth-instar desert locusts, *Schistocerca gregaria*, gave various ultrastructural changes in ovarioles, including a disintegrated follicular epithelial cell layer, vacuolated cytoplasm and the appearance of lysosomal bodies. In males, electron micrographs showed loosely disrupted testicular tissues with vacuolated testicular epithelia. In both sexes the neurosecretory cells in the pars intercerebralis exhibited trapped neurosecretion without normal liberation into their connecting nerves and the mitochondria appeared to be losing their cristae.

Keywords: *S. Gregaria*; Ovaries; Testes; Neurosecretory Cells; Ultrastructure; Lufenuron; Chitin Synthesis Inhibitors.

404. Effect of Bacillus Thuringiensis and Farnesol on Haemocytes Response and Lysozymal Activity of the Black Cut Worm Agrotis Ipsilon Larvae

Hanan H. Awad

Asian Journal of Biological Sciences, 5 (3): 157-170 (2012)

The aim of the present study was to follow up the defense reaction of the haemocytes from larvae treated with bacteria and farnesol. The lysozymes are a powerful tool of the humoral defense mechanism. The insecticidal activity of *Bacillus thuringiensis* and farnesol on the 4th larval instar of *Agrotis*

epsilon showed a significant dose and time-dependent increase in mortality. The haemocyte population after bacteria and farnesol treatments was morphologically studied and clarified the haemocytes immune response using scanning electron microscopy (SEM). A marked significant increase was observed in the lysozyme activity of control with time. This may be due to the aging process of the larval instar. The lysozyme activity of the haemocytes showed significant increases at 6 h and 12 h. However, the activity decreased significantly at 24 to 72 h, reaching nearly half that of the control value 72h after the larvae were treated with farnesol. The presented results emphasize the importance of the insect hemocytes lysozyme activity which is considered as a safe measure for insect pest control.

Keywords: Bacillus Thuringiensis; Farnesol; Lysozyme; Haemocyte Response; Sem.

Dept. of Entomology

405. Arthropod Ectoparasites of Domestic Animals

El-Sayed Hassan Shaarub

Book Published by Lambert Academic Publishing, 570 page (2012)

Crude oil production under deep water presents serious operational problems; its main implication is the paraffin blockage with serious economical consequences due to possible obstruction of flow pipes or production lines. Also, there are an increasing number of crude oil fields that produce both crude oil and water, naturally occurred or injected as a second stage recovery to maintain the reservoir operating pressure and fluid flow profile. The water in crude oil emulsion so produced will then be stabilized by the variety of surfactant indigenous to the crude oil called emulsifying agent. It is more economic to separate water before transportation. Polymers have been used extensively in the petroleum industry as pour point depressant and demulsifiers for economical transportation of crude oil since the former can prevent the deposition in the pipe lines which may cause blockage of the transportation lines. Emulsifiers are class of surfactants used to destabilize the emulsions by reducing the interfacial tension at the emulsion interface, often by neutralizing the effect of the other, naturally occurring surfactants which are stabilizing the emulsion.

406. Seasonal Abundance, Number of Annual Generations and Effect of an Entomopathogenic Fungus on Phlebotomus Papatasi (Diptera: Psychodidae)

Mohamed M. El-Shazly, Mustafa M. Soliman and Alia Zayed

Environmental Entomology, 41(1): 11-19 (2012) IF: 1.561

The monthly density of the sand fly, Phlebotomus Papatasi Scopoli (Diptera: Psychodidae), was monitored during 2009 at Burg El-Arab, a rural district located close to the Mediterranean coast of Egypt. The number of annual generations and the efficacy of microbial control by the entomopathogenic fungus, Metrahizium anisopliae (Metsch.) Sorok (Ma79), were determined in the laboratory under atmospheric conditions, simulating those of the animal shelters in the study area. We used two collecting techniques; CDC light traps and oiled paper traps, to quantify sand fly density inside houses and in the open field.

Adult flies exhibited a seasonal range from April to December. The seasonal pattern was bimodal, with one peak in July and the second one in October. Calculations of the correlation coefficient (r) revealed a significant role of temperature and relative humidity in the monthly abundance of the sand flies in the study area. P. papatasi colony completed seven annual generations under semifield conditions, but the mean developmental time of each immature stage and the mean total duration of development from egg to adult for each generation varied according to the prevailing temperature. The longest generation time was observed in winter (the mean SD was 118 11.70 d) and the shortest one occurred at the highest temperatures in summer (the mean SD was 25.21 2.04 d). In microbial control studies, the entomopathogenic fungus, M. anisopliae, was used at 15 X 10⁸ spores/g food as a standard dose against the second instar larvae of P. papatasi at the different seasons during 2009. Mortality reached 100% in winter and decreased to 56.0% as the prevailing temperature increased during the summer season.

Keywords: Sand Flies; Monthly Abundance; Burg El-Arab; Egypt; Metarahizium Anisopliae.

Dept. of Geology

407. Mineralogical and Geochemical Investigations of the Middle Eocene Ironstones, El Bahariya Depression, Western Desert, Egypt

Walid Salama, Mourtada El Aref and Reinhard Gaupp

Gondwana Res, 22: 717-736 (2012) IF: 6.659

The Middle Eocene ironstone succession is located in the northeastern part of El Bahariya Depression, Western Desert, Egypt. This succession is subdivided into lower and upper sequences and consists of two main shallow marine ironstone facies associations. The first is a lagoonal manganiferous mud and fossiliferous ironstone facies association and consists mainly of goethite and hematite, detrital minerals (quartz, rutile and feldspars), manganese minerals (todorokite, psilomelane, pyrolusite, birnessite, aurorite and manjiroite) and authigenic clay minerals (kaolinite and illite). The second is a peritidal microbially mediated stromatolitic and nummulitic ooidal- oncoloidal ironstone facies association consists of goethite, apatite and secondary minerals that include quartz, jarosite, psilomelane and pyrolusite. Organic materials such as proteinaceous compounds, lipids, cellulose and carotenoids were detected in the cortices of the ferruginous ooids and oncoids. The marine ironstone facies were exposed to subaerial weathering and subsurface alteration processes. The weathering resulted in the formation of lateritic iron ores and paleosols during humid climatic periods. The lateritic iron ores consist mainly of colloform goethite, hematite and psilomelane. The identification of cavity-filling sulfate, nitrate, carbonate and silicate minerals in the marine ironstones and the lateritic iron ore may indicate more recent alteration under arid climatic conditions. The subsurface alteration is attributed to the oxidation of sulfides, primarily pyrite and weathering of glauconitic clastic rocks in the underlying Cenomanian Bahariya Formation during the interaction with acidic heated groundwater. The formation of ferrous and ferric sulfate and silicate minerals and mobilization of trace metals are the products of the alteration process. Enrichments in Ba, Co, K, Pb and Sr are correlated with manganese oxides, whereas anomalous P, V, Cr, Ni, Zn, As, Mo and U are correlated with iron oxyhydroxides.

Keywords: Mineralogy; Geochemistry; Ironstone; El Bahariya Depression; Egypt.

408. Neoproterozoic Nascent Island Arc Volcanism from the Nubian Shield of Egypt: Magma Genesis and Generation of Continental Crust in Intra-Oceanic Arcs

Ayman E. Maurice, Fawzy F. Basta and Ali A. Khiamy

Lithos, 132-133: 1-20 (2012) IF: 3.246

The Neoproterozoic Wadi Ranga metavolcanic rocks, South Eastern Desert of Egypt, constitute a slightly metamorphosed bimodal sequence of low-K submarine tholeiitic mafic and felsic volcanic rocks. The mafic volcanic rocks are represented by massive and pillow flows and agglomerates, composed of porphyritic and aphyric basalts and basaltic andesites that are mostly amygdaloidal. The felsic volcanic rocks embrace porphyritic dacites and rhyolites and tuffs, which overlie the mafic volcanic rocks. The geochemical characteristics of Wadi Ranga volcanic rocks, especially a strong Nb depletion, indicate that they were formed from subduction-related melts. The clinopyroxene phenocrysts of basalts are more akin to those crystallizing from island-arc tholeiitic magmas. The tholeiitic nature of the Wadi Ranga volcanics as well as their LREE depleted or nearly flat REE patterns and their low K₂O contents suggest that they were developed in an immature island arc setting. The subchondritic Nb/Ta ratios (with the lowest ratio reported for any arc rocks) and low Nb/Yb ratios indicate that the mantle source of the Wadi Ranga mafic volcanic rocks was more depleted than N-MORB-source mantle. Subduction signature was dominated by aqueous fluids derived from slab dehydration, whereas the role of subducted sediments in mantle-wedge metasomatization was subordinate, implying that the subduction system was sediment-starved and far from continental clastic input. The amount of slab-derived fluids was enough to produce hydrous magmas that follow the tholeiitic but not the calc-alkaline differentiation trend. With Mg# > 64, few samples of Wadi Ranga mafic volcanic rocks are similar to primitive arc magmas, whereas the other samples have clearly experienced considerable fractional crystallization. The low abundances of trace elements, together with low K₂O contents of the felsic metavolcanic rocks indicate that they were erupted in a primitive island arc setting. The felsic volcanic rocks are characterized by lower K/Rb ratios compared to the mafic volcanic rocks, higher trace element abundances (~2 to ~9 times basalt) on primitive arc basalt-normalized pattern and nearly flat chondrite-normalized REE patterns, which display a negative Eu anomaly. These features are largely consistent with fractional crystallization model for the origin of the felsic volcanic rocks. Moreover, SiO₂-REE variations for the Wadi Ranga volcanic rocks display steadily increasing LREE over the entire mafic to felsic range and enriched La abundances in the felsic lavas relative to the most mafic lavas, features which are consistent with production of the felsic volcanic rocks through fractional crystallization of basaltic melts. The relatively large volume of Wadi Ranga silicic volcanic rocks implies that significant volume of silicic magmas can be generated in immature island arcs by fractional crystallization and indicates the significant role of intra-oceanic arcs in the production of Neoproterozoic continental crust. We emphasize that the geochemical characteristics of these rocks such as their low LILE and nearly flat REE patterns can successfully discriminate them

from other Egyptian Neoproterozoic felsic volcanic rocks, which have higher LILE, Zr and Nb and fractionated REE patterns.

Keywords: Immature; Island; Arcs; Felsic; Volcanic Rocks Arabian; Nubian Shield Eastern Desert.

409. Cryogenian Ophiolite Tectonics and Metallogeny of the Central Eastern Desert of Egypt

Yasser Abd El-Rahman, Ali Polat, Yildirim Dilek, Tim M. Kuskyf, Mohamed El-Sharkawi and Amir Said

International Geology Review, 54, (16): 1-15 (2012) IF: 2.067

The Central Eastern Desert (CED) is characterized by the widespread distribution of Neoproterozoic intra-oceanic island arc ophiolitic assemblages. The ophiolitic units have both back-arc and forearc geochemical signatures. The forearc ophiolitic units lie to the west of the back-arc related ones, indicating formation of an intra-oceanic island arc system above an east-dipping subducted slab. Following final accretion of the Neoproterozoic island arc into the western Saharan Metacraton, cordilleran margin magmatism started above a new W-dipping subduction zone due to a plate polarity reversal. The western arc-forearc belt is delineated by major serpentinite bodies running, marking a suture zone. Ophiolitic units in the back-arc belt to the east show an increase in the subduction geochemical signature from north to south, culminating in the occurrence of bimodal volcanic rocks farther south. This progression in subduction magmatism resulted from diachronous opening of a back-arc basin from north to south, with a bimodal volcanic arc evolving farther to the south. Formation of the BIFs was related to opening of an ocean basin to the north, whereas development of the VMS was related to rifting of the island arc in the south. Gold occurs as vein-type mineral deposits, concentrated along arc-forearc belt. The formation of these gold ore was controlled by the circulation of hydrothermal fluids through serpentinites that resulted in Au mobilization, as constrained by the close spatial association of auriferous quartz veins with serpentinites along the western arc-forearc belt.

Keywords: Ophiolites; Forearc; Back-Arc; Neoproterozoic; Volcanogenic Massive Sulfides; Banded Iron Formations; Gold-Quartz Veins; Eastern Desert.

410. Oxygen and Carbon Isotopic Records in Holocene Freshwater Mollusc Shells from the Faiyum Palaeolakes, Egypt: Palaeoenvironmental and Palaeoclimatic Implications

F.A. Hassan, M.A. Hamdan, R.J. Flower and K. Keatings

Quatern Int, 266: 175-187 (2012) IF: 1.874

Stable oxygen and carbon isotopes of freshwater mollusc shells from a sequence of dated palaeolake deposits in the Faiyum Depression, Egypt, provide an outline record of lake development during the Holocene. It is argued that the carbonate O₁₈ record provides a proxy for climate change and that the isotope changes are driven by variations in monsoon precipitation in Nile eadwaters and in local evaporation processes. Shells from sediments dated to ca. 10,000 to 7700 cal BP had low values for oxygen and carbon isotopes indicating higher precipitation in the local area and intensified monsoonal activity, leading to higher Nile flood discharge and flooding of the entire Faiyum Depression. This was followed by a transitional period characterized by marked variability but with precipitation on

average less than before. From ca. 6000 to 4300 cal BP, precipitation was decreased until a dramatic reduction in Nile flood discharge occurred late in the fifth millennium BP. This reduction signalled the onset of arid conditions in the Faiyum, partly as a consequence of changes in Nile headwaters that was concomitant with declining lake levels in East Africa. Lake level decline in the Faiyum was further aggravated after 2700 BP as the Nile inflow further weakened and regulation increased.

411. Stacked, Lower Miocene Tide-Dominated Estuary Deposits in A Transgressive Succession, Western Desert, Egypt

Safiya M. Hassan, Ronald J. Steel, Ahmed El Barkooky, Mohamed Hamdan, Cornel Olariu and Mark A. Helper

Sedimentary Geology, 282: 241-255 (2012) IF: 1.537

The net transgressive Lower Miocene Moghra Formation of Egypt is a sandy estuarine complex consisting of a series of stratigraphic units that reflect repeated transgressive to regressive shoreline movements across the Burdigalian (Lower Miocene) coastal landscape. The transgressive part of each unit is preserved atop a deep erosional scour surface and consists of tidal-fluvial sandstones with tree logs and vertebrate bones that transition up to cross-stratified, tidal estuarine channel deposits and then to open-marine, shelf mudstones and limestones. In contrast, the regressive part is thinly developed and consists of thin-bedded, fossiliferous shelf mudstones that pass upward to thin, tide-influenced delta front deposits. Each of the nine transgressive-regressive units of the Moghra Formation is capped by a river-scour surface that severely truncates the underlying regressive half-unit. Regional tectonic subsidence and an overall decreasing influx of clastic sediment accounts for the accumulation of the Moghra Formation and its overall transgressive character. The high frequency relative base-level changes reflected by the transgressive-regressive units (averaging 350 kyr) that punctuate the overall transgressive stratigraphic trend are thought to have been driven by (1) sea-level changes caused by recently documented variations in East Antarctic ice-sheet volume during the Lower Miocene, and/or by (2) variation in the large-scale influx of sediment to the region (during continuous tectonic subsidence). The relative importance of the sea-level (eustatic fall) vs. supply drive (deep fluvial scour) mechanisms for producing the repeated and widespread Burdigalian incision surfaces in the Moghra succession cannot easily be determined.

Keywords: Moghra Formation; Burdigalian; Egypt; Estuaries; Tide; Dominated.

412. Glass-Ceramics Materials from Basaltic Rocks and Some Industrial Waste

G.A. Khatera, A. Abdel-Motelib, A.W. El Manawib and M.O. Abu Safia

J Non-Cryst Solids, 358, Issue 8: 1128-1134 (2012) IF: 1.537

Preparation of cheap technical glass-ceramic materials by crystallizing glasses derived from Saudi basaltic rocks and ceramic waste materials were investigated. The wastes of ceramic sanitary plants in Saudi Arabia were used. The wastes were formed during the manufacturing of the sanitary ware and used in glass batches, in amounts ranging between 10–50 wt.% of batch

constituents. Batches were melted and then cast into disc and rod shapes and subjected to heat-treatment, to induce crystallization. Different techniques were used in the present study including differential thermal analysis, optical and scanning electron microscope, X-ray diffraction, indentation, micro hardness, bending strengths and water absorption. The obtained glass-ceramic materials were mainly composed of pyroxenes, anorthite, olivine and magnetite, of ultra-fine grained and uniform textures as showed by SEM. The obtained glass-ceramic materials are characterized by high values of hardness ranging between 9624 and 10074 MPa, zero water absorption and bending strengths values ranged between 92 and 135 MPa, which makes them suitable for many applications under aggressive mechanical conditions.

Keywords: Basaltic Rocks; Ceramic Waste; Crystallization; Glass-Ceramics; Pyroxenes.

413. Mechanisms of Volcaniclastic Aggradation in Fluvial Systems Influenced by Explosive Volcanism: an Example from Neoproterozoic Hammamat Group, Wadi Queih Area, Central Eastern Desert, Egypt

Ezz El Din Abdel Hakim Khalaf

Journal Of African Earth Sciences, 68: 44-66 (2012) IF: 1.025

Wadi Queih basin records different continental settings that interacted with explosive volcanism. This paper discusses the contrasting aggradational mechanisms in fluvial systems strongly influenced by explosive volcanism which took place during sedimentation of the Queih basin. Six main facies associations composed of 12 lithofacies have been recognized in the Neoproterozoic succession filling the Queih basin: (1) lava flows and pedogenically modified pyroclastics facies association, (2) debris-flow-dominated alluvial fan facies association, (3) sheet flood-dominated alluvial fan facies association, (4) crevasse play facies association, (5) lacustrine facies association and (6) loess facies association. These facies assemblages are typical of low-sinuosity rivers flowing through unsymmetrical half graben basin. Petrographical and geochemical data of the Queih sediments indicate a predominantly continental volcanic block provenance and stable craton to fault-bounded basement uplift. Low values of Chemical and Plagioclase Index of Alteration (CIA and PIA) are consistent with low intensity source rock weathering under prevailing semi-arid to arid climate. During deposition of the lower member of the Queih basin, common fall and flow tuff events occurred, indicating syn-eruptive conditions. In contrast, deposition of the upper member occurred in a fluvial aeolian setting without input of primary volcaniclastic detritus, indicating inter-eruptive conditions. The change in depositional mode from the lower to upper is considered to be due to a change in the balance between the sedimentation rate and the rate of lake-level rise. Lithofacies stacking and rapid lateral changes of lithological units in conjunction with interformational unconformities and basin margin faults suggest tectonically induced sedimentation. Volcanism can also influence basin evolution and the delicate balance between erosion, sedimentation and prevalent transport processes is affected the Queih basin by volcanic input. Thus, the Queih basin records the response of fluvial system to large, volcanism-induced sediment loads.

Keywords: Alluvial Aggradation; Explosive Volcanism; Paleosedimentological Model; Basin Type And Stacking Pattern.

414. The Structure and Significance of Early Holocene Laminated Lake Sediments in the Faiyum Depression (Egypt) with Special Reference to Diatoms

R.J. Flower, K. Keatings, M. Hamdan, F.A. Hassan, J.F. Boyle, K. Yamada and Y. Yasuda

Diatom Research, 7: 1-14 (2012) IF: 0.656

Lake Qarun lies in the Egyptian Faiyum Depression and is the modern remnant of a much larger Holocene lake. Variations in water level occurred during the Holocene as a result of palaeoclimate changes and, since c. 4000 bp, there have been hydrological interventions. Past lake levels have been inferred from the locations of archaeological sites, former beaches and exposed lake sediments, but there is no continuous Holocene palaeolimnological record for the lake. To explore the potential of this record, three sediment cores (10.4–21.4 m long) were collected from terrestrial locations on the southern margin of the lake in 2008. The basal sections of all three cores consisted of thinly laminated diatom marl sediments overlying coarse sand. The nature of these laminations was investigated in thin sections from two cores (QARU9 and -10). Quantitative very high-resolution diatom analysis revealed seasonal succession patterns of *Aulacoseira* and *Stephanodiscus* species within diatom rich laminae. Elemental microprobe analysis of one thin section (QARU10) confirmed the presence of alternating Ca- and Si-rich laminae. The results indicate annually deposited sediment sequences with seasonality signals provided by microlayers of diatoms, calcite and clastic material. According to diatom counting, mean varve thicknesses equated to 6.0 (QARU9) and 9.4 (QARU10) annual diatom laminae accumulated cm¹. Radiocarbon dates from a third core (adjacent to QARU9) indicated that the QARU9 thin section material was bracketed between 8693 and 9935 cal bp. Diatom microstratigraphy was used to infer seasonality in varve forming processes. Gross sediment stratigraphy indicated that varve forming conditions had persisted for >1500 years. The presence of early Holocene varved sediments in palaeo-Lake Qarun provides an exceptional palaeoenvironmental archive for northeast Africa.

Keywords: Diatoms; Sediment; Lake Qarun; Laminae; Varves; Ancient Egypt.

415. Impacts of Human Activities on the Sedimentological and Geochemical Characteristics of Mabahiss Bay, North Hurghada, Red Sea, Egypt

Osama Elsayed Ahmed Attia, Ahmed M. Abu Khadra, Ahmed H. Nawwar and Gamal E. Radwan

Aaohn J, (2012) 5: 481-499 (2012) IF: 0.509

In Mabahiss Bay, north Hurghada City, Red Sea, Egypt, the bathymetric measurements show the irregular topography of the bottom. The bottom sediments are mainly composed of sand fractions (average 73.5%). Gravel and sand contents decrease with depth. On the other hand, silt and clay percents show indirect relation with depth. Abnormally, there are some spots found near the coast where the percent of both silt and clay increases. They also show carbonate sediments (average 90.15%) increasing

toward the bay center. The narrow belt adjacent to the shore area has lower carbonate content reflecting the effect of clastic sediments input into the area. The sediments in the study area have more than one source as indicated from the results of the mechanical analysis. Wide range of grain size distributions, clay spots and low carbonate content near the shore indicate change in the nature of sedimentary environment (i.e., pollution) which may be caused by land filling accompanied with urbanization and building of touristic resorts and centers. The organic matter content in the sediments is much higher than that of the other areas in the Red sea (average 4.8%) with considerable accumulation in the inner most parts of the bay. This may be due to relative abundance of organic productivity, direct discharge of domestic waste in some spots along the coast of the study area, and/or local contamination of hydrocarbons (i.e., tar balls thrown out on shore by weak waves through the few inlets of the study area). The average concentrations of lead, nickel, copper and cadmium are 44, 34, 51 and 3.1 ppm, respectively. The suggested origin of these metals is either organic (localized oil pollution), or using of antifouling and anticorrosive paints from fishing and tourist boats. Other metals, particularly manganese (average 77 ppm), cobalt (average 51 ppm) and zinc (average 16 ppm) as well as sodium (average 0.32%) and potassium (av. 0.10%) show a common trend of increasing concentration toward the outermost parts of the bay. Some parts along shoreline have increasing concentrations, even if these parameters having a common trend of increase towards the center of the bay. This may be either due to sewage and wastewaters discharges from many outlets of tourist centers and fishermen and cargo boats, and/or terrestrial sediments input. Direct comparison of the present levels of heavy metals in Mabahiss Bay with other published data along the Red Sea and Gulf of Suez shows that the study area has higher concentrations. Dredging, land filling, localized oil pollution, using of antifouling and anticorrosive paints from fishing and tourist boats (where the bay is used as harbor for many of fishermen and cargo boats), sewage, variable amounts of municipal wastewater from many outlets of tourist centers considered to be the sources of pollution within Mabahiss bay. There are many effects of pollution on Mabahiss Bay environment among which: (1) death of fishes, seaweeds, birds, marine mammals, etc., (2) damage of beaches and other recreational areas, (3) damage of marine ecosystem by eliminating or decreasing population of certain species, (4) hazard to human from ingesting contaminated food and more.

Keywords: Red Sea; Heavy Metals; Bottom Sediments; Pollution.

416. Palynology and Palaeoenvironments of Middle Jurassic to Cenomanian Successions, Alamein-Ix Well, North Western Desert, Egypt

Sameh S. Tahoun, Mohamed I.A. Ibrahim and Suzan Kholeif

Revista Española De Micropaleontología, 44 (1-3): 57-78 (2012)

This paper presents the palynological results of the late Callovian middle Cenomanian sediments in the Alamein-IX well drilled in the northern part of the Western Desert of Egypt. The studied section yielded five formations from base to top, namely Masajid, Alam El Bueib, Alamein, Kharita and Bahariya. Fifty one miospore and thirty three dinoflagellate cyst species were identified. Biostratigraphically important taxa were used to differentiate the sequence into five informal palynostratigraphic biozones, which were established mainly by miospores in the

lower Cretaceous interval and mostly by dinoflagellate cysts in the middle-upper Jurassic interval. The palynozones belong to the Callovian-Oxfordian, Neocomian-Barremian, Aptian, middle-upper Albian and early-middle Cenomanian ages, respectively. Palynology was used to identify the Cimmerian event as a hiatus between the Jurassic and Cretaceous and is characterized by the absence of late Oxfordian, Kimmeridgian, Portlandian, Berriasian and Valanginian deposits. The paleoenvironments of the sedimentary successions fluctuated from shallow marine (Masajid Formation) through marginal marine (nearshore to coastal) to deeper conditions (Alam El Bueib Formation) and shallow marine (Alamein Formation) and finally marginal marine (Kharita and lower Bahariya formations).

Keywords: Palynology; Paleoenvironment; Callovian-Cenomanian; Alamein; Western Desert; Egypt.

417. Archaeometallurgical Expeditions to the Sinai Peninsula and the Eastern Desert of Egypt (2006, 2008)

Ali Abdel-Motelib, Michael Bode, Rita Hartmann, Ulrich Hartung, Andreas Hauptmann and Kristina Pfeiffer

Metalla, 19: 3-59 (2012)

In this study we report on two archaeometallurgical expeditions (2006, 2008) of an interdisciplinary Egyptian-German team to the Sinai Peninsula and the Eastern Desert in Egypt. 27 mining, smelting and habitation sites were visited which date from the Late Chalcolithic to the Late Bronze Age. It was intended to clarify the prehistoric copper production in these regions and its influence on the supra-regional copper exchange between southern Canaan and Egypt, mainly between Maadi (near Cairo) and Hujayrat al-Ghuzlan and Tall Magass, Aqaba. In addition to the field work analytical investigations (chemical and lead isotope analyses) were performed on ores, slags and metal objects collected. Provenance studies revealed that Sinai ore was probably imported to the Nile valley along with copper ore from the Wadi Arabah deposits Timna and Faynan and from Anatolia as well. The enormous potential of Sinai copper ore deposits is impressively demonstrated by gigantic metallurgical remains from the Early and Late Bronze Age. Recent mining activities in the Um Bogma area probably destroyed previous activities. Copper was apparently smelted in Sinai in wind-powered furnaces known from the entire Eastern Mediterranean. Copper-metallurgical activities in the Eastern Desert are limited. Ancient deposits were probably exploited for green pigments, or for gold.

Keywords: Sinai Peninsula; Eastern Desert; Survey; Copper Deposits; Metallurgy

418. The Holocene Evolution of the Quesna Turtle Back: Geological Evolution and Archaeological Relationships Within the Nile Delta

Joanne M. Rowland and Mohamed Hamdan

Studies In African Archaeology 11; Pozna Archaeological Museum 2012, : 11-24 (2012)

Five seasons of fieldwork have been carried out by an Egypt Exploration Society (EES) Delta Survey project under the direction of the first author. A discrete element of this project is a renewed approach to investigations both at the SCA registered site of Quesna quarries and also on the low ground around the sand

gezira (turtle back) on which the site sits. The modern town of Quesna is 65 km northwest of Cairo on the agricultural road to Alexandria, with the archaeological area c. 4 km to the east of this road. The results of geophysical survey and excavation on the gezira have been published elsewhere (Rowland 2008; 2007; Rowland and Zakrzewski 2008; Rowland and Strutt 2007; Rowland and Wilson 2006; Rowland and Billing 2006) and therefore only a brief explanation of the site is given here. The SCA commenced a programme of excavation at the site of Quesna throughout the 1990s, following the discovery of a brick-built mausoleum in the south of the site during sand quarrying in the area. Excavation proceeded throughout the 1990s within what transpired to be a Late Period to Ptolemaic mausoleum, with rooms stacked with burials up to six-deep. Some burials had been placed in limestone sarcophagi, others mummified and wrapped in linen. One inscribed black stone sarcophagus is now at the Egyptian Museum in Cairo (Gomaà and Hegazy 2001: 52-80).

Keywords: Nile Delta; Quesna; Archaeology.

419. Upgrading of Egyptian Nonsulfide Zinc Ore by Gravity Separation Techniques

M. Z. Farag, N. A. Abdel-Khalek, M. S. Hassan, M. M. El Aref and A. W. El Manawi

Journal of Metallurgical Engineering (Me), 1, (1): 6-13 (2012)

This paper aimed at evaluation and beneficiation of a nonsulfide zinc ore from Um Gheig deposits in the eastern desert of Egypt using gravity separation process. The zinc ore of Um Gheig is called "calamines". It consists of a mixture of zinc carbonates (smithsonite, hydrozincite) and zinc silicates (hemimorphite), with variable amounts of Pb bearing minerals. The ore sample has 47.5 % ZnO, 1.55% PbO and ~29.3 % L.O.I. Liberation study, using mineralogical and SEM investigations, indicated that maximum liberation can be obtained by grinding the ore to 0.125 mm. Beneficiation techniques involved crushing and grinding of the ore to 100 % -0.125 mm. This was followed by classification of the ground ore using a 0.080 mm screen. Shaking table was used to upgrade the coarse fraction (-0.125+0.080 mm) while the fines below 0.080 mm was separated by Falcon concentrator. The results of shaking table showed that a high grade concentrate can be obtained at the following optimum parameters: inclination angle (4 degree), stroke length (2.5 cm), feed rate (150 gm/min) and water flow rate (25 l/min). At such optimum conditions maximum grade (62.2 % ZnO) and operational recovery (~ 93.8 %) were obtained. In the mean time, Falcon concentrator gave a concentrate of 54.85 % ZnO with 76.6% operational recovery from the fine fraction below 0.080 mm.

Keywords: Nonsulfide Zinc Ore; Mineralogy; Petrography; Liberation Size; Gravity Separation; Shaking Table.

420. Mineral Chemistry of the Neoproterozoic Alaskan-Type Akarem Intrusion with Special Emphasis on Amphibole: Implications for the Pluton Origin and Evolution of Subduction-Related Magma

Yasser Abd El-Rahman, Hassan M. Helmy, Tomoyuki Shibata and Masako Yoshikawa

Lithos, 155: 410-425 (2012) IF: 3.246

Akarem Intrusion is one of Alaskan-type ultramafic-mafic complexes of the Neoproterozoic age. The olivine and

pyroxene-rich ultramafic core is surrounded by hornblende gabbro and hornblende margin with gradational contacts. The calculated liquids in equilibrium with clinopyroxene show enrichment in Th, U and LREE over the HREE, similar to arc magma formed from the mantle metasomatized by fluids from subducted sediments. Both olivine and pyroxene compositions indicate fractional crystallization from the ultramafic core to the mafic margin. However, amphiboles show systematic increase in concentrations of compatible elements, such as V and shift in REE patterns from a bowed-up shape to bowed-down shape from the mafic margin to the ultramafic core. Such variation in trace elements of amphiboles indicates progressive crystallization of amphiboles from the mafic margin to the ultramafic core. The formation of the Akarem Intrusion started with an early fractional crystallization stage which led to the formation of a stratified magma chamber. The circulation in the magma chamber resulted in the solidification of the mafic magma along the margin where the early-stage amphiboles crystallized along with plagioclase. Subsequently, an evolved liquid from the crystallizing mafic margin percolated into the liquid-rich ultramafic core to form the later generation of interstitial amphiboles. The calculated trace element composition of the liquids in equilibrium with amphibole shows a progressive development of Nb and Ti negative anomalies and increase in La/Yb ratios from the margin to the core of the intrusion. Such variations manifest the role of amphibole fractionation in the evolution of the geochemical signature of arc magma.

Keywords: Alaskan-Type Intrusion; Ultramafic-Mafic Complexes; Amphibole; Arc Magma; Neoproterozoic; Egypt.

421. Characterization of the Aquifer System in the Northern Sinai Peninsula, Egypt

Mohamed ElKashouty, Magdy Hosney ElSayed, Yehia El Godamy, Mohamed Gad and Morquesd Mansour

Journal of Environmental Chemistry and Ecotoxicology, 4(3): 41-63 (2012)

Northern Sinai has received great attention with respect to future agricultural development, especially after initiation of El Salam canal, as a source of irrigation. The research aim is to highlight on the nature and potentiality of the Quaternary aquifer in the northern Sinai. To achieve this target, a 256 groundwater samples were collected and analyzed chemically with respect to major ions, SiO₂, B³⁺, PO₄³⁻, NO₃⁻, Br⁻, I⁻, Pb²⁺, Fe³⁺, Cd²⁺, Ni²⁺, Cu²⁺, Zn²⁺ and Co²⁺. Five infiltration tests were accomplished at five soil sites. Two pumping and one reanalyzed tests were carried out to determine the hydrogeological parameters of the Quaternary aquifer. The granulometric investigation was measured for 15 sub soils of five soil sites. The total dissolved solids (TDS) concentration of the Quaternary aquifer is increased in the northern part of the sub area A. It reflects the impact of seawater intrusion. In the sub area B, the TDS concentration is decreased towards the northern part, due to recharge from El Salam canal (fresh water). There is hydrogeological interconnection between El Salam canal and aquifer system in the northern Sinai. In sub area C, the TDS concentration is increased towards the northwestern part (Suez canal), caused by seawater intrusion from Suez Canal. The PO₄³⁻, NO₃ and most of the toxic metals (Pb²⁺, Fe³⁺, Mn²⁺, Cd²⁺, Ni²⁺, Cu²⁺, Zn²⁺ and Co²⁺) concentrations in groundwater were recorded in medium to high concentrations in sub areas (B and C). It attributes to leakage of septic tank, seepage from El

Salam canal, agricultural activity and geomechanics. The dendrogram investigation, principle component analysis and correlation study were discussed and interpreted according to geography, geology, hydrogeology and anthropogenic sources.

Keywords: Hydrogeology; Hydrogeochemistry; Modeling; Northern Sinai.

Dept. of Geophysics

422. Magnetic, Geo-Electric and Groundwater and Soil Quality Analysis Over A Landfill from A Lead Smelter, Cairo, Egypt

Mohamed H. Khalil

Journal of Applied Geophysics (J Appl Geophys) 86: 146-159 (2012) IF: 1.444

A detailed groundmagnetic survey, geoelectric vertical electric sounding (VES) and groundwater and soil quality analysis were conducted in the area of the abandoned landfill of the Awadallah lead (Pb) smelter, northeastern Cairo, Egypt. The integration between the applied techniques located successfully the buried solid waste, demarcated the groundwater and its possible contamination and determined the lead level in soil. Magnetic survey comprised 50 magnetic profiles each 190 m length. Vertical derivatives, wavelength filters, and continuation filters characterized the eastern and central parts of the landfill by high intense magnetic anomalies reflecting metal and lead wastes, whereas the western part was characterized by low intense anomalies indicating change in the landfill composition to non-magnetized material. The geoelectric survey comprised 16 VES with a maximum AB/2 of 100 m. The inverted data demarcated effectively the groundwater aquifer with depth ranged from 11 to 18 m and true resistivities ranged from 96 to 118 m. The second layer (Holocene-Q3) of semi-permeable silty and sandy clay cap (true resistivities 29–51 m and thickness 9–17 m) constituted a considerable role in limiting the possible contamination from the landfill. The analyzed groundwater parameters pH, Eh, TDS, SEC and DO indicated a good water quality with homogenous aquifer characteristics, whereas the lead concentration in groundwater (0.033–0.036 mg/L) was slightly exceeding the safe limits identified by the U.S. EPA (0.015 mg/L). Lead in soil samples revealed elevated concentrations (3130 mg/kg at VES-3) around the Awadallah smelter, whereas a gradual decrease in concentrations was recorded in the northwestern direction.

Keywords: Lead (Pb) Ground Magnetic VES Vertical Derivatives Wavelength Filters Continuation Filters.

423. An Approach for Velocity Determination from Merging Archie and Raymer–Hunt–Gardner Transform in Reservoir of Clean Nature

Karter H. Makar and Mostafa H. Kamel

Petroleum Science and Engineering, 86-87: 297-301 (2012)

IF: 0.869

This paper introduces an empirical equation to approximately quantify the P-wave velocity especially in the absence of many logs and core usually used instantaneously to evaluate such parameter. Further, using the proposed equation with the help of Poisson's ratio, the S-wave velocity can be easily evaluated. The

proposed equation is based mainly on merging the well-known Archie equation (1942) with the Raymer–Hunt–Gardner equation (1980). This equation takes into account the effects of both matrix and fluid transit times (t_{ma}, t_f - with known type of lithology; sandstone, limestone and/or dolomite) as well as the formation water resistivity (RW), resistivity of fully saturated (R0), formation factor coefficients in terms of tortuosity factor (a) and cementation exponent (m). Further mathematical treatment for finding the VP/VS ratio from Anderson et al. (1973) of Poisson's ratio, the S-wave velocity could then be estimated. Comparison is made and agreement within an error not exceeding ± 4 between predicted and actual values is reached. Successfulness of applying the proposed approach is restricted with the accuracy of finding RW and good selection of R0. Field examples from USA and the Gulf of Suez Basin of Egypt are illustrated to indicate the potentiality and validity of the suggested approach.

Keywords: Archie–Raymer Relationship; Compressional Velocity; Shear Velocity; Resistivity; Velocity Relationship; Quick; Look Approach.

424. An Enhancement of the Formation Factor Parameters 'A' and 'M'

Walid M. Mabrouk, Khalid S. Soliman and Mohamed A. Tawfic
Explor Geophys, 43(2): 87-94 (2012) IF: 0.634

The use of incorrect values of the formation constants a, tortuosity factor and m, cementation exponent, in Archie's water saturation equation, can result in the overlooking of potential producible zones. Usually, assumptions are made to approximate a and m where often m is 2, while a may be 0.81 or 1.0, depending on the type of lithology. When core is available, accepted laboratory practices exist to calculate a and m, however, these laboratory steps are generally not considered routine analysis and, in order to save time and money, may not be conducted. Core analysis for a and m require saturating to 100% multiple plugs of varying porosity with water of known resistivity. The resistivity of each water saturated core is graphed on a log-log graph with porosity to determine a and m. This work illustrates a simple method of calculating a and m that is dependent on sonic transit time and bulk density and on knowing one cementation exponent value from core measurements. The method is tested and applied on a large number of samples to ensure its ability to determine formation factor parameters a and m.

Keywords: Cementation Exponent; Formation Factor Parameters; Formation Resistivity Factor; Tortuosity.

425. Parametric Inversion of Residual Magnetic Anomalies Due to Simple Geometric Bodies

El-Sayed M. Abdelrahman, Eid R. Abo- Ezz and Khalid S. Essa
Explor Geophys, 43: 178-189 (2012) IF: 0.634

We have developed a simple method to determine the depth, inclination parameter and amplitude coefficient of a buried structure from a residual magnetic anomaly profile using a new formula representing the magnetic anomaly expressions produced by most geological structures. The method is based on defining the anomaly value at the origin and four characteristic points and their corresponding distances on the anomaly profile. Using all possible combinations of the four characteristic points and their

corresponding distances, a procedure is developed for automated determination of the best fit model parameters including the shape (shape factor) of the buried structure from magnetic data. The method was applied to synthetic data with and without random errors and tested on two field examples from Canada and India. In both cases, the model parameters obtained by the present method, particularly the shape and depth of the buried structures, were found to be in good agreement with the actual parameters. The present method has the capability of avoiding highly noisy data points and enforcing the incorporation of points of the least random errors to enhance the interpretation results.

Keywords: Interpretation; Magnetic Data; New Formula; Noise; Numerical Methods.

426. A Fast Interpretation method for Inverse modeling of Residual Gravity Anomalies Caused by Simple Geometry

Khalid S. Essa

Journal of Geological Research, 2012: 1-10 (2012)

An inversion technique using a fast method is developed to estimate, successively, the depth, the shape factor and the amplitude coefficient of a buried structure using residual gravity anomalies. By defining the anomaly value at the origin and the anomaly value at different points on the profile, the problem of depth estimation is transformed into a problem of solving a nonlinear equation of the form $f(z) = 0$. Knowing the depth, the shape factor can be estimated and finally the amplitude coefficient can be estimated. This technique is applicable for a class of geometrically simple anomalous bodies, including the semi-infinite vertical cylinder, the infinitely long horizontal cylinder and the sphere. The efficiency of this technique is demonstrated with gravity anomaly due to a theoretical model, in each case with and without random errors. Finally, the applicability is illustrated using the residual gravity anomaly of Mobrun ore body, situated near Noranda, QC, Canada. The interpreted depth and the other model parameters are in good agreement with the known actual values.

Keywords: A Fast Interpretation Method; Residual Gravity Anomalies; The Depth; The Other Model Parameters.

Dept. of Geophysics

427. New Techniques for Potential Field Data Interpretation

Khalid S. Essa

New Achievements in Geoscience, Intech, chapter 2, 21-44 (2012)

We have developed a least-squares minimization approach to depth determination from residual magnetic anomaly. The problem of depth determination from magnetic data has been transformed into finding a solution to a nonlinear equation of the form $f(z)=0$. Formulas have been derived for a sphere, horizontal cylinder, dike and for a geologic contact. The advantages of the present method over previous techniques, which use only a few points, distances, standardized curves and nomograms are: (1) all observed values can be used, (2) the method is semi-automatic and (3) the method is not sensitive to errors in the magnetic anomaly. Finally, the advantage of the proposed method over previous least-squares techniques is that any initial guess for the

depth parameter works well.-Also, another least-squares approach has been developed to determine, successively, the depth, index parameter and amplitude coefficient of a buried thin dyke using moving average residual anomalies obtained from magnetic data using filters of successive graticule spacings.

The problem of depth determination is transformed into the problem of solving a nonlinear equation, $f(z) = 0$. Knowing the depth and applying the least-squares method, the index parameter is determined by solving a nonlinear equation of the form $f(z) = 0$. Finally, knowing the depth and the index parameter, the amplitude coefficient is determined in a least-squares sense using a simple linear equation. In this way, the depth, index parameter and amplitude coefficient are determined individually from all observed magnetic data.

The method is applied to synthetic data with random errors, complicated regionals and interference from neighboring magnetic rocks and tested on two field examples from Brazil and Canada. Finally, the window curves method has been developed to determine simultaneously the shape and depth of a buried structure from the third moving average residual gravity anomalies.

The method involves using simple models convolved with the same third moving average regional filter as applied to the observed gravity data. As a result, his method can be applied not only to residuals but also to measured gravity data. The method is applied to theoretical data with and without random errors and tested on a known field example from the U.S.A. In all cases, the shape and depth solutions obtained are in good agreement with the actual ones.

Keywords: the least-squares approach; the depth; index parameter; and amplitude coefficient; the window curves method.

Dept. of Mathematics

428. Higgs Mass Corrections in the Susy B L Model with Inverse Seesaw

A. Elsayed , S. Khalil and S. Moretti

Phys Lett B, 715: 208-213 (2012) IF: 3.955

In the context of the Supersymmetric (SUSY) B L (Baryon minus Lepton number) model with inverse seesaw mechanism, we calculate the one-loop radiative corrections due to right-handed (s)neutrinos to the mass of the lightest Higgs boson when the latter is Standard Model (SM)-like. We show that such effects can be as large as $O(100)$ GeV, thereby giving an absolute upper limit on such a mass around 180 GeV.

The importance of this result from a phenomenological point of view is twofold. On the one hand, this enhancement greatly reconciles theory and experiment, by alleviating the so-called 'little hierarchy problem' of the minimal SUSY realization, whereby the current experimental limit on the SM-like Higgs mass is very near its absolute upper limit predicted theoretically, of 130 GeV.

On the other hand, a SM-like Higgs boson with mass below 180 GeV is still well within the reach of the Large Hadron Collider (LHC), so that the SUSY realization discussed here is just as testable as the minimal version.

Keywords: Particle Physics; Supersymmetry; Higgs Mass Correction; U(1)B-L; Right; Handed Neutrino.

429. Muon Anomalous Magnetic Moment and E in B L Model with Inverse Seesaw

Mohamed S. Hanafy, Amira F.Y. El-Kady and Doaa A.H. Korym

Eur Phys J C, 8 (5):: 485-505 (2012) IF: 3.631

We study the anomalous magnetic moment of the muon, a_μ and lepton flavor violating decay e in TeV scale B L extension of the Standard Model (SM) within inverse seesaw mechanism. We show that the B L contributions to a_μ are severely constrained; therefore, the SM contribution remains intact. We also emphasize that the current experimental limit of $BR(e \rightarrow \mu \gamma)$ can be satisfied for a wide range of parameter space and it can be within the reach of MEG experiment.

Keywords: Muon Anomalous Magnetic Moment; Lepton Flavor Violation; Inverse Seesaw.

430. On Shifted Jacobi Spectral Method for High-Order Multi-Point Boundary Value Problems

E.H. Doha , A.H. Bhrawy and R.M. Hafez

Commun Nonlinear Sci, 17: 3802-3810 (2012) IF: 2.806

This paper reports a spectral tau method for numerically solving multi-point boundary value problems (BVPs) of linear high-order ordinary differential equations. The construction of the shifted Jacobi tau approximation is based on conventional differentiation. This use of differentiation allows the imposition of the governing equation at the whole set of grid points and the straight forward implementation of multiple boundary conditions. Extension of the tau method for high-order multi-point BVPs with variable coefficients is treated using the shifted Jacobi Gauss-Lobatto quadrature. Shifted Jacobi collocation method is developed for solving nonlinear high-order multi-point BVPs. The performance of the proposed methods is investigated by considering several examples. Accurate results and high convergence rates are achieved.

Keywords: Multi-Point Boundary Value Problem; High-Order Differential Equation; Nonlinear Boundary Value Problems; Tau Method; Collocation Method.

431. An Efficient Direct Solver for Multidimensional Elliptic Robin Boundary Value Problems using A Legendre Spectral-Galerkin Method

E.H. Dohaa and A.H. Bhrawy

Comput Math Appl, 64: 558-571 (2012) IF: 1.747

In this paper, a Legendre-Galerkin method for solving second-order elliptic differential equations subject to the most general nonhomogeneous Robin boundary conditions is presented. The homogeneous Robin boundary conditions are satisfied exactly by expanding the unknown variable using a polynomial basis of functions which are built upon the Legendre polynomials. The direct solution algorithm here developed for the homogeneous Robin problem in two-dimensions relies upon a tensor product process. Nonhomogeneous Robin data are taken into account by means of a lifting. Such a lifting is performed in two successive steps, the first one to account for the data specified at the corners and the second one to account for the boundary values prescribed in the interior of the sides. Numerical results

indicating the high accuracy and effectiveness of these algorithms are presented.

Keywords: Spectral-Galerkin Method; Helmholtz Equations; Nonhomogeneous Robin Conditions; Tensor Product; Direct Solution Method; Fast Spectral Solver.

432. Benjamin–Feir Instability in Nonlinear Dispersive Waves

M.A. Helal and A.R. Seadawy

Comput Math Appl, 64 (2012): 3557-3568 (2012) IF: 1.747

In this paper, the authors extended the derivation to the nonlinear Schrödinger equation in two-dimensions, modified by the effect of non-uniformity.

The authors derived several classes of soliton solutions in 2 + 1 dimensions. When the solution is assumed to depend on space and time only through a single argument of the function, they showed that the two-dimensional nonlinear Schrödinger equation is reduced either to the sine-Gordon for the hyperbolic case or sinh-Gordon equations for the elliptic case.

Moreover, the authors extended this method to obtain analytical solutions to the nonlinear Schrödinger equation in two space dimensions plus time.

This contains some interesting solutions such as the plane solitons, the N multiple solitons, the propagating breathers and quadratic solitons. The authors displayed graphically the obtained solutions by using the software Mathematica 5.

Keywords: BenjaminFeirInstability; Nonlinear Dispersive; Waves Soliton Solutions.

433. A New Jacobi Operational Matrix: an Application for Solving Fractional Differential Equations

E.H. Doha, A.H. Bhrawy and S.S. Ezz-Eldien

Appl Math Model, 36: 4931-4943 (2012) IF: 1.579

In this paper, we derived the shifted Jacobi operational matrix (JOM) of fractional derivatives which is applied together with spectral tau method for numerical solution of general linear multi-term fractional differential equations (FDEs).

A new approach implementing shifted Jacobi operational matrix in combination with the shifted Jacobi collocation technique is introduced for the numerical solution of nonlinear multi-term FDEs.

The main characteristic behind this approach is that it reduces such problems to those of solving a system of algebraic equations which greatly simplifies the problem.

The proposed methods are applied for solving linear and nonlinear multi-term FDEs subject to initial or boundary conditions and the exact solutions are obtained for some tested problems. Special attention is given to the comparison of the numerical results obtained by the new algorithm with those found by other known methods.

Keywords: Multi-Term Fractional Differential Equations; Nonlinear Fractional Differential Equations; Operational Matrix; Jacobi Polynomials; Spectral Method.

434. Towards A Unified Method for Exact Solutions of Evolution Equations an Application to Reaction Diffusion Equations with Finite Memory Transport

H.I. Abdel-Gawad

Journal of Statistical Physics, 147: 506-518 (2012) IF: 1.397

We present a brief report on the different methods for finding exact solutions of nonlinear evolution equations. Explicit exact traveling wave solutions are the most amenable besides implicit and parametric ones. It is shown that most of methods that exist in the literature are equivalent to the “generalized mapping method” that unifies them. By using this method a class of formal exact solutions for reaction diffusion equations with finite memory transport is obtained. Attention is focused to the finite-memory-transport-Fisher and Nagumo equations.

Keywords: Exact Solutions; Unified Method; Reaction Diffusion Equation; Finite Memory Transport.

435. Efficient Solutions of Multidimensional Sixth-Order Boundary Value Problems using Symmetric Generalized Jacobi-Galerkin Method

E. H. Doha and W. M. Abd-Elhameed

Abstract and Applied Analysis, 1-19 (2012) IF: 1.318

This paper presents some efficient spectral algorithms for solving linear sixth-order two-point boundary value problems in one dimension based on the application of the Galerkin method. The proposed algorithms are extended to solve the two-dimensional sixth-order differential equations. A family of symmetric generalized Jacobi polynomials is introduced and used as basic functions. The algorithms lead to linear systems with specially structured matrices that can be efficiently inverted. The various matrix systems resulting from the proposed algorithms are carefully investigated, especially their condition numbers and their complexities. These algorithms are extensions to some of the algorithms proposed by Doha and Abd-Elhameed 2002 and Doha and Bhrawy 2008 for second- and fourth-order elliptic equations, respectively. Three numerical results are presented to demonstrate the efficiency and the applicability of the proposed algorithms.

Keywords: Sixth; Order Boundary Value Problems; Jacobi Polynomials.

436. Efficient Spectral-Petrov–Galerkin Methods for the Integrated forms of Third- and Fifth-Order Elliptic Differential Equations using General Parameters Generalized Jacobi Polynomials

E.H. Doha, W.M. Abd-Elhameed and Y.H. Youssri

Appl Math Comput, 218: 7727-7740 (2012) IF: 1.317

This article analyzes some algorithms for solving numerically the integrated forms of third and fifth-order differential equations in one variable subject to homogeneous and nonhomogeneous boundary conditions using a dual Petrov–Galerkin method. Two new families of general parameters generalized Jacobi polynomials are introduced and used for this purpose. Numerical results indicating the high accuracy and effectiveness of the proposed algorithms are presented.

Keywords: Dual; Petrov; Galerkin Method; Generalized Jacobi Polynomials; Nonhomogeneous Dirichlet Conditions; Integrated Forms.

437. Numerical Studies for Fractional-Order Logistic Differential Equation with Two Different Delays

N. H. Sweilam, M. M. Khader and A. M. S. Mahdy

J Appl Math, 2012: 1-14 (2012) IF: 0.656

A numerical method for solving the fractional-order logistic differential equation with two different delays FOLE is considered. The fractional derivative is described in the Caputo sense. The proposed method is based upon Chebyshev approximations.

The properties of Chebyshev polynomials are utilized to reduce FOLE to a system of algebraic equations. Special attention is given to study the convergence and the error estimate of the presented method.

Numerical illustrations are presented to demonstrate utility of the proposed method. Chaotic behavior is observed and the smallest fractional order for the chaotic behavior is obtained.

Also, FOLE is studied using variational iteration method VIM and the fractional complex transform is introduced to convert fractional Logistic equation to its differential partner, so that its variational iteration algorithm can be simply constructed. Numerical experiment is presented to illustrate the validity and the great potential of both proposed techniques.

Keywords: Fractional-Order Logistic Differential Equation With Two Different Delays; The Caputo Fractional Derivative; Chebyshev Polynomials.

438. On C-Supplemented Subgroups of Finite Groups

Mohamed Asaad

Journal of Algebra, 362: 1-11 (2012) IF: 0.613

Let G be a finite group. A subgroup H of G is said to be C -supplemented in G if there exists a subgroup K of G such that $G = HK$ and $H \cap K = H \cap G$, where $H \cap G = \langle g \in G \mid g \in H \rangle$ is the largest normal subgroup of G contained in H . We investigate the structure of G under the assumption that some families of subgroups of G are C -supplemented in G .

Keywords: Complemented Subgroup; C -Supplemented Subgroup; Solvable Groups; Supersolvable Groups; Saturated Formations.

439. Some Solubility Criteria in Factorised Groups

M. Asaad, A. Ballester Bolinches and R. Esteban-Romero

B Aust Math Soc, 86: 22-28 (2012) IF: 0.545

In this paper, solubility of groups factorised as a product of two subgroups which are connected by certain permutability properties is studied.

Keywords: Factorised Group; Mutually M -Permutable Product; Soluble Group.

440. Finite Groups Whose Minimal Subgroups are Weakly H-Subgroups

M. M. Al-Mosa Al-Shomrani

Acta Mathematica Scientia, (6): 2295-2310 (2012) IF: 0.357

Let G be a finite group. A subgroup H of G is called an H -subgroup in G if $Ng(H)Hg \subseteq H$ for all $g \in G$. A subgroup H of G is called a weakly H -subgroup in G if there exists a normal subgroup K of G such that $G = HK$ and HK is an H -subgroup in G . In this paper, we investigate the structure of the finite group G under the assumption that every subgroup of G of prime order or of order 4 is a weakly H -subgroup in G . Our results improve and generalize several recent results in the literature.

Keywords: C -Normal Subgroup; H -Subgroup; P -Nilpotent Group; Supersolvable Group.

441. on Weakly π -Subgroups of Finite Groups

M. Asaad, A. A. Heliel and M. M. Al-Mosa Al-Shomrani

Communication Algebra, 40: 3540-3550 (2012) IF: 0.347

Let G be a finite group. A subgroup H of G is called an π -subgroup in G if $N_G(H) = H \times H$ for all $x \in G$. A subgroup H of G is called weakly π -subgroup in G if there exists a normal subgroup K of G such that $G = HK$ and $H \cap K$ is an π -subgroup in G . In this article, we investigate the structure of the finite group G under the assumption that all maximal subgroups of every Sylow subgroup of some normal subgroup of G are weakly π -subgroups in G . Some recent results are extended and generalized.

Keywords: Fitting Subgroup; Generalized Fitting Subgroup; P -Nilpotent Group; C -Normal Subgroup; Saturated Formation; Subgroup; Supersolvable Group; Sylow Subgroup.

442. Quantum Entanglement Probability from Golden Mean Renormalization Semi Groups

M, A. Helall and M.S. EI faschie

Fract. Spacetime Noncommut. Geom. Quant. High Energ. Phys., 2: 34-40 (2012)

We derive Hardy's quantum entanglement probability using the golden mean renormalisations group method in the modified form of coarse graining on two dimensional Lattice with four point blocks. We draw a constructive analogy between the orthodox quantum mechanical solution of the problem and the suggested renormalisation procedure as well as two further solutions. The first solution is based on classical probability theory and the second on purely geometrical-topological considerations. The general conclusion gained from all of the results so obtained is that Hardy's probability $y = \Phi^5$, where Φ involves the golden mean because it is the Hausdorff dimension of a random Cantor set which is at the root of quantum mechanics. On the other hand entanglement is the natural outcome of a zero measure random Cantor set. In other words the limit set of the topology of orthodox quantum mechanics is a Cantorian geometry with a zero length for which the classical common sense notion of spatial separation is meaningless. Consequently quantum mechanics is a complete description of physical reality and only lacks a geometrical-topological interpretation along the lines of the present work.

Keywords: Quantum; Entanglement; Golden Mean; Hardy's Probability; Cantor Set.

443. Heap Slicing using Type Systems

Mohamed A. El-Zawawy

Lecture Notes In Computer Science, : 592-606 (2012)

Using type systems, this paper treats heap slicing which is a technique transforming a program into a new one that produces the same result while working on a heap sliced into independent regions. Heap slicing is a common approach to handle the problem of modifying the heap layout without changing the program semantics. Heap slicing has applications in the areas of performance optimization and security.

Towards solving the problem of heap slicing, this paper introduces three type systems. The first type system does a pointer analysis and annotates program points with pointer information. This type system is an augmentation of a previously developed type system by the author.

The second type system does a region analysis and refines the result of the first type system by augmenting the pointer information with region information. The region information approximately specifies at each program point for each memory cell the region where the cell exists. The third type system uses the information gathered by the region type system to do the principal transformation of heap slicing.

The paper also presents two operational semantics; one for single-region heap scenario and the other for multi-regions heap scenario. These semantics are used to prove the soundness of the type systems.

Keywords: Heap Slicing; Type Systems; Semantics of Programming Languages; Operational Semantics; Region Analysis; Pointer Analysis.

444. Numerical Studies for Solving Fractional-Order Logistic Equation

N.H. Sweilam, M.M. Khader and A.M.S. Mahdy

International Journal of Pure And Applied Mathematics, 78 (8): 1200-1210 (2012)

In this paper, finite difference method (FDM) and variational iteration method (VIM) have been successfully implemented for solving nonlinear fractional-order Logistic equation (FOLE). We have applied the concepts of fractional calculus to the well known population growth model in chaotic dynamic.

The fractional derivative is described in the Caputo sense. The result is generalized of the classical population growth model to arbitrary order.

The resulted non-linear system of algebraic equations using FDM is solved with the well known Newton iteration method. Where the condition of convergence is verified. Using initial value, the explicit solutions of population size for different particular cases have been derived. Numerical results show that the proposed methods are extremely efficient to solve this complicated biological model.

Keywords: Fractional-Order Logistic Equation; Caputo Derivative; Finite Difference Method; Variational Iteration Method.

445. On the Numerical Solution for the Linear Fractional Klien-Gordon Equation using Legendre Pseudospectral Method

N. H. Sweilam, M. M. Khader and A. M. S. Mahdy

International Journal of Mathematics and Computer Applications Research, 2, 4: 1-10 (2012)

Fractional differential equations have recently been applied in various areas of engineering, science, finance, applied mathematics, bio-engineering and others. However, many researchers remain unaware of this field. In this paper, an efficient numerical method for solving the linear fractional Klien-Gordon equation is considered. The fractional derivative is described in the Caputo sense. The method is based on Legendre approximations. The properties of Legendre polynomials are utilized to reduce the proposed problem to a system of ordinary differential equations, which solved using the finite difference method. Numerical solutions are presented and the results are compared with the exact solution.

Keywords: Fractional Klien; Gordon Equation; Caputo Fractional Derivative; Finite Difference Method; Legendre Polynomials.

446. Exact Solution for Some Nonlinear Reaction Diffusion Equations

Nasser S. Elazab

Ijbas/Ijens, 12 No:06: 96-98 (2012)

In this paper we present a generalized method to obtain exact solutions of nonlinear partial differential equations. As a particular case, we obtain exact solutions for reaction diffusion equation. A new class of multiple-soliton or wave trains obtained.

Keywords: Exact Solution; Reaction Diffusion Equations.

447. Exact Solutions of Burgers Equation with Space Dependent Coefficients by the Extended Unified Method

Nasser S. Elazab

Ijbas/Ijens, 12 (06) : 91-95 (2012)

A brief report on the different methods for finding exact traveling wave solutions of nonlinear evolution equations is presented. In a very recent work it had been shown that most of methods that exist in the literature are equivalent to the "generalized mapping method" that unifies them. This method is extended here to find a class of formal exact solutions to Burgers equation with space-dependent coefficients.

Keywords: Exact Solutions; Extended Unified Method; Burgers Equation; Variable Coefficients.

448. Dynamic Verification for File Safety of Multithreaded Programs

Mohamed A. El-Zawawy and Nagwan M. Daoud

Int. J. of Computer Science and Network Security, 12(5):14-20 (2012)

In this paper, we present a new semantics to check file safety of multithreaded programs. A file-safe program is one that

reaches a final configuration under the proposed semantics. We extend the While language with file operations and multi-threading commands and call the new language whilef.

This paper shows that the file safety is an undecidable property for whilef. The file safety becomes a decidable property in a special case shown in this paper.

The case happens when users provide pointer information. If the file is safe we call it a strongly safe file program. We modify the syntax and the semantics of the language and call it SafeWhilef.

Keywords: File Safety; Operational Semantics; Rewriting Logic; Multithreaded Programs.

449. New Error-Recovery Techniques for Faulty-Calls of Functions

Mohamed A. El-Zawawy and Nagwan M. Daoud

Computer And Information Science, 5, (3);: 67-75 (2012)

In this paper, we introduce type systems to detect faulty calls of functions in a program. The intended meaning of the faulty call is calling a function with a mismatch to the number of its arguments.

We use error-detecting semantics that when detects the faulty calls, doesn't proceed to the next state. Type systems are used in the process of analysis and in repairing. The paper presents two type systems: the safety type system which checks the safety of a given program and the repairing type system which corrects errors.

The repairing process is made by replacing the faulty call of function with a correct one. In the repairing process simple interactive input/output statements are used. The interaction (input/output) helps to get the lost parameters by interacting with the user; informing him about the number of lost parameters. The user can then input these parameters.

Keywords: Type Systems; Semantics of Programming Languages; Faulty Function Calls.

450. Type Systems Based Data Race Detector

Mohamed A. El-Zawawy and Hamada A. Nayel

Computer And Information Science, 5, (4) (2012)

Multi-threading is a methodology that has been extremely used. Modern software depends essentially on multi-threading. Operating systems, famous examples, are based on multi-threading; a user can write his document, play an audio file and downloading a file from internet at the same time. Each of these tasks called a thread.

A common problem occurs when implementing multi-threaded programs is a data-race. Data race occurs when two threads try to access a shared variable at the same time without a proper synchronization. A detector is software that determines if the program contains a data-race problem or not.

In this paper, we develop a detector that has the form of a type system. We present a type system which discovers the data-race problems. We also prove the soundness of our type system.

Keywords: Multi; Threaded Programs; Type Systems; Data-Race; Semantics of Programming Languages.

451. Abstraction Analysis and Certified Flow and Context Sensitive Points-to Relation for Distributed Programs

Mohamed A. El-Zawawy

Lecture Notes In Computer Science, 83-99 (2012)

This paper presents a new technique for pointer analysis of distributed programs executed on parallel machines with hierarchical memories. One motivation for this research is the languages whose global address space is partitioned. Examples of these languages are Fortress, X10, Titanium, Co-Array Fortran, UPC and Chapel.

These languages allow programmers to adjust threads and data layout and to write to and read from memories of other threads. The techniques presented in this paper have the form of type systems which are simply structured.

The proposed technique is shown on a language which is the while language enriched with basic commands for pointer manipulations and also enriched with commands vital for distributed execution of programs. An abstraction analysis that for a given statement calculates the set of function abstractions that the statement may evaluate to is introduced in this paper.

The abstraction analysis is needed in the proposed pointer analysis. The mathematical soundness of all techniques presented in this paper are discussed. The soundness is proved against a new operational semantics presented in this paper. Our work has two advantages over related work.

In our technique, each analysis result is associated with a correctness proof in the form of type derivation. The hierarchical memory model used in this paper is inline with the hierarchical character of concurrent parallel computers.

Keywords: Abstraction Analysis; Certified Code; Flow And Context Sensitive Points-To Relation; Distributed Programs; Semantics Of Programming Languages; Operational Semantics.

452. An Efficient Class of Fdm Based on Hermite formula for Solving

N. H. Sweilam, M. M. Khader and M. Adel

International Journal of Mathematics And Computer Applications Research (IjmcAR), (2012)

In this article, a numerical study is introduced for the fractional reaction-subdiffusion equations by using an efficient class of finite difference methods. The proposed scheme is based on Hermite formula.

The stability analysis and the convergence of the proposed methods are given by a recently proposed procedure similar to the standard John von Neumann stability analysis. Simple and accurate stability criterion valid for different discretization schemes of the fractional derivative, arbitrary weight factor and arbitrary order of the fractional derivative, are given and checked numerically. Finally, numerical examples are carried out to confirm the theoretical results.

Keywords: Finite Difference Methods; Hermite Formula; Fractional Reaction; Subdiffusion equation; Stability and convergence analysis.

453. On the Stability Analysis of Weighted Average Finite Difference Methods for Fractional Wave Equation

N. H. Sweilam, M.M. Khader and M. Adel

Fractional Differential Calculus, 2, 1: 17-29 (2012)

In this article, a numerical study for the fractional wave equations is introduced by using a class of finite difference methods. These methods are extension of the weighted average methods for ordinary (non-fractional) wave equations. The stability analysis of the proposed methods is given by a recently proposed procedure similar to the standard John von Neumann stability analysis. Simple and accurate stability criterion valid for different discretization schemes of the fractional derivative, arbitrary weight factor and arbitrary order of the fractional derivative, is given and checked numerically. Numerical test example and comparisons have been presented for clarity.

Keywords: Weighted Average Finite Difference; Approximations; Fractional Order Wave Equation; Stability Analysis.

454. Crank-Nicolson Finite Difference Method for Solving Time-Fractional Diffusion Equation

N. H. Sweilam, M. M. Khader and A. M. S. Mahdy

Journal of Fractional Calculus and Applications, 2, (2): 1-9 (2012)

In this paper, we develop the Crank-Nicolson finite difference method (C-N-FDM) to solve the linear time-fractional diffusion equation, formulated with Caputo's fractional derivative. Special attention is given to study the stability of the proposed method which is introduced by means of a recently proposed procedure akin to the standard Von-Neumann stability analysis. Some numerical examples are presented and the behavior of the solution is examined to verify stability of the proposed method. It is found that the C-N-FDM is applicable, simple and efficient for such problems.

Keywords: Crank-Nicolson Finite Difference Method; Time-Fractional Diffusion Equation; Von-Neumann Stability Analysis.

455. Computational Methods for Fractional Differential Equations Generated by Optimization Problem

N. H. Sweilam, M. M. Khader and A. M. S. Mahdy

J. of Fractional Calculus and Applications, 3(S): 1-12 (2012)

In this paper, numerical studies for fractional differential equations (FDEs) which are generated by optimization problem are studied using the pseudo-spectral method based upon Legendre approximations and fractional finite difference method (FDM). The fractional derivatives are presented in terms of Caputo sense. The application of the proposed methods to the generated system of FDEs leads to algebraic system which can be solved by the Newton iteration method. The methods introduce promising tool for solving many systems of the non-linear fractional differential equations. Two numerical examples are provided to confirm the accuracy and the effectiveness of the proposed methods. A comparison with the fourth order Runge-Kutta (RK4) is given.

Keywords: Nonlinear Programming; Penalty Function; Dynamic System; Caputo Fractional Derivatives; Legendre Polynomials; Finite Difference; Rung; Kutta Method.

456. Numerical Studies for Solving Fractional Riccati Differential Equation

N. H. Sweilam, M. M. Khader and A. M. S. Mahdy

Applications and Applied Mathematics: an International Journal, 7, (2): 595-608 (2012)

In this paper, finite difference method (FDM) and Pade'-variational iteration method (Pade'-VIM) are successfully implemented for solving the nonlinear fractional Riccati differential equation. The fractional derivative is described in the Caputo sense. The existence and the uniqueness of the proposed problem are given. The resulting nonlinear system of algebraic equations from FDM is solved by using Newton iteration method; moreover the condition of convergence is verified. The convergence's domain of the solution is improved and enlarged by Pade'-VIM technique. The results obtained by using FDM is compared with Pade'-VIM. It should be noted that the Pade'-VIM is preferable because it always converges to the solution even for large domain.

Keywords: Fractional Riccati Differential Equation; Caputo Fractional Derivative; Finite Difference Method; Variational Iteration Method; Pade' Approximation.

457. On the Numerical Solution of Hammerstein Integral Equations using Legendre Approximation

N. H. Sweilam, M. M. Khader and W. Y. Kota

Int. J. of Applied Mathematical Research, 1 (1): 65-76 (2012)

In this study, Legendre collocation method is presented to solve numerically the Fredholm-Hammerstein integral equations. This method is based on replacement of the unknown function by truncated series of well known Legendre expansion of functions. The proposed method converts the equation to matrix equation, by means of collocation points on the interval $[1; 1]$ which corresponding to system of algebraic equations with Legendre coefficients. Thus, by solving the matrix equation, Legendre coefficients are obtained. Some numerical examples are included to demonstrate the validity and applicability of the proposed technique.

Keywords: Fredholm-Hammerstein Integral Equations; Integral Equation; Legendre Collocation Matrix Method; Legendre Polynomials; Volterra Integral Equation.

458. Numerical Studies for the Variable-Order Nonlinear Fractional Wave Equation

N. H. Sweilam, M. M. Khader and H. M. Almarwm

Fractional Calculus & Applied Analysis, 15(4): 669-683 (2012)

In this paper, the explicit finite difference method (FDM) is used to study the variable order nonlinear fractional wave equation. The fractional derivative is described in the Riesz sense. Special attention is given to study the stability analysis and the convergence of the proposed method. Numerical test examples are presented to show the efficiency of the proposed numerical scheme.

Keywords: Variable Order Fractional Calculus; Nonlinear Fractional Wave Equation; Explicit Finite Difference Method; Convergence and Stability Analysis.

459. Hahn Difference Operator and Associated Jackson Norlund Integrals

M.H. Annaby, A.E. Hamza and K.A. Aldwoah

J. Optimiz Theory App, (2012) IF: 1.062

This paper is devoted for a rigorous investigation of Hahn's difference operator and the associated calculus. Hahn's difference operator generalizes both of the difference operator and Jackson's q -difference operator. Unlike these two operators, the calculus associated with Hahn's difference operator receives no attention. In particular, its right inverse has not been constructed before. We aim to establish a calculus of differences based on Hahn's difference operator. We construct a right inverse of Hahn's operator and study some of its properties.

Keywords: Hahn's Operator; Difference Equations; Q -Difference Equations; Norlund Sums; Jackson Q -Integral.

460. Stability of Abstract Dynamic Equations on Time Scales

Alaa E Hamza and Karima M Oraby

Advances In Difference Equations, 143: 1-15 (2012) IF: 0.845

In this paper, we investigate many types of stability, like uniform stability, asymptotic stability, uniform asymptotic stability, global stability, global asymptotic stability, exponential stability, uniform exponential stability, of the homogeneous first-order linear dynamic equations of the form $x(t) = Ax(t), t \geq t_0, x(t_0) = x_0$, where A is the generator of a C_0 -semigroup $\{T(t); t \geq 0\}$ on X , the space of all bounded linear operators from a Banach space X into itself. Here, \mathbb{T} is a time scale which is an additive semigroup with the property that $ab \in \mathbb{T}$ for any $a, b \in \mathbb{T}$ such that $a > b$. Finally, we give an illustrative example for a nonregressive homogeneous first-order linear dynamic equation and we investigate its stability.

Keywords: Stability; Semi-Groups of Operators; Dynamic Equations.

Dept. of Physics

461. A New Boson with A Mass of 125 Gev Observed with the Cms Experiment at the Large Hadron Collider

The CMS collaboration

Science, 338: 1569-1575 (2012) IF: 31.2

The Higgs boson was postulated nearly five decades ago within the framework of the standard model of particle physics and has been the subject of numerous searches at accelerators around the world. Its discovery would verify the existence of a complex scalar field thought to give mass to three of the carriers of the electroweak force—the W^+ , W^- and Z^0 bosons—as well as to the fundamental quarks and leptons. The CMS Collaboration has observed, with a statistical significance of five standard deviations, a new particle produced in proton-proton collisions at the Large Hadron Collider at CERN. The evidence is strongest in

the diphoton and four-lepton (electrons and/or muons) final states, which provide the best mass resolution in the CMS detector. The probability of the observed signal being due to a random fluctuation of the background is about 1 in 3×10^6 .

The new particle is a boson with spin not equal to 1 and has a mass of about 125 giga-electron volts. Although its measured properties are, within the uncertainties of the present data, consistent with those expected of the Higgs boson, more data are needed to elucidate the precise nature of the new particle.

Keywords: Higgs Bosons; Large Hadron Collider.

462. Search for Signatures of Extra Dimensions in the Diphoton Mass Spectrum at the Large Hadron Collider

S. Chatrchyan et al

Physical Review Letter, 108: 111801-111816 (2012) IF: 7.37

A search for signatures of extra spatial dimensions in the diphoton invariant-mass spectrum has been performed with the CMS detector at the LHC. No excess of events above the standard model expectation is observed using a data sample collected in proton-proton collisions at $\sqrt{s} = 7$ TeV corresponding to an integrated luminosity of 2.2 fb^{-1} . In the context of the large-extra-dimensions model, lower limits are set on the effective Planck scale in the range of 2.3–3.8 TeV at the 95% confidence level. These limits are the most restrictive bounds on virtual-graviton exchange to date. The most restrictive lower limits to date are also set on the mass of the first graviton excitation in the Randall-Sundrum model in the range of 0.86–1.84 TeV, for values of the associated coupling parameter between 0.01 and 0.10.

Keywords: Extra Dimension; Diphoton; Large Hadron Collider.

463. Search for the Standard Model Higgs Boson in the Decay Channel $H \rightarrow ZZ \rightarrow 4\ell$ in pp Collisions at $\sqrt{s} = 7$ TeV

S. Chatrchyan et al

Physical Review Letter, 108: 111804-111804 (2012) IF: 7.013

A search for a Higgs boson in the four-lepton decay channel $H \rightarrow ZZ$, with each Z boson decaying to an electron or muon pair, is reported. The search covers Higgs boson mass hypotheses in the range of $110 < m_H < 600$ GeV. The analysis uses data corresponding to an integrated luminosity of 4.7 fb^{-1} recorded by the CMS detector in pp collisions at $\sqrt{s} = 7$ TeV from the LHC. Seventy-two events are observed with four-lepton invariant mass $m_{4\ell} > 100$ GeV (with 13 below 160 GeV), while 67.1 ± 6.0 (9.5 ± 1.3) events are expected from background.

The four-lepton mass distribution is consistent with the expectation of standard model background production of ZZ pairs. Upper limits at 95% confidence level exclude the standard model Higgs boson in the ranges of 134–158 GeV, 180–305 GeV and 340–465 GeV. Small excesses of events are observed around masses of 119, 126 and 320 GeV, making the observed limits weaker than expected in the absence of a signal.

Keywords: Higgs Bosons Decay; 4 Leptons; Large Hadron Collider.

464. Magnetic Characterization of Nickel-Rich NiFe Nanowires Grown by Pulsed Electrodeposition

Mohamed Shaker Salem, Philip Sergelius, Robert Zierold, Josep M. Montero Moreno and Detlef Görlich and Kornelius Nielsch

J. Mater. Chem., (2012) IF: 5.968

Nickel-rich NiFe nanowires with well-controlled diameters and compositions are fabricated in various porous alumina templates by using a pulsed electrochemical deposition technique. The average pore diameter of the templates is tuned either by coating the pore walls with thin silica layers using an atomic layer deposition (ALD) technique or by applying a chemical pore widening process. The composition of the alloy is controlled by varying the frequency of the deposition pulse. The coercivity of the nanowire array is influenced by its texture and the amount of iron content in the alloy. The effective field and the saturation magnetization are found to be reinforced with the decrease in Ni content. A distinct enhancement of the axial coercivity and squareness of permalloy, Ni₈₀Fe₂₀, nanowire array are obtained by decreasing the average nanowire diameter. The processes of magnetization reversal in Ni₈₀Fe₂₀ nanowire array are investigated. The temperature dependence of Ni₈₀Fe₂₀ nanowire coercivity is interpreted in accordance with magnetization fluctuation over a single energy barrier.

Keywords: Magnetic Nanowires; Porous Alumina; Magnetization Reversal.

465. Exclusive $\gamma\gamma \rightarrow \mu^+\mu^-$ Production in Proton-Proton Collisions at $\sqrt{s} = 7$ TeV

The CMS collaboration

Journal Of High Energy Physics, : 1-38 (2012) IF: 5.83

A measurement of the exclusive two-photon production of muon pairs in proton-proton collisions at $\sqrt{s} = 7$ TeV, $pp \rightarrow p + p + \mu^+ \mu^-$ is reported using data corresponding to an integrated luminosity of 40 pb⁻¹. For muon pairs with invariant mass greater than 11.5 GeV, transverse momentum $p_T > 4$ GeV and pseudorapidity $|\eta| < 2.1$, a fit to the dimuon $p_T^{(\pm)}$ distribution results in a measured cross section of $\sigma(pp \rightarrow p + p + \mu^+ \mu^-) = 3.38^{+0.58}_{-0.55}$ (stat.) ± 0.16 (syst.) ± 0.14 (lumi.) pb, consistent with the theoretical prediction evaluated with the event generator Lpair. The ratio to the predicted cross section is $0.83^{+0.14}_{-0.13}$ (stat.) ± 0.04 (syst.) ± 0.03 (lumi.). The characteristic distributions of the muon pairs produced via fusion, such as the muon acoplanarity, the muon pair invariant mass and transverse momentum agree with those from the theory.

Keywords: Photon Production; Large Hadron Collider; Hadron-Hadron Scattering.

466. Measurement of the Production Cross Section for Pairs of Isolated Photons in Pp Collisions At $\sqrt{s} = 7$ TeV

The CMS collaboration

Journal of High Energy Physics, : 1-37 (2012) IF: 5.83

The integrated and differential cross sections for the production of pairs of isolated photons is measured in proton-proton collisions at a centre-of-mass energy of 7 TeV with the CMS detector at the LHC. A data sample corresponding to an integrated luminosity of 36 pb⁻¹ is analyzed. A next-to-leading-order perturbative QCD

calculation is compared to the measurements. A discrepancy is observed for regions of the phase space where the two photons have an azimuthal angle difference $\Delta\phi > 2.8$ rad.

Keywords: Hadron-Hadron Scattering; Large Hadron Collider; Photon Production.

467. Measurement of the Inclusive Production Cross Sections for forward Jets and for Dijet Events with One forward and One Central Jet in Pp Collisions at $\sqrt{s} = 7$ TeV

The CMS collaboration

Journal of High Energy Physics, (2012) IF: 5.83

The inclusive production cross sections for forward jets, as well for jets in dijet events with at least one jet emitted at central and the other at forward pseudorapidities, are measured in the range of transverse momenta $p_T = 35$ – 150 GeV/c in proton-proton collisions at $\sqrt{s} = 7$ TeV by the CMS experiment at the LHC. Forward jets are measured within pseudorapidities $3.2 << 4.7$ and central jets within the $|\eta| < 2.8$ range. The differential cross sections $d^2/dp_T d\eta$ are compared to predictions from three approaches in perturbative quantum chromodynamics: (i) next-to-leading-order calculations obtained with and without matching to parton-shower Monte Carlo simulations, (ii) pythia and herwig parton-shower event generators with different tunes of parameters and (iii) cascade and jet models, including different non-collinear corrections to standard single-parton radiation. The single-jet inclusive forward jet spectrum is well described by all models, but not all predictions are consistent with the spectra observed for the forward-central dijet events.

Keywords: Hadron; Hadron Scattering; Large Hadron Collider.

468. Comment on “Thermal Expansion Behaviors of Bismuth Nanowires”

A. R. Esmail

Journal of Physical Chemistry C, 116: 14176-14177 (2012) IF: 4.805

In a recent publication of Tang et al.,¹ the following set of 5 equations was mentioned to calculate the lattice parameters, a , b and c , of the hexagonal structure of bismuth (Bi) nanowires.

Keywords: Surface Science; Physical Properties; Nanoparticles.

469. Target Size Dependence of Relativistic Hadron Emission from ^{32}S Nuclear Collisions At 3.7 and 200A GeV

A Abdelsalam, B M Badawy and M E Hafiz

J. Phys G Nucl Partic, 39: 105104-0 (2012) IF: 4.178

The behavior of the relativistic hadron (shower particle) multiplicity for ^{32}S -nucleus interactions is investigated. The experiment is carried out at 3.7A GeV (Dubna energy) and 200A GeV (SPS energy) to search for the incident energy effect on the interactions inside the different emulsion target nuclei. Data are presented in terms of the number of emitted relativistic hadrons in both forward and backward angular zones. The dependence on the target size is presented. For this purpose the statistical events are separated into groups according to the interactions with H, CNO,

Em and AgBr target nuclei. These separation of events, into these groups, is executed based on predictions of Glauber's multiple scattering theory. Features suggestive of a decay mechanism seem to be a characteristic of the backward emission of relativistic hadrons. The results strongly support the assumption that the relativistic hadrons may already be emitted during the de-excitation of the excited target nucleus, in a behavior like that of compound nucleus disintegration. Regarding the limiting fragmentation hypothesis beyond 1 GeV, the target size is the main parameter affecting the backward production of relativistic hadrons. The backward shower particle multiplicity can indicate the impact parameter. The incident energy is a principle factor responsible for the forward relativistic hadron production, implying that this system of particle production is a creation system. However, the target size is an effective parameter as well as the projectile size considering the geometrical concept seen in the nuclear fireball model. The forward shower particle multiplicity distributions may behave in a similar trend at Dubna energy and SPS for low target sizes. For heavy target sizes, the SPS energy reveals the creation of hadrons with nearly equal probabilities over a wide range of multiplicity, extending to more than 300 hadrons per event. The data are analyzed in the framework of the FRITIOF model.

470. Doping of Adsorbed Graphene from Defects and Impurities in SiO₂ Substrates

Razvan A. Nisto, Marcelo A. Kuroda, Ahmed A. Maarouf and Glenn J. Martyna

Physical Review B, Rapid Communication, 86 » Issue 4: 41409-41409 (2012) IF: 3.691

The performance of novel graphene-based devices often strongly depends on the electrical quality of the supporting oxide. To elucidate the general governing principles underlying this behavior, we use first-principles simulations to generate representative classes of experimentally known defect centers in passivated silicon dioxide substrates and study their charge transfer with adsorbed graphene. We find that many of the open-shell structural perturbations generated near the interface self-passivate during annealing, leading to occupied-unoccupied pairs of midgap states in the silicon dioxide band structure, but no doping of the graphene occurs. However, dangling bonds or paramagnetic defect centers stable to thermal annealing do lead to partially occupied midgap energy states that are energetically misaligned with the Dirac point of graphene allowing charge to flow to or from the carbon layer. In particular, dangling oxygen bonds in the oxide strongly p dope the graphene. We also study doping from charge donating impurities within the substrate lattice as these also act to limit the performance of graphene-based devices.

Keywords: Graphene; Doping; Substrate; Electronic; Properties; First-Principles; Calculations.

471. Correlation Between-Particle Preformation Probability and the Energy Levels of Parent Nuclei

M. Ismail and A. Adel

Phys Rev C, 86: 14616-14616 (2012) IF: 3.308

A realistic density-dependent nucleon-nucleon (NN) interaction with a finite-range exchange part which produces the nuclear matter saturation curve and the energy dependence of the nucleon-nucleus optical potential model is used to calculate the

preformation probability, S , of decay from Po isotopes to superheavy nuclei. The variation of S with the neutron number for the isotopes of Po, Rn, Ra, Th and U elements is studied below and above the magic neutron number $N = 126$. We found a strong correlation between the behavior of S and the energy levels of the parent nucleus at and just below the Fermi level. S has a regular behavior with the neutron number if the neutron pair of particles, emitted from adjacent isotopes, comes from the same energy level or from a group of levels, assuming that the order of levels in this group is not changed. Irregular behavior of S with the neutron number occurs if the levels of the adjacent isotopes change or holes are present in lower levels.

Keywords: Decay; Preformation Probability; Superheavy Elements.

472. Penetration Factor in Deformed Potentials: Application to Decay with Deformed Nuclei

M. Ismail, A. Y. Ellithi and M. M. Botros

Phys Rev C, 86: 44317-44317 (2012) IF: 3.308

A new averaging process of the calculation of decay half-lives for heavy and superheavy nuclei is studied in the framework of a deformed density-dependent cluster model. The potential between a spherical particle and a deformed daughter nucleus is calculated numerically from the double-folding model by the multipole expansion method. The nuclear potential is calculated at each-particle emission angle applying the Bohr-Sommerfeld condition at each case. The penetration factors and the half-lives for all the emission angles are evaluated with the new averaging process and compared with older values based on a fixed value of the nuclear potential depth. Finally, the half-lives of 83 even-even heavy nuclei in the atomic-number range 82–118 are calculated by the two methods and compared with their experimental values and the corresponding half-lives of the spherical daughter nuclei.

Keywords: Decay; Deformed Nuclei; Superheavy Nuclei

473. Quantized Linear Model At Finite Temperature and Nucleon Properties

M. Abu-Shady and H. M. Mansour

Phys Rev C, 85: 55204-55204 (2012) IF: 3.308

The nucleon properties due to the restoration of the chiral symmetry at nonzero temperature T are investigated within the framework of the linear model. The field equations are solved using the coherent-pair approximation. In this approach, the quantum fields are treated in a nonperturbative fashion. We minimize the expectation value of the chiral Hamiltonian using the ansatz of the coherent-pair ground-state configuration. The obtained results show that the nucleon mass and mean-square radius of the proton and the neutron increase monotonically with the temperature T and that the pion-nucleon coupling constant g_{NN} decreases with temperature values that are near the value of the critical temperature T_c . The nucleon mass and mean-square radius of the proton are examined in the (x, T) plane, showing a sensitive dependence on the coherence parameter x . This means that an increase of both the coherence parameter x and the temperature T leads to an increase in the values of the nucleon mass and the mean-square radius of the proton. This is evidence for the quark-gluon deconfinement phase transition.

Keywords: Nucleon Properties; Sigma Model;

474. Static and Dynamic Mechanical Properties of Poly(Vinyl Chloride) Loaded with Aluminum Oxide Nanopowder

M. Abu-Abdeen

Materials and Design, 33: 523-528 (2012) IF: 2.2

A series of nanocomposites from poly(vinyl chloride) loaded with different concentrations of Al₂O₃ nanopowder was prepared. The tensile mechanical properties of these composites were studied at different temperatures namely; stress-strain curves. The elastic modulus was calculated and found to decrease with increasing both filler loading and temperature. The strain at a certain stress at different temperatures was studied and the thermal activation energy for polymer chains was calculated. The complex viscosity as well as the storage modulus was found to decrease with increasing the filler loadings at different frequencies. The relaxation time of the polymer matrix was calculated and found to be independent of the concentration of the filler but it decreased linearly with increasing frequency. The glass transition temperature was found to increase with increasing both filler loading and frequency.

Keywords: Polymer Matrix; Mechanical; Nanopowder; Pvc; Rheological Properties; Dma.

475. The Unusual Effect of Temperature on Stress Relaxation and Mechanical Creep of Polycarbonate at Low Strain and Stress Levels

M. Abu-Abdeen

Materials And Design, 34: 469-473 (2012) IF: 2.2

The effects of temperature, strain level during stress relaxation tests and stress level during mechanical creep tests on the viscoelastic characteristics of polycarbonate films were investigated. When the testing temperature increased the un-relaxed elastic modulus was found to increase during relaxation tests (at low strain levels <2.0%) and the initial strain was found to decrease during creep tests (at low stress levels <20 MPa), in an unusual behavior. A transition from poly-domain to a more coiled and more entangled chains poly-domain configuration took place at low strain and stress levels. At high strain and stress levels (P2.0% and P20 MPa) a usual behavior of the un-relaxed stress and initial strain was observed and a transition from poly-domain to mono-domain configuration took place. The thermal energy required for the transition from poly-domain to another poly-domain and from poly-domain to the mono-domain during both relaxation and creep tests were calculated. Besides, both the relaxation and creep strengths were calculated and studied.

Keywords: Pc; Stress Relaxation; Mechanical Creep.

476. Microscopic Study on Proton Elastic Scattering of Light Exotic Nuclei at Energies Below Than 100 Mev- Nucleon

M.Y.H. Farag, E.H. Esmael and H.M. Maridi

Eur. Phys. J. A, 3-17 (2012) IF: 2.19

The proton elastic scattering data on some light exotic nuclei, namely, ⁶He, ⁹Li and ^{10,11,12}Be, at energies below than 100 MeV/nucleon are analyzed using the single folding optical

model. Thereal, imaginary and spin-orbit parts of the optical potential (OP) are constructed only from the folded potentials and their derivatives using M3Y effective nucleon-nucleon interaction.

These OP parts, their renormalization factors and their volume integrals are studied. The surface and spin-orbit potentials are important to fit the experimental data. Three model densities for halo nuclei are used and the sensitivity of the cross-sections to these densities is tested.

The imaginary OP within high-energy approximation is used and compared with the single folding OP. This OP with few and limited fitting parameters, which have systematic behavior with incident energy, successfully describes the proton elastic scattering data with exotic nuclei.

Keywords: Elastic Scattering of Light Exotic Nuclei

477. Evolution of Al Plasma Generated by Nd-Yag Laser Radiation at the Fundamental Wavelength

H. Hegazy, F.M. Abdel-Rahim and S.H. Allam

Appl Phys B, 108: 665-673 (2012) IF: 2.189

The aim of the present work is to evaluate the effect of the laser beam energy on the properties of the plasma generated by focusing an intense laser beam on an Al solid target in air at atmospheric pressure. Plasma is generated using a Brilliant Nd-YAG pulsed laser from Quantel at the fundamental wavelength; its pulse energy is 750 mJ and the pulse duration is 6 ns. The emission spectrum is collected using an echelle spectrometer equipped with an ICCD camera of Andor type.

The spectrum is recorded at several delay time intervals from 0 to 10 ns. Measurements of temperature and electron density of the produced plasmas at different laser energies and at different delay times are performed in the present study.

Keywords: Measurements Of Temperature; Electron Density Of The Produced Plasmas At Different Laser Energies.

478. Energy Levels, Oscillator Strengths and Transition Probabilities for Si-Like P II, S III, Cl IV, Ar V and K VI

A. Abou El-Maaref, M.A.M. Uosif, S.H. Allam and Th.M. El-Sherbini

Atomic Data and Nuclear Data Tables, 98: 589-615 (2012)

IF: 2.16

Fine-structure calculations of energy levels, oscillator strengths and transition probabilities for transitions among the terms belonging to 3s23p², 3s3p³, 3s23p³d, 3s23p⁴s, 3s23p⁴p, 3s23p⁴d, 3s23p⁵s and 3s23p⁵p configurations of silicon-like ions P II, S III, Cl IV, Ar V and K VI have been calculated using configuration-interaction version 3 (CIV3). We compared our data with the available experimental data and other theoretical calculations. Most of our calculations of energy levels and oscillator strengths (in length form) show good agreement with both experimental and theoretical data. Lifetimes of the excited levels are also given.

Keywords: Energy Levels And Oscillator Strengths.

479. Influence of the Nitrogen Content on the Optical Properties of Cnx Films

F.H. Abd El-kader, M.A. Moharram, M.G. Khafagi and Fathia Mamdouh

Spectrochimica Acta Part A: Molecular And Biomolecular Spectroscopy, 97: 1115-1119 (2012) IF: 2.098

Polycrystalline carbon nitride thin films were prepared by electrolysis of methanol-urea solution at different concentrations of urea to methanol and applied voltage 800 volts for 10 h. Grazing incidence X-ray diffraction (GIXRD) revealed that the crystalline structure of carbon nitride films at moderate nitrogen content changed from amorphous phase to polycrystalline a-C₃N₄ and b-C₃N₄ phases. The optical transmission analysis of the films revealed that the band gap value for indirect allowed transitions increased with increasing nitrogen content, while the associated phonon energy value showed the opposite behavior. The refractive index and the extinction coefficient of the samples deposited with different concentrations were determined as a function of wavelength. The refractive index decreases with increasing both nitrogen content and crystallinity. The refractive index dispersion for the investigated samples is discussed in terms of the single oscillator model and oscillator parameters.

Keywords: Carbon Nitride; Grazing Incidence X-Ray Diffraction; Optical Properties.

480. The Memory Effect of Dy₂:8Sr₀:2Fe₅O₁₂ (DySrIG) Nanoparticles

M A Ahmed, Samiha T Bishay, S I El-Dek and S Solyman

Smart Materials And Structures, 21: 1-6 (2012) IF: 2.089

Dy₂:8Sr₀:2Fe₅O₁₂ (DySrIG) was prepared using the citrate-nitrate auto-combustion method. Single phase garnet with cubic structure was obtained at 1100 C. Thermal hysteresis (heating-cooling) study was performed for the following physical properties: crystal structure using x-ray diffraction (XRD); magnetic susceptibility using Faraday's method; dielectric measurements including dielectric constant as well as ac conductivity using an LCR meter. The results of the study reveal hysteresis loops in all the parameters which agree with those appearing in differential scanning calorimetry (DSC) and the former were interpreted according to the accompanying changes in the structural characterizations. The study clarifies that the investigated nanoparticles of DySrIG possess an electric memory effect with thermalization, where their dielectric parameters have sensitive changes with temperature in the range 25–400C and return to their original values at room temperature again. Accordingly, DySrIG could be recommended in thermal electric sensor applications (thermistors).

Keywords: Garnet; Nanoparticles; Memory Effect.

481. Novel Structural and Magnetic Properties of Mg Doped Copper Nano Ferrites Prepared by Conventional and Wet Methods

M.A. Ahmed, H.H. Afify, I.K. El Zawawia and A.A. Azab

J Magn Magn Mater, 324: 2199-2204 (2012) IF: 1.78

Nanoferrites of the general formula Cu_{1-x}Mg_xFe₂O₄ with 0x0.6 were prepared by standard ceramic and wet methods. The

structure was studied by X-ray diffraction and IR spectroscopy. The density and lattice constant were calculated and reported. The particle size of the prepared nanoferrites ranged from 8.7 to 41.1 nm. It was found that the lattice parameter decreases with increasing cation substitution of Mg²⁺ due to the difference of ionic radius and atomic mass. The dc magnetic susceptibility was measured out using Faraday's method. The magnetic hysteresis measurement was performed using a vibrating sample magnetometer. Magnetic constants such as Curie temperature, effective magnetic moment, saturation magnetization, remanent magnetization and coercivity were obtained and reported. The magnetic constants decrease with increasing Mg²⁺, except the remanent magnetization which increased.

Keywords: Cu; Mg Nanoferrite; Sol; Gel; Citrate; Co-Precipitation; Magnetic Susceptibility; Hysteresis.

482. Modification of Composite Ceramics Properties Via Different Preparation Techniques

M.A. Ahmed, N.Okasha and N.G.Imam

J Magn Magn Mater, 324(2012): 4136-4142 (2012) IF: 1.78

Modifying the proportion of the base composition by substituting with suitable dopants and improving the preparation conditions is expected to change the performance of composites. In the present study, 0.5(Ni_{0.5}Zn_{0.5}Fe₂O₄)/0.5(BaTiO₃) composite was prepared by the conventional ceramic technique and the citrate method. Ceramic particles, when prepared via different routes, would demonstrate different properties, even with the same starting compositions. With the help of X-ray diffraction, scanning electron microscope (SEM), magnetic properties and electric properties of the composites have been compared. A critical comparison of those methods is needed to make the best choice for given boundary conditions of targeted eventual material properties, raw materials, investment, processing and waste disposal costs.

Keywords: Multiferroics Composite; Citrate Technique; Ceramic Technique; Ferromagnetic Property; Ferroelectric Property.

483. Structural and Electrical Properties of Nanometric Ni-Cu Ferrite Synthesized by Citrate Precursor Method

M.A. Ahmed, S.F. Mansour and M. Afifi

J Magn Magn Mater, 324 (2012): 4-10 (2012) IF: 1.78

Nanometric nickel copper ferrites Ni_{1-x}Cu_xFe₂O₄, 0x0.45 were prepared by the citrate precursor method. X-ray diffraction measurements confirm the formation of single phase cubic spinel structure. The lattice parameter (a) is increased with increasing Cu²⁺ ion substitution. The crystallite size was calculated from XRD data and compared with that obtained from TEM micrographs. A significant increase in the density is observed with increasing Cu content. The IR absorption spectra were used for the detection and confirmation of the chemical bonds in spinel ferrites. The dielectric constant and dielectric loss showed a decrease with increasing frequency for all samples. The decrease in the ac conductivity was ascribed to the increase in hopping length.

Keywords: Ni- Nanoferrite; Structural Properties; Ir Spectra; Dielectric Properties; Conductivity.

484. Enhancement of the Magnetic Properties of Al/La Multiferroic

M.A. Ahmed, N. N. Okasha and B. Hussein

J Magn Magn Mater, 324 (2012): 2349-2354 (2012) IF: 1.78

Nanosized multiferroic $\text{La}_{1-x}\text{Al}_x\text{FeO}_3$ (0.00 x 0.20) samples were successfully synthesized by the citrate technique without subsequent heat treatment. All the prepared samples revealed single phase orthorhombic structure of space group Pbnm. XRD data revealed that the lattice parameters (a) decrease with increasing Al content. The magnetic susceptibility (χ_M) was enhanced significantly from 0.36 to 0.68 emu/g mole from LaFeO_3 to $\text{La}_{0.8}\text{Al}_{0.2}\text{FeO}_3$ respectively. The values of magnetization (M) and effective magnetic moment (m_{eff}) were found to increase with increasing Al content. The enhancement of the physical and structural properties of the investigated multiferroic is possibly due to the changes in the lattice parameters, tolerance factor as well as crystallite size caused by aluminum substitution.

Keywords: Al/La Nanomultiferroic; Tolerance Factor; Structural Investigation; Magnetic Property.

485. Physical Characterizations of Semi-Conducting Conjugated Polymer-Cnts Nanocomposites

M. Abu-Abdeen, Ayman S. Ayesh and Abdullah A. Al Jaafari

Journal of Polymer Research, 19: 1-9 (2012) IF: 1.733

Carbon nanotubes (CNTs) were prepared using Alcoholic Catalyst Chemical Vapor Deposition (ACCVD) technique in order to investigate the effects of their addition on the optical, electrical and mechanical properties of Poly (3-octylthiophene-2,5-diyl) (P3OT) matrix. The absorption spectra of the prepared CNTs and CNT-P3OT nanocomposites were measured in the spectral range 200 nm–3,000 nm at room temperature. The optical energy gap was determined from the obtained UV/Vis absorption spectrum. Optical results reveal that the prepared CNTs are almost single walled. Besides, the addition of CNTs to P3OT polymer matrix will decrease the optical energy gap and enhance the optical absorbance of P3OT matrix. On the other hand, the addition of CNTs to P3OT matrix will increase the electrical conductivity of P3OT matrix up to four orders of magnitude above the percolation threshold (0.44 wt% CNTs). Additionally, I–V characteristics indicate that the conduction mechanism is Ohmic at low applied voltage range while it is due to the trap charge limited at high applied voltage range. Furthermore, the behavior of dc conductivity with temperature was also investigated and the obtained results reveal that the activation energy decreases with CNTs content. Finally, mechanical results reveal that the elastic modulus values increase with the increasing of CNTs content in P3OT matrix.

Keywords: Accvd; Cnts; P3ot; Optical; Dc Conductivity; Stress–Strain.

486. Effect of Neutron Rearrangement on Subbarrier Fusion Reactions

A. Adel, V.A. Rachkov, A.V. Karpov, A.S. Denikin and M. Ismail

Nucl Phys A, 876: 119-130 (2012) IF: 1.54

The role of neutron transfer is investigated in the fusion process near and below the Coulomb barrier within the empirical channel

coupling approach. The possibility of neutron transfer with positive Q-values considerably increases the barrier penetrability. The enhancement of fusion cross sections for $^{58}\text{Ni}+^{64}\text{Ni}$, $^{32}\text{S} + ^{64}\text{Ni}$, $^{40}\text{Ca} + ^{48}\text{Ca}$ and $^{40}\text{Ca} + ^{124}\text{Sn}$ is well reproduced at subbarrier energies by the empirical channel coupling approach including the coupling to the neutron-transfer channels. The predictions of the fusion cross sections for several combinations of colliding nuclei are also proposed which may shed additional light on the effect of neutron transfer in fusion processes. A huge enhancement of deep subbarrier fusion probability was found for light neutron-rich weakly bound nuclei. This may be quite important for astrophysical primordial and supernova nucleosynthesis.

Keywords: Fusion Reactions; Neutron Transfer; Empirical Channel Coupling.

487. Comparative Study of Coulomb Barrier Parameters for Deformed Nuclei Using Double-Folding Model And Proximity Approach

M. Ismail and I.A.M. Abdul-Magead

Nucl Phys A, 888: 34-43 (2012) IF: 1.54

In the present paper we discuss the differences between the fusion barrier parameters (the height of Coulomb barrier V_B and its radius R_B) computed by two methods namely; the proximity approach for coplanar and non-coplanar systems of interacting nuclei and double folding model. The minimum separation distance, s , between the deformed surfaces of interacting nuclei was determined exactly from numerical calculations and the results of Coulomb parameters were compared with previous calculations based on approximated determination of s . We considered the three interaction systems $^{48}\text{Ar} + ^{238}\text{Pu}$, $^{150}\text{Nd} + ^{150}\text{Nd}$ and $^{86}\text{Kr} + ^{180}\text{Hf}$ and found that V_B and R_B , evaluated by using the proximity approach, have too strong-dependence for the system $^{150}\text{Nd} + ^{150}\text{Nd}$ at relative orientation angles of the nuclei symmetry axes $\theta = 90^\circ$.

Keywords: Coulomb Barrier; Proximity Approach; Double-Folding Model

488. Structural and the Thermal Degradation Studies on Thin Films of the Nanocomposite System Pvp–Ce(So4)2_4H2o

Ahmad-Fouad Basha and Mohammad A. F. Basha

Polymer Bulletin, 68: 151-165 (2012) IF: 1.532

Newly prepared and well-characterized nanocomposite thin films of polyvinylpyrrolidone (PVP) containing 2, 5, 10 and 15 wt% cerium (IV) sulfate have been subjected to structural and thermal stability investigations using the transmission electron microscopy (TEM), atomic force microscope (AFM), X-ray diffraction (XRD), differential scanning calorimetry (DSC) and thermogravimetric analysis (TGA). The nanostructural nature of the investigated films was confirmed from the estimated average size of the particles. Better crystallinity was achieved with the addition of 15 wt% cerium disulfate to PVP. The thermograms of DSC and its derivative for the investigated composites indicated the development of a new endothermic peak of decomposition nature and the values of peak position and associated enthalpy

were found to be composition dependent, indicating a decrease in thermal stability of PVP with the increase of dopant concentration. Thermograms of TGA and its derivative revealed that the weight loss in the composite samples is composition dependent and two main steps of degradation were clearly evident, the first assigned mainly to dehydration processes at relatively lower temperature range (30–200 °C) and the second at higher temperatures up to 400 °C attributed to decomposition processes. Thermodynamic parameters, such as activation energy, entropy, enthalpy and Gibbs free energy, were also determined on the basis of thermogravimetric data.

Keywords: Polyvinylpyrrolidone; Cerium Disulfate; Magnetic Nano; Composites.

489. Numerical Investigation of the Electron Dynamic Dependence on Gas Pressure in the Breakdown of Hydrogen by Krf Laser Radiation

Yosr E.E.-D. Gamal, Khaled A. Elsayed and M.A. Mahmoud
Opt Laser Technol, 44, Issue 7: 2154-2160 (2012) IF: 1.515

This paper presents a numerical investigation of the measurements that were carried out by Yagi et al. [12] to study the breakdown of molecular hydrogen induced by short laser of wavelength 248 nm and pulse duration 20 ns. The aim of the study is to give detailed description of the physical processes which contributed to the breakdown of molecular hydrogen at focus intensities between 4 $\times 10^{12}$ W/cm² and 8.0 $\times 10^{12}$ W/cm² over gas pressure range extended from 150 to 7000 Torr. The applied computer simulation model is based on the numerical solution of the time dependent Boltzmann equation and set of rate equations that describe the rate of change of the formed excited states population. The experimentally measured rate constants and cross sections for the various physical processes involved in the model are used in the calculations. Provision is made for the electron impact ionization and photoionization of the excited states. The former process is incorporated parametrically in the calculation owing to the lack of quantitative description of this process. Computations are performed at each gas pressure. The calculated threshold intensities are found to be in good agreement with the experimentally measured ones, both showing a noticeable increase in the higher pressure region. Moreover, calculation of the electron energy distribution function (EEDF) and its parameters demonstrated the exact correlation between gas pressure and the physical processes responsible for determining the breakdown threshold intensity.

Keywords: Laser Induced Breakdown. Molecular Hydrogen. Time Dependent Boltzmann Equation.

490. X-Ray Diffraction and Differential Scanning Calorimetry Studies of BaTiO₃/Polyvinylidene Fluoride Composites

M.Y.F. Elzayat, S. El-Sayed, H.M. Osman and M. Amin
Polymer Engineering And Science, : 1945-1950 (2012) IF: 1.302

Barium titanate/polyvinylidene fluoride (BaTiO₃)_x(PVDF)_{100-x} composite samples were prepared and characterized using X-ray diffraction (XRD) and differential scanning calorimetry (DSC) techniques. In this work, the ratio of the constituents of this composite was altered and the structural and thermal changes were studied. Also, the variation of tetragonality of BaTiO₃ (BT) in the

composite samples as a function of BT content was studied for the first time. The results show that all the samples are in the a-phase and the hindrance to the PVDF crystallization increases with the increase of BaTiO₃ (BT) ratio in the composite. Tetragonal distortion of BT nanoparticles in the composite increases with the increase in BT ratio up to 30%, where it gets a saturation value. Also, it seems that stretching the samples enhances the BT tetragonality. Both melting and crystallization behaviors of the composite samples show double-melting endotherms (reorganization) and crystallization exotherms. The inclusion of BT in the composite samples results in a decrease in the melting temperature of the samples. POLYM. ENG. SCI., 52:1945–1950, 2012. 2012 Society of Plastics Engineers.

491. The Thermal, Structural and Optical Properties of C-Irradiated Poly (Vinyl Alcohol)/ Poly (Ethylene Glycol) Thin Film

S. A. Nouh, A. G. Nagla, M. H. Othman, S. A. Eman and Z. I. Lotfi

Applied Polymer Science, 124: 654-660 (2012) IF: 1.289

Poly(vinyl alcohol)/poly(ethylene glycol)(PVA/PEG) copolymer was prepared using casting technique. The obtained PVA/PEG thin films have been irradiated with gamma rays with doses ranging from 1.5 to 20 Gy. The resultant effect of gamma irradiation on the thermal properties of PVA/PEG has been investigated using thermogravimetric analysis (TGA) and differential thermal analysis (DTA). The onset temperature of decomposition T_0 and activation energy of thermal decomposition E_a were calculated, results indicating that the PVA/PEG thin film decomposes in one main weight loss stage. Also, the gamma irradiation in dose range 4–12 Gy led to a more compact structure of PVA/PEG copolymer, which resulted in an improvement in its thermal stability with an increase in the activation energy of thermal decomposition. The variation of transition temperatures with gamma dose has been determined using DTA. The PVA/PEG thermograms were characterized by the appearance of an endothermic peak due to melting of crystalline phase. In addition, structural property studies using X-ray diffraction and infrared spectroscopy were performed on both nonirradiated and irradiated samples. Furthermore, the transmission of the PVA/PEG samples and any color changes were studied. The color intensity (E) was greatly increased with increasing the gamma dose and was accompanied by a significant increase in the blue and green color components. VC 2011 Wiley Periodicals.

Keywords: C-Irradiation; Polymers; Thermal; X-Ray; FTIR; Optical Properties.

492. Investigation of the Rheological, Dynamic Mechanical and Tensile Properties of Single-Walled Carbon Nanotubes Reinforced Poly(Vinyl Chloride)

M. Abu-Abdeen

Journal of Applied Polymer Science, 124: 3192-3199 (2012)
IF: 1.289

Polymer nanocomposites consisting of single-walled carbon nanotubes (SWCNTs) and poly(vinyl chloride) were prepared by casting technique. The complex viscosity increased with increasing SWCNTs content and it had a percolation

concentration threshold equal to 0.45 wt % of SWCNTs. The storage modulus, G' , increased with increasing either SWCNTs content or frequency. A gradual decrease in the terminal zone slope of G' for the nanocomposites with increasing SWCNTs content may be explained by the fact that the nanotube–nanotube interactions will be dominant at higher CNTs content and lead to the formation of the interconnected or network-like structures of SWCNTs in the polymer nanocomposites. The rheological loss factor indicates two relaxation peaks at frequencies of 0.11 and 12.8 Hz due to the interaction between SWCNTs and polymer chains and glass transition, respectively. Dynamic mechanical properties were measured for the prepared composites. The results indicate that the storage modulus changes steadily and the tan peaks are less intense for high SWCNTs content. Tensile tests were measured and depicted by an increase in the elastic modulus with increasing SWCNTs content, but it decreases for all composites as the testing temperature increased.

Keywords: Pvc; Swents; Dma; Nanocomposites; Rheology; Mechanical Properties.

493. Electrical Properties of Cu Substituted Co Nano Ferrite

Hatem El-Gohary and Riyad Eid

Physica Scripta, 17: 523-532 (2012) IF: 1.204

The samples $\text{Co}_{1-x}\text{Cu}_x\text{Fe}_2\text{O}_4$ (0.0 ≤ x ≤ 0.6) were prepared using the standard ceramic method. The dielectric constant (ϵ'), dielectric loss ($\tan \delta$) and ac conductivity (σ) were measured at room temperature as a function of the frequency. The results of the dielectric properties were explained on the basis of Maxwell–Wagner behaviour. The effect of Cu^{2+} ion substitution on the ac electrical conductivity and dielectric properties at different frequencies, 0.1–1000 kHz, were studied. The data revealed that ϵ' and $\tan \delta$ increased as the Cu^{2+} ion increased, due to the increase in the number of vacancies at the iron site. The Cu^{2+} ions change the conduction from an n- to a p-type. The Seebeck coefficient (dV/dT) mVK⁻¹ gives a positive sign (p-type) for all samples up to 500 K, except for x = 0.6, for which it gives a negative sign. This indicates that the conduction is predominantly caused by electrons hopping between Fe^{3+} and Fe^{2+} . The mobility was calculated and found to increase with an increasing Cu content.

Keywords: Cu Co Ferrite; Nanoferrite; Electrical Properties.

494. AC conductivity and dielectric properties of bulk tungsten trioxide (WO₃)

M.M. El-Nahass, H.A.M. Ali, M.Saad eldin and M.Zaghlol

P Acad Nat Sci Phila, 407(2012): 4453-4457 (2012) IF: 1.063

AC conductivity and dielectric properties of tungsten trioxide (WO_3) in a pellet form were studied in the frequency range from 42 Hz to 5 MHz with a variation of temperature in the range from 303 K to 463 K. AC conductivity was found to be a function of where is the angular frequency and s is the and s is the frequency exponent. The values of s were found to be less than unity and decrease with increasing temperature, which supports the correlated barrier hopping mechanism (CBH) as the dominant mechanism for the conduction in WO_3 . The dielectric constant (ϵ') and dielectric loss (ϵ'') were measured. The

Cole–Cole diagram determined complex impedance for different temperatures.

495. Dielectric Behavior and Low Temperature Phase Transition in NH_4IO_3

M.M. Abdel Kader, F. El-Kabbany, H.M. Naguib and W.M. Gamal

Phase Transitions, (2012) IF: 1.06

The electrical properties namely ac conductivity (σ), T) and the complex dielectric permittivity (ϵ'') are measured at selected frequencies (5–100 kHz) as a function of temperature (95 K–5280 K) for polycrystalline samples of NH_4IO_3 . The ferroelectric hysteresis loops and the X-ray diffraction pattern are also measured. The analysis of the data indicates that the compound undergoes a structural phase transition at 103 K and the behavior of (σ , T) obeys the power law.

The trend of the temperature dependence of the angular frequency exponent s (0.5 ≤ s ≤ 1) suggests that the quantum mechanical tunneling model is the most likely one that describes the conduction mechanism.

The core results of the article are: (1) the low temperature ac electrical parameters are measured for NH_4IO_3 ; (2) the data indicate that the compound undergoes a structural phase transition at 103 K; (3) the originality of this transition has been confirmed by X-ray diffraction; (4) no evidence for the existence of a ferroelectric transition at 103 K as mentioned earlier; and (5) the quantum mechanical tunneling is proposed as the main mechanism of the electric conduction.

Keywords: Proton Conductivity; NH_4IO_3 ; Ac Conductivity; Dielectric Permittivity; Phase Transitions; X-Ray Diffraction.

496. Environmental Risk Assessment of Radon From Ceramic Tiles

A.F. Maged, L.Z. Ismail and N.L.A. Moussa

Radionuclides, 47, 3: 403-411 (2012) IF: 1

Radon-222 exhalation from different ceramic tiles depends upon the radium (^{226}Ra) concentration and porosity. Raw zirconium sand is one of the substances widely used in the ceramic industry and it is naturally radioactive.

This can produce unjustified concern and subsequently perturb the market of these products. The radon exhalation rates for all ceramic tile companies were in the ranges 28–44 mBq.m⁻².h⁻¹ and 2.0 to 4.8 mBq.kg⁻¹.h⁻¹.

The porosity of ceramic tiles is in the range 0.19–0.28. The radium activity of ceramic tiles was found to be in the range 16–38 Bq.kg⁻¹ for the glazed surface and 23–64 Bq.kg⁻¹ for the clay surface, respectively.

The average equivalent dose in contact with the ceramic surface was found to be 22 mSv.y⁻¹. The exposure at working level at the ceramic tile surface was in the range 2.4–3.8 WL. This gives a risk indication to people who spend a long time in closed ceramic tile stores, who should avoid staying for a long time in such places.

Keywords: Radon-222 / Track Density; Exhalation Rate; Ceramic Tiles; Porosity.

497. Energy Dependence for Relativistic Hadron Emission From 32S Nuclear Collisions

A. Abdelsalam, B.M. Badawy and M.E. Hafiz

Can J Phys, 90: 515-523 (2012) IF: 0.857

In this experiment, 32S interaction with emulsion nuclei is examined at 3.7A and 200A GeV. Backward relativistic hadron production seems to be an exact decay system, depending on the target size. For emulsion nuclei, the decay constant of this system nearly equals 1.3. Independent of the projectile size and energy, the backward relativistic hadrons are produced with probability values of 20%–30%. For projectile nuclei with mass numbers greater than or equal to 6 and at any incident energy, the average multiplicity of these backward hadrons tends to a saturation value of 0.4. Regarding the multiplicity range of forward relativistic hadrons, reaching 60 hadrons per event at 3.7A GeV and extending to 400 hadrons per event at 200A GeV, energy plays a fundamental role in forward relativistic hadron production. The results strongly support the assumption that relativistic hadrons are created as a result of energy from participant nucleons.

498. Magnetoelectric Characteristics of Dy₂.8Sr_{0.2}Fe₅O₁₂ garnet (Dysrig)

M.A. Ahmed, S.T. Bishay and S.I. El-dek

European Phys. J: App. Phys., 59: 20401-20407 (2012) IF: 0.77

The effect of dc magnetic field on the capacitance, impedance and resistance of Dy₂.8Sr_{0.2}Fe₅O₁₂ (DySrIG) prepared using the citrate-nitrate auto-combustion method was studied at room temperature. The measurements were carried out in two ways; the first one in which the dc magnetic field and the ac electric field are parallel (*//*) to each other and the second one in which the magnetic field and ac electric fields are perpendicular to each other. The magnetoelectric impedance of Dy₂.8Sr_{0.2}Fe₅O₁₂ increases by about 80% in the case (at 1650 Oe and 450 kHz) with respect to its values at zero magnetic field. The results of the study encourage the use of this garnet nanomaterial in magnetic sensors, in new devices including tunable filter and spintronic applications.

Keywords: Magnetoelectric; Garnet; Dysrig.

499. Low Percolation Threshold of Functionalized Single-Walled Carbon Nanotubes Polycarbonate Nanocomposites

Ayman S. Ayesh, S.S. Ibrahim and M Abu-Abdeen

Journal of Reinforced Plastics and Composites, 31(16): 1113-1123 (2012) IF: 0.727

A series of polycarbonate films loaded with different concentrations of UV-ozone pretreated single-walled carbon nanotubes were prepared. The electrical and mechanical properties of these composites were investigated. The improvement of the single-walled carbon nanotubes dispersion in polycarbonate (PC) matrix leads to a dramatic enhancement in the electrical conductivity with low percolation threshold (0.5 wt% of single-walled carbon nanotubes loading). Results obtained from the analysis of the dielectric parameters at room temperature and domain frequency range reveal that single-walled carbon nanotubes increases the dielectric constant, dielectric loss and AC conductivity of the composites. The dielectric relaxation behavior

of these composites is mostly due to polymer molecular relaxation when the single-walled carbon nanotubes content is below the percolation threshold whereas it is almost due to the charge conductivity relaxation above 0.8 wt% single-walled carbon nanotubes. The calculated values of the elastic modulus obtained from the stress–strain curves also show a percolation behavior with a threshold of 0.08 wt% single-walled carbon nanotube.

Keywords: Single; Walled Carbon Nanotubes; Polycarbonate; Nanocomposites; Percolation; Electrical; Mechanical.

500. Structure–Electrical Conductivity of Polyvinylidene Fluoride/Graphite Composites

MH Abd-El Salam, GM Elkomy H Osman MR and Nagy F El-Sayed

Journal of Reinforced Plastics and Composites, 31 (20): 1342-1352 (2012) IF: 0.727

Graphite powder was introduced into polyvinylidene fluoride via the solution mixing technique. The composites were then subjected to hot compression molding. The effect of dispersion of graphite particles and electrical conductivity of the composites were investigated. Solution mixing enabled homogeneous dispersion of graphite powder within the polyvinylidene fluoride matrix as revealed by transmission electron microscopy. X-ray diffraction and Fourier transform infrared spectroscopy analysis revealed that graphite incorporation induced the β -phase of polyvinylidene fluoride. The DC conductivity results showed that the conductivity increased with an increase in graphite content. Beyond a critical concentration of graphite, percolation threshold, (c_c ≈ 2.3 vol%) the conductivity increases by five orders of magnitude at 3.9 vol% of graphite powder composite. The electrical conductivity was approximately constant for the composites with the higher graphite loading. Consequently, adding more graphite powder did not significantly alter the electrical conductivity. The correlation between the dispersion of graphite particles and electrical conductivity was discussed. The AC conductivity of composites was investigated in a wide range of frequencies from 50 Hz to 5 MHz and at temperatures ranging from room temperature to 180°C. The conductivity of the composites exhibited strong frequency dependence particularly in the vicinity of the electrical percolation threshold. AC obeyed the power law of the form: $\sigma_{AC} \propto \omega^s$, where ω is the angular frequency and s and A the characteristic parameters. The values of the exponent (s) were found to decrease with increasing temperature which is consistent with the correlated barrier hopping model.

Keywords: Polyvinylidene Fluoride; Graphite; Transmission Electron Microscopy; X-Ray; Conductivity.

501. Shell Corrections for Heavy and Superheavy Nuclei

M. ISMAIL and A. ADEL

Int J Mod Phys E, 21(6) 1-16 (2012) IF: 0.597

The shell and pairing correction energies are calculated for heavy and superheavy nuclei (SHN) by means of the Strutinsky's method. The single-particle (s.p.) energy levels are obtained from the diagonalization of the Woods–Saxon s.p. Hamiltonian in the deformed harmonic oscillator basis for both neutrons and protons. The residual pairing interaction is calculated by means of the usual

Bardeen–Cooper–Schrieffer (BCS) approximation. A two-dimensional deformation space describing axially and reflection-symmetric shapes of nuclei has been used. Based on the shell and pairing correction energies, the signatures of the magic numbers appear at the spherical shell closures $Z = 82, 114, 164$ and $N = 126, 184, 228$ and 308 . There are also signatures for some other shell closures at, e.g., $Z = 108$ and $N = 162$ which appear only when the deformation degrees of freedom is taken into account.

Keywords: Shell Correction; Superheavy Nuclei; Magic numbers.

502. Nuclear Matter Equation of State and Three-Body forces

Hesham M. M. Mansour and Khaled S. A. Hassaneen

Physics of Atomic Nuclei, 2(2): 14-21 (2012) IF: 0.568

The energy per particle, symmetry energy, pressure and free energy are calculated for symmetric nuclear matter using BHF approach with modern nucleon–nucleon CD-Bonn, Nijm1, Argonne v18 and Reid 93 potentials. To obtain saturation in nuclear matter we add three-body interaction terms which are equivalent to a density-dependent two-nucleon interaction a la Skyrme force. Good agreement is obtained in comparison with previous theoretical estimates and experimental data.

Keywords: Nuclear matter; Equation of state; Three; Body forces.

503. Effect of Blend Ratio on the Thermal and Optical Properties of Poly (Methyl Methacrylate)/Poly (Vinyl Acetate) Films

F.H.Abd-El Kader, W.H.Osman and R.S.Hafez

Materials Science, 8(12): 493-502 (2012) IF: 0.229

Films of poly (methyl methacrylate) / Poly (vinyl acetate) (PMMA/PVAc) with different concentrations were prepared by using cast technique. The samples were investigated by differential thermal analysis (DTA), thermogravimetric analysis (TGA) and UV/visible spectra. A single glass transition temperature for each blend was observed in DTA thermograms, which reflects the existence of miscibility of such system. Thermogravimetric characterization and the calculated values of activation energies revealed that the blend sample of 75 wt% PVAc content has a more thermal stability than the other blends. The variation of band tail energy with the composition of the blend indicated that the model based on electronic transitions between localized states is preferable. The refractive index dispersion curves were simulated by both Cauchy and single effective oscillator models. The calculated color parameters such as L^* , U^* , V^* and C^* for 25 wt% PVAc blend sample were found to be dependent on addition of malachite green and irradiation.

Keywords: Thermal Analysis; Optical Parameters; Irradiation; Malachite Green; Color Detection.

504. Structural and Magnetic Properties of Electroceramic Magnetolectric Nanocomposites

M. A. Ahmed, N. Okasha and N. G. Imam

African Review of Physics, : 7-17 (2012)

Magnetolectric composite materials were prepared by sintering a mixture of a piezoelectric and piezomagnetic phase using double

sintering ceramic process. This paper deals with the preparation and measurements of some physical properties of $(1-x)\text{Ni}_0.5\text{Zn}_0.5\text{Fe}_2\text{O}_4 + (x)\text{BaTiO}_3$ nanocomposite. The formation of the nanocrystallite composite was confirmed by X-ray diffraction and scanning electron microscopy (SEM). The values of the lattice parameters and average crystallite size were calculated from the obtained measurements and reported. The hysteresis measurements were carried out to determine saturation magnetization (M_s), remanence magnetization (M_r) and coercivity (H_c) of the samples. The variation of the magnetic susceptibility (M) behavior with temperature as a function of field intensity was also studied and the magnetic constants were calculated and reported. The variation of the physical properties was correlated to the ratio of $(1-x)\text{Ni}_0.5\text{Zn}_0.5\text{Fe}_2\text{O}_4 + (x)\text{BaTiO}_3$. Critical ratio was obtained at which the prepared nanocomposites become more applicable.

Keywords: Structural; Magnetic; Magnetolectric Nanocomposite

505. Novel Behavior of the Transport Properties of Magnetolectric (Me) Nanocomposite

M. A. Ahmed, N. Okasha and N. G. Imam

Prime Journal of Engineering and Technology Research, 1(1): 19-25 (2012)

Magnetolectric (ME) biferroic nanocomposite with the composition $(x)\text{BaTiO}_3 + (1-x)\text{Ni}_0.5\text{Zn}_0.5\text{Fe}_2\text{O}_4$; $0.0 \leq x \leq 0.7$, were prepared using ceramic technique. The presence of two phases, namely ferrite; $\text{Ni}_0.5\text{Zn}_0.5\text{Fe}_2\text{O}_4$ (NZF) and ferroelectric; BaTiO_3 (BT) was confirmed by X-ray diffraction. The effects of frequency, composition and temperature on the ac and dc electrical conductivity were studied. The variation of dielectric constant (ϵ') in the frequency range 100 kHz to 5 MHz at different temperatures was investigated. The conduction phenomenon was explained on the basis of electron hopping model where the value of (ϵ') increases drastically with increasing BaTiO_3 content in the composite. The observed values of Seebeck coefficient indicate that the conduction is due to electron hopping mechanism which is in agreement with that obtained from dielectric measurements.

Keywords: Multiferroic; Ferroelectric; Ferromagnetic; Nanocomposite.

506. First Order Studies of Nanometric Biferroic

M. A. Ahmed, U. Seddik and N. G. Imam

World J of Condensed Matter Physics, 2,: 66-74 (2012)

Magnetolectric biferroic nanocomposite with composition $0.5\text{Ni}_0.5\text{Zn}_0.5\text{Fe}_2\text{O}_4 + 0.5\text{BaTiO}_3$ was synthesized by ceramic technique. The structural and electrical characterizations of the investigated nanocomposite are discussed and reported. The formation of nanosized composite with two separate phases was confirmed by X-ray diffraction, scanning electron microscopy (SEM) and Fourier transform infrared spectroscopy (FT-IR). The variation of dielectric constant, dielectric loss factor and the ac conductivity (ac) of $0.5\text{Ni}_0.5\text{Zn}_0.5\text{Fe}_2\text{O}_4 + 0.5\text{BaTiO}_3$ was investigated as a function of both frequency and temperature. Thermal hysteresis (first-order transition) was obtained during heating (300 - 830 K) and cooling runs (830 - 300 K). The exact transition temperature and the amount area of the thermal

hysteresis depend on applied ac electric field. The delay (lagging) time between heating and cooling processes was estimated from the hysteresis loop area versus frequency. The conduction mechanism in the investigated samples was explained according to different models. This study enhances the use of this prepared system in memory applications.

Keywords: Biferroic; Nanocomposite; Nickel-Zinc Ferrite; Barium Titanate; Dielectric; Hysteresis; First-Order Transition.

507. Signatures for Z'B-L Gauge Boson at Large Hadrons Collider using Monte Carlo Simulation Data

H.M.M.Mansour

International Journal of Scientific & Engineering Research, 3:(2012)

In the present work we search for Z'B-L heavy neutral boson in the dielectron events produced in proton-proton collisions at LHC using Monte Carlo simulation programs. To detect Z'B-L at LHC we used the data which are produced from pp collision of Pythia8 produced events at different energies for LHC then we use the angular distribution for the dielectron produced from Z'B-L decay channel's to detect the Z'B-L signal. B-L extension of the SM model predicts the existence of a Z'B-L heavy neutral massive boson at high energies and from our results which we had simulated for Z'B-L in the B-L extension of standard model we predict that a Z'B-L boson will be found at LHC and has a mass in the range from 1 TeV to 1.5 TeV.

Keywords: Gauge Bosons; Large Hadron Colliders; Monte Carlo Simulation; Z Prime Particles; Cross Sections; Branching Ratios; Extended Standard Model.

508. Nuclear and Neutron Matter Properties using Bhf Approximation

Hesham M. M. Mansou and Khaled S. A. Hassaneen

Journal of Nuclear and Particle Physics, 2(2): 14-21 (2012)

Results of cold and hot symmetric nuclear matter and pure neutron matter calculations are presented. The Brueckner-Hartree-Fock (BHF) approximation + two body density dependent Skyrme potential which is equivalent to three body interaction are used. Various modern nucleon-nucleon (NN) potentials are used in the framework of BHF approximation, e.g.: CD-Bonn potential, Nijm1 potential, Reid 93 potential and Argonne V18 potential. The bulk properties of asymmetric nuclear matter are computed such as the equation of state (EOS) at (T = 0), pressure at (T = 0, 5 and 10 MeV), single particle potential, free energy at (T = 5 and 10 MeV), nuclear matter incompressibility and the symmetry energy. Also the bulk properties of pure neutron matter are computed such as the EOS at (T = 0), pressure at (T = 0, 3 and 6 MeV), single particle potential, free energy at (T = 3 and 6MeV). Good agreement is obtained in comparison with previous theoretical estimates and experimental data.

Keywords: Keywords bhf approximation; Symmetric nuclear Matter And Pure Neutron Matter; Finite Temperature; Three-Body Forces.

509. A Comparative Study on the Physical Properties of MnFe₂O₄ Nanoferrite Using Novel Eco Friendly Methods

M. A. Ahmed, S. F. Mansour, S. I. El-Dek and N. Okasha

Journal of Solids and Structures, 6, 1: 37-53 (2012)

Nanocrystalline MnFe₂O₄ powder was synthesized by a simple and novel chemical route, which is based on the use of different chelating agents such as fresh coconut water, egg white, sucrose, glycerin and fresh Lemon juice adding to metal ions. In this work, X-ray diffraction analyses (XRD), dc magnetic susceptibility (M) measurements and transmission electron microscope (TEM) have been employed to assure the formation of MnFe₂O₄ nanosized particles and to obtain additional information about their physical characterizations using different types of safety materials. The magnetic properties of these nanoparticles are clearly size dependent. The variation of the lattice parameter with the type of chelating agent originates from the change in the inversion parameter. The largest and lowest values of μ were obtained for the Lemon and glycerine prepared samples respectively.

Keywords: MnFe₂O₄ Nanoferrite; Coconut; Egg White; Sucrose; Glycerin; Lemon Juice; Crystal Structure; Magnetic Properties.

510. Spectrometric Measurement of Plasma Parameters Utilizing the Target Ambient Gas O I and N I Atomic Lines in Libs Experiment

Ashraf M. El Sherbini¹, Abdel Aziz Saad Al Amer, Ahmed T. Hassan and Tharwat M. El Sherbini

Optics And Photonics Journal, 2012, 2,: 286-293 (2012)

In this article, we shall report the results of the spectroscopic measurements of the plasma parameters utilizing the spectral lines emitted from the air atoms surrounding plasma (O I line at 777.19 nm and N I at 746.83 nm).

The plasma was created via irradiation of plane solid aluminum target in open air by a high peak power Nd: YAG laser pulses at fundamental wavelength of 1064 nm. The emission spectra were recorded using Echelle type spectrograph in conjunction with a time gated ICCD camera at different delay time from 1 to 5 ns and at a fixed gate time of 1 ns. The plasma electron density was measured utilizing the Stark broadening of the N I and O I lines and then compared to the reference density as deduced from the optically thin H-line at 656.27 nm appeared in the same emission spectra.

The results show that under our experimental conditions the air lines are subjected to moderate absorption. The plasma electron temperature was measured utilizing the relative spectral intensity of the air (O I to N I) lines after correcting their spectral radiance against absorption.

The standard temperature was measured utilizing the Al II ionic lines. A comparison to the reference temperatures shows a very close agreement after correcting the emission spectral radiance of the air lines against self absorption, which emphasizes the importance of correction process.

Keywords: Libs; Self Absorption; O I-N I Lines; Plasma Parameters.

511. Measurements of Plasma Electron Temperature Utilizing Magnesium Lines Appeared in Laser Produced Aluminum Plasma in Air

Ashraf M. El Sherbini Abdel Aziz S. Al Aamer, Ahmed T. Hassan and Tharwat M. El Sherbini

Optics and Photonics Journal, 2012, 2,: 278-285 (2012)

We have utilized the relative intensity of magnesium lines originated from the Mg I at 285.2 nm and Mg II at 280.27, 279.55 nm to measure the plasma electron temperature. The plasma was produced via interaction of Nd:YAG laser with solid aluminum target contains traces of magnesium.

The magnesium lines were found to suffer from optical thickness which manifests itself on the form of scattered points around the Saha-Boltzmann line. We have utilized a simple method used for rapid calculation to the amount of absorption to these lines via comparison of the electron densities as deduced from magnesium lines to that evaluated from the optically thin hydrogen H line at 656.27 nm appeared in the same spectra under the same condition.

A correction to the magnesium spectral lines intensities was carried out; hence the corrected temperatures were re-evaluated. The measurements were repeated at different delay times ranging from 1 to 5sec. This work emphasizes on the importance of correcting the emitted spectral line intensity against the effect of self absorption before using them in the calculation of plasma electron temperature in laser induced breakdown spectroscopy (LIBS) experiments.

Keywords: Libs; Self absorption; Mg-Lines; Plasma parameters.

512. Observed Enhancement in Libs Signals from Nano Vs. Bulk ZnO Targets: Comparative Study of Plasma Parameters

Ashraf M. EL Sherbini, Abdel-Nasser M. Aboufotouh, Farid F. Rashid, Sami H. Allam, Ashraf EL Dakrouri and Tharwt M. EL Sherbini

World Journal of Nano Science and Engineering, 2012, 2,: 181-188 (2012)

In this article, we will report an experimental evidence of enhanced LIBS emission upon replacing a Bulk-Based ZnO target by the corresponding Nano-Based target. The plasma was initiated via interaction of a Nd:YAG laser at the fundamental wavelength with both targets in open air under the same experimental conditions. The measurements show an enhanced emission from the Zn I-lines at the wavelengths of 328.26, 330.29, 334.55, 468.06, 472.2, 481.01, 636.38 nm. The measurements were repeated at different delay times in the range from 1 to 5s at constant irradiation level and fixed gate time of 1s. The average enhancement over the different Zn I-lines was found to increase exponentially up to 8-fold with delay time. The electron density to each plasma was measured utilizing the H-line appeared in the emitted spectra from each plasma and was found to give similar values. The electron temperatures were measured via Boltzmann plot method utilizing the relative intensities of the Zn I-lines and were found to give very close values. Moreover, the relative population density of the ground state of the zinc atoms (relative concentration) was measured spectroscopically utilizing the Boltzmann plot method and was found to increase in a very similar trend to that of enhancement. The results of the

spectroscopic analysis conclude that these signal enhancements can be attributed to the higher concentration of neutral atoms in the Nano-Based material plasma with respect to the corresponding Bulk-based ZnO material.

Keywords: Libs; Enhancement; ZnO Nonmaterial; H-Line; Zn I-Lines; Spectroscopy.

513. The Thermal and Mechanical Studies of Pvp/2-Hec Blend Films

M.F.H. Abd El-kader and M. Abu-Abdeen

Australian J. of Basic and Applied Sciences, 6 (13): 454-462 (2012)

Solid polymer blend films based on polyvinyl pyrrolidone (PVP) and 2-hydroxyethyl cellulose (2-HEC) were prepared in various concentrations by solution cast technique. X-ray diffraction, differential scanning calorimetry (DSC), thermogravimetric analysis (TGA) and stress-strain of individual polymers and their blended samples were studied. X-ray diffraction patterns demonstrate miscibility between the PVP and 2-HEC in amorphous region for blend system. DSC characterization on PVP/2-HEC blends revealed a single Tg in each composition and its position was slightly shifted towards higher temperatures with increasing PVP content, which further supports single-phase behavior. It was found from TGA and its derivatives that the mass loss of most samples is accomplished in two decomposition stages in the temperature range of investigation, indicating different degradation mechanisms. Making use of Coats-Redfern relation, TG data allowed the calculation of some thermodynamic parameters such as activation energy, entropy, enthalpy and Gibbs's free energy. Stress-strain data indicated that the blends became more brittle as PVP content increased. The elastic modulus was found to increase as the amount of PVP increased, while the strain at break decreased in an opposite behavior. Meanwhile, the tensile strength had a maximum value at 30 wt % PVP content in blend samples.

Keywords: Polymers; Differential scanning calorimetry (Dsc); Thermogravimetric analysis (Tga); Mechanical testing.

514. The Accuracy of Neglecting the S-Dependence and its Effect on the Direct Parts of A-Interaction Potential

M.Y. Ismail, M.M. Osman and H. Elgebaly

Journal of Applied Sciences Research, 8(3): 1817-1823 (2012)

The study shows the effect of the local density and the accuracy of neglecting s-dependence on direct part of interaction potential. The large error in neglecting s-dependence produced at ($R < 2$ fm) for BDM3Y3 -Ried force. In the surface and tail region (R3) the error is less than 50%.

Keywords: Interaction potential; Double; Folding model.

515. Effect of Neutron Transfer in the Fusion Process Near and Below the Coulomb Barrier

V. A. Rachkov, A. Adel, A. V. Karpov, A. S. Denikin and V. I. Zagrebaev

Nuclear Structure and Dynamics, 1491: 381-382 (2012)

Near-barrier and sub-barrier fusion of weakly bound neutron-rich isotopes of lithium is explored within the empirical channel

coupling model. Several combinations of colliding nuclei are proposed, for which strong enhancement of the sub-barrier fusion is predicted owing to coupling with neutron transfer channels.

Keywords: Fusion Reactions; Neutron Transfer; Empirical Channel Coupling Model.

516. ZnO Nanostructures Induced by A Microwave Plasma

Noori S. Anad, Gamal Abdel Fattah, Khaled A. Elsayed and Lotfi Z. Ismail

New York Science Journal, : 1-7 (2012)

Microwave induced hydrogen plasma is used for the deposition of ZnO thin films at low ambient gas pressure by controlling the oxygen content in the gas mixture. The emission spectra have been observed. In-situ optical emission spectroscopy was used to identify the chemical reaction mechanism. Structural quality of the so-obtained nanoparticles was studied with X-ray diffraction (XRD) and high-resolution scanning electron microscopy (SEM). The results showed that ZnO nanorods were single crystals. The alignment of these nanorods with respect to the substrates depends on the lattice mismatch between ZnO and the glass substrate. The crystallite grain size is ~ 24 nm and the average diameter of nanorods is 70 nm with length of 1-2 μ m. The deposited ZnO thin films have a wide energy band gap that equals 3 eV.

Keywords: ZnO nanostructure; Nanorods; Band gap.

517. Laser Gain Calculations of the Excited Ion Mn Xv

W. O. Younis, S. H. Allam and Th. M. El-Sherbini

International Review of Physics, 6 (5) 433-438 (2012)

Rate coefficients for electron impact excitation, de-excitation and total depopulation of the excited ion Mn XV of the sodium isoelectronic sequence are calculated according to the analytical formulas of Vriens and Smeets. A simple modification has been made by substituting effective quantum numbers in Vriens formulas to be applicable for the ions under consideration. The energy levels and transition probabilities have been calculated using Hibbert's configuration interaction computer package (CIV3). Level population densities are then calculated by solving the coupled rate equations involving the 19 levels $1s2s2p6nl$, where $n=3,4,5$ and $l=0,1,2,3$. Positive gain coefficients are displayed for the transitions $2p65p(2P1/2)2p64d(2D3/2)$, $2p65p(2P3/2)2p64d(2D3/2)$, $2p65p(2P3/2)2p64d(2D5/2)$, $2p65p(2P1/2)2p65s(2S1/2)$ and $2p65p(2P3/2)2p65s(2S1/2)$ at three selected electron temperatures namely 1/4, 1/2 and 3/4 the ionization potential of each ion respectively. Copyright © 2012 Praise Worthy Prize S.r.l. – All rights reserved.

Keywords: Rate coefficients; Level populations; Laser gain.

518. Structural Characteristics and Electrical Properties of Copper Doped Manganese Ferrite

L.M. Salah a, A.M. Moustafa and I.S. Ahmed Farag

Ceramics International, 38: 5605-5611 (2012) IF: 1.751

A series of $Mn_{1-x}Cu_xFe_2O_4$ ferrite samples with $0.2 \leq x \leq 0.5$ were prepared using the co-precipitation method. X-ray analysis

confirmed the formation of single phase cubic spinel structure for all concentrations. Rietveld refinement revealed that the $Mn_{1-x}Cu_xFe_2O_4$ with all concentrations of x belongs to normal spinel structure.

The lattice parameters as well as the X-ray density decrease with increasing the copper concentration and this may be due to the difference in the ionic radii between Mn^{2+} and Cu^{2+} . The decrease in the crystallite size with increasing the copper content is attributed to the higher formation temperature.

The IR absorption spectra analyses were used for the detection and confirmation of the chemical bonds in spinel ferrites. The ac electrical conductivity, real part of the dielectric constant and the loss tangent $\tan \delta$ were studied as a function of the applied frequency and temperature.

It was found that the AC electrical conductivity increases with increasing temperature, this increase may be related to the increase in the drift mobility of the charge carriers, which are localized at ions or vacant sites. The AC conductivity increased with increasing copper concentration which may be ascribed to the decrease in hopping length. The dielectric constant and dielectric loss showed a decrease with increasing frequency and increase with increasing temperature for all compositions. The dielectric behavior is explained by using the mechanism of polarization process.

Keywords: Powders; Solid state reaction; X-Ray Methods; Ferrite; Electrical Properties.

519. Saturation Properties of Isospin Asymmetric Nuclear Matter

W.M. Seif

Nucl Phys A, 878: 14-36 (2012) IF: 1.54

The saturation properties of the isospin asymmetric nuclear matter, ANM, are studied microscopically using the density dependent M3Y-Paris and M3Y-Reid effective interactions in their CDM3Y-K versions. To do so, two-dimensional expansion of the energy per nucleon of ANM with respect to its density, and isospin asymmetry, I (np), has been used within a suitable density range. Within this framework, the ANM saturation density, energy per nucleon and incompressibility as functions of the isospin asymmetry, I , up to its eighth order are derived in simple analytical formulas.

These formulas link explicitly the ANM saturation properties to the CDM3Y-K density dependence forms through 24 characteristic quantities and coefficients which represent the different order partial derivatives of the energy with respect to I .

The results show that the different terms up to I^8 , but with only 18 characteristic coefficients, are needed to describe reasonably the different ANM saturation properties. Up to four times the saturation density of nuclear matter, some properties such as the energy per nucleon of ANM and pure neutron matter are well expressed by their expansion up to only the quadratic term in I . Based on both Paris and Reid effective interactions and within the symmetric nuclear matter saturation incompressibility range of $K_0 = 220-250$ MeV, the different coefficients of the ANM incompressibility are obtained with the values of $K_0 = 348 \pm 57$ MeV, $K_04 = 35 \pm 31$ MeV and $K_06 = 4 \pm 13$ MeV.

Keywords: Nuclear Equation Of State; Saturation Properties; Incompressibility.

Dept. of Zoology

520. Monocytes Conditioned Media Stimulate Fibronectin Expression and Spreading of Inflammatory Breast Cancer Cells in Three-Dimensional Culture: A Mechanism Mediated by IL-8 Signaling Pathway

Mona M Mohamed

Cell Communication And Signaling, 10:3: 1-13 (2012) IF: 5.5

Inflammatory breast cancer (IBC) is the most aggressive form of breast cancer characterized by invasion of carcinoma cells into dermal lymphatic vessels where they form tumor emboli over expressing adhesion molecule E-cadherin. Although invasion and metastasis are dynamic processes controlled by complex interaction between tumor cells and microenvironment the mechanisms by which soluble mediators may regulate motility and invasion of IBC cells are poorly understood. The present study investigated the effect of media conditioned by human monocytes U937 secreted cytokines, chemokines and growth factors on the expression of adhesion molecules E-cadherin and fibronectin of human IBC cell line SUM149. Furthermore, cytokines signaling pathway involved were also identified. RESULTS: U937 secreted cytokines, chemokines and growth factors were characterized by cytokine antibody array. The major U937 secreted cytokines/chemokines were interleukin-8 (IL-8) and monocyte chemotactic protein-1 (MCP-1/CCL2). When SUM149 cells were seeded in three dimensional (3D) models with media conditioned by U937 secreted cytokines, chemokines and growth factors; results showed: 1) changes in the morphology of IBC cells from epithelial to migratory spindle shape branched like structures; 2) Over-expression of adhesion molecule fibronectin and not E-cadherin. Further analysis revealed that over-expression of fibronectin may be mediated by IL-8 via PI3K/Akt signaling pathway. CONCLUSION: The present results suggested that cytokines secreted by human monocytes may promote chemotactic migration and spreading of IBC cell lines. Results also indicated that IL-8 the major secreted cytokine by U937 cells may play essential role in fibronectin expression by SUM149 cells via interaction with IL-8 specific receptors and stimulation of PI3K/Akt signaling pathway.

Keywords: Fibronectin; E-Cadherin; IL-8; Inflammatory Breast Cancer; Monocytes.

521. Targeting of Syndecan-1 by Microna Mir-10B Promotes Breast Cancer Cell Motility and Invasiveness Via A Rho-Gtpase- and E-Cadherin-Dependent Mechanism

Sherif A. Ibrahim, George W. Yip Christian Stock, Jun-Wei Pan Claudia Neubauer, Michaela Poeter, Danute Pupjalis, Chuay Yeng Koo, Reinhard Kelsch, Roland Schulte, Ursula Rescher, Ludwig Kiesel and Martin Gfötte

Int J Cancer, 131: 884-896 (2012) IF: 5.444

microRNAs are small endogenous noncoding RNAs, which post-transcriptionally regulate gene expression. In breast cancer, overexpression of the transmembrane heparan sulfate proteoglycan syndecan-1, a predicted target of the oncomiR miR-10b, correlates with poor clinical outcome. To investigate the potential functional relationship of miR-10b and syndecan-1,

MDA-MB-231 and MCF-7 breast cancer cells were transiently transfected with pre-miR-10b, syndecan-1 siRNA or control reagents, respectively. Altered cell behavior was monitored by proliferation, migration and invasion chamber assays and time-lapse video microscopy. miR-10b overexpression induced post-transcriptional downregulation of syndecan-1, as demonstrated by quantitative real-time PCR (qPCR), flow cytometry and 3'UTR luciferase assays, resulting in increased cancer cell migration and matrigel invasiveness. Syndecan-1 silencing generated a copy of this phenotype. Adhesion to fibronectin and laminin and basal cell proliferation was increased. Syndecan-1 coimmunoprecipitated with focal adhesion kinase, which showed increased activation upon syndecan-1 depletion. Affymetrix screening and confirmatory qPCR and Western blotting analysis of syndecan-1-deficient cells revealed upregulation of ATF-2, COX-2, cadherin-11, vinculin, actin 2, MYL9, transgelin-1, RhoA/C, matrix metalloproteinase 2 (MMP2) and heparanase and downregulation of AML1/RUNX1, E-cadherin, CLDN1, p21WAF/CIP, cyclin-dependent kinase 6, TLR-4, PAI1/2, Collagen1alpha1, JHDM1D, Mpp4, MMP9, matrilin-2 and ANXA3/A10. Video microscopy demonstrated massively increased Rho kinase-dependent motility of syndecan-1-depleted cells, which displayed increased filopodia formation. We conclude that syndecan-1 is a novel target of the oncomiR miR-10b. Rho-GTPase-dependent modulation of cytoskeletal function and downregulation of E-cadherin expression are identified as relevant effectors of the miR-10b-syndecan-1 axis, which emerges as a promising target for the development of new therapeutic approaches for breast cancer.

Keywords: Syndecans; Heparan Sulfate Proteoglycan; Cd138; Breast Cancer; Cell Motility; Microna; Oncomir; Atf-2; Runx1.

522. Efficacy and Mechanism of Action of Arachidonic Acid in the Treatment of Hamsters – Infected with Schistosoma Mansoni or Schistosoma Haematobium

Abeer M. Ashmawy, Samar S. Azab and Omayma A. Eldahshan

International Journal of Antimicrobial Agents, 8(8): 965-972 (2012) IF: 4.128

The current study addressed the evaluation of the in-vitro cytotoxic activity of *Chorisia Crispiflora* (Bombaceae) different extracts on MCF-7 breast cancer cell line, then in parallel phytochemical and molecular investigations of the most cytotoxic extract. Materials and Methods: The most cytotoxic extract against -7 breast cancer cell line was investigated for its effect on NF-B, p21 and DNA fragmentation. The compounds isolated were identified using different spectroscopic techniques. Results: The most active extract was the ethyl acetate, where it exhibited cytotoxic effect at IC50; 5.2 and 4.2g/ml compared with doxorubicin for 48 & 72 hours. Further investigations on the extract were achieved in parallel for detection of the active principles responsible for that effect and for assessing the molecular mechanisms underlying extract may interfere with several cell signaling pathways. Protocatechuic acid, apigenin 7-rhamnoside, apigenin 7-glucoside, kaempferol 3-rutinoside and apigenin 7-neohesperidoside were isolated and identified through different spectroscopic methods. The anticancer effect on MCF-7 breast cancer cell line was produced as result of down regulation of NF-B and up regulation of p21 levels at time and concentration dependent manner. Conclusions: *Chorisia crispiflora* extract may down regulate NF-B and up regulate p21 levels at time and

concentration dependent manner and also may assume that activated NF-B antagonizes P53 induces P21 function, possibly through the cross-competition for transcriptional coactivators. The phenolics isolated from the extract may responsible for the anticancer effect produced.

Keywords: Schistosoma mansoni; Schistosoma haematobium; Arachidonic acid.

523. Study for the Stability and Corrosion Inhibition of Electrophoretic Deposited Chitosan on Mild Steel Alloy in Acidic Medium

Rasha A. Ahmed, R. A. Farghali and A.M. Fekry

International Journal of Electrochemical Science, 7: 7270-7282 (2012) IF: 3.729

Electrophoretic deposition (EPD) of chitosan (CS) on mild steel substrates was done from a chitosan-acetic acid solution. To increase the protective ability of chitosan coating, the coated samples were immersed in glutaraldehyde solution for 5 minutes. The electrophoretic deposition (EPD) of chitosan on mild steel substrates was investigated by FTIR, scanning electron microscopy, potentiodynamic polarization measurements and electrochemical impedance spectroscopy (EIS). The results of EIS showed that the resistance (Rt) or film stability increases with increasing immersion time in 0.5 M H2SO4 solution indicating a decrease in corrosion rate of the tested alloy with time. EIS measurements under open-circuit conditions confirmed well polarization results. CS showed very good inhibition efficiency (IE) in 0.5 M sulphuric acid solution reaches to 98.1%. The method enabled the formation of adherent, protective and uniform coatings.

Keywords: Chitosan; Eis; Polarization; Sem; Mild Steel.

524. Hepatitis C Virus-Multispecific T-Cell Responses Without Viremia or Seroconversion Among Egyptian Health Care Workers at High Risk of Infection

Sayed F. Abdelwahab, Zainab Zakaria, Maha Sobhy, Eman Rewisha, Mohamed A. Mahmoud, Mahmoud A. Amer, Mariarosaria Del Sorbo, Stefania Capone, Alfredo Nicosia, Antonella Folgori, Mohamed Hashem and Samer S. El-Kamary

Clinical and Vaccine Immunology, 19 (5): 780-786 (2012) IF: 2.546

Hepatitis C virus (HCV)-specific cell-mediated immunity (CMI) has been reported among exposed individuals without viremia or seroconversion. Limited data are available regarding CMI among at-risk, seronegative, aviremic Egyptian health care workers (HCW), where HCV genotype 4 predominates. We investigated CMI responses among HCW at the National Liver Institute, where over 85% of the patients are HCV infected. We quantified HCV-specific CMI in 52 seronegative aviremic Egyptian HCW using a gamma interferon (IFN- γ) enzyme-linked immunospot assay in response to 7 HCV genotype 4a overlapping 15-mer peptide pools covering most of the viral genome. A positive HCV-specific IFN- γ response was detected in 29 of 52 HCW (55.8%), where 21 (40.4%) had a positive response for two to seven HCV pools and 8 (15.4%) responded to only one pool. The average numbers of IFN- γ total spot-forming cells (SFC) per million peripheral blood mononuclear cells (PBMC) (\pm standard

error of the mean [SEM]) in the 29 responding and 23 nonresponding HCW were 842 ± 141 and 64 ± 15 , respectively ($P < 0.001$). Flow cytometry indicated that both CD4(+) and CD4(-) T cells produced IFN- γ . In summary, more than half of Egyptian HCW demonstrated strong HCV multispecific CMI without viremia or seroconversion, suggesting possible clearance of low HCV exposure(s). These data suggest that detecting anti-HCV and viremia to determine past exposure to HCV can lead to an underestimation of the true disease exposure and that CMI response may contribute to the low degree of chronic HCV infection in these HCW. These findings could have strong implications for planning vaccine studies among populations with a high HCV exposure rate. Further studies are needed to determine whether these responses are protective.

Keywords: Hepatitis C Virus; Cell-Mediated Immunity; Flow Cytometry.

525. Evaluation of the Antiepileptic Effect of Curcumin and Nigella Sativa Oil in the Pilocarpine Model of Epilepsy in Comparison with Valproate

Neveen A. Noor, Heba S. Aboul Ezz, Abdel Razik Faraag and Yasser A. Khadrawy .

Epilepsy Behav, 24: 199-206 (2012) IF: 2.335

The present study aimed to investigate the effect of curcumin and Nigella sativa oil (NSO) on amino acid neurotransmitter alterations and the histological changes induced by pilocarpine in the hippocampus and cortex of rats. Epilepsy was induced by i.p. injection of pilocarpine and the animals were left for 22 days to establish spontaneous recurrent seizures.

They were then treated with curcumin, NSO or valproate for 21 days. Pilocarpine induced a significant increase in hippocampal aspartate and a significant decrease in glycine and taurine levels. In the cortex, a significant increase in aspartate, glutamate, GABA, glycine and taurine levels was obtained after pilocarpine injection.

Treatment of pilocarpinized rats with curcumin and valproate ameliorated most of the changes in amino acid concentrations and reduced the histopathological abnormalities induced by pilocarpine. N. sativa oil failed to improve the pilocarpine-induced abnormalities. This may explain the antiepileptic effect of curcumin and suggest its use as an anticonvulsant.

Keywords: Pilocarpine Curcumin Nigella Sativa Oil Valproate Amino Acid Neurotransmitters Histopathology Botanical.

526. Adjuvant Selection for Vaccination Against Murine Schistosomiasis

R. El Ridi and H. Tallima

Scandinavian Journal of Immunology, 76, 552-558 (2012) IF: 2.23

Schistosoma mansoni cercariae penetrate mouse epidermis, detach the glycocalyx and transform into schistosomula, triggering innate immune responses by host keratinocytes and Langerhans cells. Schistosomula leave the dermis and enter blood capillaries, releasing excretory-secretory products (ESP), which induce readily detectable primary adaptive immunity responses, dominated by T helper (Th) 1 and 17 cytokines. Partial protection against murine schistosomiasis may be achieved using subunit antigens and Th1 cytokine-inducing adjuvants.

Conversely, resistance to primary and/or secondary schistosomiasis in rats, mice and humans is associated with production of Th2 cytokines.

Accordingly, we reasoned that effective vaccination against murine primary schistosomiasis might be achieved provided selection of an adjuvant capable of skewing the *S. mansoni* larval ESP-mediated Th1/Th17 immune responses towards a Th2 profile. In an aim to select such an adjuvant, we administered the prototypical Th1 and Th2, respectively C57BL/6 and BALB/c, mice with polyinosinic-polycytidylic acid (Poly I:C), peptidoglycan (PGN), or thymic stromal lymphopoietin (TSLP) before exposure to *S. mansoni* cercariae.

Serum antibody reactivity and ex vivo spleen cells (SC) immune responses to larval ESP, in a recombinant or multiple antigen peptide form, were assessed one week after infection. Injection with Poly I:C failed to increase interleukin (IL)-4 and led to elevated gamma interferon (IFN- γ) levels released by unstimulated or ESP-stimulated SC. Treatment with PGN triggered heightened amounts of IL-4, IL-17 and IFN- γ released by unstimulated or ESP-stimulated C57BL/6 SC. In contrast, TSLP succeeded in directing the ESP-mediated immune responses towards a Th2-biased profile in prototypical Th1 and Th2 mice.

Keywords: Schistosoma Mansoni; Adjuvants; Type 2 Cytokines.

527. First Record of *Lecithochirium Grandiporum* (Digenea: Hemiuridae) Infecting the Lizard Fish *Saurida Tumbil* From the Red Sea

Kareem Morsy, Abdel-Rahman Bashtar, Fathy Abdel-Ghaffar and Wesam Baksh

Parasitol Res, 111: 2339-2344 (2012) IF: 2.149

The present study was the first investigation of digenetic trematode parasites of *Saurida tumbil*, a commercially important fish species of the Red Sea, during the period from January to December 2011. Thirty-nine out of 103 (37.8 %) of the examined fish were found to harbor the digenetic trematode *Lecithochirium grandiporum* (family: Hemiuridae) infecting the pyloric portion of stomach and middle part of intestines of the lizard fish. The morphology and morphometric characterizations of this digenetic trematode were described by light and scanning electron microscopy. The parasite possessed a body which was elongated and rounded anteriorly, but truncated posteriorly and its body measured 1.63 ± 0.20 ($1.2-1.93$) mm (invaginated ecsoma), 2.11 ± 0.20 ($1.83-2.35$) mm (evaginated ecsoma) in length with a maximum width of 0.4 ± 0.02 ($0.31-0.52$) mm at ovarian level. They were characterized by a subterminal oral sucker which measured 0.15 ± 0.02 ($0.12-0.18$) mm in diameter and was smaller than the ventral sucker which was circular and large with a wide aperture, hence the specific name *grandiporum*. A multilobated digitiform vitellarium which was a distinctive feature for this species was also observed. The number of parasite per fish was one to six. Prevalence and intensity of infection were positively correlated with host size (increasing with host size increasing). Host sex does not seem to affect the prevalence of infection. The present study was considered as a first record from the Red Sea in Egypt.

Keywords: *Lecithochirium grandiporum*; Digenea; Hemiuridae; *Saurida tumbil*; Red sea

528. A New Species of the Genus *Heterobothrium* (Monogenea: Diclidophoridae) Parasitizing the Gills of Tiger Puffer Fish *Tetraodon Lineatus* (Tetraodontidae) A Light and Scanning Electron Microscopic Study

Kareem Morsy, Hoda Saady, Fathy Abdel-Ghaffar, Abdel-Rahman Bashtar, Heinz Mehlhorn, Saleh Al Quraishy and Asmaa Adel

Parasitol Res, 110: 1119-1124 (2012) IF: 2.149

In the present study, the morphology and morphometric characterization of *Heterobothrium lineatus*, a monogenean gill parasite infecting the gills and wall of the bronchial cavity of the tiger pufferfish *Tetraodon lineatus*, were described by means of light and scanning electron microscopy for the first time from the River Nile at Qena Governorate, South Valley, Egypt.

In wet mount preparation, the adult worms exhibited an elongated body with anterior pointed and posterior broad ends. The adult worm measured $1.15-1.76$ mm (1.53 ± 0.2) in length and $0.30-0.42$ mm (0.35 ± 0.02) in width. Light and scanning electron microscopic observations showed the presence of two buccal organs situated anteriorly around the mouth opening.

The opisthohaptor was subdivided into four pairs of clamps but had no isthmus separating it from the body proper. The present *Heterobothrium* species differs from all other described species in the genus, by its lower dimensions of the worm measurements and the presence of a copulatory organ armed with 12-15 genital hooks.

Furthermore, it is easily distinguished from *Heterobothrium tetradonis* and *Heterobothrium okamotoi* by the absence of a distinct isthmus and resembles *Heterobothrium lamothei* described from the gills of *Sphoeroides testodineus* in Mexico in its general appearance and the presence of rectangular haptor with the fourth pair of clamps smaller than the previous ones.

Keywords: *Heterobothrium*; Monogenea; *Tetraodon Lineatus*; Light And Scanning Electron Microscopy.

529. First Record of Anisakid Juveniles (Nematoda) in the European Seabass *Dicentrarchus Labrax* (Family: Moronidae) and their Role as Bio-Indicators of Heavy Metal Pollution

Kareem Morsy, Abdel-Rahman Bashtar, Fathy Abdel-Ghaffar, Heinz Mehlhorn, Saleh Al Quraishy, Magda El-Mahdi, Ali Al-Ghamdi and Nesma Mostafa

Parasitol Res, 110: 1131-1138 (2012) IF: 2.149

This study assessed the anisakid nematode distribution pattern in the fish collected from coasts of Mediterranean Sea, Egypt, during the period September 2010-April 2011.

Two hundred thirty out of 300 (76.7%) *Dicentrarchus labrax* (European seabass) marine fishes belonging to family Moronidae were dissected and found to be infected with larva three nematodes. The larvae had been studied by light and scanning electron microscopy.

The present work represents the first record of the presence of the parasite in this fish in the Mediterranean Sea. The concentrations of some heavy metals (Pb, Zn, Fe, Cd, Cu, Mn, Ni) in parasites as well as in tissues of fish were measured. The presented results showed that the nematode parasites are able to accumulate heavy metals in their tissues and in some cases that they are able to

accumulate large amounts of heavy metals in a higher amount than host tissues. This demonstrated their sustainability as bioindicators of environmental pollution by removing heavy metals and help in the survival of fish.

Keywords: Anisakids; Nematoda; Dicentrarchus Labrax; Heavy Metal Pollution; Light And Scanning Electron Microscopy.

530. Ultrastructure and Molecular Phylogenetic of A New Isolate of *Pleistophora pagri* Sp. Nov. (Microsporidia, Pleistophoridae) from *Pagrus pagrus* in Egypt

Kareem Morsy, Fathy Abdel-Ghaffar, Heinz Mehlhorn, Abdel-Rahman Bashtar and Rewaida Abdel-Gaber

Parasitol Res, 111: 1587-1597 (2012) IF: 2.149

The spore morphology and molecular systematic of a new microsporidian which was isolated from the common sea bream *Pagrus pagrus* (F: Sparidae Linnaeus, 1758) from the Red Sea, Egypt have been studied. Fifty-six out of 300 (18.7 %) of this fish were infected with microsporidian parasites.

The infection was appeared as whitish, ellipsoid, round, or elongated nodules embedded in the epithelial lining of the peritoneum and also in the intestinal epithelium. Light microscopic study revealed that nodules were encapsulated by a fibrous layer encircling numerous mature spores measuring 1.7 ± 0.6 ($1.5-2.7$) \times 1.5 ± 0.3 ($1.2-1.8$) μ m in size. Ultrastructure of spores was characteristic for the genus *Pleistophora*: dimorphic, uninucleate spores (each spore possesses three to five polar filament coils) and a posterior vacuole.

Also, the early recognizable stages of the parasite within nodules include uninucleated, binucleated and multinucleated meronts followed by detachment of the plasmalemma of the sporont producing sporoblasts which mature to spores that consist of a spore coat and spore contents.

Also, we analyzed the small subunit ribosomal gene (SSUrDNA) using PCR and sequencing specimens from the marine populations of *P. pagrus* fish from the Red Sea. From blast searches, sequence analysis and phylogenetic analysis, we did not find corresponding GenBank entries to our species. Comparison of the nucleotide sequences showed that the sequence of our microsporidium was most similar to five *Pleistophora* species with degrees of identity (>91.5 %).

It was most similar (97.8 % identity) to that of *Pleistophora hypessobryconis* (account no. GU126672) differing in 19 nucleotide positions and with lower divergence value, *Pleistophora ovariae* (96.2 % identity, account no. AJ252955), *Pleistophora hippoglossoides* (91.9 % identity, account no. AJ252953), *Pleistophora mulleri* (91.9 % identity, account no. EF119339) and *Pleistophora typicalis* (91.9 % identity, account no. AJ252956). So, they likely represent new species named *Pleistophora pagri* sp. n. with accession number JF797622 and a GC content of 53 %.

Keywords: *Pleistophora pagri* Sp. Nov.; Microsporidia; *Pagrus pagrus*; Phylogeny.

531. *Sarcocystis Acanthocolubri* Sp. N. Infecting three Lizard Species of the Genus *Acanthodactylus* and the Problem of Host Specificity. Light and Electron Microscopic Study

Kareem Morsy, Abdel-Rahman Bashtar, Fathy Abdel-Ghaffar, Heinz Mehlhorn, Saleh Al Quraishy, Ali Al-Ghamdi, Eglal Koura and Sherein Maher

Parasitol Res, 110: 355-362 (2012) IF: 2.149

In the present investigation, macroscopic sarcocysts of *Sarcocystis acanthocolubri* were observed in muscles of 42 (4.3%) out of 975 *Acanthodactylus* sp. lizards collected from different geographical areas in Egypt. The infection rate was 6.4% in *Acanthodactylus boskianus*, 2.1% in *Acanthodactylus sculentus* and 5% in *Acanthodactylus paradalis*. The highest infection rate was recorded in the lizards captured from Baltem (10% in *A. boskianus* and 8% in *A. paradalis*). The infection rate was usually higher in females (7.4%) than in males (3.8%). Moreover, the highest infection rate was recorded in summer (7.53%), autumn (3.57%) and spring (3.11%) and the lowest was recorded in winter (0.91%). Also, old animals had higher infection rates (10.8%) than young ones (0–2.7%). Macrocytes measured 0.95×10.12 μ m. Both macroscopic and microscopic sarcocysts were enclosed only by a primary cyst wall, which had many finger-like, stalkless and nonbranched protrusions giving it a striated appearance. The primary cyst wall measured 3.9 μ m. A dark granulated ground substance was found directly underneath the protrusions and is extended interiorly dividing the cyst cavity into many compartments containing the parasites (metrocytes and merozoites). Metrocytes were found directly under the ground substance and usually multiply asexually by endodyogeny producing two merozoites from each metrocyte. Both metrocytes and merozoites had the apical complex structures characteristic to the genus *Sarcocystis*. Transmission experiments with three snake species indicated that the snake *Spalerosophis diadema* is the proper final host belonging to the family Colubridae. The prepatent period was 16 days, while the patent period was 35 days. The results obtained from the present investigation revealed that this is a new species which was named *Sarcocystis acanthocolubri*.

Keywords: *Sarcocystis Acanthocolubri*; *Acanthodactylus*; *Spalerosophis Diadema*; Light and Electron Microscopic Study.

532. Effects of A Neem Seed Extract (Mitestop®) on Mallophages (Featherlings) of Chicken: in Vivo and in Vitro Studies

Saleh Al-Quraishy, Fathy Abdel-Ghaffar, Khaled A. S. Al-Rasheid, Julia Mehlhorn and Heinz Mehlhorn

Parasitol Res, 110: 617-622 (2012) IF: 2.149

Mallophages of birds (featherlings) are mostly very tiny and can even as adults better be recognized by their movements than by their elongate body shape when using just the naked eye. Since some species (e.g., the “shaft louse” *Menopon gallinae*, the elongate feather louse *Lipeurus caponis*, or *Columbicola* sp.) may pierce the pulp of feathers or the skin by their biting or scratching mandibles and thus lick the excreted blood, they may be extremely dangerous especially to young birds, even if they only feed by nibbling along the feather surface and/or eat epidermal debris. The present paper reports on the successful treatment of

different races of fowls being severely infested with both above cited species. This in vivo treatment was done either by a short dipping of the whole fowl into the 1:33 dilution (with tap water) of a neem seed extract (MiteStop®) or by spraying them with the freshly diluted product. It was seen that the dead mallophages dropped down from the feathers as soon as they were dry again. As a precaution, a second treatment was done by some owners 1 week after the first one in order to eliminate all stages, which eventually might have hatched from untouched nits during the time interval between the two treatments. When controlling the treated fowls 4 weeks after their treatment, in no case (treated once or twice), living motile stages were diagnosed indicating the high efficacy of this nontoxic neem seed extract. When treating in vitro cutoff feathers contaminated with *L. caponis*, it was seen under the stereomicroscope, that the mallophages tried to run away from the 1:33 water-diluted active compound indicating that there is also a repellent effect. Treated *L. caponis* stopped leg movements within 3 min and died on their feathers within 1–20 min. Then, the last slight trembling movements of their legs and convulsions of their intestine stopped finally.

Keywords: Neem Seed; Mitestop; Mallophages; Chicken.

533. Morphological and Molecular Biological Characterization of *Pleistophora Aegyptiaca* Sp. Nov. Infecting the Red Sea Fish *Saurida Tumbil*

Fathy Abdel-Ghaffar, Abdel-Rahman Bashtar, Kareem Morsy, Heinz Mehlhorn, Saleh Al Quraishy, Khaled AL-Rasheid and Rewaida Abdel-Gaber

Parasitol Res, 110: 741-752 (2012) IF: 2.149

One hundred three out of 225 (45.8%) of the Red Sea fish *Saurida tumbil* were infected with microsporidian parasites. The infection was recorded as tumor-like masses (whitish macroscopic cysts) or xenomas often up to 2 cm in diameter and embedded in the peritoneal cavity. Generally, the infection was increased during winter 63.8% (86 out of 135) and fall to 18.9% (17 out of 90) in summer.

Light microscopic study revealed that xenomas were encapsulated by a fibrous layer encircling numerous sporophorous vesicles filled with mature spores measuring 1.7 ± 0.6 ($1.5-2.7$) \times 1.5 ± 0.3 ($1.2-1.8$) μ m in size. Ultrastructural microscopic study showed the presence of smooth membranes of the sarcoplasmic reticulum forming a thick, amorphous coat surrounding various developmental stages of the parasite. The various recognizable stages of the parasite were uninuclear, binucleated and multinucleated meronts followed by detachment of the plasmalemma of the sporont from the sporophorous vesicle producing sporoblasts. Mature spores consist of a spore coat and spore contents.

The spore contents consist of the uninucleated sporoplasm and a posterior vacuole located at the posterior end. The polar tube consists of a straight shaft and a coiled region (26–32 coils) arranged in many rows along the inside periphery of the spore. The polaroplast consisted of an anterior region of closely and loosely packed membranes. Molecular analysis based on the small subunit rDNA gene was performed to determine the phylogenetic position of the present species.

The percentage identity between this species and a range of other microsporidia predominantly from aquatic hosts demonstrated a high degree of similarity (>92%) with eight *Pleistophora* species. Comparison of the nucleotide sequences and divergence showed that the sequence of the present microsporidium was most similar

to that of *Pleistophora anguillarum* (99.8% identity) differing in 13 nucleotide positions. So, the present species was recorded and phylogenetically positioned as a new species of *Pleistophora*.

Keywords: *Pleistophora Aegyptiaca* Sp. Nov.; *Saurida Tumbil*; Small Subunit Rdna; Light and Scanning Electron Microscopy.

534. Biting and Bloodsucking Lice of Dogs treatment by Means of A Neem Seed Extract (Mitestop, Wash Away Dog)

Heinz Mehlhorn, Volker Walldorf, Fathy Abdel-Ghaffar, Saleh Al-Quraishy, Khaled A. S. Al-Rasheid and Julia Mehlhorn

Parasitol Res, 110: 769-773 (2012) IF: 2.149

Dogs infested with lice belonging either to the group of Mallophaga (hairlings, i.e., *Trichodectes canis*) or Anoplura (bloodsucking lice, e.g., *Linognathus setosus*) were washed with the neem seed preparations MiteStop® or Wash Away Dog. It was found that a single treatment with one of these products killed both motile stages and those developing inside eggs (nits) being glued at the hair. In both cases the product had been left for 20 min onto the hair before it was washed away just with normal tap water.

Keywords: Lice; Neem Seed; Mitestop; Wash Away.

535. Observations on Effects of A Neem Seed Extract (Mitestop®) on Biting Lice (Mallophages) and Bloodsucking Insects Parasitizing Horses

Saleh Al-Quraishy, Fathy Abdel-Ghaffar, Khaled A. S. Al-Rasheid, Julia Mehlhorn and Heinz Mehlhorn

Parasitol Res, 110: 335-339 (2012) IF: 2.149

The hair of 300 horses belonging to short hair and long hair races had been routinely treated during the last 3 years with a neem seed extract (MiteStop®) in order to kill mallophages (e.g., specimens of the genus *Werneckiella*). It was found that in all cases, a hidden infestation with these biting lice had existed, which became visible when the product (diluted 1:20 with tap water) was brushed onto the hair. The mallophages left the body surface and became visible as a fine “wooly looking” layer at the tips of the hair. Furthermore, this treatment stopped the forming of dandruff of the skin of the horses, which, in case of heavy mallophage infestations, had looked like being powdered. Another interesting result of the treatment was reported by the riders. They described that the product had a considerable repellent effect on bloodsucking tabanids, mosquitoes, ceratopogonids, simuliids, as well as on licking flies. This repellency effect was noted to last for up to 7 days if the horses were not washed.

Keywords: Neem Seed Extract; Mitestop; Mallophages; Horses.

536. Research and Increase of Expertise in Arachnology and Entomology Are Urgently Needed

Heinz Mehlhorn, Khaled A. S. Al-Rasheid, Saleh Al-Quraishy and Fathy Abdel-Ghaffar

Parasitol Res, 110: 259-265 (2012) IF: 2.149

Considering the contents of international journals of parasitology dealing with broader topics inside this field show that rather a few

papers appear with studies in the discipline of arachno-entomology. In the journals Journal of Parasitology, Parasitology Research and Trends in Parasitology, the relations of published papers on protozoology, helminthology and arachno-entomology showed that in all three journals, papers on protozoans were the most common, while those on helminths of any kind reached the second place being rather as common as the protozoan papers in Parasitology Research and in the Journal of Parasitology. In Trends of Parasitology, however, the papers on helminths reached only about 25% of the numbers published on protozoan topics. But in all three journals—and this is important—the papers on arachnoentomological themes were scarce reaching less than the half of the protozoan papers in Parasitology Research and only about 15% in the Journal of Parasitology and in the Trends of Parasitology. These disproportions between the three great subdivisions of targets in the focus of parasitological research are dangerous, since this lack exists already for several decades and thus led to a backlog of unsolved increasing problems that are caused by ticks, mites, insects and/or parasitic crustaceans especially in times of intensive globalization and global warming. Studies on the biology, vectorship, invasion and spreading of wanted vectors and on the control of pests and parasites belonging to the field of arachno-entomology are urgently needed.

Keywords: Arachnoentomology; Parasitology Research; Control of Pests.

537. Treatment with A Neem Seed Extract (Mitestop®) of Beetle Larvae Parasitizing the Plumage of Poultry

Volker Walldorf, Heinz Mehlhorn, Saleh Al-Quraishy, Khaled A. S. Al-Rasheid, Fathy Abdel-Ghaffar and Julia Mehlhorn

Parasitol Res, 110: 623-627 (2012) IF: 2.149

Beetles of the species *Alphitobius diaperinus*, *Dermestes bicolor* and *Dermestes lardarius* may transmit severe agents of diseases on poultry and may in addition harm as larvae the skin and feathers thus leading to severe economic losses. The present study deals with a control measurement using a neem seed extract (MiteStop®) being diluted with tap water. It was shown that spraying of a 1:33 dilution kills both larvae and adults of these part-time parasites as was previously shown for other parasites such as mites, ticks and blood sucking or biting insects.

Keywords: *Alphitobius Diaperinus*; Neem Seed Extract; Beetle Larvae.

538. Efficacy of A Single Treatment of Head Lice with A Neem Seed Extract: An in Vivo and in Vitro Study on Nits and Motile Stages

Fathy Abdel-Ghaffar, Saleh Al-Quraishy, Khaled A. S. Al-Rasheid and Heinz Mehlhorn

Parasitol Res, 110: 227-280 (2012) IF: 2.149

An anti-lice shampoo (Licener®) based on a neem seed extract was tested in vivo and in vitro on its efficacy to eliminate head louse infestation by a single treatment.

The hair of 12 children being selected from a larger group due to their intense infestation with head lice were incubated for 10 min with the neem seed extract containing shampoo. It was found that after this short exposition period, none of the lice had survived,

when being observed for 22 h. In all cases, more than 50–70 dead lice had been combed down from each head after the shampoo had been washed out with normal tap water.

A second group of eight children had been treated for 20 min with identical results. Intense combing of the volunteers 7 days after the treatment did not result in the finding of any motile louse neither in the 10-min treated group nor in the group the hair of which had been treated for 20 min.

Other living head lice were in vitro incubated within the undiluted product (being placed inside little baskets the floor of which consisted of a fine net of gauze). It was seen that a total submersion for only 3 min prior to washing 3× for 2 min with tap water was sufficient to kill all motile stages (larvae and adults). The incubation of nits at 30°C into the undiluted product for 3, 10 and 20 min did not show differences.

In all cases, there was no eyespot development or hatching larvae within 7–10 days of observation. This and the fact that the hair of treated children (even in the short-time treated group of only 10 min) did not reveal freshly hatched larval stages of lice indicate that there is an ovicidal activity of the product, too.

Keywords: Head Lice; Neem Seed Extract; In Vivo And In Vitro Study.

539. Why is it Crucial to Test Anti-Lice Repellents

Margit Semmler, Fathy Abdel-Ghaffar, Saleh Al-Quraishy, Khaled A. S. Al-Rasheid and Heinz Mehlhorn

Parasitol Res, 110: 273-276 (2012) IF: 2.149

It is difficult to stop lice propagation just by treating infested heads, since reinfections are possible just a few hours after a successful elimination of all lice from a child's head by application of an active anti-lice product. Therefore, several products have been developed that claim to have a louse repellent activity; however, definite proofs are scarce. The present study involving two louse repellents (Linicin® Preventive Spray, Picksan® NoLice) and three substances (at 10% dilution) known for their general repellency activity shows that there are much more difficulties to repel lice when compared to other insects or even ticks. Thus, it must be feared that several repellents on the market might have used a problematical test system and thus might not be as effective as they claim.

Keywords: Lice; Anti Louse; Linicin.

540. The Effects of Flumethrin (Bayticol® Pour-On) on European Ticks Exposed to Treated Hairs of Cattle and Sheep

Heinz Mehlhorn, Brbel Schumacher, Antje Jatzlau, Fathy Abdel-Ghaffar, Khaled A. S. Al-Rasheid and Chandra Bhushan

Parasitol Res, 110: 2181-2186 (2012) IF: 2.149

Tick infestations in cattle and sheep pose serious health problems when agents of diseases are transmitted. In addition, blood feeding of ticks induces enormous economic losses due to reduced weight gain of infested animals. The present study was designed to investigate the effects of exposure to hairs clipped from cattle and sheep treated with flumethrin (Bayticol®) on European ticks. The dose used was 10 ml/100 kg body weight for both animal species. At intervals of 7 days (days 7, 14, 21, 28 and 35), hairs were cut off from treated and untreated animals along the backline and from the feet just above the claws. These hairs

were mingled with stages of the tick species *Ixodes ricinus*, *Dermacentor reticulatus* and *Rhipicephalus sanguineus*. It was found that in the cases of *I. ricinus* and *D. reticulatus*, all specimens died within 5–12 h when coming into contact with cattle hair from the feet or back of animals treated 3 weeks ago and within 6 to 9 h after contact to sheep hair from back or feet. After 4 weeks, the specimens of both tick species that had contact with hair of treated sheep and cattle, independent from the origin backline or feet, were dead after 8 h except for one tick that had contact to hair from feet of cattle. It remained fully motile after a 12-h contact even for the observation time on another 5 days. When having contact to hair of animals treated 5 weeks before, several specimens of *Ixodes* and *Dermacentor* survived an exposition of 12 h. There were more survivors in the case of ticks tested on hair of the feet than in the case of contacts with hair of the backline. The exposure of *R. sanguineus* to hair obtained from animals treated 2 weeks earlier resulted in death in 2–4 h. However, most *R. sanguineus* ticks when coming in contact with treated hairs (collected from animals treated 3, 4 or 5 weeks earlier) from back or feet survived for at least 5 days even after exposure for 12 h. These experiments confirmed the positive protection results obtained in former studies with typical cattle ticks in the tropics and/or subtropics. In addition to the killing effects described above, it was noted that flumethrin had a significant repellent effect. If ticks were mingled with treated hair, they tried to flee away and did not seek shelter inside the hair as the controls did in untreated hair.

Keywords: Flumethrin- Ticks; *Ixodes Ricinus*; *Dermacentor Reticulatus*.

541. Morphology and Small Subunit Ribosomal Dna Sequence of *Henneguya* Suprabranchiae (Myxozoa), A Parasite of the Catfish *Clarias Gariepinus* (Clariidae) from the River Nile, Egypt

Kareem Morsy, Fathy Abdel-Ghaffar, Abdel-Rahman Bashtar, Heinz Mehlhorn, Saleh Al Quraishy and Rewaida Abdel-Gaber

Parasitol Res, 111: 1423-1435 (2012) IF: 2.149

Forty-three out of 120 (35.8 %) *Clarias gariepinus* fish were found to be naturally infected with *Henneguya* suprabranchiae. The infection appeared as clusters of ovoid to ellipsoidal plasmodia being embedded within the hyaline cartilage of the suprabranchial organ of the fish. Histological studies indicate tissue distortion at the sites of infection.

The continuous growth of the plasmodium led to deformation of the filament structure as well as disorganization and displacement of the gill lamellae. Also, a severe atrophy occurred in the hyaline cartilage of the gills and also in the gill lamellae. Based on the structure and measurements of fresh spores by light microscopy, this parasite was identified as *H. suprabranchiae*. Spores are oval in shape and they measure $13 (11-14) \times 3 (2-5) \mu\text{m}$ length by width. It has two polar capsules inside, each measures $3 (2.5-5) \times 1 (1.5-4) \mu\text{m}$ length by width. Each polar capsule has a spirally coiled (7–9 turns) polar filament.

The ultrastructural analysis showed that the plasmodia were surrounded by single-unit membrane. The generative cells and the early developmental stages were arranged at the periphery of the plasmodia, while immature and mature spores were centrally arranged.

The developmental stages characterizing sporogenesis, capsulogenesis and valvogenesis of the present parasite were

ultrastructurally studied. The small subunit 18 S rDNA (SSU rDNA) gene sequences from different isolates was sequenced and compared with the sequence of the same gene from the *Henneguya* sp. isolated from GenBank.

The phylogenetic position of the present *Henneguya* sp. within the genus was determined using sequence analysis of all related taxa available in GenBank and the phylogenetic tree derived from this study is elucidated and compared with the current taxonomy of the available myxosporeans. Comparison of the nucleotide sequences and divergence showed that the SSU rDNA gene of this *Henneguya* species revealed 92.2 % sequence identity with *Henneguya exilis* (acc. no. AF021881) differing in 30 nucleotides with lower divergence value.

Keywords: *Henneguya* Suprabranchiae; Myxozoa; *Clarias Gariepinus*; Small Subunit Ribosomal Dna.

542. First Report of *Kudoa* Species (Myxozoa: Kudoidae) Infecting the Spotted Coral Grouper *Plectropomus Maculates* from the Red Sea. A Light and Ultrastructural Study

Fathy Abdel-Ghaffar, Kareem Morsy, Heinz Mehlhorn, Abdel-Rahman Bashtar, Mohamed Abdallah Shazly, Abdel-Hakem Saad and Rewaida Abdel-Gaber

Parasitology Research, 111: 1579-1585 (2012) IF: 2.14

In the present study, out of 200, 120 (60 %) *Plectropomus maculates* fish were found to be naturally infected with *Kudoa* sp. The infection was intensive and appeared as clusters of ovoid to ellipsoidal plasmodia being restricted to the cardiac muscles. More than 100 plasmodia were counted per infected heart and measured $1.53 \pm 0.2 (1.2-2.5) \times 0.65 \pm 0.2 (0.63-0.80) \text{mm}$. On the basis of spore morphology, the parasite was identified as *Kudoa* sp. The spore measures $4.8 \pm 0.3 (4.7-6.8) \times 4.0 \pm 0.3 (4.6-6.5) \mu\text{m}$. The four polar capsules were pyriform in shape measuring $1.4 \pm 0.2 (1.3-3.5) \times 1.2 \pm 0.2 (1.1-2.2) \mu\text{m}$. Transmission electron microscopy showed that the plasmodia were bordered by a single membrane which invaginates into pinocytotic canals. Adjacent to the plasmodial wall, the generative cells and the early pansporoblasts were located peripherally. The developmental stages characterizing sporogenesis, capsulogenesis and valvogenesis of the present parasites were ultrastructurally studied.

Keywords: *Kudoa*; Myxozoa; A Light And Ultrastructural Study.

543. Influence of Atrazine and Roundup Pesticides on Biochemical and Molecular Aspects of *Biomphalaria Alexandrina* Snails

Fayez A. Barky, Hala A. Abdelsalam, Momeana, Mahmoud and Salwa A.H. Hamdi

Pestic Biochem Phys, 104: 9-18 (2012) IF: 1.713

The excessive use of pesticides in agriculture has sparked the interest of scientists in investigating the harmful effects of these compounds. The present study evaluates the pesticides Atrazine and Roundup (glyphosate) on biochemical and molecular aspects of *Biomphalaria alexandrina* snails. The results showed that LC10 of these two pesticides caused considerable reduction in survival rates and egg production of treated snails. Additionally, Atrazine proved to be more toxic to *B. alexandrina* snails than Roundup. Intreated snails, glucose concentration (GL) in the hemolymph as well as lactate (LT) and free amino acid (FAA) in soft tissues of

treated snails increased while glycogen (GN), pyruvate (PV), total protein (TP), nucleic acids (DNA and RNA) levels in snail's tissues decreased.

The activities of glycogen phosphorylase (GP), superoxide dismutase (SOD), catalase (CAT) and glutathione reductase (GR), succinic dehydrogenase (SDH), acetylcholinesterase (AChE), lactic dehydrogenase (LDH) and phosphatases (ACP and ALP) enzymes in homogenate of snail's tissues were reduced in response to the treatment with the two pesticides while lipid peroxide (LP) and transaminases (GOT and GPT) activity increased ($P < 0.001$).

The changes in the number, position and intensity of DNA bands induced by pesticides may be attributed to the fact that pesticide can induce genotoxicity through DNA damage. It was concluded that the pollution of the aquatic environment by Atrazine and Roundup pesticides, would adversely affect the metabolism of the B. alexandrina snails and have adverse effects on its reproduction.

Keywords: Biomphalaria Alexandrina; Atrazine; Roundup; Some Enzymatic Activities; Biochemical and Molecular Aspects.

544. Lethality, Accumulation and Toxicokinetics of Aluminum in Some Tissues of Male Albino Rats

Sayed M. Rawy, Gamal M. Morsy and Majda M Elshibani

Toxicology And Industrial Health, (s): 2-10 (2012) IF: 1.423

In the present work, the lethality percentiles including median lethal doses (LD₅₀), accumulation, distribution and toxicokinetics of aluminum in the liver, kidney, intestine, brain and serum of male albino rats, following a single oral administration were studied throughout 1, 3, 7, 14 and 28 days. The estimated LD₅₀ at 24 h was 3.45 g Al/kg body weight (b. wt.).

The utilized dose of Al was 1/50 LD₅₀ (0.07 g Al/kg b. wt.). Aluminum residues, in Al-treated rats, were significantly decreased in response to the experimental periods and were negatively correlated with time. In addition, the hepatic, renal, intestinal, brain and serum Al contents were significantly higher than the corresponding controls at all experimental periods, except the brain that showed significant depletion when compared with its corresponding control after 28 days. Kinetically, the highest average of Al area under concentration-time curves (AUC_{total}, g/g day) and area under moment concentration-time curves (AUMC_{total}, g/g day²) recorded in the brain followed by kidney, serum, intestine and liver.

The longest elimination half-life time (t_{1/2}, day) and the mean residence time (MRT, day) were recorded in the brain followed by the liver, kidney, serum and intestine. On the other hand, the slowest clearance rates (Cl_s, L/day) of Al, in order, were recorded in brain, kidney, serum, intestine and the liver.

The elimination rate constant (L_z, day⁻¹) of Al from the brain was less than that in the intestine and serum was less than that in the liver and kidney.

The computed maximum concentrations (C_{max}) of Al in the intestine > kidney > serum > brain > liver were recorded after 3, 3.8, 2.2, 5.4 and 3.8 days, respectively. The computed starting concentration (C₀, g) of Al in serum was higher than its level in the intestine followed by the brain, kidney and liver.

Keywords: Lethality Percentiles; Accumulation; Toxicokinetics; Aluminum; Rats; Elimination Half-Life Time; Total Clearance; Mean Residence Time.

545. Genotoxic Evaluation for the Tricyclic Antidepressant Drug, Amitriptyline

Mohamed S. Hassanane, Naglaa Hafiz, Walaah Radwan and Akmal A. El-Ghor

Drug Chem Toxicol, 35 (4): 450-455 (2012) IF: 1.082

Tryptizol® [amitriptyline HCl (AT); El-Kahira Pharmacological and Chemical Co., Cairo, Egypt], a widely used antidepressant drug in Egypt, was evaluated for its genotoxicity. The evaluation was performed in somatic (bone marrow) and germ (spermatocytes) cells, as well as the sperm morphology (i.e., head and tail) and count of the resulting sperm. Three doses were tested (low, medium and high); they were chosen according to the drug manufacturer. The low-dose group received orally 1 mg/kg body weight (b.w.) daily for a total period of 1 month; the medium-dose group received 1 mg/kg b.w. daily for 15 days and 2 mg/kg b.w. daily for another 15 days; and the high-dose group received 1 mg/kg b.w. daily for 10 days, then 2 mg/kg b.w. daily for another 10 days and, finally, 4 mg/kg b.w. daily for 10 more days. The results showed that AT treatment induced structural and numerical chromosome abnormalities in somatic cells (bone marrow) and germ cells (spermatocytes). Moreover, AT significantly reduced both the mitotic index and meiotic activity after the different treatments used. AT was found to increase significantly the incidence of sperm-cell head and tail abnormalities. The sperm-cell count was also significantly decreased with the 3 doses tested. In general, results of chromosome abnormalities in both somatic and germ cells as well as sperm morphology and count showed that the effect of AT was dose dependent. The results of the current study showed that AT is a genotoxic agent for both somatic and germ cells and should be taken under special precautions and medical supervision.

Keywords: Genotoxic; Antidepressant; Amitriptyline.

546. Fasciola Gigantica Fatty Acid Binding Protein (Fabp) As A Prophylactic Agent Against Schistosoma Mansoni Infection in Cd1 Mice

Ibrahim Rabia Aly, M. Diab, A. M. El-Amir, M. Hendawy and S. Kadry

Korean J Parasitol, 50 (1): 37-43 (2012) IF: 1.042

Although schistosomicidal drugs and other control measures exist, the advent of an efficacious vaccine remains the most potentially powerful means for controlling this disease. In this study, native fatty acid binding protein (FABP) from *Fasciola gigantica* was purified from the adult worm's crude extract by saturation with ammonium sulphate followed by separation on DEAE-Sephadex A-50 anion exchange chromatography and gel filtration using Sephacryl HR-100, respectively. CD1 mice were immunized with the purified, native *F. gigantica* FABP in Freund's adjuvant and challenged subcutaneously with 120 *Schistosoma mansoni* cercariae. Immunization of CD1 mice with *F. gigantica* FABP has induced heterologous protection against *S. mansoni*, evidenced by the significant reduction in mean worm burden (72.3%), liver and intestinal egg counts (81.3% and 80.8%, respectively) and hepatic granuloma counts (42%). Also, it elicited mixed IgG1/IgG2b immune responses with predominant IgG1 isotype, suggesting that native *F. gigantica* FABP is mediated by a mixed Th1/Th2 response. However, it failed to induce any significant differences in the oogram pattern

or in the mean granuloma diameter. This indicated that native *F. gigantica* FABP could be a promising vaccine candidate against *S. mansoni* infection.

Keywords: Schistosoma Mansoni; Fasciola Gigantica; Fabp; Heterologous Protection; Th1/Th2 Immunity.

547. Hazardous Effects of Acrylamide on Immature Male and Female Rats

Sayed M. Raw, Mohamed-Assem. S. Marie, Sohair R. Fahmy and Salma A. El-Abied

African Journal of Pharmacy and Pharmacology, 6 (18): 1367-1386 (2012) IF: 0.839

Acrylamide (ACR) is an industrial chemical which induces neurotoxic effects in experimental animals and humans. The present study was carried out to investigate the hematological, biochemical, neurological and histopathological effects of ACR on immature male and female rats. Animals were divided into 2 main groups; immature male group and immature female group and all rats were treated for 28 consecutive days. Each main group subsequently was divided into 2 subgroups: (I) Untreated control group that received a daily oral administration of distilled water and (II) ACR treated rats which received a daily oral administration of ACR (15 mg/kg/body weight). The results obtained indicate that ACR administration induced some behavioral disorders in the movement of immature male and female rats as well as loss of body weight. ACR induced a significant decrease in hemoglobin (Hb), erythrocytes (RBCS), hematocrit (HCT) and lymphocyte levels of young female rats. ACR significantly increased serum glucose, total cholesterol and triglycerides concentrations of both immature male and female rats. While, significant increase in the total urea concentration was noticed only in the immature male rats following ACR administration. Moreover, ACR induced marked increase in the activities of aspartate aminotransferase (AST) and alanine aminotransferase (ALT) in the immature male and female rats. On the other hand, the activities of serum alkaline phosphatase (ALP) and acetylcholinesterase (AChE) were significantly decreased in both treated groups. ACR caused a significant increase in norepinephrin (NE), glutamate, aspartate and taurine, while it reduced dopamine (DA) and serotonin (5-HT) levels. In conclusion, the present study showed that, ACR induced hazardous effects on immature male and female rats. So, we recommended that children must avoid fast or junk foods.

Keywords: Acrylamide; Hematological; Biochemical; Neurological. Histopathological; Immature.

548. Immunomodulatory and Chemo Preventive Activity of Bacillus Subtilis Sulphated Levan

Faten S. Bayoumi, Azza M.El Amir, El Deeb S.O, Hassan Abd el Zaher and Haiam S.A

Life Science Journal, 9 (4): 2846-2856 (2012) IF: 0.073

The aim of this study was to investigate the possible immunomodulatory and chemopreventive effects of a bacterial polysaccharide drug (Bacillus subtilis sulphated Levan; BSL) relevant for prevention of tumour development during the initiation stage. Initiation is the first stage of carcinogenesis. The activity of BSL could be tested via a series of in vivo and in vitro

assays; direct scavenging of ROS (Reactive oxygen species), modulation of the carcinogen metabolizing mechanisms, either via inhibiting phase-I drug metabolizing enzymes (particularly CYP 450; Cytochrome P450), which converts of pro-carcinogens to active carcinogens, or via enhancing phase-II conjugating enzymes (e.g. GSTs, Glutathione-S-Transferase), for removing carcinogens. In order to examine the anti-initiation activity of BSL, in vitro experiments; its effect on the CYP 450, GST and GSH (Glutathione) using Hep-G2 cells and its DPPH (1,1-diphenyl-2-picrylhydrazyl) scavenging capacity was performed. In vivo experiments on adult Swiss albino male mice was performed to investigate its effect on the level of GST, GSH, MDA (Malondialdehyde), GST-P immunochemical and HDAC (Histone Deacetylase) using hepatocarcinogenesis in the mice by i.p. injection of diethyl-nitrosamine (DEN). In addition, BSL activity was also compared with garlic as a natural compound with chemopreventive action. Results: Through the in vitro studies, statistical inhibition of both CYP1A and GSH activities was noticed in relation to the different doses of BSL. In addition, scavenging capacity of BSL against DPPH radicals was inactive. In vivo studies showed that GST activity of saline and control groups were not significantly altered by administration of garlic, while, BSL administration significantly ($P < 0.05$) enhanced this activity to 2.4-fold of the control. BSL was proved to have an antioxidant activity proved by enhancing the antioxidant protein GSH content to 1.2-fold in induced group of mice with cancer induction. Also, decreased level of LOP (Lipid peroxidation) values was significantly ($P < 0.05$) noticed by BSL administration and was insignificantly altered by garlic administration. GST-P immunohistochemical staining in the mice livers showed absence of initiated cells in mice administered BSL alone and highly decreased initiated cells when administered BSL before and after DEN injection (the carcinogenic material used). In comparison, treatment with garlic before and after DEN decreased the appearance of the initiated cells to lesser extent than BSL. Results showed that BSL had a highly significant ($P < 0.05$) inhibitory effect on HDAC activity (play an essential role in the regulation of cell proliferation and apoptosis). It decreases HDAC activity to 2 fold of control, while, garlic did not possess any inhibitory effect. Conclusion: BSL was represented as a promising cancer chemopreventive agent against initiation of hepatocarcinogenesis.

Keywords: Bacterial Polysaccharide Drug; Gst-P Immunochemical; Cytochrome P450; Carcinogens; Initiation Stage.

549. Evaluation of C- Reactive Protein as A Probable Factor for Cancer Diagnosis

Safinaz Elshabrawy, Alyaa Farid, Mohamed El- Beddini, Ahmed Osman and Somaya El- Deeb

Life Science Journal, 9 (4): 2796-2803 (2012) IF: 0.073

C- reactive protein (CRP) is a definitive marker of inflammation produced and synthesized in the liver in response of interleukin-6 (IL-6). It was studied in 10 healthy individuals and 97 patients with different types of diseases including kidney failure (KF), cardiovascular disease (CVD), hepatocellular carcinoma (HCC), Non-Hodgkin lymphoma (NHL), lung cancer (L.C), colon and bladder carcinoma (C.C), ovary and cervix carcinoma (O.C) and breast cancer (B.C). Routine blood tests were assayed for the 107 studied cases such as some liver enzymes (aspartate aminotransferase (AST) and alanine aminotransferase (ALT)), some kidney function factors (urea and creatinine) and some

tumor markers (alfafeto protein (AFP), carcinoembryonic antigen (CEA), cancer antigen 19.9 (CA19.9), cancer antigen 15.3 (CA15.3) and cancer antigen 125 (CA125)) specific to the different studied types of cancers. This study examined the relationship between circulating levels of CRP and various parameters of blood analysis in addition to the level of various tumor markers. It was found that CRP is associated with both KF and CVD cases. The studied specific tumor markers were significantly high in HCC (AFP), NHL (CEA), L.C (CEA) and B.C (CA15.3) studied cases ($P < 0.05$) but it showed no significance in the C.C (CA19.9) and O.C (CA125) studied cases. It was evident that CRP levels are closely related to CA19.9 and CA125 tumor markers in case of C.C and O.C, respectively.

Keywords: C- Reactive Protein; Acute Phase Proteins; Inflammation; Cancer; Tumor Markers.

550. Anatomical Studied on the Cranial Nerves of Liza Ramada (Family: Mugilidae) Nervus Glossopharyngeus

Dakrory, A.I; Ali, R.S and Issa.A.Z.

Life Science Journal, 9 (2): 86-93 (2012) IF: 0.073

This study deals with the nervus glossopharyngeus of Liza ramada. The microscopic observations showed that, the nervus glossopharyngeus arises by one root and leaves the cranial cavity through its own foramen. It gives visceromotor fibres for the first levator arcualis branchialis muscles. It has single extracranially located epibranchial (petrosal) ganglion. The ramus pretrematicus carries general viscerosensory fibres for the epithelial lining of the pharynx and special ones for the taste buds. The ramus posttrematicus carries both general viscerosensory fibres for the epithelial lining of the pharynx and special ones for the gill filaments, as well as visceromotor fibres for the first adductor arcualis branchialis and the first obliquus ventralis muscle.

Keywords: Nervus Glossopharyngeus- Liza Ramada.

551. Redescription of three Cichlidogyrids (Monogenea: Ancyrocephalidae) and One Gyrodactylid (Monogenea: Gyrodactylidae) Infecting Oreochromis Niloticus (Cichlidae) from the River Nile

Kareem Morsy, FathyA. Abdel-Ghaffar, Abdel-Rahman Bashtar, Mohamed Shazli, Hamed Fayed and Faten Adel

Life Science Journal, 9 (3): 2600-2611 (2012) IF: 0.073

In the present study, the morphology and morphometric characterization of four species of monogeneangill parasites infecting the skin and gills of Oreochromis niloticus belonging to family Cichlidae collected from the River Nile at Giza governorates, Egypt were described by means of light microscopy. Thirty six out of 68 specimens of this fish were found to be naturally infected at a rate of 53%. three Cichlidogyrids (family: Ancyrocephalidae) and one Gyrodactylid (family: Gyrodactylidae) were identified. Cichlidogyrus tilapiae Paperna, 1960 was characterized by a copulatory organ found in the midline of the body, with accessory sclerite situated roughly parallel with the copulatory tube and never seen completely isolated from it. In all worms examined, the proximal end of the accessory sclerite was found in contact with the base of the copulatory tube, indicating that there was a connection between

the base of the copulatory tube and the proximal part of the accessory sclerite. Cichlidogyrus longicornis longicornis which was characterized from all species of this genus by having two long projections of the complex bar and its copulatory organ had a slightly long ejaculatory tube. Cichlidogyrus tubicerrus magnus possessed a haptor with two pairs of anchors, its ventral anchor was attached to the V-shaped bar that had a number of tooth-like projections on the inner margin. The dorsal anchor was attached to a complex bar (dorsal bar), which consists of three articulated pieces. The central piece was slightly bent and the other two pieces were attached to the central one in such a way that their points of attachments divide the bar in three equal parts. Gyrodactylus cichlidarum Paperna, 1968 possessed a haptor resembled a cub holding a variety of hamuli, bars and supportive additional sclerites. The hamuli withdrawn inside a transparent tegumental sheath, the hamulus blade emerged from an opening decorating the distal area of a cone-shaped, transparent, tegumental sheath. Oreochromis niloticus fish represents a normal host for all these species except for Cichlidogyrus tubicerrus magnus which represented as a new host for this parasite. These species were redescribed by using light micrographs, line drawings and measurements which can be used as a guide material for the identification of these species by following researchers.

Keywords: Monogenea; Oreochromis Niloticus; Cichlidogyrus Spp.; Gyrodactylus Spp; Light Microscopy.

552. First Description of the Adult Stages of Postorchigenes Sp. (Trematoda: Lecithodendriidae) and Malagashitrema Sp. (Trematoda Homalometridae) Infecting the Common Chameleon Chamaeleo Chamaeleo (Reptilia: Chamaeleonidae) in Egypt

Kareem Morsy, Nadia Ramadan, Salam Al Hashimi, Medhat Ali and Abdel-Rahman Bashtar

Life Science Journal, 9 (4): 399-405 (2012) IF: 0.073

In the present study, the morphological and morphometric characterization of two species of digenetic trematodes infecting the large intestines of the common chameleon Chamaeleo chamaeleo (Reptilia: Chamaeleonidae) were described by means of light microscopy as a first description. 30 and 37 out of 115 (26.1 % and 32.1%) of this lizard species were found to be naturally infected with Postorchigenes sp. (Trematoda: Lecithodendriidae) and Malagashitrema sp. (Trematoda: Homalometridae) respectively. Postorchigenes sp. possesses a body which is oval, spinulate with an oral sucker bigger than acetabulum. The prevalence of Postorchigenes sp. reported from the present study were agreed with the previous studies carried out by Kennedy et al. (1987) who described a three species of digenea from seven species of lizards in Indonesia. Malagashitrema sp. possesses oral sucker larger than acetabulum. The presence of Malagashitrema sp. proved that Malagashitrema is a genus with species linked to Chamaeleo spp. These trematodes adapted to different areas, making their presence are possible in different geographical regions in the world and appears to be a species adapted to Chamaeleo spp.

Keywords: Digenea; Postorchigenes Sp; Malagashitrema Sp; Chamaeleo Chamaeleo; Light Microscopy.

553. Evaluation of Different Immunological Techniques for Diagnosis of Schistosomiasis Haematobium in Egypt"

A. Mahfouz, N. Mahana, ZI. Rabee and A. El Amir

Biotechnology, 1-10 (2012)

The detection of soluble egg antigen (SEA) in serum and urine could be more valuable in diagnosis; hence early treatment would be applied before irreparable damage occurs. In this study, *Schistosoma* (S.) eggs were isolated from the intestine of infected hamsters and purified by Sodium Dodecyl Sulfate-Polyacrylamide Gel Electrophoresis (SDS-PAGE). The purified SEA was injected in rabbits to raise specific polyclonal antibodies (pAb) against *S. haematobium*. The purified pAb was further used as a primary capture to coat ELISA plates. The secondary capture of pAb was by conjugation with horse-raddish peroxidase (HRP). According to parasitological examination, this study included 150 *S. haematobium* infected patients, 50 other parasites infected patients and 30 negative control samples. Latex agglutination technique (LAT) was performed for both serum and urine in comparison to sandwich and dot-ELISA on 150 infected individual. Comparison was evaluated between LAT, sandwich and Dot-ELISA in serum samples, it showed 92%, 98% and 98.66% sensitivity and 92.50%, 96.25% and 98.75% specificity, respectively, while in urine samples showed 88.66%, 90.66% and 94.66% sensitivity and 91.25%, 93.75% and 96.25% specificity, respectively. It was clear that, the sensitivity of LAT in urine was significantly higher than the parasitological examinations. From the obtained results and with consideration to sandwich and Dot-ELISA assays, LAT assay has an important value as an applicable, fast and accurate diagnostic technique for schistosomiasis in the field.

Keywords: Schistosoma; Lat; Sandwich Elisa; Dot; Elisa.

554. The Sensitivity of Liver, Kidney & Testis of Rats to Oxidative Stress Induced by Different Doses of Bisphenol A

Iman M. Mourad and Yasser A. Khadrawy

International J. of Life Science and Pharma Research, 2(2) : 19-28 (2012)

Bisphenol A (BPA) is a world wide used endocrine disruptor that is incorporated in many plastic industries. The exposure of humans to such substances starts early during the fetal life, postnatal life and extends throughout the life of the individual. Many agencies raised warnings against the excessive use of such substances.

The aim of the present study is to evaluate the extent to which BPA can affect the liver, kidney and testis by measuring the oxidative stress induced by two different doses of BPA in these organs. Adult male rats were subjected to different oral doses of BPA (25 mg/kg for 6 weeks and 10mg/kg for 6 and 10 weeks, 5 days a week).

The oxidative stress arising from BPA was evaluated in liver, kidney and testis tissues. In addition, serum uric acid level as a marker of kidney function together with the activities of aspartate aminotransferase (AST) and alanine aminotransferase (ALT) as markers of liver function were measured.

The results of the present study showed significant changes in the antioxidant mechanisms in the liver and testis with the high dose

of BPA (25 mg/kg). The low dose showed significant changes after 10 weeks in the case of the liver and 6 weeks in the case of the testis. In addition, significant increases in serum uric acid level were observed after the administration of the two doses of BPA for 6 weeks and in AST and ALT activities after the high dose (25mg/kg). It could be concluded that BPA-induced toxicity is mediated by oxidative stress which was prominent in liver and testis after the short and long term exposure to both the high and low dose.

Keywords: Bisphenol A; Oxidative Stress; Liver; Kidney; Testis.

555. Investigation of Telomerase Activity in Inflammatory and Non Inflammatory Breast Cancer

Ayman Maher Ibrahim, Salwa Farouk Sabe and Mohamed El-Shinawi

Journal of Cancer Science And Therapy, 4(11): 360-367 (2012)

Inflammatory breast cancer (IBC) is an aggressive type of breast cancer disease that has a high incidence in Egypt than western countries. It is characterized by rapid progression, involvement of dermal lymphatic emboli and extensive lymph node involvement. Basic and translational studies are needed to define IBC disease biology and identify specific biomarkers have been limited by the paucity of patient samples. Hence, the current study aimed to introduce the telomerase activity level as a novel diagnostic marker for breast cancer and specifically for IBC to be differentiated from non-IBC. **Methods:** Breast cancer patients were enrolled from Ain Shams University hospitals in Cairo, divided into two groups: IBC (n=26) and non-IBC (n=27). Tissue samples were collected during modified radical mastectomy. TRAP (Telomerase repeat amplification protocol) assay was used to assess the telomerase activity in inflammatory and non-inflammatory breast cancer tissue samples. Immunohistochemistry was used to investigate the expression of hTERT subunit of telomerase in paraffin embedded tissue samples of both types of patients. **Results:** IBC showed Telomerase activity ranged from 12.2 to 367.1 units with a mean value of 78 and a median value of 43, while telomerase activity in non-IBC ranged from 6.1 to 109.34 units with a mean value of 41.1 and a median value of 24. On the other hand, normal tissues showed telomerase activity below 5 (P<0.001). Using immunohistochemistry, the hTERT expression was higher in IBC than non-IBC and no expression at all in normal tissues. Moreover, a positive mild correlation was found between the telomerase activity and the number of metastatic lymph nodes in both IBC (r=0.53) and non-IBC (r=0.54). **Conclusions:** Telomerase could be a promising marker at the diagnostic and therapeutic levels in breast cancer and specifically in IBC.

Keywords: Breast Cancer; Cancer Death; Erythema; Telomerase.

Dept. of Zoology

556. Evaluation of *Procambarus Clarkii* and *Ergosquilla Massavensis*

Salwa A.H. Hamdi

Book Published by Lap Lambert Academic Publishing, 73 (2012)

Both fresh and marine edible crustaceans *Procambarus clarkii* and *Ergosquilla massavensis*, respectively, are now important components of our local aquatic fauna in Egypt that have a small

yet growing economic importance in our markets. So, the purpose of the present work was, therefore, to assess the protein, amino acids, fatty acids, minerals, vitamins, protein electrophoresis and dendrogram analysis of their extracts for the first time in Egypt which may be in the future play an important role in some pharmaceutical industries and may be used as a specific health foods (functional supplement). In the present study, nutritional analysis of muscle and exoskeleton extracts of *P. clarkii* and *E. massavensis* indicated the presence of a high amount of protein, 9 essential amino acids and 9 non essential amino acids including taurine which has a very scientific action and benefit for men. Also, the results showed the presence of 9 unsaturated fatty acids which included essential fatty acids linoleic acid (omega 6) and alpha linolenic acid (omega 3) which have many functions for man (food supplement) in addition to 4 saturated fatty acids. The minerals recorded were (Cu, Zn, Mn, Fe, Mg, Ca, K and P) and the vitamins were (vit. A, D, E, B1, B2, B6, B12).

Also, The aim of this work is to estimate the nutritive quality of mantis shrimp *Erugosquilla massavensis* and to study the interrelationships between this newly introduced commercial edible crustacean and pollution, for which 2 sites along Suez Canal (Ismailia & Suez).

The estimation of the concentrations of Cu, Zn, Cd and Pb in the tissues of *E. massavensis* caught in the Suez Canal is an attempt to ascertain whether these concentrations exceed the permissible limits and to identify any potential public health risks that could be associated with dietary intakes of seafood from Suez Canal.

The present results reveal that the muscles proteins (50.76 and 48.85%, respectively) and lipids from the two localities (15.25 and 16.47%, respectively) of the male shrimps from Ismailia and Suez regions are higher than in females (36.89% and 35.14% for proteins and 10.25 and 10.54% for lipids, respectively). While, carbohydrates displayed more or less similar percentages in muscles of both sexes.

Moreover, in term of nutritive quality, *E. massavensis* is ranked as protein rich edible crustacean. 12 and 61.50 mg/kg in Ismailia and Suez regions, respectively). The present study suggests that *E. massavensis* can be used as a bioindicator of water pollution and that a close monitoring program is needed to ensure the safety to consume this crustacean species a food source.

Keywords: Evaluation; *procambarus clarkii*; *Erugosquilla massavensis*; Egypt.

557. Protective Effects of Honey and Zizyphus Extract in Male Albino Rats

Sohair Fahmy and Amel Soliman

Book Published by Lambert Academic Publishing, 176 (2012)

Medicinal plants have been used as remedies for human diseases for centuries. The reason for using them as medicine lies in the fact that they contain chemical components of therapeutic value. Kava refers to both the South Pacific herb (*Piper methysticum* G. Forster) and the products prepared from its rhizomes and roots that contain the psychoactive kavalactones.

Several reports suggest that, occasionally, even normal doses of kava can cause severe liver injury. Carbon tetrachloride (CCl₄) is the best characterized system of xenobiotic-induced hepatotoxicity. *Zizyphus spina-christi* belongs to the family Rhamnaceae and grows throughout Upper Egypt and Sinai. *Zizyphus* species are commonly used in folklore medicine for the

treatment of various diseases such as digestive disorders, weakness, liver complaints. Honey, a natural product formed from nectar by honeybees, has been a subject of renewed research interest in the last few years. Evidence indicates that honey can exert several health-beneficial effects such as Gastroprotective, hepatoprotective, reproductive and antioxidant effects.

558. Herbal Treatment of Anxiety Anxiolytic Action of Kava Extract: Implication of Acetylcholine and Amino Acid Neurotransmitters

Neveen Amin Noor

Book Published by Lambert Academic Publishing, 98 (2012)

Generalized anxiety disorder (GAD) is a prevalent and impairing disorder, associated with extensive psychiatric and medical comorbidity. The current pharmacotherapies of anxiety are based on antidepressants and benzodiazepines. However, these drugs have limitations like slow onset of action, development of drug dependence, tolerance, amnesia and sedation. Therefore, the use of alternative therapies has increased substantially over the last decade. Kava is an intoxicating beverage made from the root extract of *Piper methysticum* and has been known as anxiolytic drug.

The German health authorities banned kava extract containing products based on the suspicion of a potential liver toxicity. However, the risk-to-benefit ratio of kava extracts remains good in comparison to that of other anxiolytic drugs. To specialists in phytotherapy, this book provides detailed study to investigate the role played by amino acid neurotransmitters and acetylcholinesterase, in different rat brain areas, in the anxiolytic action of kava and the withdrawal effect of kava on them. Another aspect of this study is to demonstrate the effect of kava on some liver and kidney function parameters.

Keywords: Anxiety; Kava; Amino acids; Acetylcholinesterase; Cortex; Hippocampus; Striatum; Hypothalamus; Rat.

559. The Rapeutic Effect of the Egyptian Freshwater Mussel Extract in Rats Efficacy of the Egyptian Freshwater Mussel Extract Against Monosodium Glutamate Toxicity in Male Rats

Amel Soliman and Sohair Fahmy

Book Published by Lambert Academic Publishing, 176 (2012)

Antioxidant and anti-inflammatory agents play a critical role in body protection by scavenging active oxygen and free radicals and neutralizing lipid peroxides. Therefore, there is need for a natural product that protects the body but cost-effective, safe and without side effects. Pharmacological effects due to the properties of their constituents. Freshwater bivalves occurring in Egypt represent a neglected animal group and little is known about them or their diversity; perhaps due to the fact that they have no apparent economic or medical importance.

Egyptian freshwater mussels (*Coelaturaeegyptiaca*) are a Molluscan Bivalve belonging to Unionoidae common in the Egyptian River Nile. This book aimed to evaluate the possible effect of *C. aegyptiaca* extract for the first time in Egypt, in order to establish whether it would exacerbate or ameliorate the adverse effects of MSG on some serum parameters and oxidative markers in the liver, kidney, testis and brain of rats using vitamin C as a positive control group.

560. The Possible Protective Role of Protein Isolated from Peganum Harmala Protective Effect of Isolated Protein

Amel Soliman, Helal AbouDahab and Hanaa El Badawy

Book Published by Lambert Academic Publishing, 232 (2012)

Proteins have excellent potential as antioxidant additives in foods because they can inhibit lipid peroxidation through multiple pathways including inactivation of reactive oxygen species, scavenging free radicals, chelation of pro-oxidative transition metals, reduction of hydroperoxides and alteration of the physical properties of food systems.

Numbers of herbs are traditionally used in different countries during drug of toxin induced hepatic and renal disorders, such as 43kDa protein molecule isolated from leaves of *Cajanus indicus* L., which provide maximum protection for liver, kidney and other organs in vivo against different toxins.

561. Genotoxic Effects of Metal Pollution in Two Fish Species, *Oreochromis Niloticus* and *Mugil Cephalus*, from Highly Degraded Aquatic Habitats

Wael A. Omara, Khalid H. Zaghoul, Amr A. AbdelKhalek and S. Abo-Hegab

Mutation Research/Genetic Toxicology and Environmental Mutagenesis, 746: 7-14 (2012) IF: 3.035

In Egypt, Lake Qaroun and its neighbouring fish farms are in a serious environmental situation as a result of pollution by agricultural sewage and domestic non-treated discharges. The present study aims to evaluate genotoxic effects of toxic metals in cultured and wild Nile tilapia, *Oreochromis niloticus* and mullet, *Mugil cephalus* collected from these contaminated aquatic habitats, in comparison with fish from a non-polluted reference site. Heavy-metal concentrations (Cu^{2+} , Zn^{2+} , Pb^{2+} , Fe^{2+} and Mn^{2+}) in water and sediment samples were recorded.

The condition factor (CF) was taken as a general biomarker of the health of the fish and genotoxicity assays such as the micronucleus (MN) test and a DNA-fragmentation assay were carried out on the fish species studied. In addition to micronuclei, other nuclear abnormalities (NA) were assessed in fish erythrocytes. Degradation of the studied aquatic habitats revealed species specific effects.

A significant decrease in CF values associated with a significant elevation in MN and NA frequencies was observed in fish collected from the polluted areas compared with those from the reference site.

Moreover, mixed smearing and laddering of DNA fragments in gills and liver samples of both fish species collected from the polluted areas indicate an intricate pollution condition. Results of the present study show the significance of integrating a set of biomarkers to identify the effects of anthropogenic pollution. High concentrations of heavy metals have a potential genotoxic effects and genotoxicity is possibly related to agricultural and domestic activities.

Keywords: Aquatic Pollution; Metal Toxicity; Dna Damage; Micronucleus Test.

562. Effects of Experimentally Induced Maternal Hypothyroidism and Hyperthyroidism On the Development of Rat Offspring: it- the Developmental Pattern of Neurons in Relation to Oxidative Stress and Antioxidant Defense System

O.M. Ahmed R.G. Ahmed, A.W. El-Gareib, A.M. El-Bakry and S.M. Abd El-Tawab

International Journal of Developmental Neuroscience, 30: 517-537 (2012) IF: 2.418

Excessive concentrations of free radicals in the developing brain may lead to neurons maldevelopment and neurons damage and death. Thyroid hormones (THs) states play an important role in affecting the modulation of oxidative stress and antioxidant defense system.

Thus, the objective of this study was to clarify the effect of hypothyroidism and hyperthyroidism in rat dams on the neurons development of different brain regions of their offspring at several postnatal weeks in relation to changes in the oxidative stress and antioxidant defense system.

The adult female rats were administered methimazole (MMI) in drinking water (0.02% w/v) from gestation day 1 to lactation day 21 to induce hypothyroidism and exogenous thyroxine (T4) in drinking water (0.002% w/v) beside intragastric incubation of 50–200 T4 $\mu\text{g}/\text{kg}$ body weight (b. wt.) to induce hyperthyroidism. In normal female rats, the sera total thyroxine (TT4) and total triiodothyronine (TT3) levels were detectably increased at day 10 post-partum than those at day 10 of pregnancy. Free thyroxine (FT4), free triiodothyronine (FT3), thyrotropin (TSH) and growth hormone (GH) concentrations in normal offspring were elevated at first, second and third postnatal weeks in an age-dependent manner. In hypothyroid group, a marked depression was observed in sera of dam TT3 and TT4 as well as offspring FT3, FT4 and GH, while there was a significant increase in TSH level with the age progress.

The reverse pattern to latter state was recorded in hyperthyroid group. Concomitantly, in control offspring, the rate of neuron development in both cerebellar and cerebral cortex was increased in its density and complexity with age progress. This development may depend, largely, on THs state. Both maternal hypothyroidism and hyperthyroidism caused severe growth retardation in neurons of these regions of their offspring from the first to third weeks. Additionally, in normal offspring, seven antioxidant enzymes, four non-enzymatic antioxidants and one oxidative stress marker (lipid peroxidation, LPO) followed a synchronized course of alterations in cerebrum, cerebellum and medulla oblongata.

In both thyroid states, the oxidative damage has been demonstrated by the increased LPO and inhibition of enzymatic and non-enzymatic antioxidants in most examined ages and brain regions. These disturbances in the antioxidant defense system led to deterioration in the neuronal maturation and development. In conclusion, it can be suggested that the maldevelopment of neurons and dendrites in different brain regions of offspring of hypothyroid and hyperthyroid mother rat dams may be attributed, at least in part, to the excess oxidative stress and deteriorated antioxidant defense system in such conditions.

Keywords: Development; Hypothyroidism; Hyperthyroidism; Neurons; Reactive Oxygen Species Generation and Antioxidant Defense System.

563. Anatomical, Histological and Histochemical Adaptations of the Avian Alimentary Canal to the ir Food Habits: I-Coturnix Coturnix

Mostafa Zaher, Abdel-Wahab El-Ghareeb, Hamida Hamdi and Fathia AbuAmod

Life Science Journal, 9 (3): 253-275 (2012) IF: 0.073

The present work is the first in a series of studies aiming at establishing a connection between the food habits of aves and the anatomical, histological and histochemical structures of their alimentary canal. In this study the gross anatomy, histology and histochemistry of the alimentary canal of common quail, *Coturnix coturnix*, a granivorous bird, have been investigated. This study revealed that, the oesophagus is not ably long with a well developed crop; thus stomach is differentiated into a glandular proventriculus and a muscular ventriculus or gizzard. The gizzard is much more developed having a thick hard cuticle, its wall consists of two strong smooth muscles, the small intestine is divided into duodenum, jejunum and ileum and the transition from the jejunum to ileum is indicated by the vitelline (Meckel's) diverticulum and the ileum was the longest part of the small intestine. The large intestine consists of paired well developed caeca and a short rectum. The present histological studies revealed that the alimentary tract showed the usual four laminae: serosa, muscosa, submucosa and mucosa. The oesophageal mucosa of the quail was thrown into numerous longitudinal folds. The mucosa of oesophagus is lined with stratified squamous epithelium. The proventricular glands are simple tubular to simple branched tubular glands. The mucosal surface of the ventriculus is indented by deep, broad crypts into which simple to branched tubular gastric glands open. A thick gastric keratinoid material covers the mucosa of the ventriculus. The intestinal mucosa is thrown into intestinal villi which show a marked variation in density, shape and size in the different regions of the intestine. The goblet cells gradually increase in frequency from the duodenum to the rectum. Also, the histochemical study revealed the existence of a high amount of mucopolysaccharides in the oesophageal glands, PAS and Alcian blue positive mucin granules as well (neutral and acid mucin, respectively). The ventriculus mucosa is covered by a thick keratinized laminated layer of koilin membrane which is formed of proteinous material similar to keratin and stained positive for PAS and Alcian blue indicating the presence of neutral and acid mucin within its contents. The proventriculus mucosa shows folds lined by simple columnar cells containing PAS and Alcian blue positive mucin granules. The goblet cells and crypts of Lieberkühn have acid and neutral mucopolysaccharide secretions and the luminal surface of the columnar cells and the lamina propria of the intestine contains proteins.

Keywords: Anatomical; Histological; Histochemical; Alimentary Canal; Birds.

564. Anatomical, Histological and Histochemical Adaptations of the Reptilian Alimentary Canal to the ir Food Habits: I. Uromastix Aegyptiaca

Moustafa Zaher, Abdel-Wahab El-Ghareeb, Hamida Hamdi, Azza Essa and Suad Lahsik

Life Science Journal, 9 (3): (2012) IF: 0.073

A series of studies was carried out to elucidate the relationship between the microscopic anatomy of the alimentary canal and the

food habits in reptiles. Three reptiles were chosen according to different feeding habits, *Uromastix* is a herbivorous, Chameleon is an insectivorous, while *Crocodylus* is a carnivorous reptile. So, it is obvious that the anatomy as well as the histology of the alimentary tract of reptiles demonstrate certain specific characteristics of functional adaptations as a reflection of the herbivorous, carnivorous and insectivorous mode of feeding. The anatomical and histological study of the alimentary canal of *Uromastix aegyptiaca* was carried out. A comparison between the different histological structures found and those known in other reptiles was done. The straight oesophagus is lined with ciliated epithelium and goblet cells, leading to the stomach which consists of two portions, fundic or oxyntic and pyloric or mucous. The small intestine is comparatively short although the animal is purely herbivorous. It consists of the duodenum and ileum. The duodenal mucosa is in the form of leaf-like villi provided with shallow branched Lieberkühn crypts at their bases. The ileum is devoid of found glands. The large intestine is formed of a well developed large caecum, colon and rectum. At the posterior edge of the caecum there is a small blind sac which is considered as the appendix. The caecum which is devoid of glands is lined with simple columnar cells of a special type. While the ileo-caecal valve is in the form of a characteristic well developed protrusion, the caeco-colic valve is formed of a flap arising from one side. The mucosa of the colon is folded and lined with goblet and columnar cells, while that of the rectum is, more or less, straight and is rich in goblet cells and lymph spaces. The distribution and localization of different carbohydrate categories (PAS-positive material, mucopolysaccharides) were studied in the mucosal epithelium of the alimentary canal of *Uromastix aegyptiaca*. The goblet cells of the oesophagus are rich in acid mucopolysaccharides, those of the small and large intestine contained smaller amounts. Neutral mucopolysaccharides were found in small to moderate amounts, being most obvious in the gastric mucosa. Mode of feeding as well as habitat, show, more or less a close similarity in the histochemical pattern of their gut mucosa as regards to the distribution and localization of proteins and nucleic acids.

Keywords: Anatomy; Histology; Histochemistry; Alimentary Canal; Reptiles.

565. Prenatal and Perinatal Acrylamide Disrupts the Development of Cerebrum and Medulla Oblongata in Albino Rats

Bayoumy, E. M. and Sayed Abd El- Monem

African Journal of Biotechnology, 5 (2012) 353-360 (2012)

A series of studies was carried out to elucidate the relationship between the microscopic anatomy of the alimentary canal and the food habits in reptiles. Three reptiles were chosen according to different feeding habits, Acrylamide is known to cause neurotoxicity in experimental animals and humans. The literature on its neurotoxic effect in adult animals is huge, but the effect of acrylamide on the embryonic and postnatal development is relatively less understood. The present study examined its effects on the development of oxidative stress of cerebrum and medulla oblongata in albino rats. Acrylamide was orally administered to non-anesthetized pregnant females by gastric intubation 10 mg/kg/day. The animals were divided into 3 groups as follows: group A - newborn from control animals, group B - newborns from mothers treated with acrylamide from day 7 (D7) of gestation till birth (prenatal intoxicated group), group C - newborns from mothers treated with acrylamide from D7 of

gestation till D28 after birth (perinatally intoxicated group). Acrylamide administered either prenatally or perinatally was shown to induce significant increase of thiobarbituric acid-reactive substances (TBARS) and oxidative stress (significant reductions in glutathione (GSH), total thiols, superoxide dismutase (SOD) and peroxidase activities) in the developing cerebrum and medulla oblongata. The results of this study showed that prenatal and perinatal acrylamide or its metabolites disrupts the biochemical machinery, cause oxidative stress and induce structural changes in the developing rat cerebrum and medulla oblongata.

Keywords: Acrylamide; Postnatal Development; Cerebrum; Medulla Oblongata; Oxidative Stress.

Faculty of Veterinary Medicine

Dept. of Biochemistry

566. Beta Adrenergic Overstimulation Impaired Vascular Contractility Via Actin-Cytoskeleton Disorganization in Rabbit Cerebral Artery.

Hyoung Kyu Kim, Won Sun Park, Mohamad Warda, So Youn Park, Eun A. Ko, Min Hee Kim, SeungHun Jeong, Hye-Jin Heo, Tae-Hoon Choi, Young-Won Hwang, Sun-Il Lee, Kyung Soo Ko, ByoungDoo Rhee, Nari Kim and Jin Han.

Plos One, 7 (8): 1-14 (2012) IF: 4.092

Beta adrenergic overstimulation may increase the vascular damage and stroke. However, the underlying mechanisms of beta adrenergic overstimulation in cerebrovascular dysfunctions are not well known. We investigated the possible cerebrovascular dysfunction response to isoproterenol induced beta-adrenergic overstimulation (ISO) in rabbit cerebral arteries (CAs). **METHODS:** ISO was induced in six weeks aged male New Zealand white rabbit (0.8-1.0 kg) by 7-days isoproterenol injection (300g/kg/day).

We investigated the alteration of protein expression in ISO treated CAs using 2DE proteomics and western blot analysis. Systemic properties of 2DE proteomics result were analyzed using bioinformatics software. ROS generation and following DNA damage were assessed to evaluate deteriorative effect of ISO on CAs. Intracellular Ca(2+) level change and vascular contractile response to vasoactive drug, angiotensin II (Ang II), were assessed to evaluate functional alteration of ISO treated CAs.

Ang II-induced ROS generation was assessed to evaluate involvement of ROS generation in CA contractility. **RESULTS:** Proteomic analysis revealed remarkably decreased expression of cytoskeleton organizing proteins (e.g. actin related protein 1A and 2,-actin, capping protein Z beta and vimentin) and anti-oxidative stress proteins (e.g. heat shock protein 9A and stress-induced-phosphoprotein 1) in ISO-CAs.

As a cause of dysregulation of actin-cytoskeleton organization, we found decreased level of RhoA and ROCK1, which are major regulators of actin-cytoskeleton organization. As functional consequences of proteomic alteration, we found the decreased transient Ca(2+) efflux and constriction response to angiotensin II and high K(+) in ISO-CAs. ISO also increased basal ROS generation and induced oxidative damage in CA; however, it decreased the Ang II-induced ROS generation rate. These results indicate that ISO disrupted actin cytoskeleton proteome network through down-regulation of RhoA/ROCK1 proteins and increased

oxidative damage, which consequently led to contractile dysfunction in CA.

Keywords: Proteome; Cerebral Artery; Actin; Rabbit.

567. Phenological and Liver Antioxidant Profiles of Adult Nile Tilapia (*Oreochromis Niloticus*) Exposed to Toxic Live Cyanobacterium (*Microcystis Aeruginosa* Kützing) Cells

Hanan M. Khairy, Marwa A. Ibrahim and Mai D. Ibrahim

Z Naturforsch C, 620-628 (2012) IF: 0.772

Blue-green algae (cyanobacteria) constitute the greater part of the phytoplankton. *Microcystis aeruginosa* is amongst the most ubiquitously distributed cyanobacterial species and almost invariably produces cyclic heptapeptide toxins called microcystins (MCs). The present study was designed to investigate the phenological and liver antioxidant profiles of the Nile tilapia *Oreochromis niloticus* chronically exposed to toxic live *M. aeruginosa* cells. Fish were grown in the absence and presence of *M. aeruginosa* in three different concentrations for seven days and subsequently reared for another 30 days in the absence of the cyanobacteria. While cyanobacteria did not cause any fish mortality, there was a progressive development of yellowish discoloration in the livers of exposed fish. In the livers, the activities and levels of superoxide dismutase (SOD), lactate dehydrogenase (LDH), glutathione (GSH) and lipid peroxidation products like malondialdehyde (MDA) were elevated in response to the concentration of *M. aeruginosa*. Moreover, DNA fragmentation and DNA-protein cross links were measured. These parameters can thus be considered potential biomarkers for the fish exposure to *M. aeruginosa*. The present study sheds light on cyanobacterial blooms like health, environmental and economic problem, respectively.

Keywords: Cyanobacteria; *Oreochromis niloticus*; Oxidative Stress.

Dept. of Clinical Pathology

568. Antiviral and Immune Stimulant Activities of Glycyrrhizin Against Duck Hepatitis Virus

H Soufy, S Yassein, AR Ahmed, MH Khodier, MA Kutkat, SM and Nasr and FA Okda

African Journal of Traditional, Complementary and Alternative Medicines, 9 (3): 389-395 (2012) IF: 0.707

This study was conducted to investigate the effect of glycyrrhizin as an immune stimulant against duck hepatitis virus (DHV). In vitro study was carried out to determine cytotoxic and antiviral effects of glycyrrhizin in VERO cells. In vivo study was performed on 40 one-day-old White Pekin ducklings. –and the birds were divided into 4 groups: control, glycyrrhizin treated, vaccinated with live attenuated DHV vaccine and glycyrrhizin treated and vaccinated; to investigate the changes in immunity and challenge test. Blood samples were collected from each duckling for evaluation of cellular and humeral immunity. The in vitro results revealed that glycyrrhizin had antiviral and no toxic effects till 106 dilutions. Higher antibody titer was observed from the 5th week till the end of experiment in glycyrrhizin and vaccinated group. Treatment with glycyrrhizin alone or with DHV vaccine demonstrated a pronounced lymphocytic

proliferation response after 4 days postinoculation till the end of experiment, while vaccinated group revealed a pronounced proliferation response after 24 days post-inoculation. Treatment with glycyrrhizin alone or combination with DHV vaccine revealed good immune stimulant and antiviral effect against DHV.

569. Immunostimulant Effect of Egyptian Propolis in Rabbits

Somya A. Nassar, Amira H. Mohamed, Hamdy Soufy, Soad M. Nasr and K.M. Mahran

The Scientific World Journal, (2012)

The present experiment was conducted to study the effect of ethanolic extract of Egyptian propolis given alone or in combination with inactivated *Pasteurella multocida* vaccine on rabbits challenged with a virulent strain of *Pasteurella multocida*. Fifty-six New-Zealand rabbits, 6–8 weeks old and non-vaccinated against pasteurellosis, were randomly divided into eight equal groups. The first group was kept as a control for the experiment. The other groups received different treatments with propolis extract, inactivated vaccine, or both. The experiment continued for seven weeks during which clinical signs, body weight and mortality rate were monitored and blood samples were collected weekly for evaluating the leukogram, serum biochemistry and immune response in all groups of animals. At the end of the seventh week, the animals were subjected to challenge with a virulent strain of *Pasteurella multocida*. Two weeks later, tissue specimens were collected from different organs for histopathological examination. Results showed that rabbits of the groups treated with both propolis and the vaccine by different routes appeared healthy after challenge. It has been concluded that alcoholic extract of propolis administered in combination with inactivated *Pasteurella multocida* vaccine has no adverse effects on the general health conditions and enhances immune response in rabbits.

Keywords: Egyptian Propolis; *Pasteurella Multocida*; Rabbits; Immunostimulant Effect; Leukogram; Serum Biochemistry.

570. : Effect of Bactocell® and Revitylte-Plus™ as Probiotic Food Supplements On the Growth Performance, Hematological and Biochemical Parameters and Humoral Immune Response of Broiler Chickens

Azza H. Abd-El-Rahman, H.H. Kamel, Walaa M. Ahmed, Olfat S.H. Mogoda and Amira H. Mohamed

World Applied Sciences, 18 (3): 305-316 (2012)

This study was designed to compare between the effect of Bactocell® and Revitylte-Plus™ as probiotic supplements on the growth performance, hematological and biochemical constituents of blood and humoral immune response of broiler chickens. Three hundred, one day old broiler chicks were divided into three equal groups, first group (C) fed on a balanced ration and considered the control group, second group (L) fed on a balanced ration and provided with the probiotic Revitylte-Plus™ at a rate of 1 gm/4 liter of drinking water and the third group (P) fed on a balanced ration supplemented with the probiotic Bactocell® at a rate of 1kg/ton ration. On the 5th week of age, each of the previous groups was subdivided into 2 equal subgroups. One of which (C+S, L+S and P+S) is infected with

Salmonella kentucky (8×10^{12} microorganisms/ml for 2 successive days given in (1ml in the first day and 0.5 ml in the second day). The experimental groups became (group C, L, P and C+S, L+S and P+S). Groups C+S, L+S and P+S were infected with *Salmonella kentucky* (8×10^{12} microorganisms/ml) for 2 successive days (1ml in the first day and 0.5 ml in the second day). The period of the experiment extended for 2 weeks after infection through which at intervals throughout the time of the experiment, body weight (BW), food conversion rate (FCR), hemogram, some serum biochemical parameters and humoral immunity using ELISA technique were investigated. Results revealed significant increase in body weight and FCR in the non-infected groups L and P on the 3rd week and in group P till the end of the experiment, while the infected groups showed significant decrease in body weight along the experiment. Hemogram of the infected groups revealed macrocytic hypochromic anemia, leucocytosis associated with heterophilia, lymphocytosis and monocytosis. Serum biochemical parameters showed elevated Aspartate amino transferase (AST) and Alkaline phosphatase (ALP), hypoglycemia, elevated total proteins and globulins, hypocholesterolemia (HDL and LDL) and low triglycerides when compared with the control. Results of ELISA assay revealed significant elevation in humoral immune response in the P+S, L+S and C+S group respectively, the study concluded that use of probiotics improve the immune response of birds against salmonella infection and Bactocell® is better than Revitylte-Plus™ as it increased BW, improved FCR, caused low mortalities and induced more immunoglobulins.

Keywords: Broilers Chickens; Probiotic; Body Weight Gain; Fcr; Hemogram; Serum Biochemistry; Electrophoresis; Elisa.

Dept. of Fish Diseases and Management

571. Experimental Exposure of African Catfish *Clarias Gariepinus* (Burchell, 1822) to Phenol: Clinical Evaluation, Tissue Alterations and Residue Assessment

Mai D. Ibrahim

Journal of Advanced Research, 3: 177-183 (2012) IF: 3

There is lack of information regarding; the toxicological and pathological consequences of phenol stressed *Clarias gariepinus*; as well as; the susceptibility of the stressed fish to disease occurrence. Static renewal bioassay was experimentally conducted to evaluate the toxic effects of phenol on the African catfish *C. gariepinus*. Ninety-six-hour acute toxicity tests revealed that the median lethal concentration of phenol (LC50) is 35 mg/L by immersion. Four experimental fish groups were assigned for 3 weeks exposure test; three were exposed 20%, 50% and 70% LC50, the fourth control fish group received a vehicle of dechlorinated water. Abnormal signs including cessation of feeding, nervous manifestations; skin expressed perfuses mucous, black patches with skin erosion and ulcerations in the later stages. All observations were correlated to the time and dose of exposure. Post mortem examination revealed adhesion of the internal organs. For tissue alterations; Skin, gills, brain, liver and kidney showed variable degrees of degenerative changes and necrosis. Muscle residues shown in mean \pm SE were 4.3 ± 0.05 and 6.65 ± 0.05 ppm in groups that received 20 and 50% LD50, respectively. Infection with *Aeromonas hydrophila* resulted in high percent of mortalities with a non significant difference

between the challenged fish groups. The study cleared that phenol is toxic to *C. gariepinus* under experimental conditions.

Keywords: Phenol Toxicity; African Catfish *Clarias Gariepinus*; Median Lethal Concentration; Clinical Studies; Pathology; Tissue Residue Assay.

572. Epidemiological Investigation of Renibacterium Salmoninarum in three Oncorhynchus Spp. in Michigan from 2001 to 2010

Mohamed Faisal, Carolyn Schulz, Alaa Eissa, Travis Brenden, Andrew Winters, Gary Whelane, Martha Wolgamood, Edward Eischg and Jan VanAmbergh

Preventive Veterinary Medicine, 107: 260-274 (2012) IF: 2.046

Bacterial kidney disease (BKD) has caused mortalities and chronic infections in wild and farm-raised salmonids throughout the world. In the Laurentian Great Lakes of North America, BKD was associated with several large-scale mortality events of *Oncorhynchus* spp. throughout the 1980s and 1990s.

In response to these mortality events, the state of Michigan implemented several enhanced biosecurity measures to limit the occurrence of BKD in state-operated hatcheries and gamete-collection weirs. The objectives of this study were to assess if infection levels (prevalence and intensity) of *Renibacterium salmoninarum*, the causative agent of BKD, have changed in broodstock and pre-stocking fingerlings of three feral *Oncorhynchus* spp. (Chinook salmon (*O. tshawytscha*), coho salmon (*O. kisutch*) and steelhead (*O. mykiss*)) over a decade, following the implementation of the enhanced biosecurity measures. Between 2001 and 2010, a total of 3,530 broodstock salmonids collected from lakes Huron and Michigan tributaries during spawning runs and 4,294 propagated prestocking salmonid fingerlings collected from three state of Michigan fish hatcheries were tested for the presence of *R. salmoninarum* antigens using the enzyme-linked immunosorbent assay.

Substantial declines in the overall prevalence of the bacterium were detected in each of the examined broodstocks. Most propagated pre-stocking fingerlings also exhibited substantial declines in *R. salmoninarum* prevalence. Prevalence was typically higher in Chinook salmon from Lake Michigan than from Lake Huron; prevalence was also generally higher in the Hinchinbrooke strain of coho salmon than in the Michigan-adapted strain. For most strains and stocks examined, intensity of *R. salmoninarum* infection was found to have declined.

Keywords: *Renibacterium Salmoninarum*; Bacterial Kidney Disease; Michigan; *Oncorhynchus Salmonid*; Disease Prevalence.

573. Laboratory Exposure of Oreochromis Niloticus to Crude Microcystins (Containing Microcystin-Lr) Extracted from Egyptian Locally Isolated Strain (Microcystis Aeruginosa Ku^r Tzing): Biological and Biochemical Studies

Mai D. Ibrahim Hanan M. Khairy and Marwa A. Ibrahim

Fish Physiol Biochem, 38: 899-908 (2012) IF: 1.528

Cyanobacterial blooms exert negative impacts on fisheries and water management authorities. Recently, it has gained global attention, as elevated earth warming and environmental pollution are accelerating algal growth. *Oreochromis niloticus* (*O.*

niloticus) is a worldwide and the most commonly cultured fish in Egypt. The biological interaction of the living organisms to the surrounding environment must continuously be assessed to predict future effects of the ongoing hazards on fish. The study was designed to examine the possible biological and biochemical response of *O. niloticus* exposed to different concentrations of microcystins crude extract (containing microcystin-LR). Three equal groups of *O. niloticus* were assigned for intraperitoneal injection of three different doses: 100, 200 and 400g ml dried aqueous microcystins extract, for 10 days. Clinical, condition factor (K) and hepatosomatic index (HIS) were estimated. Biochemical alterations were evaluated via lipid peroxidation, DNA fragmentation assay and electrophoretic analysis of fragmented DNA using agarose gel electrophoresis. The results showed that there were discernible behavioral and clinical alterations. Significant differences in K and HIS were observed between treatments. Also, significant elevations were observed in lipid peroxidation level and in the DNA fragmentation percentage in the exposed fish to the doses of 200 and 400g ml of microcystins crude extract. The current study addresses the possible toxic effects of microcystins crude extract to *O. niloticus*. The results cleared that microcystins crude extract (containing MC-LR) is toxic to *O. niloticus* in time- and dose-dependent manners.

Keywords: Microcystins Crude Extract; *Oreochromis Niloticus* Clinical Picture; Condition Factor (K); Hepatosomatic Index (His); Lipid Peroxidation; Malondialdehyde (Mda); Dna Fragmentation Test; Agarose Gel Electrophoresis

574. Spread of the Emerging Viral Hemorrhagic Septicemia Virus Strain, Genotype Ivb, in Michigan, Usa

Mohamed Faisal, Megan Shavaliar, Robert K. Kim, Elena V. Millard, Michelle R. Gunn, Andrew D. Winters, Carolyn A. Schulz, Alaa Eissa, Michael V. Thomas, Martha Wolgamood, Gary E. Whelan and James Winton

Viruses - Basel, 4: 734-760 (2012) IF: 1.5

In 2003, viral hemorrhagic septicemia virus (VHSV) emerged in the Laurentian Great Lakes causing serious losses in a number of ecologically and recreationally important fish species. Within six years, despite concerted managerial preventive measures, the virus spread into the five Great Lakes and to a number of inland water bodies. In response to this emerging threat, cooperative efforts between the Michigan Department of Natural Resources (MI DNR), the Michigan State University Aquatic Animal Health Laboratory (MSU-AAHL) and the United States Department of Agriculture-Animal and Plant Health Inspection Services (USDA-APHIS) were focused on performing a series of general and VHSV-targeted surveillances to determine the extent of virus trafficking in the State of Michigan. Herein we describe six years (2005–2010) of testing, covering hundreds of sites throughout Michigan's Upper and Lower Peninsulas.

A total of 96,228 fish representing 73 species were checked for lesions suggestive of VHSV and their internal organs tested for the presence of VHSV using susceptible cell lines. Of the 1,823 cases tested, 30 cases from 19 fish species tested positive for VHSV by tissue culture and were confirmed by reverse transcriptase polymerase chain reaction (RT-PCR). Gene sequence analyses of all VHSV isolates retrieved in Michigan demonstrated that they belong to the emerging sublineage "b" of the North American VHSV genotype IV.

These findings underscore the complexity of VHSV ecology in the Great Lakes basin and the critical need for rigorous legislation and regulatory guidelines in order to reduce the virus spread within and outside of the Laurentian Great Lakes watershed.

Keywords: Michigan; Viral Hemorrhagic Septicemia Virus; Laurentian Great Lakes; Emerging Disease.

Dept. of Food Hygiene and Control

575. Incorporating Essential Oils of Marjoram and Rosemary in the Formulation of Beef Patties Manufactured with Mechanically Deboned Poultry Meat to Improve the Lipid Stability and Sensory Attributes

Hussein M.H. Mohamed and Hayam A. Mansour

Lwt-Food Science and Technology, 45: 79-87 (2012) IF: 2.545

The effect of addition of essential oils of marjoram (*Origanum marjorana* L.) and rosemary (*Rosmarinus officinalis* L.) at concentration of 200 mg/kg to beef patties formulated with 200 g/kg mechanically deboned poultry meat (MDPM) was studied. The proximate composition, lipid oxidation, sensory characteristics and microbial counts of beef patties manufactured with 200 g/kg MDPM (percentage of lean portion) were assessed during frozen storage at 18 °C. Beef patties formulated with MDPM (200 g/kg) showed significant ($P < 0.05$) reduction in protein content and significant ($P < 0.05$) increase in fat content.

Incorporating MDPM in beef patties formulation significantly ($P < 0.05$) increased the TBARS (Thiobarbituric acid reactive substance) values and significantly ($P < 0.05$) reduced the flavor and overall acceptability scores. Addition of essential oils of marjoram and rosemary at level of 200 mg/kg significantly ($P < 0.05$) reduced the TBARS and significantly ($P < 0.05$) increased the sensory scores of beef patties during frozen storage period. Overall, the study indicated the potential use of natural herbal essential oils to protect against lipid oxidation and improve the sensory attributes of beef patties formulated with MDPM.

Keywords: Beef Patties; Natural Herbal Extracts; Mechanically Deboned Poultry Meat; Lipid Oxidation; Sensory Attributes.

576. Accelerated Inactivation of Geobacillus Stearothermophilus Spores by Ohmic Heating

Romel Somavat, Hussein M.H. Mohamed, Yoon-Kyung Chung, Ahmed E. Yousef and Sudhir K. Sastry

J Food Eng, 108: 69-76 (2012) IF: 2.414

Until recently, ohmic heating was commonly thought to kill microorganisms through a thermal effect. However a growing body of evidence suggests that non-thermal effects may occur. Our aim was to determine the kinetics of inactivation of *Geobacillus stearothermophilus* spores (ATCC 7953) under ohmic and conventional heating using a specially constructed test chamber with capillary sized cells to eliminate potential sources of error and ensure that identical thermal histories were experienced both by conventionally and ohmically heated samples.

Ohmic treatments at frequencies of 60Hz and 10kHz were compared with conventional heating at 121, 125 and 130°C for four different holding times. Both ohmic treatments showed a

general trend of accelerated spore inactivation. It is hypothesized that vibration of polar dipicolinic acid molecules (DPA) and spore proteins to electric fields at high temperature conditions may result in the accelerated inactivation.

Keywords: Ohmic Heating; Conventional Heating; *Geobacillus Stearothermophilus*; Spores; Inactivation Kinetics.

577. The Real Inactivation Kinetics of Bacillus Coagulans Spores in Tomato Juice

Jing Peng, Jae-Hyung Mah, Romel Somavat, Hussein Mohamed, Sudhir Sastry and Juming Tang

J Food Protect, 75 (7): 1236-1242 (2012) IF: 1.937

The thermal characteristics of the spores and vegetative cells of three strains of *Bacillus coagulans* (ATCC 8038, ATCC 7050 and 185A) in tomato juice were evaluated. *B. coagulans* ATCC 8038 was chosen as the target microorganism for thermal processing of tomato products due to its spores having the highest thermal resistance among the three strains.

The thermal inactivation kinetics of *B. coagulans* ATCC 8038 spores in tomato juice between 95 and 115°C were determined independently in two different laboratories using two different heating setups.

The results obtained from both laboratories were in general agreement, with z-values (z-value is defined as the change in temperature required for a 10-fold reduction of the D-value, which is defined as the time required at a certain temperature for a 1-log reduction of the target microorganisms) of 8.3 and 8.7°C, respectively. The z-value of *B. coagulans* 185A spores in tomato juice (pH 4.3) was found to be 10.2°C. The influence of environmental factors, including cold storage time, pH and preconditioning, upon the thermal resistance of these bacterial spores is discussed. The results obtained showed that a storage temperature of 4°C was appropriate for maintaining the viability and thermal resistance of *B. coagulans* ATCC 8038 spores. Acidifying the pH of tomato juice decreased the thermal resistance of these spores. A 1-h exposure at room temperature was considered optimal for preconditioning *B. coagulans* ATCC 8038 spores in tomato juice.

578. Structural Changes in Listeria Monocytogenes Treated with Gamma Radiation, Pulsed Electric Field and Ultra-High Pressure

Hussein M.H. Mohamed, Beatrice H.S. Diono and Ahmed E. Yousef

J Food Safety, 32: 66-73 (2012) IF: 0.72

Understanding the mode of action of gamma radiation, pulsed electric field (PEF) and ultra-high pressure (UHP) against targeted pathogens should help improve implementation of these technologies. *Listeria monocytogenes* Scott A was treated with radiation, PEF and UHP at doses that caused equal lethality (3-log inactivation).

These doses were 0.57 kGy at 5°C (radiation), 30 kV/cm at 22°C for 216 µs (PEF) and 400 MPa at 24 ± 1°C for 6 min (UHP). When structural changes in cells of *L. monocytogenes* were compared using transmission electron microscopy (TEM), the nucleoid region of irradiated cells appeared to have spread throughout the cytoplasm. UHP-treated cells showed aggregated cytoplasm, indicating extensive protein denaturing. Structural

differences between PEF-treated and untreated cells were minimal, as revealed by TEM. Electrophoresis of genomic DNA from irradiated *L. monocytogenes* showed considerable fragmentation.

These DNA lesions were not detected when *L. monocytogenes* was treated with PEF or UHP. When irradiated cells were analyzed by pulsed field gel electrophoresis, the banding pattern changed into smearing. In conclusion, radiation, PEF and UHP targeted different loci in the cell and thus synergy between these treatments against *L. monocytogenes* is likely.

579. Fate of Aflatoxin M1 During Manufacture and Storage of Egyptian Karish Soft Cheese

Salwa A Aly and Diekmann H

International Journal of Biology, Pharmacy and Allied Science, 1(5): 780-785 (2012)

Aflatoxin M1 (AFM1) is an important mycotoxin frequently found in milk and dairy products. Egyptian karish cheese from raw cow's milk artificially contaminated with AFM1 at level of 100 ng/L (ppt) was fermented to reach pH 3.8 ± 0.04 . The samples were stored at 4°C for up to 3 weeks.

Analysis of AFM1 in karish cheese samples was carried out using immunoaffinity column coupled to indirect competitive enzyme-linked immunosorbent assay (ELISA) method. AFM1 in cheese showed a significant increase ($P < 0.01$) compared with those initially added to raw milk.

The level of AFM1 in cheese samples were 3.5 ± 0.07 fold. During the refrigerated storage AFM1 was rather more stable, the percentage losses were zero, 3.75 ± 0.05 , 6.25 ± 0.16 and 13.75 ± 0.24 by the end of storage with pH 4.1 ± 0.08 , 3.1 ± 0.01 , 2.5 ± 0.03 and 2.2 ± 0.01 , respectively.

Changes in AFM1 content of cheese samples were statistically insignificant ($P > 0.01$) during 3 weeks storage. The results indicate that the necessary precaution has to be taken to minimize the AFM1 contamination in milk.

Keywords: Soft Karish Cheese; Aflatoxin M; Stability During Storage.

Dept. of Medicine and Infectious Diseases

580. Clinical Survey and Selection of the Rapetic Approach for Emergent Feline Urological Syndrome

Wael M. Kelany

Life Science Journal, 9 (1s): 151-156 (2012) IF: 0.073

The management of cases of the emergent feline urological syndrome (FUS) is described with particular reference to urethral obstruction in the tom cat. Treatment of the obstructive episode, medical therapy in the post-obstruction period and the prevention of recurrence of blockage in the longer term are discussed. The target of the present investigation was rapid confirmation of diagnosis of feline urological syndrome with epidemiological studies and to choose the suitable life saving therapeutic regimen. Also, the important aim was prevention of recurrence of such cases. The present study was carried out on forty seven tom cats (42 clinically diseased tom cats and 5 apparently healthy tom cats). Clinical manifestations were stranguria ($n = 23$), bloody urine ($n = 23$) and frequent licking of the urinary opening ($n = 17$), frequent attempts to urinate end with failure ($n = 17$), isuria ($n =$

19), excessive salivation ($n = 15$), increased respiratory and pulse rates and vomiting ($n = 13$). Clinical examination was revealed severely distended urinary bladder and abdominal tenderness. Ultrasonographic examination revealed severe distension of urinary bladder, turbidity inside urinary bladder (floating debris) and dilation of renal pelvis (Hypoechoogenicity). Therapeutic approaches in order were either gentle manual compression of the bladder with milking of penile urethra or catheterization or cytocentesis followed by Perineal urethrostomy. It was concluded that confirmation of emergent feline urological syndrome by rigid urinary bladder during palpation. FUS was aggravated when vomiting was presented and accompanied by dilation of renal pelvis detected by ultrasonography. The most selected therapeutic regimen by the present investigation was catheterization (64.3%).

Keywords: Feline; Urological; Syndrome; Survey; Therapeutic.

581. First Isolation and Identification of Ovine Herpesvirus 2 Causing Malignant Catarrhal Fever Outbreak in Egypt

Iman M. Bastawecy and Abd El-Samee, A.A.

Life Science Journal, 9 (3): 798-804 (2012) IF: 0.073

Ovine herpesvirus 2 (Ov HV-2) was isolated for the first time from cattle and water buffalos during an outbreak of malignant catarrhal fever (MCF) in Egypt, 2012. The isolated virus was characterized as herpesvirus with negative staining electron microscopy (EM). Further identification using polymerase chain reaction (PCR) and nucleotide sequencing of the PCR product. GenBank confirmed it as ovine herpesvirus 2, complete genome with query coverage 100% and maximum identity 100% and ovine herpesvirus 2 strain BJ 1035, complete genome with query coverage 100% and maximum identity 99%. Separation of susceptible animals from sheep and goats specially during lambing is recommended and euthanasia of animals which were clinically infected with MCF is advised.

Keywords: Ovine Herpesvirus 2; Malignant Catarrhal Fever; Isolation; Electron Microscopy; Sequencing.

582. Epidemiology and Diagnosis of Feline Intestinal Lymphosarcomas in Egypt

Fayez Awadalla Salib, Haithem Ali Farghali and Sherein S.A. Elgayed

Journal of Advanced Veterinary Research, 2 (2012): 160-168 (2012)

Feline intestinal lymphosarcomas are mostly caused by Feline Leukemia Virus (FeLV). Unfortunately, there is no available vaccine for FeLV in Egypt. The diagnosis of feline intestinal lymphosarcomas depends upon abdominal palpation, x-rays examination, ultrasonography, direct ELISA and histopathology of masses excised during laparotomy. The recorded clinical signs in intestinal lymphosarcoma affected cats were variable including vomiting, fever, anorexia, ascites, anemia, dyspnea, constipation and emaciation. The affected lymph nodes were mesenteric, mediastinal and retropharyngeal. The prevalence of intestinal lymphosarcomas in the examined cats was 4.03 % (11 out of 273 cats). The prevalence was higher in queens than toms (2.93 % and 0.73 % respectively). The Siamese cats had higher prevalence than the Sherazy ones (2.56 % and 1.47 % respectively). X-ray films and ultrasonographic images performed on the eleven cats

suffered from intestinal lymphosarcomas revealed ascities and abdominal masses. The comparison of ELISA and histopathology (of excised masses) results showed that 9 out of 11 intestinal lymphosarcoma affected cats were infected with FeLV that proved not all cases of intestinal lymphosarcoma were caused by FeLV. The sensitivity, specificity and accuracy of ELISA to diagnose intestinal lymphosarcoma in cats were 81.81 %, 100 % and 92 % respectively. Gross autopsy of the collected lymph nodes, livers, kidneys revealed that gross lymphadenopathy involving one or more nodes, hepatomegaly and kidney enlargement. Microscopically, the examined tissues specimens showed that the normal architecture of the examined lymph nodes, livers and kidneys has been replaced by a diffuse infiltrate of both lymphocytes and lymphoblasts. The vast majority of the cells are small lymphocyte-type cells with round basophilic nuclei and a sparse rim of cytoplasm. The eleven intestinal lymphosarcoma affected cats exposed to abdominal exploratory surgery (laparotomy) died at one to three months post-surgery. It is concluded that the vaccination of kittens and cats against FeLV in Egypt is very important to prevent the highly fatal intestinal lymphosarcomas.

Keywords: Lymphosarcoma; Felv; Cat; Diagnosis; Egypt.

583. in Vitro Evaluation of Sheep Rumen Fermentation Pattern after Adding Different Levels of Eugenol – Fumaric Acid Combinations

T A M Baraka and M A Abdl-Rahman

Vet. World, 5(2): 110-117 (2012)

In vitro gas production technique was used to evaluate the effect of three different levels of eugenol + fumaric acid combinations on rumen fermentation. Rumen contents were collected from five rams immediately after slaughtering and used for preparation of inoculums of mixed rumen microbes that were used in generation of five treatment systems, negative control with no additives (T1), fumaric acid 0.5 mg L⁻¹ (T2) and fumaric acid 0.5 mg L⁻¹ in combination with three different doses of eugenol, 100, 200 and 400 mg L⁻¹ (T3, T4 and T5 respectively). Incubations were conducted in triplicates with gas production, pH, ammonia nitrogen (NH₃-N), total and 3 fractional volatile fatty acids (VFAs) concentrations, cellulase activity, amount of substrate degraded, microbial yield (Y_p), fermentation efficiency (FE) and VFAs utilization index (NGGR) were determined after 24 hours of ATP incubation.

The results revealed that, different levels of eugenol + fumaric acid combinations were associated with decreased pH value, NH₃-N concentrations and methane production and increased valeric and isovaleric 3 acids molar proportions. T3 and T4 were associated with increased propionates at the expense of acetates (low A/P), decreased methane production and increased FE, microbial yield (Y_p) and VFAs utilization.

In contrast, ATPT5 showed decreased total VFAs concentrations, cellulase activity, the amount of substrate degraded, microbial mass generated and VFAs utilization. In conclusion, the authors recommend using 200 mg L⁻¹ eugenol + fumaric acid combination as an alternative for antibiotic feed additives to optimize rumen fermentation pattern. Further investigations are required to apply this work in vivo experiments.

Keywords: Eugenol; Fermentation Efficiency; Fumaric Acid; Rumen Microbes.

Dept. of Microbiology

584. Methicillin-Resistant Staphylococcus Aureus: an Emerging Pathogen of Pets in Egypt with A Public Health Burden

K. A. Abdel-moein, M. El-Hariri and A. Samir

Transbound Emerg Dis, 59: 331-335 (2012) IF: 1.809

Community-acquired methicillin-resistant Staphylococcus aureus (CA-MRSA) has emerged to be a pathogen of public health burden causing infections with significant concern. This study was conducted to investigate methicillin-resistant Staphylococcus aureus (MRSA) infection in pet dogs and cats as an emerging zoonosis that could be disseminated in the community. A total of 184 (nasal, oral, ear and wound) swabs were collected from 70 pet dogs and 48 pet cats, whereas 50 nasal and oral swabs were collected from 28 apparently healthy companion persons in intimate contact with pets and without history of hospitalization. All samples were cultured for the isolation and identification of Staphylococcus aureus using selective media, biochemical and serological tests, while isolates were identified as MRSA after antimicrobial susceptibility testing and determination of the MIC. PCR was applied using specific primers to confirm MRSA. Three MRSA isolates have been recovered from two dogs of 70 (2.9%) and one isolate from 28 examined persons (3.6%), while none of the examined cats yielded MRSA. Furthermore, we found that two MRSA isolates recovered from one diseased dog seemed to be hospital-associated methicillin-resistant Staphylococcus aureus (HA-MRSA), whereas the other dog isolate as well as the human isolate were considered as community-acquired (CAMRSA). The occurrence of MRSA in apparently healthy and/or diseased pet dogs makes it an emerging veterinary pathogen which could be considered a public health burden if it is disseminated in our community outside hospitals.

Keywords: Pets; Mrsa; Emerging Zoonosis; Community.

585. Prevalence of Clostridium Perfringens Type A Isolates in Commercial Broiler Chickens and Parent Broiler Breeder Hens in Egypt

K.M. Osman, Y.A. Soliman, Z.M.S. Amin and M.A.K. Aly

Scientific and Technical Review, World Organization for Animal Health (Oie), 31 (3): 931-941 (2012) IF: 1.099

The aim of this study was to determine the presence of genes coding for alpha (cp), beta (cp), epsilon (tx), iota (A), enterotoxin (cp) and beta2 (cp2) toxin in Clostridium perfringens isolates from broiler chickens and parent broiler breeder hens, using multiplex polymerase chain reaction (PCR) assay. The incidence of C. perfringens in the intestinal segments and the effects of age were also investigated.

The highest percentage of isolates from the broiler chickens and parent broiler breeder hens was found in the duodenum, with an incidence of 41.7% and 58.4%, respectively and the lowest percentage of isolates came from the ileum, with an incidence of 15.6% and 31.3%, respectively.

Chickens harboured C. perfringens in the intestine and this increased with age. Clostridium perfringens was detected in 35.4% (17/48) of asymptomatic broiler chickens and 22.1% (17/77) of asymptomatic parent broiler breeder hens.

The bacterium was detected in 100% of the broiler chickens and parent broiler breeder hens with clinical signs (31/31 and 60/60,

respectively). The multiplex PCR assay indicated that in 99 (79.2%) of the 125 samples that tested positive for *C. perfringens* the strains isolated were type A and were shown to carry the cp gene (99/99, or 100%).

The gene encoding cp2-toxin was present in 62.6% (62/99) of the isolates. A significant association was found between *C. perfringens* possessing the cp2-toxin gene and necrotic enteritis in broiler chickens and parent broiler breeder hens, suggesting that this gene might play a key role in the pathogenesis of the disease in Egypt. Therefore, the authors suggest that the presence of the cp2-toxin gene in *C. perfringens* isolates found in broiler chickens and parent broiler breeder hens during this study poses a risk of transmission to humans through the food chain.

Keywords: Breeders; Broilers; Chickens; Cp; Cp; Cp; 2 Gene; Cp Toxins; Egypt; Tx; A; Necrotic enteritis; Poultry.

586. Chlamydiaceae in Riverine Buffalo (*Bubalus Bubalis*) and Cows (*Bos Taurus*) in Egypt with and Without Signs of Reproductive Disease.

Osman KM, Ali HA, Eljakee JA. and Galal HM

New Zeal Vet J, (2012) IF: 0.887

The presence of anti-Chlamydiaceae antibodies in 77% of the animals with signs of reproductive disease and the detection of Chlamydiaceae in 72% of vaginal swabs of the animals suggest a pathogenic role by Chlamydiaceae in riverine buffalo and cows. The main Chlamydiaceae found in the genital tract of cattle in Egypt were *Cp. psittaci* and *Cp. abortus*.

Keywords: Chlamydia Abortus; Chlamydia Psittaci; Reproductive disorder; Riverine buffalo; Cow.

587. Preparation and Evaluation of Elisa Polyvalent Salmonella Antigen for Detection of Salmonella Infection Among Poultry

Mona I. El-Enbaawy, Zakia A.M. Ahmed, M.A. Sadek and H.M. Darwish

World Applied Sciences Journal, 20 (6): 806-811 (2012)

Avian salmonellosis due to *Salmonella* B and D serogroups has a great importance because of its public health and economical impact in poultry industry. Serological diagnosis of *Salmonella* infection currently relies on laboratory-based ELISA for detection of antibodies against most predominant *Salmonella* serotypes. The present study was conducted to prepare sonicated polyvalent *Salmonella* antigen (group B and D) from local isolates. ELISA procedure was developed for the detection of *Salmonella* infection in experimentally infected chickens. For ELISA validation, the efficacy test was accomplished by reaction with known positive and negative serum. The results revealed that, relative sensitivity and specificity of ELISA using the polyvalent sonicated *Salmonella* antigen with chicken cloacae samples compared to bacteriological diagnosis were 100 and 55.5 %, respectively. The data indicated that the polyvalent *Salmonella* antigen isn't suitable for clinical testing and detection of *Salmonella* infection among poultry by ELISA as it showed a very low level of specificity.

Keywords: Polyvalent sonicated antigen; Elisa; Relative sensitivity; Relative specificity.

588. Molecular Characterization of E. Coli Isolated from Chicken, Cattle and Buffaloes

J.K. El-Jakee, R.M. Mahmoud, A.A. Samy, Mona A. El-Shabrawy, M.M. Effat and W.A. Gad El-Said

International Journal of Microbiological Research, 3 (1): 64-74 (2012)

E. coli plays an important role in maintaining intestinal physiology. However, there are pathogenic strains that cause distinct syndromes of diarrheal disease. In this study we used a collection of 28 *E. coli* isolated from cattle, buffaloes and chicken obtained in the same geographical area to perform a detailed analysis of the molecular epidemiology of O157 and non O157 strains by using PCR for identifying general similarities and differences in the genetic composition of *E. coli* populations. The isolates showed a degree of diversity in PCR of *stx1*, *stx2* and *eae*. 12 strains had *stx1* gene, 16 strains had *stx2* gene and 10 strains had *eae* gene. 76.92% of cattle isolates had *stx2* and 38.46% possessed both *stx1* and *stx2*, also *stx1* was detected from 38.46% of the examined cattle strains. Using restriction enzyme (RE) it is clear that between 3 to 6 fragments were obtained with *HindIII* digested DNA of chicken and buffalo isolates and between 3 to 5 fragments of cow isolates. Among *EcoRI* between 5 to 9 fragments were obtained with digested genomic DNA of chicken and cattle and 7 to 9 fragments of buffalo isolates. *HindIII* and *EcoRI* ribotyping could reveal only minor differences in non O157:H7 strains belonging to the same serotypes. This indicates that ribotyping which is regarded to be a useful tool for epidemiological investigation, was not able to discriminate between STEC isolates belonging to the same serotype. It is believed that in future a better understanding of molecular diversity of *E. coli* strains of different sources would provide and assist the design of approaches to epidemiological studies.

Keywords: *Escherichia coli*; O157; *Stx1*; *Stx2* and *eae* genes; Restriction enzyme.

589. Antimicrobial Susceptibility and Molecular Typing of Multiple Chlamydiaceae Species Isolated from Genital Infection of Women in Egypt

Kamelia M. Osman, Hadia A. Ali, Jakeen A. Eljakee, Maha M. Gaafar and Hussein M. Galal

Microbial Drug Resistance, 18, Number 4 440-445 (2012)
IF: 2.153

This study investigated the existence of vaginal Chlamydia infection and the prevalence of the disease in asymptomatic gynecologically diseased women in Egypt. In addition, the antibiotics penicillin, tetracycline and erythromycin were evaluated for their in vitro anti-chlamydial activity of the isolated strains. Vaginal swabs (n = 160) were collected from females gynecologically diseased using cotton swabs. Samples were tested for Chlamydia by Vero cells tissue culture, chicken embryo, Gimenez staining, direct fluorescein-conjugated monoclonal antibody staining and immunoperoxidase. Polymerase chain reaction (PCR) analyses conducted for the presence of chlamydial DNA was used to detect its specific DNA by the *omp2* gene. PCR analyses conducted for the presence of chlamydial DNA revealed that 112/160 (70%) were positive for Chlamydiaceae. The specific DNA defined by the *omp2* gene identified them as *Chlamydia trachomatis* (17/112, 15.2%), *Chlamydia psittaci*

(56/112, 50.0%) and *Chlamydia abortus* (40/112, 35.7%). The antibiotics penicillin, tetracycline and erythromycin at different concentrations were effective in inactivating the viability of Chlamydiaceae isolates.

Keywords: Antimicrobial Susceptibility; Chlamydiaceae; Genital Infection of Women In Egypt.

590. Prevalence of *Chlamydia psittaci* Infections in the Eyes of Cattle, Buffaloes, Sheep and Goats in Contact with a Human Population

K. M. Osman H. A. Ali, J. A. ElJakee and H. M. Galal

Transboundary and Emerging Diseases, (2012) IF: 1.809

This work is an example of cooperation between veterinary and human medicine being fully complementary and at the same time, indispensable to improve our knowledge on animal chlamydiosis. This study investigated the existence of ocular chlamydiae and determined the prevalence of its presence, chlamydiosis, in asymptomatic and diseased farm animals and adjacent humans. Data were obtained by the *omp2* gene family Chlamydiaceae-specific PCR. Two hundred cattle, buffaloes, sheep and goats and 44 human specimens were also examined. Conjunctival swabs from both the eyes were collected from all animals and humans using cotton swabs. Samples were tested for chlamydiae by Vero cell tissue culture, chicken embryo, modified Gimenez staining, direct fluorescein conjugated monoclonal antibody staining (FA), immunoperoxidase, CFT and PCR. The PCR-RFLP revealed that *Chlamydia psittaci* demonstrated in the conjunctival samples of cattle (68% asymptomatic and 88% diseased), of buffalo (68% asymptomatic and 72% diseased), of sheep (68% asymptomatic and 80% diseased), of goat (76% asymptomatic and 92% diseased) and of humans (77% asymptomatic and 82% diseased). The *Cp. psittaci* was the only chlamydiae demonstrated in all of the ocular conjunctival samples, which confirms the prevalence of *Cp. psittaci* in this population of animals and adjacent humans. Statistically, the animal species factor was calculated and was found to be of no significance. Yet, there appeared to be a significant difference in the percentage of animal that tested positive using the different methods. Detection of *Cp. psittaci* in most samples confirms the prevalence of *Cp. psittaci* in this population of animals and adjacent humans.

Keywords: *Chlamydia psittaci*; Cattle; Buffalo; Sheep.

591. Blood Heat Shock Proteins Evoked by Some *Salmonella* Strains Infection in Ducks

Kamelia Osman, Ihab Ibrahim, Ashgan Yousef, Tanios Nabil and AlAtfeehy Nayerah

World J Microb Biot, 370: 859-866 (2012) IF: 1.532

Bacterial heat-shock response is a global regulatory system required for effective adaptation to changes (stress) in the environment. An in vitro study was conducted to investigate the impact of a sublethal temperature (42°C) on heat shock protein (HSP) expression in 6 *Salmonella* strains (*Salmonella* Enteritidis, *S. Typhimurium*, *S. Virchow*, *S. Shubra*, *S. Haifa* and *S. Eingedi*). The 6 *Salmonella* strains were isolated from the tissues of ducklings that had died from avian salmonellosis. To determine the induction of HSP in the 6 *Salmonella* strains, they were exposed to the selected temperature level for 24 h and further kept for 48 h at culturing condition of 42°C. Growth under a sublethal

temperature of 42°C increased the expression of several proteins of *Salmonella*, including a 63 kDa protein in addition to the generation and/or overexpression of 143 proteins which were specific to heat shock, concurrent to this acquired thermotolerance. The 6 *Salmonella* strains responded to 24 h of thermal stress at an elevated temperature 42°C by synthesizing different heat shock proteins (HSP) with molecular weights ranging between 13.62 and 96.61 kDa. At 48 h, the 6 *Salmonella* strains synthesized different HSPs with molecular weights ranging between 14.53 and 103.43 kDa. It follows that *Salmonella* would produce HSPs during the course of the infectious process. Salmonellosis produced several proteins after 24 and 48 h of infection. Seven of these proteins (100, 80, 60, 40, 30, 20 and 10 kDa) were recognized in the serum obtained from the ducklings infected with *S. Enteritidis*, *S. Typhimurium*, *S. Virchow*, *S. Shubra*, *S. Haifa* and *S. Eingedi* after 24 h of infection. After 48 h, the 1–7 kDa HSP became more evident and indicated their de novo generation.

Keywords: *Salmonella* Serovars; Heat Shock Proteins.

592. The Prevalence of Multidrug Resistance of Various Numbers of Antimicrobial Classes, Multiple Resistance Patterns and Distribution of *Salmonella* Isolates from Human and Avian Clinical Cases of Diarrhoea

Kamelia M. Osman, Sherif H. Marouf, Ahmed Samir and Nayerah AlAtfeehy

Journal of Chemotherapy, 24(5): 300-304 (2012) IF: 1.084

Seventy *Salmonella* isolates recovered from human (n = 5) and poultry diagnostic samples (chickens, n = 18; ducks, n = 34; turkeys, n = 7; pigeons, n = 6) were tested for antimicrobial susceptibilities. Resistance was most often observed to lincomycin (98.6%), streptomycin (81.4%), chloramphenicol (80%), nalidixic acid (58.5%), followed by trimethoprim-sulfamethoxazole (45.6%), tetracycline (44.3%) and to a lesser extent neomycin (41.4%), trimethoprim (40%), ampicillin (35.7%), amoxicillin (31.3%), gentamicin (22.8%), norfloxacin (22.8%). Resistance dropped down to 4.3% and 1.4% in colistin sulphate and ciprofloxacin, respectively. The 70 *Salmonella* isolates were MDR. A large percentage of isolates were resistant to all antimicrobials assessed: lincomycin (92%), streptomycin (76%) and chloramphenicol (75%). All of the isolates (100%) were resistant to at least one antimicrobial, contributing to 54 different susceptibility profiles. A number of MDR isolates (27/70) exhibited a penicillin/aminoglycoside/ lincosamide/ fluoroquinolone/sulfonamide resistance profile and all of these were resistant to six or nine antimicrobial classes.

Keywords: *Salmonella*; Drug Resistance; Human; Chicken; Ducks; Turkeys; Pigeons.

593. Identification of Serotypes and Virulence Markers of *Escherichia coli* Isolated from Human Stool and Urine Samples in Egypt

KM Osman, AM Mustafa, M Elhariri and GS Abdelhamed

Indian J Med Microbi, 30(3): 308-313 (2012) IF: 0.988

Haemorrhagic colitis and haemolytic-uremic syndrome are associated with Shiga-toxin producing *Escherichia coli* (STEC). There are others DEC (Diarrhoeagenic *E. coli*)

pathotypes responsible for outbreaks and other toxins associated to these. Most clinical signs of disease arise as a consequence of the production of Shiga toxin 1 (Stx1), Stx2 or combinations of these toxins. Other major virulence factors include E. coli haemolysin (hlyA) and intimin, the product of the eaeA gene that is involved in the attaching and effacing adherence phenotype.

Materials and Methods: In this study, the PCR assay was used to detect 12 E. coli genes associated with virulence (stx1, stx2, hlyA, FliC7, stb, F41, K99, sta, F17, LT-I, LT-II and eaeA).

Results: A total of 108 E. coli strains were serotyped into 64 typable strains. The investigated strains from the stool, 8/80 (10%) strains were O164:K, while the 56/110 strains isolated from the urine were O126:K71 (44/110, 40%) and O86:K61 (12/110, 11%). The distribution pattern of the detected virulence genes was observed to be in the following order: F17 (10% from the stool and 44% from the urine), Sta (10% from the stool), hlyA (10% from the stool and 44% from the urine), Stb (44% from the urine) and stx1 (27% from the urine). The 8 faecal strains encoded a combination of the F17, Sta and hlyA genes, while the 56 urine strains encoded a combination of the F17 + Stb + hlyA (44/110, 40%) and Stx1 only (12/60, 20%).

Conclusion: This is the first report on the molecular characterization of E. coli diarrhoeagenic strains in Egypt and the first report on the potential role of E. coli in diarrhoea and urinary tract infections in a localized geographic area where the people engage in various occupational activities.

Keywords: E. Coli Virulence Markers; Human Diarrhoea; Pathogenic E. Coli; Urine.

594. Emergence of an Antimicrobial Resistant Pseudomonas Aeruginosa from Human and Animal Clinical Samples: A Zoonotic and Public Health Hazard

Kamelia M. Osman, Nagwa S. Ata, Riham H. Hedia, Azza S.M. Abu Elnaga, M. El-Hariri and Magda A.K. Aly

Global Veterinaria, : 1-7 (2012)

There is very little factual evidence to clarify the nature and extent of the multi-drug resistance (MDR) producing PER-1 Extended-spectrum β -lactamase (PER-1 ESBL) Pseudomonas aeruginosa problem in Egypt. The obtained results revealed that all isolates from human origin were totally resistant to ampicillin (100%) while the same isolates were totally sensitive to imipenem (100%). Most isolates were resistant to amoxicillin and less resistant to amoxicillin/clavulanic acid, but most isolates were sensitive to piperacillin while they were less sensitive to aztreonam. Results of detection of antimicrobial resistance of P. aeruginosa producing PER-1 ESBL revealed positive amplification of the 966 bp of PER-1 ESBL from the extracted DNA (only 3 PER-1 ESBL were positive isolates and 16 PER-1 ESBL were negative isolates). The results of detection of MDR to P. aeruginosa producing PER-1 ESBL revealed that the gene appeared to be chromosomally located and present in isolates from human burns and from the internal organs of diseased chicken. The prevalence of resistance gene reported here suggests that P. aeruginosa from cattle operations, poultry farms and veterinary or/and human clinics may be important contributors to environmental reservoirs of resistance genes. It also highlights the importance of spreading of the beta-lactamase-mediated resistance mechanisms between countries and continents.

Keywords: Pseudomonas Aeruginosa; Blaper-1; Antipseudomonal Agents; Chicken; Milk; Calves.

595. Protein Expression Diversity Amongst Different Serovars of Salmonella Enterica using Quantitative Real Time Pcr

K.M. Osman, M.I. Radwan, Zeinab M.S. Amin Girh, M.A. Bakry and A.S. Hakim

Global Veterinaria, 8 (6): 565-573 (2012)

The present endeavor was initiated to focus the study on closely related Salmonella serovars Gallinarum, Shubra, Typhimurium, Newport, Agona, Saintpaul and Kentucky, which are associated with the majority of infections of mammalian and avian hosts in Egypt. The objective was to consider the level of variation in the protein expression patterns of the five resolved over-regulated proteins [Salmonella pathogenicity island 1 effector protein (SPI 1 effector protein), response regulator protein (RRP), T cell inhibitor protein (STI), rfbS and heat shock protein 90 (HSP 90)]. These selected 5 genes showed over-expression on the level of protein in S. Gallinarum versus S. Enteritidis. Primers were designed using gene-specific sequences deposited in Gene Bank after aligning each gene with the same gene in different Salmonella serovars to choose the highly conserved regions. Different expression levels for the five proteins, HSP90, SPI1, TCI, rfbS and RRP, were examined among seven Salmonella serovars using QRT-PCR. The gene expression data were normalized to the 16S rRNA gene as reference house keeping gene. There was an over expression in the level of the mRNA in case of the 5 examined proteins in S. Gallinarum over the other Salmonella serovars. Hypothetically, this emphasizes the involvement of such proteins in host specificity or virulence in a specific host.

Keywords: Hsp90; Spi1; Tci; Rfbs; Rrp; Salmonella Serovars.

Dept. of Obstetrics, Reproduction & Artificial Insemination

596. Differential Effects of Linoleic and Alpha-Linolenic Fatty Acids on Spatial and Temporal Mitochondrial Distribution and Activity in Bovine Oocytes

Waleed F. Marei, D. Claire Wathes A and Ali and Fouladi-Nashta

Reproduction, Fertility and Development, 24(5):(2012) IF: 2.109

Using specific stains and confocal microscope imaging, the patterns of mitochondrial distribution, mitochondrial inner membrane potential and reactive oxygen species (ROS) levels during bovine oocyte maturation were determined in the presence or absence of physiological concentrations of linoleic acid (LA; 100 μ M) or α -linolenic acid (ALA; 50 μ M). Mitochondrial distribution in control oocytes at 0 h was mainly peripheral and changed to a diffused pattern after 1 h of culture; this was maintained up to 24 h. Mitochondrial clusters were observed during the early hours of maturation (1–4 h); the majority of these were arranged in perinuclear fashion. LA supplementation resulted in: (1) delayed redistribution of the mitochondria from a peripheral to a diffuse pattern and a decreased percentage of oocytes showing perinuclear mitochondrial clusters, (2) decreased

mitochondrial inner membrane potential at 1 and 24 h compared with the control and (3) higher ROS levels, associated with a lower nuclear maturation rate. In contrast, ALA supplementation had no effect on mitochondrial distribution and activity and decreased ROS levels compared with the control; this was associated with an increased nuclear maturation rate. In conclusion, LA induced alterations in mitochondrial distribution and activity as well as increasing ROS levels, which mediate, at least in part, the inhibitory effect on oocyte maturation. *Reproduction, Fertility and Development*, 2012, 24, 679–690.

Keywords: Jc-1; Mitochondria; Mitotracker; Oocyte Maturation.

597. *In Vitro* Fertilization of Ovine Oocytes Vitrified by Solid Surface Vitrification at Germinal Vesicle Stage

Adel R. Moawad, Patricia Fisher, Jie Zhu, Inchul Choi, Zsuzsanna Polgar, Andras Dinnyes and Keith H.S. Campbell

Cryobiology, 65: 139-144 (2012) IF: 2.062

Cryopreservation of immature oocytes at germinal vesicle (GV) stage would provide a readily available source of oocytes for use in research and allow experiments to be performed irrespective of seasonality or other constraints. This study was designed to evaluate the recovery, viability, maturation status, fertilization events and subsequent development of ovine oocytes vitrified at GV stage using solid surface vitrification (SSV). Cumulus oocyte complexes (COCs) obtained from mature ewes were randomly divided into three groups (1) SSV (oocytes were vitrified using SSV), (2) EXP (oocytes were exposed to vitrification and warming solutions without vitrification) or (3) Untreated (control). Following vitrification and warming, viable oocytes were matured *in vitro* for 24h. After that, nuclear maturation was evaluated using orcein staining. Matured oocytes were fertilized and cultured *in vitro* for 7 days. Following SSV, 75.7% (143/189) oocytes were recovered. Of those oocytes recovered 74.8%, 107/143 were morphologically normal (viable). Frequencies of *in vitro* maturation were significantly ($P < 0.01$) decreased in SSV and EXP groups as compared to control. *In vitro* fertilization rates were significantly ($P < 0.01$) decreased in SSV (39.3%) group as compared to EXP (56.4%) and control (64.7%) groups. Cleavage at 48h post insemination (pi) and development to the blastocyst stage on day 7 pi were significantly ($P < 0.001$) decreased in SSV oocytes as compared to EXP and control groups. In conclusion, immature ovine oocytes vitrified using SSV as a simple and rapid procedure can survive and subsequently be matured, fertilized and cultured *in vitro* up to the blastocyst stage, although the frequency of development is low.

Keywords: Oocytes; Vitrification; Gv; Ovine; Ssv; Ivf.

598. Antioxidant Capacity of Follicular Fluid in Relation to Follicular Size and Stage of Estrous Cycle in Buffaloes

K.H. El-Shahat and M. Kandil

Theriogenology, 77, Issue 8: 1513-1518 (2012) IF: 1.963

The present study was designed to evaluate the changes in the concentrations of different antioxidants, such as glutathione (GSH), glutathione reductase (GR), superoxide dismutase (SOD) and catalase (CAT), in the follicular fluid collected from different

follicular size categories in relation to stage of estrous cycle in buffaloes. In addition, malondialdehyde (MDA) as an indicator for lipid peroxidation was also estimated. Fifty pairs of buffalo ovaries were collected from a local slaughterhouse. Based on ovarian structures, the cycle was divided into follicular and luteal phase. The follicles on each pair were classified into three groups; small (3 mm), medium (4–9 mm) and large (10 mm). The concentrations of SOD, CAT, GSH and GR in the follicular fluid of each group as well as MDA were estimated. Results indicated that there was a significant decrease ($P < 0.05$) in the average numbers of small follicles obtained at the follicular phase than those obtained at the luteal phase of the cycle. However, the mean numbers of the large sized follicles was significantly increased ($P < 0.05$) in the follicular phase than in the luteal phase. Large follicles obtained at the luteal phase had a significantly higher ($P < 0.05$) concentration of GSH than that obtained from small ones. A significant ($P < 0.05$) effect of follicular size on GR concentrations was observed. The concentration of SOD tended to be higher in large follicles obtained at the follicular phase than that collected at the luteal phase (56.7 \pm 3.7 vs. 28.1 \pm 6.7 U/mL, respectively). On the contrary, a significantly higher concentration ($P < 0.05$) of SOD was recorded in small follicles as compared with medium and large follicles collected at the luteal phase. CAT concentrations did not significantly differ among different follicular sizes between follicular and luteal phases as well as within each phase. Malondialdehyde concentration was significantly decreased ($P < 0.05$) in the follicular fluid obtained from small follicles collected at the follicular phase compared with those obtained at the luteal phase. In conclusion, the present study showed that the concentrations of enzymatic antioxidants except for CAT vary according to the follicle size and the stage of the estrous cycle suggesting their possible role in the process of follicular development during estrous cycle in buffaloes.

Keywords: Antioxidant; Follicles; Estrous Cycle; Buffaloes.

599. Role of Hyaluronic Acid in Maturation and Further Early Embryo Development of Bovine Oocytes

W.F. Mareia, b, F. Ghafaric and A.A. Fouladi-Nashtaa

Theriogenology, 78 (2012): 670-677 (2012) IF: 1.963

Hyaluronic acid (HA), an important component of the extracellular matrix, plays a crucial role for cumulus cell expansion. Genes and proteins involved in HA synthesis and its receptor CD44 are expressed in cumulus oocyte complexes (COCs) in different animal species and increase during maturation. Hyaluronidase enzymes (Hyal) degrade HA into smaller biologically active HA fragments. To investigate the effects of the molecular size and concentration of HA on oocyte maturation and further embryo development, bovine oocytes were matured *in vitro* in the presence or absence of HA, Hyal-2 or 4-methylumbelliferone (4-MU); an HA synthesis inhibitor. The rates of oocyte nuclear maturation to metaphase II stage and development of embryos to blastocyst stage and blastocyst quality were recorded. Hyal-2 inhibited cumulus cell expansion without affecting oocyte maturation and further embryo development. Whereas, 4-MU at 1 mM reduced cumulus cell expansion, oocyte maturation rate and further embryo development; an effect which was partially abrogated by exogenous HA supplementation. These data suggest that HA production by cumulus cells during maturation is essential not only for cumulus cell expansion, but also for oocyte maturation and further embryo development. This

effect is not affected by HA-degradation by Hyal-2. *Theriogenology* 78 (2012) 670–677.

Keywords: Hyaluronidase; 4-Methylumbelliferone; Oocyte Maturation; Blastocyst.

600. Hormonal and Biochemical Serum Assay in Relation to the Estrous Cycle and Follicular Growth in Arabian Mare

Amal M. Abo-El maaty and K. H. El-Shahat

Asian Pacific J Reproduction, 1(2): 105-110 (2012)

The current study is an endeavor for profound understanding hormonal and biochemical constituents during the estrous cycle of Arabian mare serum. **Methods:** Ten Arab brood mares of previous foaling records were scanned with ultrasound each other day and blood samples were collected with each ultrasound examination. Follicles and corpus luteum diameter were measured. The follicles were classified according to their diameter into small, medium, dominant, first and second largest. Hormonal concentrations of thyroxin, progesterone, estradiol and testosterone were assayed. Superoxide dismutase (SOD), malondialdehyde (MDA), nitric oxide (NO) and total antioxidants concentrations (TAC) were measured. Besides, total proteins, albumin, globulin, glucose, total cholesterol, triglycerides and levels were assayed. **Results:** The data revealed that the serum progesterone levels in mare were significantly ($P < 0.05$) higher in luteal phase than those recorded at time of estrus. The reverse was true for estradiol. However, the levels of testosterone and thyroxin did not significantly change during estrus cycle in mare. No significant difference was observed in the serum level of total protein, albumin and globulin in both phases of estrous cycle. Similar finding was observed in SOD concentrations. In contrast, the concentrations of glucose, cholesterol and triglyceride tended to be significantly ($P < 0.05$) higher in estrus stage than those recorded at luteal one. The same finding was observed in NO levels. On other hand, TAC assay significantly increased ($P < 0.05$) in mare serum obtained from luteal phase than those obtained at estrous one. A reverse was true for MDA levels. **Conclusion:** the data indicated that the steroid hormones and metabolic constituents of mare serum (glucose, cholesterol and triglyceride) as well as NO, MDA and TAC vary according to the stage of the estrous cycle suggesting their possible role in the process of follicular development in mare.

Keywords: Mare; Estrous Cycle; Hormones; Biochemical Constituents.

601. A Comparative Study of Vitrification and Slow Freezing on Subsequent Developmental Capacity of Immature Sheep Oocytes

El-Shahat K.H and Hamam A.M.

Theriogenology Insight, 2(2): 145-152 (2012)

The present study evaluated the post warming morphologic survival and subsequent in vitro maturation and development of immature ovine oocytes cryopreserved by either conventional slow freezing or vitrification. Cumulus oocyte complexes (COC's, $n=300$) retrieved from slaughter house ovaries were serially kept for 10 min each in a freezing solution (FS) containing different concentrations of glycerol (3.3%, 6.6% and 10%) prepared in Modified dulbeccos phosphate buffered saline

supplemented with 10.0% fetal calf serum, 10% sucrose and 1.0% antibiotic-antimycotics. COCs (10-15) were then loaded in pre-sterilized 0.25 mL empty semen straws and cryopreserved by either conventional slow freezing ($n=150$) or vitrification ($n=150$). After 7-10 days of cryostorage in liquid nitrogen, COCs were warmed and evaluated for morphologic damage. Morphologically normal COCs were matured in vitro in TCM-199, evaluated for cumulus expansion and fertilized with frozen ram semen prepared in Brackett and Oliphant medium supplemented with heparin and caffeine. Inseminated oocytes were cultured in vitro for 5-6 days for embryo development. Freshly collected oocytes ($n=100$) were also matured, fertilized and cultured in vitro and kept as control. A significantly ($p < 0.05$) higher proportion of morphologically normal oocytes were recovered after vitrification-thawing than those obtained with slow cooling (73.33 vs 56.67%, respectively). Among the damaged oocytes, cracking of zona pellucida and leakage of cellular contents were the most frequently observed abnormalities. A significantly higher ($p < 0.05$) proportion of in vitro maturation was observed for vitrified-warmed oocytes in glycerol than those obtained with slow freezing. A similar trend was observed for development to morula and blastocyst stage. However, in vitro developmental competence was higher for fresh oocytes (control) than those obtained for vitrified or slow frozen oocytes. In conclusion, vitrification of sheep oocytes in 10% of glycerol yields better oocyte survival, in vitro maturation and embryo development compared to conventional slow freezing.

Keywords: Sheep; Oocyte; Vitrification; Slow.

Dept. of Parasitology

602. Molluscicidal and Mosquitocidal Activities of the Essential Oils of Thymus Capitatus L. and Marrubium Vulgare L.

M.M. Salama, E.E. Taher and M.M. El. Bahy

American Journal of Drug Discovery And Development, 2(4): 204-211 (2012)

Molluscicidal activity of Thymus capitatus and Marrubium vulgare essential oils on adult and eggs of Biomphalaria alexandrina as well as on different stages of Culex pipiens was evaluated for their effectiveness on vector control. Steam distillation of essential oils of the flowering aerial parts of both Thymus capitatus L. and Marrubium vulgare L. yielded 0.5 and 0.2%, respectively. Results of GC/MS analyses of the two samples revealed an identified components in both oils amounted to 96.27 and 90.19% of the total oil composition for T. capitatus and M. vulgare, respectively. The two oil samples appeared dominated by the oxygenated constituents (88.22 and 57.50% for T. capitatus and M. vulgare, respectively). These were mainly composed of phenols among which carvacrol (32.98%) and thymol (32.82%) were the major constituents in T. capitatus oil while in M. vulgare oil, thymol (34.55%) was the major constituent. Borneol was present only in T. capitatus oil (9.15%). T. capitatus essential oil gave LC₅₀ and LC₉₀ mortality against adult snails at 200 and 400 ppm/3 h, respectively while that of M. vulgare was 50 and 100 ppm/3 h, respectively. On the other hand, M. vulgare showed LC₅₀ ovicidal activity at 200 ppm/24 h while T. capitatus oil showed no ovicidal activity. Insecticidal activity of both two essential oils revealed LC₅₀ and LC₉₀ larvicidal activity at 100 and 200 ppm/12 h, respectively and LC₅₀ and LC₉₀,

pupicidal activity at 200 and 400 ppm/12 h, respectively. Results of this study suggest that plant essential oils may have a promising role in vector control with needed continuing investigations.

Keywords: Plant extracts; *Thymus eapitatus*; *Marrubium vulgare*; Molluscicides; *Biomphalaria alexandrina*; Larvaecides; *Culex pipiens*.

Dept. of Pathology

603. In Vitro Differentiation of Endothelial Progenitor Stem Cells Derived from Peripheral Blood of Camel

Hala M.F. El Miniawy, Dina Sabry and Laila A. Rashed

J. of Camel Practice and Research, 19(2): 1-7 (2012) IF: 0.061

The peripheral blood-derived mononuclear cells (PBMNCS) obtained from camel blood when set in culture gave rise to adherent cells. The count of colony forming unit (CFU) after culturing PBMNCS for 7 days were significantly lower in the non pregnant animals than in the pregnant ones (32.4 ± 26.7 versus 65.2 ± 18.3 , respectively). Flow cytometry analysis shows the expression of CD34 + (33.8%), CD14 + (33%) and CD29 + (22.8%), the latter is a marker for mesenchymal stem cells although direct evidence for the presence of mesenchymal progenitor cells (MPCS) in the peripheral blood does not exist. The stem/progenitor cell characteristics were evidenced by their proliferative capacities and their ability to differentiate into osteoblasts, chondrocytes and neural cells after culture for 2 months in a modified conditioned medium. The stemness capacity of the PB-MNCS of camel was proven in this study and further study was needed to establish the clinical application of these stem cells.

Keywords: Camel; Differentiation; Endothelial Progenitor Cells; Peripheral Blood; Stem Cells.

Dept. of Pharmacology

604. Synthesis, Biological Evaluation and Radioiodination of Halogenated Closo-Carboranylthymidine Analogues

Rohit Tiwari, Antonio Toppino Hitesh K. Agarwal Tianyao Huo, Youngjoo Byun, Judith Gallucci, Sherifa Hasabelnaby, Ahmed Khalil, Ayman Goudah, Robert A. Baiocchi, Michael V. DarbyRolf F. Barth and Werner Tjarks

Inorganic Chemistry, 51: 629-639 (2012) IF: 4.601

The synthesis and initial biological evaluation of 3-carboranylthymidine analogues (3CTAs) that are (radio)halogenated at the closo-carborane cluster are described. Radiohalogenated 3CTAs have the potential to be used in the radiotherapy and imaging of cancer because they may be selectively entrapped in tumor cells through monophosphorylation by human thymidine kinase 1 (hTK1). Two strategies for the synthesis of a 127I-labeled form of a specific 3CTA, previously designated as N5, are described: (1) direct iodination of N5 with iodine monochloride and aluminum chloride to obtain N5-127I and (2) initial monoiodination of o-carborane to 9-iodo-o-carborane followed by its functionalization to N5-127I. The former strategy produced N5-127I in low yields along with

di-, tri- and tetraiodinated N5 as well as decomposition products, whereas the latter method produced only N5-127I in high yields. N5-127I was subjected to nucleophilic halogen- and isotope-exchange reactions using Na⁷⁹/81Br and Na¹²⁵I, respectively, in the presence of Herrmann's catalyst to obtain N5-79/81Br and N5-125I, respectively. Two intermediate products formed using the second strategy, 1-(tert-butyl(dimethylsilyl)-9-iodo-o-carborane and 1-(tert-butyl(dimethylsilyl)-12-iodo-o-carborane, were subjected to X-ray diffraction studies to confirm that substitution at a single carbon atom of 9-iodo-o-carborane resulted in the formation of two structural isomers. To the best of our knowledge, this is the first report of halogen- and isotope-exchange reactions of B-halocarboranes that have been conjugated to a complex biomolecule. Human TK1 phosphorylation rates of N5, N5-127I and N5-79/81Br ranged from 38.0% to 29.6% relative to that of thymidine, the endogenous hTK1 substrate. The in vitro uptake of N5, N5-127I and N5-79/81Br in L929 TK1(+) cells was 2.0, 1.8 and 1.4 times greater than that in L929 TK1 cells.

Keywords: Radioiodination; Closo; Carboranylthymidine; 3Carboranylthymidine Analogues; Thymidine.

605. Residual Determination of Clothianidin and its Metabolites in three Minor Crops Via Tandem Mass Spectrometry

Bo Mi Kim, Joon-Seong Park, Jeong-Heui Choi, A.M. Abd El-Aty, Tae Woong Na and Jae-Han Shim

Food Chem, 131: 1546-1551 (2012) IF: 3.655

A determination method for clothianidin and its metabolites (MNG, TMG, TZMU and TZNG) in crown daisy, sedum and amaranth grown under greenhouse conditions has been developed. The target compounds were identified and quantitatively determined using liquid chromatography coupled to tandem mass spectrometry. The matrix-matched calibration curves, used for quantification of the field-incurred analyte residues, were linear with coefficients of determination (r^2) exceeding 0.99. The matrix effects ranged from -61.4 ± 3.6 to 328.3 ± 26.9 in three different crops. The limits of detection and quantitation were in the ranges of 0.01–0.04 and 0.04–0.16 mg/kg, respectively. The mean recoveries of the analytes ranged between 71.7% and 120.3%. The validated method developed herein was successively applied for the determination of clothianidin and its four metabolites in field-incurred samples. The parent compound, clothianidin, was identified as the main residue and the metabolite residues were variable in the treated crown daisy, sedum and amaranth samples.

Keywords: Clothianidin; Lc–Ms/Ms; Metabolites; Minor Crops; Quenchers.

606. Pepper Leaf Matrix as A Promising Analyte Protectant Prior to the Analysis of the Rmolabile Terbufos and its Metabolites in Pepper using Gc-Fpd

Md. Musfiqur Rahman, Jeong-Heui Choi, A.M. Abd El-Aty, Morad D.N. Abid, Jong-Hyounk Park Tae Woong Na, Yong-Doo Kim and Jae-Han Shim

Food Chem, 133: 604-610 (2012) IF: 3.655

During gas chromatography (GC), the matrix can deactivate the active site during the transport of the compound from the injector

to the detector. This deactivation capacity varies among matrices, as it is dependant on the concentrations of the different constituent compounds of each matrix. During the analysis of terbufos and its metabolites, two of its metabolites were highly thermolabile and were readily decomposed inside the GC system. As the matrix can mask the active site, we carried out a matrix matched calibration in an effort to protect the analyte against decomposition. As a component of our analysis, the pepper matrix was the first to be matched; however, it failed to completely protect the metabolites. Subsequently, a variety of different compounds, including 3-ethoxy-1,2-propanediol, gulonolactone and sorbitol at 10, 1 and 1 mg/mL were tested; however, none of these generated the desired effect. We surmised that some of the compounds may have decomposed inside the injection port, so we introduced a carbofrit inlet liner, which is highly inert. But, this step did not improve the protective qualities of the matrices. Finally, pepper leaf matrix was added to the pepper matrix and we observed a profound protective effect for almost all of the analytes tested. A selective detector (flame photometric detector with phosphorus filter) was used to facilitate a high matrix concentration without interaction with the analyte. After resolving the problem of these two metabolites, terbufos and its five toxic metabolites were analyzed in pepper and pepper leaf samples. The recovery rates for terbufos and its metabolites were 73–114.5% with a relative standard deviation of <12%. This method was successfully applied to field samples and terbufos sulfone, terbufos sulfoxide and terbufoxon sulfoxide were found as residues in the suspected pepper and pepper leaf samples.

Keywords: Gas chromatography; Analyte Protectant; Matrix Effect; Unstable Metabolite; Thermolabile Pesticide.

607. Determination of Spinetoram and its Metabolites in Amaranth and Parsley using Quenchers-Based Extraction and Liquid Chromatography-Tandem Mass Spectrometry

Ki Hun Park, Jeong-Heui Choi, A.M. Abd El-Aty, Soon-Kil Cho, Jong-Hyouk Park, Bo Mi Kim, Angel Yang, Tae Woong Na, Md. Musfiqur Rahman, Geon-Jae Im and Jae-Han Shim

Food Chem, 134: 2552-2559 (2012) IF: 3.655

In this study, a simultaneous method was developed for the determination of spinetoram (XDE-175-J and XDE-175-L) and its demethyl metabolites (N-demethyl-175-J and N-demethyl-175-L) and formyl metabolites (N-formyl-175-J and N-formyl-175-L) in the minor crops; amaranth and parsley. The method uses quick, easy, cheap, effective, rugged and safe (QuEChERS)-based extraction. Afterwards, the analytes were quantified and confirmed via liquid chromatography–electrospray ionisation tandem mass spectrometry (LC–ESI–MS/MS) in the positive ion mode using multiple reaction monitoring (MRM). Calibration curves were linear over the calibration ranges for all the analytes tested with $r^2 > 0.993$. Limits of detection and quantitation were 0.01 and 0.03 mg/kg for all the tested analytes in amaranth and parsley, respectively. Recovery values, at spiking levels 0.05 and 0.25 mg/kg, ranged from 71.0% to 115.2% with relative standard deviations <15%, except for N-formyl-175-J in both amaranth and parsley. This method was applied to field-incurred samples and was shown to provide an adequate sensitivity and performance for the simultaneous determination of spinetoram and metabolites. To the best of our knowledge, this is the first

time spinetoram and its metabolites were quantified using LC–MS; MS in minor crops.

Keywords: Simultaneous Determination; Spinetoram; Metabolites; Minor Crops; Lc–Esi–Ms; Ms.

608. Synthesis, Chemical and Enzymatic Hydrolysis and Aqueous Solubility of Amino Acid Ester Prodrugs of 3-Carboranyl Thymidine Analogs for Boron Neutron Capture Therapy of Brain Tumors

Sherifa Hasabelnaby, Ayman Goudah, Hitesh K. Agarwal, Mosaad S.M. Abd alla and Werner Tjarks,

European Journal of Medicinal Chemistry, 55: 325-334 (2012) IF: 3.346

Various water-soluble L-valine-, L-glutamate- and glycine ester prodrugs of two 3-Carboranyl Thymidine Analogs (3-CTAs), designated N5 and N5-2OH, were synthesized for Boron Neutron Capture Therapy (BNCT) of brain tumors since the water solubilities of the parental compounds proved to be insufficient in preclinical studies. The amino acid ester prodrugs were prepared and stored as hydrochloride salts. The water solubilities of these amino acid ester prodrugs, evaluated in phosphate buffered saline (PBS) at pH 5, pH 6 and pH 7.4, improved 486600 times compared with parental N5 and N5-2OH. The stability of the amino acid ester prodrugs was evaluated in PBS at pH 7.4, Bovine serum and Bovine cerebrospinal fluid (CSF). The rate of the hydrolysis in all three incubation media depended primarily on the amino acid moiety and, to a lesser extent, on the site of esterification at the deoxyribose portion of the 3-CTAs. In general, 30-amino acid ester prodrugs were less sensitive to chemical and enzymatic hydrolysis than 50- amino acid ester prodrugs and the stabilities of the latter decreased in the following order: 50-valine > 50- glutamate > 50-glycine. The rate of the hydrolysis of the 50-amino acid ester prodrugs in Bovine CSF was overall higher than in PBS and somewhat lower than in Bovine serum. Overall, 50-glutamate ester prodrug of N5 and the 50-glycine ester prodrugs of N5 and N5-2OH appeared to be the most promising candidates for preclinical BNCT studies.

Keywords: 3-Carboranyl Thymidine Analogs; Amino Acid Ester Prodrugs; Boron Neutron Capture Therapy; Glioblastoma Multiforme.

609. Synergistic Effect of Washing and Cooking on the Removal of Multi-Class Pesticides From Various Food Samples

Angel Yang, Jong-Hyouk Park, A.M. Abd El-At, Jeong-Heui Choi, Jae-Ho Oh, Jung-Ah Do, Kisung Kwon, Ki-Hoon Shim, Ok-Ja Choi and Jae-Han Shim.

Food Control, 28: 99-105 (2012) IF: 2.656

The principal objective of this study was to investigate the effect of household processing, including washing and cooking on pesticide residue levels in various food samples. For this study, 31 food materials were selected and 44 pesticide residues were monitored using the “quick, easy, cheap, effective, rugged and safe” QuEChERS extraction-based and liquid chromatography tandem mass spectrometry (LC-MS/MS) methods. Eight pesticides, including acetamiprid, azoxystrobin, fenobucarb, fosthiazate, iprobenfos, lufenuron, propiconazole and trifloxystrobin were detected in nine food samples including

colored rice, glutinous rice (white rice), glutinous rice (unpolished rice), green chili, ginger, butterbur, chinamul, spinach and perilla leaf. Results indicated that residue levels in positive food commodities declined substantially following washing and cooking. However, the residual level of acetamiprid increased in green chilis after boiling and stir-frying. In sum, household processing (washing and cooking) tended to substantially reduce or eliminate pesticide residues in a synergistic manner. These applications are necessary to protect consumers from the negative health effects of pesticide residues detected in food commodities.

Keywords: Pesticide Residues; Quechers; Washing; Cooking; Household Processing; Lc; Ms/Ms.

610. Development of Quechers-Based Extraction and Liquid Chromatography-Tandem Mass Spectrometry Method for Quantifying Flumethasone Residues in Beef Muscle

Ki Hun Park, Jeong-Heui Choi, A.M. Abd El-Aty, Soon-Kil Cho, Jong-Hyoun Park, Ki Sung Kwon, Hee Ra Park, Hyung Soo Kim, Ho-Chul Shin, Mi Ra Kim and Jae-Han Shim

Meat Sci, 92: 749-753 (2012) IF: 2.275

A rapid, specific and sensitive method based on liquid chromatography–electrospray ionization tandem mass spectrometry (LC–ESI–MS/MS) in the positive ion mode using multiple reaction monitoring (MRM) was developed and validated to quantify flumethasone residues in beef muscle. Methods were compared between the original as well as the EN quick, easy, cheap, effective, rugged and safe (QuEChERS)-based extraction. Good linearity was achieved at concentration levels of 5–30g/kg. Estimated recovery rates at spiking levels of 5 and 10g/kg ranged from 72.1 to 84.6%, with relative standard deviations (RSDs) 7%. The results of the inter-day study, which was performed by fortifying beef muscle samples (n=18) on 3 separate days, showed an accuracy of 93.4–94.4%. The precision (expressed as relative standard deviation values) for the inter-day variation at two levels of fortification (10 and 20g/kg) was 1.9–5.2%. The limit of detection (LOD) and limit of quantitation (LOQ) were 1.7 and 5g/kg, at signal-to-noise ratios (S/Ns) of 3 and 10, respectively. The method was successfully applied to analyze real samples obtained from large markets throughout the Korean Peninsula. The method proved to be sensitive and reliable and, thus, rendered an appropriate means for residue analysis studies.

Keywords: Corticosteroids; Flumethasone; Residue Analysis; Lc–Ms; Ms; Beef Muscles.

611. Flavonoid Profiling in three Citrus Varieties Native to Republic of Korea using Liquid Chromatography Coupled with Tandem Mass Spectrometry: Contribution to Overall Antioxidant Activity

Hae Gyeong Kima, Gon-Sup Kimb, Semin Parka, Jung Han Leea, On Nuri Seoa, Soo Jung Leec, Jae Hoon Kimd, Jae-Han Shime, A. M. Abd El-Atyf, Jong Sung Jing and Sung Chul Shin

Biomed Chromatogr, 26: 464-470 (2012) IF: 1.966

A mixture of flavonoid components was isolated from the fruit peel of three varieties of citrus native to Republic of Korea, Citrus

leioarpa Hort. ex Tanaka (CLHT), Citrus aurantium L. (CAL) and Citrus erythrosa Hort. (CEH), via 70% methanol extraction followed by ethyl acetate elution over a silica gel cartridge. The flavonoid components of the mixture were analyzed via high-performance liquid chromatography–tandem mass spectrometry (HPLC-MS/MS) in positive-ion mode and a comparison of the reported data. Among 17 characterized components, two flavanones, four flavones and two coumarin derivatives in the fruit peel of the three varieties were identified for the first time. The individual characterized components were quantified via HPLC-UV. The flavanones dominated in CAL, whereas the flavones prevailed in CLHT and CEH. The antioxidant activity of the flavonoid mixture of the fruit peel was determined via DPPH•, ABTS•+ and reducing power assays. The antioxidant activity of CEH and CAL was greater than that of CLHT.

Keywords: Citrus; Flavonoids; Coumarin; Hplc-Ms; Ms; Antioxidant Activity.

612. Determination of Chlorfenapyr in Leek Grown Under Greenhouse Conditions with GcEcd and Confirmation by Mass Spectrometry

Rahman MM, Choi JH, Abd El-Aty AM, Park JH, Park JY, Im GJ and Shim JH.

Biomed Chromatogr, 26(2): 172-177 (2012) IF: 1.966

A simple analytical method was developed for the determination of chlorfenapyr residues in leeks grown under greenhouse conditions. Residues were extracted by salting out, analyzed by gas chromatography with microelectroncapture detection and confirmed via gas chromatography–mass spectrometry. The calibration curves were found to be linear with correlation coefficients (r²) in excess of 0.998. The limits of detection and quantification were 0.0015 and 0.005mg kg⁻¹, respectively. For validation purposes, recovery studies were carried out at low and high levels. Yield recovery rates were 87.27–89.64% with a relative standard deviation <6%. A maximum of 0.32mg kg⁻¹ of chlorfenapyr residue was detected in leek sample sprayed three times at 7 day intervals until 7 days prior to harvest. The results of this study suggest that chlorfenapyr is acceptable for application in/on leeks under the recommended dosage regimen.

Keywords: Chlorfenapyr; Gas Chromatography; Leek; Greenhouse.

613. Characterization of Secondary Volatile Profiles in Nigella Sativa Seeds from Two Different Origins using Accelerated Solvent Extraction and Gas Chromatography-Mass Spectrometry

Xue Liua, A.M. Abd El-Aty, S.-K. Chod, Angel Yanga, Jong-Hyoun Parka and Jae-Han Shim

Biomed Chromatogr, 26: 1157-1162 (2012) IF: 1.966

The extraction and identification of bioactive compounds from herbs is of great interest. In this study, accelerated solvent extraction (ASE) technique was used to analyze the secondary volatile profiles in Nigella sativa seeds obtained from two different origins, Egypt and Bangladesh. The main extraction parameters, including extraction temperature, pressure and static extraction time, were investigated and optimized. Identification and quantification of the major constituents in nonpolar extracts (hexane) were achieved by means of GC-FID/GC-MS analysis

with external standards. The two seeds showed a similar variety of chemical composition; however, the secondary volatiles profile of Bangladesh seed was higher than that of the Egyptian seed. A total of 25 compounds were identified from the ASE extract under the following optimum extraction conditions: 100 °C, 1500 psi and 5 min, for extraction temperature, pressure and static time, respectively. The proposed technique can be used for the characterization of *N. sativa* varieties or cultivars.

Keywords: Black Seeds; Chemical Constituents; Thymoquinone; Accelerated Solvent Extraction; Gas Chromatography; Mass Spectrometry.

614. Pharmacokinetics of Tulathromycin in Lactating Goats

A.M.M. Amer, P.D. Constable, A. Goudah and S.A. El Badawy
Small Ruminant Research, 108: 137-147 (2012) IF: 1.295

Tulathromycin is a novel long acting semi synthetic macrolide antibiotic of the triamilide group that is used to treat respiratory diseases in cattle and pigs. Tulathromycin may therefore be useful in treating respiratory diseases of goats. The objective of this study was to characterize the pharmacokinetics of tulathromycin in lactating goats. Five lactating goats received single IV and IM injections of tulathromycin (2.5 mg/kg) with a 6 week interval between injections. Plasma, milk and urine concentrations of tulathromycin were determined using a microbiological assay method and pharmacokinetic values were calculated. Following a single IV injection of tulathromycin formulation, tulathromycin had a high mean volume of distribution (16.1 L/kg), excellent penetration into milk, slow plasma clearance (126 mL kg⁻¹ h⁻¹) and a long elimination half time (88 h). Plasma protein binding was 23%. Tulathromycin was rapidly absorbed following a single IM injection; the mean maximum plasma concentration (0.73 mg/mL) was rapidly reached at 0.5 h and mean bioavailability was 95.8%. Tulathromycin concentrations exceeded 0.1 mg/mL in milk and 0.01 mg/mL in plasma for at least 7 days. We conclude that the pharmacokinetics of a single IM injection of tulathromycin (2.5 mg/kg) in lactating goats are similar to those in nonlactating goats and yearling cattle administered a similar dose of tulathromycin SC. Tulathromycin may therefore be effective in the treatment of respiratory disease in goats. Long withdrawal times (>19 days) are required for milk intended for human consumption when tulathromycin is administered accidentally to lactating dairy goats.

Keywords: Goat; Macrolide; Pharmacokinetics; Tulathromycin.

615. Separation of Multi-Class Pesticide Residues from Fatty Food Matrices Prior to Analysis using Gas Chromatography

Ji-Yeon Park, Angel Yang, Jong-Hyouk Park, A. M. Abd El-Aty, Jae-Ho Oh, Jung-Ah Do, Kisung Kwon, Ki-Hoon Shim, Ok-Ja Choi and Jae-Han Shim

Journal of the Korean Society for Applied Biological Chemistry, 55: 541-549 (2012) IF: 0.365

Separation of pesticides and other chemical contaminants from fatty food matrices prior to subsequent steps in the analytical process remains a challenging issue and much effort has been invested to further enhance this method. The aim of the present

study was to develop a simple multi-residue method involving a quick, easy, cheap, effective, rugged and safe (QuEChERS) extraction method for the identification and quantification of 41 pesticide residues in cooked fatty food matrices, including heated soybean oil, roasted sesame and boiled soybean using gas chromatography-micro/electron capture detector (GC-ECD). The analytes were subsequently confirmed via GC-mass spectrometry (MS). The responses of analytes were linear with excellent correlation coefficients (r^2) ranging from 0.993 to 1.000 (calculated from absolute peak areas). For the majority of the tested pesticides, the mean recoveries ranged from 68.5 and 121.4% with relative standard deviations ranging from 0.4 to 18.7%. Instrument limits of detection and quantification ranged from 0.004 to 0.30 g/kg and 0.0125 to 1.00 g/kg, respectively. The developed method presented in this study was applied successfully to determine pesticide residue levels in cooked fatty food matrices. None of the samples contained detectable amounts of pesticide residues.

Keywords: Fatty Food Matrices; Gas Chromatography; Multiresidues; Pesticides; QuEChERS (Quick; Easy; Cheap; Effective; Rugged; Safe).

616. Determination of Dinotefuran in Pepper using Liquid Chromatography: Contribution to Safety Evaluation

Lina Hem, A. M. Abd El-Aty, Jong-Hyouk Park and Jae-Han Shim

Journal of the Korean Society for Applied Biological Chemistry, 55: 765-768 (2012) IF: 0.365

This paper presents a simple and sensitive method for detection and quantification of neonicotinoids (dinotefurans) in pepper. Extraction of pesticide was carried out with acetonitrile and water partition and passed through cleanup. The residue levels were determined by high performance liquid chromatography with UV detection and liquid chromatography-tandem mass spectrometry (LC-MS/MS) confirmation. The analytical method was very good within a wide range of concentrations with linearity (r^2) of 1.00. The recovery at two fortification levels ranged between 91.2 to 97.5% with relative standard deviation less than 6.0%. The method was successfully applied for determination of the analyte in pepper grown under greenhouse conditions.

Keywords: Dinotefuran; Half-Life; High Performance Liquid Chromatography; Mass Spectrometry; Neonicotinoids; Safety.

617. Residual Pattern of Acequinocyl and Hydroxyacequinocyl in Perilla Leaf Grown Under Greenhouse Conditions using Uplc-Pda with Tandem Mass Confirmation

Tae Woong Na, Md. Musfiqur Rahman, Jong-Hyouk Park, Angel Yang, Ki Hun Park, A. M. Abd El-Aty and Jae-Han Shim

Journal of the Korean Society for Applied Biological Chemistry, 55: 567-662 (2012) IF: 0.365

Persistence and degradation behaviors of acequinocyl and hydroxyacequinocyl were determined in perilla leaf grown under greenhouse conditions. Acequinocyl (15%, SC) was sprayed on perilla leaf at the recommended dose rate of 37.5 g/250 L water/10a with single and double dose applications. Leaf samples were collected randomly at 0 (2 h after application), 1, 3, 5 and 7

days post-application from two different plots. The samples were extracted with acetonitrile, purified through a solid phase extraction procedure and analyzed via ultra performance liquid chromatography coupled with photo diode array detector (UPLCPDA). Residues were confirmed via liquid chromatography tandem mass spectrometry (LC-MS/MS) in positive-ion electrospray ionization (ESI+) mode. Calibration curves were linear over the concentration ranges for the analytes with $r^2=0.992$. The limits of detection and quantification were 0.05 and 0.165 mg/kg for both acequinocyl and hydroxyacequinocyl. The method was validated in triplicate at two fortification concentrations in the matrix. Good recoveries were observed for the target analytes, ranging between 94.95 and 113.26% with relative standard deviations less than 6%. The rates of disappearance of total acequinocyl on perilla leaf for single and double doses were described as first-order kinetics with half-lives of 2.8 and 3.1-days, respectively.

Keywords: Acequinocyl; Hydroxyacequinocyl; First Order Kinetics; Residual Pattern; Ultra Performance Liquid Chromatography; Photo Diode Array Detector.

618. Synthesis of New Ester Entities of Nsaids with Nitric Oxide Releasing Properties

Gehan H. Hegazy and Gehan M.Kamel

Life Science Journal, 9(3): 1113-1120 (2012) IF: 0.073

All the NSAIDs are suffering from deadlier GIT toxicity. The free carboxylic group is thought to be responsible for this toxicity. In this work, the main motto was to develop new chemical entities as potential anti-inflammatory agents with no gastric toxicity. In this work we esterified some commonly used NSAIDs as ibuprofen, mefenamic acid and indomethacin to p-aminophenol. These compounds were then converted to their nitrate derivative to combined benefits of both esterification and nitrate releasing properties on the GIT. The newly synthesized compounds were biologically evaluated as anti-inflammatory and analgesic. The ulcerogenicity of these compounds was also determined. All the synthesized compounds show similar activity to the parent one. These compounds elicited less ulcerogenicity compared to their parent one.

Keywords: Nsaids; Esters; Nitric Oxide; Gastric Toxicity.

619. Pharmacokinetics and Bioavailability of Tulathromycin Following Intravenous, Intramuscular and Subcutaneous Administrations in Healthy Rabbits

K. Abo-El-Sooud, N. A. Afifi and A. M. Abd-El-Aty

Veterinary World, 5(7): 424-428 (2012)

This work was performed to investigate the pharmacokinetics of the triamilide antibiotic, tulathromycin in healthy rabbits. Materials and Methods: Ten rabbits in each group were given a single dose of 2.5 mg/kg body weight (bw) of tulathromycin via intravenous (IV), intramuscular (IM) and subcutaneous (SC) administrations. The concentration of tulathromycin in plasma was determined by microbiological assay *Bacillus subtilis* ATCC6633 as the test organism. Results: Following IV administration, the total body clearance (Cl) was 321.70 ml/kg/h, the volume of distribution at steady-state (V_d) was 13.26 L/kg and the value of the elimination half-life ($t_{1/2}$) was 29.29 h. After SC administration, the

total body clearance (Cl), mean residence time (MRT) and maximum plasma concentration (C_{max}) were significantly higher (36.22 h, 52.54 h and 882.19 ng/ml) than after IM route (31.69 h, 45.89 h and 714.72 ng/ml), respectively. Tulathromycin was bound to the extent of 36% to plasma protein of healthy rabbits. The absolute bioavailabilities were 88.07 and 94.25% after IM and SC injections. Conclusion: Thus a single dose of tulathromycin is promising treatment for most respiratory disease in rabbits.

Keywords: Pharmacokinetics; Tulathromycin; Bioavailability; Rabbits.

620. Pharmacokinetics and Bioavailability of Azithromycin Following Intramuscular and Oral Administrations in Broiler Chickens

K. Abo-El-Sooud, Eman Fahmy, N.A. Afifi and A.M. Abd El-Aty

Research & Reviews In Biosciences, 6(9): 264-270 (2012)

The pharmacokinetics of azithromycin were investigated in broiler chickens after intravenous (i.v.), intramuscular (i.m.) and oral (p.o.) administrations to estimate an appropriate dosage regimen of azithromycin. Moreover, to determine the bioavailability after the extravascular routes and the serum protein binding capacity with azithromycin's molecules. Three equal groups of 5 chickens each were given a single dose of 20 mg/kg body weight (bw) of azithromycin via i.v., i.m. and p.o. administrations. Serum concentrations of azithromycin were determined by a modified agar diffusion bioassay using *Bacillus subtilis* ATCC 6633 as the test organism. Following compartmental analysis, a three-compartment open model best described the concentration-time data of azithromycin after i.v. administration. The total body clearance (Cl_{tot}) was 0.77 L/kg/h, the volume of distribution at steady-state (V_{dss}) was 47.75 L/kg and the value of the elimination half-life ($t_{1/2}$) was 31.91 h. After i.m. administration, the elimination half-life ($t_{1/2el}$) and mean residence time (MRT) were significantly higher (38.95 h and 47.16 h) than after p.o. route (31.50 h and 39.93 h), respectively. Azithromycin was bound to the extent of 24.42 % to serum protein of chickens. The absolute bioavailabilities were 95.17 and 83.52 % after i.m. and p.o. administrations, respectively. Based on the fortunate pharmacokinetic characteristics, a single dose of azithromycin at 20 mg/kg (bw) via i.m. and p.o. administrations every 72 h for susceptible bacterial infections in chickens is greatly recommended.

Keywords: Pharmacokinetics; Azithromycin; Bioavailability; Chickens.

621. In Vitro Assessment of Different Antibacterials Against Nanobacteria Isolated from Kidney Stones

K. Abo-EL-Sooud, M.M. Hashem and ZAQ. Gab-Allaha

Insight Nanotechnology, 2 (1): 1-6 (2012)

Nanobacteria (NB) are implicated in stone formation in the urinary tract and antibacterials have been used with some success for the treatment of pathological calcification-related diseases, therefore, therapy to eliminate NB is a major concern. Material and Methods: Twelve antibacterial agents from various categories were tested against in vitro inhibition of NB, isolated from human kidney stones. The tested antibacterials were oxytetracycline, doxycycline, ampicillin, lincomycin, spectinomycin,

trimethoprim, neomycin, erythromycin, florfenicol, streptomycin, gentamicin and colistin. A modified microdilution inhibitory assay was used to achieve the unique growth conditions and long multiplication times of NB. This modified microdilution method included inoculation of 96-well plates and determination of inhibition by periodic measurement of the absorbance for 30 days in Dulbecco's modified Eagle's medium (DMEM) supplemented with 10% gamma-irradiated fetal calf serum (-FBS) under cell culture conditions. Bactericidal or bacteriostatic effects were distinguished by subsequent subculture in drug-free media and monitoring for increasing absorbance. Results: NB isolated from kidney stones were inhibited by trimethoprim, oxytetracycline, colistin, neomycin and doxycycline at levels achievable in serum and urine. The other antibacterials tested against NB exhibited an inhibitory concentration above clinically attainable levels. All tested antibacterials were bactericidal.

Keywords: Nanobacteria; Antibacterial Agents; In Vitro Inhibition; Bactericidal.

622. Effect of Different Sites of Intramuscular Injection on Elimination, Bioavailability and Tissue Residues Profile of Gentamicin in Broiler Chickens

K. Abo-EL-Sooud, Z.G.A. Swielim, Z.E.F. Khalifa and Z.S.M. EL-Gammal

Insight Poultry Research, 2 (1): 1-7 (2012)

The site of intramuscular (IM) injections can affect the serum and tissue concentration profiles and so alter bioavailability of drug. The variation in the pattern of absorption can be attributed to regional differences in blood flow to skeletal muscles. The pharmacokinetics and systemic bioavailability of gentamicin in broiler chickens were compared after single intravenous (IV) and (IM) in (two sites) thigh and pectoral muscles injections of 5 mg/kg body weight (b.w.). Tissue residue profiles (kidney, liver, lung and muscles) of gentamicin were also compared after both sites of IM injections. The concentrations of gentamicin in serum and tissues were measured by microbiological assay using *Bacillus subtilis* ATCC 6633 as test organism. Following IV injection, serum concentration-time curves were best described by a two compartment open model. The decline in serum drug concentration was bi-exponential with half-lives of (t_{1/2}) 0.09 h and (t_{1/2}) 2.25 h for distribution and elimination phases, respectively. After IM injections in thigh and pectoral muscles, serum concentrations were significantly lower in those injected gentamicin through thigh muscles. The peak serum concentrations of gentamicin (C_{max}) were 32.44 and 39.34 µg/ml and were obtained at 0.44 and 0.42 h (T_{max}), respectively and the elimination half-lives (t_{1/2el}) were 1.74 and 2.39 h, respectively. The systemic IM bioavailabilities were 83 and 105.20%, after thigh and pectoral muscles injections, respectively. In vitro protein binding percent of gentamicin was 3.4%. The tissue levels following IM injections in thigh and pectorals muscles were highest in kidney, liver and respectively and decreased in the following order: serum, lung and muscle. No gentamicin residues were detected in tissues and serum after 12 h with both routes of administration, gentamicin was found in both the liver and kidney after 48 h. We recommend that injectable antibiotics should be injected in pectoral muscles in poultry farms to achieve high efficacy and avoid rapid elimination by renal portal system.

Keywords: Intramuscular; Gentamicin; Bioavailability; Renal Portal System.

623. Screening of the Anti-Nanobacterial Activity of Essential Oils and Extracts of Some Edible Plants

K.Abo-El-Sooud, M.M.Hashem and A.Q.Gab-Allaha

Natural Products-An Indian Journal, 8(7): 276-283 (2012)

In the present investigation the anti-nanobacterial activity of twenty five extracts and oils of edible plants had been evaluated for their abilities to inhibit the in vitro multiplication of nanobacteria (NB), isolated from human kidney stones. A modified micro-dilution inhibitory test was used to achieve the unique growth conditions and long multiplication times of NB. This method included an inoculation of 96-well plates and determination of inhibition by periodic measurement of the absorbance for 30 days in Dulbecco's modified Eagle's medium (DMEM) supplemented with 10% gamma-irradiated fetal calf serum (-FBS) under cell culture conditions. Bactericidal or bacteriostatic plant effects were distinguished by subsequent subculture in extract-free media and monitoring for increasing absorbance. For screening of anti-nanobacterial susceptibility in each tested plant, both positive and negative controls were set to determine MIC (minimum inhibitory concentration) and MBC (minimum bactericidal concentration) values. Among all essential oils sesame, cinnamon and almond oils were found to be highly bactericidal at 250 µg/ml whereas cinnamon was the most potent bacteriostatic oil at 31.25 µg/ml followed by sesame and anise oils. From all extracts, fenugreek, sewak and black cumin were bactericidal and only khella had bacteriostatic against NB. The results reflect a hope for the development of many more novel chemotherapeutic agents or templates from such plants which in future may serve as an alternative medicine.

Keywords: Nanobacteria; Essential Oils; Extracts; Edible Plants.

624. The Effect of Bacillus Subtilis Spores - Based Probiotic and Florfenicol on the Colonization of Salmonella Enteritidis in Intestine of the Broilers

M.M. Hashem; A. Ramdan, H.Y. El Zorba1 Soad A. Abd El Wanis and A.M. El Mahdy

Researcher, (2012)

The current study investigated the effect of dietary supplementation of *Bacillus* spores based probiotic and drinking water supplementation of florfenicol on *Salmonella enteritidis* colonization in the intestine of broiler chicks, also recorded the clinical signs which appeared during the experiment. A total of 220 broiler chicks (one day old, Ross) free from *Salmonella* infection divided into 5 equal groups, the broilers were then subjected to the following treatments: 1st group was given *Salmonella enteritidis*, *Bacillus* spores based probiotic and florfenicol, 2nd group was given *Salmonella enteritidis* and florfenicol, 3rd group was given *Salmonella enteritidis* and *Bacillus* spores based probiotic. 4th group was given *Salmonella enteritidis* only and used as positive control group. 5th group was given neither *Salmonella enteritidis* nor treatments and used as negative control group. The statistical analysis for results by Duncan multiple range test and ANOVA test showed that, there was a significant difference at $p < 0.05$ between groups using *Bacillus* spores based probiotic, florfenicol, combination of both treatments and positive control group in colony counts of *Salmonella enteritidis* in intestine of broiler chicks. Furthermore, the results showed that broiler chicks fed with probiotic supplements had a minimal viable colony count of

Salmonella enteritidis bacteria in the intestinal tract. Bacillus spores based probiotic fed birds was able to resist Salmonella enteritidis infection with few mild clinical signs. Improved resistance to other bacterial disease is expected from the supplementation of Bacillus spores based probiotic in the formulation of feeds for broilers.

Keywords: Bacillus Spores Based Probiotic; Florfenicol; Salmonella Enteritidis; Broiler Chicks.

625. Antiuro lithiatic Activity of Edible Plants and Products

K.Abo-El-Sooud, M.M.Hashem, Mona M.E.Eleiwa and A.Q.Gab-Allaha

Natural Products-An Indian Journal,8(4): 168-174(2012)

Urolithiasis is known to be an affliction to mankind from ancient eras and remains a major issue regarding health and well being today. Stone disease affects 10 to 12% of the population in industrialized countries with a peak incidence between 20 and 40 years of age.

There are many theories that explain the pathogenesis of stone formation, for example, the supersaturation theory and the inhibitors theory.

Supersaturation occurs when there is an overabundance of solute in a solution. Although, urolithiasis is a multifactorial disease, nutrition, especially fluid intake, with several underlying disorders of metabolism: that is why diet is an important treatment, especially in the prevention of recurrences. Epidemiological studies reveal that about 80% of all kidney stones are composed of calcium salts (75% calcium oxalate), while about 5% are pure uric acid. Kidney stones have previously been linked to higher rates of high blood pressure, obesity, diabetes and other heart disease risk factors.

Researchers have speculated that the dietary approaches to hypertension (DASH) style diet could, also prevent kidney stones. The main components of the DASH diet includes fruit, vegetables, nuts and legumes, low fat dairy, whole grains and lower intakes of salt, sweetened drinks, red meat and processed meat. The DASH-style diet may reduce stone risk by increasing urinary citrate and volume. The small associations between higher DASH score and lower relative supersaturation of calcium oxalate and uric acid suggesting that unidentified stone inhibitors in dairy products and/or plants.

One of the important phenomena that characterizes urolithiasis is its high recurrence. Thus, a protective system is required including extracorporeal shock wave lithotripsy and medicament treatment. Unfortunately, these means remain costly and in most cases are invasive and with side effects. Therefore, great interest has arisen among both physicians and patients towards identifying effective measures to achieve analgesia during renal colic, promote stone passage or stone dissolution and prevent stone recurrence by natural products (phytotherapy).

Recent years have shown a dramatic expansion in the knowledge of molecular mechanism of phytotherapeutic agents used to treat urolithiasis. The discovery and elucidation of the mechanism of action, in particular the clinical role of these herbal remedies, has made an important contribution to treatment for urinary stone disease as an alternative or adjunct therapy. We present a literature review of edible and herbal products in renal stone management.

Keywords: Antiuro lithiatic; Phytotherapy; Edible plants; Juices.

Dept. of Poultry Diseases

626. Early Immune Dynamics Following Infection with Salmonella Enterica Serovars Enteritidis, Infantis, Pullorum and Gallinarum; Cytokine and Chemokine Gene Expression Profile and Cellular Changes of Chicken Cecal Tonsils

A.M. Settaa, P.A. Barrow, P. Kaiser and M.A. Jonesa

Comp Immunol Microb, 35(5): 397-410 (2012) IF: 2.337

Salmonella enterica subspecies enterica infection remains a serious problem in a wide range of animals and in man. Poultry-derived food is the main source of human infection with the non-host-adapted serovars while fowl typhoid and pullorum disease are important diseases of poultry. We have assessed cecal colonization and immune responses of newly hatched and older chickens to Salmonella serotypes Enteritidis, Infantis, Gallinarum and Pullorum. S. Enteritidis and S. Infantis colonized the ceca more efficiently than S. Gallinarum and S. Pullorum. Salmonella infection was also associated with increased staining for B-lymphocytes and macrophages in the cecal tonsils of infected birds. S. Enteritidis infection in newly hatched birds stimulated the expression of CXCLi1 and CXCLi2 chemokines in the cecal tonsils, while S. Gallinarum up-regulated the expression of LITAF. In older chickens, S. Enteritidis infection resulted in a significantly higher expression of CXCLi2, iNOS, LITAF and IL-10 while S. Pullorum appeared to down-regulate CXCLi1 expression in the cecal tonsils. Data from spleens showed either no expression or down-regulation of the tested genes.

Keywords: Cytokines; Innate Immunity; Caecal Tonsils; Salmonella; Chickens.

627. Immune Dynamics Following Infection of Avian Macrophages and Epithelial Cells with Typhoidal and Non-Typhoidal Salmonella Enterica Serovars; Bacterial Invasion and Persistence, Nitric Oxide and Oxygen Production, Differential Host Gene Expression, Nf-B Signalling and Cell Cytotoxicity

Ahmed Settaa, Paul A. Barrow, Pete Kaiser and Michael A. Jonesa

Vet Immunol Immunop, 146: 212-224 (2012) IF: 2.076

Poultry-derived food is a common source of infection of human with the non-host adapted salmonellae while fowl typhoid and pullorum disease are serious diseases in poultry. Development of novel immune-based control strategies against Salmonella infection necessitates a better understanding of the host-pathogen interactions at the cellular level. Intestinal epithelial cells are the first line of defence against enteric infections and the role of macrophages is crucial in Salmonella infection and pathogenesis. While gene expression following Salmonella infection has been investigated, a comparison between different serovars has not been, as yet, extensively studied in poultry. In this study, chicken macrophage-like cells (HD11) and chick kidney epithelial cells (CKC) were used to study and compare the immune responses and mechanisms that develop after infection with different Salmonella serotypes. Salmonella serovars Typhimurium, Enteritidis, Hadar and Infantis showed a greater level of invasion and/or uptake characters when compared with S. Pullorum or S. Gallinarum. Nitrate and reactive oxygen species were greater in

Salmonella-infected HD11 cells with the expression of iNOS and nuclear factor-B by chicken macrophages infected with both systemic and broad host range serovars. HD11 cells revealed higher mRNA gene expression for CXCLi2, IL-6 and iNOS genes in response to *S. Enteritidis* infection when compared to *S. Pullorum*-infected cells. *S. Typhimurium*- and *S. Hadar*-infected HD11 showed higher gene expression for CXCLi2 versus *S. Pullorum*-infected cells. Higher mRNA gene expression levels of pro-inflammatory cytokine IL-6, chemokines CXCLi1 and CXCLi2 and iNOS genes were detected in *S. Typhimurium*- and *S. Enteritidis*-infected CKC followed by *S. Hadar* and *S. Infantis* while no significant changes were observed in *S. Pullorum* or *S. Gallinarum*-infected CKC.

Keywords: Cytokines; Immunity; Chicken; Salmonella; Macrophages; Epithelial Cells.

628. A Survey on Salmonella Species Isolated from Chicken Flocks in Egypt

Wafaa A. Abd El-Ghany, S0umaya SA. El-Shafii and IVLE. Hatem

Asian J Anim Vet Adv, 7 (6): 489-501 (2012) IF: 0.869

This study was carried out to investigate serologically and molecularly the prevalent species of Salmonellae present in four broiler chicken flocks in Kalubia governorate, Egypt. A bacteriological examination was done on a total of 1073 samples that collected from 293 chickens (127 apparently healthy, 62 diseased with whitish watery diarrhea and 104 dead broiler chickens). These samples included cloacal swabs, gall bladders, yolk sacs, spleens and livers. The colonial morphology, microscopical and biochemical identifications of isolates revealed presence of 51 strains of Salmonellae representing; 10 (2.55%) from apparently healthy chickens, 18 (7.03%) from diseased broilers and 23 (4.69%) from dead birds. Positive Salmonellae strains were present as percentages of 3.84, 4.15, 5.06 and 5.18% from flocks 1, 2, 3 and 4, respectively. Using slide agglutination test, serotyping of the isolated strains according somatic (O) and flagellar (H) antigens detected presence of 19 *S. Enteritidis* (37.25%); 10 *S. Infantis* (19.60%); 1 *S. Chiredzi* (1.96%); 4 *S. Kentucky* (7.84%); 15 *S. Typhimurium* (29.41%) and 2 *S. Tsevie* (3.92%). There was a variation in the presence of Salmonella species serotypes in each of the examined flocks. Molecular characterization using polymerase chain reaction (PCR) produced positive amplification of 284 bp fragments of *invA* genes (100%) specific for all members of Salmonella species. From the previous results, it could be concluded that there are different Salmonellae serotypes including *S. Enteritidis*, *S. Infantis*, *S. Chiredzi*, *S. Kentucky*, *S. Typhimurium* and *S. Tsevie* circulating in broiler chicken farms in Kalubia governorate, Egypt and the most prevalent ones are *S. Enteritidis* and *S. Typhimurium*.

Keywords: Salmonella; Chickens; Egypt; Broiler Chickens.

629. Serological and Molecular Typing of Clostridium Perfringens and its Toxins Recovered from Weaned Rabbit'S Flocks in Egypt

Khelfa D. E. -D. G., Wafaa A. Abd El-Ghany and Heba M. Salem

Life Sci J, 9(4): 2263-2271 (2012) IF: 0.073

This study was carried out for serological and molecular typing of *Clostridium perfringens* (*C. perfringens*) and its toxins recovered

from apparently healthy, diseased and dead weaned rabbits, as well as their feed and water. Identified 42 *C. perfringens* organisms representing 35 from rabbits and 7 from feed and water were subjected for determination of toxigenicity by intravenous inoculation (I/V) in Swiss mice. Toxigenic *C. perfringens* organisms were typed serologically using Nagler's test, dermonecrotic reaction in albino Guinea pigs and toxin antitoxin serum neutralization test (SNT) in Swiss mice. For confirmation of serological results, detection of alpha gene of *C. perfringens* was done using conventional polymerase chain reaction (PCR), followed by using multiplex PCR to detect the toxin's types. Distribution of different *C. perfringens* types of surveyed rabbit's farms at different Egyptian governorate was carried out. In addition, the in-vitro antibiotic sensitivity of different *C. perfringens* types against different antimicrobial agents was performed. The results showed that 34 (97.14%) of *C. perfringens* recovered from rabbits were toxigenic, while 1.0 (2.86%) was none. Four out of 6 (66.66%) *C. perfringens* isolates from feed were toxigenic and 2 (33.33%) isolates were non-toxigenic. Only one (100%) *C. perfringens* isolate from water was toxigenic. Identical proving results were obtained using serological typing tests. Single and mixed types of toxigenic *C. perfringens* constituted 17 out of 35 (48.57%) for each, whereas only one type was none (2.86%). Single *C. perfringens* was representing 8 (22.85%) type A, 3 (8.57%) type B, 4 (11.43%) type D and 2 (5.71%) type E, whereas mixed types were 11 (31.42%) types (A and D), 2 (5.71%) types (A and E) and 4 (11.42%) types (B and D). Four *C. perfringens* isolates from feed were 3 type A (50%) and 1.0 type D (16.6%). The only *C. perfringens* isolate from water was type A (100%). Conventional PCR proved detection of alpha gene of *C. perfringens*, whereas multiplex PCR proved that *C. perfringens* type (A) was positive for alpha toxin at 324 base pair (bp), type (B) was positive for alpha toxin at (324 bp), beta toxin at (196 bp) and epsilon toxin at (655 bp), type (D) was positive for alpha toxin at (324 bp) and epsilon toxin at (655 bp) while type (E) was positive for alpha toxin at (324 bp) and iota toxin at (446 bp). The result of distribution of different *C. perfringens* types at different Egyptian governorate was recorded. In vitro antibiotic sensitivity test of single or mixed types of identified *C. perfringens* revealed sensitivity to amoxicillin/clavulanic acid and ampicillin and resistance to colistine, erythromycin and lincomycin.

Keywords: Weaned Rabbits; Clostridium Species; Egypt; Serotyping; Pcr; Sensitivity Test.

630. Recent Status of Clostridial Enteritis Affecting Early Weaned Rabbits in Egypt

Khelfa D. E. -D. G., Wafaa A. Abd El-Ghany and Heba M. Salem

Life Sci J, 9(4): 2272-2279 (2012) IF: 0.073

A surveillance study for diagnosis of Clostridial enteritis affecting early weaned rabbits was carried out on eight Egyptian governorates. Diagnosis based on history, clinical examination, palpation, post-mortem lesions, histopathological examination, as well as isolation of different Clostridial species (spp.) causing Clostridial enteritis. Two samples representing rectal swabs, liver and intestine were collected from each examined rabbit. A total of 718 samples expressing 329 surveyed rabbits (95 apparently healthy, 204 clinically affected and 30 freshly dead ones). Equal number (19) of feed and water samples were collected from each surveyed farm. All the samples were subjected for Clostridial isolation and spp. identification after cultural and biochemical

characterization. Tissue samples from liver and intestine of freshly dead rabbits were subjected for histopathological examination. Results revealed that, the most prevalent observed signs were severe diarrhea, bloat accompanied with variable mortalities. Post-mortem lesions were severe enteritis and typhlitis with different degrees of necrosis and hemorrhages associated with gaseous contents. Both kidneys and livers showed congestion and enlargement with peripheral hepatic necrosis. The rate of isolation of Clostridial spp. recovered from 756 rabbits, feed and water samples was 311 (41.13%). Only 135 (41.03%) out of 329 examined rabbits was positive for Clostridial spp. that was distributed as the following; 109 (80.74%) exhibited single Clostridial spp., 4 (2.96%) showed mixed infection with more than one Clostridial spp. and 22 (16.29%) were un-typable. From 135 positive Clostridial spp.; *Clostridium perfringens* (C. perfringens), C. tertium, C. sporogenes, C. bifermentans, C. septicum and C. difficile were recovered as 35 (25.92%), 32 (23.70%), 19 (14.07%), 14 (10.37%), 5 (3.70%) and 4 (2.96%), respectively. Mixed types (C. perfringens and C. tertium) were represented as 2 (1.48%), (C. perfringens and C. sporogenes) 1 (0.74%) as well as (C. perfringens and C. difficile) 1 (0.74%). Seven (18.42%) out of 38 examined feed and water samples was positive for Clostridial spp. where C. perfringens was the only Clostridial spp. that isolated at a rate of 6/19 (31.57%) from feed and 1.0/19 (5.26%) from water samples. The distribution of Clostridial spp. among surveyed rabbit's farms at different Egyptian governorates was detected. On histopathological examination, fibrosis in the portal area of liver as well as infiltration with inflammatory cells and also diffuse inflammatory cells, oedema and necrosis was observed in intestines.

Keywords: Weaned Rabbits; Enteritis; Clostridium Species; Egypt.

631. A Trial to Prevent Salmonella Enteritidis Infection in Broiler Chickens using Autogenous Bacterin Compared with Probiotic Preparation

Wafaa A. Abd El-Ghany, Soumaya S.A. El-Shafii M.E. Hatem and Rehab E. Dawood

Journal of Agricultural Science, 4, (5), 91-108 (2012)

This study was carried out to investigate the efficacy of the locally prepared autogenous Salmonella Enteritidis (S. Enteritidis) bacterin as well as a probiotic preparation in the prevention of broiler chickens from S. Enteritidis infection. A total of three hundred and ten, one day-old Hubbard broiler chicks were used. At day old, ten chicks were sacrificed and examined bacteriologically to prove their freedom from S. Enteritidis infection. Three hundred birds were divided into four equal groups. Chickens in group (1) were kept as blank control negative non infected non treated birds, while those of group (2) were challenged non treated birds. Group (3) was vaccinated intramuscularly by the autogenous bacterin at the first day of age in a dose of 0.2 ml/bird and boosted as a second dose at 10 days of age in a dose 0.5 ml/bird, however, group (4) was given a commercial probiotic preparation as 1gm/ 4 liter of the drinking water from the first day of age and continued for 5 successive days. All birds in groups 2, 3 and 4 were challenged orally by 0.5 ml containing 109 CFU/ml S. Enteritidis at 20 days of age. All the groups were kept under complete observation for three weeks for recording signs, mortalities, gross lesions, shedding rate of S. Enteritidis, re-isolation of the organism, the performance as well as detection of the titer of antibodies serologically using

microagglutination test and enzyme linked immunosorbent assay (ELISA) test. The results showed that the both the bacterin and the probiotic are equally effective in reducing signs, mortalities, gross lesions, the shedding rate and the re-isolation of S. Enteritidis and also increasing in the performance of chickens. The effect of the bacterin and the probiotic was significant (P<0.05) when compared with the infected non treated chickens. Moreover, the serological investigation revealed an improvement in the titer of antibodies after vaccination and probiotic treatment. In conclusion, double doses of locally prepared autogenous S. Enteritidis bacterin and the probiotic preparation were effective and safe methods for prevention of S. Enteritidis infection in broiler chickens.

Keywords: Salmonella Enteritidis; Prevention; Bacterin; Probiotic.

632. The Effect of Clostridium Difficile Experimental Infection on the Health Status of Weaned Rabbits

Khelfa D.G., Wafaa A. Abd El-Ghany and Heba M. Salem

Journal of Applied Sciences Research, 8(8): 4672-4677 (2012)

In this study, a trial to detect the effect of Clostridium difficile (C. difficile) experimental infection on the health status of weaned rabbits was carried out. Thirty, 5 week old weaned New Zealand rabbits were used. Rabbits were kept for a week under observation for adaptation and ensuring absence of any clinical signs, mortalities and anaerobic infections. Rabbits were randomly divided into 3 equal groups; 10 rabbits for each. Each rabbit in group (1) was subcutaneously (S/C) inoculated with 1 ml containing 1×10^8 colony forming unit (CFU) of C. difficile, while each one in group (2) was orally inoculated with 2 ml (3×10^{10} CFU). Group (3) was kept as non-infected control one. During 3 weeks observation period; clinical signs, mortalities, gross lesions, histopathological changes and C. difficile re-isolation were detected. The results indicated absence of clinical signs in C. difficile S/C challenged rabbits, while signs of bloat and brownish diarrhea were observed in orally challenged ones. No mortalities were recorded in rabbits of both challenged groups. Lesions observed in sacrificed orally challenged rabbits were enlargement and congestion of liver and kidneys as well as mild degree of enteritis. The challenging C. difficile was re-isolated from sacrificed rabbits at the end of the study. It could be concluded that C. difficile is an organism of economic importance for newly weaned rabbits as it can badly affect rabbits' health status.

Keywords: Rabbits; C. Difficile; Signs; Lesions; Isolation.

633. Exacerbating Effect of Newcastle Disease Virus (Ndv) Infection on Sub Clinical Caecal Coccidiosis in Broilers Vaccinated Against Ndv

Shaban Kh.S.

Researcher, 4(1): 55-59 (2012)

This study reports the effect of experimental infection with NDV on the sub clinical caecal coccidiosis in broiler birds vaccinated against NDV. For this purpose 300 one-day-old broiler chickens were randomly divided into 3 equal groups (G1, G2 and G3) of 100. The birds were placed on floor pens in separated rooms. At 15 days of age G3 was infected intra crop with a dose of 12500 sporulated oocysts of a field strain of caecal E. species, which

suspected to be *E. tenella* isolated from clinically affected broiler flock with cecal coccidiosis. G1 and G2 were not challenged and remained as control negative for coccidia. Management and nutrition were the same in all groups. All groups of birds were vaccinated at 4th day of age with Infectious Bronchitis (IB) virus vaccine (H120 strain) by eye drop method. At 7th day of age NDV vaccines (Inactivated and Hitchener B1) were given by subcutaneous (SC) and eye drop routes respectively for G2 and G3. The infectious bursal disease virus (IBDV) vaccine and Inactivated H5N2 Avian Influenza (AI) virus vaccine were given at 13th day of age for all groups by eye drop and SC routes respectively. At 17th day of age G2 and G3 were also vaccinated against NDV with Lasota strain vaccine by eye drop while G1 was not vaccinated with any one of NDV vaccines and remained as a blank. The challenging NDV was given for all groups at 25th day of age by intramuscular (IM) injection. The birds of G1 exhibited 100% mortality with obvious PM lesion of NDV infection. The birds of G2 showed torticollis in one bird only. The birds of the G3 started dying with bloody diarrhea a day post challenging with NDV and the clinical signs, postmortem (PM) findings and response to treatment were used to confirm coccidiosis. The rapid onset of the clinical disease and the high mortality rate (36% over a period of 5 days) was considered to have been induced by the challenging NDV administration. The diagnosis of sub clinical coccidiosis and institution of prophylactic anticoccidial therapy would have obviated the clinical disease in the field.

Keywords: Chicken; Coccidiosis; Ndv; Subclinical Coccidiosis; Coccidiosis.

634. Immunosuppressive Potential of Acute Caecal Coccidiosis as Well as Anticoccidial Vaccine on Antibody Titers Induced by Newcastle Disease and Infectious Bursal Disease Viruses Vaccines in Broiler Chickens

Shaban KH. S

Researcher, 4(4): 32-36 (2012)

This study was designed to evaluate the effect of the most prevalent and highly virulent coccidial infection (caecal coccidiosis) as well as anticoccidial vaccination on haemagglutinating antibody titers of Newcastle Disease virus (NDV) and Infectious Bursal Disease Virus (IBDV) antibody ELISA titers resulted from vaccination program in broiler chickens. For this purpose, 180 day old Hubbard broiler chicks were randomly divided into 3 equal groups (G1, G2 and G3), each of 60 chicks. At 3rd day of age birds of G1 was vaccinated with anticoccidial vaccine via crop and at 14th day of age birds of G2 was infected with high dose (50000) of sporulated *E. tenella* oocysts intra crop, while birds of G3 remain as control (Non coccidia vaccinated or infected). At 14th, 21th and 28th days of age, mean HI antibody titers of G3 were higher than G2 and G1 groups. At 21th and 28th days of age, mean HI antibody titers for NDV as well as mean ELISA antibody titers for IBDV of G2 were significantly lower than other groups ($p < 0.05$). At 35th and 42th days of age HI titers of G3 and G1 were higher than G2, but the differences were not significant ($p > 0.05$). The mean HI antibody titers for NDV as well as mean ELISA antibody titers for IBDV of G1 had non-significant lowering values than those of G3 at all ages ($p > 0.05$). It was concluded that coccidial infections as well as anticoccidial vaccination are able to reduce humeral

immunological reactions of broiler chickens as indicated by the significant reduction in mean HI antibody titers for NDV and mean ELISA antibody titers for IBDV as well as the significant lowering in the protection percentage against challenge with VVND and virulent IBDV in these chickens. Since this effect was more prominent in infected group than in anticoccidial vaccinated one, in the cases of coccidiosis outbreaks in the farm with higher levels of coccidial infections, involvement of mixed virulent species (*E. tenella*, *E. necatrix*, *E. acervulina*, *E. maxima*..... ect.) and other environmental stressors, more severe and prolonged immunosuppression are expected.

Keywords: Immunosuppression; Chickens; Ibdv; Ndv; Coccidiosis; Anticoccidial Vaccine.

Dept. of Surgery Anesthesiology and Radiology

635. Radiographic Evaluation of Early Periprosthetic Femoral Bone Contrast and Prosthetic Stem Alignment After Uncemented and Cemented Total Hip Replacement in Dogs

Ayman A. Mostafa, Svenja Dru^o en, Ingo Nolte and Patrick Wefstaedt

Vet Surg, 41: 69-77 (2012) IF: 1.265

To radiographically evaluate periprosthetic femoral bone contrast and assess alignment of the prosthetic stem after uncemented and cemented total hip replacement (THR). Study Design: Prospective clinical study. Animals: Dogs ($n = 15$). Methods: Dogs were classified into uncemented ($n=8$) and cemented ($n=7$) THR groups. Radiographs were analyzed using image processing software to evaluate femoral bone contrast (gray scale value, GV) for each and combined modified Gruen zone(s) immediately and 4 months after THR. Modified Gruen zones were classified into 5 zones to analyze retrospectively the regional radiographic GV of the femur around uncemented and cemented prosthetic stem. Alignment of prosthetic stem was assessed immediately and 4 months postoperatively. Variables were compared by use of 2-tailed t-test, with $P < .05$ considered significant. Results: Zone 1 showed significant decrease in the mean bone GV 4 months after uncemented THR. No differences in zones 1-5 after 4 months of cemented THR. Combined zones showed significant decrease in overall mean bone GV 4 months after uncemented THR. No changes were observed 4 months after cemented THR. Number of limbs with varus-aligned femoral stem markedly increased after 4 months of uncemented THR. Conclusions: Regional bone contrast and prosthetic stem alignment vary with the design of THR.

Keywords: Radiographic; Periprosthetic; Femoral; Contrast; Stem; Alignment.

636. Efficacy of Diclofenac Sodium Either Alone Or Together with Cefotaxime Sodium, for Control of Postoperative Pain, in Dogs Undergoing Ovariohysterectomy

Abu-Seida and Ashraf M. A.

Asian J Anim Vet Adv, 7 Issue 2, (2012) IF: 0.869

There is not much data about diclofenac sodium as an anti-inflammatory drug in veterinary practice, therefore the objectives of this study were to assess the efficacy and adverse effects of diclofenac sodium on its own and together with cefotaxime Na as

postoperative pain control in dogs. A prospective, randomized, blinded, clinical trial was assigned to one of four groups according to postoperative injections: Group 1 (given diclofenac and cefotaxime), group 2 (control), group 3 (given cefotaxime only) and group 4(given diclofenac only). Examinations were performed postoperatively using a pain scale modified from University of Melbourne at 0,1,2,3,4,5,6,8,12.24 h. Statistical analysis of results was done.

The results of the present study showed that groups (1 and 4) had mean pain scores which were not significantly different from each other and different from groups (2 and 3) significantly. From three hours post-operative till twenty four hours post-operative groups (2 and 3) recorded mean pain scores which were significantly higher than groups (1 and 4). On the other hand, groups 2 and 3 were not statistically different from each other. Also groups 1 and 4 were not statistically different. In conclusion, diclofenac sodium is an excellent analgesic for postoperative pain control in healthy dogs undergoing ovariohysterectomy.

Keywords: Diclofenac; Cefotaxime; Pain; Dogs; Ovariohysterectomy.

637. Anatomical and Ultrasonographical Studies on Tendons and Digital Cushions of Normal Phalangeal Region in Camels

A.M Adu Seida, A.M. Mostafa and A.R. Tolba

Journal Of Camel Practice And Research, 19(2): 1-7 (2012)
IF: 0.061

In the present study, anatomical and ultrasonographical findings have been evaluated to be compared to abnormal digits in further studies.

This study was carried out on 10 feet specimens of both fore and hind limbs from freshly slaughtered camels of both sexes and of different ages and body weights and digits of three apparently normal camels. Transverse and sagittal ultrasonographical examinations were carried out in all digits from fetlock joint to nails using Toshiba ultrasound device connecting with 6-8 MHz linear Transducer.

Ten specimens of the digits were dissected anatomically to compare anatomical and ultrasonographical findings. All anatomical and ultrasonographical findings of common digital extensor tendon, superficial and deep digital flexor tendons, digital cushions and sole were described. In conclusion, ultrasonography is a highly impressive cross sectional diagnostic imaging in camels digits.

Keywords: Anatomy; Ultrasonography; Tendons; Digital Cushions; Camels.

638. Case Report: the lotomy in A Dairy Buffalo After Ultrasonographic Diagnosis of Teat Stenosis

Sameh S.F. Mehanny

Journal of Buffalo Science, 3, (1): 17-35 (2012)

Teat cistern stenosis was surgically treated by thelotomy and excision of the fibrous stenosis following teat ultrasonography to determine location and extent of the lesion in a dairy water buffalo.

Keywords: Ultrasonography; Teat Cistern; Thelotomy.

639. Ultrasonographic Diagnosis of Some Scrotal Swellings in Bulls

Ashraf M. A. Abu-Seida

Pak Vet J, 32(3): 378-381 (2012) IF: 1.255

Information regarding the use of ultrasonography in the diagnosis of testicular and scrotal affections is scarce in bovine. In the present study, eight bulls suffering with scrotal swellings were examined ultrasonographically. The recorded affections included; ruptured urethra with scrotal swelling, testicular hypoplasia, malignant Sertoli cell neoplasm, hydrocele and scrotal hernia. In case of ruptured urethra, the scrotum appeared as thick hyperechoic skin, the testes showed normal echogenicity and the surrounding tissue showed diffuse anechoic areas separated by hyperechoic threads. The hypoplastic testis was less echogenic and its rete testis was more echogenic, than the normal one. The neoplastic testis had several anechoic areas, hyperechoic masses and areas of normal testicular echogenicity. In hydrocele, the scrotal skin appeared as clear hyperechoic line with anechoic fluid accumulated in the vaginal cavity of the scrotum and both testes had normal echotexture. In scrotal hernia, a hyperechoic omental loop was seen adjacent to high echogenic testis. In conclusion, ultrasonography is a good tool for differential diagnosis of different scrotal swellings in bulls.

Keywords: Bulls; Scrotum; Swellings; Ultrasonography.

640. Trans-Abdominal Intra-Prostatic Injection of Ethanol and Oxytetracycline Hcl Under Ultrasonographic Guidance as A New Approach for Treatment of Benign Prostatic Hyperplasia in Dogs

Ashraf M. Abu-Seida and Faisal M. Torad

Asian J Anim Vet Adv, 7 Issue: 11: 1055-1066 (2012) IF: 0.869

The aim of the present study is to assess the efficacy of trans-abdominal intra-prostatic injection of ethanol and oxytetracycline Hcl under ultrasonographic guidance for treatment of canine BPH. Under sedation with xylazine Hcl (1mg/kg i/v), aseptic precautions and ultrasonographic guidance, canine BPH was diagnosed in twelve dogs. Ten dogs were allocated randomly into one of the following groups: Group I, five dogs were injected trans-abdominally with ethanol (5-10 ml) after aspiration of the intra-prostatic cyst if present. Group II, five dogs were injected trans-abdominally with oxytetracycline Hcl (5-10 ml) after aspiration of the intra-prostatic cyst if present. Ultrasonographic follow up was performed in all injected dogs for two months. Repeated injections were carried out on dogs that did not respond well after one month of the first injection. Postmortem examination was carried out on two dogs which were euthanized by the request of the owners as the dogs were in severe pain due to other affections.

The Results indicated that there was obvious reduction of the prostatic size in both groups after one month of injection and disappearance of the clinical signs. Ethanol is more potent than oxytetracycline Hcl as sclerosant in canine BPH. All data about the cases, clinical signs, abdominal and rectal examinations and ultrasonographic and postmortem findings were recorded. In conclusion; trans-abdominal intra-prostatic injection of either ethanol or oxytetracycline Hcl is an easy, quick, effective, safe, minimally invasive and cheap technique for treatment of canine BPH. Ethanol is more potent than oxytetracycline Hcl as sclerosant in canines BPH.

Keywords: Ethanol; Oxytetracycline; Ultrasonography; Prostatic Hyperplasia; Dogs.

641. Ultrasound-Guided Paravertebral Regional Anesthesia in Water Buffalo

M.M. Shokry and E.A. Berbish

Buffalo Science, 2012, 1.; 107-109 (2012)

Adequate flank regional anaesthesia was achieved using ultrasound-guided nerve block of the 13th thoracic, 1st and 2nd lumbar spinal nerves after their exits from their intervertebral foraminae with only 5 ml of lidocaine 2%. Twelve successful trials were conducted on 4 buffaloes without any complications.

Keywords: Ultrasound; Paravertebral; Analgesia; Spinal Nerves.

Dept. of Toxicology and forensic Medicine

642. The Protective Effect of Green Tea Extract on Lead Induced Oxidative and Dna Damage on Rat Brain

A.A. Khalafa, Walaa A. Moselhy and Marwa. Abdel-Hamedc

Neurotoxicology, 33(3): 280-289 (2012) IF: 3.096

The role of green tea in protection against neurotoxicity induced by lead acetate was investigated in rats. Five equal groups, each of ten rats were used. The first group was served as control, the second, third and fourth groups were given lead acetate, lead acetate and green tea and green tea only, respectively, for one month, the fifth group was administered lead acetate for one month followed by green tea for 15 days. Lead acetate as given orally at a dose of 100 mg/kg b. wt, while green tea was given in drinking water at a concentration of 5 g/L. Lead acetate administration induced loss of body weight and decreased concentration of reduced glutathione and SOD activity in brain tissues as well as significantly high DNA fragmentation and pathological changes. Co-administration of green tea with lead acetate significantly alleviated these adverse effects.

Keywords: Albino Rats Lead Neurotoxicity Green Tea Oxidative Stress.

Dept. of Veterinary Hygiene and Manament

643. Detection of Avian Influenza (H5n1) in Some Fish and Shellfish from Different Aquatic Habitats Across Some Egyptian Provinces

A.E. Eissa, H. A. Hussein and M.M. Zaki

Life Science, 9(3): 2702-2712 (2012) IF: 0.073

The global climatic changes impact on air, water and earth could extend scope of Avian Influenza (H5N1) virus to another broad sector of creatures including aquatic animals, especially those with direct relationship to aquatic birds. In the current study, Avian Influenza virus (H5N1) was detected in hemolymph of the Red Swamp crayfish (*Procambrus clarkii*) from three different provinces across the Nile Delta. Most of the positive cases were from the neighborhood of migratory bird natural stop stations. The virus was also detected in the Mediterranean Cone Shell (*Conus mediterraneus*) and the Pufferfish *Lagocephalus sceleratus* (Gmelin, 1789) during its course of invasion to the Mediterranean

Sea. Two out of three poultry manure samples collected prior to earthen pond fertilization at three different localities were proved to be positive for the H5N1 virus. Tissue / mucous samples collected from earthen pond raised tilapias were negative for the virus. Catfish (*Clarias gariepinus*) has presented a striking model for aquatic species carrying the virus in their blood. The current results are suggestive for an important epidemiological role played by aquatic animals in spread of avian influenza (H5N1) virus across the Egyptian aquatic habitat.

Keywords: Avian Influenza; H5n1; Crayfish; Nile Tilapia; Catfish; Poultry Manure.

644. Effect of Yeast as Feed Supplement on Behavioural and Productive Performance of Broiler Chickens

Kassem G. El Iraqi and Rabie H. Fayed

Life Science Journal, 9(4): 4026-4031 (2012) IF: 0.073

This study was conducted to evaluate the effects of new patent probiotic inactivated *Saccharomyces cerevisiae* Var. *ellipsoideus* (Thepax®) and other commercial yeast "*Saccharomyces cerevisiae*" either live or dry feed additives, on behavioral and productive performance of broiler chickens. A total of 496 day-old Cobb chicks were used and divided into 4 groups, 2 replicates for each. Chicks in group one were fed on commercial basal diet as a control group, the chicks in other three groups were fed on the same diet enriched with 0.5 gm Live yeast / kg diet for group two (T1), 1 gm. dry yeast /kg diet for group three (T2) and 1 gm inactivated yeast /kg diet for group four (T3) (this dose of inactivated yeast was 0.5 g/ kg in grower diet). During 5 weeks experimental period, behavioral measurements as frequency and duration of feeding and drinking behavior; comfort behavior including wing and leg stretch, preening, ground scratch, body shaking and resting behaviour were observed and recorded. Broiler performance including weekly feed intake, weekly body weight gain, final feed intake, final body weight, feed conversion ratio, dressing weight, dressing percentage, mortality rate and European efficiency index were calculated. Significant differences were observed between different yeast types in ingestive behavior, comfort behaviour, feed intake, final body weight, food conversion ratio, dressing weight, dressing percentage, mortality rate and European performance index. It can be concluded that the inactivated yeast probiotic can be included in broiler diets for their beneficial effect and to improve their behavioral and productive performance.

Keywords: Behavior; Broiler; Inactivated Yeast; Probiotics; Performance; Thepax.

645. Efficacy of Composting Dead Poultry and Farms Wastes Infected with Avian Influenza Virus H5n1

Zakia AM Ahmed, H.A. Hussin, M.A. Rohaim and Shimaa Abo El Soud Nasr

American-Eurasian J. Agric. and Environ. Sci., (2012)

Composting had proven to be an environmentally sound method for disposing dead birds. The composting process management and monitoring its thermal profile, moisture content, nutrient ingredients were determined and recorded during day 1 to 33. Isolation and characterization of H5N1 avian influenza

virus(AIV) in freshly dead birds and their wastes before, during and after composting was carried out using RT-PCRbased assay and sequence analysis. In composting the temperature was increased gradually from 40-60°Cthrough days 5 to 15 then declined after day 15 till end composting.

The dry conditions and increasedtemperature were important virus determinants. Failure of re-isolation of virus in consequence to increasedtemperature during composting was proven when tested at day 15, end composting and dryness period. AIVwas characterized before composting in the birds trachea and compost mix. Positive isolation, characterizationand sequence analysis of fragment 4 of H5 gene revealed clustering of the virus with those field strainscirculating among chicken population in Egypt in 2011. Testing thecomposting mix at the day 15 and end ofcomposting by RT-PCR assay revealed negative amplification confirming the efficacy of composting processfor destroying AIV. Composting within the newly designed closed composte achieved unfavorable thermaland dryness conditions for H5N1 surviving with no isolation and characterization of AIV H5N1 from field deadbirds and their wastes. The study proposes composting as a reliable, environmentally safe way to disposepoultry waste infected with H5N1 AIV.

Keywords: Aiv H5n1; Amino Acids Sequencing; Composting Ingredients; Surviving Determinants; Rt; Pcr.

646. Review Article; Occupational Hazards in Fish Industry

Zakia A.M. Ahmed, Mai I. Dosoki and Shaimaa Abo A. Nasr

World Journal of Fish And Marine Sciences, (2012)

The current review is directed to workers in aquaculture, fish handlers, consumers, private andgovernmental fish industry producers and researchers. They should consider the possible occupational hazardsand follow regulations and legislations adopted.

The occupational hazards, safety concerns and risks to healthin the aquaculture industry are based on the types of operation, scale of production and the specific speciesof interest. Hazard is a biological, chemical, or physical agent with the potential to cause an adverse healtheffect. Fish grown in excreta-fertilized or wastewater ponds may be contaminated with pathogens. Transgenicfish is hazardous because of their potential allergenicity and toxicity.

Awareness of the health hazards involvedin the handling of industrial fish is important, particularly for those working in the vicinity of fishingcommunities. Farmhands and other workers in aquafarms are susceptible to many injuries, noise, sting from fishspines, sprain and fracture which are of physical hazards. Spoiled wet fish in storage may produce poisonousgases. Fish muscle can hold different concentration of Hg representing health risk to fertile women. Cadmiumand lead concentrations are higher in fish scales and vertebral column than in the other parts of the fish. The

author's objective is to improve the health and safety of workers in aquaculture through the recognition,evaluation, control ormitigation of human health risk in the aquaculture industry. Focusing on the possible roleof aquatic farming in the spread of communicable human diseases.

Keywords: Chemical Pollution; Microbial Toxins; Occupational Hazards; Risk Assessment; Transgenic Fish.

647. Ecomonitoring of Climate Impact on Tilapia Niloticus Performance and Development of Different Histopathological Changes

Zakia A.M. Ahmed, Faten F. Mohammed and A. Abdel-Rahman

Global Veterinaria, (2012)

Monitoring water quality was so important to assess and manage the risk associated with climatechange impact and consequent stress. Assessing seasonal impact on aquaculture water quality parameters andfish performance (final body weight and organosomatic indices) was estimated in 10 earthen ponds aquaculturein ALFayoum province. Water and fish samples were collected during summer, spring and autumn 2009. Biomarkers as organs-somatic indices (SI) and histopathological alterations were determined. Results revealedthat, spring season characterized by significant differences in mean values of water quality parameters Vsautumn and summer with absence of seasonal significant differences in dissolved oxygen (DO) values. Significant differences were recorded in final body weight (FBW), organs-somatic indices (SI) and tissue lesionsin all examined vital organs. Histopathological investigation during winter (December and January) revealed, gill arch showed dense aggregation of eosinophilic granular cells (EGCs) with leucocytes infiltration and edematous fluid exudation. The gill filaments showed lamellar hyperplasia with fusion of secondary gill lamellaeand proliferation of lamellar epithelium. Fish gills were among the most recognized organs affected by waterquality changes. Liver showed small foci of vacuolar degeneration of hepatocytes with small multifocalaggregation of mononuclear cells. Diffuse hepatocellular degeneration with congestion of hepatportal blood vessel. Spleen showed lymphoid depletion with congestion of sinusoids and necrosis of the splenic ellipsoid. Spleen tissue showed individual case of encysted metacercaria. Brain edema, congestion of cerebral bloodcapillaries, neuronal degeneration and necrosis were the most oblivious brain tissue alterations. It'srecommended to examine water periodically and randomly harvest fish for rapid evaluation of affected fishbiomarkers. Owners must be alert to the expected seasonal alteration on the water quality of earthen pondsaquaculture from the socio-economic aspect.

Keywords: Water Quality; Seasonal Change; Biomarkers; Histological Alterations; Earthen Ponds, Organosomatic Indices.

648. Microbial Ecology of Composting Dead Poultry and their Wastes

Zakia A.M. Ahmed, Z.M. Sedik, M.D. Alharery, M.A. Khalaf, Shaimaa A. Nasr and H.A. Abdelrahman

Global Veterinaria, (2012)

Composting is environmentally acceptable disposal route, with potential financial benefits. EmergedAvian influenza virus epidemics in Egypt 2005-2009 potentiate proposing composting as soundmethod. Constructing a newly designed movable closed composting unit for dead poultry with AIV H5N1 andtheir wastes was one of main project goals for hygienic disposal. Field litter samples before compostingconfirmed existence of 4 species of Gram negative and 3 species of Gram positive bacteria as well as Aspergilluspecies with absence of anaerobes. Efficient composting was attained at temperature ranged 40-60°C, relativehumidity 60-74%. The litter carbon content ranged from 43.77-54.72% with mean 49.25 % and carbon: nitrogenranged

(C:N) from 21.54-24.33%. Composting reduced total colony count 80 % and total fungi count 66.10%, Salmonella Spp. and Clostridium spp. count (70.59 and 73.68% respectively). End compost had the highest C:N value 24.33%, moisture content 22.34%, total nitrogen 2.21%, total phosphorus 0.54 % and total potassium 0.79%. Compost product is used for agronomic purpose (1:2) after had been subjected to chemical and microbial examination. The well-grown edible obtained vegetable had no phototoxic impact to pose health risk. Composting is recommended for hygienic disposal of dead birds and their wastes with more environmental safe level than traditional methods used in Egypt.

Keywords: Composting; Litter; Bacteria; Fungi Load; Thermal Profile; Anaerobes; Environmental; Safe Level.

Dept. of Veterinary Hygiene and Management

649. Molecular Histopathology

Hussein A. Kaoud

Histopathology-Reviews and Recent Advances, Intech, chapter No 13, 255-282 (2012)

Molecular pathology is an emerging discipline within pathology which is focused in the study and diagnosis of disease through the examination of molecules within organs, tissues or bodily fluids. Molecular pathology shares some aspects of practice with both anatomic pathology and clinical pathology, molecular biology, biochemistry, proteomics and genetics and is sometimes considered a "crossover" discipline. It is multi-disciplinary in nature and focuses mainly on the sub-microscopic aspects of disease, as well as upcoming, molecular diagnostic applications is greatly advantageous for today's practice of pathology.

Keywords: Molecular pathology; genetics; multi-disciplinary; diagnostic applications.

Dept. of Virology

650. Recovery and Molecular Characterization of Live Camel pox Virus from Skin 12 Months After Onset of Clinical Signs Reveals Possible Mechanism of Virus Persistence in Herds

A.A. Yousif and A.A. Al-Naeem

Vet Microbiol, 159: 320-326 (2012) IF: 3.327

Potentially pathogenic orthopoxviruses (OPVs) persist in nature and re-emerge for reasons we do not fully understand. New information pertaining to Orthopoxvirus (OPV) persistence in nature would significantly improve surveillance and control programs. In a recent investigation of a Camel pox virus (CMLV) outbreak in Eastern Saudi Arabia, atypical minute pox-like skin lesions (AMPL) persisted on 42.9% of convalescent camels (8.8% of herd) for more than a year after the onset of clinical signs. In order to investigate whether AMPL were related to CMLV infection, AMPL homogenates were inoculated on the chorioallantoic membranes (CAM) of specific-pathogen-free (SPF) embryonating chicken eggs (ECE). Live CMLV was recovered from AMPL homogenates. The sequences of the ATIP gene of viruses isolated in the beginning of the outbreak and one year later from AMPL were identical and similar to the Kazakhstan isolate CMLV M-96. Virus identity was confirmed

by sequence analysis of the CMLV A33R, A27L, B5R and L1R orthologous genes. Uninfected adult camels that came in contact with animals showing AMPL became infected within two weeks. Since AMPL were easily missed by veterinarians and camel drivers, it was concluded that CMLV survival in persistent skin lesions may be a key mechanism in maintaining the virus in previously infected camel herds during inter-epizootic periods.

Keywords: Persistence; Orthopox; Camel pox; Skin; Sequencing; Isolation.

651. A Case of Mistaken Identity Vaccinia Virus in A Live Camel pox Vaccine

A.A. Yousif and A.M. Al-Ali

Biologicals "Journal of the International Alliance for Biological Standardization" (Elsevier), 40: 495-498 (2012) IF: 1.698

Live-attenuated (LA) and inactivated adjuvant (IA) camel pox virus (CMLV) vaccines are produced in several countries worldwide. A tissue culture attenuated CMLV isolate (Jouf-78) is used to produce a LA vaccine in Saudi Arabia (Hafez et al., 1992). DNA extracts from the Saudi LA vaccine used as positive controls for a routine ATIP PCR produced 1596 bp amplicons. ATIP amplicon sequences were similar to Vaccinia virus (VACV) Lister strain. PCR and sequence analysis of two extracellular enveloped virus (EEV)-specific (A33R and B5R) and two intracellular mature virus (IMV) (L1R and A27L) orthologous genes from the vaccine DNA extracts confirmed the finding. CMLV sequences were not detected in the vaccine DNA extracts. A Swiss Smallpox vaccine containing VACV Lister strain was used as a control during the initial testing of the Saudi CMLV vaccine. High antigenic similarity between VACV and CMLV and a possible contamination event during production may have caused this issue. Environmental and health impact studies were recommended because early VACV vaccines produced in some European countries contained nonhighly attenuated strains that were not adequately screened for adventitious agents.

Keywords: Orthopox; Camel pox; Vaccinia; Lister; Sequencing; Contamination.

Dept. of Zoonoses

652. Fish as A Possible Reservoir for Zoonotic Giardia Duodenalis Assemblages

Nahed H. Ghoneim, Khaled A. Abdel-Moein and Hossam Saeed

Parasitol Res, 110: 2193-2196 (2012) IF: 2.149

Giardiasis is a re-emerging infectious disease of worldwide significance caused by *Giardia duodenalis*. This study investigated the occurrence of zoonotic *G. duodenalis* assemblages in fish to explore the possible role of fish in the epidemiology of human giardiasis. For this purpose, 92 fish (*Tilapia nilotica* and *Mugil cephalus*) collected from (fish farms and Nile River) at different governorates in Egypt were examined for the presence of *G. duodenalis* in their feces by using enzyme linked immunosorbent assay, then positive fecal samples were tested by duplex PCR for identification of triose phosphate isomerase (tpi) gene specific for zoonotic assemblages A and B. The overall prevalence of *G. duodenalis* in the examined fish was 3.3%, while the detection rates among the examined fish species were 2.9% and 4.2% for *T. nilotica* and *M. cephalus*, respectively. *G. duodenalis*

was detected in the feces of both farmed and wild fish whereas all isolates were genotyped as assemblage A. In conclusion, the occurrence of zoonotic *G. duodenalis* assemblage A in the examined fish species at two different aquatic environments underlines the possibility of fish to be an additional reservoir for zoonotic *G. duodenalis* assemblage that contributes in the contamination of water with this pathogen and thus the role of fish in the epidemiology of human giardiasis cannot be ruled out.

Keywords: Fish; Giardia; Zoonoses.

Institute of Statistical Studies and Research

Dept. of Applied Statistics and Econometrics

653. General Stochastic Restricted SUR Ridge and SUR Robust Ridge Estimators with Robust Cross Validation

El-Houssainy A. Rady, Sayed M. El Saye, Alaa A. Abdel-Aziz, Naglaa A. Morad and Tarek M. Omara

Journal of Statistical Theory and Applications, 11: 63-86 (2012)

If we consider that, the SUR model suffered from outliers, multicollinearity and it involved a degree of uncertainty associated with restrictions on the parameters. Three estimators introduced to avoid this problem. The first estimator, General Stochastic Restricted SUR Ridge Estimator with ridge parameter depends on robust cross validation instead of classic robust cross validation. The second estimator, General Stochastic Restricted SUR Robust Ridge Estimator which uses S-estimators with Ridge Regression under stochastic restriction and ridge parameter depends on robust cross validation. The third estimator, General Stochastic Restricted SUR Robust Estimator which depends on S-estimators. We introduced algorithm to compute General Stochastic Restricted SUR Ridge estimator, General Stochastic Restricted SUR Robust estimator and General Stochastic Restricted SUR Robust Ridge estimator. And we conducted a set of simulation study which used the ASE (average squared error) criterion to measure the goodness of fit at the several factors.

Keywords: General Stochastic Restricted Sur Estimator; General Stochastic Restricted Sur; Robust Estimators; General Stochastic Restricted Sur Ridge Estimators; General Stochastic; Restricted Sur Robust Ridge Estimators.

654. Generalized Method of Moments of Random Coefficient Model

El-Houssainy Abd Elbar Rady, Ahmed H. Youssef and Tarek Abdul-Aziz Al-Doub

Far East Journal of Theoretical Statistics, 3.8: 9-18 (2012)

In panel data, estimation is a popular point, researchers used many techniques to face the estimation in panel data; such as Generalized Least Square (GLS) technique which had been used by Swamy [13] and Generalized Method of Moment (GMM) had been used by Hansen [7] and Verbeek [15]. GLS is a technique for estimating the unknown parameters in the linear regression model. It can use in situations where Ordinary Least Squares (OLS) is statistically inefficient, or gives misleading inferences. Whereas GMM method is a very general statistical technique obtaining estimates of parameters of statistics models; many

estimators are known as special cases of GMM, such as OLS, Instrumental Variables (IV) and 2 Stage Least Squares (2SLS). The present work is concerned to derive GMM for Swamy model to obtain a new estimator and variance.

Keywords: Panel Data; Generalized Least Square; Generalized Method of Moment; Ordinary Least Squares.

655. A Monte Carlo Simulation Study for (GLs) and (Gmm) Estimation

El-Houssainy Abd Elbar Rady, Ahmed H. Youssef and Tarek Abdul-Aziz Al-Doub

Advances and Applications in Statistics, 26(7), 1-23 (2012)

Estimation in panel data is a common problem. Many approaches have been developed to face the estimation problems in panel data such as Generalized Least Square (GLS) and Generalized Method of Moment (GMM). The (GLS) technique used by Swamy [9] depends on Ordinary Least Square (OLS), whereas GMM used by Hansen [8] and Verbeek [4] depends on two-stage Least Squares (2-SLS). This study aims to set a comparison between these two techniques using Simple Panel Data (SPD) and Multiple Panel Data (MPD) in linear regression. The purpose of this comparison is to determine which technique is considered a better estimation technique through a simulation study using various sample sizes, models, parameters and standard deviations. Moreover, the following criteria were used to evaluate the two techniques: bias, Mean Square Error (MSE), variances and the negative variances. Results of the study have revealed that (GMM) is more capable and accurate in estimation than (GLS) methodology.

Keywords: Panel Data, Generalized Least Square; Generalized Method of Moment Simple Linear Regression; Multiple Linear Regression; Simulation Study; Estimation Technique; Bias; Mean Square Error; Negative Variances.

Dept. of Computer Sciences and Information

656. Threshold Based AntNet Algorithm for Dynamic Traffic Routing of Road Networks

Ayman M. Ghazy, Fatma EL-Licy and Hesham A. Hefny

Egyptian Informatics Journal, 13: 111-121 (2012) IF: 2

Dynamic routing algorithms play an important role in road traffic routing to avoid congestion and to direct vehicles to better routes. AntNet routing algorithms have been applied, extensively and successfully, in data communication network. However, its application for dynamic routing on road networks is still considerably limited.

This paper presents a modified version of the AntNet routing algorithm, called "Threshold based AntNet", that has the ability to efficiently utilize a priori information of dynamic traffic routing, especially, for road networks. The modification exploits the practical and pre-known information for most road traffic networks, namely, the good travel times between sources and destinations. The values of those good travel times are manipulated as threshold values.

This approach has proven to conserve tracking of good routes. According to the dynamic nature of the problem, the presented approach guards the agility of rediscovering a good route. Attaining the thresholds (good reported travel times), of a given source to destination route, permits for a better utilization of the

computational resources, that, leads to better accommodation for the network changes.

The presented algorithm introduces a new type of ants called "check ants". It assists in preserving good routes and, better yet, exposes and discards the degraded ones. The threshold AntNet algorithm presents a new strategy for updating the routing information, supported by the backward ants.

Keywords: Swarm Intelligence; Dynamic Traffic Routing; Antnet; Forward ant; Backward ant; Check ant.

657. Modular Approach with Rough Decision Models

Ahmed T. Shawky, Hesham A. Hefny and Ashraf H. Abd Elwhab

International Journal of Data Mining & Knowledge Management Process (Ijdkp), 2 (5): 83-95 (2012)

Decision models which adopt rough set theory have been used effectively in many real world applications. However, rough decision models suffer the high computational complexity when dealing with datasets of huge size. In this research we propose a new rough decision model that allows making decisions based on modularity mechanism. According to the proposed approach, large-size datasets can be divided into arbitrary moderate-size datasets, then a group of rough decision models can be built as separate decision modules. The overall model decision is computed as the consensus decision of all decision modules through some aggregation technique. This approach provides a flexible and a quick way for extracting decision rules of large size information tables using rough decision models.

Keywords: Rough Sets; Fuzzy Sets; Modularity; Data Mining.

658. Using Modularity with Rough Decision Models

Ahmed T. Shawky, Hesham A. Hefny and Ashraf H. Abd-Elwahab

International Journal of Artificial Intelligence & Applications (Ijaia), 3 (1): 15-31 (2012)

Many real world applications need to deal with imprecise data. Therefore, there is a need for new techniques which can manage such imprecision. Computational Intelligence (CI) techniques are the most appropriate for dealing with imprecise data to help decision makers. It is well known that soft computing techniques like genetic algorithms, neural networks and fuzzy logic are effective in dealing with problems without explicit model and characterized by uncertainties Using fuzzy set theory considered as major techniques, which allows decision makers to take a good decision using imprecise inexact data and knowledge. Now using rough set is getting quite necessary to be used for its ability to mining such type of data. In this research, we are looking forward to propose a novel technique, which depends on the integration between fuzzy set concepts and rough set theory in mining relational databases. The proposed model allows introducing modularity mechanism, by building a virtual modular decision tables according to variety of decision makers points of view. And introduce decision grouping mechanism for getting the optimizing decision. This approach provides flexibility in decision making verifies all decision standards and determines decision requirements, through modularizing rough decision table, extraction of rough association rules and developing mechanisms for decision grouping.

Keywords: Rough Sets; Fuzzy Sets; Modularity; Data Mining.

Dept. of Computer Sciences and Information

659. Using Modularity with Rough Information Systems

Ahmed T. Shawky, Hesham A. Hefny and Ashraf H. Abd Elwhab

Advances in Computer Science, Engineering & Applications, (2012)

We are looking forward to propose a novel technique, which depends on using modular techniques and integration between fuzzy set concepts and rough set theory in mining rough systems In this research We propose a set of algorithms For a novel model allows introducing modularity mechanism; by introduce decision grouping mechanism for getting the optimizing decision. This approach provides flexibility in decision making verifies all decision standards and determines decision requirements, through modularizing rough information system, extraction of rough association rules and developing mechanisms for decision grouping.

660. Construct Fuzzy Decision Trees Based on Roughness Measures

Mohamed A. Elashiri, Hesham A. Hefny and Ashraf H. Abd Elwhab

Advances in Communication, Network and Computing, (2012)

Data mining is a process of extracting useful patterns and regularities from large bodies of data. Decision trees (DT) is one of data mining techniques used to deal with classical data. Fuzzy Decision Trees (FDT) is generalization of crisp decision trees, which aims to combine symbolic decision trees with approximate reasoning offered by fuzzy representation. Given a fuzzy information system (FIS), fuzzy expanded attributes play a crucial role in fuzzy decision trees. In this paper the problem is slowness and complexities of the fuzzy decision trees, but its rules are more accurate. Our target is to simplify computational procedures and increase the accuracy rules or to keep the high grade of accuracy and to select an efficient criterion to select fuzzy expanded attributes based on rough set theory.

661. Mas: Qualitative and Quantitative Reasoning

Ammar Mohammed and Ulrich Furbach

Programing Multi-Agents System - Lecture Notes in Computer Science, (2012)

In a former work, we have presented/implemented a framework for modeling and verifying multi-agent systems, using hybrid automata To specify properties of those systems, one needs a specification language that brings, at the same level of specification, both the qualitative and quantitative requirements. For this aim, there have been proposed several temporal logics with either event or state based approach. Both approaches have their pros and cons which should not be played off against each other. This paper contributes to present a variant of temporal logics which combines the expressiveness of both approaches. Using this proposed logic, we are able reason about many properties in a concise and intuitive manner. In particular, we concentrate on those types of properties that can be verified using reachability analysis. Hence these properties can be verified directly within our implemented framework.

Dept. of Mathematical Statistics**662. Characterizations of Continuous Distributions by the ir Mean Inactivity Times**

I. Elbatal, A.N. Ahmed and M. Ahsanullah

Pak. J. Statist., 28(3): 279-292 (2012) IF: 0.286

In this paper we introduce characterization results of a class for continuous distributions by properties relating to the reversed hazard rate (RHR) and the mean in activity time (MIT). A general procedure to characterize some continuous distributions by using reversed failure (hazard) rate function is obtained. The theoretical results are illustrated by obtaining new characterizations of some probability models including Gamma and Beta Distributions

Keywords: Reversed Hazard Rate; Mean Inactivity Time; Characterizations.

663. A Vikor Approach for Project Selection Problem

Mohamed F. El-Santawy and A. N. Ahmed

Life Science Journal-Acta Zhengzhou University Overseas Edition, 9(4): 5878-5880 (2012) IF: 0.073

Profitable investments lead to the growth and prosperity of each corporation. Various objectives are usually taken into account when projects are analyzed, including economic desirability, technical issues and environmental and social factors. Many conflicting criteria should be considered when comparing projects to choose among or rank them. The merit of MCDM techniques is that they consider both qualitative parameters as well as the quantitative ones. In this article, a MCDM project selection problem found in real-life international company is presented. The technique used named Vlse Kriterijumska Optimizacija I Kompromisno Resenje in Serbian (VIKOR) is applied for ranking the projects.

Keywords: Multi-Criteria Decision Making; Project Selection; Vikor.

664. An Information Entropy Weighting Method Combined to Topsis Approach for Ranking Consulting Firms

Mohamed F. El-Santawy and A. N. Ahmed

Life Science Journal-Acta Zhengzhou University Overseas Edition, 9(2s): 116-119 (2012) IF: 0.073

The purpose of this paper is to select and rank consulting firms by suggesting new multi-criteria decision making approach. The new technique employs an Information Entropy Weighting (IEW) method to allocate weights when no preference exists among criteria involved.

The Technique for Order Preference by Similarity to an Ideal Solution (TOPSIS) technique is combined to the new weighting method to rank the consulting firm. A MCDM problem of consulting firms found in real-life international company is presented. The new approach so-called SDVMOORA is employed to solve the MCDM problem.

Keywords: Consulting Firms; Information Entropy; Multi-Criteria Decision Making; Topsis.

665. Analysis of Project Selection by using Sdv-Moora Approach

Mohamed F. El-Santawy and A. N. Ahmed

Life Science Journal-Acta Zhengzhou University Overseas Edition, 9(2s): 129-131 (2012) IF: 0.073

Various objectives are usually taken into account when projects are analyzed, including economic desirability, technical issues and environmental and social factors. As the decision maker tries to maximize or minimize outcomes associated with each objective depending on its nature, so a Multi-Criteria Decision Making (MCDM) problem arises.

In this article, a new method is developed to assign weights to criteria when there is no preference among them based on the Standard Deviation (SDV) and Multi-Objective Optimization on the basis of Ratio Analysis (MOORA) technique. A MCDM project selection problem found in real-life international company is presented. The new approach so-called SDV-MOORA is employed to solve the MCDM problem.

Keywords: Multi-Criteria Decision Making; Moora; Project Selection; Standard Deviation.

666. Cv-Vikor: A New Approach for Allocating Weights in Multi-Criteria Decision Making Problems

Mohamed F. El-Santawy and A. N. Ahmed

Life Science Journal-Acta Zhengzhou University Overseas Edition, 9(4): 5875-5877 (2012) IF: 0.073

Multi-Criteria analysis, often called Multi-Criteria Decision-Making (MCDM) or Multi-Criteria Decision Aid methods (MCDA), is a branch of a general class of Operations Research (OR) models which deal with the process of making decisions in the presence of multiple objectives. These methods, which can handle both quantitative and qualitative criteria, share the common characteristics of conflict among criteria, incommensurable units and difficulties in design/selection of alternatives. The technique used in this paper named Vlse Kriterijumska Optimizacija I Kompromisno Resenje in Serbian (VIKOR) is combined to the Coefficient of Variation (CV) to constitute a new approach called CV-VIKOR. The Coefficient of Variation (CV) is employed to allocate weights when no preference existed among the criteria considered. Also, a given numerical example is solved to illustrate the proposed method.

Keywords: Coefficient Of Variation; Multi-Criteria Decision Making; Vikor.

667. Evaluating Consulting Firms using Vikor

Mohamed F. El-Santawy and A. N. Ahmed

Life Science Journal-Acta Zhengzhou University Overseas Edition, 9(4): 5872-5874 (2012) IF: 0.073

Many companies usually ask for consulting firm service. Thus evaluating and selecting a suitable consulting firm becomes an important issue. In this article, a Multi-Criteria Decision Making (MCDM) problem is presented and a real-life international company is illustrated. The technique used in solution named Vlse Kriterijumska Optimizacija I Kompromisno Resenje in Serbian (VIKOR) is applied for ranking the consulting

firms. Many quantitative criteria are considered to compare firms in order to rank them.

Keywords: Consulting Firms; Multi-Criteria Decision Making; Vikor.

668. Personnel Training Selection Problem Based on Sdv-Moora

Mohamed F. El-Santawy and A. N. Ahmed

Life Science Journal-Acta Zhengzhou University Overseas Edition, 9(2s): 123-125 (2012) IF: 0.073

Selection of qualified human resources is a key success factor for an organization. The adequate personnel training have a dramatic effect on improving the employees' performance, which will be reflected on the growth and competence of the whole organization, especially in large-size and multinational companies and organizations. Personnel selection problem is a well known Multi Criteria Decision Making (MCDM) problem which involves many conflicting attributes. In This article a MCDM problem is presented and a real-life international company personnel selection problem of a new manner is illustrated. A modified Technique for Multi-Objective Optimization on the basis of Ratio Analysis (MOORA) method combined to Standard Deviation weight method is presented to solve the MCDM problem.

Keywords: Multi-Criteria Decision Making; Moora; Personnel; Standard Deviation.

669. A Sdv-Moora Technique for Solving Multi-Criteria Decision Making Problems with No Preference

Mohamed F. El-Santawy and A. N. Ahmed

Life Science Journal-Acta Zhengzhou University Overseas Edition, 9(4): 5881-5883 (2012) IF: 0.073

The Standard Deviation (SDV) is a well known measure of dispersion, which suits the problem of allocating weights in MCDM. In this paper we try to address this problem by employing the Standard Deviation to allocate weights, then combining the proposed method to a well-known technique called Multi-Objective Optimization on the basis of Ratio Analysis (MOORA). The new approach so-called SDV-MOORA can be used when no preference among the criteria considered. Also, it is validated and illustrated by ranking the alternatives of a given numerical example.

Keywords: Facility Locations; Multi-Criteria Decision Making; Moora; Standard Deviation.

670. A Multi-Objective Chaotic Harmony Search Technique for Structural Optimization

Mohamed F. El-Santawy and A. N. Ahmed

International Journal of Computing Science, 1, (3) 9-12 (2012)

In this paper, a new Multi-Objective Evolutionary technique is introduced. The new method incorporates Harmony Search optimization to Chaos search. The well known Fitness Sharing method is employed to adopt the size of the external archive used by the technique during search. The proposed method is applied to Structural optimization which is one of the most challenging areas

in Multi-Objective Optimization. The proposed technique is applied to two-bar truss problem and the solution resulted shows superiority of the proposed method over the constraint method in terms of closeness and spread.

Keywords: Chaos; Harmony Search Algorithm; Multi-Objective Optimization; Structural Optimization; Two-Bar Truss.

671. Ranking Facility Locations Using Vikor

Mohamed F. El-Santawy, A. N. Ahmed and Mohamed Abd El-Baset Metwaly

Computing and Information Systems Journal, 16,(2): 45-48 (2012)

Many organizations want to expand their operations through allocating new facilities. The facility location decision process combines the identification, analysis, evaluation of and selection among alternatives. Facility location problem implies more than one dimension, many factors should be considered when comparing alternatives to choose among or rank them. In this article a Multi-Criteria Decision Making (MCDM) problem of facility location is presented and an international company's facility location problem of a new manner is illustrated. The well-known VIKOR technique is employed to solve the MCDM problem.

Keywords: Facility Location; Multi-Criteria Decision Making; Vikor.

672. Optimal Design of Failure Step Stress Partially Accelerated Life Tests with Type II Censored Inverted Weibull Data

Amal S. Hassan and Abeer K. Al-Thobety

International Journal of Engineering Research and Applications, 2, (3) : 3242-3253 (2012)

This article provides the optimum simple failure step stress partially accelerated life tests (FSS-PALTs) and statistical inferences for the model parameters and acceleration factor in which items are run at both accelerated and use conditions. It is assumed that the lifetime of the test items follows inverse Weibull distribution under type II censoring. The maximum likelihood estimators (MLEs), asymptomatic variance-covariance matrix and the confidence bounds of the model parameters and acceleration factor are obtained via MathCAD¹⁴. The optimum test plan specifies the optimal stress switching point is determined by minimizing the generalized asymptotic variance of the MLEs for the model parameters. Finally, the numerical studies are applied to illustrate the proposed procedures.

Keywords: Failure Step Stress Test; Generalized Asymptotic Variance; Inverse Weibull Distribution.

673. On Characterization of A Certain Family of Distributions Based on Some Recurrence Relations

Ali A. A-Rahman

International J. of Contemporary Mathematical Sciences, 7:2167-2177 (2012)

In this paper, three recurrence relations for a certain class of probability distributions are presented. The first one is a recurrence relation between conditional moments of $h(X)$ given X

> y. The second is the relationship between the moments and where is the order statistic from a sample of size n. The last one is the relationship between the conditional moments and t). Some results concerning Modified Weibull, Weibull, Rayleigh, exponential, Linear failure rate, 1 type Pearsonian distributions, Burr, Pareto power and uniform distributions are obtained as special cases.

Keywords: Characterization; Left Truncated Moments; Order Statistics; Recurrence Relations; Modified Weibull; Rayleigh; Exponential; Linear Failure Rate; 1 Type Pearsonian Distribution; Burr; Pareto; Power; Beta; Uniform Distributions.

674. Identifying A Certain Class of Distributions using Some Recurrence Relations

Ali A. A-Rahman

International Journal of Mathematical Archive, 3(8): 2997-3003 (2012)

In this paper, three recurrence relations for a certain class of probability distributions are presented. The first one is a recurrence relation between conditional moments of $h(X)$ given $X < y$. The second is the relationship between the moments is the order statistic from a sample of size n. The last one is the relationship between the conditional moments. Some results concerning exponentiated Weibull, modified Weibull, exponentiated Pareto, inverse Weibull, inverse Rayleigh, linear failure rate distribution, Burr, power and uniform distributions are obtained as special cases.

Keywords: Characterization; Right Truncated Moments; Order Statistics; Recurrence Relations; Exponentiated Weibull; Exponentiated Pareto; Modified Weibull; Inverse Weibull; Inverse Rayleigh; Linear Failure Rate; Burr; Power; Beta; Uniform Distributions.

675. Some Characteristic Properties of the Exponential Family

Samir-El-Sherif, S A Sayeda and A H Hanan

Journal Of Statistics And Mathematics, 3(2): 330-335 (2012)

In this paper, two recurrence relations characterizing a certain class of distribution family are presented. The first one is a recurrence relation between conditional moments of (X) given $X < y$. The second is a relationship between the conditional moments and where Y_k is the kth order statistic from a sample of size n. Finally the concept of conditional variance of (Y_k) given $Y_k > t$ is used to characterize this family. Some results concerning Modified Weibull, Weibull, Rayleigh, exponential, Linear failure rate, 1st type Pearsonian distributions, Burr, Pareto, Power and uniform distributions are obtained as special cases.

Keywords: Characterization; Truncated Moments; Conditional Variance; Order Statistics; Recurrence Relations; Modified Weibull; Linear Failure Rate; Pearson Distribution Of The First Type; Burr; And Power Distributions.

676. Bayesian Estimation for Burr Distribution Type Iii Based on Trimmed Samples

A. M. Abd-Elfattah and A. H. Alharbey

International Scholarly Research Network, 2012: 1-18 (2012)

Trimmed samples are widely employed in several areas of statistical practice, especially when some sample values at either or both extremes might have been contaminated. The problem of estimating the parameters of Burr distribution type III based on a trimmed samples and prior information will be considered. In this paper, we study the estimation of unknown parameters based on doubly censored type II.

The problem discussed using maximum likelihood method and Bayesian approach to estimate the shape parameters of Burr type III distribution. The numerical illustration requires solving nonlinear equations, therefore, MathCAD 2001 statistical package used to assess these effects numerically.

Keywords: Trimmed Samples; Burr Distribution Type Iii; Bayesian Approach.

677. Maximum Likelihood Estimation for Unknown Parameters of A Feller Pareto Distribution using Type I Censored Data

Amal El Beshlawy, Ibrahim Alaraby, Mohamed S.E.M. Abdel Kader, Dina H. Ahmed and Hossam E.M. Abdelrahman

Pioneer Journal of Theoretical and Applied Statistics, (2012)

The Feller-Pareto (FP) family traces its roots back to Feller (1971) but it was first defined and investigated by Arnold and Laguna (1977).

The FP family is a very general unimodal distribution which includes a variety of distributions as special cases and is known under several other names: in econometrics it is called a generalized beta distribution of second kind (GB2), whereas in actuarial science the term transformed beta distribution is used. It may also be considered as a generalized F distribution.

Arnold (1983) introduced an additional location parameter to the distribution that is further referred to as a Feller-Pareto distribution. In this paper we estimate the unknown parameters of a Feller-Pareto distribution derived by Arnold (1983), from censored type I samples using the method of maximum likelihood, asymptotic variance matrix is given as well as a numerical illustration and different special cases may be obtained from the present result.

Keywords: Fisk Distribution; Feller; Pareto Distribution; Order Statistics; Maximum Likelihood Estimation; Censored Type I.

678. On Comparing Different Chaotic Maps in Differential Evolutionary Optimization

Mohamed F. Ell-Santawy and A.N. Ahmed

Annals. Computer Science Series, X, fasc 25-28 (2012)

This paper presents a comparison between new approaches introducing different chaotic maps with ergodicity, irregularity and the stochastic property in Differential Evolution algorithm (DE). The members of the new family so-called Chaotic Differential Evolution (CDE) algorithms employ chaos in order to improve the global convergence by escaping the local solutions.

Keywords: Chaos; Chaotic Maps; Differential Evolution Algorithm; Optimization.

679. onSome Properties of the Discrete Nbu Class Based on Generating Function Order

Elbatal M. Ahsanullah

Journal of Statistical Theory and Applications, 11, (3): 209-223 (2012)

A new discrete class of life distributions is studied. This class is defined based on comparing the residual life time to the whole life in the probability generating function order giving the discrete new better than used in the probability generating function order ageing class (d_{NBUp}). Fundamental properties of this class are given including some closure properties and characterizations. Finally, we consider new results about comparisons of age and block replacement policies when the underlying distribution belongs to (d_{NBUp}) aging classes.

Keywords: Life Distributions; DNbug Ageing Class; Characterization Of Life Distributions; Block Replacement Policies.

680. On Some Reliability Characterizations of Member of the Pearson and Ord Families of Distributions

I. Elbatal

International Journal of Mathematical Archive, 3(4): 1316-1323 (2012)

In this paper we characterize the Pearson family of distributions by finding a relationship between the reversed hazard rate (RHR) and the mean inactivity time (MIT). We present characterization of discrete distribution using Ord-Carver system (discrete Pearson family).

Keywords: Reversed Hazard Rate; Mean Inactivity Time; Characterizations; Exponential Distribution. Induced Distributions.

681. A Chaos Embedded Differential Evolution Algorithm for Multi-Objective Optimization

Mohamed F. El-Santawy and A. N. Ahmed

Computing And Information Systems Journal, 16, No 2: 34-39 (2012)

In Multi-Objective Optimization, the problem of identifying the whole Pareto-optimal set is very crucial. In this paper, we developed a new Multi-Objective Evolutionary technique. The new method incorporates Differential Evolution algorithm to have search for better exploration and so better quality of solution.

In order to obtain more diversified solution set we used the well known Fitness Sharing method to adopt the size of the external archive maintained by the technique during search. Several test functions are employed for experiments. The simulation results show that the proposed algorithm is efficient.

Keywords: Chaos; Differential Evolution Algorithm; Multi-Objective Optimization.

682. Maximum Likelihood Estimation for the Bivariate Generalized Exponential Distribution Parameters using Type I Censored Data

Samir K. Ashour, Essam A. Amin and Hiba Z. Muhammed

Journal of Applied Sciences Research, 8(4): 1893-1900 (2012)

Recently a new distribution, named a bivariate generalized exponential (BVGE) distribution has been introduced by Kundu and Gupta (2009a). In this paper we obtain the maximum likelihood estimates for the unknown parameters of the bivariate generalized exponential distribution and their approximate variance covariance matrix based on time (right) censored samples. To illustrate the new results two numerical examples are given. The results in the case of complete samples obtained by Kundu and Gupta (2009a) can be considered as a special case from the present work as well as many special cases.

Keywords: Bivariate Generalized Exponential Distribution; Censored Samples; Fisher Information; Maximum Likelihood Estimate; Joint And Marginal Moments; Moment Generating Function.

683. Modified Goodness of Fit Tests for Exponentiated Pareto Distribution Under Selective Ranked Set Sampling

Amal S. Hassan

Australian J. of Basic and Applied Sciences, 6(1): 173-189 (2012)

This article deals with modified empirical distribution function (EDF) goodness of fit tests for exponentiated Pareto (EP) distribution. The performance of several modified goodness of fit tests such as Kolmogorov-Smirnov, Cramer-von Mises, Anderson-Darling, Watson and test statistics are investigated. The performances of these selected tests are studied under two sampling techniques which are simple random sampling (SRS) and ranked set sampling (RSS). Tables of critical values for the proposed tests statistics under RSS are given. The power of the modified test statistics under SRS and RSS is investigated for a number of alternative distributions. A simulation study is conducted to compare the power functions of these tests under RSS relative to SRS. The results of the power studies showed that the Anderson-Darling test statistic the most powerful goodness-of-fit test among the competitors.

Keywords: Anderson-Darling Test Statistic; Cramer-Von Mises Test Statistic; Exponentiated Pareto; Kolmogorov-Smirnov Statistic; Watson Statistic; Critical Values; Ranked Set Sample.

684. Reliability Estimation of Stress-Strength Model with Non-Identical Component Strength: the Exponentiated Pareto Case

Amal S. Hassan and Heba M. Basheikh

International Journal of Engineering Research and Applications, 2, 3: 2774-2781 (2012)

This article deals with the Bayesian and non-Bayesian estimation of reliability of an s-out-of-k system with non-identical component strengths which are subjected to a common stress. Assuming that both stress and strength are assumed to have an exponentiated Pareto distribution with common and known shape

parameter. Five non-Bayesian methods of estimation will be used which are maximum likelihood, moments, percentile, least squares and weighted least squares. The Bayesian estimation will be studied under squared error and LINEX loss functions using Lindley's approximation. Based on a Monte Carlo simulation study, comparison are made between the different estimators of system reliability by obtaining their absolute biases and mean squared errors. Comparison study revealed that the maximum likelihood estimator works the best among the competitors.

Keywords: Bayes Estimator; Exponentiated Pareto Distribution; Least Squares Estimator; Maximum Likelihood Stress–Strength Model.

685. Parameters Estimation for the Class of Weighted Weibull Distribution Under Type II Censored Samples

Elsayed A. Elsherpieny

Int. J. of Science and Advanced Technology, 2 No 6: 61-64 (2012)

Maximum likelihood estimators for the three unknown parameters of weighted Weibull distribution and the corresponding asymptotic variance covariance matrix are obtained under type II censored sample. Shahbaz et al. (2010) results may be considered as a special case from these results. Numerical illustrations will be carried out.

Keywords: A Class Of Weighted Distribution; Maximum Likelihood Estimators; Type II Censored Sample; Asymptotic Variance Covariance Matrix.

686. Optimal Progressive Group-Censoring Plans for Weibull Distribution in Presence of Cost Constraint

A. F. Attia and S. M. Assar

International Journal of Contemporary Mathematical Sciences, 7: 1337-1349 (2012)

This article discusses a life test under progressive type-I group-censoring. We use maximum likelihood method to obtain the point estimator of the unknown parameter of lifetime distribution. We proposed that scale parameter is known and fixed. In order to obtain a precise estimate of shape parameter of the Weibull distribution, one needs to design an optimal life test. Thus, this article proposes an approach to determine the number of test units, number of inspections and length of inspection interval of a life test under a pre-determined budget of experiment such that the asymptotic variance of estimator of shape parameter is minimum. The method will be applied to a numerical example and the sensitivity analysis will be investigated.

Keywords: Grouped Data; Progressive Censoring; Sensitivity Analysis; Type-I Censoring; Variance Optimality.

687. Maximum Likelihood Estimation of three Unknown Parameter of Beta-Weibull Distribution Under Type II Censored Samples

Mahmoud M.R. and Mandouh R.M.

Journal of Applied Sciences Research, 8(4): 2221-2231 (2012)

This paper is concerned with the maximum likelihood estimation (mle) of the beta-Weibull (BW) distribution. Maximum likelihood

equations are derived for estimating the distribution parameters from type II censored samples. Asymptotic variance covariance matrix is given for this type sample. Also, mle of hazard rate function of BW will be obtained. A simulation study is included.

Keywords: The Beta-Weibull Distribution; Censored Type II; Maximum Likelihood Estimates; Fisher Information Matrix; Asymptotic Variance Covariance Matrix.

688. Maximum Likelihood Estimation of Two Unknown Parameter of Beta-Weibull Distribution under Type II Censored Samples

M. R. Mahmoud and R. M. Mandouh

Applied Mathematical Sciences, 6: 2369-2384 (2012)

In this paper, the maximum likelihood estimates (mles) are obtained for the two unknown parameters of the Beta-Weibull (B-W) distribution under type II censored samples. Also, asymptotic variances and covariance matrix of the estimators are given. An iterative procedure is used to obtain the estimators numerically using MathCad Package. To study the properties of maximum likelihood estimators simulation results are included for different sample sizes.

Keywords: The Beta-Weibull Distribution; Censored Type II; Maximum Likelihood Estimates; Variance Covariance Matrix.

689. Parameter Estimation Beta-Weibull Distribution Based on Censored Samples

R.M. Mahmoud and R.M. Mandouh

Journal of Applied Sciences Research, 8(1): 390-400 (2012)

This paper studies the maximum likelihood estimation in the case of beta-Weibull distribution from type II censored samples. Asymptotic variance covariance matrix will be obtained. A simulation study has been performed, using MathCad software to investigate the properties of the MLEs.

Keywords: The Beta-Weibull Distribution; Censored Type II; Maximum Likelihood Estimates; Asymptotic Variance Covariance Matrix.

Dept. of Operational Research

690. Constrained Optimization Based on Modified Differential Evolution Evolution Algorithm

Ali Wagdy Mohamed and Hegazy Zaher Sabry

Information Sciences, 194: 171-208 (2012) IF: 2.833

This paper presents a novel Constrained Optimization based on Modified Differential Evolution algorithm (COMDE). In the new algorithm, a new directed mutation rule, based on the weighted difference vector between the best and the worst individuals at a particular generation, is introduced. The new directed mutation rule is combined with the modified basic mutation strategy DE/rand/1/bin, where only one of the two mutation rules is applied with the probability of 0.5. The proposed mutation rule is shown to enhance the local search ability of the basic Differential Evolution (DE) and to get a better trade-off between convergence rate and robustness. Two new scaling factors are introduced as uniform random variables to improve the diversity of the population and to bias the search direction. Additionally, a

dynamic non-linear increased crossover probability is utilized to balance the global exploration and local exploitation. COMDE also includes a modified constraint handling technique based on feasibility and the sum of constraints violations. A new dynamic tolerance technique to handle equality constraints is also adopted. The effectiveness and benefits of the new directed mutation strategy and modified basic strategy used in COMDE has been experimentally investigated. The effect of the parameters of the crossover probability function and the parameters of the dynamic tolerance equation on the performance of COMDE have been analyzed and evaluated by different experiments. Numerical experiments on 13 well-known benchmark test functions and five engineering design problems have shown that the new approach is efficient, effective and robust. The comparison results between the COMDE and the other 28 state-of-the-art evolutionary algorithms indicate that the proposed COMDE algorithm is competitive with and in some cases superior to, other existing algorithms in terms of the quality, efficiency, convergence rate and robustness of the final solution.

Keywords: Differential Evolution; Constrained Optimization; Directed Mutation; Dynamic Non-Linear Crossover; Dynamic Tolerance.

691. Comments on "Solving A Capacitated Fixed-Charge Transportation Problem by Artificial Immune and Genetic Algorithms with A Prüfer Number Representation" by Molla-Alizadeh-Zavardehi, S. Et Al. Expert Systems with Applications (2011)

Mahmoud M. El-Sherbiny

Expert Syst Appl, 39: 11321-11322 (2012) IF: 2.203

In this work presented are some comments concerning the paper titled Spanning tree-based artificial immune and genetic algorithms with a Prüfer number for solving a capacitated fixed charge transportation problem was proposed by Molla-Alizadeh-Zavardehi, S. et al., which was published in Expert Systems with Applications 38 (2011) 10462–10474. The comments are related to the mathematical model of the capacitated fixed charge problem, transportation graph of the example and the total cost of the example.

Keywords: Fixed Charge Transportation; Artificial Immune Algorithm; Genetic Algorithms; Spanning Tree; Prüfer Number.

692. Alternate Mutation Based Artificial Immune Algorithm for Step Fixed Charge Transportation Problem

Mahmoud Moustafa El-Sherbiny

Egyptian Informatics Journal, 13: 123-134 (2012) IF: 2

Step fixed charge transportation problem (SFCTP) is considered as a special version of the fixed-charge transportation problem (FCTP). In SFCTP, the fixed cost is incurred for every route that is used in the solution and is proportional to the amount shipped. This cost structure causes the value of the objective function to behave like a step function. Both FCTP and SFCTP are considered to be NP-hard problems. While a lot of research has been carried out concerning FCTP, not much has been done concerning SFCTP. This paper introduces an alternate Mutation

based Artificial Immune (MAI) algorithm for solving SFCTPs. The proposed MAI algorithm solves both balanced and unbalanced SFCTP without introducing a dummy supplier or a dummy customer. In MAI algorithm a coding schema is designed and procedures are developed for decoding such schema and shipping units. MAI algorithm guarantees the feasibility of all the generated solutions. Due to the significant role of mutation function on the MAI algorithm's quality, 16 mutation functions are presented and their performances are compared to select the best one. For this purpose, forty problems with different sizes have been generated at random and then a robust calibration is applied using the relative percentage deviation (RPD) method. Through two illustrative problems of different sizes the performance of the MAI algorithm has been compared with most recent methods.

Keywords: Fixed Charge Transportation; Convergence; Step Fixed Charge; Transportation; Artificial Immune Algorithm.

693. On using Vikor for Ranking Personnel Problem

Mohamed F. El-Santawy and Ramadan A. Zean El-Dean

Life Science Journal-Acta Zhengzhou University Overseas Edition, 9(4): 1534-1536 (2012) IF: 0.073

Personnel selection problem implies more than one dimension to be optimized. Many conflicting criteria should be considered when comparing alternatives to choose among or rank them. In this article, a Multi-Criteria Decision Making (MCDM) problem is presented and a real-life international company personnel selection problem of a new manner is illustrated. The technique used in solution named Vlse Kriterijumska Optimizacija I Kompromisno Resenje in Serbian (VIKOR) is applied for ranking the alternatives.

Keywords: Multi; Criteria Decision Making; Personnel; Vikor.

694. A Sdv-Moora Approach for Ranking Facility Locations

Mohamed F. El-Santawy and Ramadan A. Zean El-Dean

Life Science Journal-Acta Zhengzhou University Overseas Edition, 9(2s): 120-122 (2012) IF: 0.073

The suitability of a specific location for proposed facility operations depends largely on what location factors are selected and evaluated as well as their potential impact on corporate objectives and operations. Facility location problem is a typical Multi Criteria Decision Making (MCDM) problem which involves many conflicting attributes. In this paper we try to tackle this well known problem by combining the Standard Deviation to allocate the weights, then combining the proposed method to Multi-Objective Optimization on the basis of Ratio Analysis (MOORA) technique. An international company's facility location problem of a new manner is illustrated. The new approach so-called SDV-MOORA is employed to solve the MCDM problem.

Keywords: Facility Locations; Multi-Criteria Decision Making; Moora; Standard Deviation.

695. Selection of A Consulting Firm by using Sdv-Moora

Mohamed F. El-Santawy and Ramadan A. Zean El-Dean

Life Science Journal-Acta Zhengzhou University Overseas Edition, 9(2s): 126-128 (2012) IF: 0.073

Many companies usually ask for consulting firm service to cautiously deal with critical problems, such that introducing new product, pricing, marketing strategies. Thus evaluating and selecting a suitable consulting firm becomes an important issue. Many criteria must be considered when evaluating consulting firms, some of them are qualitative others are quantitative. In This article a Multi-Criteria Decision Making (MCDM) problem of a real-life international company is presented. The MCDM problem of selecting consulting firm existed in the company is tackled by a new proposed method. A modified Technique for Multi-Objective Optimization on the basis of Ratio Analysis (MOORA) method combined to Standard Deviation weight method is presented to solve the MCDM problem.

Keywords: Consulting Firm; Multi-Criteria Decision Making; Moora; Standard Deviation.

696. A Decision Support System for Performance Evaluation

Ramadan Abdel Hamid ZeinEldin

International Journal of Computer Applications, (2012)

This paper presents a model based decision support system (DSS) for evaluating performance. Performance evaluation in business is difficult. Multicriteria methods are used for evaluation of performance of public and private organizations. The proposed system is based on financial ratios and some methods such as Analytic Hierarchy Process (AHP), Technique for Order Preference by Similarity to Ideal Solution (TOPSIS) and Simple additive weighting (SAW). AHP is a theory of measurement through pairwise comparisons and relies on the judgements of experts to derive priority scales and it is used to determine the criteria weights. TOPSIS is used to help select the best alternative with a finite number of criteria. SAW is the most widely used method because it is simple and easy to use and understand. The developed decision support system is implemented with a real application.

Keywords: Decision Support System; Model Base; Ahp; Topsis; Saw; Performance.

697. Chaotic Differential Evolution Optimization

Mohamed F. El-Santawy, A. N. Ahmed and Ramadan A. Zean El-Dean

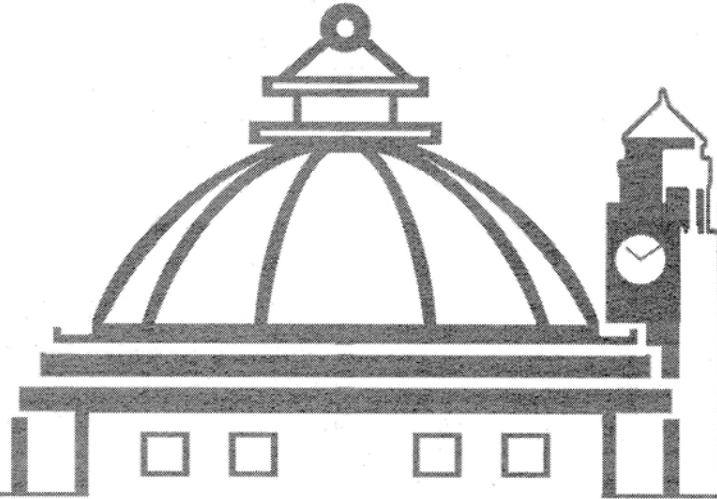
Computing and Information Systems Journal, (2012)

In this paper, a hybrid differential evolution (DE) algorithm based on chaos is proposed. In this algorithm, Chaos Search gives more perturbations, which provides more opportunities for the algorithm to find the global optimum. Two test functions are employed for experiments. The simulation results show that the proposed algorithm is efficient.

Keywords: Chaos; Differential Evolution Algorithm; Evolutionary Algorithms; Multimodal Functions.



**International Publications Awards
Cairo University**



Authors' Index

Authors' Index

A

- | | | | |
|--------------------------------|--|----------------------------------|---------------------------------------|
| Abd El -Fattah, Alaa: | 27 | AboulEzz, Heba: | 131 |
| Abd El Gwad, Soha: | 58, 59 | Aboul-Enein, Ahmed: | 4, 8, 10 |
| Abd El Wahab, Sahar: | 34, 36 | Aboufotouh, Abdou: | 34 |
| Abd El-Aty, Abd El-Aty: | 155, 156, 157,
158, 159 | Aboufotouh, Abdel-Nasser: | 128 |
| Abd El-Ghani, Monier: | 50 | Abowarda, Mohamad: | 144 |
| Abd El-Ghany, Wafaa: | 162, 163 | Abu Elela, Shahenda: | 103 |
| Abd El-Kader, Fawzy: | 121, 126 | Abu El-Ela, Faten: | 8 |
| Abd El-Kader, Mahmoud: | 128 | Abu-Abdeen, Mohammed: | 120, 122, 123,
125, 128 |
| Abd El-Rahman, Yasser: | 105 | Abu-Seida, Ashraf: | 164, 165 |
| Abd El-Rahman, Hamid: | 91 | Abu-Taleb, Amira: | 51 |
| Abd El-Wahab, Abeer: | 29, 30 | Adel, Mohamed: | 116 |
| AbdRabo, Fawzia: | 27 | Adel, Ahmed: | 128 |
| AbdRahmanb, Mariam: | 87 | Adham, Fatma: | 102 |
| Abdel Azim, Sabry: | 79 | Affi, Nehal: | 159 |
| Abdel Ghani, Nour: | 54, 62, 65, 72,
74, 79, 89, 91,
95, 98 | Affiy, Abd El Moneim: | 3, 5, 6, 7, 8, 14 |
| Abdel Hadi, El-Sayed: | 160 | Ahmad, Yahia: | 61 |
| Abdel Kader, Mohamed: | 124 | Ahmed, Abdul Hady: | 171, 172, 173,
174 |
| Abdel Kawy, Wael: | 37, 38 | Ahmed, Sayeda: | 28, 29 |
| Abdel Samd, Hanan: | 29 | Ahmed, Fouad: | 9 |
| Abdel Wahab, Mohamed: | 43 | Ahmed, Mohamed: | 121, 122 |
| Abdel?Riheem, Nadia: | 91 | Ahmed, Ahmed: | 55, 60, 64, 69,
84, 99 |
| Abdel-Alim, Ahmed: | 36 | Ahmed, Ashour: | 65 |
| Abd-Elfattah, Abdallah: | 173 | Ahmed, Ahmed: | 84 |
| Abdel-Fattah, Azza: | 86, 95 | Ahmed, Zakia: | 150, 166, 167 |
| Abdel-Gawad, Hamdy: | 112 | Ahmed, Alaa: | 144 |
| Abd-Elhameed, Waled: | 112 | Ahmed, Mohamed: | 121, 124, 125,
126, 127 |
| Abdelhamid, Ismail: | 75 | Ahmed, Esayed: | 175 |
| Abdelhamid, Abdou: | 66, 83, 89, 90, 91 | Alharery, Mahmoud: | 149, 167 |
| Abdel-Kader, Nora: | 74, 80 | Ali, Rehab: | 4, 6 |
| Abdel-Mageed, Ibrahim: | 24 | Ali, Shimaa: | 60, 69 |
| Abdel-Moein, Nadia: | 9, 13 | Ali, Mohamed: | 50 |
| Abdel-Moein, Khaled: | 149, 168 | Allam, Samy: | 120, 128, 129 |
| Abdel-Moniem, Ebtsam: | 13 | Alsayed, Alsayed: | 5, 13, 20 |
| Abdel-Rahim, Emam: | 6, 9, 11 | Aly, Salwa: | 148 |
| Abdelrahman, El-Sayed: | 110 | Ameer, Magda: | 61 |
| Abdel-Rahman, Ali: | 172, 173 | Amer, Wafaa: | 50 |
| Abdelrazek, Fathy: | 83, 90 | Amer, Mahmoud: | 131 |
| Abdelsalam, Hala: | 136 | Amer, Aziza: | 158 |
| Abdelsalam, Abdallah: | 118, 125 | Amin, Ahmed: | 90 |
| Abdullah, Aboubakr: | 63 | Amin, Mohamed: | 123 |
| Abdullatif, Amal: | 42 | Asaad, Mohamed: | 113 |
| Abo Taleb, Sawsan: | 15, 17 | Ashour, Samir: | 173, 174 |
| Abo-Ezz, Eid: | 110 | Assar, Salwa: | 175 |
| Abo-Hegazy, Samir: | 25 | Atta, Nada: | 54, 56, 57, 58,
60, 61, 63, 67, 69 |
| AbouDahab, Helal: | 142 | Attaby, Fawzy: | 84, 86, 95 |
| | | Attia, Osama: | 107 |
| | | Awad, Mervat: | 44 |
| | | Awad, Mohamed: | 59, 64, 84, 91 |
| | | Awad, Hanan: | 103 |

B

Badawi, Mona:	19
Badawy, Waheed:	56, 66, 72, 81, 98
Badie, Adel:	31
Badran, Snaa:	27
Baraka, Taher:	149
Baraka, Amine:	58, 90
Barsoum, Barsoum:	89
Basha, Mohamed:	122
Basha, Ahmed:	122
Basta, Fawzy:	105
Borham, Taha:	39

D

Dakrory, Ahmed:	139
Darweesh, Ahmed:	84
Darwish, Elham:	88, 96
Dawood, Kamal:	83
Dawoud, Mohamed:	51
Doha, Eid:	111, 112

E

Eihusseiny, Mona:	52
Eissa, AlaaEldin:	146
Eissa, AlaaEldin:	166
El Amir, Azza:	137, 138, 140
El Anadouli, Bahgat:	60, 64, 69, 99
El Aref, Mohamed:	108
El Badawy, Hanaa:	142
El Badawya, Shaima:	158
El Barkooky, Ahmed:	106
El Baroty, Gamal:	3
El Deeb, Somaya:	138
El Hadidy, Azza:	50
El Iraqi, Kassem:	166
El Manawi, Abdel Hamid:	106, 108
El Miniawy, Hala:	155
El Nashar, Rasha:	54, 57, 62, 64
El Ridi, Rashika:	130, 131
El Shemy, Hany:	3, 8, 9, 11, 12
El Sherbini, Ashraf:	127, 128
El Sherbiny, Tharwat:	120, 127, 128, 129
El Zorba, Hesham:	160
El. Shafee, Ezzeldin:	72, 76
El-Ansary, Aida:	74, 96
El-Assal, Salah El-Din:	32, 33

Elazab, Nasser:	114
El-Bahy, Mohamed:	154
Elbatal, Ibrahim:	171, 174
El-Beltagi, Hossam:	3, 5, 7, 8, 13
Elbially, Nihal:	45, 47, 48
El-Deab, Mohamed:	54, 58, 60, 66, 69, 99
Eldebss, Taha:	65
El-Dessouky, Maher:	94
El-Dieb, Samia:	27
El-Enbaawy, Mona:	150
El-Gamel, Nadia:	56
El-Gammal, Samar:	160
El-Gawad, Karima:	41
El-Gebaly, Reem:	45, 47, 48
El-Gendy, Essam:	25
El-Ghor, Mohamed:	137
El-Helaly, Mostafa:	40, 41
El-Idreesy, Tamer:	65, 91
El-Jakee, Jakeen:	150
El-Kabbany, Farouk:	124
El-Kady, Amira:	36
Elkholy, Said:	86
Ellithi, Ali:	117, 118
El-Mahy, Wessam:	44
Elmougy, Mahamed:	40, 42
Elnagar, Salah:	29
Elsabee, Maher:	68, 78, 82, 86, 88, 98, 99
El-Samee, Abd El-Monem:	148
Elsayed, Gamal:	30
Elsayed, Khaled:	123
Elsayed, Wael:	103
Elsayed, Ahmed:	111
El-Sayed, Ashraf:	22
Elshaghabee, Foad:	27
Elshahat, Khaled:	153, 154
El-Sharkawi, Mohamed:	105
El-Sheikh, Mohamed:	29
Elshemey, Wael:	46, 49
El-Sherbiny, Mahmoud:	176
El-Sherif, Samir:	28, 29
El-Sherif, Ahmed:	75, 80, 81, 98
El-Shobaky, Hala:	72
Eltaweel, Safaa:	82
Elwahy, Ahmed:	83, 84, 98
El-Zalabani, Soheir:	73, 81
El-Zawawy, Mohamed:	114, 115
Esawy, Sherif:	14
Esmael, Ihab:	120
Esmail, Ahmed:	118
Essa, Khalid:	110

F

Fahmi, Abdel Gawad:	75, 83, 87, 88, 90, 97
Fahmy, Mona:	69, 71
Fahmy, Sohair:	138, 141
Farag, Mohamed:	120
Farag, Ahmed:	65, 85, 99
Farahat, Ahmed:	5, 13
Farid, Alyaa:	138
Fathy, Hayam:	18
Fayed, Rabie:	166
Fayez, Mohamed:	18, 19
Fekry, Amany:	61
Frag, Eman:	62, 63, 81, 96

G

Gaber, Ahmed:	31, 32, 33
Gad, Ahmed:	22, 23
Gad El-Said, Wageh:	150
Gad-Allah, Ahmed:	91
Galal, Ahmed:	54, 56, 57, 58, 60, 61, 63, 67, 69, 75
Galal, Hussein:	150
Gamala, Wafia:	124
Geweely, Neveen:	53
Ghazawy, Nervina:	103
Ghoneim, Nahed:	168
Gomaa, Elham:	15, 16
Goniem, Azza:	61
Goudah, Ayman:	155, 156, 158
Guirguis, Osiris:	45, 46, 47, 48

H

Hafez, Ranya:	126
Haitham, Mohammed:	49
Hamadan, Mohamed:	105, 106, 107, 108
Hamdi, Salwa:	136, 140
Hamed, Hamed:	35
Hamed, Hamed:	35
Hashem, Mohamed:	28, 41
Hashem, Mohamed:	159, 160
Hassan, Amal:	172, 174
Hassan, Hazem:	10
Hassan, Hanaa:	76
Hassan, Safaa:	74
Hassan, Walid:	61, 98
Hassan, Rania:	50
Hassib, Hekmat:	80

Hatem, Mohamed:	21
Hatem, Mahmoud:	162, 163
Heakal, Fakiha:	55, 58
Hefny, Hesham:	169, 170
Hegazi, El-Saeed:	35, 36
Hegazi, Ayman:	33, 34, 36
Hegazi, Nabil:	18, 19
Hegazy, Gehan:	159
Helal, Mohamed:	112, 113
Helmy, Shahinaz:	30, 31
Hilal, Rifaat:	68, 76
Hosny, Wafaa:	80
Hussein, Basim:	122

I

Ibrahem, Mai:	144, 145, 146, 167
Ibrahim, Hosny:	67, 92
Ibrahim, Sherif:	130
Ibrahim, Marwa:	144, 146, 166
Ibrahim, Hend:	15
Ibrahim, Ayman:	140
Ismail, Ismai:	45
Ismail, Lotfi:	123, 124, 129
Issa, Yousry:	67, 80, 86, 91, 92, 93

K

Kamel, Mostafa:	109
Kaoud, Hussein:	168
Kelany, Wael:	148
Kesba, Hosny:	20
Khadra, Ahmed:	107
Khalaf, Ezz El Din:	106
Khalaf, Mahmoud:	167
Khalaf, Abdel Azim:	166
Khalil, Ali:	106, 108
Khalil, Neveen:	50, 52
Khater, Motaza:	91
Khatab, Magda:	34
Khatab, El AmiraHend:	44
Kheder, Nabila:	68, 85
Khelfa, DiaaEddin:	162, 163
Kilany, Omima:	35
Kobeasy, Mohamed:	9

M

Maarouf, Ahmed:	119
Mabrouk, Walid:	110
Madbouly, Samy:	54, 75

Mady, Mohsen:	45, 46, 47, 48	Nasser, Ghanem:	22, 23
Mahana, Noha:	140	Noha, Saleh:	49
Mahmoud, Mahmoud:	175	Noor, Neveen:	131, 141
Mahmoud, Adel:	24	NourEldien, Faten:	63, 78, 96, 97
Mahmoud, Ghada:	12, 13, 41		
Mahran, Khaled:	145	O	
Makar, Karter:	109		
Mansour, Ahmed:	65, 72, 79	Omar, Mohamed:	62, 81
Mansour, Hayam:	147	Osman, Hamdy:	123, 125
Mansour, Hesham:	119, 126, 127	Osman, Ahmed:	138
Marei, Waleed:	152, 153	Osman, Kamelia:	149, 150
Marie, Mohamed:	138	Osman, Wafaa:	126
Medany, Shymaa:	66, 81	Othman, Mohamed:	123
Mekky, Ahmed:	84		
Metwally, Abd El Alim:	25, 26	R	
Mikhail, Maurice:	36		
Moawad, Adel:	153	Rady, El-Houssainy:	169
Mohamed, Samira:	35	Rageh, Monira:	45, 47, 48
Mohamed, Nadia:	69, 71	Rahoma, Walid:	43
Mohamed, Gehad:	62, 63, 70, 73, 77, 78, 79, 81, 89, 94, 95, 96, 97	Ramadan, Hassan:	15
Mohamed, Riham:	56, 64, 71, 77, 82	Rashad, Ferial:	18
Mohamed, Sabrein:	91	Rawi, Sayed:	138
Mohamed, Thoraya:	86, 87	Risha, El-Sayed:	28
Mohamed, Mona:	130	Riyadh, Sayed:	85
Mohamed, Hussein:	147	Rizk, Mamoud:	89, 91
Mohamed, Amira:	145	Romeih, Ehab:	27
Mohamed, Ali:	175	Romeilah, Ramy:	7
Mohamed, Mohamed:	124		
Mohammed, Faten:	167	S	
Mohammed, Waleed:	111		
Mohareb, Rafat:	67, 71, 82, 89, 93, 94	Saad, Gamal:	70, 82, 87
Moharram, Hatem:	75	Sabaa, Magdy:	64, 77, 82, 87
Mohsen, Ashraf:	26	Sabet, Salwa:	140
Monib, Mohamed:	18	Sabry, Hegazy:	175
Morsi, Mohamed:	59	Said, Amir:	105
Morsy, Gamal:	137	Sakr, Osama:	24
Mostafa, Ehab:	20, 21	Saleh, Waleed:	18
Mostafa, Ayman:	164, 165	Saleh, Mahmoud:	59, 91
Mourad, Eman:	140	Saleh, Ahmed:	53
Moussa, Tarek:	52	Salem, Mohamed:	118
		Salih, Said:	91
N		Samer, Mohamed:	20, 21, 22
		Samir, Ahmed:	149
Nagiub, Hazem:	124	Sanad, Manar:	19
Naguib, Hala:	68, 70, 88	Sanad, Manar:	19
Naoum, Magdi:	87	Setta, Ahmed:	161
Nasr, Shimaa:	167	Seufi, Alaaeddeen:	102
Nassar, Farid:	24	Shaabana, Mohamed:	65, 83, 84
Nassar, Mohamed:	15	Shaban, Ayman:	34
Nassar, Dalia:	16	Shaban, Khalid:	163, 164
Nassar, Rania:	16	Shafik, Magdy:	25
		Shaheen, Mohamed:	36
		Shahein, Mohamed:	42

Shahin, Mohamed:	113
Shalaby, Emad:	8, 12, 13, 14
Shallan, Magdy:	10
Shaurub, El-Sayed:	103, 104
Shawali, Ahmed:	66, 67, 83, 84, 87
Shawali, Ahmad:	82, 86
Shehab, Ola:	67, 92
Shehata, Said:	41, 42, 43
Shehata, Mohamed:	73, 74, 79, 84
Sherif, Sherif:	70, 93
Shokry, Mohamed:	165
Shoukry, Mohamed:	73, 74, 75, 76, 79, 80, 84
Soliman, Khalid:	110
Soliman, Ahmed:	74
Soliman, Amal:	141, 142
Suloma, Ashraf:	40
Sweilam, Nasser:	75, 113, 114, 115, 116
Swielim, Gamal:	160

T

Tahoun, Tahoun:	75, 107
Talaat, Neveen:	14, 18
Tolba, Ayman:	165

Y

Yassein, Safaa:	144
Yehia, Taher:	34
Yehia, Ramy:	52, 53
Yousef, Shahinaz:	44
Yousif, Ausama:	168
Youssri, Youssri:	112

Z

Zaki, Manal:	166
Zayed, Mohamed:	55, 56, 62, 73, 77, 81
Zein, Haggag:	32
Zein El-Abdeen, Hayman:	43, 44
Zeineldin, Ramadan:	176, 177
Zohdy, Hussein:	85

General Scientific Research Department
Information System Unit

Cairo University- University Administration Building,
Tharwat St., Giza, Egypt, Postal code: 12613.

Phone: +(202) 35704943 - 35676918 - 35675597

Fax: +(202) 37745324

Web site: <http://gsrd.cu.edu.eg>
www.cu.edu.eg

E-mail: resinfo@cu.edu.eg